TECHNICAL REPORT SL-85-8

STRUCTURAL ELEMENT TESTS IN SUPPORT OF THE KEYWORKER BLAST SHELTER PROGRAM

by

T. R. Slawson, H. M. Taylor, Jr.,
F. D. Dallriva, S. A. Kiger

Structures Laboratory

DEPARTMENT OF THE ARMY
Waterways Experiment Station, Corps of Engineers
PO Box 631, Vicksburg, Mississippi 39180-0631

US Army Corps of Engineers

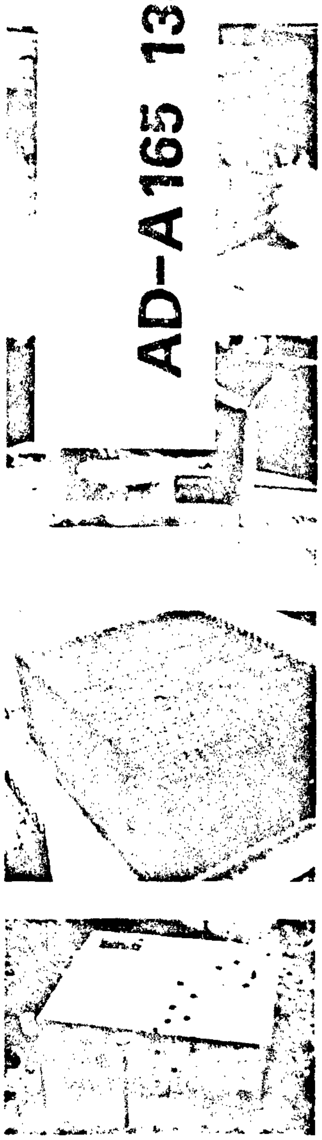

Best Available Copy

October 1985

Final Report

Prepared for Federal Emergency Management Agency
Washington, DC 20472

and Defense Nuclear Agency
Washington, DC 20305

Under Interagency Agreement No. E87830072 and
DNA Subtask Y99QAXSC, Work Unit 00080

STRUCTURES LABORATORY

TECHNICAL REPORT SL-85-8

STRUCTURAL ELEMENT TESTS IN SUPPORT OF THE KEYWORKER BLAST SHELTER PROGRAM

by

T. R. Slawson, H. M. Taylor, Jr.,
F. D. Dallriva, S. A. Kiger

Structures Laboratory

DEPARTMENT OF THE ARMY
Waterways Experiment Station, Corps of Engineers
PO Box 631, Vicksburg, Mississippi 39180-0631

October 1985

Final Report

Prepared for Federal Emergency Management Agency
Washington, DC 20472

and Defense Nuclear Agency
Washington, DC 20305

Under Interagency Agreement No. E87830072 and
DNA Subtask Y99QAXSC, Work Unit 00080

Unclassified

SECURITY CLASSIFICATION OF THIS PAGE (When Data Entered)

REPORT DOCUMENTATION PAGE		READ INSTRUCTIONS BEFORE COMPLETING FORM
1. REPORT NUMBER Technical Report SL-85-8	2. GOVT ACCESSION NO. AD-A165136	3. RECIPIENT'S CATALOG NUMBER
4. TITLE (and Subtitle) STRUCTURAL ELEMENT TESTS IN SUPPORT OF THE KEYWORKER BLAST SHELTER PROGRAM		5. TYPE OF REPORT & PERIOD COVERED Final report 6. PERFORMING ORG. REPORT NUMBER
7. AUTHOR(s) T. R. Slawson, H. M. Taylor, Jr., F. D. Dallriva, S. A. Kiger		8. CONTRACT OR GRANT NUMBER(s)
9. PERFORMING ORGANIZATION NAME AND ADDRESS US Army Engineer Waterways Experiment Station Structures Laboratory PO Box 631, Vicksburg, Mississippi 39180-0631		10. PROGRAM ELEMENT, PROJECT, TASK AREA & WORK UNIT NUMBERS Interagency Agreement No. E87830072 and DNA Subtask Y99QAXSC Work Unit 00080
11. CONTROLLING OFFICE NAME AND ADDRESS Federal Emergency Management Agency 500 C Street, SW, Room 716 Washington, DC 20472 and Defense Nuclear Agency Washington, DC 20305		12. REPORT DATE October 1985 13. NUMBER OF PAGES 322 15. SECURITY CLASS. (of this report) Unclassified
14. MONITORING AGENCY NAME & ADDRESS(if different from Controlling Office)		15a. DECLASSIFICATION DOWNGRADING SCHEDULE
16. DISTRIBUTION STATEMENT (of this Report) Approved for public release; distribution unlimited.		
17. DISTRIBUTION STATEMENT (of the abstract entered in Block 20, if different from Report)		
18. SUPPLEMENTARY NOTES Available from National Technical Information Service, 5285 Port Royal Road, Springfield, Virginia 22161. fr. back		
19. KEY WORDS (Continue on reverse side if necessary and identify by block number) Airblast simulation; ~~Blast shelter~~; Box structures; ~~Civil defense~~; ~~Concrete structures~~; Nuclear explosion simulation; Shallow-buried structures; Soil-structure interaction; Underground structures		

20. ABSTRACT (Continue on reverse side if necessary and identify by block number)

At the initiation of this study, civil defense planning called for the evacuation of nonessential personnel to safe host areas during a time of crisis, and the construction of shelters to protect the keyworkers remaining behind. The investigation documented in this report will assist the US Army Engineer Division, Huntsville, in designing a 100-man keyworker blast shelter.
(Continued)

DD FORM 1473, 1 JAN 73 EDITION OF 1 NOV 65 IS OBSOLETE

Unclassified

SECURITY CLASSIFICATION OF THIS PAGE (When Data Entered)

20. ABSTRACT (Continued).

Contd

Six static tests and twelve dynamic tests were conducted on approximately 1/4-scale models of blast shelters. Specific objectives of these tests were to evaluate the preliminary structural design, to investigate structural response in various backfills, to investigate and recommend minimum concrete strength requirements, to evaluate structural response calculations, and to develop a data base on repeated hits so that structural response computational procedures can be developed to include the effects of repeated hits.

Test results indicate that the keyworker blast shelter design will resist a peak overpressure of 150 psi from a 1-MT nuclear weapon. Based on the results of this series of static and dynamic tests, it is recommended that:

1. Minimum strength of concrete used in the keyworker blast shelter should be 3,000 psi.
2. Backfill specifications can be reduced to include soils with a minimum angle of internal friction of 25 degrees (30 degrees for foundation materials).
3. A minimum depth of burial of 4 feet (30 percent of the unsupported roof span) should be used.
4. The interior structural steel frames should be replaced with precast or cast-in-place reinforced concrete walls.

Keywords: FLD19

PREFACE

This investigation, sponsored by the Federal Emergency Management Agency (FEMA), under Interagency Agreement No. E87830072, and by the Defense Nuclear Agency (DNA) under Subtask Y99QAXSC, Work Unit 00080, "Keyworker Shelter," was conducted by personnel of the Structures Laboratory (SL), US Army Engineer Waterways Experiment Station (WES) during the period March 1983 through January 1984.

This study was performed under the general supervision of Messrs. Bryant Mather, Chief, SL, and J. T. Ballard, Assistant Chief, SL, and under the direct supervision of Dr. Jimmy P. Balsara, Chief, Structural Mechanics Division (SMD), SL. Dr. S. A. Kiger was project manager for this research. This report was prepared by Messrs. T. R. Slawson, F. D. Dallriva, and Dr. S. A. Kiger, SMD, and by Mr. H. M. Taylor, Jr., Geotechnical Laboratory, WES. Mr. Tom Provenzano, FEMA, and Dr. Kent Goering, DNA, were the program monitors.

COL Tilford C. Creel, CE, and COL Robert C. Lee, CE, were Commanders and Directors of WES during the conduct of the study. COL Allen F. Grum, USA, was the Director of WES during the preparation and publication of this report. Mr. F. R. Brown and Dr. Robert W. Whalin were Technical Directors.

CONTENTS

LIST OF ILLUSTRATIONS

Figure		Page

Figure		Page

LIST OF TABLES

Table		Page
5.4	Comparison of static ultimate capacities	87
5.5	Static load-deflection behavior	87
5.6	Comparison of Type 2 static test results	88
6.1	Experimentally determined loading wave velocities, lateral soil pressure coefficients, roof reflection factors, and reflected stress durations	110
6.2	Experimental attenuation factors	111
6.3	Dynamic soil arching	112
6.4	Static soil arching	113
6.5	Comparison of actual and predicted roof responses	114
A.1	Parameters and results of Speicher-Brode nuclear weapon	123
B.1	Data summary for the dynamic tests	135
B.2	Data summary for the static tests	136

CONVERSION FACTORS, NON-SI TO SI (METRIC)
UNITS OF MEASUREMENT

Non-SI units of measurement used in this report can be converted to SI (metric) units as follows:

Multiply	By	To Obtain
degrees (angle)	0.01745	radians
feet	0.3048	metres
feet per second	0.3048	metres per second
g's (standard free-fall)	9.806650	metres per second squared
grains per foot	0.2125948	grams per metre
inches	2.540	centimetres
inches per second	25.4	millimetres per second
inch-kips (force)	112.985	newton-metres
inch-pounds (force) per inch	4.448222	newton-metres per metre
kilotons (nuclear equivalent of TNT)	4.184	megajoules
kips per square inch	6.894757	megapascals
megatons (nuclear equivalent of TNT)	4.184	gigajoules
micro-inches per inch	1.0	microcentimetres per centimetre
pounds (force)	4.448222	newtons
pounds (force) per square inch	6.894757	kilopascals
pounds (mass) per cubic foot	16.01846	kilograms per cubic metre
pounds per square inch-seconds	0.006895	megapascal-seconds
square inches	6.4516	square centimetres
tons (force) per square foot	95.76052	kilopascals
tons (mass) per square foot	9,764.856	kilograms per square metre

STRUCTURAL ELEMENT TESTS IN SUPPORT OF THE KEYWORKER BLAST SHELTER PROGRAM

CHAPTER 1

INTRODUCTION

1.1 BACKGROUND

At the initiation of this study, civil defense planning called for the evacuation of nonessential personnel to safe (low-risk) host areas during a time of crisis, and the construction of shelters to protect the keyworkers remaining behind. Keyworker blast shelters will be used as command and control centers for emergency operations, facilities to provide continuity of government, and space to house personnel operating critical industry within high-risk areas of the country during and after a nuclear attack. Both dedicated and expedient types of shelters are planned. A dedicated shelter is one that is in place long before a nuclear crisis occurs. An expedient shelter consists of prefabricated components which can be prepositioned at key sites and constructed, using available equipment and personnel, in a short time during a crisis period. An expedient shelter will provide space for up to about 20 people while a dedicated shelter will provide 100 to 400 spaces. The US Army Engineer Division, Huntsville (HND), has been tasked by the Federal Emergency Management Agency (FEMA) to design a 100-man dedicated shelter and to build three prototype shelters. The research reported herein is in support of the HND design effort.

Structural design parameters require that the structure survive a peak overpressure of 50 psi[1] from a 1-MT nuclear weapon. The structural design criteria and protection from initial and residual radiation associated with the threat weapon require an earth-covered or buried structure. The shelter is designed to function as a box structure constructed of poured-in-place reinforced concrete. The walls, roof slab, and floor slab are one integral structure with structural steel frames providing interior supports for the one-way reinforced concrete roof slab. Beams and columns for the interior

[1] A table of factors for converting non-SI to SI (metric) units of measurement is presented on page 8.

frames consist of standard structural steel members. The floor is a reinforced concrete slab with two transverse reinforced concrete floor beams to transfer the interior column loads to the floor slab.

Using a roof slab thickness of 10 inches, a span of 11.33 feet, and limiting midspan deflection to 7 inches, the principal tension and compression steel ratios were determined using a computational procedure (Reference 1) developed at the US Army Engineer Waterways Experiment Station (WES) in the Shallow-Buried Structures Research Program. The "Vulnerability of Shallow-Buried Structures" computer code (VSBS6) incorporates the ability of the backfill to transfer load from the midspan of the roof to the supports, thereby reducing the required flexural capacity of the roof slab to resist a given ground surface loading. This allows a more economical slab section to be designed, reducing material costs. Using this procedure, compression and tension steel ratios of 0.007 were recommended.

1.2 OBJECTIVES

The objectives of this test program were to evaluate the structural design, to investigate structural response in various backfills, to investigate and recommend minimum concrete strength requirements, to validate and/or modify structural response calculations, and to extend the data base on repeated hits so that structural response computational procedures can be developed to incorporate repeated hits.

1.3 SCOPE

To accomplish the objectives of this test program, static and dynamic tests were conducted on two types of structural elements. The Type 1 element was a reinforced concrete box structure with interior supports consisting of a structural steel framing system. The Type 2 element was an open-end box element representing a section of one bay of the shelter. Both element types were approximately 1/4-scale models of the keyworker blast shelter.

Six static tests were conducted; one on a Type 1 element to evaluate the structural design configuration and five on Type 2 elements to investigate variations in concrete strength, depth of burial (DOB), and backfill material.

Twelve dynamic tests were conducted; one on a Type 1 element to evaluate the structural design configuration and eleven on Type 2 elements. The design structure's ability to withstand repeated hits was also evaluated.

Static and dynamic tests were performed in sand backfill at DOB of 0 inch and 12 inches (L/2.75); while tests in the two alternate backfills were performed at DOB equal to 12 inches (L/2.75). Multiple hits were performed at depths of burial of 6 and 12 inches in sand backfill. Table 1.1 gives a test matrix for the static and dynamic tests showing the element type and parameter investigated for each test.

The Keyworker blast shelter was designed to resist a 1-MT nuclear weapon at 50 psi; therefore, using a cube-root scaling and a 1/4-scale factor, the nuclear weapon yield simulator for the dynamic tests was designed to produce a 16-KT simulation. The weapon simulator is described in Chapter 4.

Table 1.1. Static and dynamic test matrix.

Baseline configuration: DOB = 1 ft in sand backfill. Alternate backfills: RCS = red clayey sand, CWG = clayey sand with gravel. Flume sand backfill was used unless otherwise noted.

Test	Element	Type	Parameter
S1	S1	1	Baseline Type 1 element (static)
S3	S3	2	DOB--surface flush (static)
S4	S4	2	Baseline Type 2 element (static)
S5	S5	2	Alternate backfill--RCS (static)
S6	S6	2	Low-strength concrete (static)
S7	S7	2	Alternate backfill--CWG (static)
D1	D1	1	Baseline Type 1 element (dynamic)
D2	D2	2	DOB--surface flush (dynamic)
D3	D3	2	Overpressure (dynamic)
D3A	D3	2	Overpressure, repeated hit (dynamic)
D3B	D3	2	Overpressure, repeated hit (dynamic)
D3C	D3	2	Overpressure, repeated hit (dynamic)
D4	D4	2	Baseline Type 2 element (dynamic)
D5	D5	2	Alternate backfill--RCS (dynamic)
D6	D6	2	Low-strength concrete (dynamic)
D7	D7	2	Alternate backfill--CWG (dynamic)
Multi-hit	D3, D4, D5, D6, D7	2	Repeated hit, DOB = 6 in for D7
D8	D8 , D4, D6	2	Repeated hit

CHAPTER 2

ELEMENT CONSTRUCTION DETAILS AND STRUCTURAL MATERIAL PROPERTIES

2.1 ELEMENT DETAILS

Two Type 1 test elements and twelve Type 2 test elements were built in the WES Structures Laboratory from March through June 1983.

2.1.1 Structural Details

These elements were approximately 1/4-scale reinforced concrete models of the FEMA keyworker blast shelter. The structural parameters of the models included: a clear span of 33 inches, a clear height of 30 inches, a roof thickness of 2.5 inches and an effective depth of 1.94 inches, wall and floor thicknesses of 2.25 inches and effective depths of 1.78 inches, a roof clear span-to-effective depth ratio (L/d) of 17, a roof clear span-to-thickness ratio of 13.2, and principal steel ratios of approximately 0.007 for the roof, walls, and floor slabs. Principal reinforcement consisted of 0.25-inch-diameter, Grade-60 deformed wire spaced at 3.75 inches in both faces of the roof, walls, and floor. This yielded tension and compression steel ratios of approximately 0.007. Shear reinforcement was provided by double-leg, 0.11-inch-diameter, Grade-60 deformed wire stirrups spaced at 3 inches on center with alternate rows staggered 1.5 inches. Transverse reinforcement for the roof, walls, and floor was provided by 0.11-inch-diameter, Grade-60 deformed wire spaced at 3 inches on center. A floor plan of the Type 1 element is shown in Figure 2.1. Reinforcement and structural details are shown for the Type 1 element in Figures 2.2 and 2.3. Note that a structural steel floor girder was used instead of a reinforced concrete floor beam as on the prototype. This modification was made to enable accurate measurement of the floor load distribution. Figure 2.4 shows structural and reinforcement details for the Type 2 element.

2.1.2 Type 1 Element Construction

Construction of each Type 1 element was accomplished in two stages. In the first, the floor steel was placed in the forms, the reinforcement for the walls was tied in place, and the floor girder was set in place before pouring the floor slab as shown in Figure 2.5. Stage 2 consisted of placing the

inside wall forms, installing the structural steel columns and the roof girder as shown in Figure 2.6, installing the galvanized steel decking (bottom form for the roof slab), placing the roof reinforcement mat, setting the outside wall forms, and pouring the walls and roof in one pour. Figure 2.7 shows the Type 1 element with all steel in place prior to setting the outside wall forms and pouring. Figure 2.8 is a close-up showing the 26-gage galvanized steel decking and steel placement details. The galvanized steel decking was used as bottom formwork for the roof slab and as a means to prevent spalling concrete from reaching the floor. Two 35-1/2- by 90-1/2-inch sheets of corrugated steel decking were required to make the bottom roof form. Each sheet of decking extends from the 2-inch angle (embedded along the top of each side wall as shown in Figure 2.1) to the interior support (the roof girder). The sheets of decking were welded to the angle and the roof girder with approximately 1/8-inch tack welds spaced 1-1/2 inches on center and 1 inch from the edge of the decking. The two sheets of corrugated decking were lapped 1-1/2 inches at the centerline of the roof girder. The 2- by 2- by 1/4-inch angle that is part of the wall-to-steel decking connection is secured to the wall by means of 1/4-inch-diameter by 2-inch-long studs that were welded to the angle. The angle and stud assembly was tied into the wall before concrete was poured.

2.1.3 Type 2 Element Construction

Construction of the open-end Type 2 elements consisted of building the inside forms (open end up), placing the reinforcement steel mats, installing interface pressure gage mounts, placing the outside forms, and pouring the structures. Figure 2.9 shows the inside formwork with the reinforcement tied in place and the interface pressure gage mounts installed. The twelve Type 2 elements were cast from six batches of concrete with one static and one dynamic element cast from each batch.

2.2 STRUCTURAL MATERIAL PROPERTIES

2.2.1 Concrete

Two concrete mixes were designed to investigate the effects of concrete strength on structure resistance and performance. One static Type 2 element (S6) and one dynamic Type 2 element (D6) were cast with concrete designed to have a 28-day compressive strength of 2,500 psi. The average 28-day strength

was 2,785 psi. The remaining ten Type 2 and the two Type 1 static and dynamic elements were cast with concrete designed to have a 28-day compressive strength of 4,000 psi. The 28-day strengths ranged from 3,400 to 5,360 psi. Table 2.1 gives complete results of the concrete cylinder testing for the static and dynamic test models.

Both concrete mixes were designed using a Type I portland cement obtained from a local commercial supplier. The fine aggregate was a natural siliceous sand, and the coarse aggregate was crushed limestone with a 3/8-inch maximum diameter. For the Type 1 elements, four cylinders were taken from each batch of concrete, which allowed testing two cylinders at 28 days and two cylinders at the element test day for each batch of concrete (each Type 1 element required three batches of concrete: one for the floor slab and two for the walls and roof slab). For the Type 2 elements, six cylinders were taken from each batch of concrete (two test elements were poured from each batch); which allowed testing two cylinders at 28 days for each pair of test elements and two cylinders for each element on the element's test day.

There appears to be considerable scatter in the 28-day compressive strengths of the 4,000-psi concrete mix design. A one-way analysis of the variance was performed on Batches 1, 2, 3, 4, 8, 10, and 12, showing an inconsistency in the concrete strengths. The actual concrete compressive strength for each test element should be considered in comparing test results.

Table 2.1 also lists experimentally determined parameters for constructing a concrete model. The elastic modulus was determined to be $64,000\sqrt{f'_c}$ psi, the Poisson's ratio was 0.21, and the strain at ultimate stress was found to be 0.00202 in/in. The concrete crushing strain was not determined in these concrete cylinder tests because the strain gages malfunctioned at strains of about 0.0025 or less. The concrete model is adequately defined in the region from strain equals zero to strain equals 0.00202 in/in by:

$$\sigma_c = f'_c \frac{1 - (0.00202 - \varepsilon_c)^2}{(0.00202)^2} \tag{2.1}$$

where

σ_c = concrete stress, psi

f'_c = concrete compressive strength, psi

ε_c = concrete strain, in/in

Since the stress-strain relation was not experimentally determined at strains larger than 0.0025 in/in, no experimental concrete model can be derived for this region. At strains greater than the strain at ultimate stress (0.00202 in/in in this case) the stress-strain function is dependent on the amount and spacing of shear steel and temperature steel (or ties) in the slab section (due to confining stresses) so the uniaxial test on unreinforced concrete cylinders does not yield the required stress-strain relation. A good approximation for the concrete stress-strain relation at large strains is given in Reference 2.

The concrete stress-strain is divided into three zones:

Zone 1: σ_c is given by Equation 2.1 for $0 < \varepsilon_c \leq 0.00202$

$$\text{Zone 2:} \quad \sigma_c = f'_c \left[1 - 0.5 \left(0.03147 + \frac{3 + 0.00202f'}{f'_c - 1000} \right)^{-1} (\varepsilon_c - 0.00202) \right] \tag{2.2}$$

for $0.00202 < \varepsilon_c \leq \varepsilon_{20c}$

where ε_{20c} = the large strain at which $\sigma_c = 0.2f'_c$

Zone 3: $\sigma_c = 0.2f'_c$ for $\varepsilon_{20c} < \varepsilon_c \leq 0.10$

Figure 2.10 graphically depicts the recommended concrete stress-strain constitutive equations.

2.2.2 Reinforcing Steel

The principal reinforcing steel consisted of Grade-60 No. 2 deformed wire that was used to model American Society for Testing and Materials (ASTM) Grade-60 No. 8 deformed bars. The results of tensile tests on the 1/4-inch deformed wire are given in Table 2.2. The mean yield stress was 68,495 psi and the mean ultimate stress was 72,790 psi. Rupture stress was not recorded on all of the tests, but rupture stress based on three samples was 56,465 psi. The elastic modulus was found to be 29,200 ksi and the initial strain hardening modulus was 430 ksi. The strain at initiation of strain hardening was 0.013 in/in and the strain at ultimate stress was approximately

0.06 in/in. These parameters can be used in constructing a steel model consisting of an elastic portion up to the yield point, a plastic portion to initiation of strain hardening, and a strain-hardening portion up to ultimate stress.

Shear reinforcement and temperature steel consisted of Grade-60 0.11-inch-diameter deformed wire that was used to model ASTM Grade-60 No. 3 deformed bars. The results of tensile tests on the 0.11-inch-diameter deformed wire are given in Table 2.3. The mean yield stress was 60,845 psi, the mean ultimate stress was 63,565 psi, and the mean rupture stress was 50,350 psi.

2.2.3 Structural Steel

Built-up sections were used to model the roof girder and the columns that made up the interior support for the shelter roof slab. The girders were made from 1/4-inch Grade-60 and 3/16-inch Grade-50 steel plate. The columns were made from 3/16-inch A36 plate. Results of tensile tests on coupons cut from these plates are given in Table 2.4. For the 1/4-inch Grade-50 steel, the mean yield stress was 62,685 psi, the mean ultimate stress was 83,635 psi, and the mean rupture stress was 63,060 psi. For the 3/16-inch Grade-50 plate, the mean yield stress was 59,945 psi, the mean ultimate stress was 73,460 psi, and the mean rupture stress was 52,385 psi. For the 3/16-inch A36 plate, the mean yield stress was 46,445 psi, the mean ultimate stress was 62,320 psi, and the mean rupture stress was 50,145. The elastic modulus was approximately 30×10^6 psi for all plates. The mean strain at the initiation of strain hardening was 0.017 in/in. The strain at ultimate stress was approximately 0.10 in/in. The mean initial strain hardening modulus was 1.06×10^6 psi.

2.2.4 Steel Models

From the data presented in the preceding sections, steel models can be constructed for the principal reinforcing steel and the structural steel as shown in Figure 2.11. The models are elastic in tension and compression until the steel yields, plastic from the yield point until the initiation of strain hardening, and strain hardening until ultimate stress is reached.

Table 2.1. Concrete strengths.

Numbers in parentheses are the average concrete compressive strength for the test element shown. The elastic modulus was determined to equal $64{,}000\sqrt{f'_c}$ (psi) using a least-squares fit to 13 data points. Poisson's ratio based on a mean of 13 data points is 0.21 with a range of 0.05. The strain at ultimate stress based on a mean of 13 data points is 0.00202 in/in with a range of 0.0004.

Test Element	Concrete Batch	28-day Compressive Strength, psi	Day-of-Test Compressive Strength, psi	Element Age When tested Days
S1	6	4,630 floor	5,780 floor	244
		4,370	6,240	
	9	4,990 walls	5,800 walls	221
		4,990	5,590	
	10	4,780 roof	6,150 roof	221
		--	6,240	
		(4,780) roof	(6,195) roof	
S3	2	4,760	5,340	163
		4,560	5,080	
		(4,660)	(5,210)	
S4	3	4,600	5,220	174
		4,690	5,250	
		(4,645)	(5,235)	
S5	4	4,440	5,390	202
		4,560	5,820	
		(4,500)	(5,605)	
S6	5	2,720	3,470	194
		2,850	3,500	
		(2,785)	(3,485)	
S7	8	3,500	4,470	189
		3,400	4,560	
		(3,450)	(4,515)	
D1	7	4,620 floor	5,520 floor	122
		4,470	5,460	
	11	5,030 walls	5,960 walls	99
		5,130	5,850	
	12	5,060 roof	6,000 roof	99
		5,360	6,300	
		(5,210) roof	(6,150) roof	
D2	1	4,460	5,290	100
		4,550	5,270	
		(4,505)	(5,280)	
D3	2	4,760	5,130	59
		4,560	4,850	
		(4,660)	(4,990)	
D4	3	4,600	5,010	78
		4,690	4,990	
		(4,645)	(5,000)	
D5	4	4,440	4,990	88
		4,560	5,250	
		(4,500)	(5,120)	
D6	5	2,720	3,250	82
		2,850	3,190	
		(2,785)	(3,220)	
D7	8	3,500	4,100	80
		3,400	4,140	
		(3,450)	(4,120)	
D8	1	4,460	5,360	125
		4,550	5,250	
		(4,505)	(5,305)	

Table 2.2. Principal steel (No. 2 deformed wire) strengths.

Sample	Yield Stress, psi	Ultimate Stress, psi	Sample	Yield Stress, psi	Ultimate Stress, psi
1	60,200	67,000	19	69,000	72,000
2	75,000	79,200	20	70,600	71,200
3	63,400	70,800	21	70,200	71,200
4	72,000	78,200	22	71,000	72,500
5	76,000	79,600	23	67,000	69,600
6	67,800	74,200	24	69,200	73,800
7	72,200	78,600	25	65,400	70,000
8	74,400	79,400	26	59,000	60,000
9	69,600	76,200	27	62,200	67,600
10	59,800	66,400	28	60,000	63,800
11	70,400	77,000	29	67,600	70,000
12	66,800	76,000	30	69,600	71,300
13	71,000	75,600	31	73,000	74,800
14	74,000	77,000	32	71,300	74,800
15	68,200	74,400	33	56,800	64,200
16	76,800	77,200	34	63,000	65,400
17	74,000	79,200	35	65,800	70,600
18	75,000	78,800	Average	68,495	72,790

Table 2.3. Shear and temperature reinforcement (0.11-inch diameter) strengths.

Sample	Yield Stress, psi	Ultimate Stress, psi	Rupture Stress, psi
1	68,005	68,005	48,960
2	56,700	60,265	49,135
3	60,440	62,875	49,830
4	59,570	62,180	50,265
5	60,875	63,395	51,310
6	55,655	58,875	46,785
7	64,355	65,050	52,005
8	59,790	63,700	50,440
9	60,440	65,225	50,875
10	62,615	66,095	53,920
Average	60,845	63,565	50,350

Table 2.4. Structural steel strengths.

The effective elastic modulus was approximately 30 × 10^6 psi. Actual experimental values calculated based on the initial slope of the stress-strain plots ran 5 to 30% higher than this. Strain by initiation of strain hardening was approximately 0.017 in/in. Strain hardening modulus was 1.06 × 10^6 psi.

Plate No. (Description)	Use	Coupon No.	Yield Stress psi	Ultimate Stress psi[a]	Rupture Stress psi
1 (1/4 in Grade 50)	Girder Flange	1L1[b]	--	85,015	70,845
	Column End Plate	1L2	62,670	83,490	69,270
		1T1[c]	62,990	83,065	56,375
		1T2	62,390	82,975	55,744
		Average	62,685	83,635	63,060
2 (3/16 in Grade 50)	Girder Web	2L1	59,540	73,655	54,410
	Girder Stiffeners	2L2	60,540	74,470	55,725
		2T1	59,845	73,315	49,740
		2T2	59,860	72,405	49,665
		Average	59,945	73,460	52,385
3 (3/16 in A36)	Column Flange	3L1	48,015	62,200	51,005
	Column Web	3L2	46,415	61,645	51,085
		3T1	46,290	63,260	50,145
		3T2	45,065	62,185	43,338
		Average	46,445	62,320	50,145

[a]Strain at ultimate stress was approximately 0.10.
[b]L = coupon cut in long direction of plate (roll direction).
[c]T = coupon cut perpendicular to roll direction.

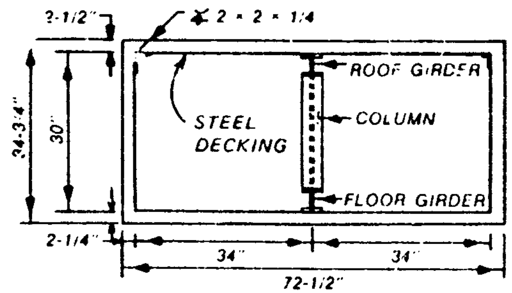

SECTION A-A

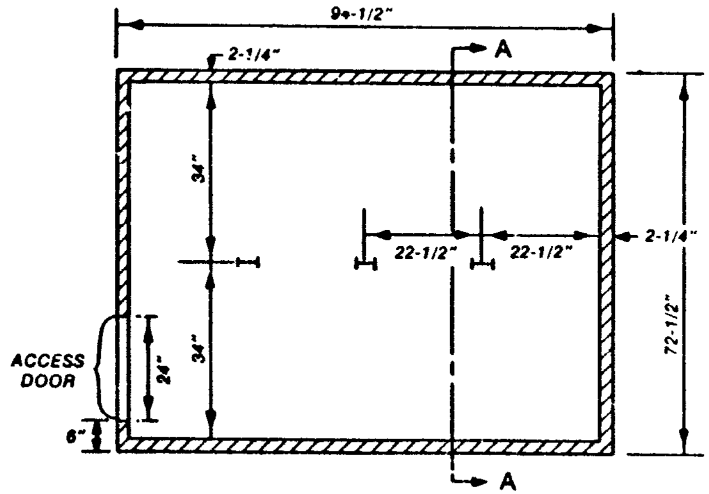

TYPE 1 FLOOR PLAN

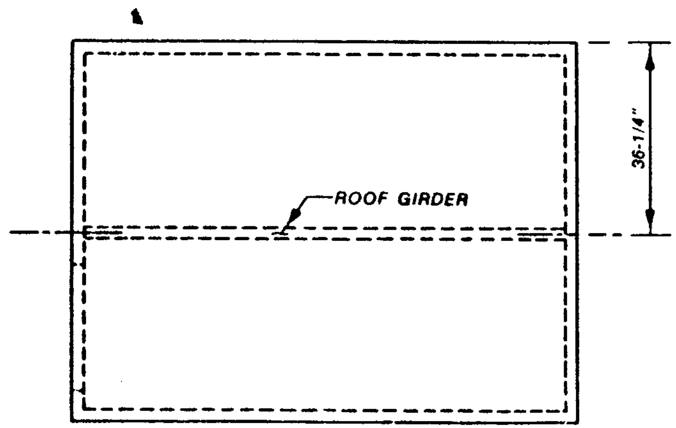

ROOF PLAN

Figure 2.1. Type 1 element: plans and section.

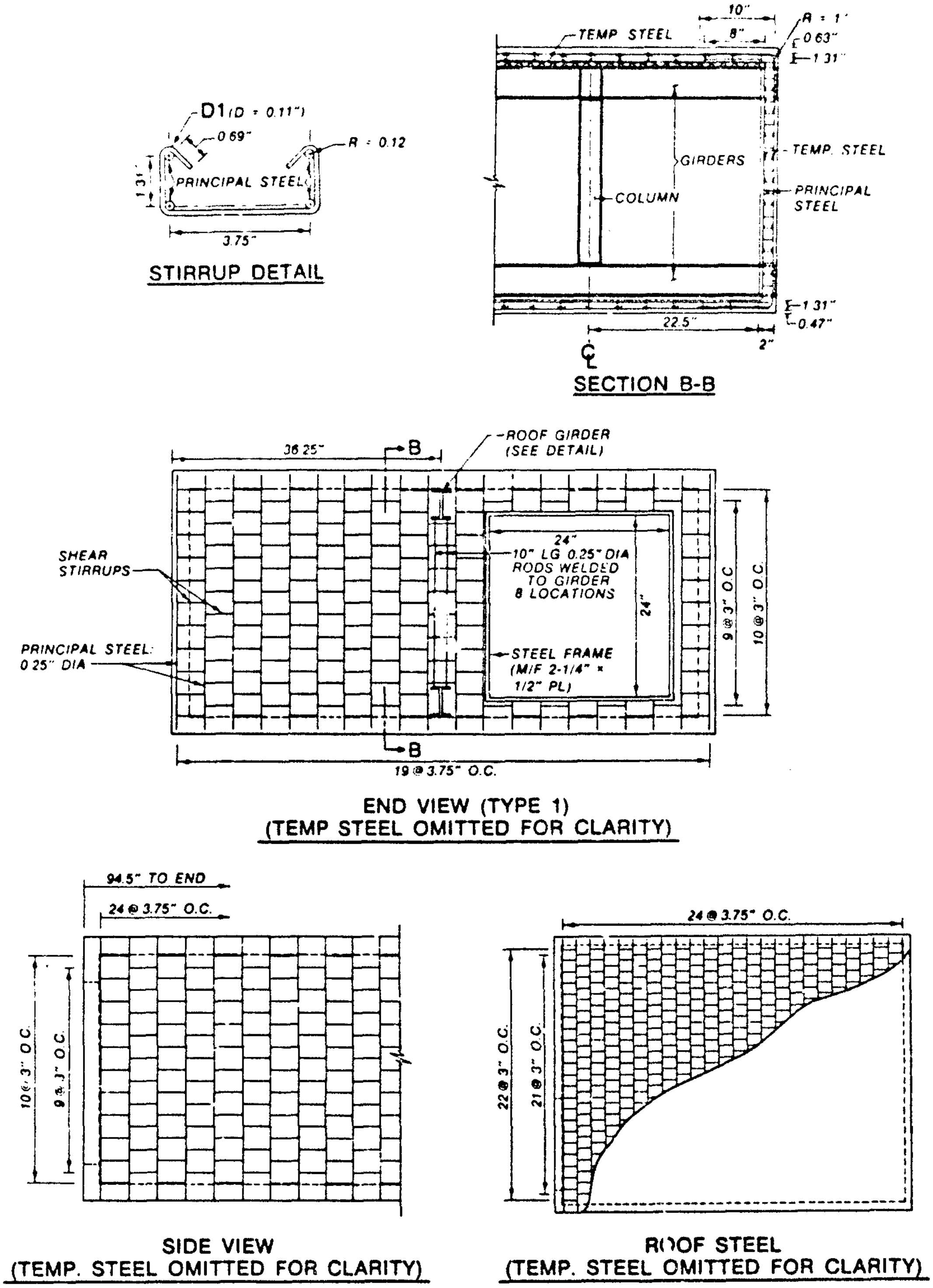

Figure 2.2. Type 1 element reinforcement details.

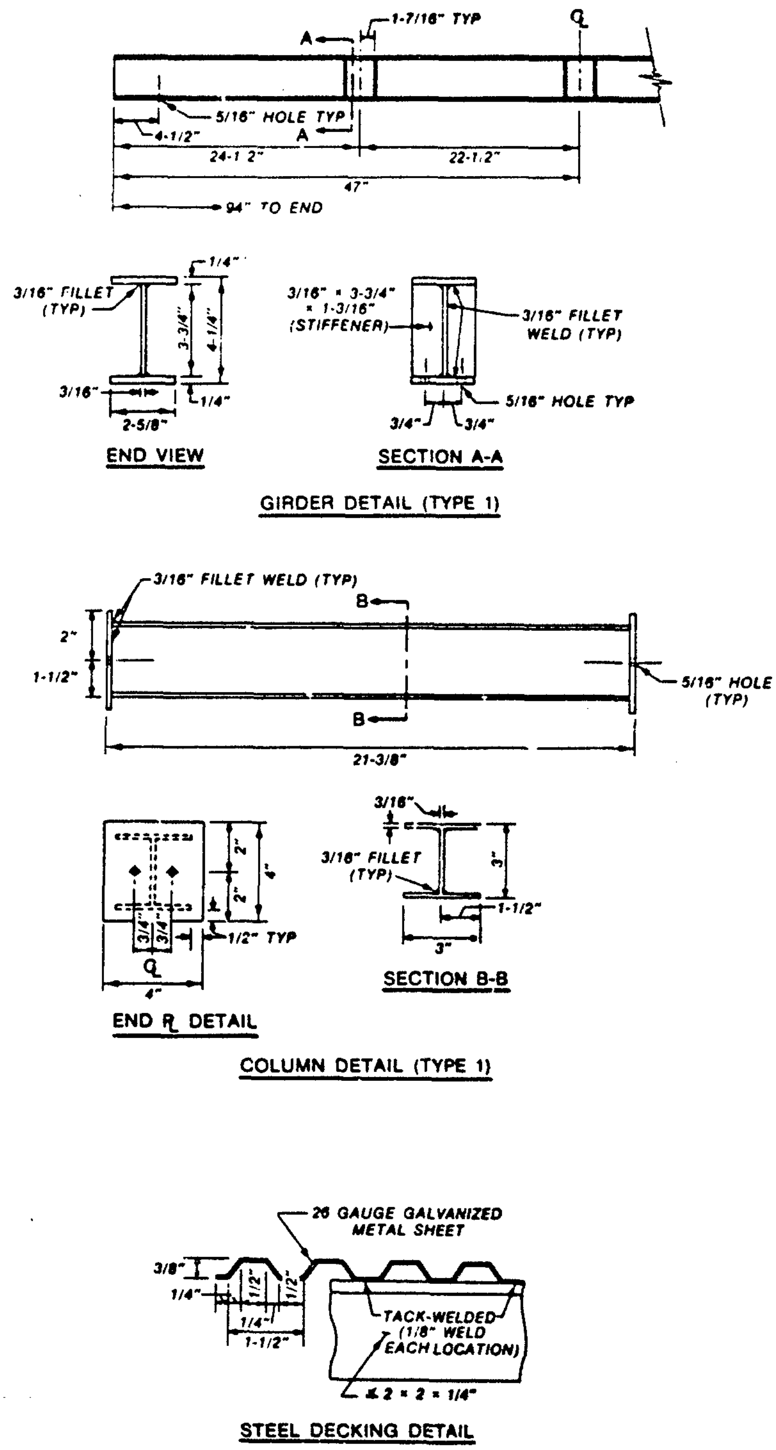

Figure 2.3. Type 1 element structural steel details.

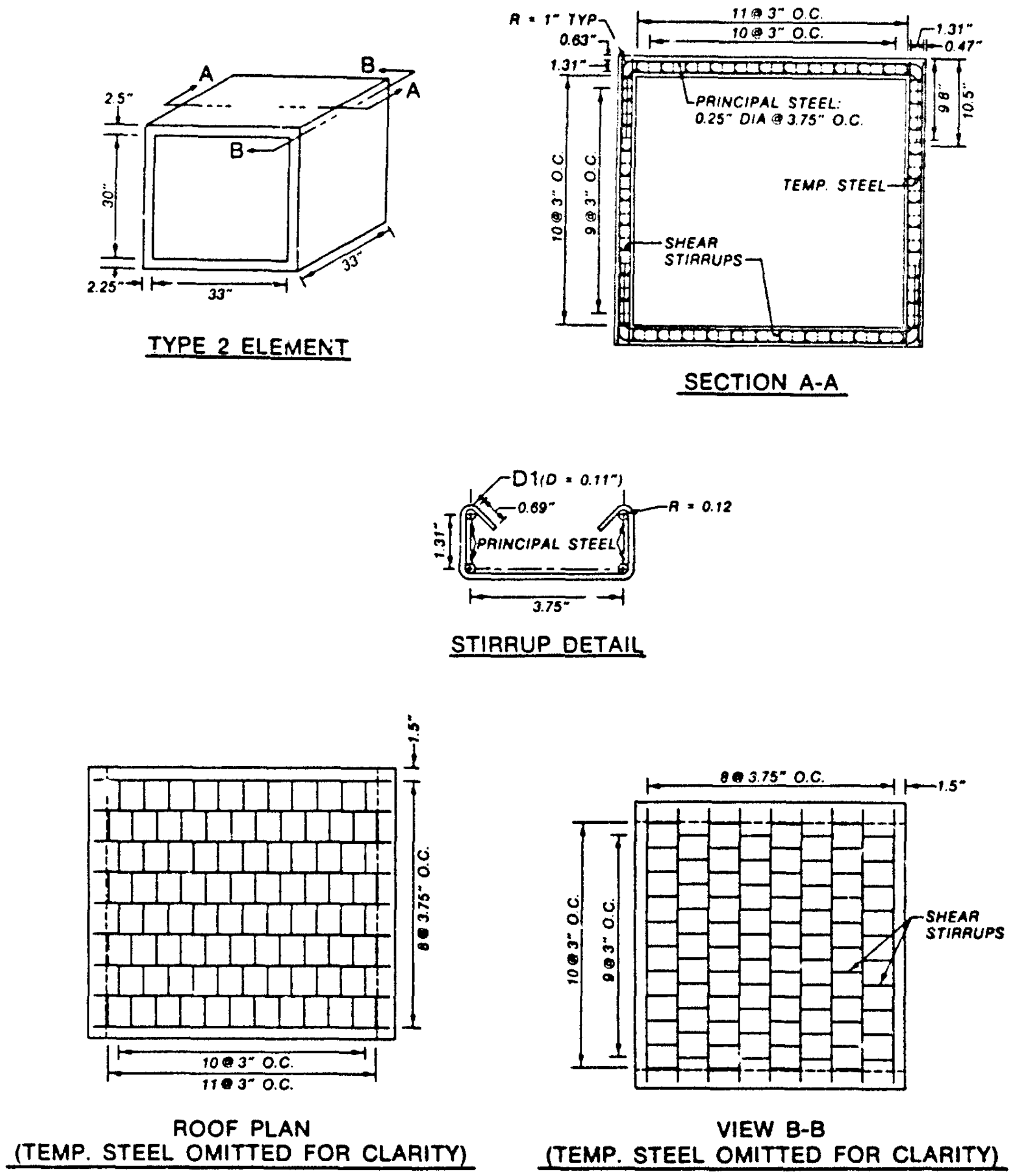

Figure 2.4. Type 2 element structural and reinforcement details.

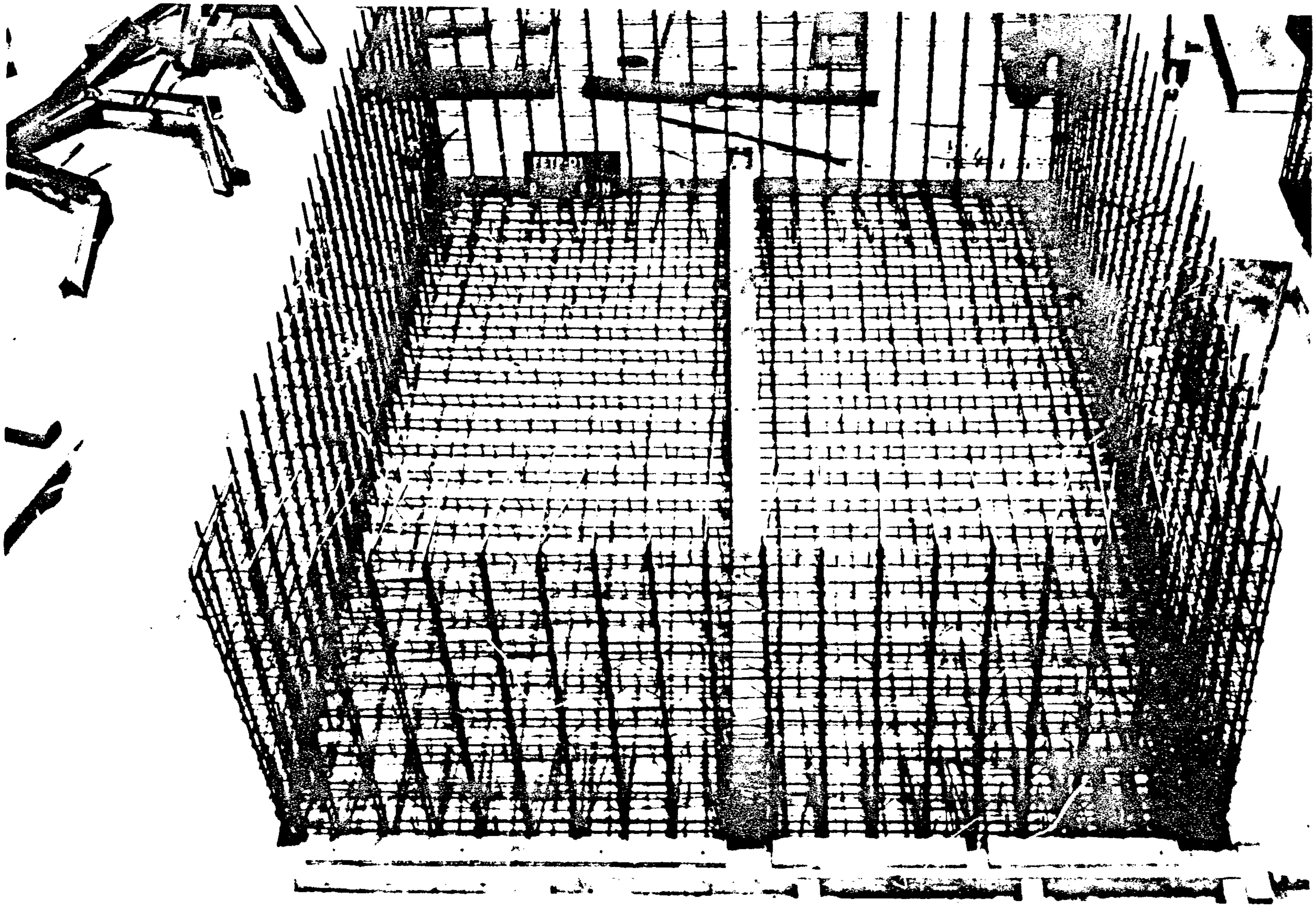

Figure 2.5. Placement of steel before pouring the Type 1 element floor slab.

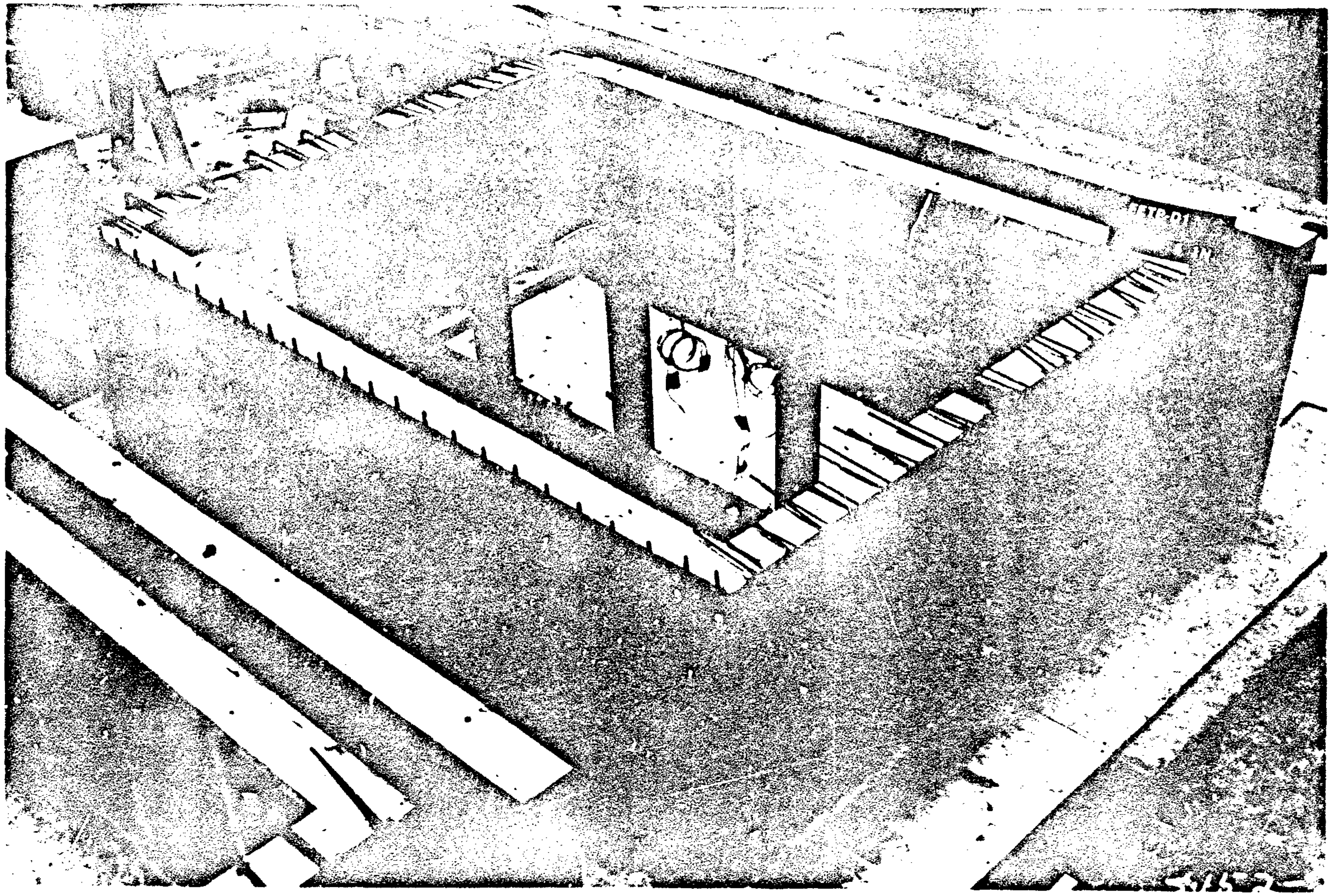

Figure 2.6. Type 1 element: placement of inside forms and structural steel frame.

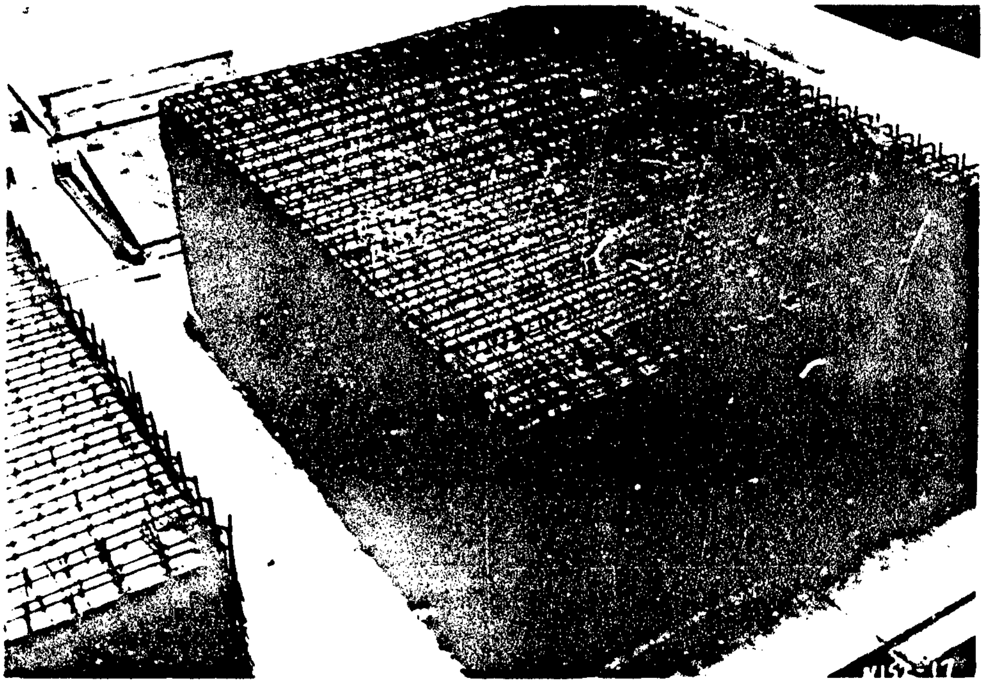

Figure 2.7. Type 1 element prior to placing outside forms and pouring the walls and roof.

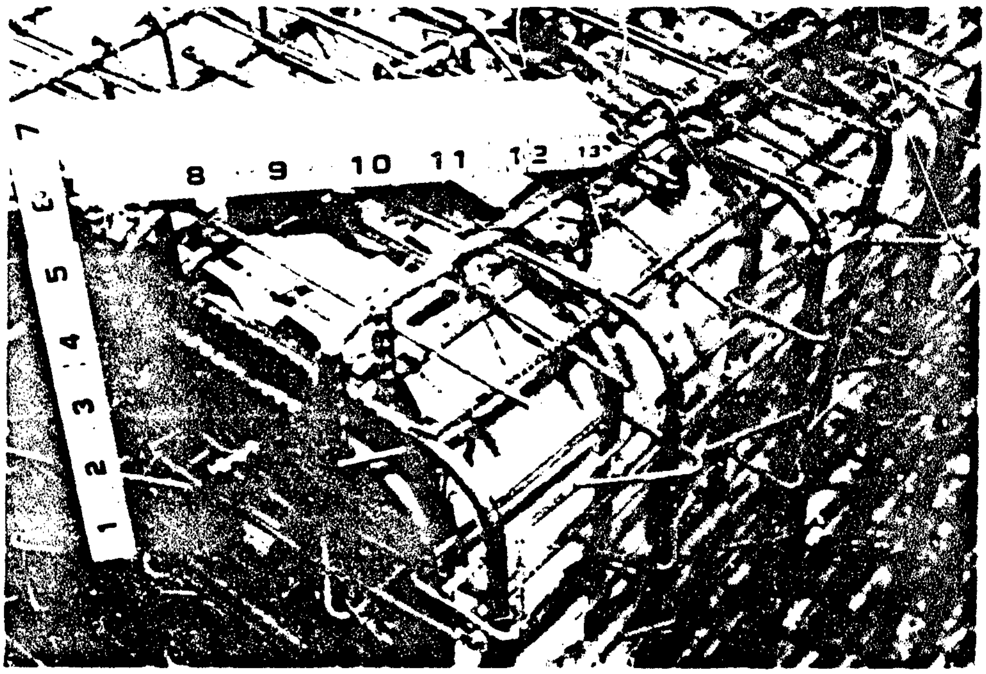

Figure 2.8. Close-up showing the galvanized steel decking and steel placement for the Type 1 element.

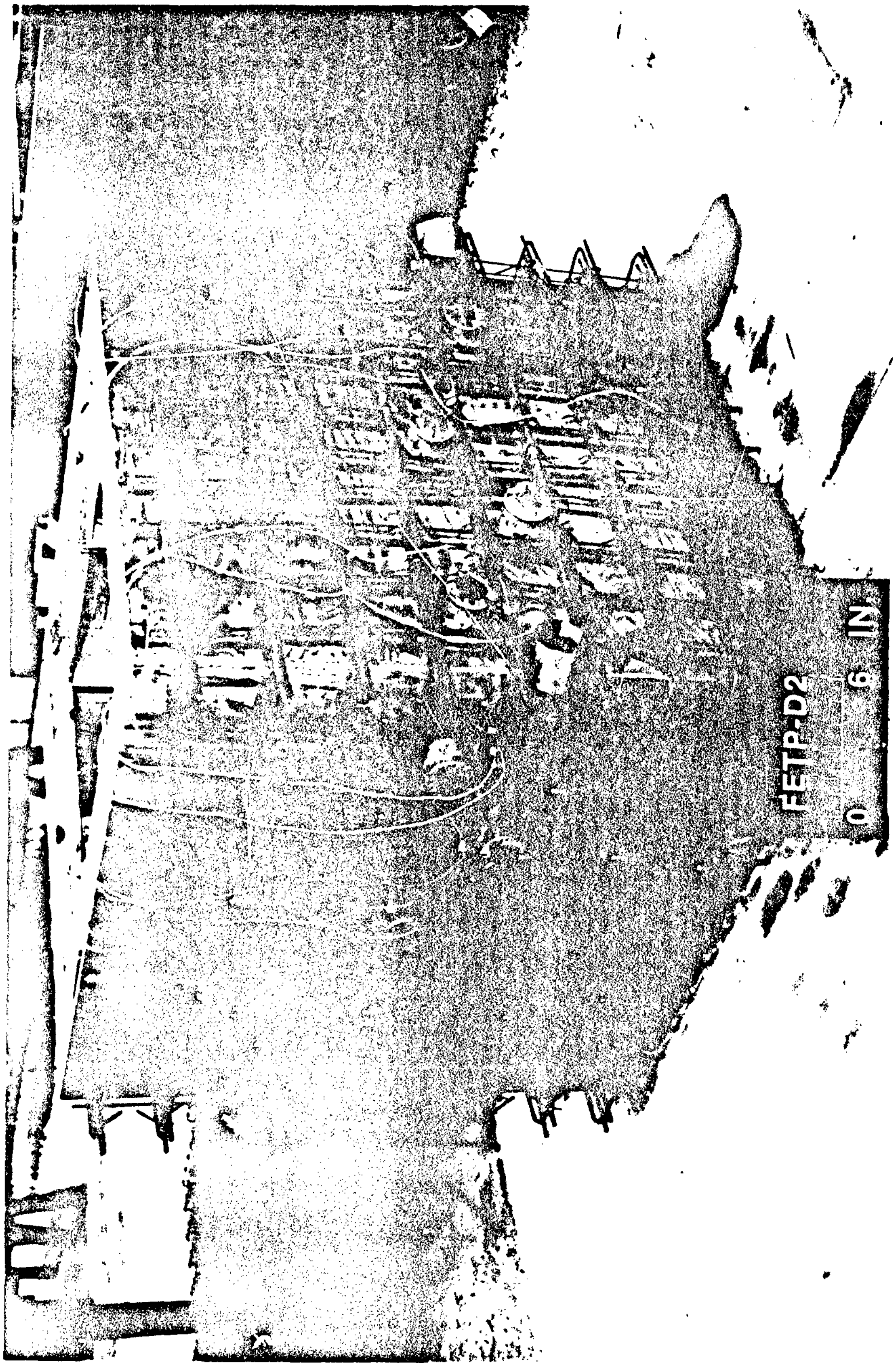

Figure 2.9. Steel placement on the inside forms for the Type 2 element.

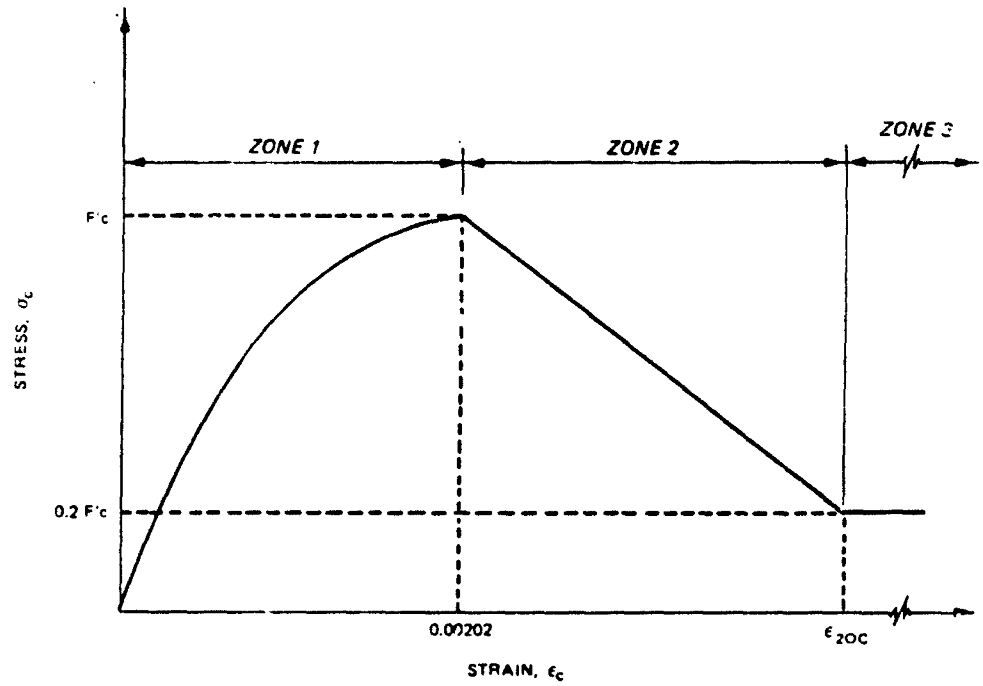

Figure 2.10. Idealized concrete stress-strain relation.

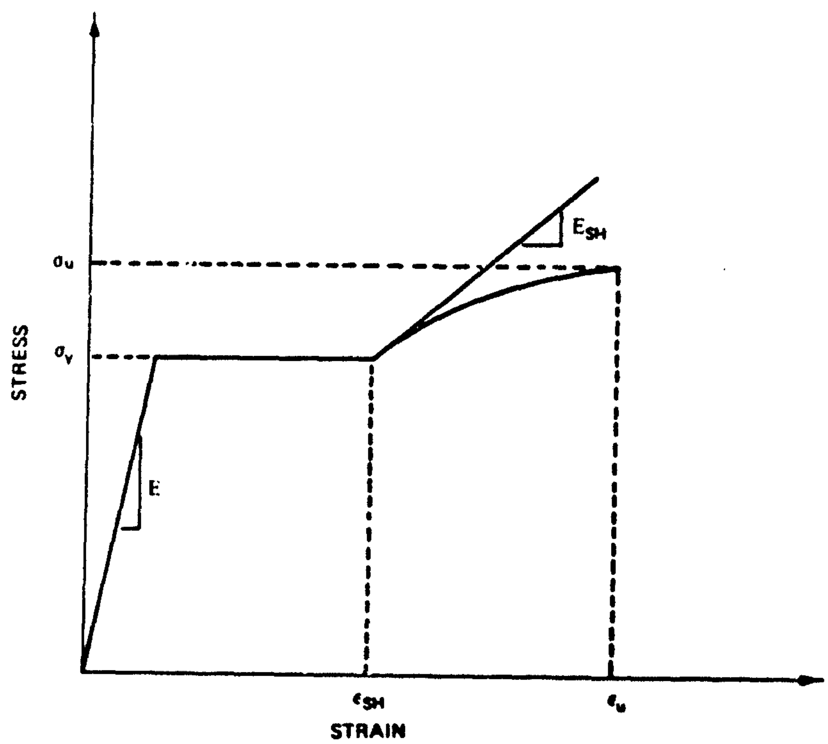

Figure 2.11. Stress-strain curve for reinforcement and structural steel.

CHAPTER 3

BACKFILL MATERIAL PROPERTIES

3.1 BACKGROUND

Prototype backfill specifications should be as unrestrictive as possible so that suitable excavated soil at the construction site can be used as backfill for the keyworker blast shelters. Backfill material types for this study were selected from locally available materials to test structural elements in cohesionless (ϕ) backfill and alternately in cohesive ($c - \phi$) materials (sand and/or gravel in a clay matrix) that are somewhat representative of near-surface soils commonly encountered in the United States.

The structural response computational procedure uses the angle of internal friction, ϕ , in calculating the soil arching factor which modifies the roof load distribution. Therefore, ϕ was of primary interest in the backfill analysis. Direct shear (S) tests were conducted on 2.5-in/in specimens, 0.5 inch high, to determine the relation between ϕ and the dry density of the backfill materials for the approximate ranges of placement water content. Other conventional laboratory soil tests were conducted to determine gradation, Atterberg limits, compaction characteristics, and water content.

3.2 BACKFILL MATERIALS

Three backfill soil types were used in the dynamic and static test programs. Flume sand was the primary backfill material. It was used in tests of Elements D1, D2, D3, D4, D6, D8, S1, S3, S4, and S6. Flume sand is a fine poorly graded (predominantly uniform) clean sand, light brown in color and classified SP by the Unified Soil Classification System (Reference 3). A red clayey sand (SC) stockpiled from a borrow excavation on Range 36, Fort Polk, La., and a clayey sand (SC) with gravel obtained from a local contractor were used as backfills in Dynamic Tests D5 and D7, respectively, and Static Tests S5 and S7, respectively.

Test bed density and moisture control in the red clayey sand and clayey sand with gravel backfills were selected to be representative of as-built prototype backfill. Densities of about 85 percent of CE-55 maximum densities were allowed in the test bed. It is recognized that these backfill conditions are conservative in allowing more potential structural response since military

construction specifications in similar backfills would require 90 to 95 percent of CE-55 maximum dry density and a range of moisture of 2 or 3 percent of optimum moisture content. Correlations of the angle of internal friction, ϕ , and dry density were conducted at 12 percent moisture content in the alternate backfills so that it would be possible to determine the range of ϕ for densities as great as 95 percent of the CE-55 maximum density. Water content and density measurements were made in the backfill as the test beds were constructed. The average minimum and maximum values for water content, wet density, and dry density are shown in Tables 3.1 and 3.2 for the dynamic and static test bed construction, respectively.

3.2.1 Flume Sand

Flume sand is the residue from a pit gravel washing process. It is a uniform fine sand typically containing 2 to 4 percent silt-size particles. The flume sand gradation is presented in Figure 3.1. Figure 3.2 shows the compaction curve for flume sand, indicating the common phenomenon for granular soils of bulking. The lower densities at water contents greater than 1 percent are due to the capillary forces resisting the rearrangement of sand grains. Because the amount of moisture influences the density obtainable for given compactive effort and normally influences the angle of internal friction, these direct shear (S) tests were conducted to determine a correlation between ϕ and dry unit weight. The direct shear test data are presented in Figure 3.3. An angle of internal friction of 38 degrees was obtained for the three densities given in Table 3.3 and Figure 3.4.

Tables 3.1 and 3.2 indicate average dry densities ranged from 97.9 to 99.7 lb/ft^3 and 97.4 to 101.2 lb/ft^3 for the dynamic and static test beds, respectively. Therefore, an angle of internal friction of 38 degrees is recommended.

3.2.2 Red Clayey Sand

The gradation for the red clayey sand (SC) is presented in Figure 3.5. This backfill material is a borderline silty-clayey sand containing about 30 percent finer than the No. 200 sieve. The results of a CE 55 compaction test on the red clayey sand are presented in Figure 3.6. A maximum dry density of 128.3 lb/ft^3 was obtained at the optimum water content of 8.5 percent.

Direct shear tests were conducted on specimens at about 13 percent

moisture content and densities representative of those obtained in the dynamic and static test program. The direct shear test data are presented in Figure 3.7.

Table 3.3 and Figure 3.8 present the ϕ angles obtained for the red clayey sand for densities of 80 and 85 percent of CE 55 maximum density. The angles of internal friction were 26 and 35 degrees for densities of 101.4 and 110 lb/ft^3, respectively. The recommended angle of internal friction is 26.5 degrees for the dry unit weights used in the static and dynamic tests.

3.2.3 Clayey Sand with Gravel

The gradation for the clayey sand with gravel is presented in Figure 3.9. This material was classified as a red clayey sand with gravel (10 percent) having 3/4-inch maximum size particles. Atterberg limits are indicated in Figure 3.9. A CE-55 compaction curve is presented in Figure 3.10 indicating a maximum dry density of 128.5 lb/ft^3 at an optimum water content of 9.3 percent.

Direct shear tests were also conducted on specimens of the clay gravel at a density of about 12 percent moisture content. The test data are presented in Figure 3.11. Angles of internal friction presented in Table 3.3 and Figure 3.12 were determined for 85 to 95 percent of the CE 55 maximum density. These data indicate ϕ varies from 28 to 36 degrees for densities ranging from 109.2 to 121.7 lb/ft^3. Recommended angles of internal friction are 29.5 degrees for the static test and 32 degrees for the dynamic test.

3.3 BACKFILL PLACEMENT

3.3.1 Dynamic Test Bed

The dynamic test bed was constructed by placing the backfill with a backhoe/front-end loader and leveling with shovels to about a 7-inch loose thickness. The sand backfill was compacted with three passes of a [illegible]oline-powered vibrator with a 17- by 18-inch base weighing approximately 4[illegible] pounds. The vibrator output energy at 3,600 rpm is rated to produce 90 pe[illegible]ent of CE-55 compactive effort for four passes on a 6-inch compacted layer.

A compaction test strip of two layers was conducted with the red clayey sand. It was determined that four passes of the same gas-powered vibrator on 7- to 8-inch loose layer thickness would produce densities at least equal to

85 percent of CE-55 maximum density. Therefore, construction of the test bed with red clayey sand backfill was similar to the construction with flume sand.

A compaction test strip of two layers was also conducted on the clayey sand with gravel. It was determined that three passes of a gas-powered tamper on a 7- to 8-inch loose layer thickness would produce densities at least equal to 90 percent of CE-55 maximum density. The clayey sand with gravel was much more difficult to level with shovels, and one pass of the vibrator was used to level the surface of the clayey sand with gravel prior to three passes with the tamper.

3.3.2 Static Test Bed

Construction using flume sand and the red clayey sand backfill in the static test bed was accomplished by hand placing the sand for the smaller Type 2 structural elements in the 6-foot-diameter small blast load generator (SBLG). Flume sand backfill was placed by clam shell for the larger Type 1 elements in the 23-foot-diameter large blast load generator (LBLG). Compaction was achieved in the SBLG by hand tamping four passes with a 23-pound hand tamp having a 6-3/4- by 11-inch foot, and by three passes of a gas-powered vibrator in the LBLG. The clayey sand with gravel was leveled with shovels, hand-tamped one pass to smooth the surface, and three passes were applied with a pneumatic tamper driven with about 100-psi line pressure. The pneumatic tamper had a foot which was 5-1/4 inches in diameter.

Table 3.1. Backfill water content and density data for dynamic tests.

Test	Backfill	Average Water Content (Min, Max)	Average Wet Density, lb/ft^3 (Min, Max)	Average Dry Density, lb/ft^3 (Min, Max)
D3	Sand	5.0 (4.4, 5.4)	102.5 (101.5, 104.0)	97.7 (96.9, 98.9)
D3A	Sand	4.16 (2.4, 5.4)	103.7 (101.3, 106.2)	99.5 (96.8, 101.7)
D3B	Sand	3.9 (3.1, 5.4)	103.2 (101.9, 105.3)	99.3 (97.6, 100.9)
D3C	Sand	3.9 (3.1, 4.8)	103.0 (102.5, 105.0)	99.4 (98.3, 102.1)
D4	Sand	5.1 (3.7, 7.2)	104.2 (101.4, 106.4)	99.3 (98.1, 101.3)
D6	Sand	4.8 (3.8, 6.3)	103.9 (100.0, 105.7)	99.1 (95.4, 100.2)
D5	Red sandy clay	12.5 (11.1, 14.1)	117.3 (114.2, 123.4)	104.3 (100.4, 108.5)
D2	Sand	5.2 (4.2, 5.8)	103.6 (101.1, 104.8)	98.8 (97.8, 99.8)
D7	Sandy clay with gravel	14.4 (13.1, 16.4)	132.7 (126.7, 135.2)	116.2 (111.2, 118.2)
Multi-hit	Sand	4.8 (3.7, 5.8)	103.4 (100.6, 106.7)	98.7 (96.2, 102.1)
D8	Sand	3.3 (2.2, 4.1)	102.8 (100.7, 107.7)	99.5 (96.5, 104.6)
D1	Sand	3.4 (1.9, 4.4)	103.1 (101.2, 106.7)	99.7 (197.4, 104.6)

Table 3.2. Backfill water content and density data for static tests.

Test	Backfill	Average Water Content (Min, Max)	Average Wet Density, lb/ft^3 (Min, Max)	Average Dry Density, lb/ft^3 (Min, Max)
S3	Flume sand	4.5 (3.7, 5.4)	104.6 (103.4, 106.4)	101.2 (98.2, 102.3)
S4	Flume sand	6.1 (5.9, 6.5)	103.4 (101.0, 105.8)	97.4 (95.3, 99.3)
S5	Red clayey sand	[illegible].1 (9.0, 19.1)	118.2 (110.3, 122.5)	103.6 (98.3, 109.0)
S6	Flume sand	4.4 (3.1, 5.1)	105.1 (96.7, 107.5)	100.7 (92.1, 104.3)
S7	Clayey sand with gravel	16.1 (15.1, 17.1)	128.9 (124.0, 133.8)	110.9 (107.7, 114.0)
S1	Flume sand	4.0 (3.0, 4.7)	103.4 (102.3, 104.6)	99.4 (98.8, 99.8)

Table 3.3. Summary of backfill angle of internal friction.

Backfill Type	Dry Density, lb/ft^3	Water Content, %	Angle of Internal Friction, Deg
Flume sand	109.9	0.0	38.0
	103.4	4.5	38.0
	98.7	4.8	38.0
Red clayey sand	102.6	12.9	26.0
	109.6	13.1	35.0
Clayey sand with gravel	121.7	12.2	36.0
	109.4	13.3	28.0

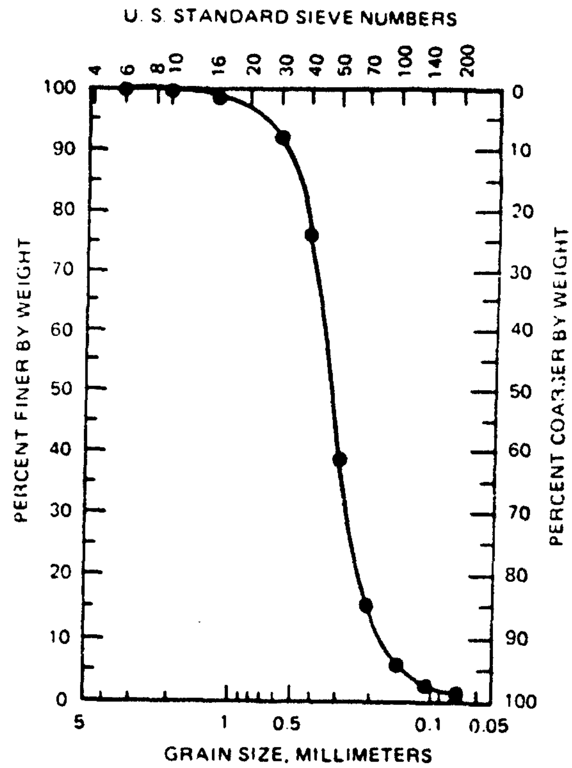

Figure 3.1. Flume sand gradation.

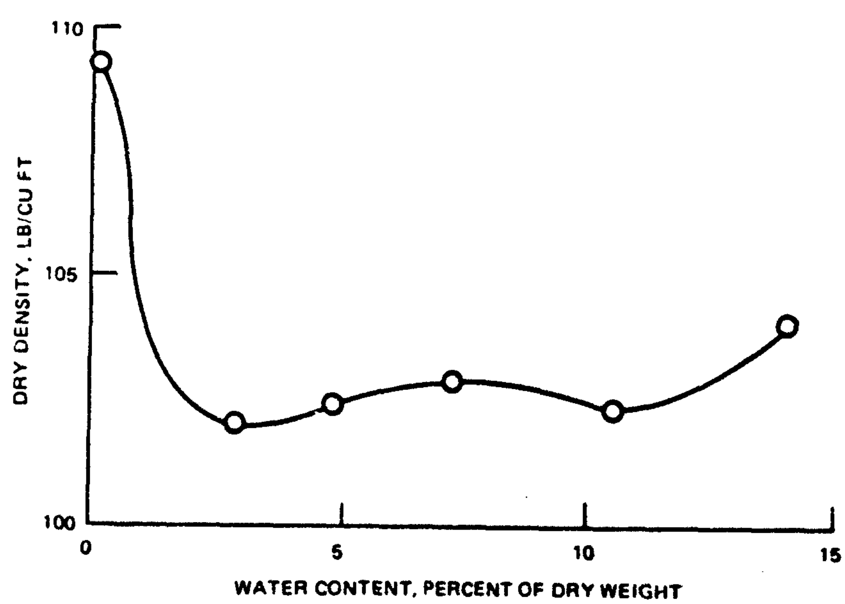

Figure 3.2. Compaction curve for flume sand using CE-55 effort.

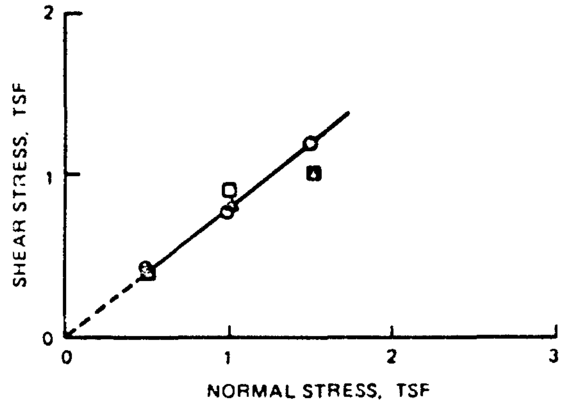

NOTE:

SYMBOL	WATER CONTENT, %	DRY DENSITY, PCF	ϕ, DEGREES
○	4.5	103.4	38
△	4.8	98.7	38
□	0.0	109.9	38

Figure 3.3. Direct shear test results for flume sand.

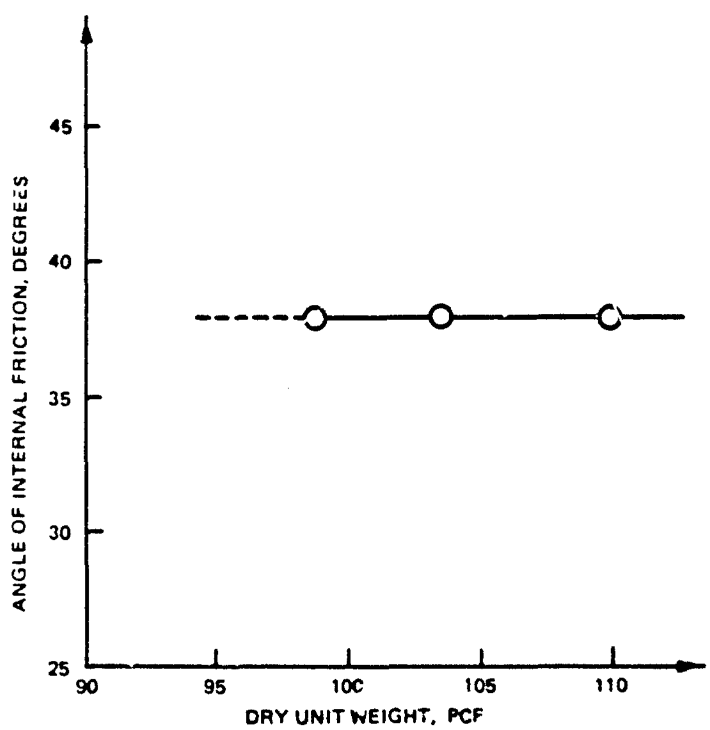

Figure 3.4. Angle of internal friction versus dry unit weight for flume sand.

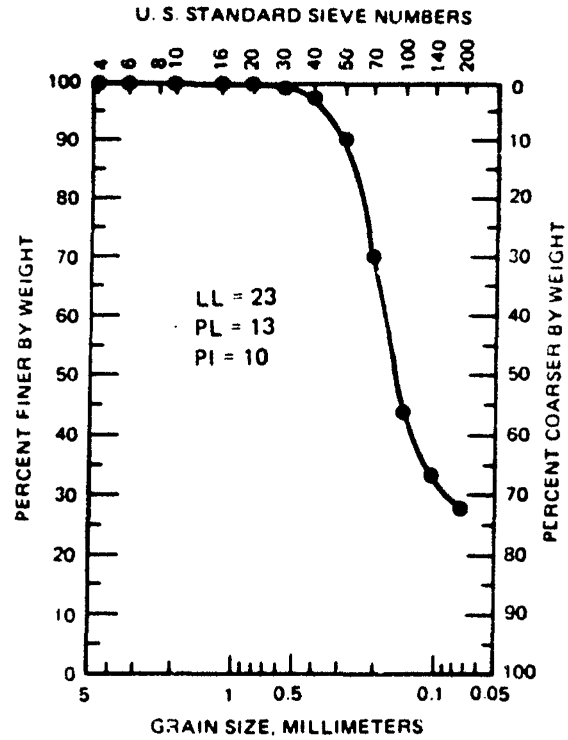

Figure 3.5. Gradation curve for red clayey sand backfill.

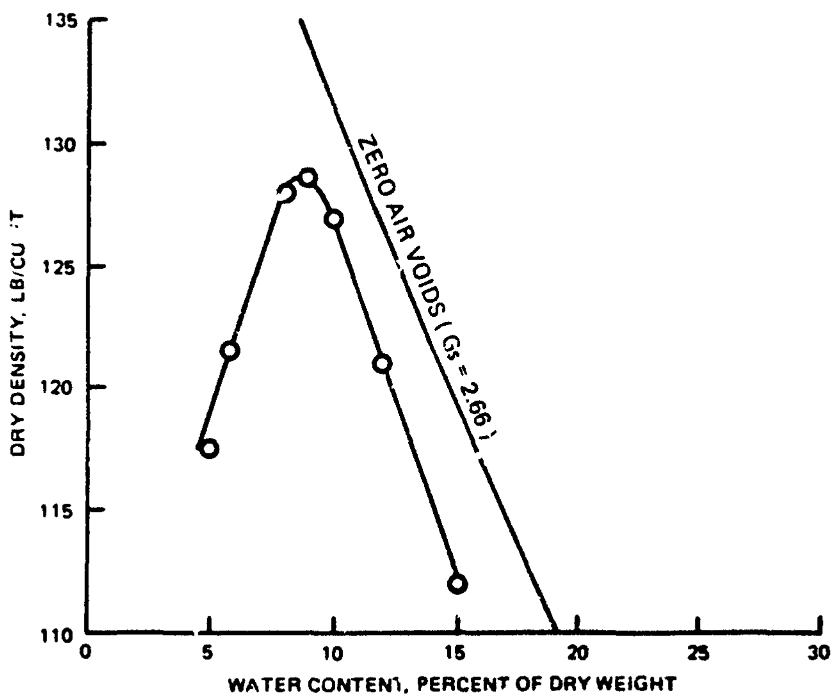

Figure 3.6. Compaction curve for red clayey sand using CE-55 effort.

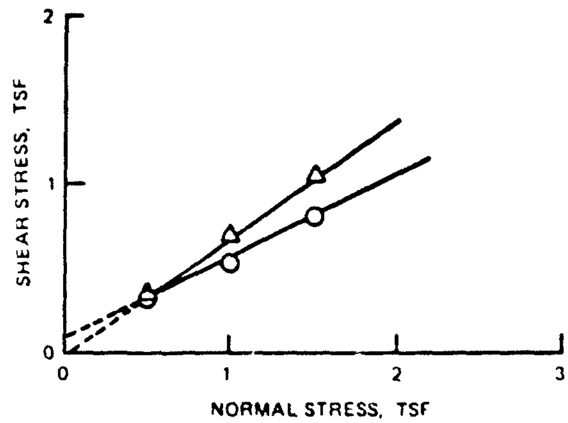

NOTE:

SYMBOL	WATER CONTENT, %	DRY DENSITY, PCF	φ, DEGREES	C, TSF
O	12.9	102.6	26	0.09
Δ	13.1	109.6	35	0.00

Figure 3.7. Direct shear test results, red clayey sand.

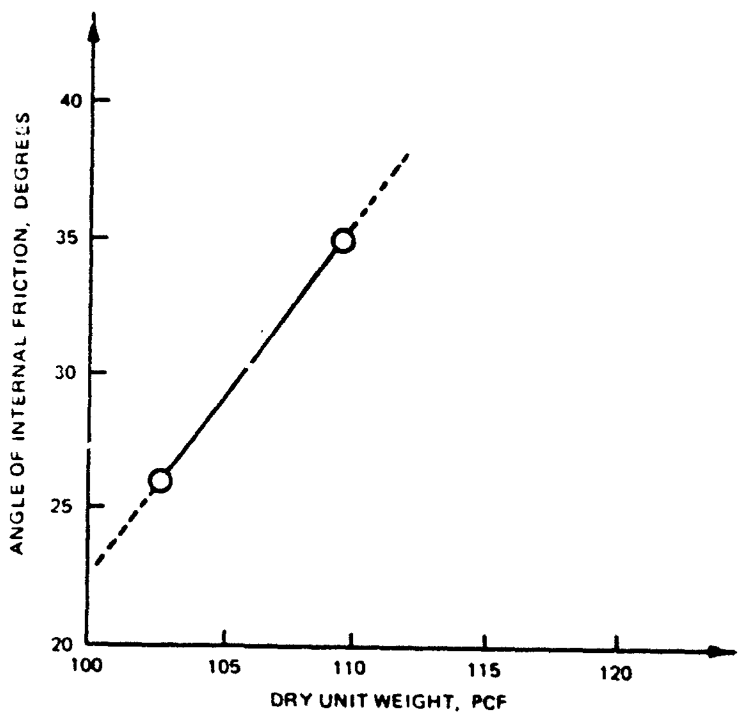

Figure 3.8. Angle of internal friction versus dry unit weight for red clayey sand.

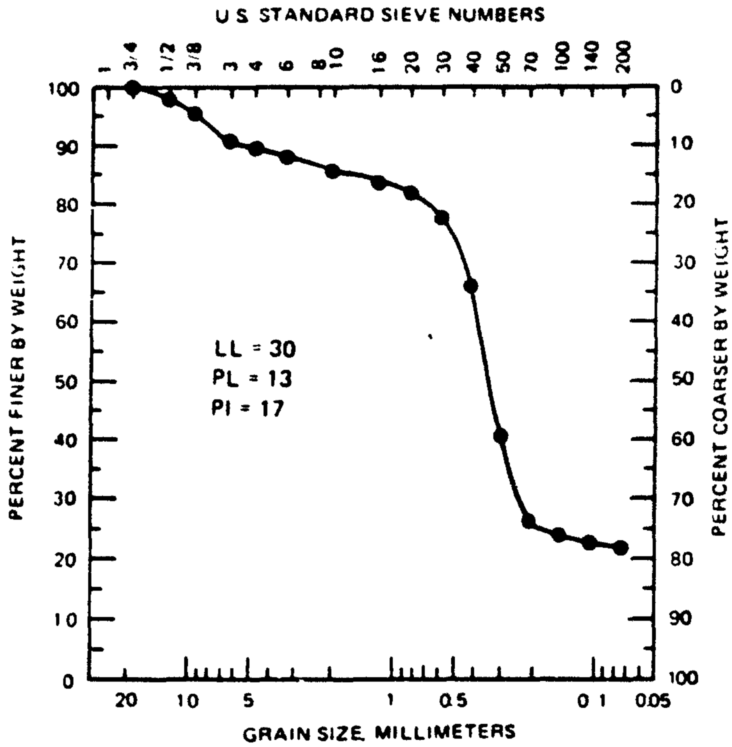

Figure 3.9. Gradation curve for clayey sand with gravel.

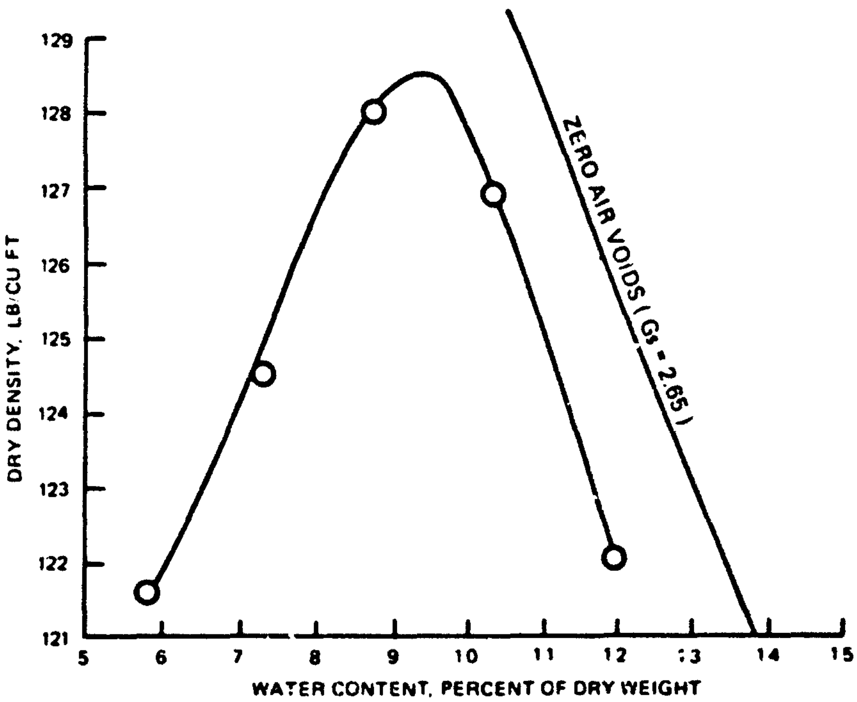

Figure 3.10. CE-55 compaction curve for clayey sand with gravel.

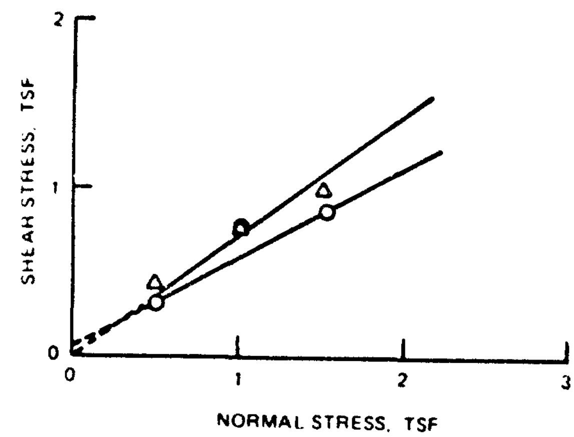

NOTE

SYMBOL	WATER CONTENT, %	DRY DENSITY, PCF	Φ, DEGREES	C, TSF
○	13.3	109.4	28	0.05
△	12.2	121.7	36	0

Figure 3.11. Direct shear test results on the clayey sand with gravel backfill.

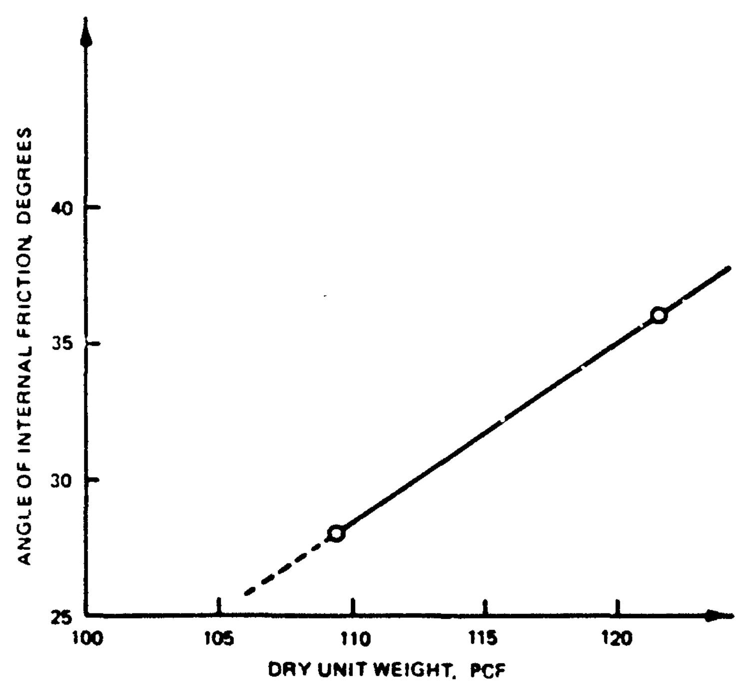

Figure 3.12. Angle of internal friction versus dry unit weight for clayey sand with gravel.

CHAPTER 4

TEST DESCRIPTION

4.1 TEST DATES, LOCATIONS, AND GENERAL DESCRIPTION

Twelve dynamic tests were performed on approximately 1/4-scale reinforced concrete box elements (one on a Type 1 element and eleven on Type 2 elements) from 1 July to 16 September 1983 at Range 36, Fort Polk, La. The dynamic loading for each test was provided by an air High Explosive Simulation Technique (HEST) charge cavity that was designed to simulate the airblast component of a 16-KT nuclear weapon at overpressures ranging from 34 to 158 psi. The weapon simulator will be discussed in detail later in this chapter.

Six static tests were performed on approximately 1/4-scale reinforced concrete box elements (one on a Type 1 element and five on Type 2 elements) from 10 October 1983 to 16 January 1984 in the laboratory at WES. The static overpressure was provided by water pressure contained in the LBLG for Test S1 (Type 1 element) and in the 6-foot generator for the five tests on Type 2 elements (S3, 4, 5, 6, 7).

Test element construction and structural material properties are described in Chapter 2 and backfill placement and material properties are described in Chapter 3. A test matrix listing all static and dynamic tests and the parameters studied in each test is shown in Table 4.1. Test configuration, instrumentation, and test procedures are described in the remainder of this chapter.

4.2 TEST CONFIGURATION

4.2.1 Dynamic Test Configuration

The test configurations for the 12 dynamic tests are shown in Figure 4.1. The test bed was constructed in a 20- by 20-foot excavation 7 feet in depth. Backfill was placed as described in Chapter 3 so that a minimum of 2 feet of compacted backfill was in place before the structures were placed in the test bed. Figures 4.2 and 4.3 show pretest photographs of dynamic tests. At this point, the structures were instrumented.

For the Type 2 element tests, thrust rods were installed between the two steel end plates to keep them from bearing on the end of the element. This

ensured that the roof of the test element acted as a one-way slab without externally applied confining stress perpendicular to the axis of one-way action.

Backfill (backfill types for each test are given in Table 4.1) was placed in 6-inch lifts until each structure was covered to the desired DOB, which is shown for each test in Table 4.1. Free-field instrumentation was installed during backfilling at the proper elevations.

After backfilling, the air HEST charge cavity was constructed on the ground surface as shown in Figure 4.4. The air HEST charge cavity consisted of a wood framing system covered with plywood that supported the initial charge cavity volume. The 18- by 15-foot cavity was 3 feet deep and covered by 3 feet of sand overburden to contain the blast and help control the pressure decay with time to simulate a 16-KT nuclear weapon detonation with overpressure ranging from 34 to 158 psi. For these tests the charge cavity parameters that controlled the weapon yield were charge density, cavity thickness, and height of overburden. From the series of calibration tests performed to develop the simulator, the required charge cavity thickness and height of overburden were determined to be 3 feet. A summary of the calibration tests is included in Appendix A. Table 4.2 lists charge densities for the dynamic tests.

The high-explosive primacord was uniformly distributed in strands running from the direction of detonation through the charge cavity in a plane 1 foot below the top of the cavity. The explosive used was pentaerythritol tetra nitrate (PETN) which was made into 50-gpf detonating cord (primacord). The strands of primacord extended 3 feet out of the charge cavity on the detonation side. These strands were bundled in groups of six strands. Each bundle of primacord was connected to one end of an 8-foot piece of 50-gpf primacord. These 8-foot strands were spliced together at the free ends enclosing a blasting cap. The blasting cap was used to initiate the detonation of the charge. This method of detonation provided a simultaneous detonation of the rows of primacord beginning at one end of the charge cavity. The charge cavity design ensures that the explosive is uniformly distributed, that the charge cavity overlapped the test element far enough to minimize edge effects, and that the structural loading was due to the propagation of a planar wave.

4.2.2 Static Test Configuration

The LBLG facility at WES was used to test the static Type 1 structure (S1). The LBLG, shown in Figure 4.5, consists of two basic components, a Central Firing Station (CFS) and a test chamber. The test chamber consists of three 22-foot, 10-inch-ID, high-strength steel rings stacked on a movable platen to form a cylindrical chamber 10 feet deep. After the model to be tested and backfill material are placed in this chamber, a ring containing baffled firing tubes and a lid are placed on the three rings of the tank below and moved into the CFS (a massive posttensioned concrete reaction structure).

Slowly applied or static loading of up to 1,000 psi can be obtained by sealing the exhaust ports of the top ring of the tank and using the tank as a pressure vessel.

More complete descriptions of the LBLG, its performance, and how it is calibrated are given in References 4 and 5.

The static tests on Type 2 elements were performed in the SBLG at WES. This device consists of a CFS and a test chamber. The test chamber consists of two 5-foot, 11-3/4-inch ID, high-strength steel rings stacked on a movable platen to form a cylindrical chamber 6 feet deep. After the model to be tested and backfill material are placed in this chamber, the pressure lid is placed on the chamber, and this assembly is moved into the CFS for testing similar to the LBLG.

Before the model was placed in the test chamber, the chamber was partially filled with backfill which was compacted and leveled to provide a uniform support for the model. The model was then placed in the test chamber, instrumented, and covered to the depth of burial given for each test in Table 4.1 with compacted backfill. The surface of the backfill was covered with a waterproof diaphragm and water was pumped in to apply a uniform load to the surface. Sketches showing the placement of the model structure in the test chamber are given in Figures 4.6 and 4.7. Figure 4.8 is a pretest photograph of Test S1 prior to placing the sand backfill. A borescope was used to view the initial roof crack patterns during Tests S1, S4, S5, S6, and S7. A camera attachment for the borescope was not available during the tests so no photographic data were recovered.

4.3 INSTRUMENTATION

Tables 4.3 and 4.4 summarize the number of channels of instrumentation

recorded in the dynamic and static tests, respectively. The data for each test were recorded on 32-channel Sangamo Sabre IV and V, FM magnetic tape recorders which were located in the instrument van (approximately 1,000 feet from the test bed) for the dynamic tests and in the instrumentation room in the LBLG building at WES for the static tests. Dynamic data were recorded at speeds of 120 in/s and later digitized at 200 kHz. A zero time channel to establish a common time reference for the data records was included in each dynamic test. Static data were recorded at tape speeds of 3.75 in/s. After digitizing, each static data record was plotted with static water pressure as the ordinate.

4.3.1 Dynamic Test Gage Locations

Gages for the dynamic tests included airblast pressure, interface pressure, soil stress, free-field acceleration, structure acceleration, strain, passive deflection, rebar strain, roof girder strain (Test D1 only) and column load (Test D1 only). Gage locations are shown in Figures 4.9 through 4.18. Table 4.5 summarizes the figures that document gage locations for the dynamic tests.

Kulite Model HKS-375 airblast pressure (BP) gages were used to measure the overpressure-time histories for the dynamic tests. They were located at ground level directly beneath the air HEST charge cavity. Airblast gage ranges used were 500 and 1,000 psi.

Soil stress measurements were made using Kulite SE Model VQV-080-LR soil stress gages (SE) which have a range of 200 psi.

Structural (A) and free-field (AFF) accelerations were measured using Endevco Model 2262 accelerometers. Ranges of the accelerometers varied from 200 to 2,000 g's.

Interface pressure measurements were made using Kulite Model VM-750 transducers with ranges of 200 and 500 psi.

Reinforcement steel strains were measured on the inside (EI) and outside (EO) principal steel using micro-measurement single-axis, metal film, 350-ohm, temperature-compensated, 1/8-inch strain gages. The model number of these gages is EA-06-125BZ-350-W and the range is ±50,000 μin/in.

Roof girder strains (Test D1 only) were measured using micro-measurement 1/4-inch strain gages (similar to those above). Gage locations (GT and GB)

are shown in Figure 4.11. The model number of these gages is EA-06-250BF-350-W and the range is ±50,000 μin/in.

Column loads (Test D1 only) were measured using pairs of 1/4-inch micro-measurement strain gages (Model No. EA-06-250BF-350-W), which were located on the column web at midheight of the column. Two columns (LC1 and LC2) were strain gaged and calibrated as load cells.

Passive deflection measurements were made using scratch gages (S1, S2) located at midspan in all dynamic tests except Test D8. These gages recorded the maximum midspan deflection and rebound.

4.3.2 Static Test Gage Locations

Gages for the static tests included water pressure, interface pressure, soil stress, deflection, rebar strain, roof girder strain (Test S1 only), and column load (Test S1 only). Gage locations are shown in Figures 4.9, 4.10, 4.11, 4.15, and 4.19 through 4.22. Table 4.6 summarizes the figures that document gage locations for the static tests.

Static water pressure measurements were made using two Norwood Model 211-34 pressure transducers that are capable of measuring a maximum of 1,000 psi. These transducers were mounted on the B-ring of the LBLG for Test S1 and on the lid of the SBLG for Tests S3, S4, S5, S6, and S7.

Deflection measurements were made at center-span in one location in Tests S3, S4, S5, S6, and S7, and at two locations in Test S1. The deflection gage used was a Transtek LVDT (Linearly Variable Differential Transformer) Model 246 with a maximum range of 6 inches.

Soil stress, interface pressure, rebar strain, roof girder strain (Test S1 only), and column load cells (Test S1 only) were identical to those used in the dynamic tests as described in Section 4.3.1.

Table 4.1. Static and dynamic test matrix.

Test[a]	Element	Element Type	DOB[b] in	Back-fill[c]	f'_c[d] psi	Parameter Investigated
S1	S1	1	12	S	6,195	Baseline
S3	S3	2	0	S	5,210	DOB = 0
S4	S4	2	12	S	5,235	Baseline
S5	S5	2	12	RCS	5,605	Backfill
S6	S6	2	12	S	3,485	Concrete strength
S7	S7	2	12	CSG	4,515	Backfill
D1	D1	1	12	S	6,150	Baseline
D2	D2	2	0	S	5,280	DOB = 0
D3	D3	2	12	S	4,990	P_{so}
D3A	D3	2	12	S	--	Repeated hit
D3B	D3	2	12	S	--	Repeated hit
D3C	D3	2	12	S	--	Repeated hit
D4	D4	2	12	S	5,000	Baseline
D5	D5	2	12	RCS	5,120	Backfill
D6	D6	2	12	S	3,220	Concrete strength
D7	D7	2	12	CSG	4,120	Backfill
Multi-hit	D3, D4, D5, D6, D7	2	12[b]	S	--	Repeated hit
D8	D8, D4, D6	2	12	S	5,305 (D8)	Repeated hit on D4 and D6

[a]Test numbers preceded by an S are static and by a D are dynamic.
[b]DOB = 6 inches for Element D7.
[c]S = flume sand, RCS = red clayey sand, CSG = clayey sand with gravel.
[d]Design 28-day concrete strengths were 2,500 psi for Elements S6 and D6 and 4,000 psi for the remaining elements. Concrete strengths presented are day-of-test strengths.

Table 4.2 Charge densities for dynamic tests.

Test	Number of Strands of 50-gpf Primacord	Charge Density, lb/ft^3
D1	88	0.0140
D2	88	0.0140
D3	20	0.0032
D3A	29	0.0046
D3B	59	0.0079
D3C	74	0.0118
D4	88	0.0140
D5	88	0.0140
D6	88	0.0140
D7	88	0.0140
Multi-hit	88	0.0140
D8	120	0.0190

Table 4.3. Number of channels of instrumentation for the dynamic tests.

Test D1 used two passive deflection (scratch) gages and the remaining dynamic tests used one for each element.

Test	Airblast Pressure	Soil Stress	Free-Field Acceleration	Structure Acceleration	Interface Pressure	Rebar Strain	Roof Girder Strain	Load Cell	Total
D1	6	7	1	4	22	26	8	2	76
D2	6	7	1	1	11	22	0	0	48
D3	4	7	1	2	16	22	0	0	52
D3A	4	7	1	2	16	22	0	0	52
D3B	4	7	1	2	16	22	0	0	52
D3C	4	7	1	2	16	22	0	0	52
D4	4	7	1	2	16	22	0	0	52
D5	6	7	1	2	16	22	0	0	54
D6	4	7	1	2	16	22	0	0	52
D7	5	7	1	2	16	22	0	0	53
Multi-hit	6	7	0	0	10	0	0	0	23
D8	6	7	1	2	16	22	0	0	54
Total									566

Table 4.4. Number of channels of instrumentation for the static tests.

Test	Water Pressure	Soil Stress	Deflection	Interface Pressure	Rebar Strain	Roof Girder Strain	Load Cell	Total
S1	2	7	2	22	26	8	2	69
S3	2	4	1	6	22	0	0	35
S4	2	6	1	11	22	0	0	42
S5	2	6	1	11	22	0	0	42
S6	2	6	1	11	22	0	0	42
S7	2	6	1	11	22	0	0	42
Total								272

Table 4.5. Gage location drawing matrix for the dynamic tests.

			Figure Numbers						
Test	Airblast Pressure	Soil Stress	Free-Field Acceleration	Structure Acceleration	Interface Pressure	Rebar Strain	Roof Girder Strain	Load Cell	Passive Deflection
D1	4.12	4.12	4.12	4.12	4.9	4.10	4.11	4.9	4.9
D2	4.13	4.13	4.13	4.13	4.14	4.15	a	a	a
D3	4.16	4.16	4.16	4.16	4.14	4.15	a	a	4.14
D3A	4.16	4.16	4.16	4.16	4.14	4.15	a	a	4.14
D3B	4.16	4.16	4.16	4.16	4.14	4.15	a	a	4.14
D3C	4.16	4.16	4.16	4.16	4.14	4.15	a	a	4.14
D4	4.17	4.17	4.17	4.17	4.14	4.15	a	a	4.14
D5	4.17	4.17	4.17	4.17	4.14	4.15	a	a	4.14
D6	4.17	4.17	4.17	4.17	4.14	4.15	a	a	4.14
D7	4.17	4.17	4.17	4.17	4.14	4.15	a	a	4.14
Multi-hit	4.18	4.18	a	a	4.18	a	a	a	4.14
D8	4.16	4.16	4.16	4.16	4.14	4.15	a	a	a

[a]Not used.

Table 4.6. Gage location drawing matrix for the static tests.

Test	Water Pressure	Soil Stress	Deflection	Interface Pressure	Rebar Strain	Roof Girder Strain	Column Load Cell
S1	a	4.19	4.9	4.9	4.10	4.11	4.9
S3	a	4.20	4.22	4.22	4.15	b	b
S4	a	4.21	4.22	4.22	4.15	b	b
S5	a	4.21	4.22	4.22	4.15	b	b
S6	a	4.21	4.22	4.22	4.15	b	b
S7	a	4.21	4.22	4.22	4.15	b	b

[a]Water pressure gages located on B-ring of LBLG for Test S1 and on the SLBG lid for Tests S3, S4, S5, S6, and S7.
[b]Not used.

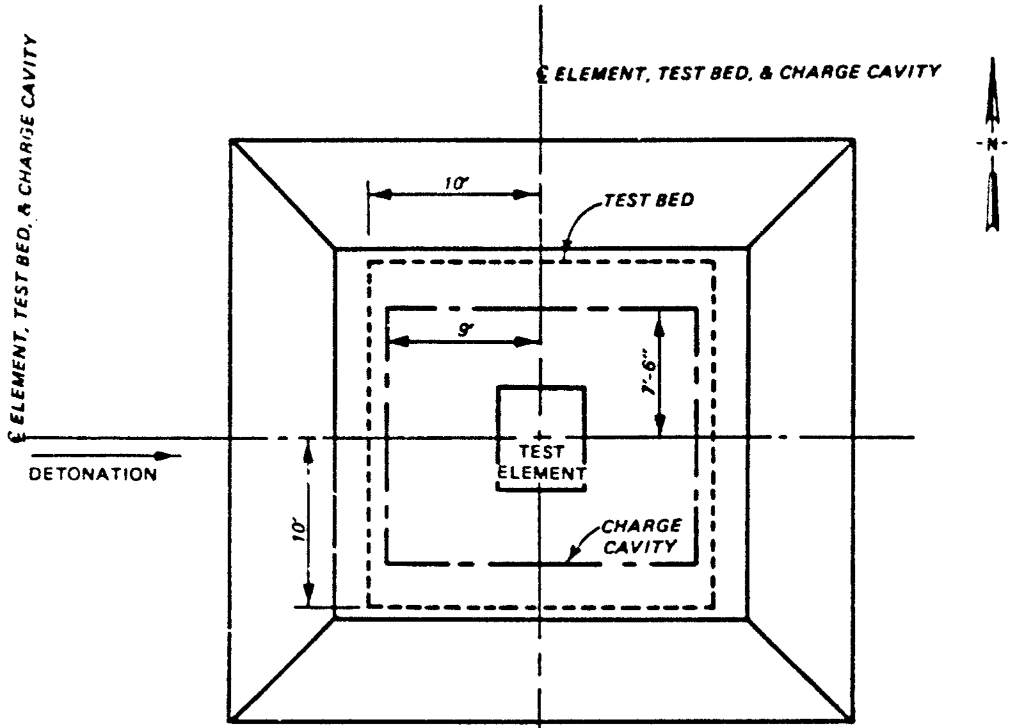

PLAN VIEW
(TYPICAL EXCEPT FOR TEST D8 AND MULTI-HIT)

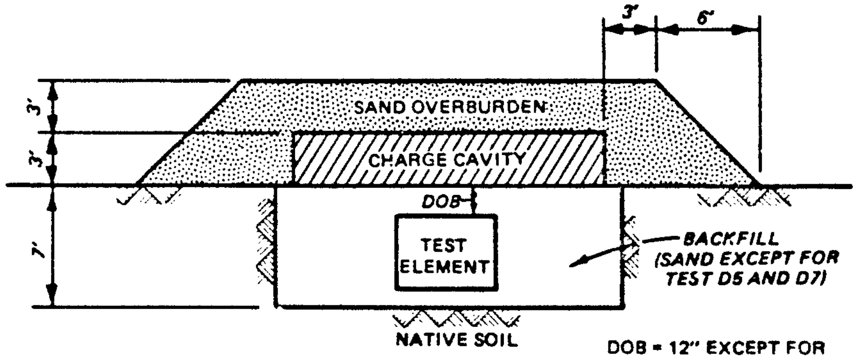

ELEVATION
(TYPICAL EXCEPT FOR TEST D8 AND MULTI-HIT WHERE MORE THAN ONE ELEMENT WAS TESTED)

Figure 4.1. Dynamic test configuration (Sheet 1 of 2).

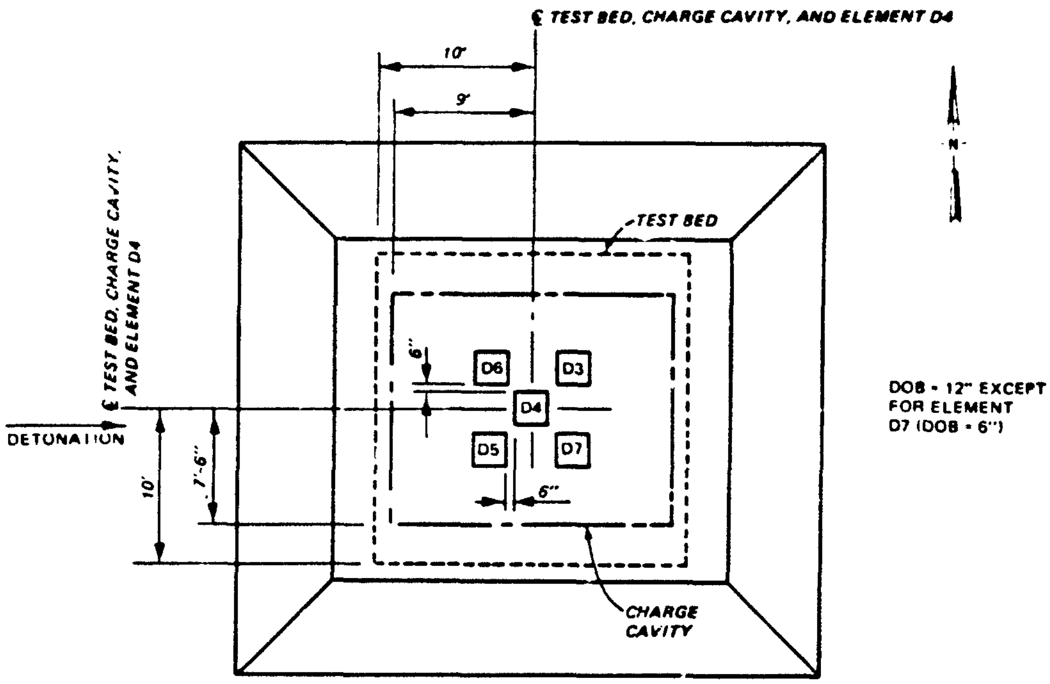

PLAN VIEW, MULTI-HIT TEST

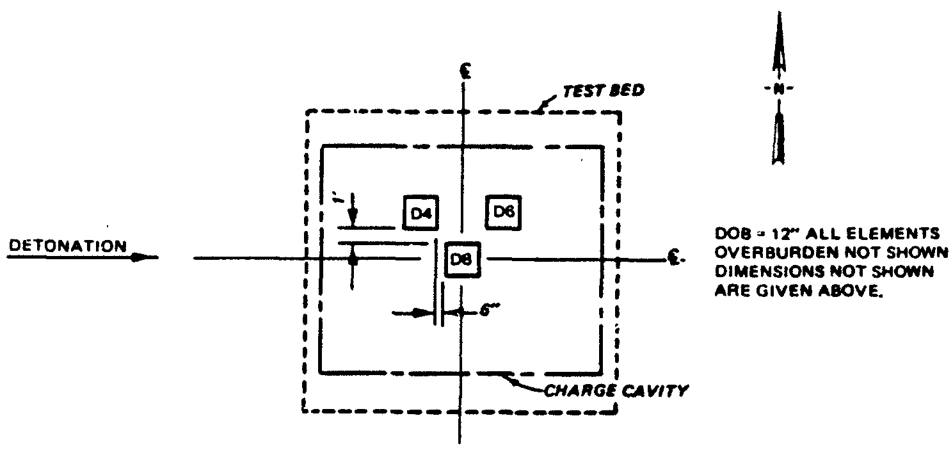

PLAN VIEW, TEST D8

Figure 4.1. (Sheet 2 of 2).

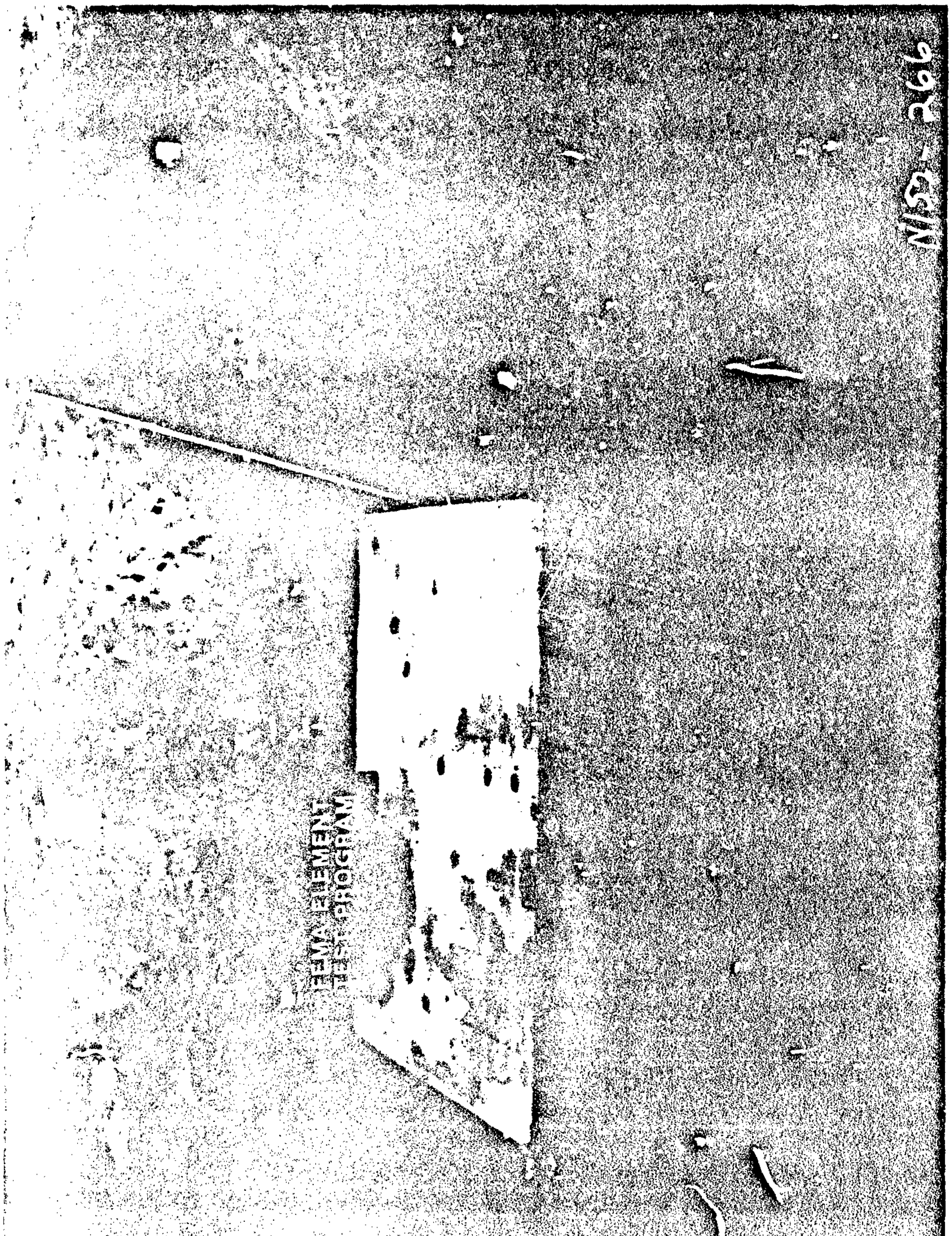

Figure 4.2. Pretest photograph of a Type 1 dynamic test.

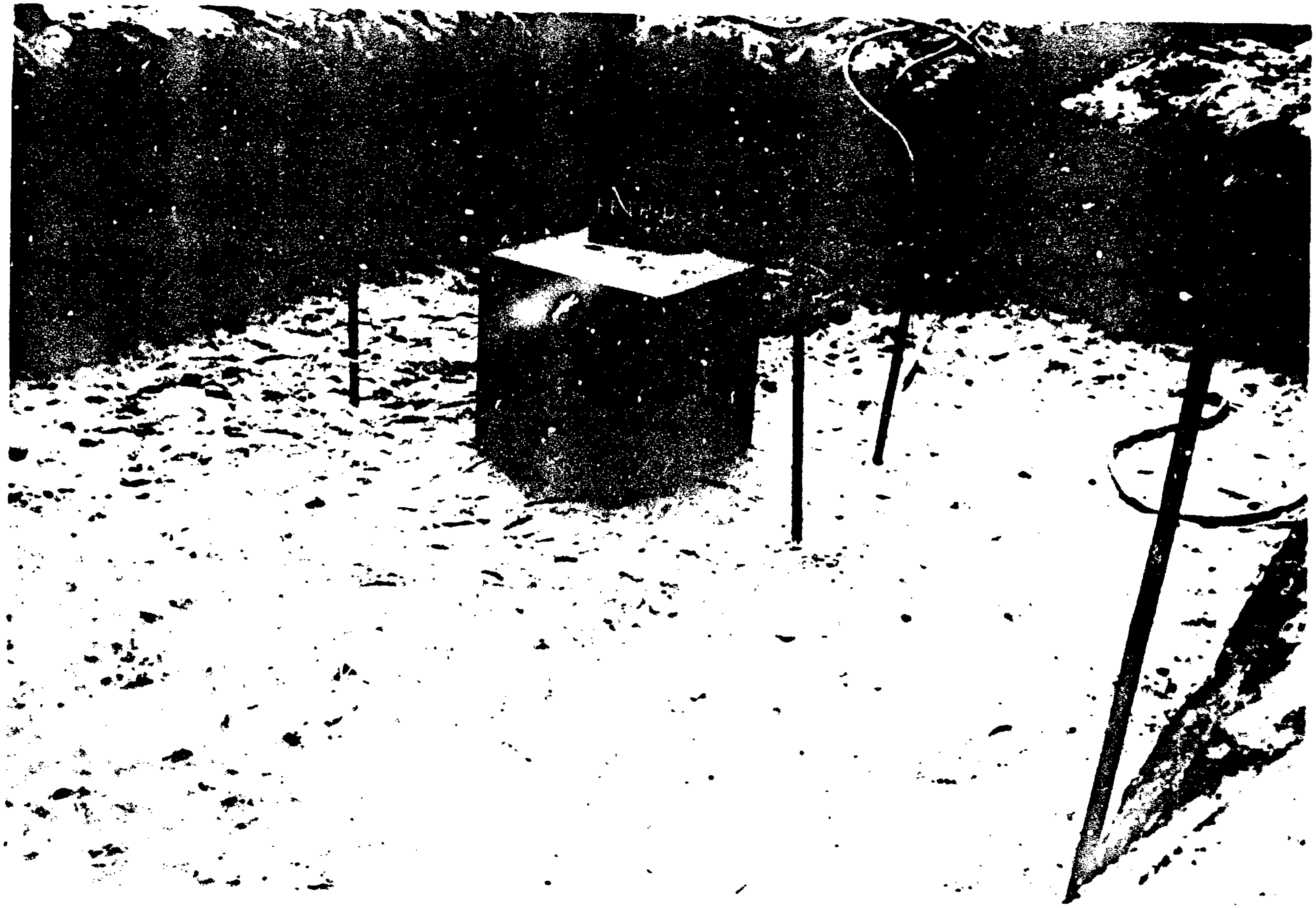

Figure 4.3. Pretest photograph of a Type 2 dynamic test.

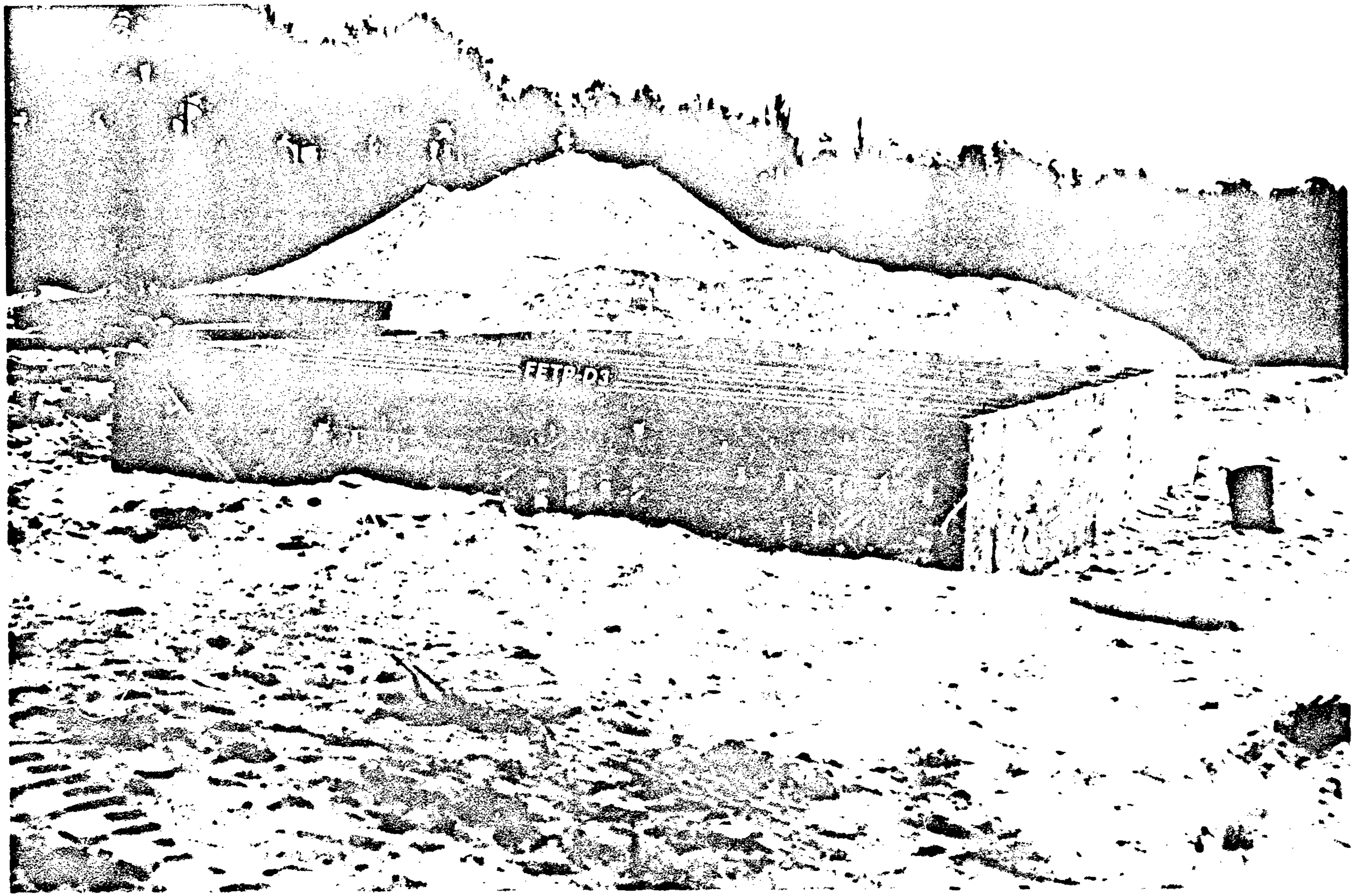

Figure 4.4. Charge cavity construction.

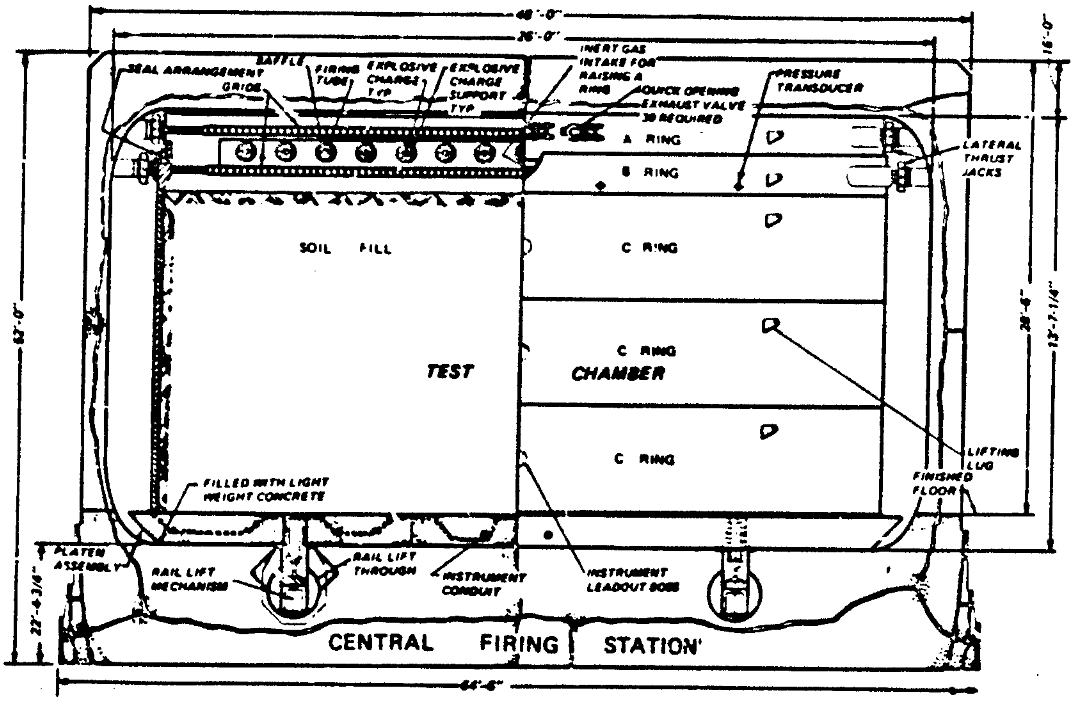

a. HALF SECTION OF THE LBLG.

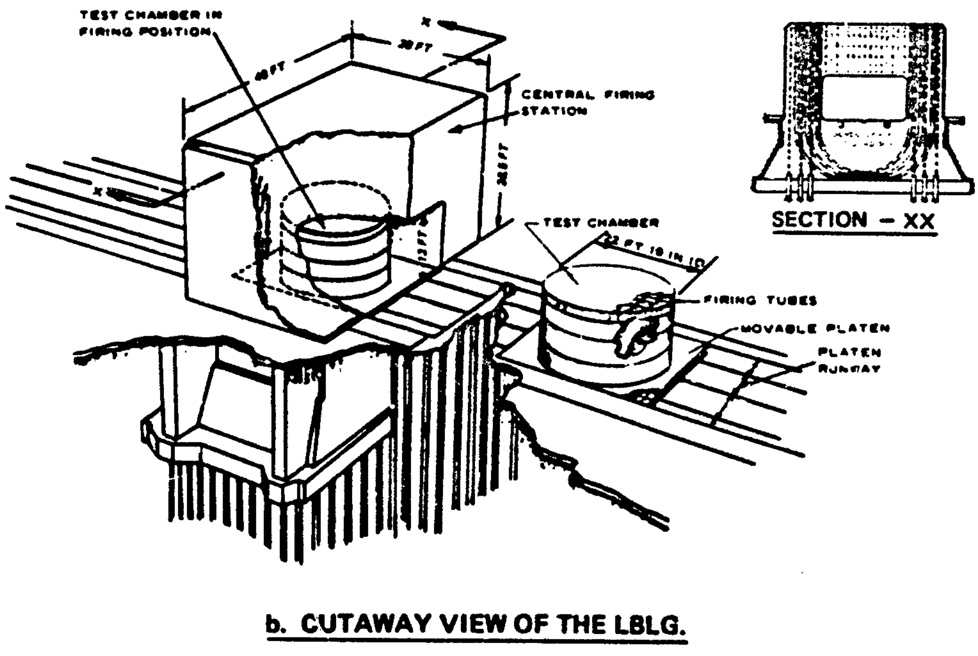

b. CUTAWAY VIEW OF THE LBLG.

Figure 4.5. LBLG.

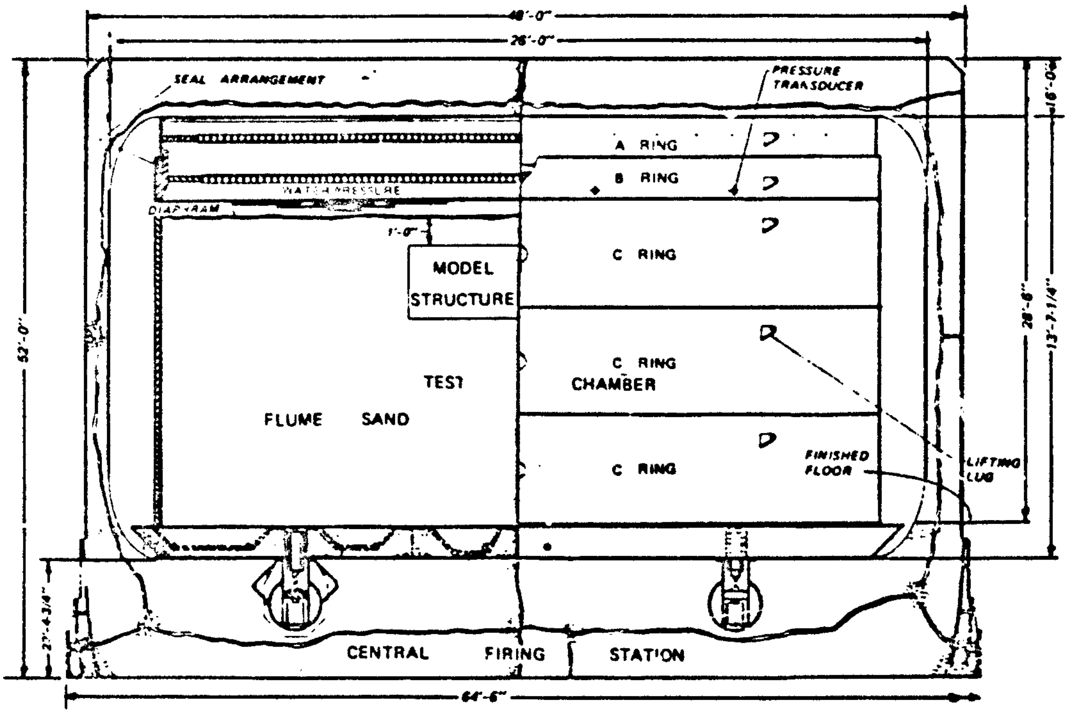

SECTION OF TEST CHAMBER

Figure 4.6. Placement of Element S1 in the LBLG.

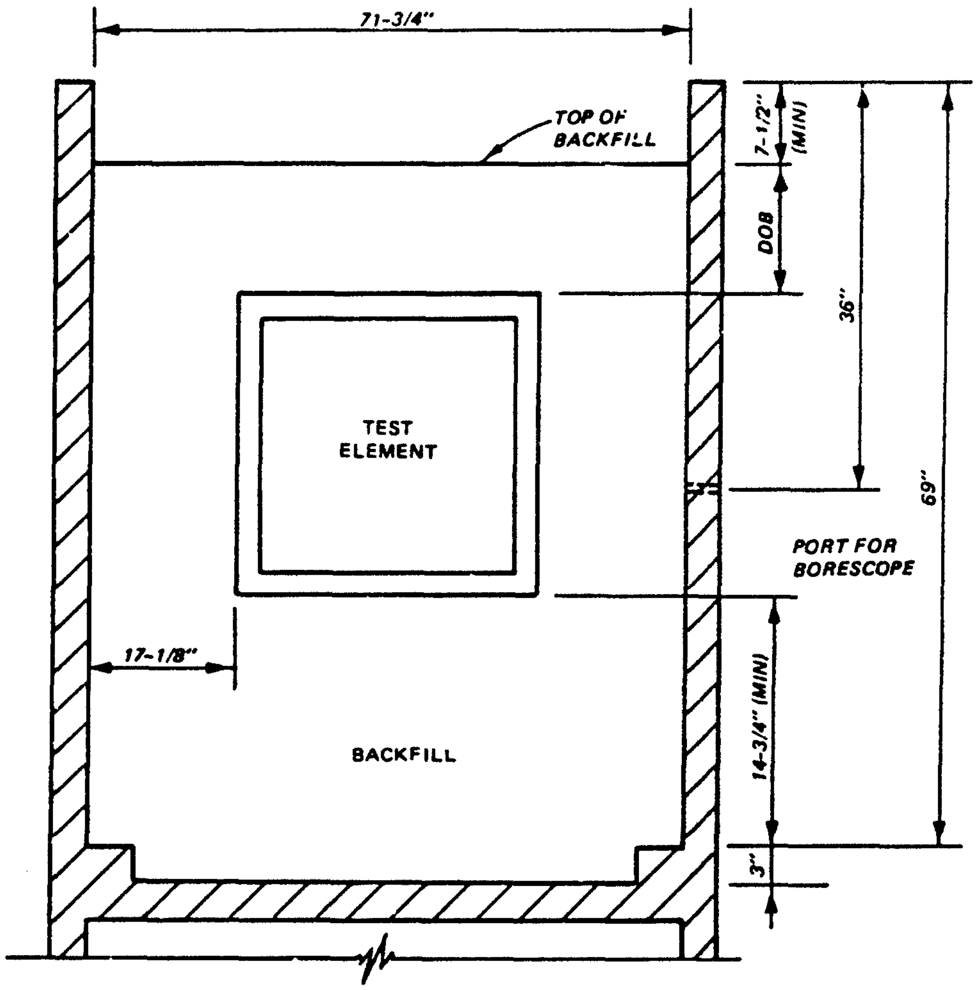

NOTE: DOB = 12" EXCEPT FOR TEST S3 (DOB = 0)

Figure 4.7. Placement of Type 2 element in the small test chamber.

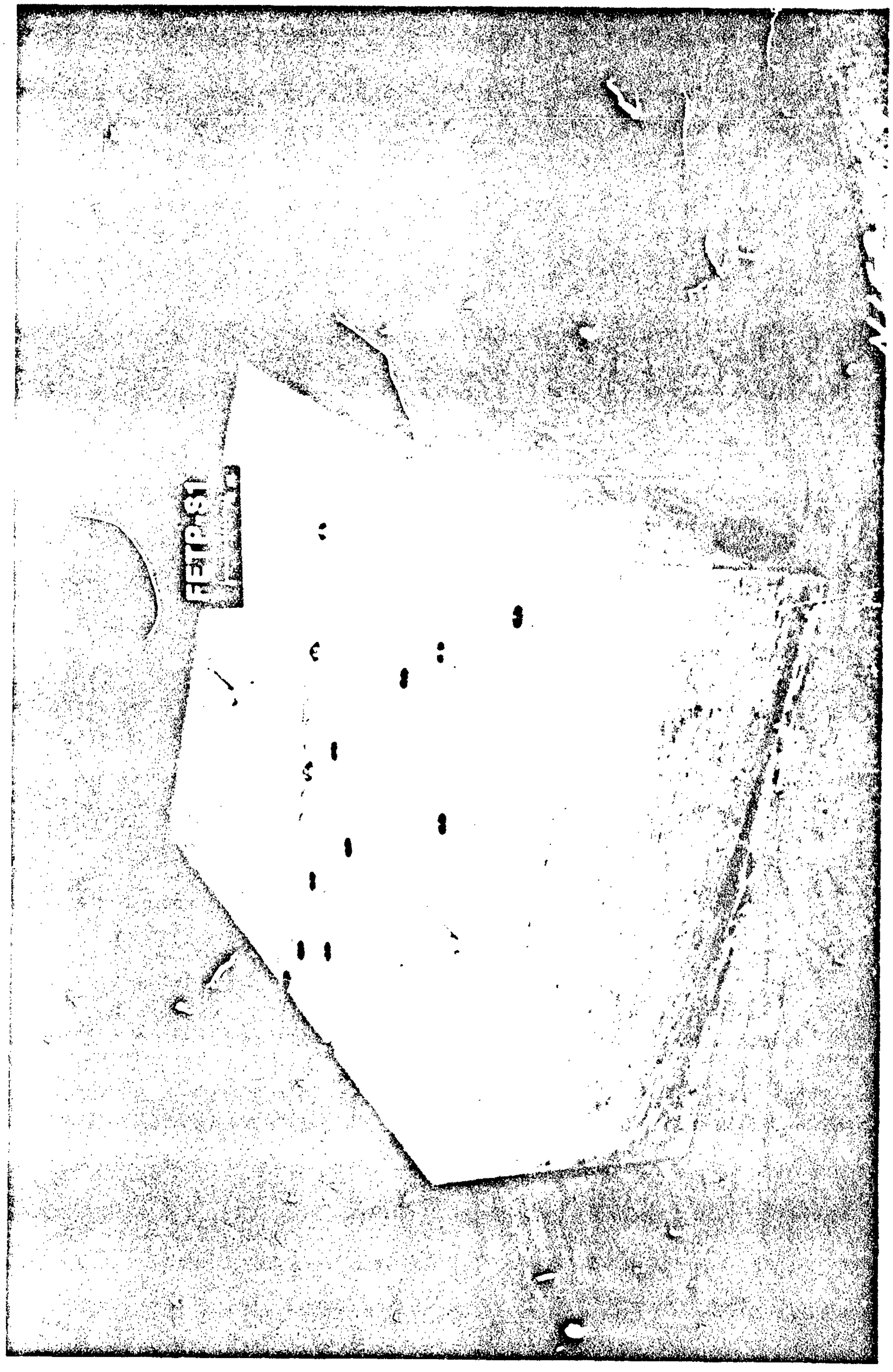

Figure 4.8. Pretest view of Element S1 prior to placing backfill.

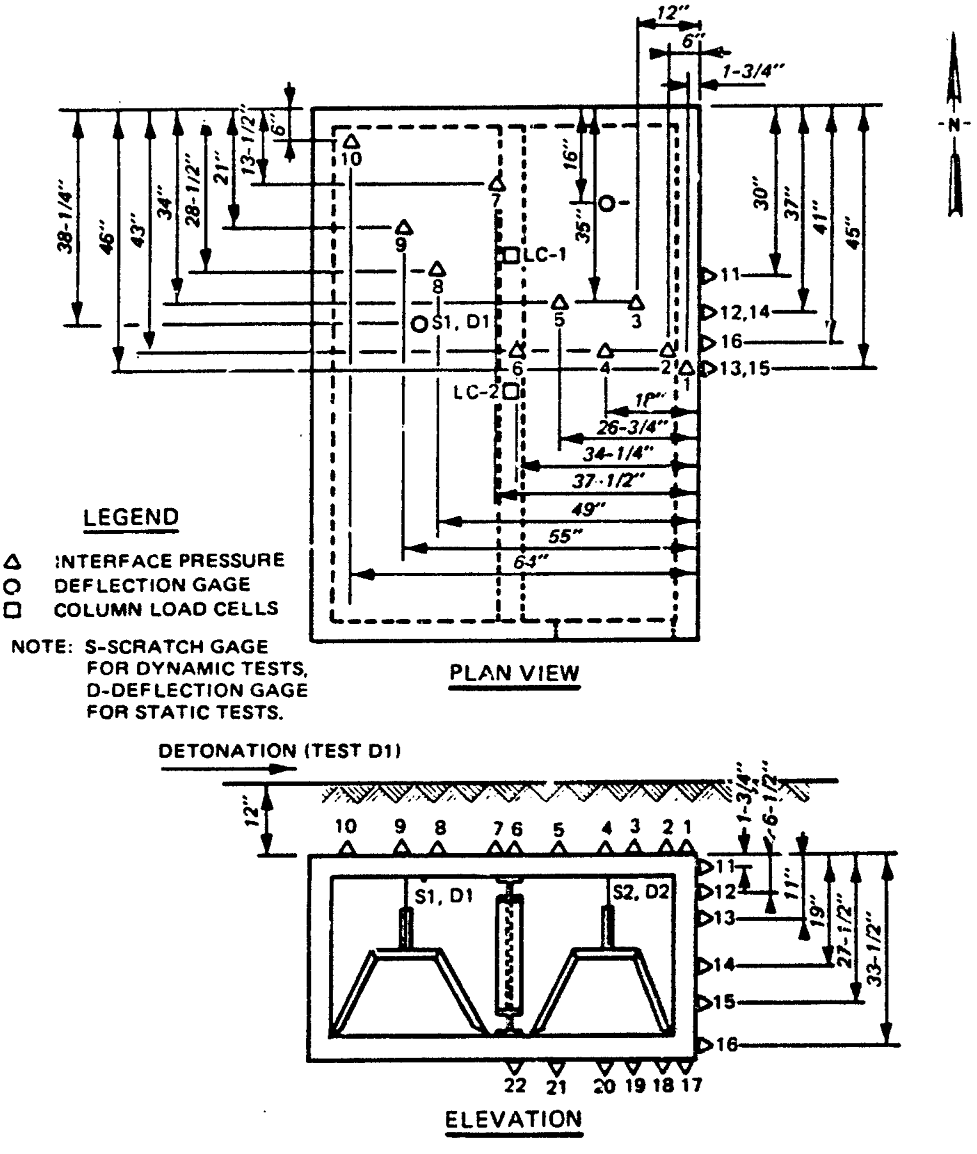

Figure 4.9. Interface pressure, deflection, and column load measurement locations for Tests D1 and S1.

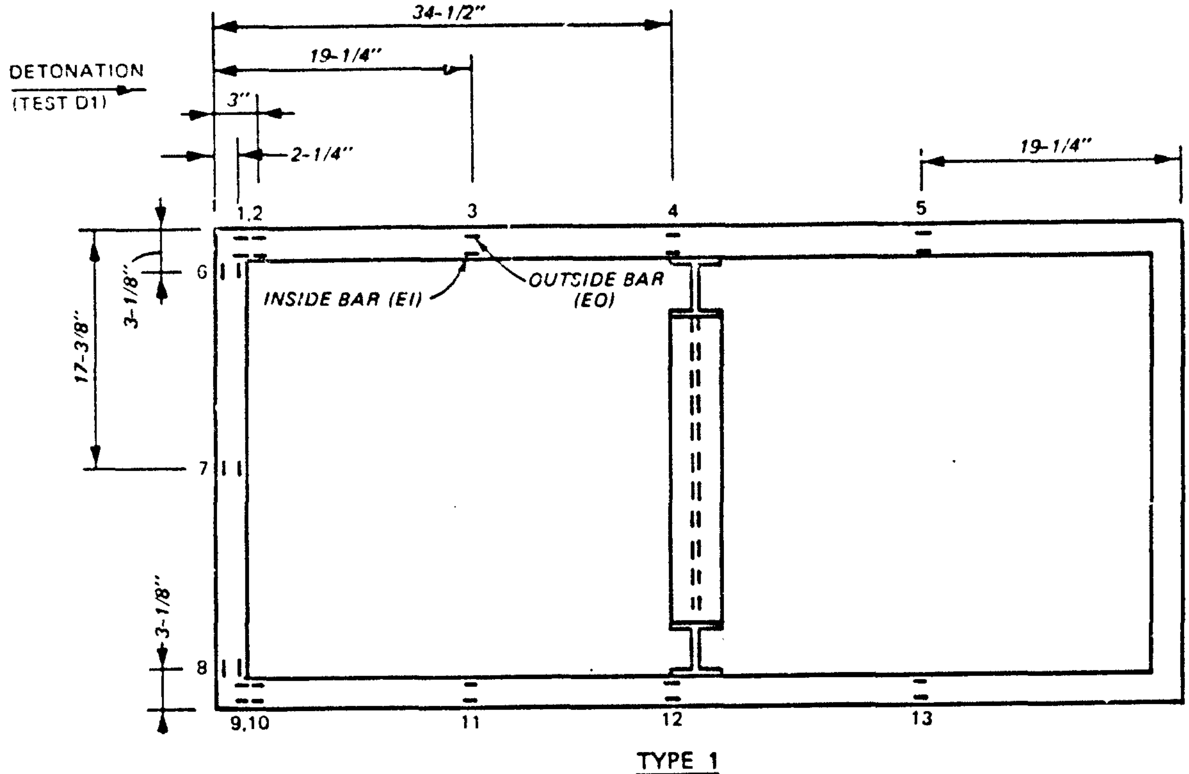

Figure 4.10. Rebar strain gage locations for Tests D1 and S1.

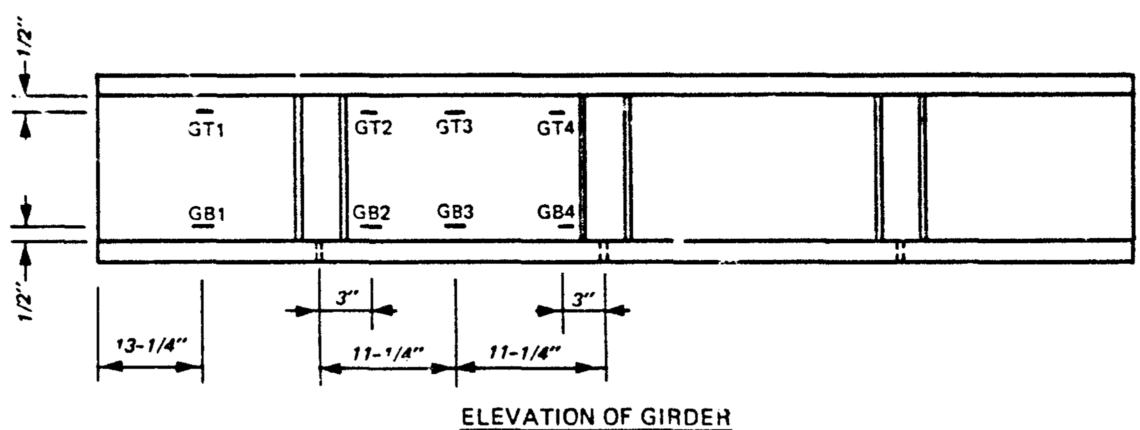

Figure 4.11. Roof girder strain gage locations for Tests D1 and S1.

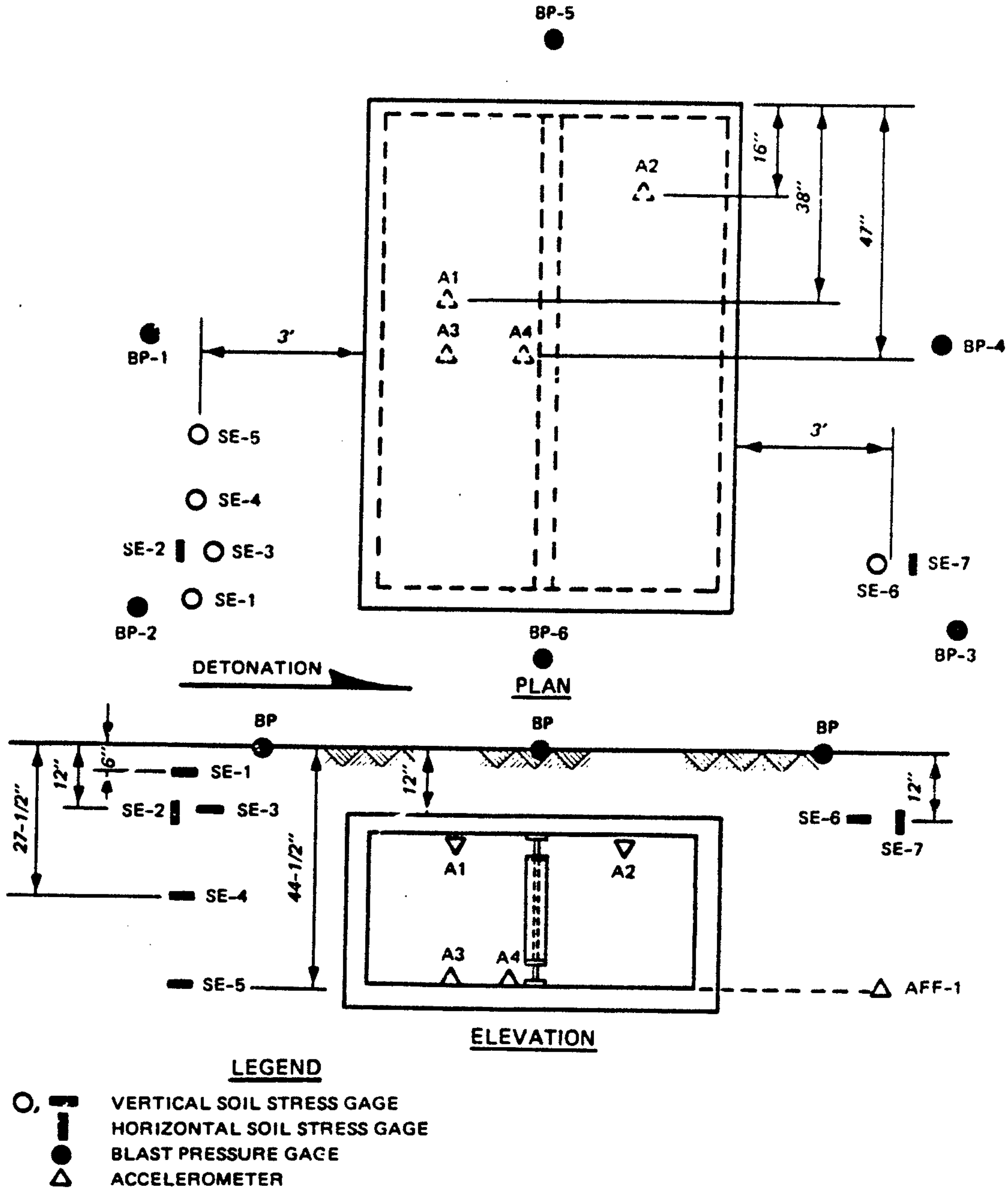

Figure 4.12. Blast pressure, soil stress, free-field acceleration, and structure acceleration gage locations for Test D1.

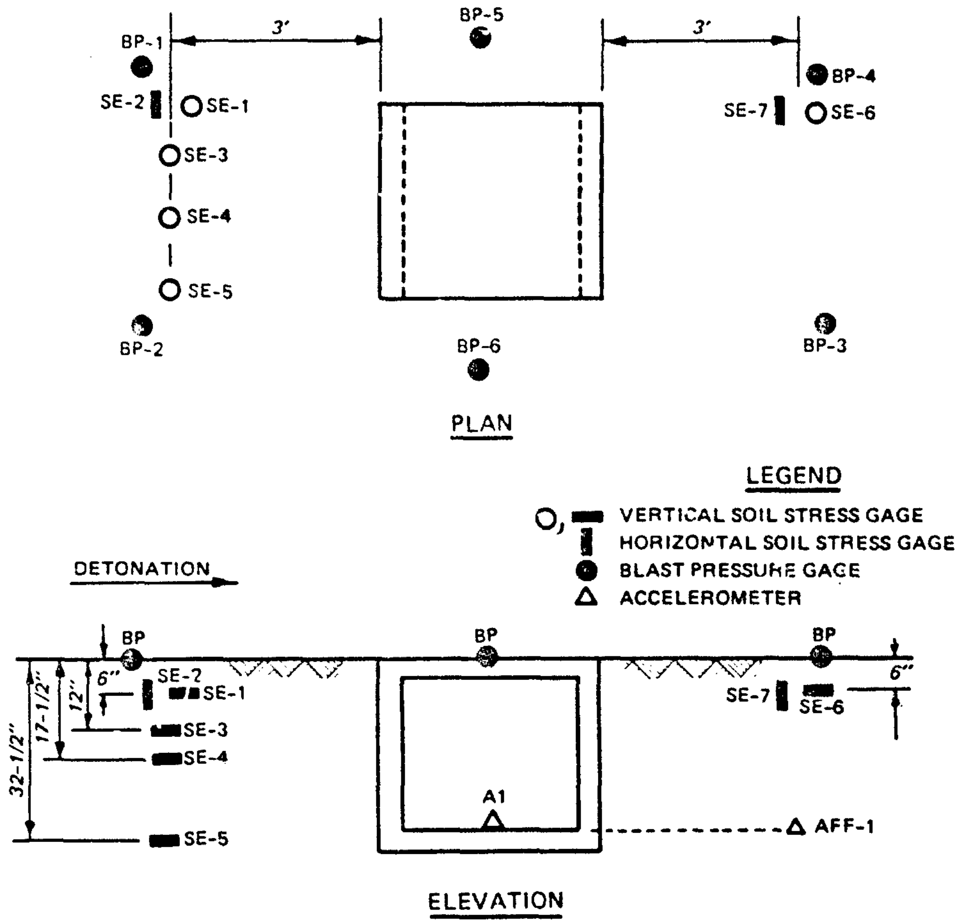

Figure 4.13. Airblast pressure, soil stress, free-field acceleration, and structure acceleration for Test D2.

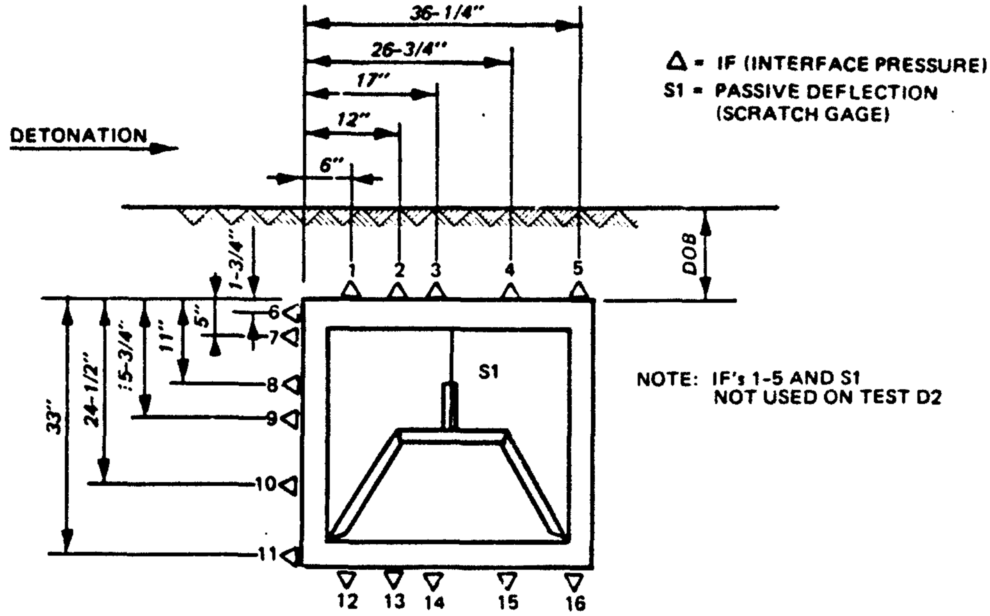

Figure 4.14. Interface pressure and deflection gage locations for Tests D2, D3, D3A, D3B, D3C, D4, D5, D6, D7, and D8.

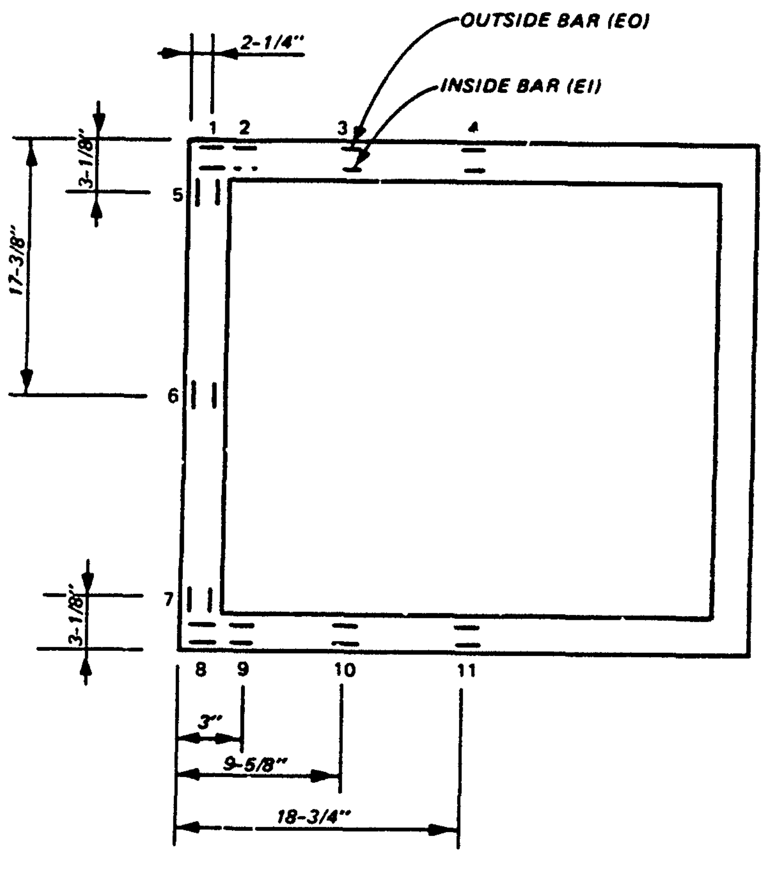

TYPE 2

Figure 4.15. Strain gage locations for the dynamic and static Type 2 element tests.

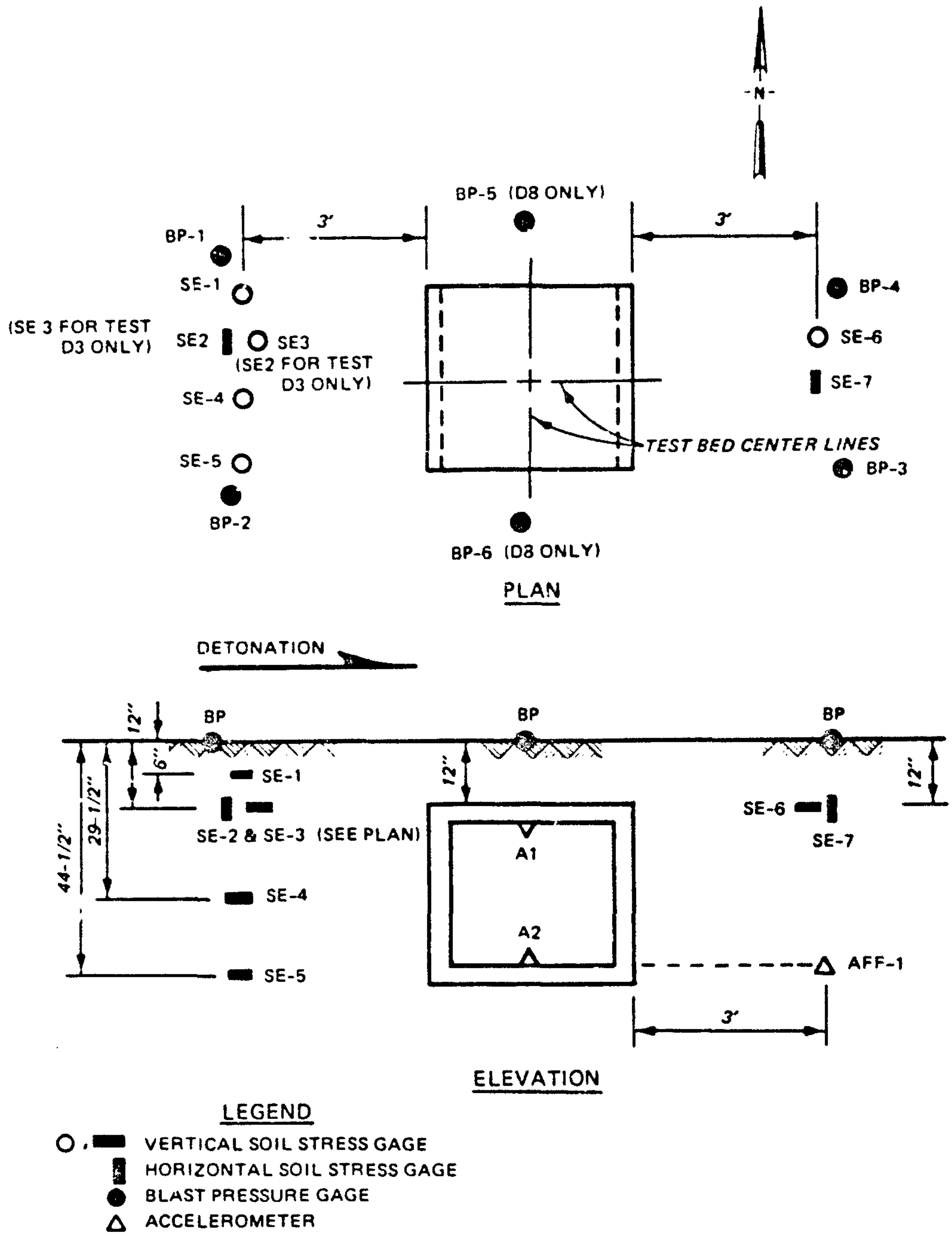

Figure 4.16. Airblast pressure, soil stress, free-field acceleration, and structure acceleration for Tests D3, D3A, D3B, D3C, and D8.

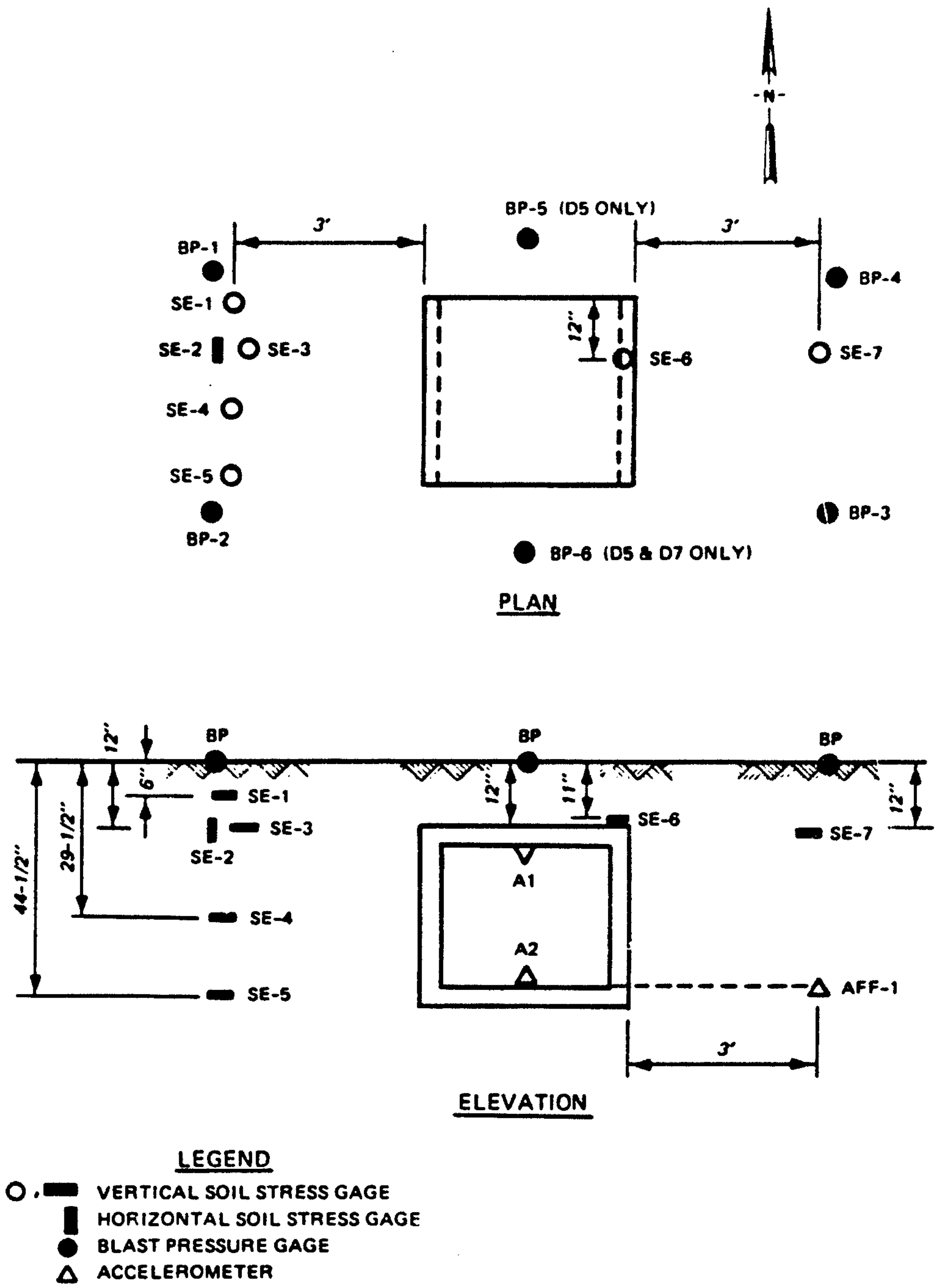

Figure 4.17. Airblast pressure, soil stress, free-field acceleration, and structure acceleration for Tests D4, D5, D6, and D7.

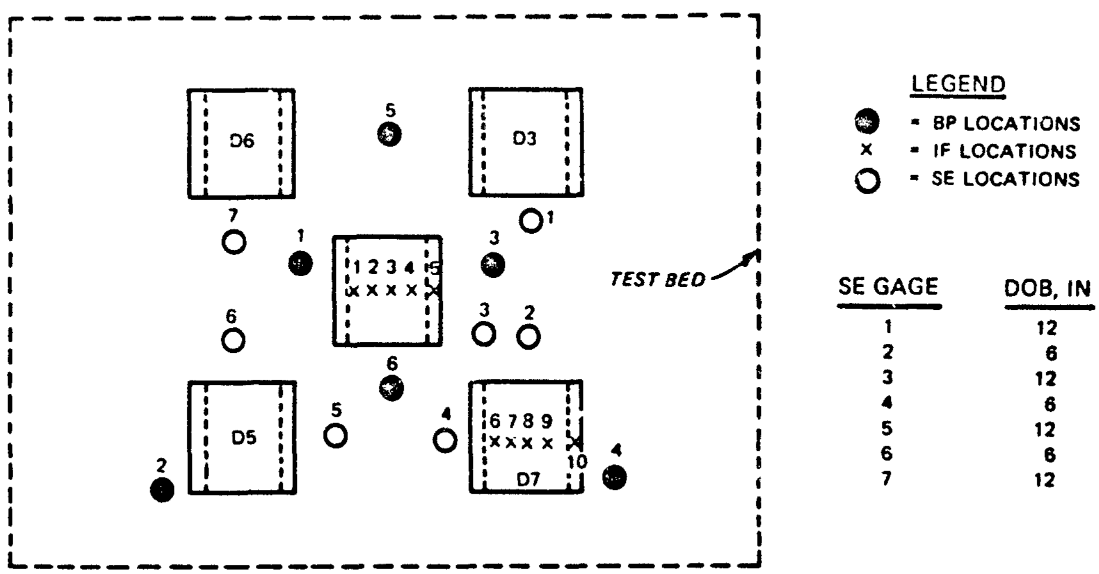

SE GAGE	DOB, IN
1	12
2	6
3	12
4	6
5	12
6	6
7	12

NOTE: IF GAGE LOCATIONS ARE TYPICAL OF THOSE SHOWN IN FIGURE 4.14 FOR ROOF IF GAGES

Figure 4.18. Blast pressure, interface pressure, and soil stress gage locations for the multi-hit test.

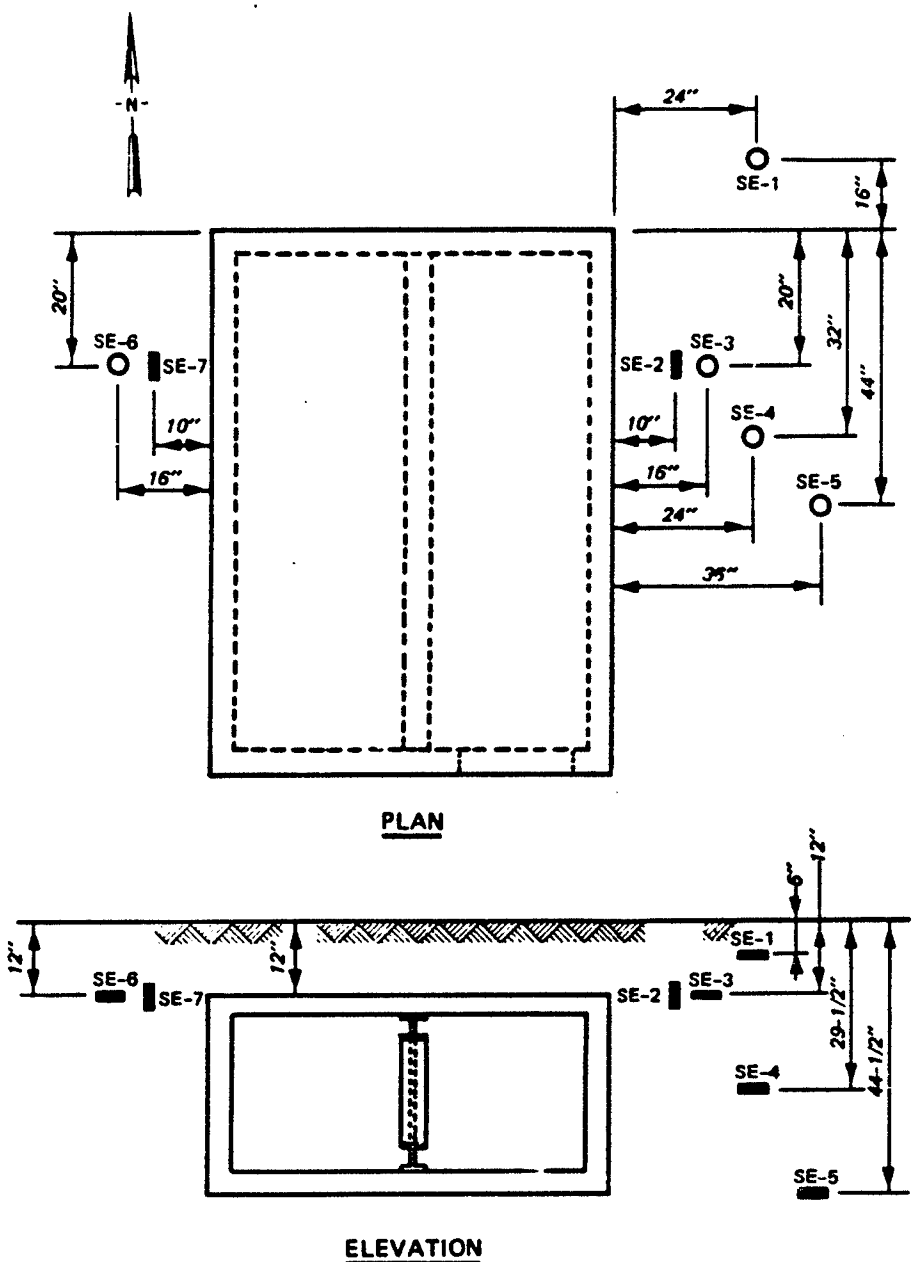

Figure 4.19. Soil stress gage locations for Test S1.

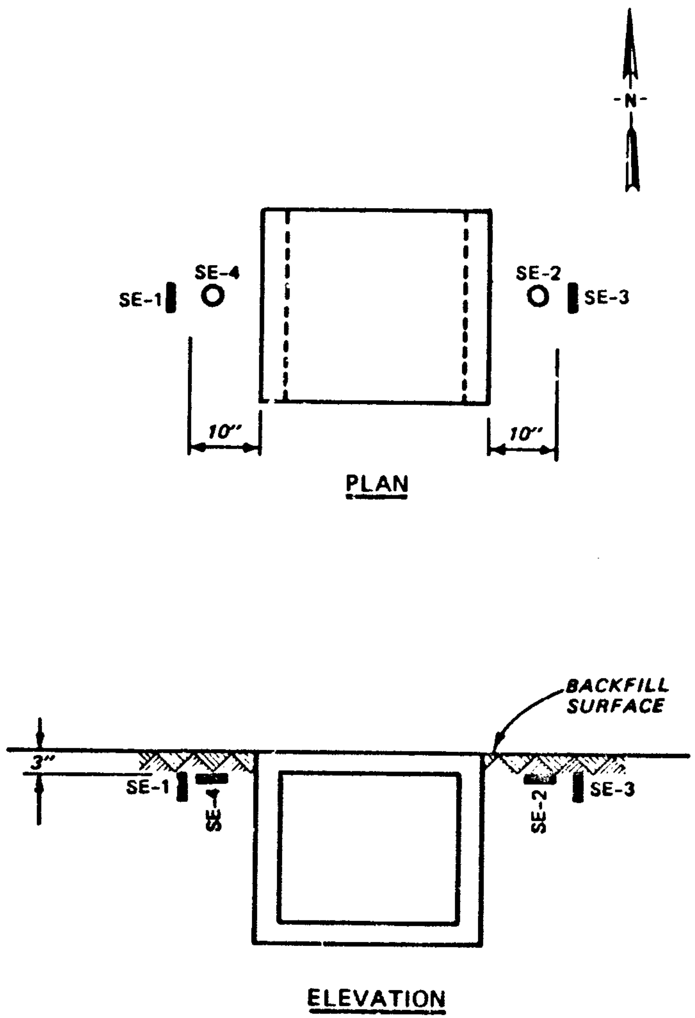

Figure 4.20. Soil stress gage locations for Test S3.

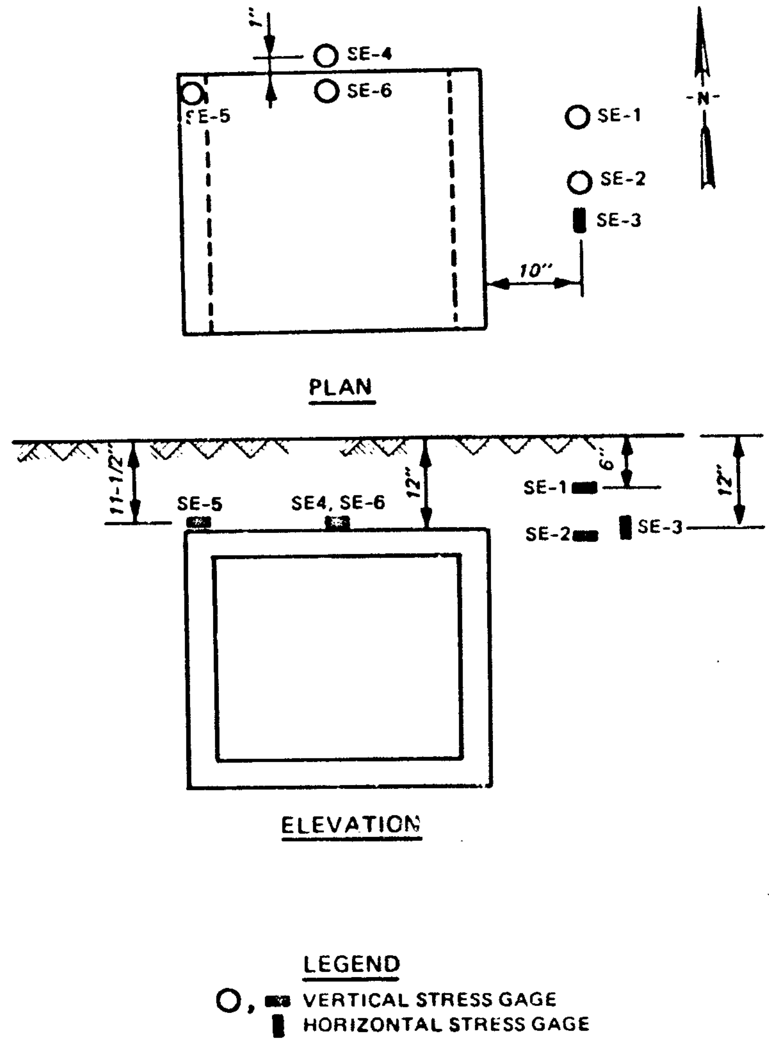

Figure 4.21. Soil stress gage locations for Tests S4, S5, S6, and S7.

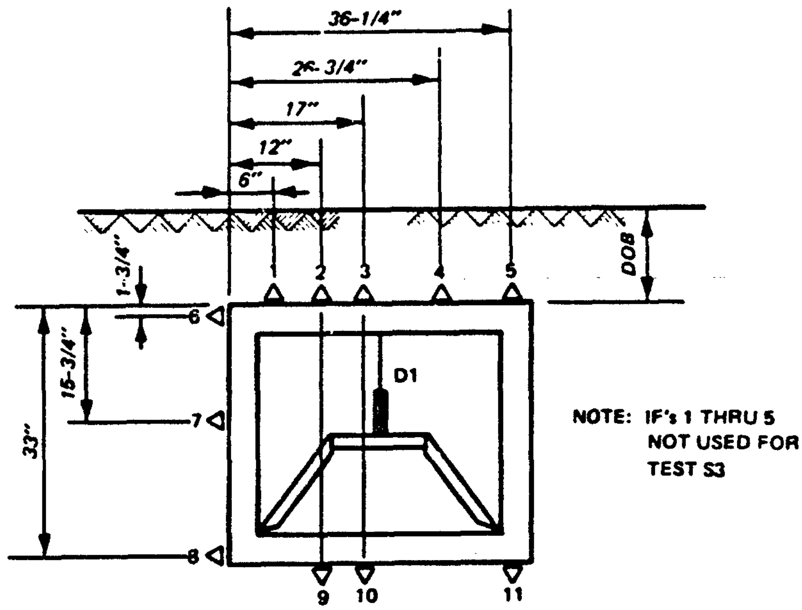

Figure 4.22. Interface pressure gage locations for Tests S4, S5, S6, and S7.

CHAPTER 5

RESULTS

5.1 DYNAMIC TEST RESULTS

The dynamic tests reported herein of approximately 1/4-scale model structures took place from 1 July to 16 September 1983. A total of 12 dynamic tests were performed as described in the preceding chapters.

5.1.1 Nuclear Weapon Simulation

The dynamic surface loading for each test was produced by the air HEST procedure discussed in Chapter 4. Typical overpressure-time records with the simulated weapon superimposed are shown in Figures 5.1 and 5.2. Figure 5.1 is a typical weapon simulation for a low-pressure test (D3). The simulated yield is 122 KT with a simulated peak overpressure of 61 psi. Figure 5.2 is a typical weapon simulation for a high-pressure test (D4). The simulation yield is 23 KT with a simulated peak overpressure of 140 psi. These weapon simulations were determined by a comparison of nuclear overpressure-time histories, as defined by S. J. Speicher and H. L. Brode (Reference 6), with 20 ms (taking time equal zero after the blast wave reaches the blast pressure gage) of an airblast pressure-time record recorded during the test. A best fit was determined for each airblast data record using the principle of least squares as determined from a computer program developed by Mlakar and Walker (Reference 7) and modified by Mr. J. T. Baylot of WES. The program was modified to fit impulse rather than pressure as in the original program. The weapon simulations for each recovered airblast data record are listed in Table 5.1.

Tests D3, D3A, D3B, and D3C were performed to determine an overpressure that would cause significant damage. After these four tests were performed, it was decided that the air HEST charge density should be 0.014 lb/ft^3 in the remaining tests where the effects of element type, backfill type, concrete strength, and DOB on structural response were compared.

5.1.2 Structural Damage

Structural response (midspan roof deflection) for each test is summarized in Table 5.2. Roof-wall joint rotations for each test are summarized in Table 5.3. Rigid body motion of the test elements was inconsistent based on

overpressure. For the most part, rigid body displacements were small (0.1 to 0.5 inch) except in Test D5, in which an average permanent rigid body displacement of 1.7 inches was recorded. Test D5 resulted in 1.13 inches of floor response. Test D5 was the only test in which it was clear that the bearing capacity of the foundation material was exceeded.

5.1.2.1 Test D1. Test D1 was a baseline test (DOB = 1 foot, sand backfill) on the Type 1 element. The test simulated a nuclear weapon with 12-KT yield at 127 psi. Maximum midspan roof response, including 5/16-inch rebound, was 9/16 inch. This occurred at Scratch Gage S1 where the permanent set was 1/4 inch. Scratch Gage S2 recorded a maximum response of 3/8 inch with 1/4-inch rebound, which yields a 1/8-inch permanent set at midspan (16 inches from the end of the structure). Two-way action near the end of the structure explains the difference in response of the roof slab at scratch gage locations S1 and S2. As shown in Figures 5.3 and 5.4, concrete cracking was minor. Tensile cracks were noted in the roof at the walls and over the interior support (structural steel frame). Since the bottom of the roof slab was covered with the corrugated steel decking, no roof cracks could be seen from inside the structure. No visible damage was noted to the roof and floor girders or the columns. No cracking was noted at the girder-to-wall connection.

5.1.2.2 Test D2. Test D2 was a surface-flush (DOB = 0) test on a Type 2 element. The test simulated a nuclear weapon with a 14-KT yield at 129 psi. As shown in Figure 5.5, the roof was severed at midspan and the walls failed at 18 inches from the floor (east wall) and 16 inches from the floor (west wall). An analysis of the strain data indicates that the midspan of the roof failed before the walls yielded (5 ms for the roof and 15 ms for the wall). All outside rebars were broken in the wall failure planes. At the west roof-wall joint, seven of nine top roof rebars were broken. At the east roof-wall joint, eight of nine top roof rebars were broken. No bottom roof steel was broken at the supports. All principal reinforcing steel was broken at midspan. Necking down of reinforcing steel was noted at all failure planes.

5.1.2.3 Test D3. Test D3 was a test on a Type 2 element in sand backfill with a DOB of 1 foot. The purpose of Test D3 was to validate the 50-psi design. Element D3 was then retested at higher overpressures to evaluate repeated hits and to establish an overpressure for the tests on different backfill types and concrete strengths. The nuclear weapon simulated in Test D3 (based on an average of the surviving airblast records had a yield of 299 KT

at 34 psi. Maximum midspan roof response was 1/16 inch with no evidence of rebound. As shown in Figure 5.6 concrete cracking was minimal. Hairline cracks formed at the top of the roof slab over the interior face of each wall as shown in Figure 5.6. Also, two hairline cracks that extend the length of the box were formed on the bottom of the roof slab as shown in Figure 5.7. These cracks were located 2-1/2 inches west of the slab midspan and 1-1/2 inches east of the slab midspan.

Test D3A was a retest of Element D3 in sand backfill with DOB equal to 1 foot. The test simulated a nuclear weapon with a yield of 343 KT at 62 psi. Maximum midspan roof response was 3/16 inch with 1/8-inch rebound yielding an additional permanent set of 1/16 inch and a total permanent set of 1/8 inch. The crack patterns formed in Test D3 remained with no additional cracking. Figure 5.8 is a posttest view of Test D3A.

Test D3B was the third test on Element D3. The DOB was 1 foot in sand backfill. The simulated nuclear weapon yield was 9,920 KT at 60 psi. Maximum midspan roof response was 5/16 inch with 9/32-inch rebound which resulted in an additional 1/32 inch of permanent deflection and a total permanent deflection of 5/32 inch. Roof crack patterns are shown in Figure 5.9. Longitudinal cracks 4 to 5 inches from midspan were formed in addition to the existing cracks from the first two tests on Element D3 (compare Figures 5.7 and 5.9).

Test D3C was the fourth test on Element D3. The DOB was 1 foot in sand backfill. The test simulated a nuclear weapon of 18 KT at 129 psi. Maximum midspan roof response was 21/32 inch with a rebound of 5/16 inch. This test resulted in an additional permanent deflection of 11/32 inch and a total permanent midspan deflection of 1/2 inch. The roof crack pattern was unchanged from Test D3B. The width of the existing cracks increased from hairline cracks to 1/16- to 1/8-inch-wide cracks. Figure 5.10 shows an end view of the roof cracks, a side view of the crack at the roof-wall connection (typical of both walls), and minor hairline cracks in the top of the floor slab.

5.1.2.4 Test D4. Test D4 was a baseline test (DOB = 1 foot in sand) on a Type 2 element. The test simulated a nuclear weapon of 18 KT at 142 psi. Maximum response including 7/32-inch rebound was 23/32 inch, which yielded a roof midspan permanent set of 1/2 inch. Midspan roof cracking occurred over a 10-inch length as shown in Figure 5.11. Some crushing of concrete was noted at midspan as shown in Figure 5.12. Figure 5.12 also shows roof cracking at the supports. Only hairline cracks were noted in the floor slab.

5.1.2.5 Test D5. Test D5 was identical to Test D4 except the backfill material used was red clayey sand instead of sand. The nuclear weapon simulation was 77 KT at 158 psi peak overpressure. Maximum midspan roof response, including 11/32-inch rebound, was 1-7/32 inches, which resulted in a permanent set of 7/8 inch. Roof cracking was similar to Test D4. The major difference in the results of Tests D5 and D4 was floor damage in Test D5. In Test D5 there was a 1-1/8 inch permanent set in the floor slab. The floor crack pattern is shown in Figure 5.13. Note that cracks along the free end of the floor slab shown in Figure 5.13 were caused by the end plate supports and should not be interpreted as a typical failure mechanism.

5.1.2.6 Test D6. Test D6 was identical to Test D4 except the concrete strength was 3,220 psi instead of 5,000 psi. The test simulated a 23-KT nuclear weapon at 141 psi peak overpressure. Maximum midspan roof response (including 5/16-inch rebound) was 1 inch, which yielded a permanent set of 11/16 inch. This test showed that the decrease in concrete strength did not significantly increase roof response. Concrete crack patterns were similar to Test D4. However, the area of crushed concrete (Figure 5.14) at the roof midspan was about 50 percent wider (1-1/2 inches versus 1 inch) on Test D5 than on Test D4.

5.1.2.7 Test D7. Test D7 was identical to Test D4 except the backfill material was a clayey sand with gravel. The nuclear weapon simulation was 58 KT at 134 psi. Maximum midspan roof response was 1-1/32 inches with 3/8-inch rebound, which yielded 21/32 inch permanent set. Crack patterns were similar to Test D4 on the roof and floor slabs.

5.1.2.8 Multi-hit Test. The multi-hit test was a retest of Elements D3, D4, D5, D6, and D7. DOB was 1 foot except for Element D7 which was buried 6 inches. Backfill was sand. The test simulated a 16-KT nuclear weapon at 134 psi peak overpressure. A posttest photograph of the multi-hit test is shown in Figure 5.15. This test was the fifth hit on Element D3. The maximum midspan roof deflection in this test was 1/2 inch with a rebound of 3/16 inch, which yields an additional permanent set of 5/16 inch and a total permanent set of 13/16 inch. This test was the second test of Elements D4, D5, D6, and D7. The maximum midspan roof deflection of Element D4 was 9/16 inch with 3/8-inch rebound, which yields an additional permanent set of 3/16 inch and a total permanent set of 11/16 inch. The scratch gage on Element D5 broke during the test so maximum response and rebound were not measured. The permanent

response measured in this test was 3/16 inch, for a total permanent set of 1-1/16 inches. No additional floor response or cracking was noted on Element D5. The maximum midspan roof deflection on Element D6 was 3/8 inch with no rebound, which yielded a total permanent set of 1-1/16 inches. Element D7 (DOB = 6 inches) suffered collapse of the roof slab and walls as shown in Figure 5.16. The west roof-wall connection failed and the west wall failed 8 inches from the top of the floor slab. The east wall failed at 23 inches from the top of the floor slab. At center span of the roof slab all nine bottom bars were broken and one top bar was broken. At the west roof-wall connection, all nine top bars and three bottom bars were broken. No bars were broken in the west wall failure plane of the east roof-wall connection. In the east wall failure plane, seven outside bars and no inside bars were broken.

5.1.2.9 Test D8. Test D8 was the first test on Element D8 and the third test on Elements D4 and D6. DOB for each element was 1 foot in sand backfill. The test simulated a 6-KT nuclear weapon at a peak overpressure of 134 psi. Figure 5.17 is a posttest view of the elements in Test D8. Element D8 had minor damage with a roof midspan permanent response of 1/2 inch (maximum response and rebound were not measured). Element D4 had a maximum roof midspan response of 3/4 inch with 7/16-inch rebound which yields an additional permanent set of 5/16 inch and a total permanent set of 1 inch. Cracking of the roof slab remained the same as in the multi-hit test for Element D4. Maximum tensile crack widths were 3/16 inch. Element D6 sustained 5-13/16 inches of additional permanent roof response for a total of 6-7/8 inches of permanent set as shown in Figure 5.18. At the roof midspan of Element D6, the area of crushed concrete varied from 1-1/2 to 2 inches wide and all bottom bars were broken. The crack width at midspan was a maximum of 1-3/8 inches. No broken tensile steel was noted at the supports. Test D8 showed that the low-strength concrete element (D6) did not have the reserve capacity to withstand three hits at approximately 130 to 140 psi peak overpressure Element D4 had adequate reserve capacity to withstand three hits.

5.1.3 Summary of the Dynamic Test Results

Based on the results of the 12 dynamic tests, the following statements can be made:

1. Tests at pressures below 100 psi resulted in very low damage levels (less than 1/2 inch midspan roof response).

2. The dynamic structural capacity in the backfills used in these tests at DOB of 1 foot (1/4-scale) was not exceeded at overpressure up to 158 psi.

3. A test at DOB equal to 0 inch (D2) and a retest at DOB equal to 6 inches (multi-hit: D7) at peak overpressures of approximately 130 psi resulted in structural collapse, while tests with DOB equal to 1 foot resulted in minor damage.

4. Tests in alternate backillls with lower shear strengths than sand resulted in acceptable performance except in Test D5 in which there was considerable floor damage. The specifications for foundation backfill material may need to be more strict than for backfill over the structure.

5. The low-strength concrete element (D6) performed adequately in two tests at more than twice the design pressure level but failed on the third test. Although no testing of the low-strength concrete was performed at 50 psi, the low-strength element appeared to have adequate reserve capacity to resist many repeated hits at the design overpressure of 50 psi.

6. The Type 2 models that were tested to failure did not appear to have adequate load-bearing capacity at deflections greater than about 1-1/2 to 2 inches. The tensile steel appeared to have fractured at the onset of tensile membrane response which resulted in large deflections and/or failure.

5.2 STATIC TEST RESULTS

The static tests reported herein of approximately 1/4-scale model structures took place from 13 October 1983 to 16 January 1984. A total of six static tests were performed as described in the preceding chapters.

5.2.1 Static Load Capacity

A comparison of the static ultimate capacities for each test is given in Table 5.4. Test S4 was a baseline test on a Type 2 element with a 4,000-psi 28-day concrete mix design and a DOB of 1 foot in sand backfill. The ultimate resistance was approximately 185 psi. Test S3 was performed to investigate the effects of soil cover. In Test S3 with no soil cover, the ultimate resistance was approximately 44 psi or only 24 percent of Test S4. Test S6 was a test identical to Test S4 except that the concrete in Element S6 was designed to have a 28-day compressive strength of 2,500 psi. The ultimate capacity of

Test S6 was 164 psi or 89 percent of that of Test S4. Test S5 was identical to Test S4 except a red clayey sand was used as backfill instead of flume sand. The ultimate capacity of S5 was 96 psi or 52 percent of Test S4. Test S7 was identical to S4 except that a clayey sand with gravel backfill was used. The ultimate capacity of S7 was 81 psi or 45 percent of S4. Test S1 was a baseline test on the Type 1 element. The ultimate capacity for Test S1 was limited to approximately 100 psi due to premature failure caused by collapse of the interior support which consisted of a structural steel frame. Test S1 was expected to have a capacity equal to or slightly greater than Test S4.

In general the data were consistent in the static tests except that Test S7 had a lower ultimate resistance than Test S5. Test S7 had the clayey sand with gravel backfill which had more shear strength than the red clayey sand backfill of Test S5. A partial explanation of this is that the concrete strength of Element S7 was approximately 1,100 psi less than S5 (4,515 versus 5,605 psi). Comparing Tests S4 and S6 (both in sand backfill) which had a difference in concrete strength of 1,750 psi (5,235 versus 3,485 psi) resulted in a reduction in ultimate capacity of 11.3 percent (185 versus 164 psi). Test S7 had an ultimate capacity 15.6 percent lower than Test S5 (81 versus 96 psi). Also, a partial explanation of the difference is scatter in the data.

5.2.2 Structural Damage and Load Response

Table 5.5 compares the load-deflection behavior of the static tests. The load-deflection points presented in Table 5.5 are as follows: Points A are deflection and load at ultimate resistance, Points B are at the point when compressive membrane action ends, Points C are at the onset of tensile membrane action, and Points D are at the peak test pressure before the test was terminated. These points are shown on a load-deflection curve in Figure 5.19. The load-deflection curves will be analyzed in the next chapter in detail. In general, the tests in the alternate backfills (S5 and S7) reached ultimate capacity at larger deflections than the tests in sand backfill. Only Test S7 developed load resistance equal to the ultimate capacity in the tensile membrane region (large deflections). Test S7 developed the lowest ultimate resistance of any of the buried tests so the tensile membrane action only had

to increase the capacity by 10 psi to reach ultimate resistance. Tests S3 and S5 showed almost no tensile membrane enhancement. Test S4 showed an increase in capacity of about 20 psi and Test S7 showed an increase in capacity of about 30 psi at large deflections.

Posttest photographs of Test S1 are shown in Figures 5.20 and 5.21. When the roof collapsed, it split into three approximately equal segments as shown in Figure 5.20. Also shown in Figure 5.20 is evidence of considerable two-way action. The center one-third section of the roof slab acted as a one-way slab with all of the roof principal steel at the walls broken, but none of the roof principal steel at the interior support broken. Figure 5.22 shows the final condition of the interior structural steel columns. All three columns had buckled. Figure 5.23 shows the roof girder from Test S1. Evidence of warping of the roof girder was noted; however, it was not clear from the test results if warping of the girder or buckling of the columns caused the premature roof collapse.

Figures 5.24 and 5.25 show typical posttest views of a Type 2 element. The only differences noted between tests were crack widths and area of crushed concrete. The results of the Type 2 static element tests are presented in Table 5.6. The only comparison in Table 5.6 that appears to be significant is that the width of crushed concrete at the roof midspan was larger in Test S5 than in any other test. Test S5 had a lower ultimate capacity than the tests buried in sand backfill (S4 and S6).

5.2.3 Summary of the Static Test Results

Based on the results of the six static tests the following statements can be made:

1. The interior structural steel frame failed before the ultimate static capacity of the roof was reached in Test S1.

2. Comparing Tests S4, S5, and S7 shows a significant difference in ultimate capacity due to backfill type.

3. Comparing Tests S4 and S6 shows no significant difference in ultimate capacity due to concrete strength in sand backfill.

4. As noted in the dynamic tests, the capacity of the roof slab was not adequate at deflections greater than the thickness of the roof slab.

5.3 RECOVERED DATA

A data summary for each test and all recovered electronic data are included in Appendix B. The data for each dynamic test are referenced to a common zero time and are displayed with time in milliseconds as the abscissa. The data for each static test are displayed with reference pressure as the ordinate.

Data recovery was good for all the tests. In the lower-pressure (<100 psi) dynamic tests there is considerable scatter in the airblast pressure data and some disagreement between airblast pressure and soil stress data. The pressure level presented in this chapter for each dynamic test is given as the average simulation based on the average of all recovered airblast pressure records. This average simulation appears to be low for Tests D3, D3A, and D3B when the soil stress records are considered. Tape machine head alignment was corrected after the first three tests, and the consistency of the data improved on the remaining dynamic tests.

Table 5.1. Weapon simulations.

The average weapon yield and peak overpressure were determined by fitting the average overpressure-time history for each test.

Test	Gage	Weapon Yield, KT	Peak Overpressure psi
D1	BP2	8	122
	BP3	7	117
	BP6	25	142
	Average	12	127
D2	BP1	26	134
	BP4	7	124
	Average	14	129
D3	BP1	145,325	20
	BP3	122	61
	BP4	14,821	23
	Average	299	34
D3A	BP1	143,539	58
	BP3	363	100
	BP4	78	30
	Average	343	62
D3B	BP1	6,351	69
	BP2	97,164,071	28
	BP3	337	114
	B94	25	37
	Average	9,920	60
D3C	BP1	17	130
	BP2	12	118
	BP3	39	153
	BP4	10	116
	Average	18	129
D4	BP1	18	128
	BP2	23	140
	BP3	25	173
D4 Continued	BP4	8	126
	Average	18	142
D5	BP1	104	137
	BP2	94	155
	BP3	109	193
	BP4	17	138
	BP6	125	168
	Average	77	158
D6	BP1	35	135
	BP2	59	146
	BP3	18	164
	BP4	6	121
	Average	23	141
D7	BP1	73	154
	BP2	55	140
	BP3	51	161
	BP4	12	118
	BP6	1,097	99
	Average	58	134
Multi-hit	BP2	33	143
	BP3	11	157
	BP4	11	139
	BP6	15	98
	Average	16	134
D8	BP2	6	125
	BP3	4	132
	BP4	5	139
	BP6	7	143
	Average	6	134

Table 5.2. Dynamic test results: midspan deflection.

The accuracy of response measurements is to the nearest 1/32 in, and measurements were made at midspan at mid-width of the roof slab.

Test	Element	Maximum Response in	Rebound in	Permanent Deflection in	Total Permanent Deflection in
D1	D1	0.56	0.31	0.25 (S1)	0.25
		0.37	0.25	0.12 (S2)	0.12
D2	D2	Collapse	0	Collapse	Collapse
D3	D3	0.06	0	0.06	0.06
D3A	D3	0.19	0.12	0.07	0.13
D3B	D3	0.31	0.28	0.03	0.16
D3C	D3	0.65	0.31	0.34	0.50
D4	D4	0.72	0.22	0.50	0.50
D5	D5	1.22	0.34	0.88	0.88
D6	D6	1.00	0.31	0.69	0.69
D7	D7	1.04	0.38	0.66	0.66
Multi-hit	D3	0.50	0.19	0.31	0.81
	D4	0.57	0.38	0.19	0.69
	D5	Scratch gage broken		0.19	1.07
	D6	0.38	0	0.38	1.07
	D7	Collapse	0	Collapse	Collapse
D8	D8	No scratch gage		0.50	0.50
	D4	0.75	0.44	0.31	1.00
	D6	5.81	0	5.81	6.88

Table 5.3. Dynamic test roof-to-wall joint rotations.

Test	Element	θ_E [a]	θ_W [b]
D1	D1	c	c
D2	D2	Collapse	Collapse
D3	D3	c	c
D3A	D3	c	c
D3B	D3	c	c
D3C	D3	0.032	0.042
D4	D4	0.041	0.031
D5	D5	0.050	0.031
D6	D6	0.042	0.052
D7	D7	0.032	0.042
Multi-hit	D3	0.050	0.039
	D4	0.055	0.039
	D5	0.050	0.033
	D6	0.042	0.055
	D7	Collapse	Collapse
D8	D8	0.021	0.027
	D4	0.027	0.043
	D6	0.333	0.361

[a] θ_E is the roof rotation at the top of the east wall in radians.
[b] θ_W is the roof rotation at the top of the west wall in radians.

[c] Rotations could not be measured on Test D1 and were not measured on Tests D3, D3A, and D3C since deflections were small.

Table 5.4. Comparison of static ultimate capacities.

Test	Ultimate Capacity, psi	Comments [a]
S1	100[b]	Type 1 element
S3	44	Surface flush
S4	185	Baseline test
S5	96	Red clayey sand backfill
S6	164	Low-strength concrete
S7	81	Clayey sand with gravel backfill

[a]Unless noted, the element type was 2, the backfill was flume sand, the concrete strength was 4,000 psi (28-day mix design), and the DOB was 1 foot.
[b]Ultimate capacity limited by failure of interior structural steel support.

Table 5.5. Static load-deflection behavior.

Test	Δ_A in	P_A psi	Δ_B in	P_B psi	Δ_C in	P_C psi	Δ_D in	P_D psi
S1[a]	0.5	100	--	--	--	--	--	--
S3	0.5	44	2.0	17	3	17	4.5	21
S4	0.7	185	2.3	65	2.3	65	4.5	85
S5[b]	1.2	96	1.6	70	2.3	68	--	--
S6	0.7	164	1.6	80	2.4	60	4.6	90
S7	1.4	81	2.0	68	3.5	70	4.5	80

[a]Test S1 collapsed at approximately 100 psi.
[b]Test S5 was stopped at 2.3 in of deflection when no increase in capacity in the tensile membrane region was observed.

Table 5.6. Comparison of Type 2 static test results.
Columns 4 and 5 represent average values at mid-structure length.

Test	Parameter Varied	Permanent Midspan Deflection, in	Width of Crushed Concrete, Top of Midspan, in	Width of Midspan Tensile Crack, in
S3	DOB = 0	4.5	2.1	1.0
S4	Baseline	4.4	2.5	1.3
S5	Backfill	2.3	2.9	0.8
S6	f'_c	4.4	2.5	1.4
S7	Backfill	4.4	2.2	1.0

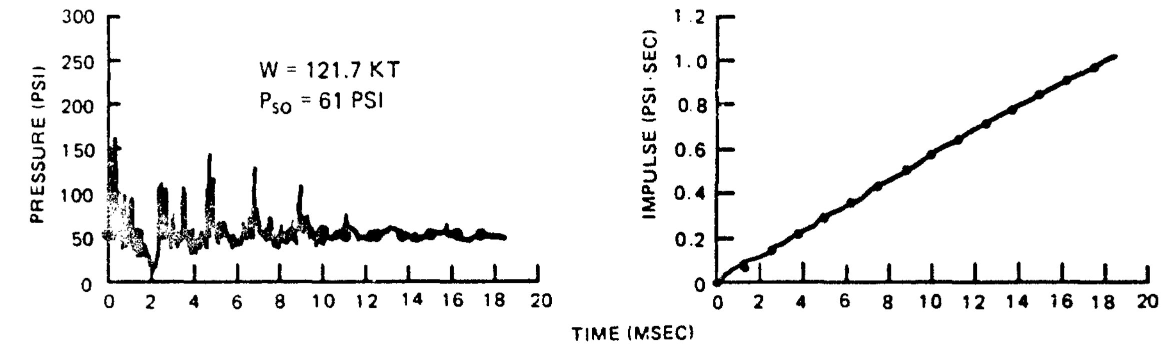

Figure 5.1. Overpressure-time, impulse-time records, and weapon fit for a low-pressure test. (Solid lines are data and dots are weapon fits.)

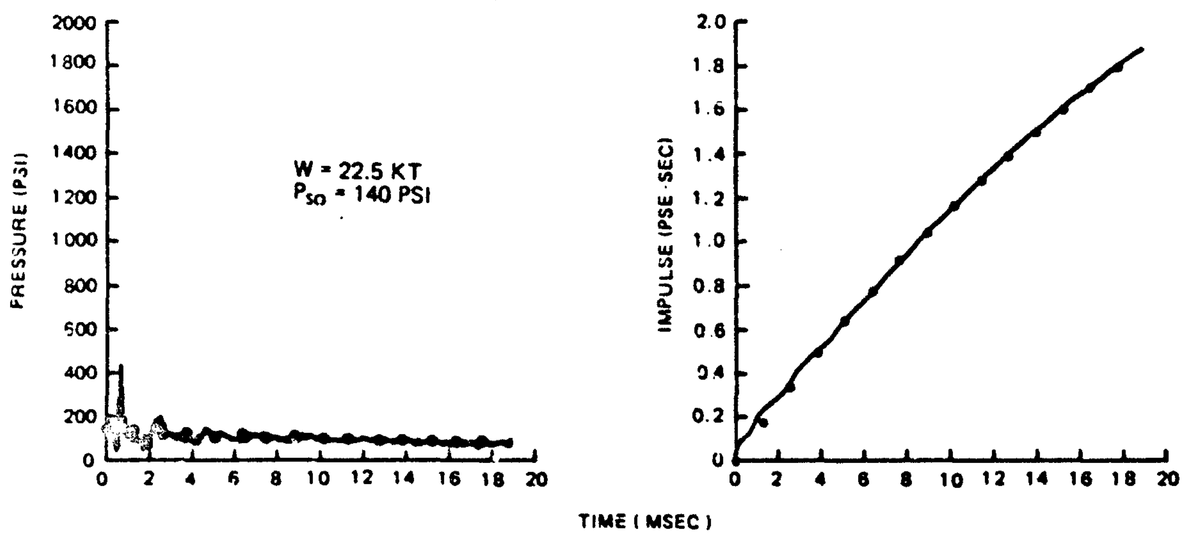

Figure 5.2. Overpressure-time, impulse-time records, and weapon fit for a high-pressure test. (Solid lines are data and dots are weapon fits.)

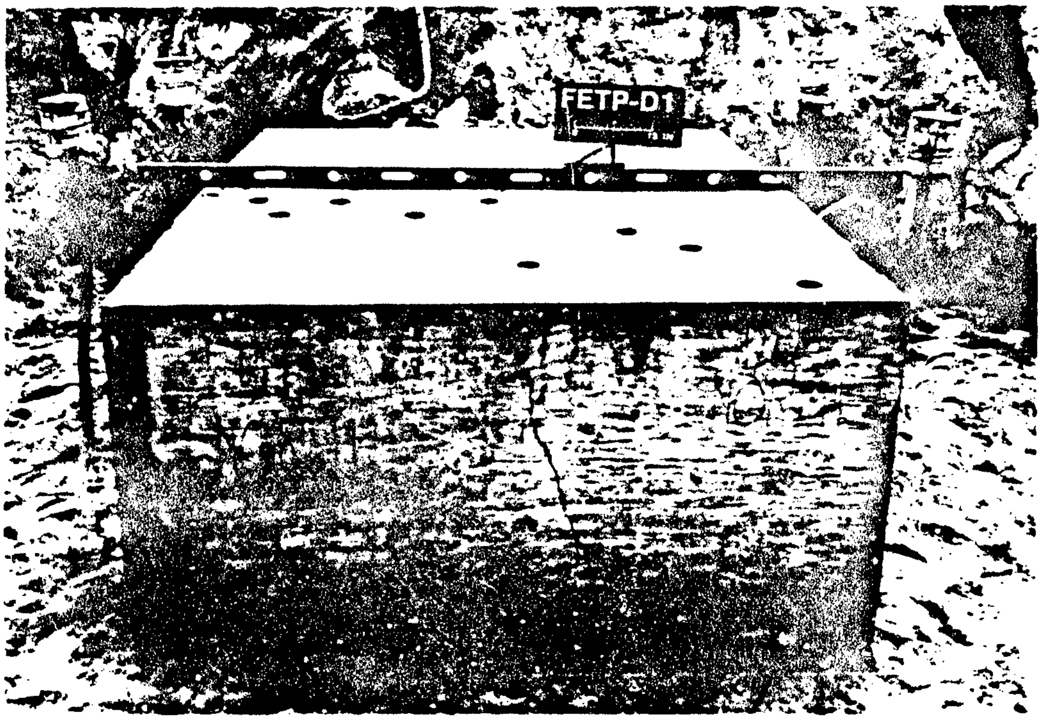

Figure 5.3. Posttest view of Type 1 element (D1).

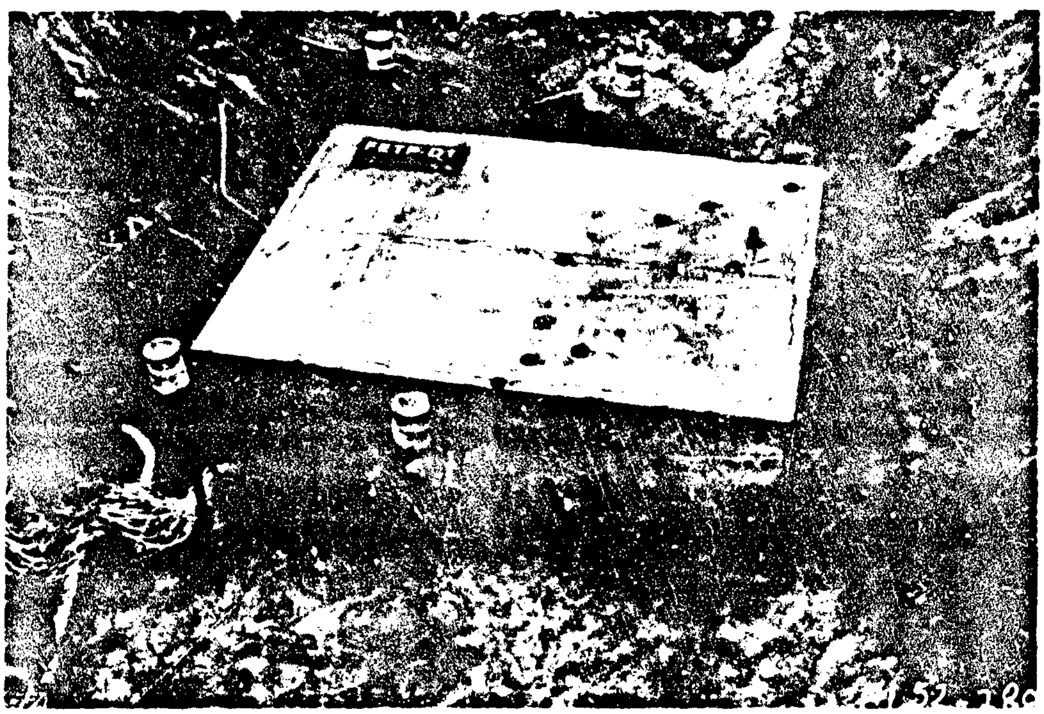

Figure 5.4. Type 1 element following Test D1.

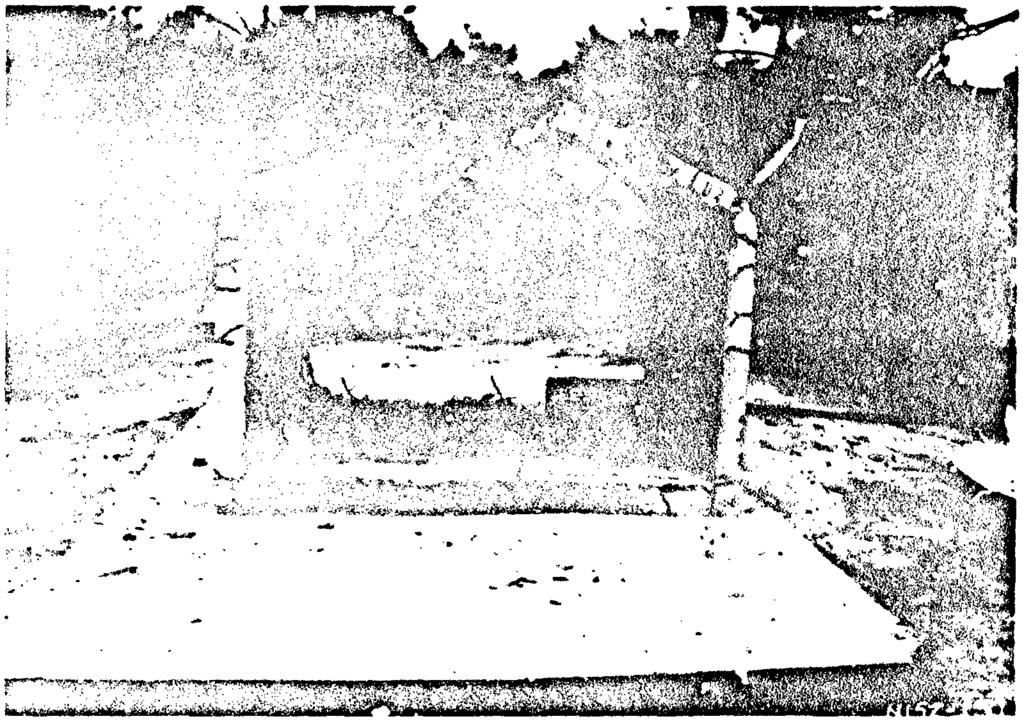

Figure 5.5. Type 2 element following Test D2.

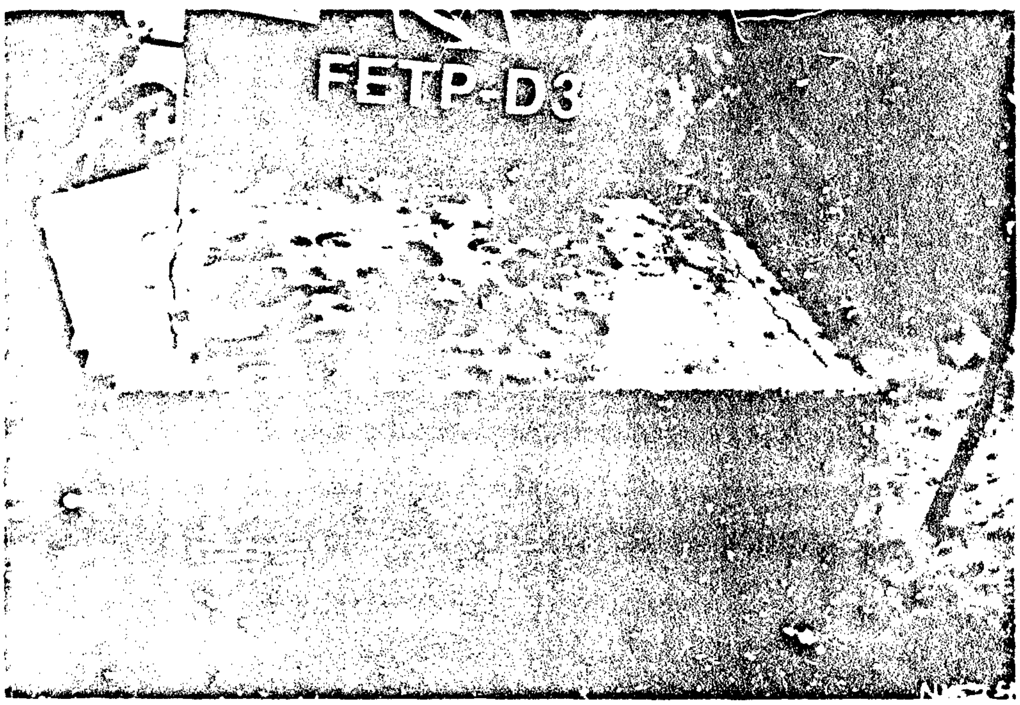

Figure 5.6. Posttest view of Test Element D3 after Test D3.

Figure 5.7. Bottom of Element D3 roof slab following Test D3.

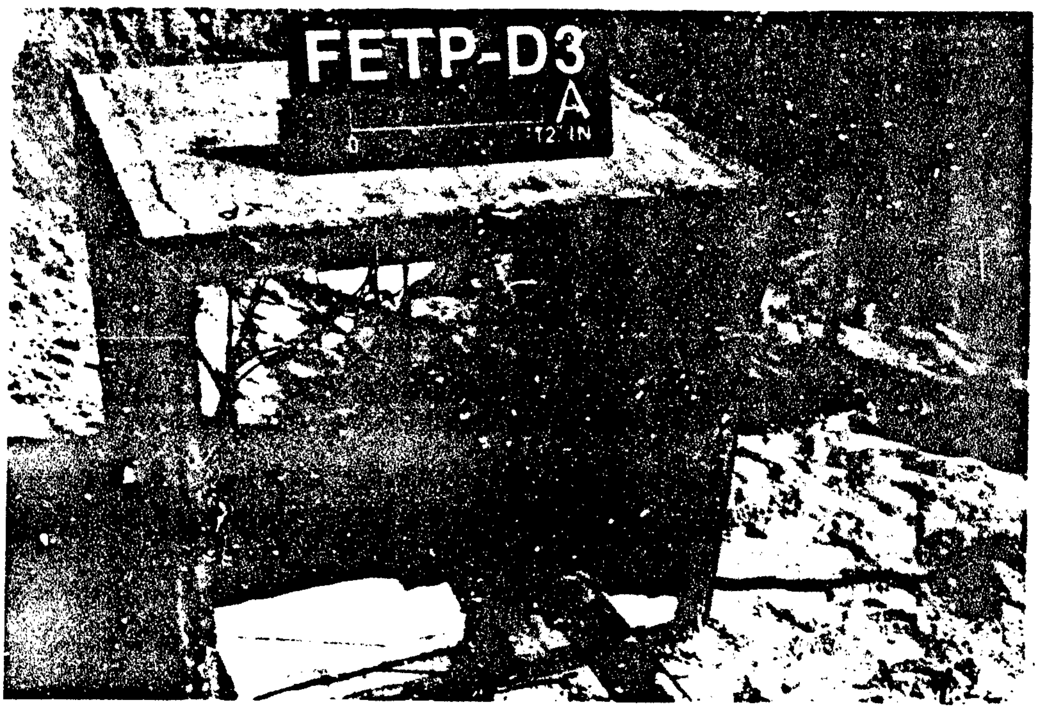

Figure 5.8. Posttest view of D3 test element after Test D3A.

Figure 5.9. Roof crack patterns, Test Element D3 following Test D3B.

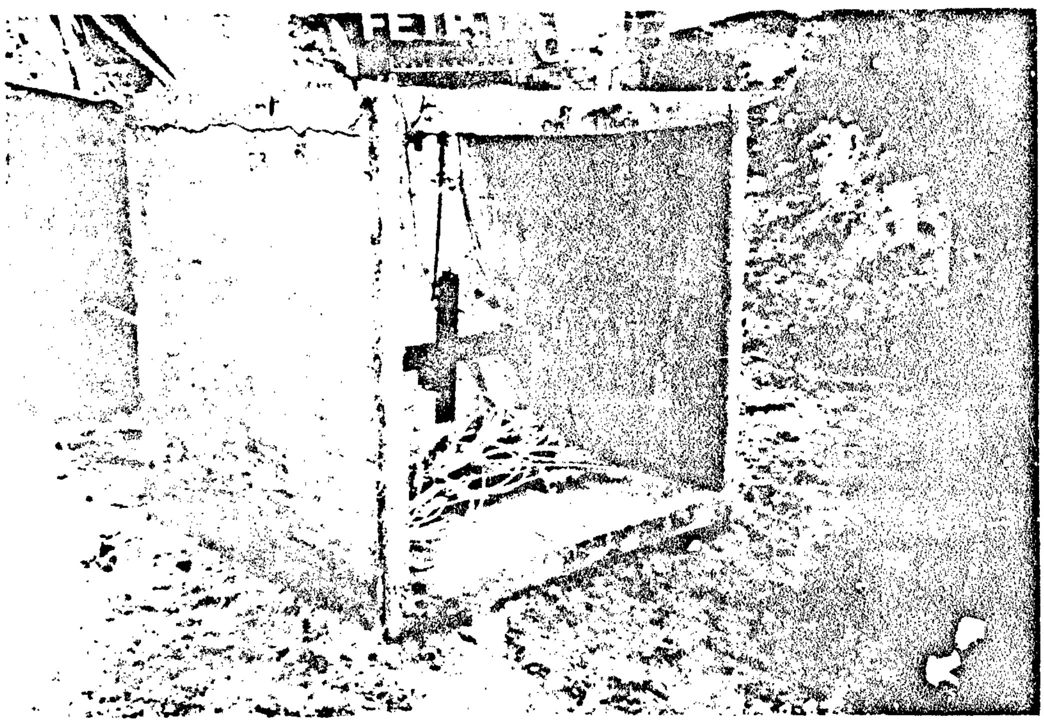

Figure 5.10. View of Test Element D3 following Test D3C.

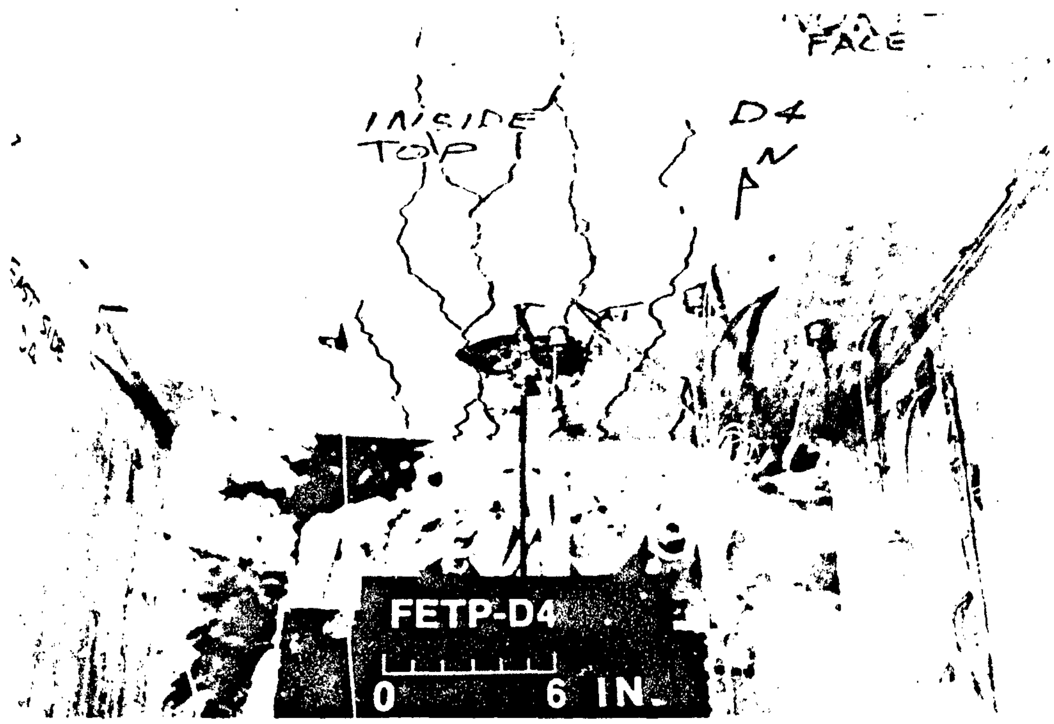

Figure 5.11. Midspan roof cracking, Test D4.

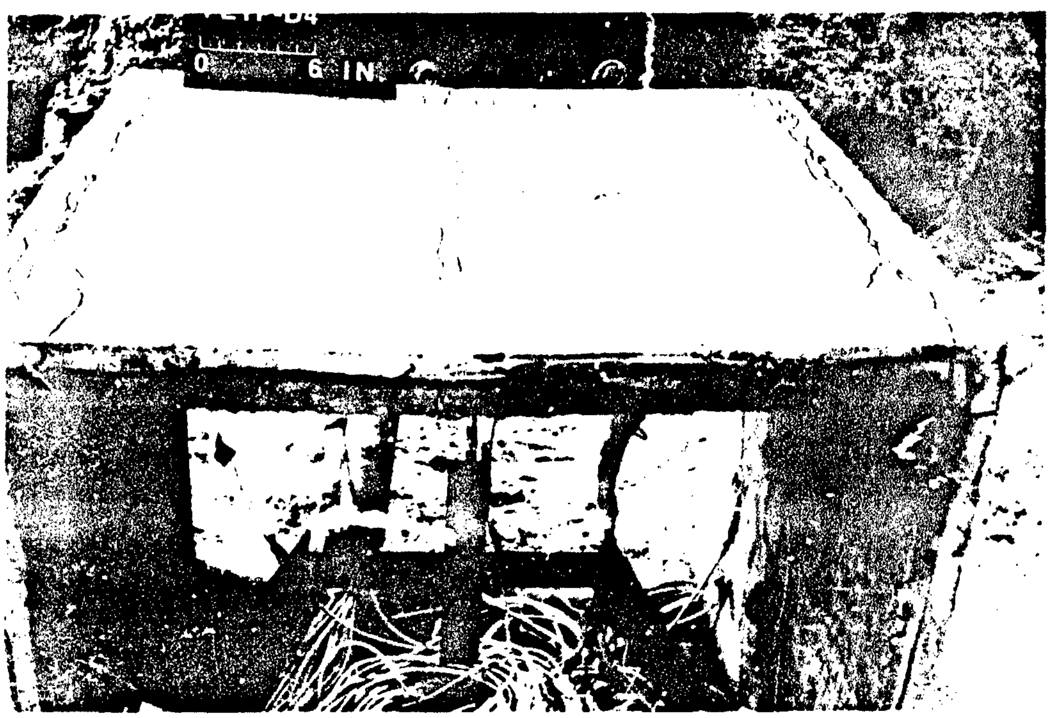

Figure 5.12. Crushing of concrete, Element D4 midspan.

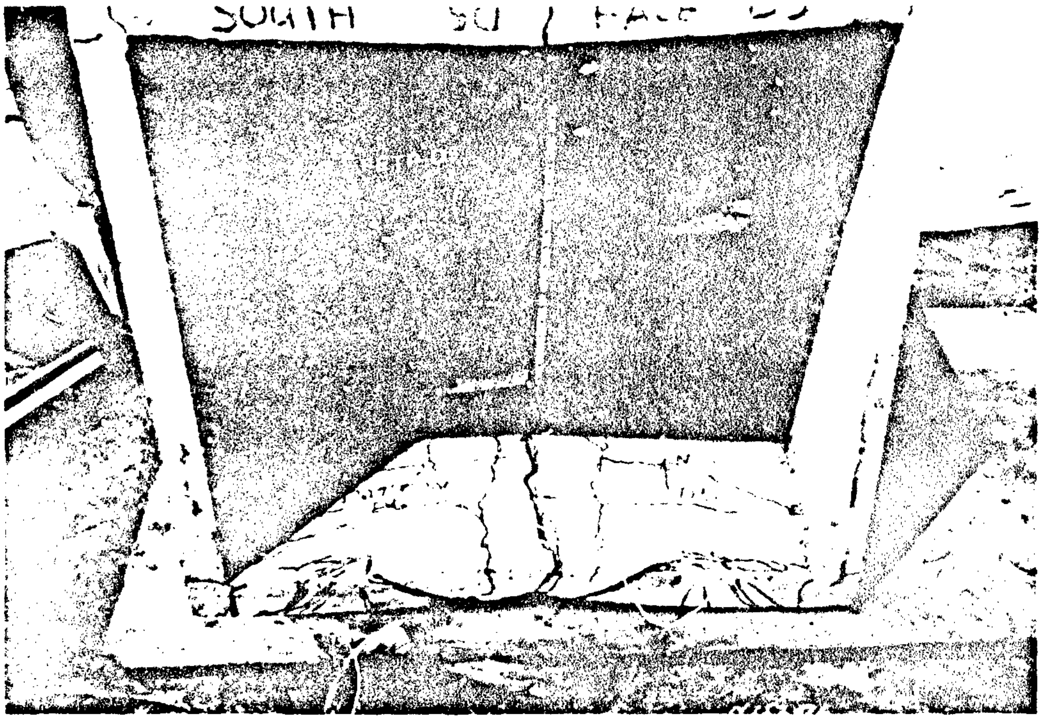

Figure 5.13. Posttest view of Test Element D5.

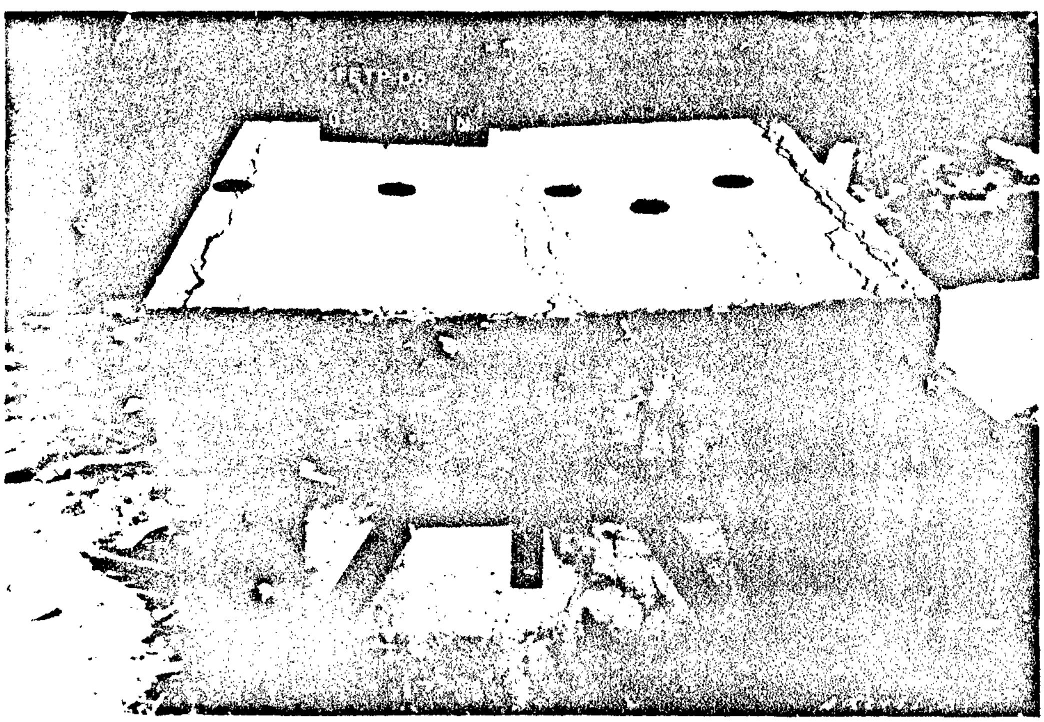

Figure 5.14. Posttest view of Test Element D6.

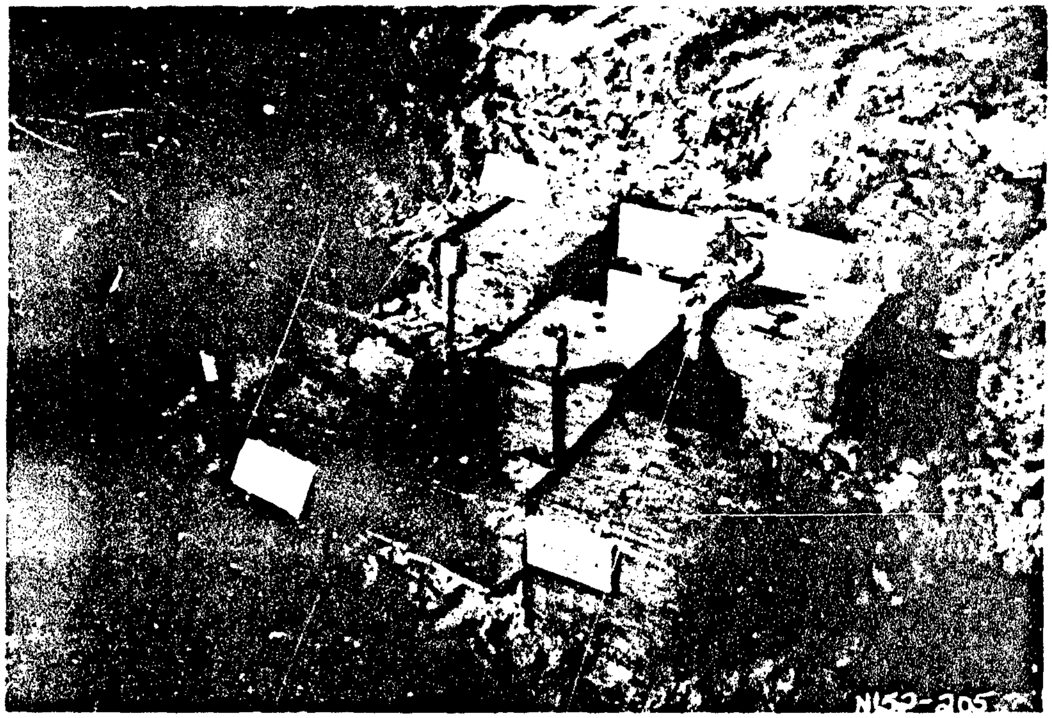

Figure 5.15. Posttest view of multi-hit test.

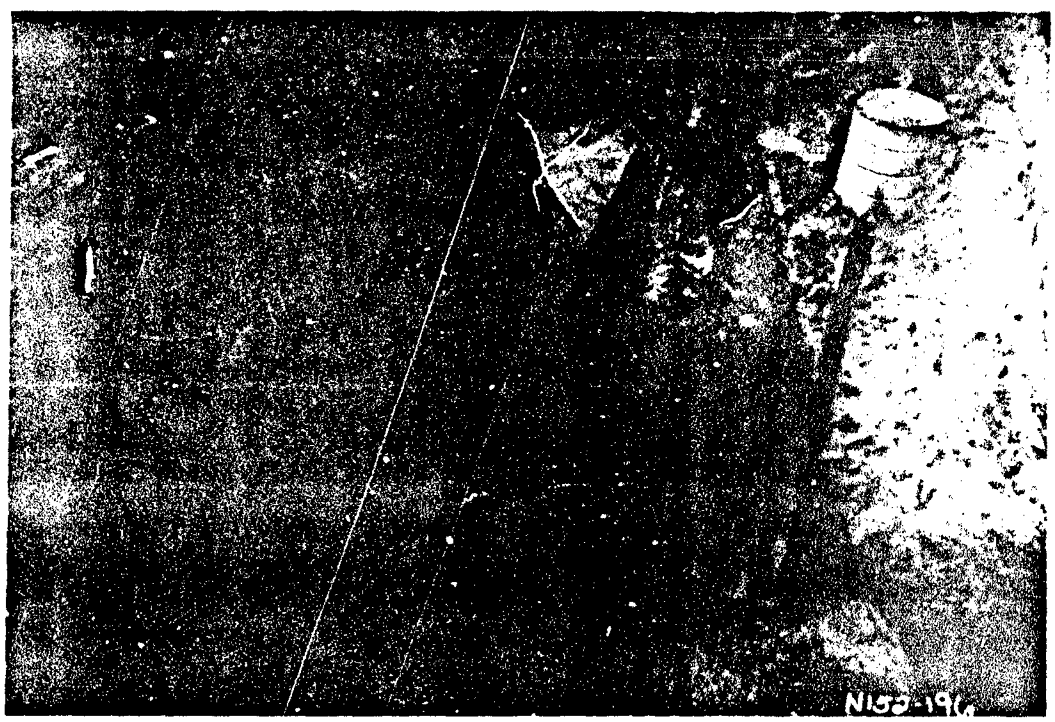

Figure 5.16. Test Element D7 following multi-hit test.

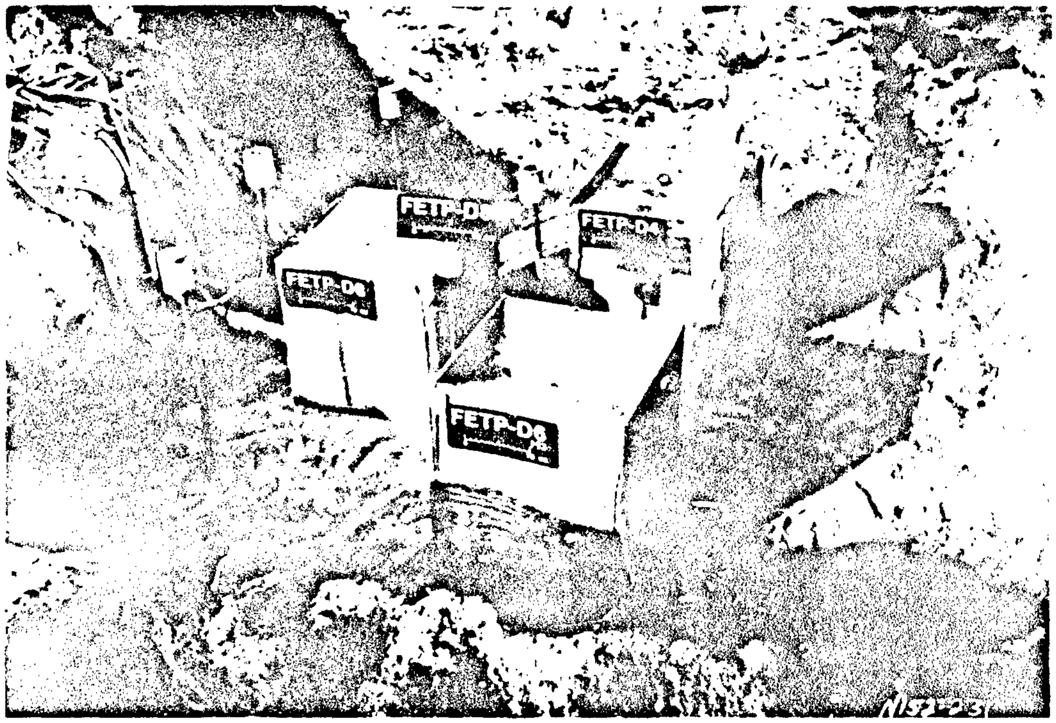

Figure 5.17. Posttest view, Test D8.

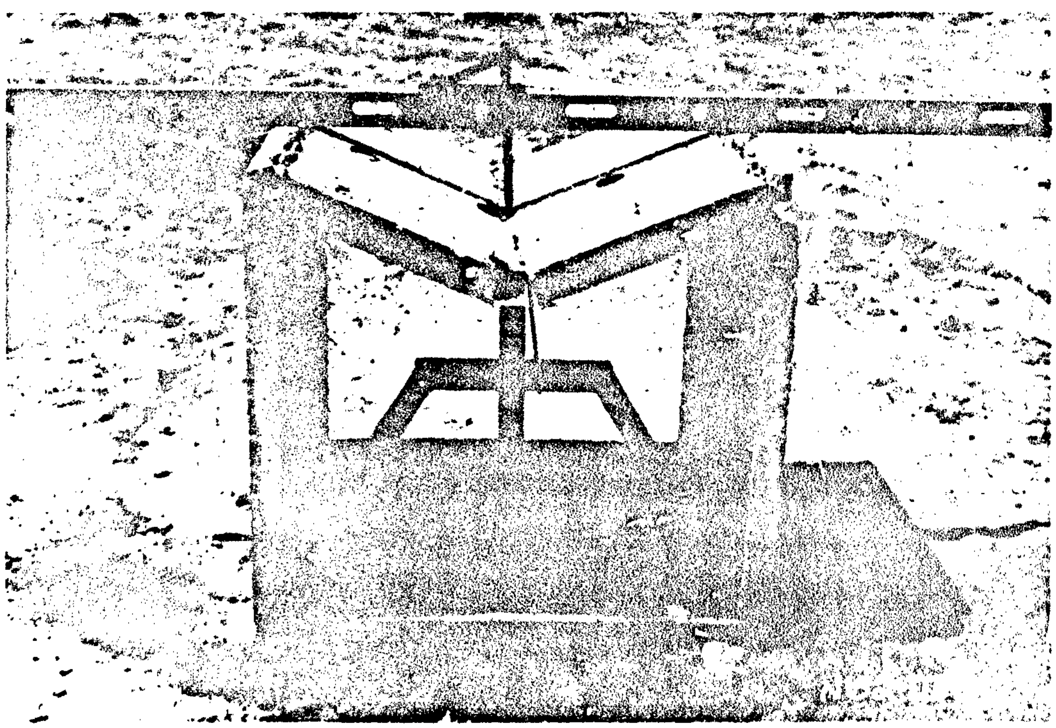

Figure 5.18. Test Element D6 following Test D8.

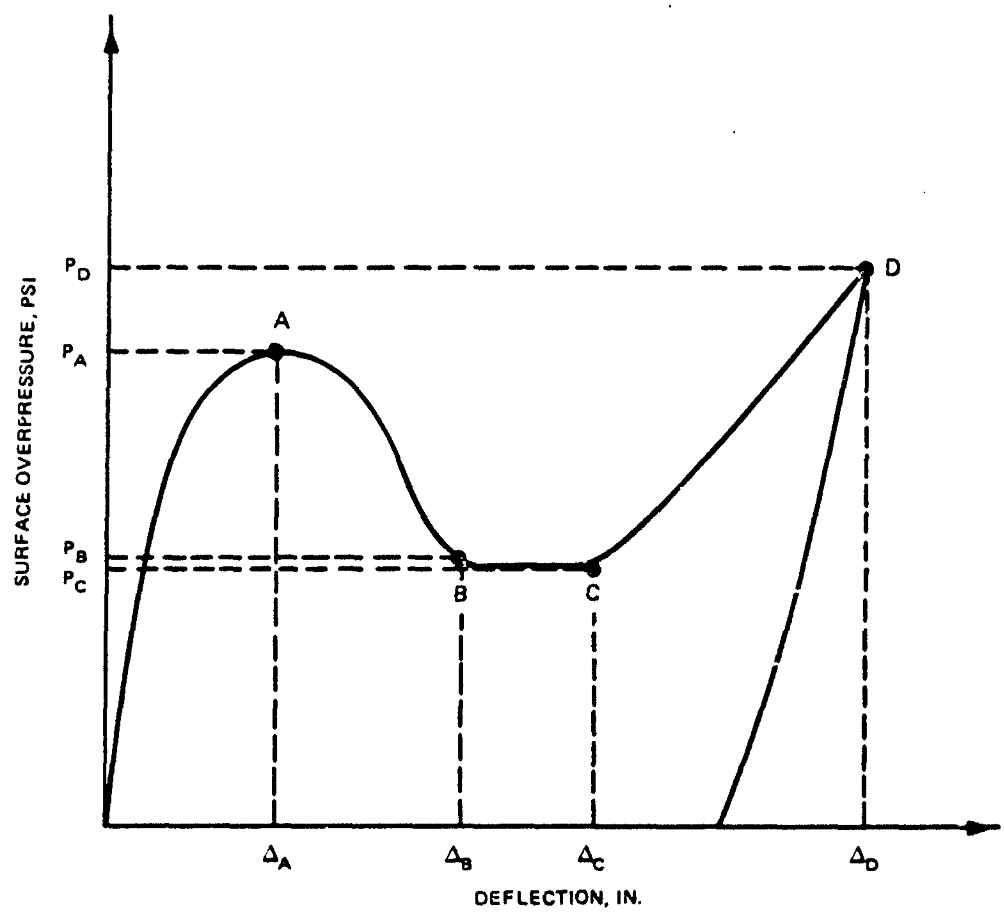

Figure 5.19. Expected load-deflection behavior for static tests.

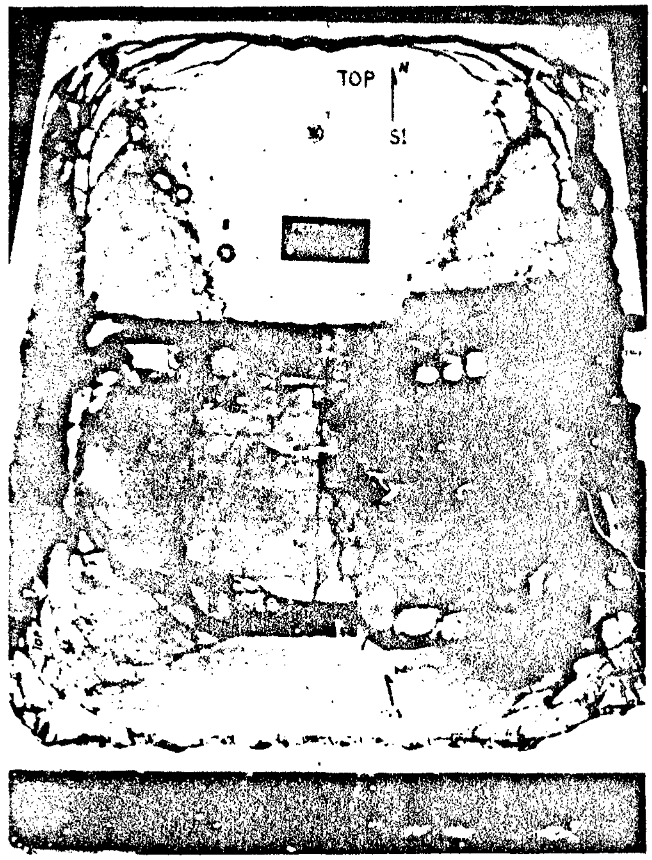

Figure 5.20. Overhead view of test element following Test S1.

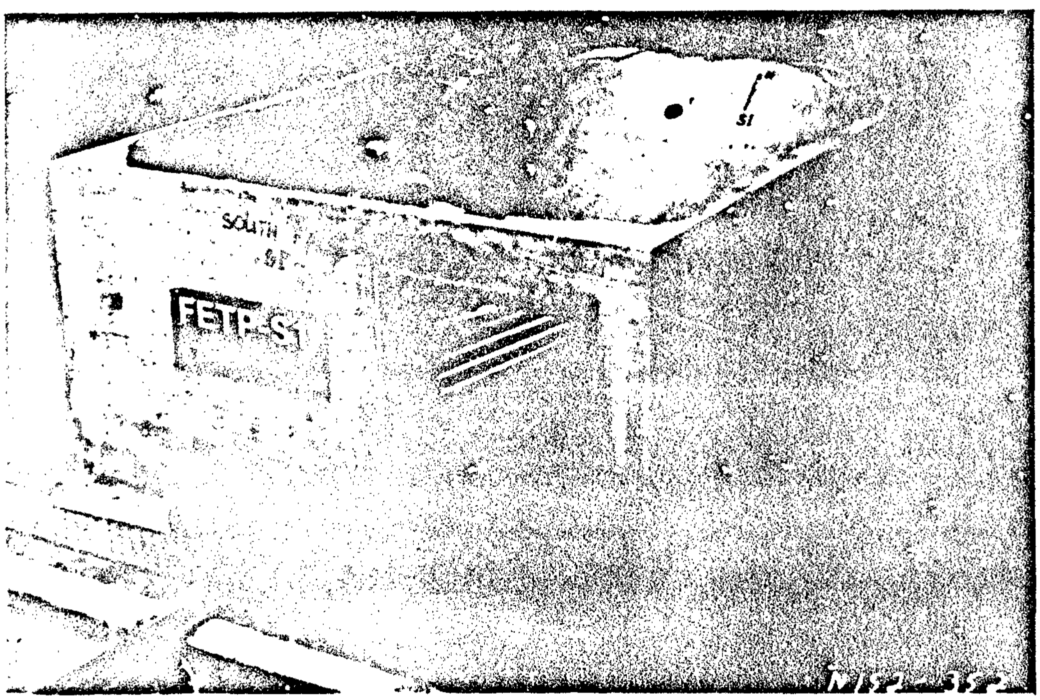

Figure 5.21. Posttest view of Test Element S1.

Figure 5.22. Interior structural steel columns following Test S1.

Figure 5.23. Roof girder following Test S1.

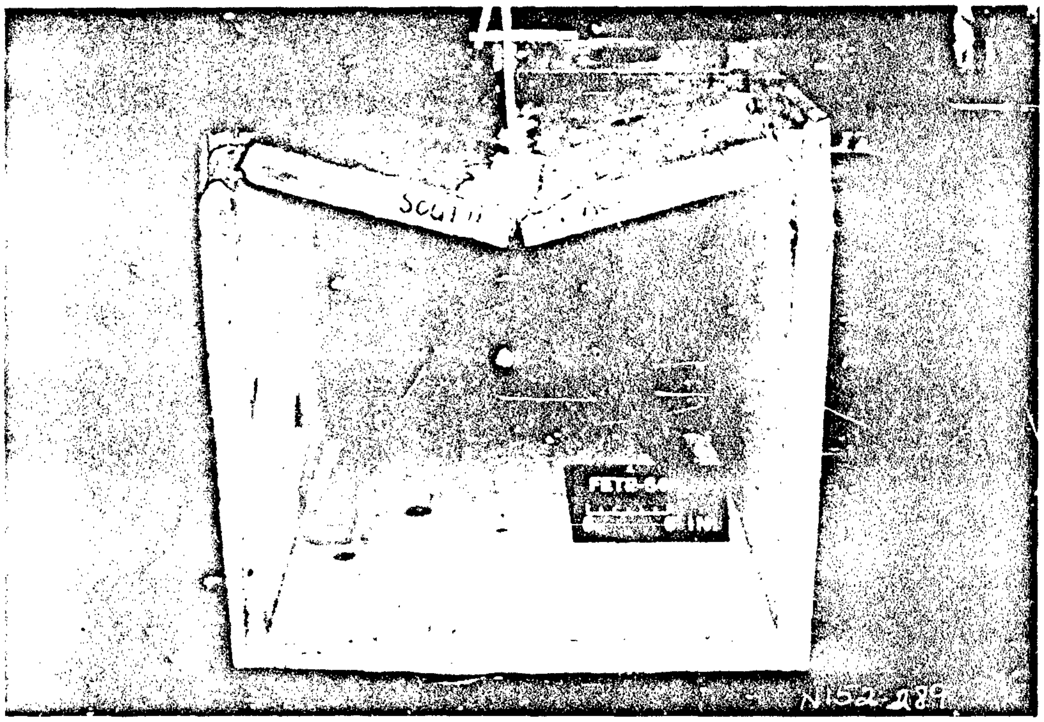

Figure 5.24. Posttest view of Type 2 element (S4).

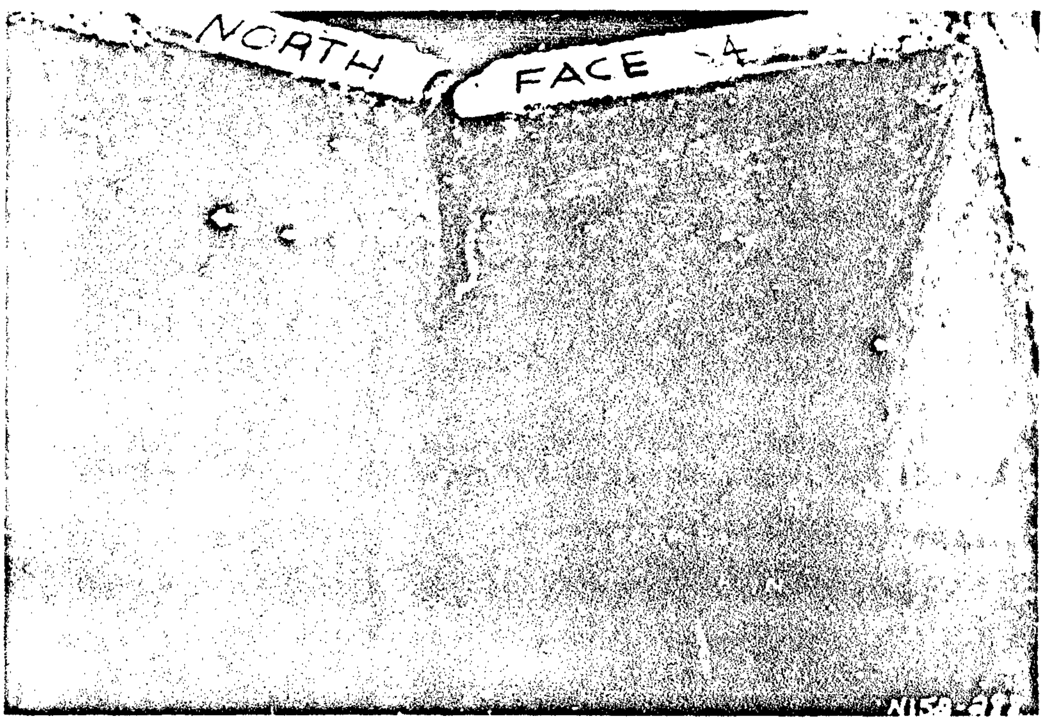

Figure 5.25. Closeup view of test element following Test S4.

CHAPTER 6

ANALYSIS

Chapter 6 includes analysis of the dynamic test data for attenuation factors, reflection factors, soil arching, loading wave velocity and lateral pressure coefficients. Also included are structural response calculations using the VSBS6 code (Reference 1), in-structure shock calculations, and an analysis of the static load-deflection behavior. Nuclear weapon simulations for each dynamic test are included in Chapter 5.

6.1 ANALYSIS OF FREE-FIELD AND STRUCTURE LOADING DATA

6.1.1 Loading Wave Velocity

Loading wave velocities (C_L) were determined from airblast and soil stress data from the dynamic tests. As described in Chapter 4, airblast pressure and soil stress measurements were made in each test. Using the loading wave arrival times for airblast pressure gages at the ground surface and soil stress gages (at depths ranging from 6 inches from the ground surface to the level of the structure floor) in line with the airblast pressure gages and perpendicular with the direction of detonation of the HEST cavity, loading wave velocities were calculated. Table 6.1 summarizes average loading wave velocities for each test. In the tests in sand backfill the loading wave velocities varied from 1,025 to 1,455 ft/s with the average being 1,269 ft/s. In the red clayey sand backfill (Test D5) the loading wave velocity was 1,309 ft/s. In the clayey sand with gravel (Test D7) the loading wave velocity was 1,111 ft/s. There was no significant difference in loading wave velocity due to backfill type. Structural response calculations should be made using a loading wave velocity of about 1,200 ft/s.

6.1.2 Lateral Soil Pressure Coefficient

The lateral soil pressure coefficient (K_o) is defined as the ratio of horizontal to vertical soil pressures. The importance of this coefficient is that the wall loading is determined by this coefficient and the magnitude of the vertical stress. From the wall loading, the externally applied in-plane thrust on the roof slab is determined, which influences the load-bearing capacity of the roof.

Table 6.1 lists the experimentally determined lateral soil pressure coefficients. They were determined using vertical and horizontal soil stress measurements in the dynamic tests. In the tests in sand backfill, K_o ranged from 0.43 to 0.67, with the average being 0.50. In the test in red clayey sand (D5) K_o was 0.50, and in the test in clayey sand with gravel (D7), K_o was 0.51. For analysis it is suggested that K_o be taken as 0.50.

6.1.3 Reflection Factor

The loads on the roof of a buried structure are increased initially due to reflection of the loading wave. This reflection increases the peak stress but the amplitude of this reflected stress decreases rapidly due to tensile wave reflections from the concrete-air interface at the bottom of the roof slab and/or from wave interactions with the free soil surface. Therefore, the duration of the reflected stress spike is a function of the roof thickness, compression wave speed in the roof (10,000 ft/s for concrete), the backfill material properties, loading wave velocity in the backfill, and the DOB.

Experimentally determined reflection factors based on free-field stress measurements at the roof level and interface stress measurements at the roof-soil boundary are presented in Table 6.1, along with observed reflected stress durations. In the tests in sand, the stress reflection factor ranged from 1.33 to 2.26, with an average of 1.51. The duration of the reflected spike ranged from 0.80 to 1.30 ms with an average of 0.97. In the test in the red clayey sand backfill (D5) the reflection factor was 1.33 with a duration of 1.63 ms. In the test in clayey sand with gravel backfill (D7) the reflection factor was 1.20 with a duration of 1.55 ms. The tests in the alternate backfills (D5 and D7) appeared to have lower reflection factors and longer durations than the tests in sand. The computational procedure (VSBS6) described in Reference 1 uses a reflection factor of 1.6 and calculates a reflected spike duration of 1.10 ms. These values show reasonable agreement with the data from the tests in sand backfill.

6.1.4 Attenuation Factor

The attenuation of peak stress with increasing depth is due to both the spatial decay of the shock front and hysteretic losses in the soil. A procedure for including hysteretic effects in computing peak stress at depth is outlined in Reference 8. In this section attenuation factors will be

determined at depths of the test element roof, midheight of the wall, and top of the floor slab using the free-field soil stress data and the procedure given in Reference 8. The results of this analysis are given in Table 6.2. There is considerable scatter and inconsistency in the experimentally determined attenuation factors. This is due in part to the nuclear weapon simulator used in these tests. The air HEST charge cavity produces very large spikes in the airblast surface loading, which are not characteristic of a nuclear detonation. This spike normally does not travel very deep into the backfill, but in these tests it affected the free-field stress as deep as the roof level as shown in Table 6.2 ($\alpha_Y > 1$). In the calculation of attenuation factors shown in Table 6.2, the peak simulated blast pressure was used with free-field data. If the actual peak blast pressures were used, the attenuation factors would be about one-fifth of the values shown in Table 6.2. The attenuation factors calculated at the test structure wall midheight and floor levels are not significantly affected by the large spikes of the airblast loading.

The theoretical attenuation factors calculated by the VSBS6 code described in Reference 1 range from 0.95 to 0.99 at all elevations in the backfill. This does not agree very well with the experimentally determined factors. This does not affect the calculation of the roof loading since the theoretical attenuation factor was approximately one at the roof level, but calculation of the wall loading is affected since there was significant attenuation of the surface loading at mid-structure height and at the floor level which differs from the code prediction.

6.1.5 Soil Arching

Soil arching is defined as the ability of a soil to transfer loads from one location to another in response to a relative displacement between the locations. A system of shear stresses is the mechanism by which the loads are transferred; thus, the shear strength of the backfill is of considerable importance in determining the effects of soil arching. The other parameters that influence soil-structure interaction are the clear span of the structure, the length of the structure, and the DOB of the structure. A more detailed description of soil arching is given in Reference 1. The effects of soil arching on roof load distribution are illustrated in Figure 6.1.

Soil arching ratios (ratio of average roof stress to free-field stress at

the roof level) were determined for the dynamic tests from a comparison of roof interface pressure data and free-field soil stress data by:

1. Fitting a parabola of the form $y = a + bx^2$ to the interface pressure data at incremental time steps to define the roof pressure distribution as a function of time.

2. Integrating the parabolic definition of the roof pressure distribution across the clear span of the roof to find the total roof loading as a function of time.

3. Dividing the total roof load by the clear span to calculate an average roof stress as a function of time.

4. Calculating the arching ratio (C_A) as the ratio of average roof stress to free-field stress as a function of time.

Soil arching ratio calculations were performed for the dynamic tests using 20 and 50 ms of data. The results of this analysis are presented in Table 6.3 and are compared to theoretical soil arching calculations as developed by Kiger (Reference 1). Figure 6.2 shows a typical soil arching ratio versus time plot.

Static soil arching calculations were also performed in a similar manner as the dynamic soil arching calculations. However, instead of calculating soil arching ratios as a function of time, the soil arching ratios were calculated and plotted as a function of static surface pressure. The results of the static soil arching analysis are compared to theoretical values in Table 6.4.

Considerable scatter exists in the dynamic and static soil arching calculations. In general, the experimental arching ratios were higher than the theoretical arching ratios. In the dynamic tests in the alternate backfills, the arching ratios were lower than in the tests in sand backfill (instead of higher, as expected). Statically the trend in arching ratio behaved as expected. The data indicate that the computational model may need improvement to more accurately predict the roof loading of buried structures.

6.2 STRUCTURAL RESPONSE AND CAPACITY CALCULATIONS

6.2.1 Analysis Using VSBS6

The VSBS6 (Reference 1) computer code is a single-degree-of-freedom computational model that includes the effects of soil-structure interaction in

calculating the response of shallow-buried, flat-roofed, reinforced concrete structures to nuclear detonations. Table 6.5 compares the actual maximum midspan roof response to the VSBS6 code predictions (Column 2). The VSBS6 code predictions were much too large in every case. The major reason for this is explained by comparison of the resistance function as calculated by VSBS6 to actual static test data (see Section 6.2.2). The VSBS6 code has been used with considerable success in predicting the response of shallow-buried structures in the Defense Nuclear Agency (DNA)-sponsored Shallow-Buried Structures Program (Reference 1). These structures were tested with highly impulsive loads and pushed to large deflections. In these tests the initial portion of the resistance function is not as important in calculating the maximum response as in the FEMA tests. In the FEMA tests the loading was due to a large weapon yield simulator (the load is quasi-static) and the initial ultimate capacity was the most important part of the resistance function in the response calculation.

A modification to the resistance function was made using compressive membrane theory as described by Park and Gamble (Reference 9). Predictions were made for the dynamic tests as shown in Column 5 of Table 6.5. The predictions show much better agreement with test results. Revision of the VSBS6 code is currently in progress at WES. The revised code will include the results of a test program designed to improve the resistance function.

6.2.2 Static Load-Deflection Behavior

Figure 6.3 compares the experimental load-deflection curve to the resistance function as calculated by the VSBS6 code and the resistance function as calculated using compressive membrane theory from Reference 9. Figure 6.3 shows that VSBS6 underpredicts the ultimate capacity of the slab by 43 percent. This is due to compressive membrane effects. Compressive membrane forces are due to jamming of the slab between the boundary restraints, which causes the slab to arch from boundary to boundary. This induces a self-generated in-plane thrust which increases the moment capacities at the critical sections.

Also, the load-deflection curve for Test S3 shows no increase in load capacity at large deflections (tensile membrane region). This was due to rupture of the tension steel which prevented both layers of principal steel acting as a tensile net to resist the static load. This indicates that the

roof slab cannot resist a dynamic load from a large-yield nuclear weapon that causes a response past the deflection at ultimate capacity of the slab. In this case the roof load exceeds the roof slab resistance at large deflections, and since the resistance function is not enhanced in the tensile membrane region, roof slab collapse results. Therefore, the design deflection for the keyworker blast shelter should be limited to small deflections (no larger than 0.5d) unless reinforcement details are revised to yield an increase in capacity at large deflections.

One inconsistency in the static tests was that the ultimate capacity of Test S5 in the red clayey sand backfill was higher than Test S7 in the higher shear strength clayey sand with gravel backfill as pointed out in Chapter 5. Test S5 had an ultimate capacity of 96 psi, while Test S7 had an ultimate capacity of 81 psi. Table 6.4 shows that more soil arching took place in Test S7 than Test S5 (Ca = 0.83 for S7 versus 0.89 for S5) as expected. The difference in capacity is explained by lower concrete strength in Test S7 (4,515 psi) than in Test S5 (5,605 psi). Ignoring in-plane thrust, the moment capacity of S7 is 1,828 in-lb/in and the moment capacity for S5 is 1,949 in-lb/in. The moment capacity for Element S7 is 94 percent of that of Element S5. Part of the difference in ultimate capacity is also explained by scatter in the data.

Test S1 failed at approximately 100 psi. The expected ultimate capacity should have been at least 185 psi. The failure was due to collapse of the interior structural steel frame. The columns in the model structure should not buckle elastically and should reach approximately 71,700 pounds before plastic buckling occurs. The test data indicate column loads in excess of this amount when the roof collapsed. The column load cell data are in error at high loads since the columns were calibrated for elastic loads only. Plastic buckling of the columns is a possible failure mode for Test S1.

The other possible failure mode for Test S1 is failure of the roof girder. The allowable design moment capacity of the roof girder is 113 in-k or an average roof load of 61.5 psi. This load was exceeded during the test. Looking at strain gage data, only GT-1 indicated any significant yielding. The posttest photo of the roof girder looks like a case of lateral buckling; however, this could have occurred after a column buckled and the roof collapsed.

Since load cell 2 (middle column) recorded the highest axial load and IF6

(near LC-2) measured the highest interface pressure, it is probable that the middle column buckled leading to catastrophic failure of the roof of Element S1.

6.3 IN-STRUCTURE SHOCK AND SURVIVABILITY

6.3.1 In-structure Shock

In-structure shock is typically represented in terms of shock spectra. Shock spectra are plots of the maximum responses (in terms of displacement, velocity, acceleration, etc.) of all possible linear oscillators with a specified amount of damping to a given input base acceleration-time history. Predictions of shock spectra for the prototype shelter were made by Applied Research Associates, Inc. (Reference 10). Figure 6.4 is the predicted vertical shock spectra for the prototype shelter due to a 1-MT surface burst at 50 psi peak overpressure.

Vertical shock spectra were generated from acceleration data recovered in the dynamic tests (approximately 1/4-scale) using a computer code developed at WES. These spectra were scaled up to the prototype shelter and were calculated using damping of 0, 5, and 10 percent of critical. A comparison of the experimentally determined shock spectra with the predicted shock spectra shows that maximum values of displacement, velocity, and acceleration are less than predicted. Shock spectra for the other tests are presented in Reference 10. Reference 11 also states that shock levels were slightly higher in the two clayey sand backfills than in the flume sand backfills. Figure 6.4 compares the predicted shock spectra as described above with experimentally determined shock spectra from tests near the design overpressure of 50 psi.

6.3.2 Survivability

Figure 6.4 represents vertical shock spectra for the prototype keyworker blast shelter at peak overpressures approximately equal to the design overpressure. These shock spectra can be used to determine if shock isolation is needed for a given piece of equipment, provided fragility curves or shock resistances for the equipment are known. Alternatively, these shock spectra can be used to write shock resistance specifications that equipment must be able to withstand. Figure 6.5 compares experimentally determined shock spectra for Tests D1 and D3 with safe response spectra for typical floor-mounted equipment

from Reference 12. Reference 12 also contains safe response spectra for other equipment that may be of interest. Figure 6.5 shows that motor generators and communication equipment may need to be shock isolated to survive.

References 13 and 14 discuss human shock tolerance. The effects of shock on personnel inside the structure depend on the magnitude, duration, frequency, and direction of the motion. Also, the position of the man at the time of shock influences its effect. References 13 and 14 conclude that a standing man will receive compressive injuries in the body-supporting bones if the upward floor acceleration exceeds 20 g's during a long-duration loading. The injury threshold increases as the duration of the load decreases. Reference 13 recommends using a maximum design acceleration of 10 g's at frequencies at or below man's resonant frequency in the standing position (10 Hz). Experimentally determined shock spectra show that, at the shelter design overpressure, no injury would occur. Since floor displacements in these tests were downward and relatively small, no compressive injury would be expected in these tests even at the 150-psi overpressure level. Since human shock tolerance is higher in the seated and prone positions than in the standing position, the probability of injury decreases.

Impact injuries occur at much lower accelerations than compressive bone fractures. Generally, impact injuries may occur at accelerations of 0.5 to 1 g for an unrestrained man in the standing or seated positions. These injuries are the results of falling and hitting the floor or other objects. Impact injuries may be reduced by padding or restraining to prevent movement.

6.3.3 Conclusions and Recommendations Based on In-structure Shock

Based on the results of 1/4-scale dynamic testing, in-structure shock in the keyworker blast shelter is within acceptable limits for occupants. Impact injuries might be a problem but can be eliminated by padding impact surfaces or restraining personnel to prevent falls. It is recommended that typical blast-shelter equipment such as generators and communication equipment be shock isolated to insure survivability.

Table 6.1. Experimentally determined loading wave velocities, lateral soil pressure coefficients, roof reflection factors, and reflected stress durations.

Test	C_L , ft/s	K_o	R	t_d , ms
D1	1,455	0.47	2.26	0.80
D2	1,200	0.67	--	--
D3	1,025	0.44	1.33	0.92
D3A	1,176	0.52	1.81	0.98
D3B	1,143	0.46	1.89	1.15
D3C	1,369	0.45	1.46	1.30
D4	1,300	0.52	1.69	1.25
D5	1,309	0.50	1.33	1.63
D6	1,333	0.52	1.40	1.30
D7	1,111	0.51	1.20	1.55
D8	1,417	0.43	1.75	1.00

Table 6.2. Experimental attenuation factors.

α_r = attentuation factor at roof level; α_m = attenuation factor at mid-structure height; and α_f = attenuation factor at floor level.

Test	α_r	α_m	α_f
D1	1.31	--	0.65
D2	--	1.05	0.89
D3	1.41	0.90	0.85
D3A	1.04	0.74	0.54
D3B	1.14	0.88	0.68
D3C	1.18	0.67	0.51
D4	1.13	0.60	0.52
D5	0.88	0.52	--
D6	0.85	0.56	0.58
D7	0.78	0.42	--
D8	0.99	--	0.93

Table 6.3. Dynamic soil arching.

Test	Experimental[a] C_a (20 ms)	Experimental[a] C_a (50 ms)	Theoretical[b] C_a	Percent Error[c] E_1	Percent Error[c] E_2
D1	0.71	0.58	0.59	16.9	1.7
D3	0.77	0.73	0.62	19.5	15.1
D3A	0.88	0.76	0.62	29.5	18.4
D3B	0.81	0.75	0.62	23.5	17.3
D3C	0.58	0.54	0.62	6.9	14.8
D4	0.70	0.68	0.62	11.4	8.8
D5	0.57	0.58	0.76	33.3	31.0
D6	0.84	0.68	0.62	26.2	8.8
D7	0.67	0.75	0.73	9.0	2.7
D8	0.52	0.43	0.62	19.2	44.2
Multi-hit					
D4	0.65	0.56	0.62	4.6	10.7
D7	0.67	0.46	0.81	20.9	76.1

[a] C_a values shown are averages based on the durations shown.

[b] Theoretical C_a values calculated using a structure length of four times the clear span for one-way arching except Test D1 (actual structure length was used).

[c] E_1 uses 20 ms of data and E_2 uses 50 ms of data.

Table 6.4. Static soil arching.

C_a values shown are average values calculated from reference pressure equals zero to ultimate capacity for each test.

Test	Experimental C_a	Theoretical C_a	Percent Error
S1	0.75	0.59	21.3
S4	0.81	0.62	23.5
S5	0.89	0.76	14.6
S6	0.88	0.62	29.5
S7	0.83	0.73	12.0

Table 6.5. Comparison of actual and predicted roof response.

Test	Actual Roof Response, in	VSBS6[a] Prediction, in	Percent Error	Modified VSBS6[b] Prediction, in	Percent Error
D1	0.56	3.57	538	0.55	1.8
D2	Collapse	10.68	--	7.70	--
D3	0.06	0.12	100	0.19	217
D4	0.72	4.95	588	0.69	4.2
D5	1.22	10.20	736	3.60	195
D6	1.00	5.27	427	1.08	8.0
D7	1.04	8.17	686	2.02	94
D8	0.50[c]	3.13	526	0.60	20

[a] Predictions made with VSBS6 using Speicher-Brode definition of a nuclear overpressure.
[b] Predictions made using VSBS6 with the resistance function modified to include compressive membrane effects.
[c] Maximum deflection was not measured in Test D8. The deflection given is permanent response, which does not include rebound.

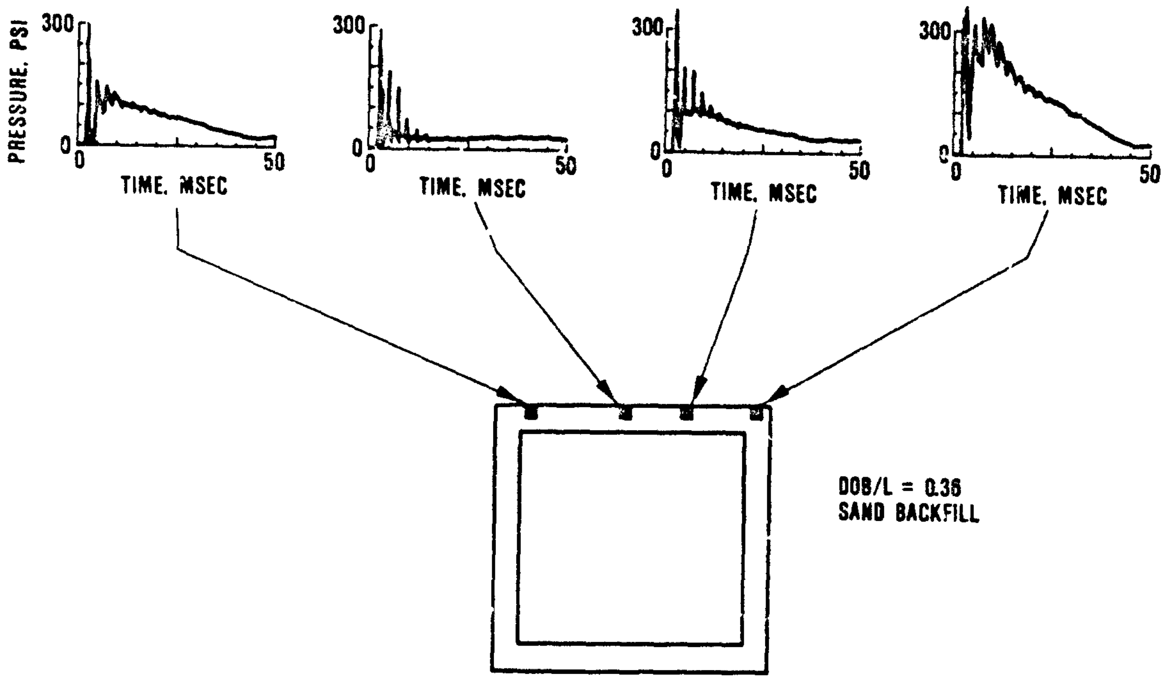

Figure 6.1. Typical dynamic test roof load distribution.

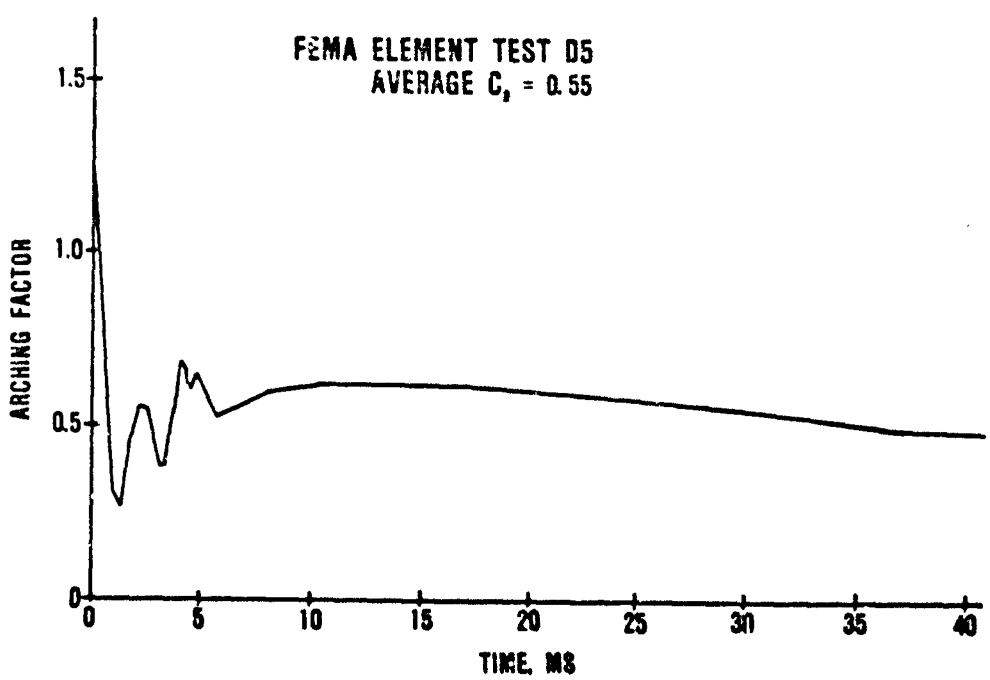

Figure 6.2. Soil arching calculated from Test D5 data.

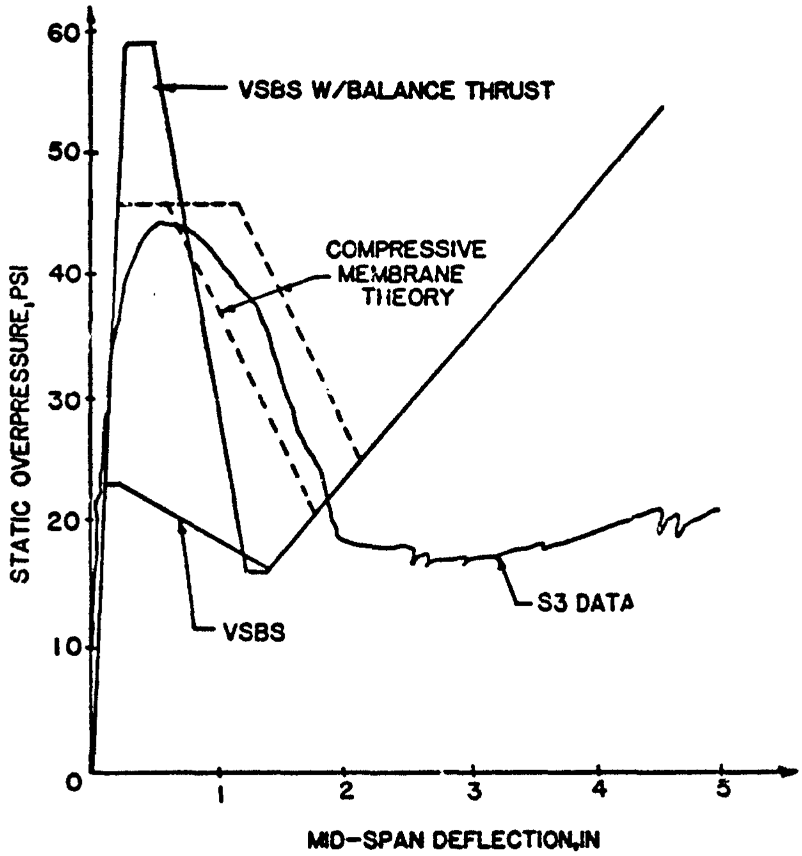

Figure 6.3. Comparison of experimental and theoretical S3 resistance functions.

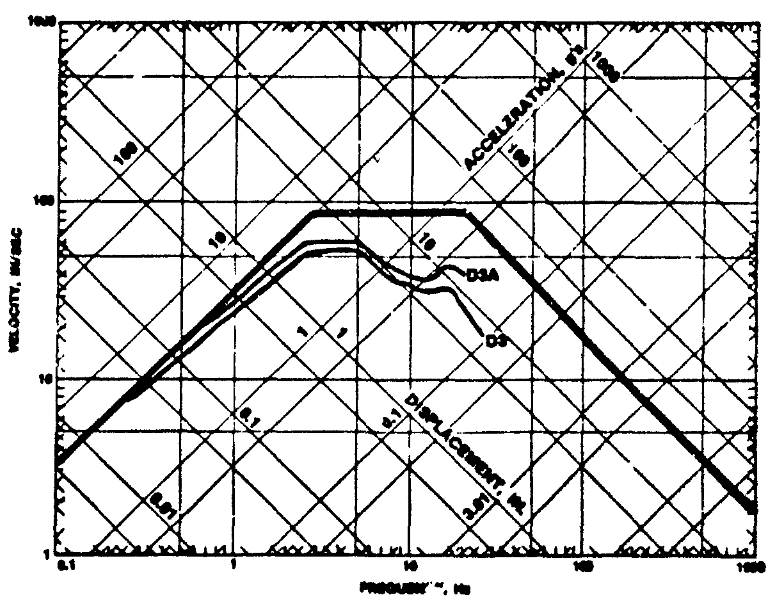

Figure 6.4. Comparison of predicted and experimental shock spectra.

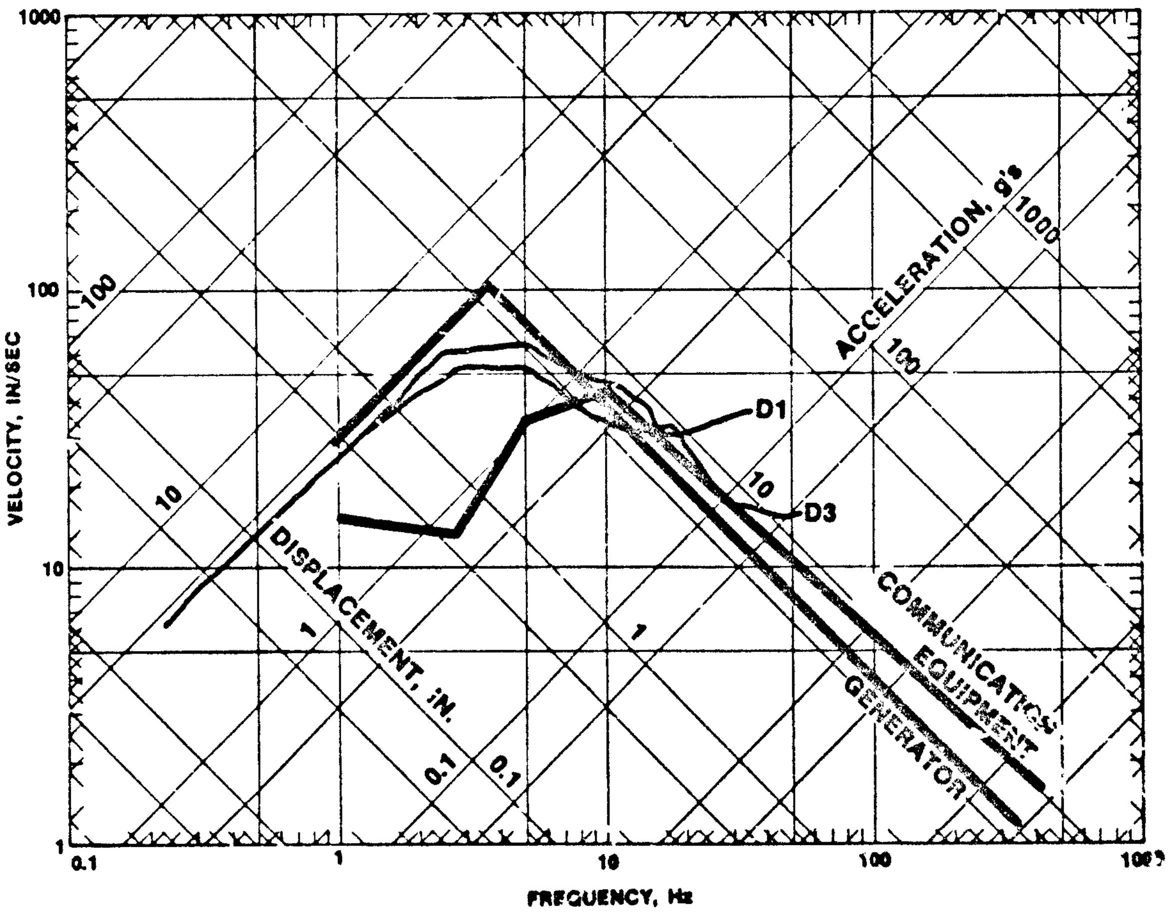

Figure 6.5. Comparison of scaled shock spectra from Tests D3 and D1 to equipment shock tolerances.

CHAPTER 7

CONCLUSIONS AND RECOMMENDATIONS

7.1 CONCLUSIONS

The structural design evaluated in these experiments will survive, with light structural damage, a peak overpressure of 150 psi from a 1-MT surface burst. It will survive, with moderate structural damage, at least three repeated loadings at a peak overpressure of 150 psi.

Shock spectra computed from floor acceleration data indicate no personnel injury will occur at peak overpressure up to 150 psi. However, some equipment may need to be isolated on pads rather than hard mounted at the higher overpressures. Maximum accelerations and relative displacements at a frequency of 10 Hz indicated by the spectra are about 8 g's and 0.5 inch at 150-psi peak overpressure. Since the initial peak motions are downward, only hard-mounted equipment is affected.

Test results in the flume sand, red clayey sand, and clayey sand with gravel backfills were very similar. However, significant floor damage occurred in the test in the red clayey sand. Backfill specifications need not be as restrictive as currently required except under the floor slab. Relaxing backfill specifications will reduce construction costs since most areas in the United States have soils that will meet the new specifications.

The structural model with low-strength concrete (compressive strength, f'_c, equal to about 3,000 psi) survived two repeated loadings at about 150 psi with approximately the same damage as the higher strength concrete element (f'_c equal to 4,500 psi). During the third loading both models survived, but the model with 3,000-psi concrete sustained much more damage than the model with 4,500-psi concrete.

For structures buried in a high-shear-strength soil backfill, active soil arching will result in pressure being transferred away from the flexible portion of the roof and onto the hard, interior support points such as walls or columns. These intense localized loads can cause a punching shear failure or buckling of column supports; thus, interior wall supports are preferred. The Type 1 structural model with an interior structural steel frame failed in the static test when the columns buckled.

All of the structural models tested responded in flexure with three

well-defined hinges, one at each support and one in the center of the roof. These very localized hinges resulted in reinforcement steel rupturing at relatively small roof deflections and little, or no, tensile membrane capacity. If the principal reinforcement steel were increased and/or repositioned it may result in the hinge patterns being less localized and a significant increase in the tensile membrane capacity that is so important for the reserve strength to resist repeated hits or significant overloads.

The static test results indicate that compressive membrane stresses are causing a significantly higher ultimate capacity than expected for the roof slabs. As a result, the VSBS6 code predictions in general overpredicted structural response for those experiments where relatively small deflection occurred (getting the correct maximum capacity was extremely important in these tests). Code predictions were much better in the experiments with relatively large roof deflection. The VSBS6 code could be improved by including the initial compressive membrane effects when calculating ultimate capacity of the roof slab.

7.2 RECOMMENDATIONS

1. Minimum compressive concrete strength requirements should be reduced from 4,000 to 3,000 psi.

2. Less restrictive backfill specifications should be adopted so that soils around and above the structure with a minimum internal friction angle (drained) of 25 degrees are acceptable. Foundation materials should have a minimum drained internal friction angle of 30 degrees to prevent excessive floor damage.

3. The minimum DOB (soil cover over the roof) should be 4 feet.

4. The possibility of modifying the placement of principal reinforcement steel to enhance tensile membrane behavior should be investigated.

5. The interior structural steel support frame should be replaced with cast-in-place or precast reinforced concrete walls.

REFERENCES

1. S. A. Kiger, T. R. Slawson, and D. W. Hyde; "Vulnerability of Shallow-Buried Flat-Roof Structures; Final Report: A Computational Procedure"; Technical Report SL-80-7, Report 6, September 1984; US Army Engineer Waterways Experiment Station, Vicksburg, Miss.

2. D. C. Kent; "Inelastic Behavior of Reinforced Concrete Members with Cyclic Loadings"; Ph. D. Thesis, 1969; University of Canterbury, Christchurch, New Zealand.

3. US Army Engineer Waterways Experiment Station; "The Unified Soil Classification System"; Technical Memorandum No. 3-357, 1953; Vicksburg, Miss.

4. G. E. Albritton; "Description, Proof Test, and Evaluation of Large Blast Load Generator Facility"; Technical Report 1707, December 1975; US Army Engineer Waterways Experiment Station, Vicksburg, Miss.

5. W. L. Huff; "Test Devices, Blast Load Generator Facility"; Miscellaneous Paper N-69-1, April 1969; US Army Engineer Waterways Experiment Station, Vicksburg, Miss.

6. S. J. Speicher and H. L. Brode; "Airblast Overpressure Analysis Expression for Burst Height, Range and Time - Over an Ideal Surface"; PSR Note 385, November 1981 (with updates through November 1982); Pacific-Sierra Research Corp., Santa Monica, Calif.

7. P. F. Mlakar and R. E. Walker; "Statistical Estimation of Simulated Yield and Overpressure"; The Shock and Vibration Bulletin, Bulletin 50, Part 2, September 1980; The Shock and Vibration Information Center, Naval Research Laboratory, Washington, DC.

8. Air Force Systems Command; "Effects of Airblast, Cratering, Ground Shock, and Radiation on Hardened Structures"; AFSCM 500-8, January 1976; Norton Air Force Base, Calif.

9. R. Park and W. L. Gamble; "Reinforced Concrete Slabs"; 1980, John Wiley and Sons, New York, N. Y.

10. Applied Research Associates, Inc.; "Multiple Burst Damage Patterns and Ground Shock Analysis of Effects on Buried Structures"; Progress Report No. 2 (Draft April 1982), Alexandria, Va.

11. T. R. Slawson, S. C. Woodson, and S. A. Kiger; "Shock Environment in a Civil Defense Blast Shelter" (In preparation); US Army Engineer Waterways Experiment Station, Vicksburg, Miss.

12. Department of the Army; "Fundamentals of Protective Design for Conventional Weapons"; TM 5-855-1, 1984; Washington, DC.

13. Boeing Aerospace Company; "Personnel and C-E Equipment Shock Tolerance"; Summary Report, 1977; Seattle, Wash.

14. Crawford, R. E. and others; "The Air Force Design Manual for Design and Analysis of Hardened Structures"; 1974; Air Force Weapons Laboratory, Kirtland Air Force Base, N. Mex.

APPENDIX A

DEVELOPMENT OF A NUCLEAR WEAPON SIMULATOR

During the period April-June 1983, six tests were conducted at Range 36, Fort Polk, La., to develop a nuclear weapon simulator for the Federal Emergency Management Agency (FEMA) Element Test Program. These tests used the High Explosive Simulation Technique (HEST) to simulate the peak overpressure and overpressure decay of a nuclear weapon detonation.

The HEST test configuration consists of a charge cavity with high explosive detonator cord uniformly distributed throughout the cavity and sand overburden placed on top of the cavity to momentarily confine the blast. The high explosive used was pentaerythrital tetranitrate made into 50-gpf detonating cord. The high explosive is detonated by a blasting cap to generate blast pressure within the charge cavity. The cavity expands, resulting in a decay in cavity pressure. The rate of pressure decay determines the simulated weapon yield for a given peak overpressure. The rate of pressure decay is a function of charge density, cavity plan area, cavity depth, overburden height, backfill material properties, and overburden material properties. The parameters varied in these tests were cavity depth (CD), overburden height (OH), HEST type (foam or air), and charge density (γ). These parameters and the results of Speicher-Brode nuclear weapon fits to the data are presented in Table A.1. Estimates of the surface-burst nuclear yield and overpressure which most closely correspond to the airblast data record were found using the principle of least squares and the Speicher-Brode definition of nuclear detonation pressure-time histories. The simulation is based on the best fit to the impulse-time history as integrated from the recovered airblast data. Figures A.1 through A.17 show the pressure-time history and impulse-time history with the nuclear weapon simulation superimposed for each test.

Table A.1. Parameters and results of Speicher-Brode nuclear weapon.

All fits are based on 20 ms of data and are fitted by least mean square on impulse. Pressure data for gages identified as average were the average of the recovered gages for each test.

						Simulation	
Test	Type	γ, lb/ft^3	CD, ft	OH, ft	Gage	W, KT	P_{so}, psi
1	Foam	0.0160	1	2	BP1	0.01	14
					BP2	0.01	18
					BP3	0.01	17
					BP4	0.01	20
					Average	0.01	17
2	Air	0.0160	1	2	BP2	0.17	135
					BP3	0.08	112
					BP4	0.18	137
					Average	0.14	128
3	Air	0.0082	1.75	2.5	BP2	1.02	100
					BP3	0.88	98
					BP4	0.85	101
					Average	0.92	100
4	Air	0.0048	3	4	BP3	92.1	62
					BP4	69.0	64
					Average	124.0	63
5	Air	0.0040	3	3	BP1	25.2	68
					BP2	4.62	63
					Average	14.9	66
6	Air	0.0032	3	3	BP2	133.5	67
					BP3	64.6	50
					BP4	20.1	52
					Average	72.7	56

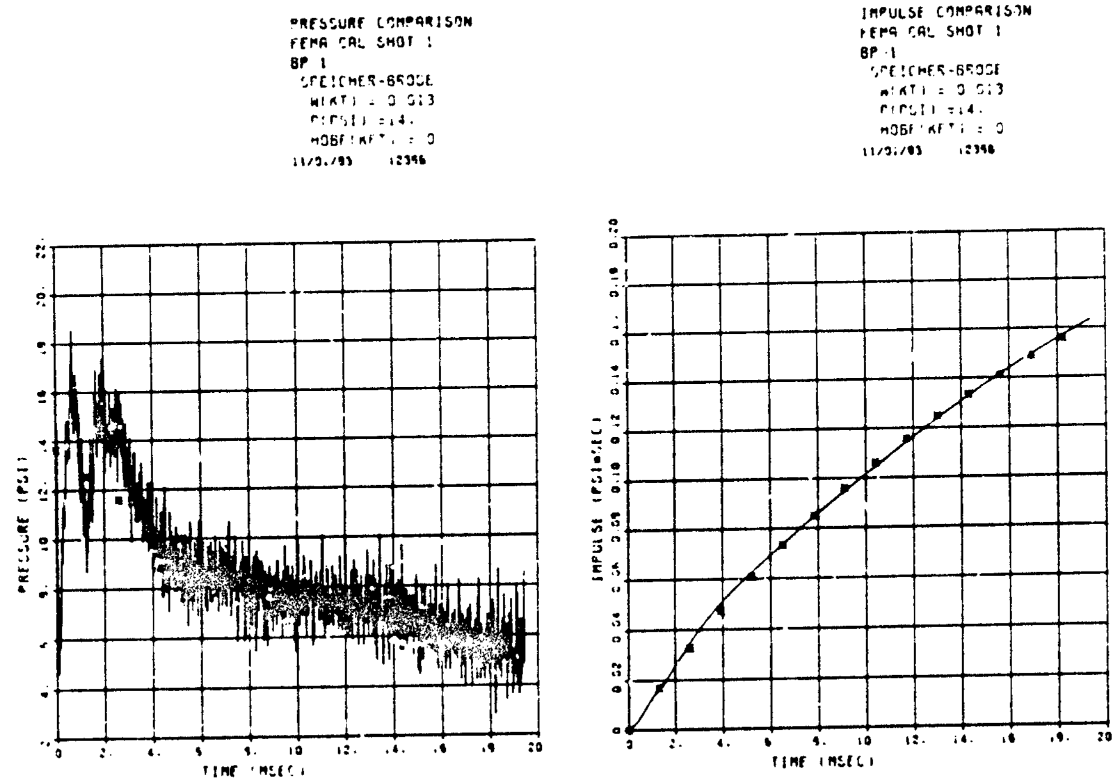

Figure A.1. Airblast- and impulse-time histories for BP1 for FEMA Calibration Shot 1.

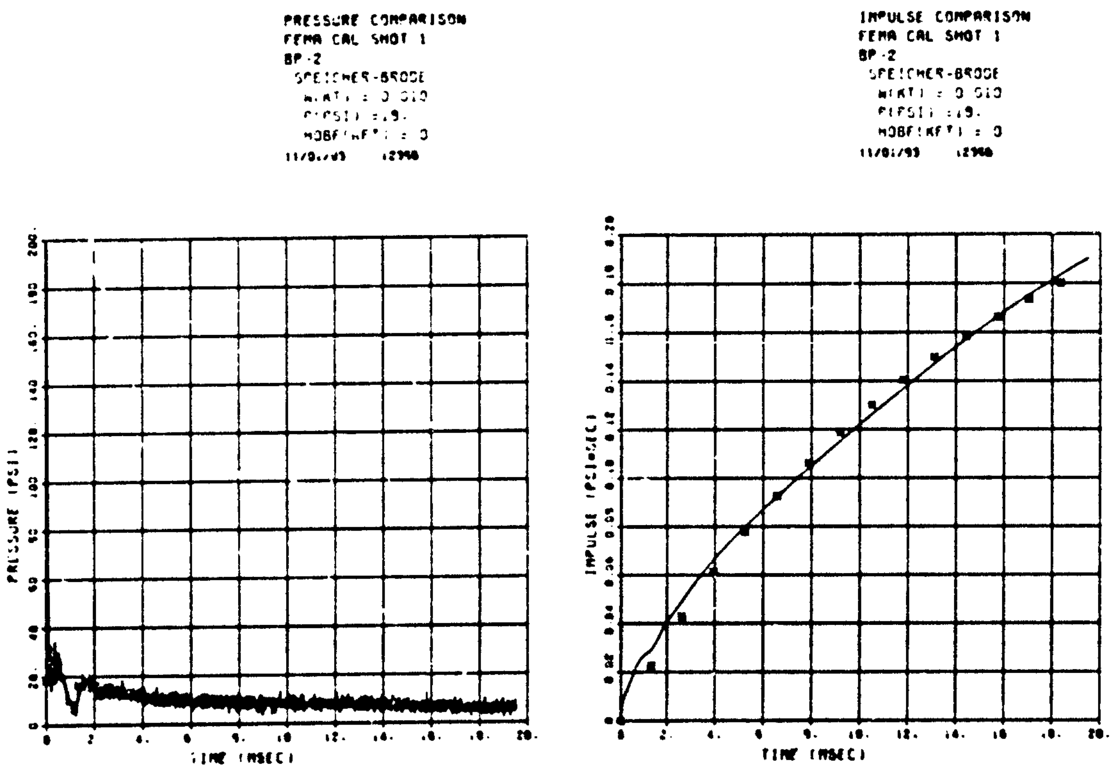

Figure A.2. Airblast- and impulse-time histories for BP2 for FEMA Calibration Shot 1.

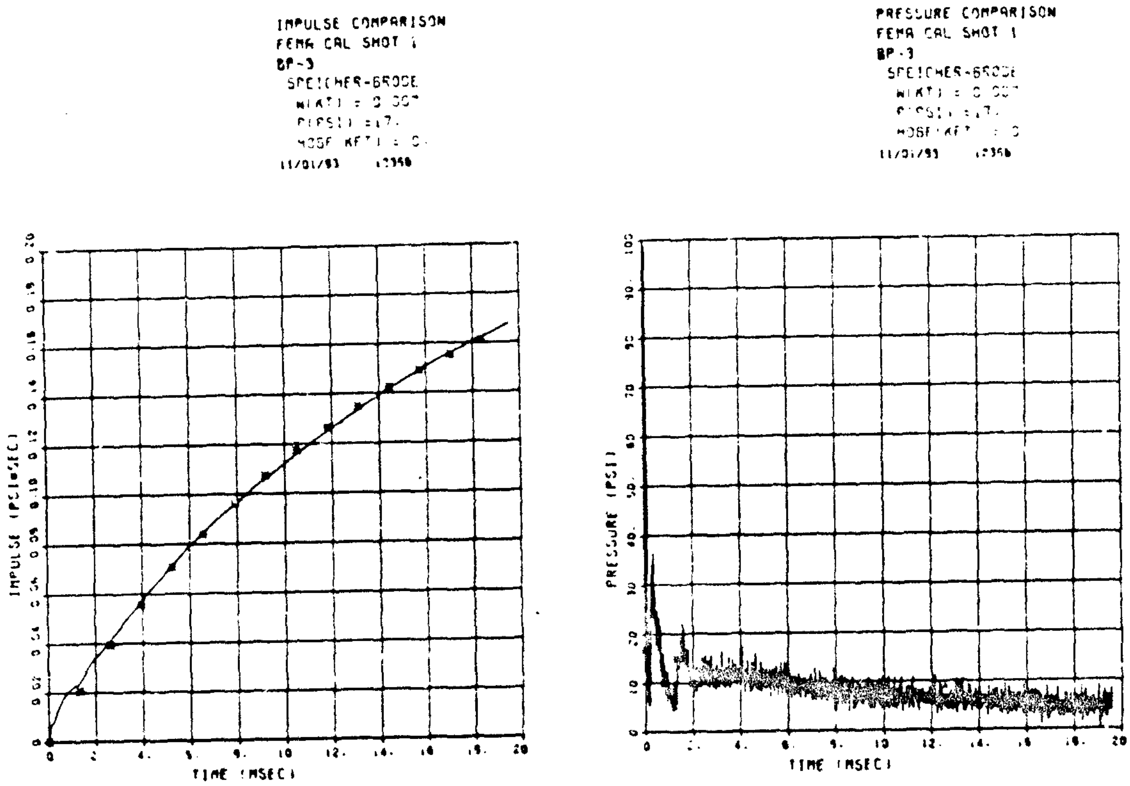

Figure A.3. Airblast- and impulse-time histories for BP3 for FEMA Calibration Shot 1.

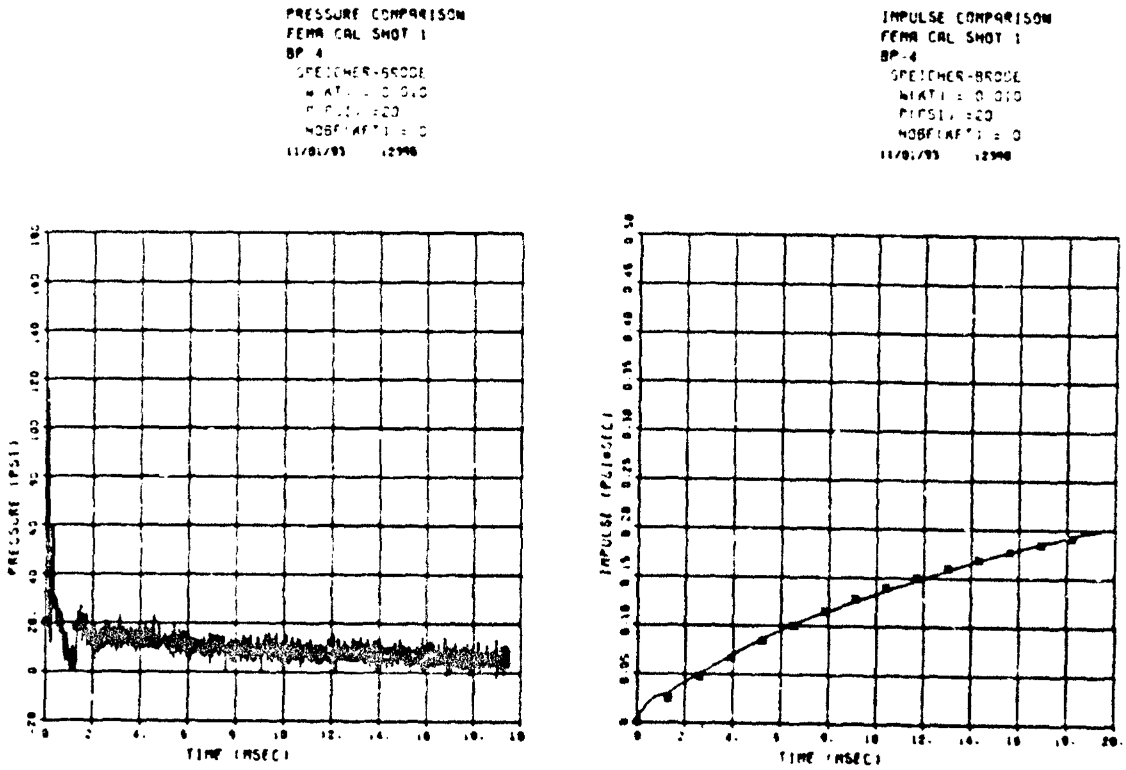

Figure A.4. Airblast- and impulse-time histories for BP4 for FEMA Calibration Shot 1.

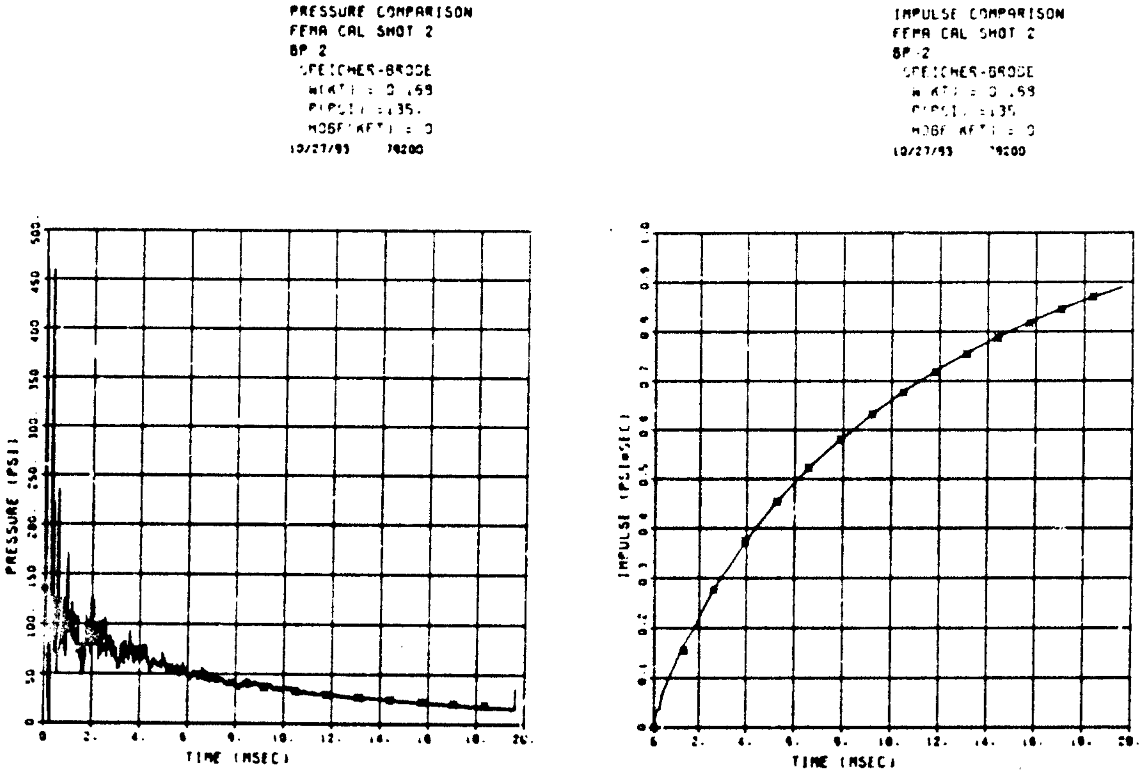

Figure A.5. Airblast- and impulse-time histories for BP2 for FEMA Calibration Shot 2.

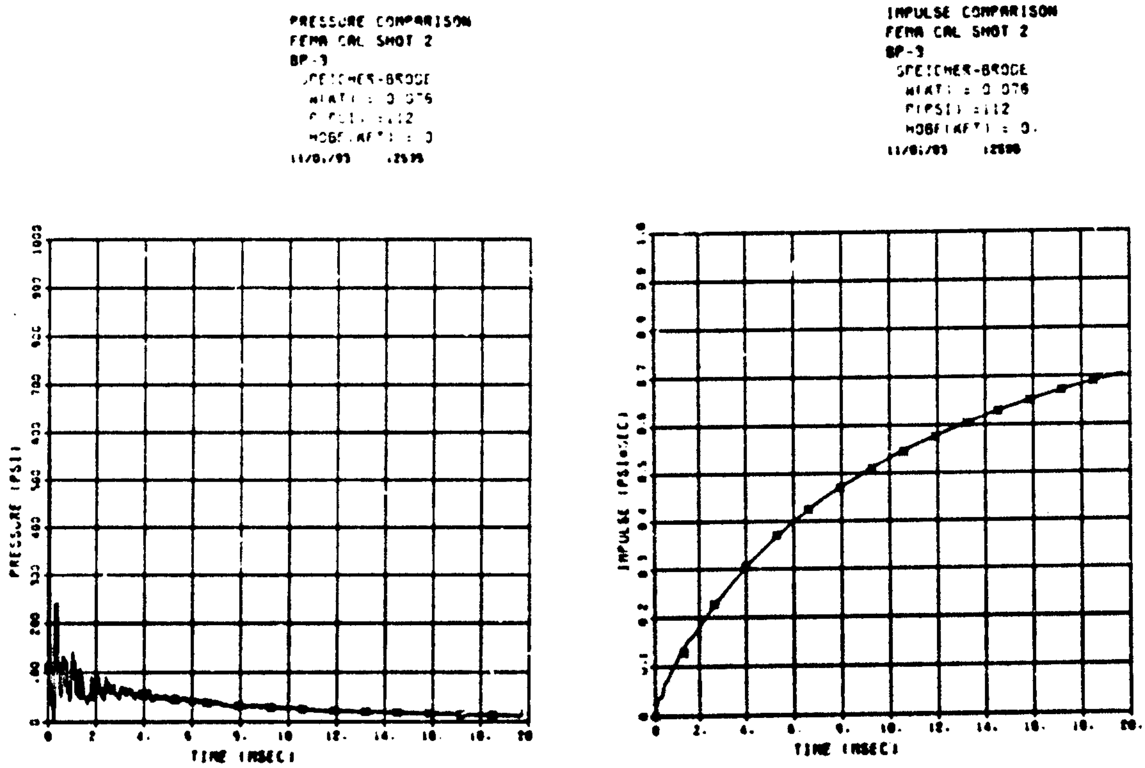

Figure A.6. Airblast- and impulse-time histories for BP3 for FEMA Calibration Shot 2.

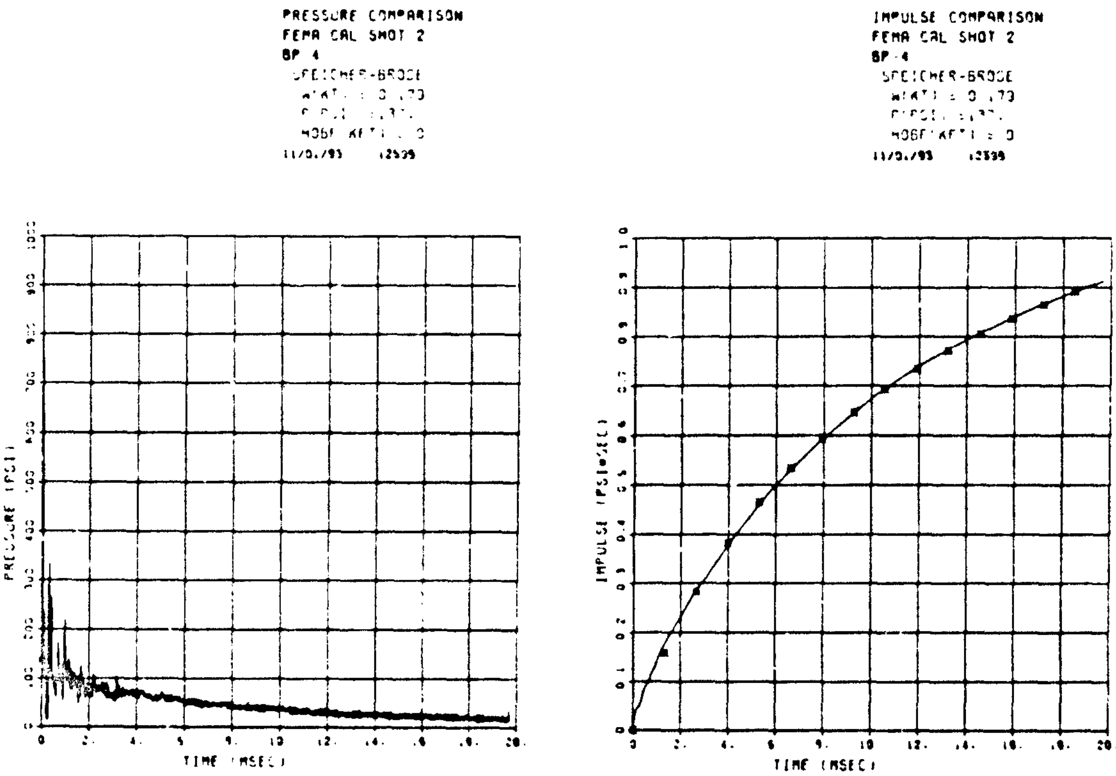

Figure A.7. Airblast- and impulse-time histories for BP4 for FEMA Calibration Shot 2.

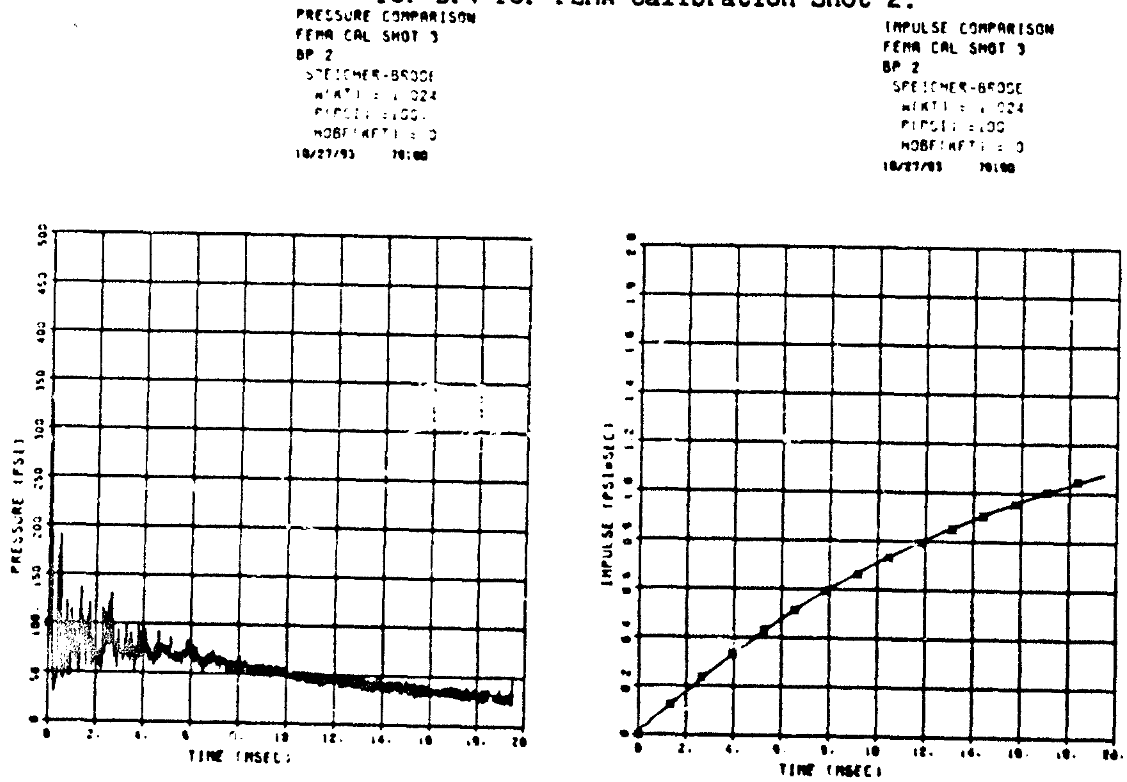

Figure A.8. Airblast- and impulse-time histories for BP2 for FEMA Calibration Shot 3.

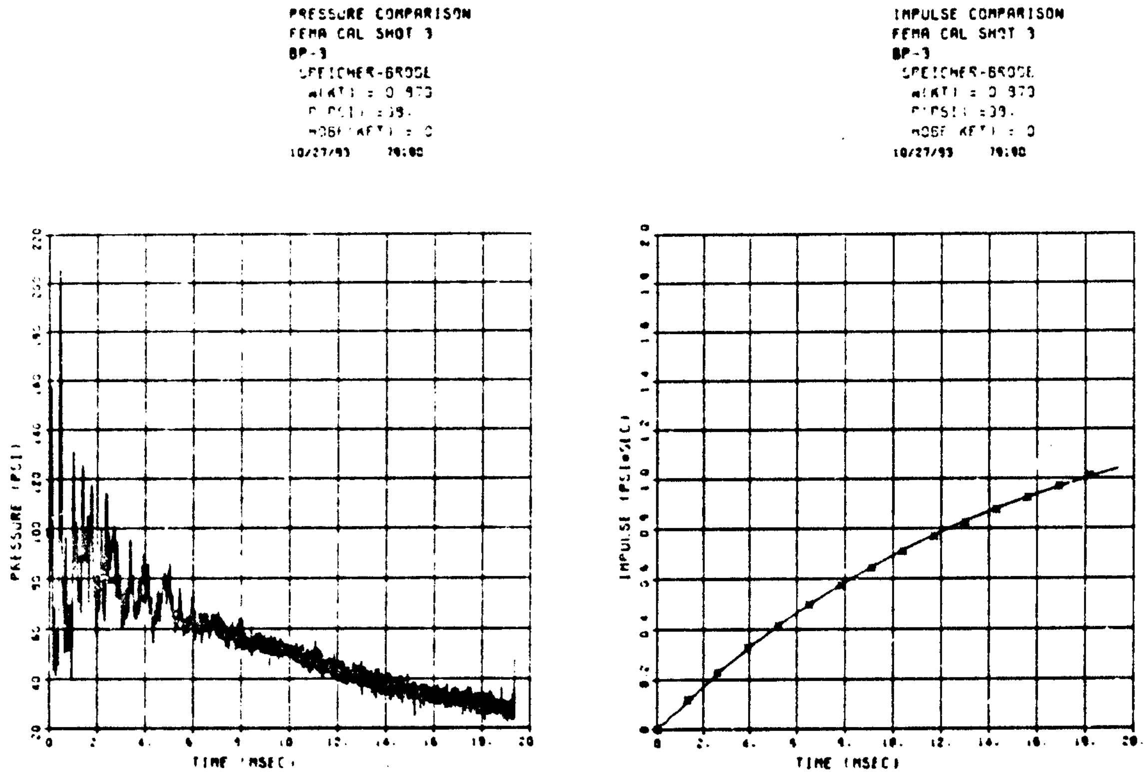

Figure A.9. Airblast- and impulse-time histories for BP3 for FEMA Calibration Shot 3.

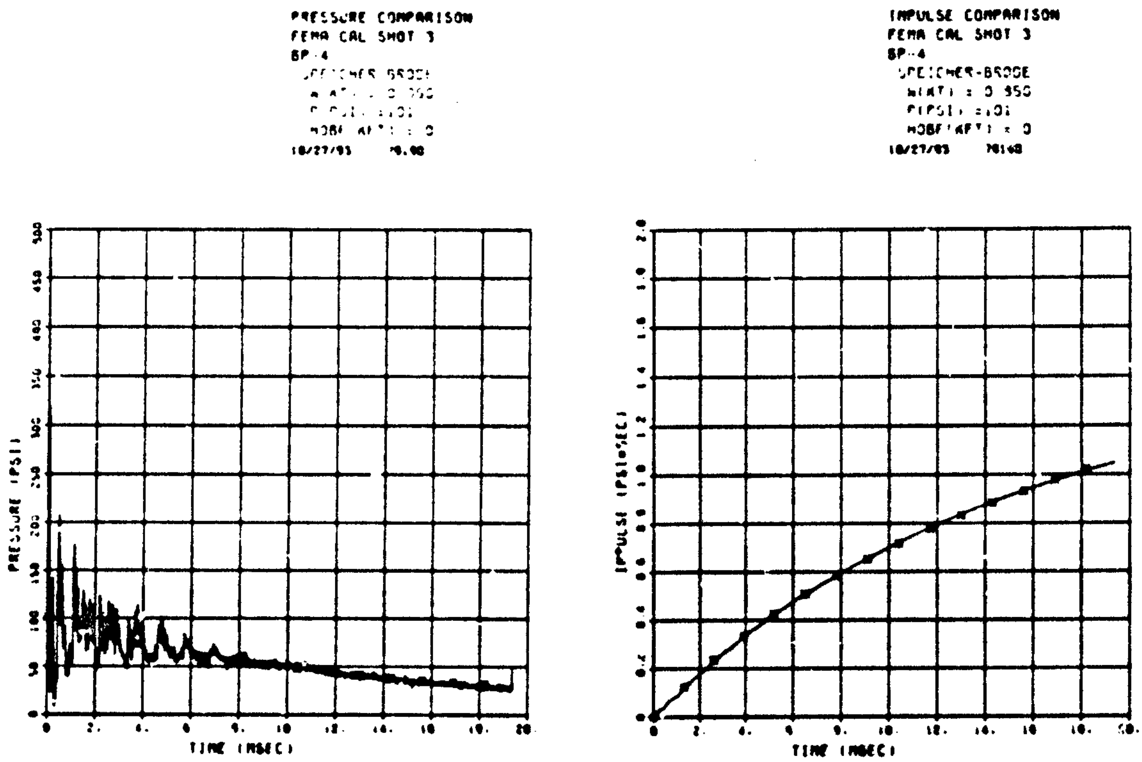

Figure A.10. Airblast- and impulse-time histories for BP4 for FEMA Calibration Shot 3.

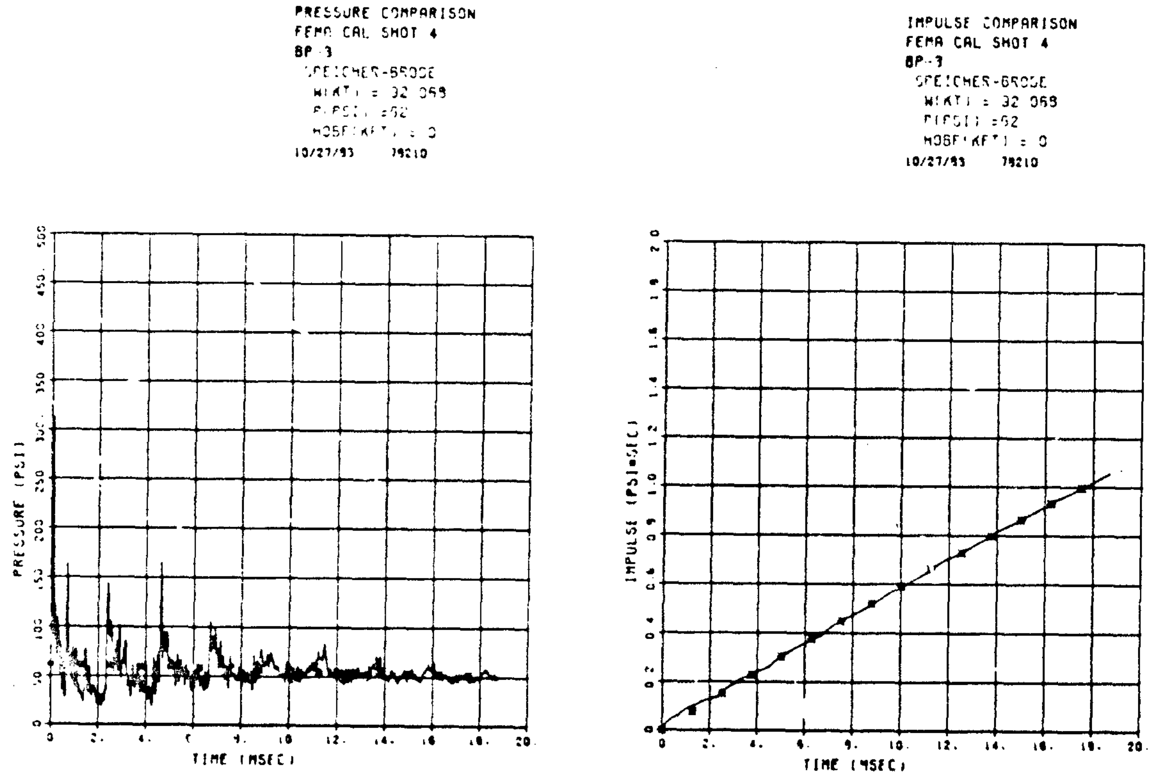

Figure A.11. Airblast- and impulse-time histories for BP3 for FEMA Calibration Shot 4.

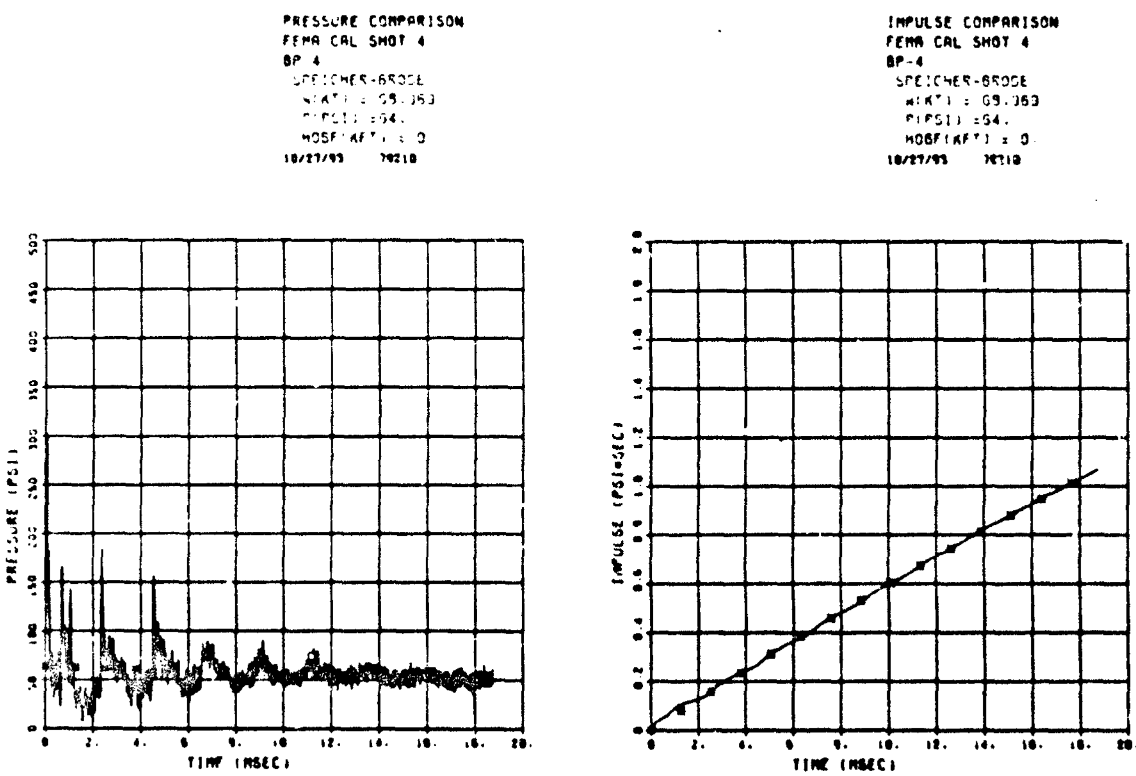

Figure A.12. Airblast- and impulse-time histories for BP4 for FEMA Calibration Shot 4.

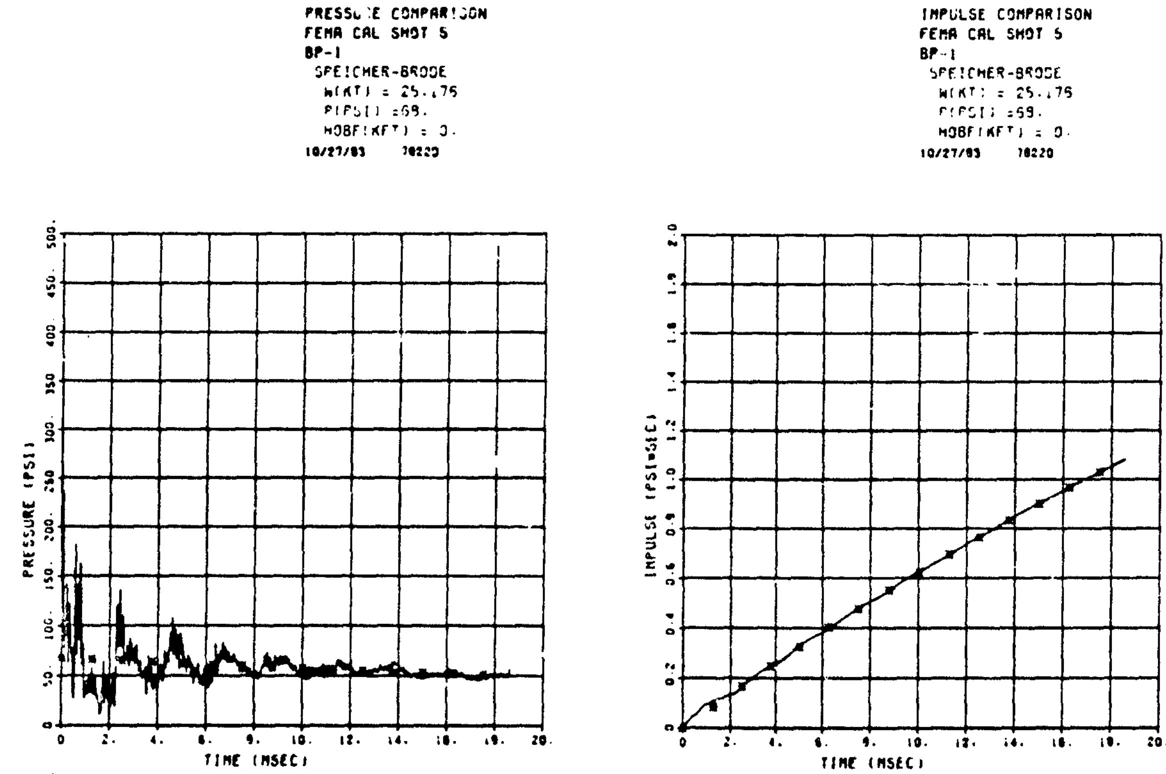

Figure A.13. Airblast- and impulse-time histories for BP1 for FEMA Calibration Shot 5.

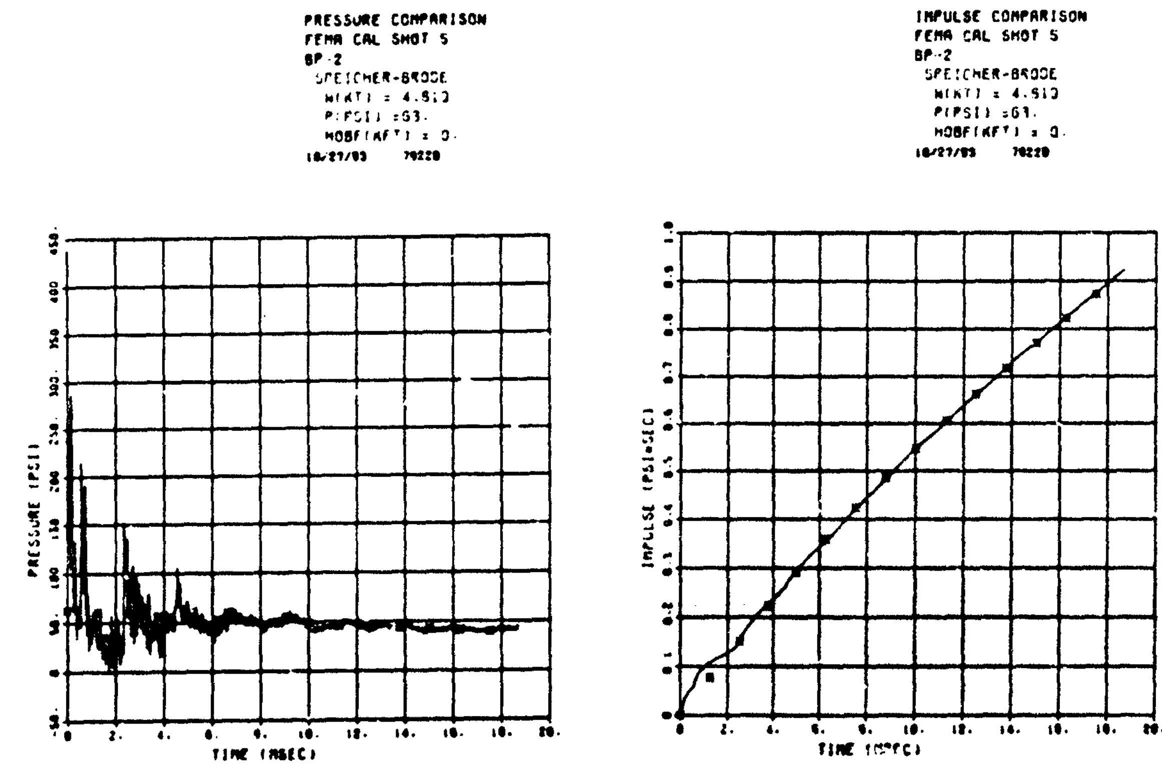

Figure A.14. Airblast- and impulse-time histories for BP2 for FEMA Calibration Shot 5.

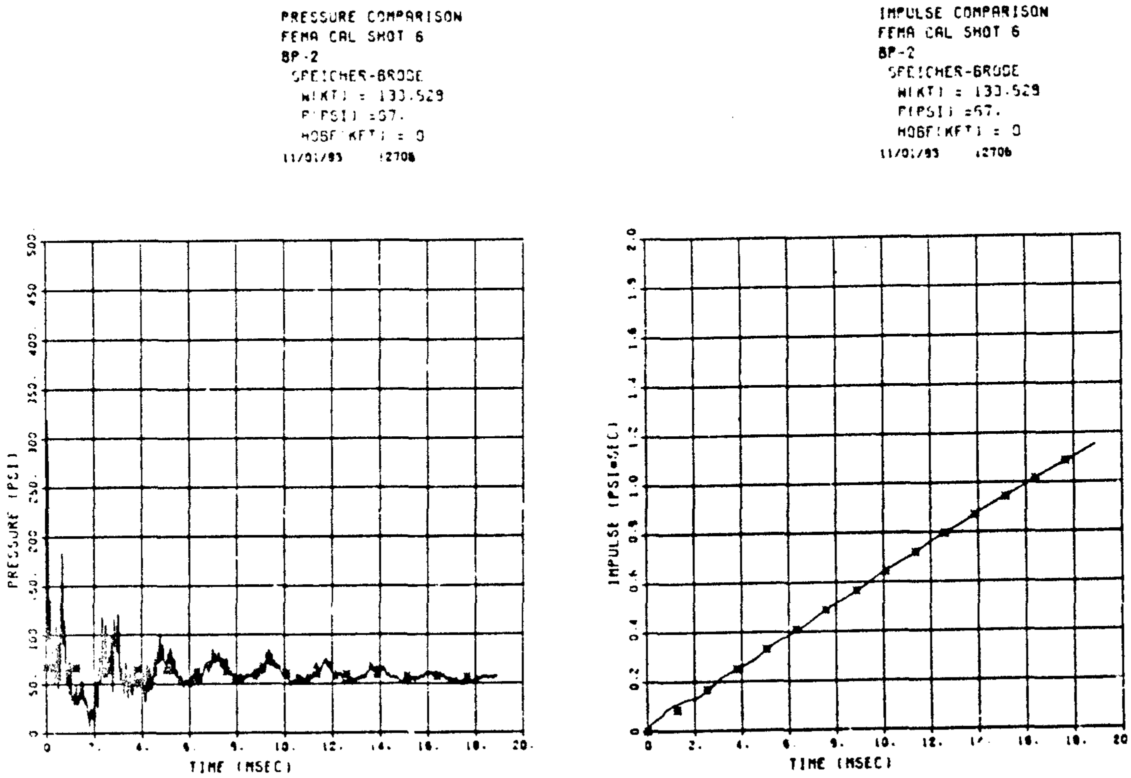

Figure A.15. Airblast- and impulse-time histories for BP2 for FEMA Calibration Shot 6.

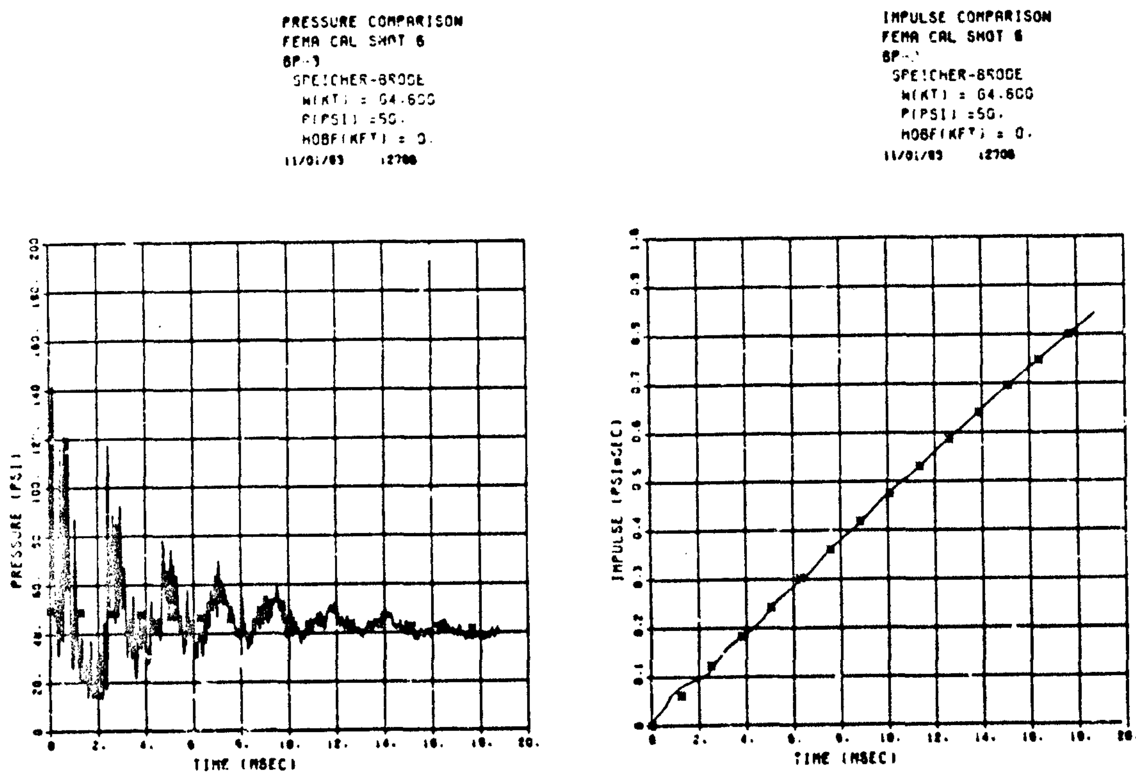

Figure A.16. Airblast- and impulse-time histories for BP3 for FEMA Calibration Shot 6.

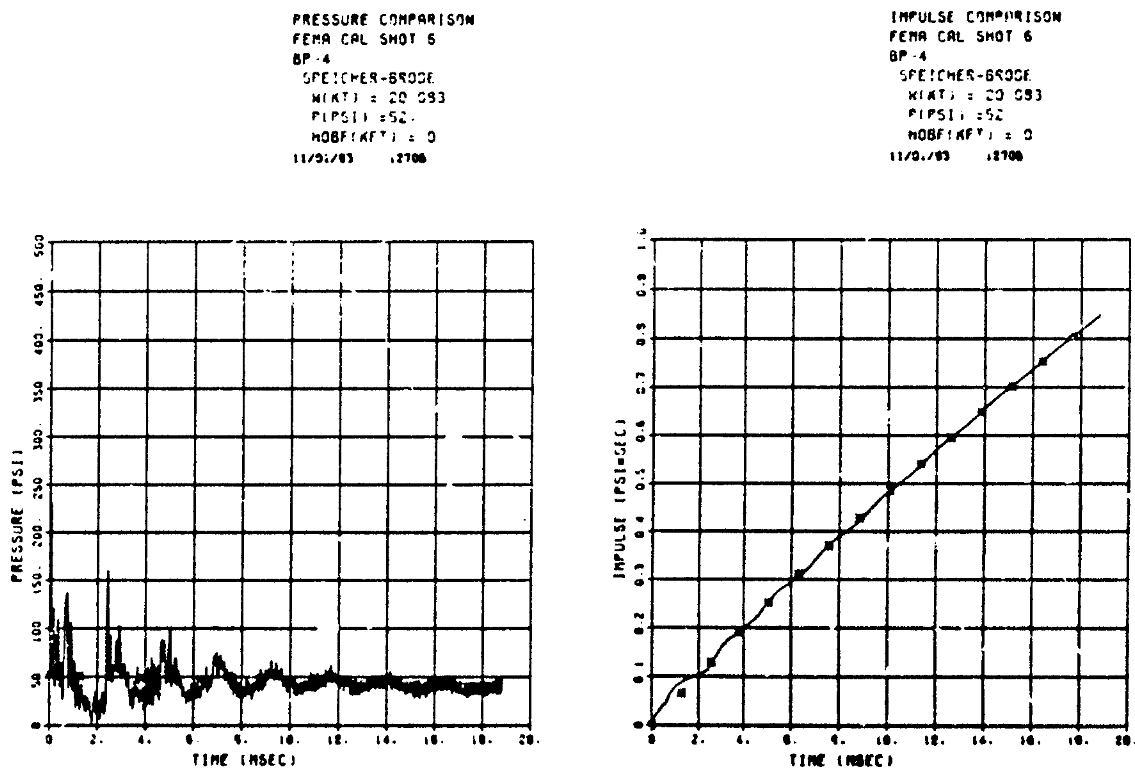

Figure A.17. Airblast- and impulse-time histories for BP4 for FEMA Calibration Shot 6.

APPENDIX B

DATA

Complete data records obtained in the element tests are presented in this appendix. Sign conventions are as follows:

1. Positive measurements of acceleration and deflection indicate motions that are vertically down except for floor accelerations, which are positive upward.

2. Positive values of interface pressure indicate soil pressures toward the structure.

3. Positive values of airblast pressure (dynamic tests) or water pressure (static tests) indicate downward pressure at the soil surface.

4. Tensile strains are positive. Compressive strains are negative.

5. Positive load cell measurements indicate compression in the steel columns.

Labels on the dynamic test data plots are explained as follows:

1. Line 1: Test name.
2. Line 2: Gage numbers.
3. Line 3: Digitization rate, baseline shift, and calibration peak.
4. Line 4: Filter option (blank implies no filter).
5. Line 5: Bookkeeping data.

Labels on static test data vary, with Line 1 being the test name and Line 2 being the gage number.

Data summaries are included for the dynamic tests in Table B.1 and for the static tests in Table B.2. Data plots for each test follow Tables B.1 and B.2. For the dynamic tests, data are plotted with time as the abscissa. For the static tests, data are plotted with reference pressure as the ordinate.

Table B.1. Data summary for the dynamic tests.

NR = not recovered, NU = not used. Numbers indicate the page number in this appendix on which each recovered data record can be found.

	Test											
Gage	D1	D2	D3	D3A	D3B	D3C	D4	D5	D6	D7	Multi-hit	D8
BP1	NR	151	160	172	184	197	209	221	232	244	NR	NR
BP2	137	NR	NR	NR	184	197	209	221	233	244	255	260
BP3	137	NR	160	172	185	197	210	221	233	244	256	260
BP4	NR	151	160	172	185	197	210	222	233	244	256	260
BP5	NR	NR	NU	NU	NU	NU	NU	NR	NU	NU	NR	NR
BP6	137	NR	NU	NU	NU	NU	NU	222	NU	245	256	261
SE1	137	151	161	173	185	198	210	222	233	245	NR	261
SE2	138	152	161	173	185	198	210	222	234	245	256	261
SE3	138	152	161	173	186	198	211	223	234	245	257	261
SE4	NR	152	161	173	186	198	211	223	234	246	257	NR
SE5	138	152	162	174	186	199	211	223	234	NR	257	262
SE6	138	153	162	174	186	199	211	223	235	NR	257	NR
SE7	139	153	162	174	187	199	212	224	235	246	256	262
APF1	139	153	162	174	187	199	212	224	235	246	NU	262
A1	139	NU	163	175	187	200	212	224	235	246	↓	262
A2	139	153	163	175	187	200	212	224	236	247	↓	263
A3	140	NU	NU	NU	NU	NU	NU	NU	NU	NU	↓	NU
A4	140	NU	NU	NU	NU	NU	NU	NU	NU	NU	NU	NU
IF1	140	NU	163	175	188	200	213	225	236	247	258	263
IF2	140	NU	163	175	188	200	213	225	236	247	258	263
IF3	141	NU	164	176	188	201	213	225	236	247	258	NR
IF4	141	NU	164	176	188	201	213	225	237	248	259	NR
IF5	141	NU	164	176	189	201	NR	226	237	248	259	263
IF6	141	154	154	176	189	201	214	226	237	248	NR	264
IF7	142	NR	165	177	189	202	214	NR	237	248	259	264
IF8	NR	NR	165	177	189	202	214	226	238	249	NR	264
IF9	NR	154	165	177	190	202	214	226	238	249	259	264
IF10	NR	NR	165	177	190	202	215	227	238	249	260	265
IF11	142	154	166	178	190	203	215	227	238	NR	NU	265
IF12	142	154	166	178	190	203	215	227	239	249	↓	265
IF13	142	NR	166	178	191	203	215	227	239	250	↓	265
IF14	143	NR	NR	178	191	203	216	228	239	250	↓	266
IF15	143	NR	166	179	191	204	216	228	239	250	↓	266
IF16	143	155	167	179	191	204	216	228	240	250	↓	266
IF17	143	NU	NU	NU	NU	NU	NU	NU	NU	NU	↓	NU
IF18	144	NU	NU	NU	NU	↓	↓	↓	↓	↓	↓	
IF19	144	NU	NU	NU	NU	↓	↓	↓	↓	↓	↓	
IF20	144	NU	NU	NU	NU	↓	↓	↓	↓	↓	↓	

	Test											
Gage	D1	D2	D3	D3A	D3B	D3C	D4	D5	D6	D7	Multi-hit	D8
IF21	144	NU	NU	NU	NU	NU	NU	NU	NU	NU	NU	NU
IF22	145	NU	NU	NU	NU	NU	NU	NU	NU	NU	NU	NU
ED1	145	155	167	179	192	204	216	NR	240	251	NU	266
EI1	NR	155	167	179	192	204	217	NR	240	251	↓	267
EO2	NR	155	167	180	192	205	217	228	240	251	↓	267
EI2	NR	156	168	180	192	205	217	NR	241	251	↓	267
EO3	145	156	168	180	193	205	217	229	241	252	↓	267
EI3	NR	NR	168	180	193	205	NR	NR	NR	252	↓	268
EO4	145	156	168	181	193	206	NR	229	241	252	↓	268
EI4	146	NR	NR	NR	NR	NR	NR	229	NR	NR	↓	268
EO5	146	156	169	181	193	206	218	229	241	252	↓	NR
EI5	NR	157	169	181	194	206	218	230	242	253	↓	268
EO6	NR	157	169	181	194	206	218	230	NR	253	↓	NR
EI6	NR	157	169	182	194	207	218	230	NR	NR	↓	NR
EO7	146	157	170	182	194	207	219	NR	NR	253	↓	NR
EI7	146	158	170	182	195	207	219	230	242	253	↓	269
EO8	147	158	170	182	195	207	NR	NR	242	254	↓	NR
EI8	147	158	170	183	195	208	219	231	242	NR	↓	NR
EO9	NR	158	171	183	195	208	219	231	243	254	↓	NR
EI9	147	159	171	183	196	208	220	231	243	254	↓	269
EO10	NU	159	171	183	196	208	220	231	NR	254	↓	269
EI10	NR	159	NR	NR	NR	NR	220	232	NR	255	↓	269
EO11	147	159	171	184	196	209	220	232	243	255	↓	270
EI11	148	160	172	184	196	209	221	232	243	255	↓	270
EO12	148	NU	NU	NU	NU	NU	NU	NU	NU	NU	↓	NU
EI12	148	↓	↓	↓	↓	↓	↓	↓	↓	↓	↓	↓
EO13	NR	↓	↓	↓	↓	↓	↓	↓	↓	↓	↓	↓
EI13	NR	↓	↓	↓	↓	↓	↓	↓	↓	↓	↓	↓
GT1	148	↓	↓	↓	↓	↓	↓	↓	↓	↓	↓	↓
GB1	149	↓	↓	↓	↓	↓	↓	↓	↓	↓	↓	↓
GT2	149	↓	↓	↓	↓	↓	↓	↓	↓	↓	↓	↓
GB2	149	↓	↓	↓	↓	↓	↓	↓	↓	↓	↓	↓
GT3	149	↓	↓	↓	↓	↓	↓	↓	↓	↓	↓	↓
GB3	150	↓	↓	↓	↓	↓	↓	↓	↓	↓	↓	↓
GT4	150	↓	↓	↓	↓	↓	↓	↓	↓	↓	↓	↓
GB4	150	↓	↓	↓	↓	↓	↓	↓	↓	↓	↓	↓
LC1	150	↓	↓	↓	↓	↓	↓	↓	↓	↓	↓	↓
LC2	151	↓	↓	↓	↓	↓	↓	↓	↓	↓	↓	↓

Table B.2. Data summary for the static tests.

The reference pressure channels (P1 and P2) were not recorded on Test S1. Therefore, all data was plotted with Gage SE1 as the reference pressure. NR = not recovered, NS = not shown, NU = not used. Numbers indicate the page number in this appendix on which each recovered data record can be found.

	Test					
Gage	S1	S3	S4	S5	S6	S7
P1	NR	NS	NS	NS	NS	NS
P2	NR	NS	NS	NS	NS	NS
SE1	270	NR	NR	297	305	314
SE2	270	NR	NR	297	306	314
SE3	271	284	NR	297	306	314
SE4	271	284	NR	297	306	314
SE5	271	NU	NR	298	306	NR
SE6	271	NU	291	298	NR	315
SE7	272	NU	NU	NU	NU	NU
D1	272	285	291	298	307	315
D2	272	NU	NU	NU	NU	NU
IF1	272	↓	291	298	307	315
IF2	273	↓	292	299	307	315
IF3	273	↓	NR	299	307	NR
IF4	NR	↓	292	299	308	316
IF5	NR	NU	292	299	308	NR
IF6	273	285	NR	300	308	316
IF7	273	285	292	300	308	316
IG8	274	285	NR	300	309	316
IF9	NR	286	NR	NR	309	317
IF10	274	286	NR	NR	NR	317
IF11	274	NR	293	300	309	NR
IF12	274	NU	NU	NU	NU	NU
IF13	275	↓	↓	↓	↓	↓
IF14	275	↓	↓	↓	↓	↓
IF15	275	↓	↓	↓	↓	↓
IF16	275	↓	↓	↓	↓	↓
IF17	276	↓	↓	↓	↓	↓
IF18	276	↓	↓	↓	↓	↓
IF19	276	↓	↓	↓	↓	↓
IF20	276	↓	↓	↓	↓	↓
IF21	277	↓	↓	↓	↓	↓
IF22	277	↓	↓	↓	↓	↓
LC1	277	↓	↓	↓	↓	↓
LC2	277	NU	NU	NU	NU	NU

	Test					
Gage	S1	S3	S4	S5	S6	S7
EO1	278	286	293	301	309	NR
EI1	278	286	293	301	310	317
EO2	NR	287	293	301	310	317
EI2	278	287	294	301	310	318
EO3	278	NR	NR	302	310	318
EI3	279	287	NR	NR	311	NR
EO4	279	287	294	302	311	318
EI4	NR	NR	294	302	311	318
EO5	279	288	294	302	NR	319
EI5	279	288	295	303	NR	319
EO6	280	288	295	303	311	319
EI6	280	288	295	303	312	319
EO7	NR	289	295	303	312	320
EI7	280	289	NR	304	312	320
EO8	NR	289	296	304	312	NR
EI8	NR	289	296	304	NR	NR
EO9	NR	290	NR	304	313	320
EI9	280	290	NR	305	313	320
EO10	281	290	296	305	313	321
EI10	281	NR	NR	NR	313	NR
EO11	281	290	296	NR	NR	321
EI11	NR	291	NR	305	NR	NR
EO12	281	NU	NU	NU	NU	NU
EI12	282	↓	↓	↓	↓	↓
EO13	282	↓	↓	↓	↓	↓
EI13	282	↓	↓	↓	↓	↓
GT1	282	↓	↓	↓	↓	↓
GB1	NR	↓	↓	↓	↓	↓
GT2	283	↓	↓	↓	↓	↓
GB2	283	↓	↓	↓	↓	↓
GT3	283	↓	↓	↓	↓	↓
GB3	283	↓	↓	↓	↓	↓
GT4	284	↓	↓	↓	↓	↓
GB4	284	↓	↓	↓	↓	↓

FEMA ELEM TEST D-1
BP-2
200000. HZ CAL= 739.4

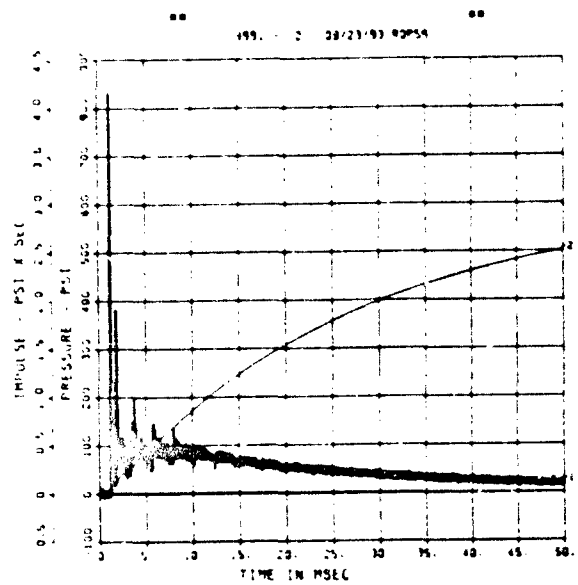

** PEAK VALUE IS [illegible] % OVER CALIBRATION **

FEMA ELEM TEST D-1
BP-3
200000. HZ CAL= 878.0

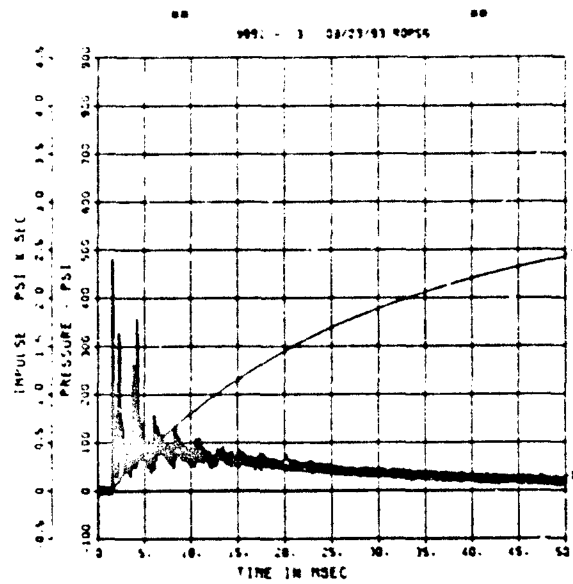

FEMA ELEM TEST D-1
BP-6
200000. HZ CAL= 992.0

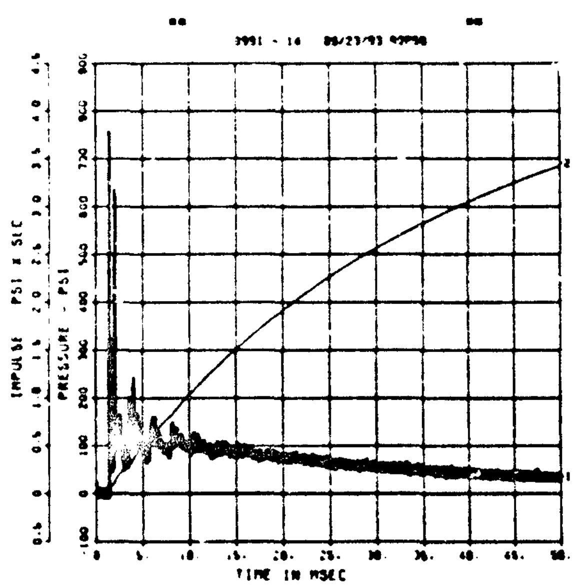

FEMA ELEM TEST D-1
SE-1
200000. HZ CAL= 414.1

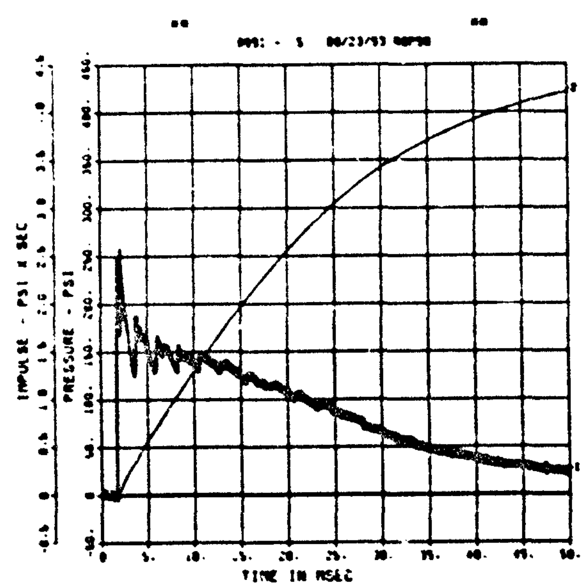

FEMA ELEM TEST D-1
SE-2
200000. HZ CAL= 139.6

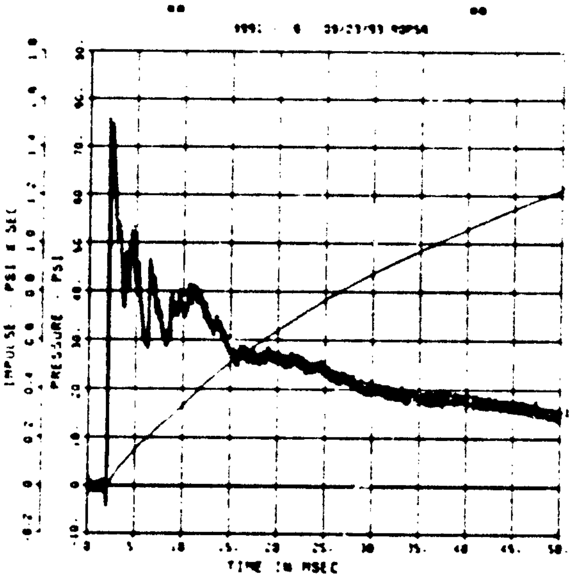

FEMA ELEM TEST D-1
SE-3
200000. HZ CAL= 253.0

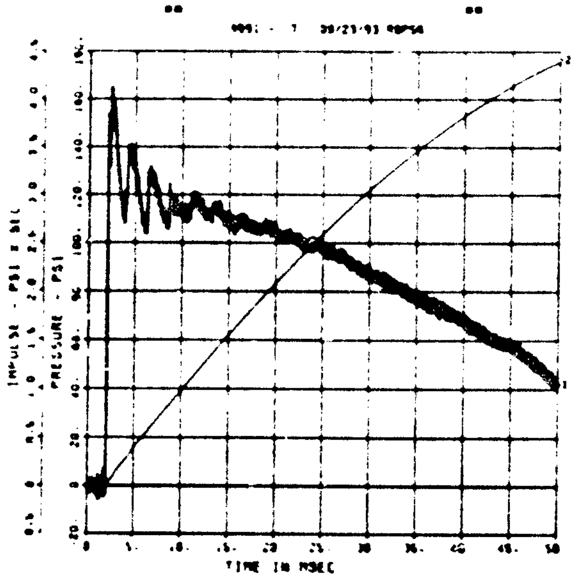

FEMA ELEM TEST D-1
SE-5
200000. HZ CAL= 81.80

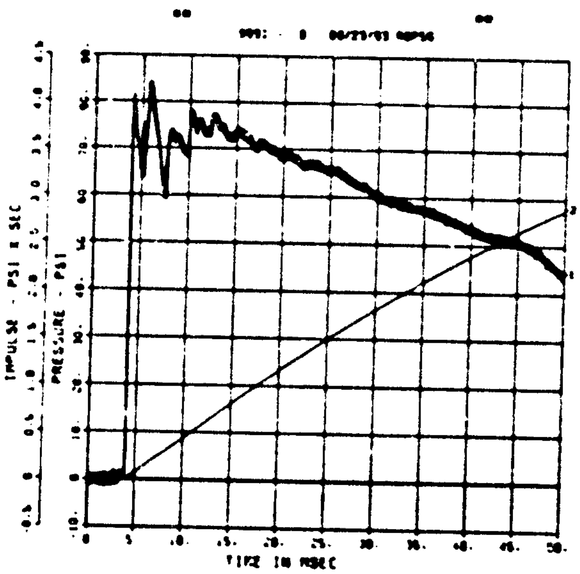

FEMA ELEM TEST D-1
SE-6
200000. HZ CAL= 133.8

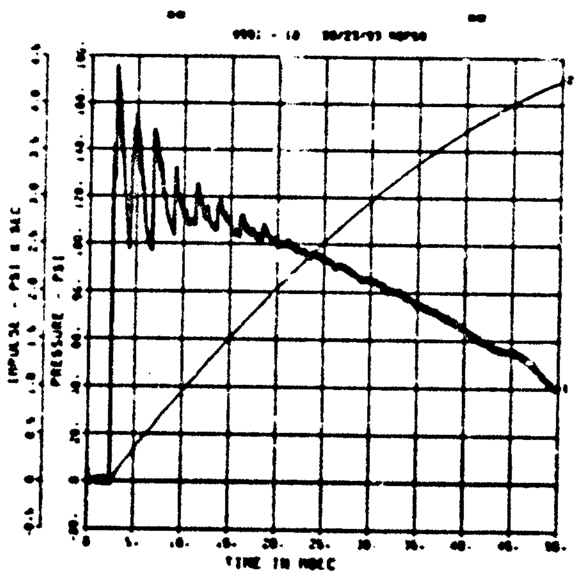

** PEAK VALUE IS 3 % OVER CALIBRATION **

** PEAK VALUE IS 32 % OVER CALIBRATION **

FEMA ELEM TEST D-1
SE-7
200000. HZ CAL= 233.3

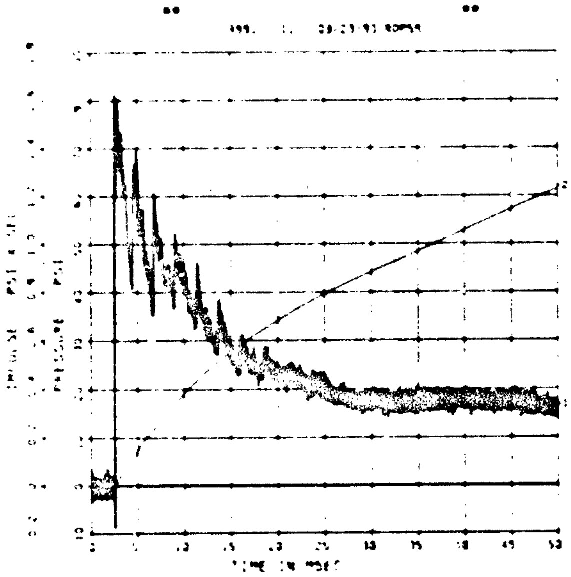

FEMA ELEM TEST D-1
AFF-1
200000. HZ CAL= 519.5

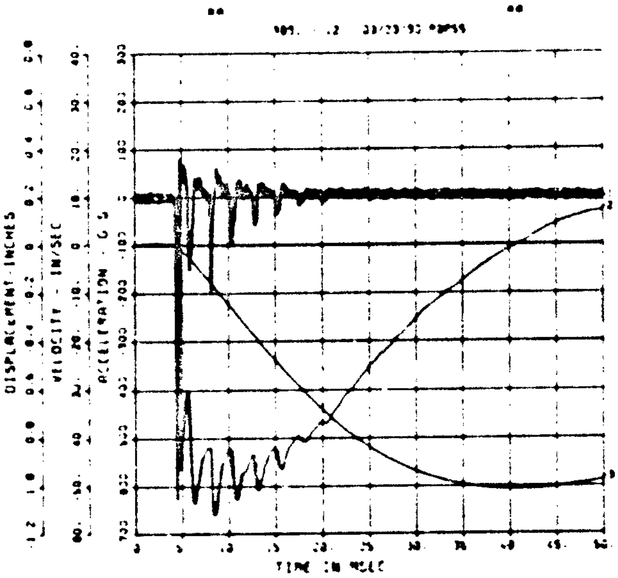

FEMA ELEM TEST D-1
A-1
200000. HZ CAL= 2281.

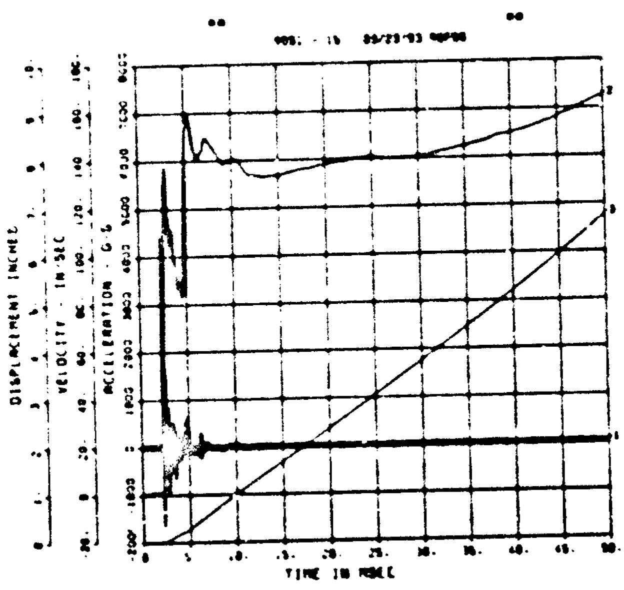

FEMA ELEM TEST D-1
A-2
200000. HZ CAL= 2212.

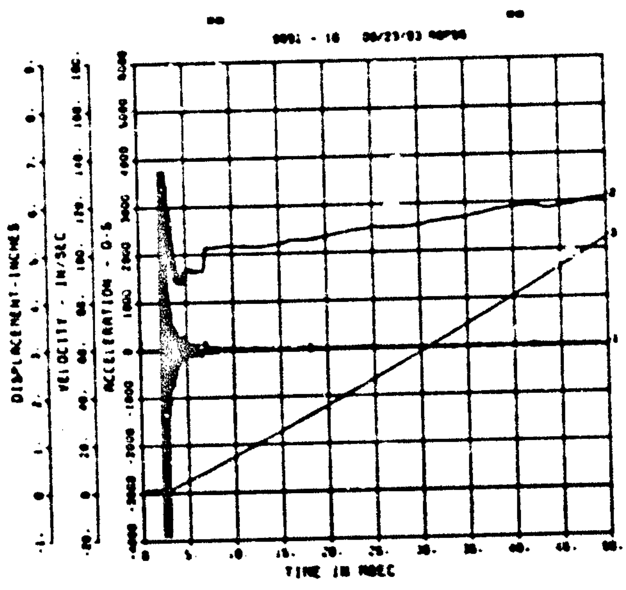

FEMA ELEM TEST D-1
A-3
200000. HZ CAL= 501.3

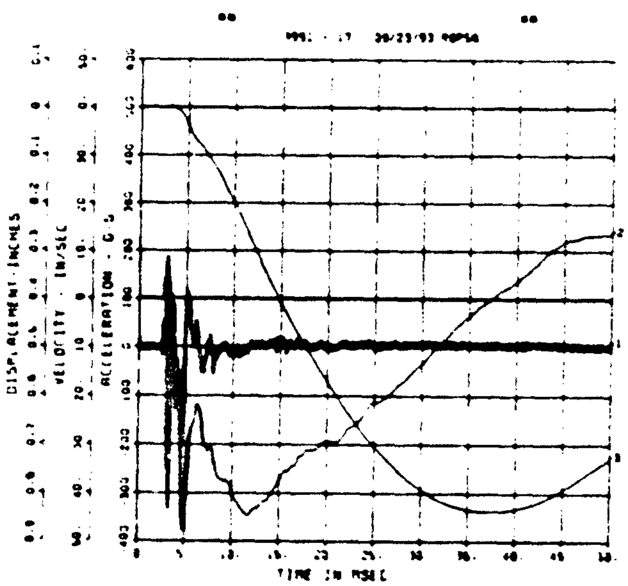

FEMA ELEM TEST D-1
A-4
200000. HZ CAL= 861.0

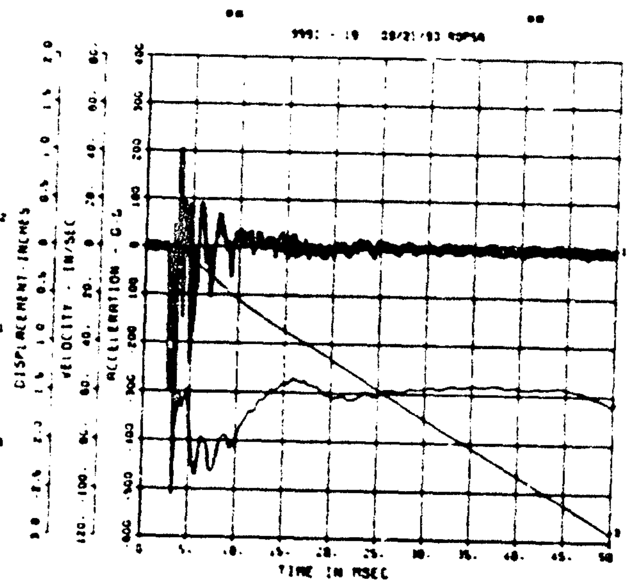

FEMA ELEM TEST D-1
IF-1
200000. HZ CAL= 375.5

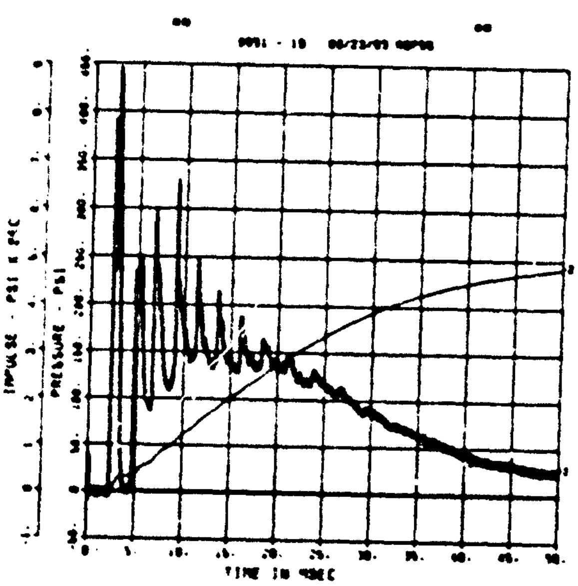

FEMA ELEM TEST D-1
IF-2
200000. HZ CAL= 398.0

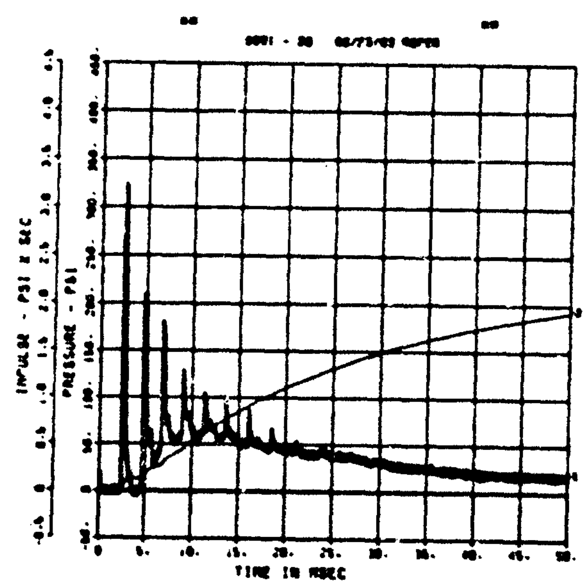

** PEAK VALUE IS 10 % OVER CALIBRATION **

FEMA ELEM TEST D-1
IF-3
200000. HZ CAL= 257.8

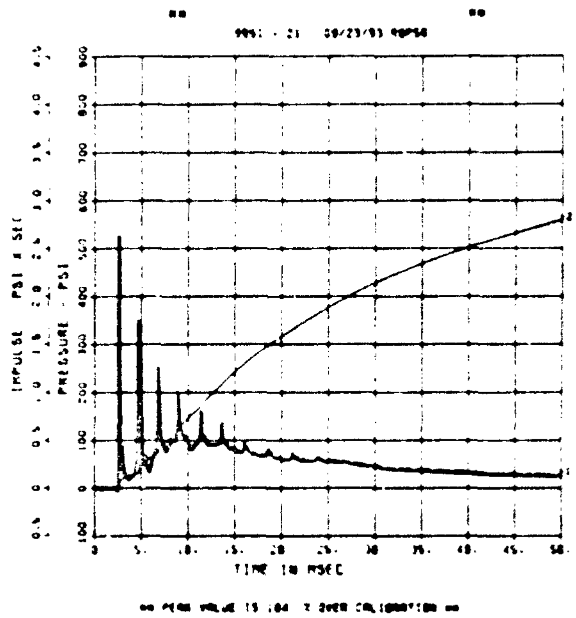

FEMA ELEM TEST D-1
IF-4
200000. HZ CAL= 348.8

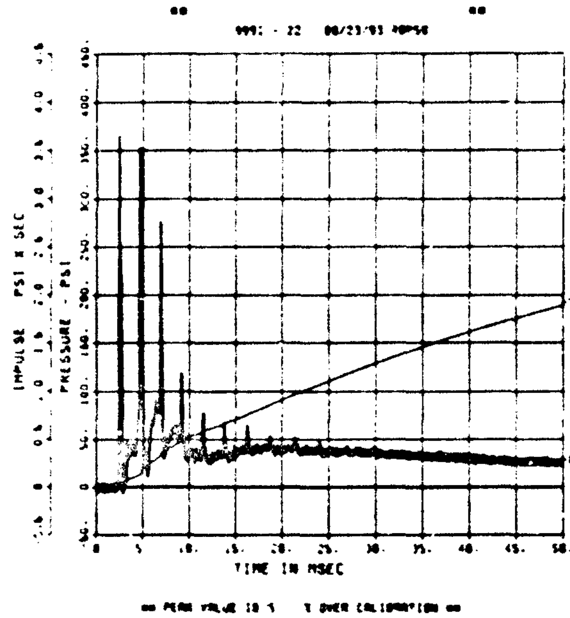

FEMA ELEM TEST D-1
IF-5
200000. HZ CAL= 351.3

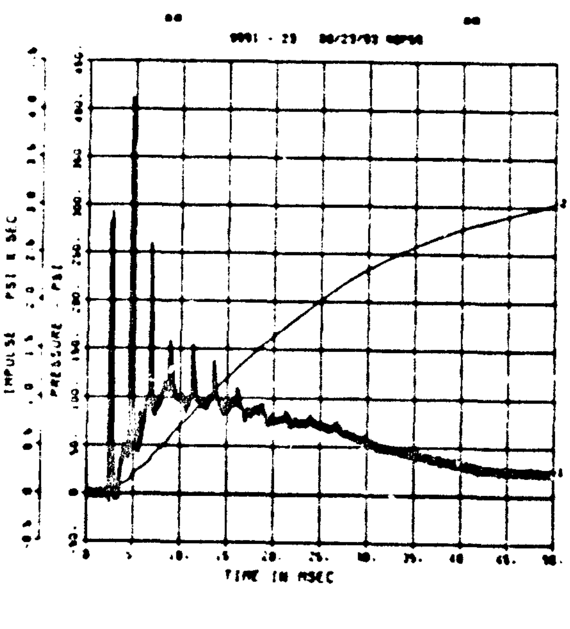

FEMA ELEM TEST D-1
IF-6
200000. HZ CAL= 358.7

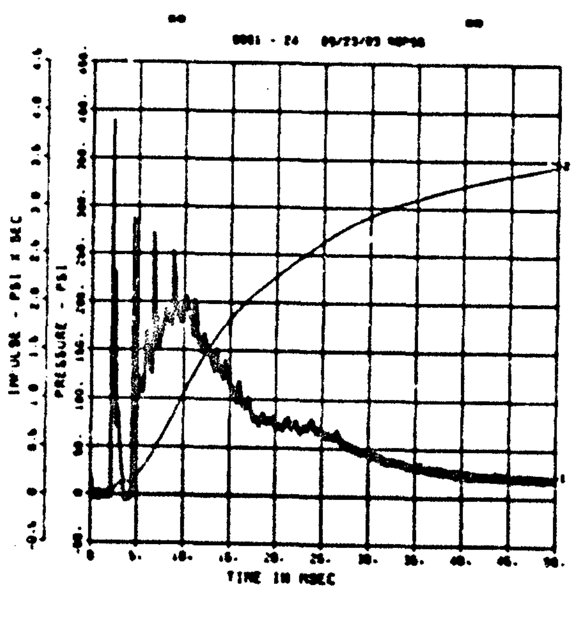

FEMA ELEM TEST D-1
IF-7
200000. HZ CAL= 184.0

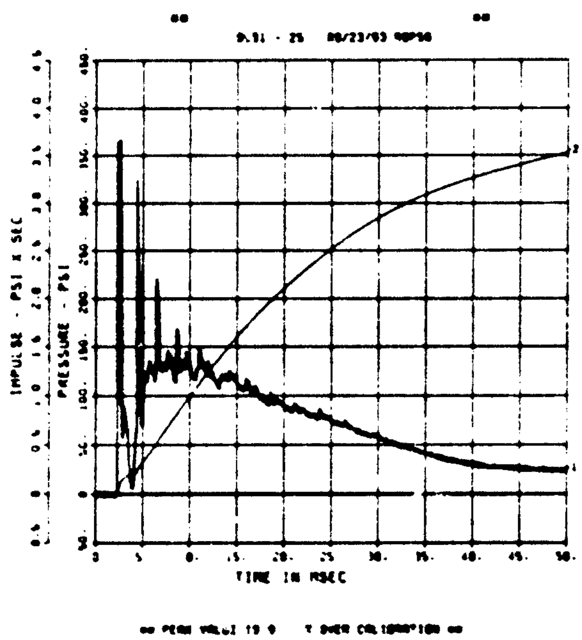

FEMA ELEM TEST D-1
IF-11
200000. HZ CAL= 126.8

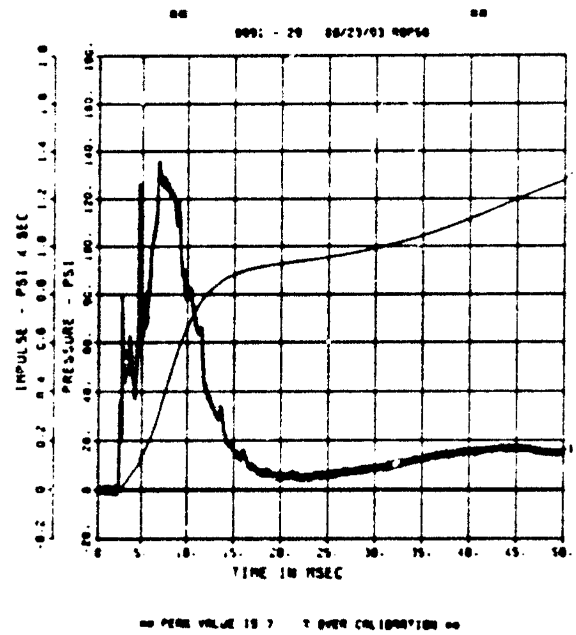

FEMA ELEM TEST D-1
IF-12
200000. HZ CAL= 125.3

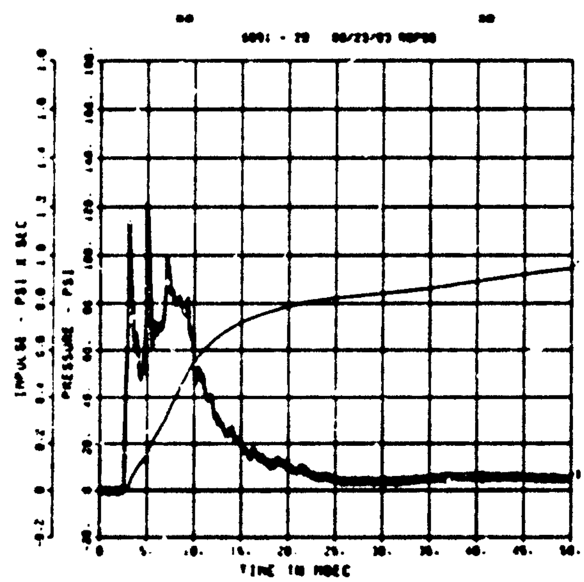

FEMA ELEM TEST D-1
IF-13
200000. HZ CAL= 128.1

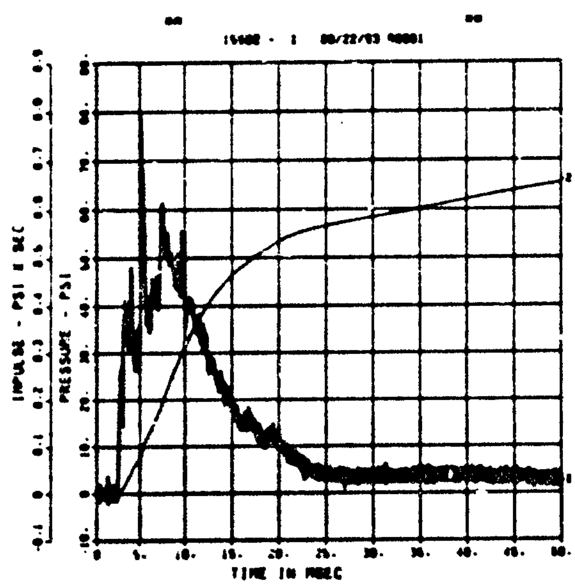

FEMA ELEM TEST D-1
IF-14
200000. HZ CAL= 85.00

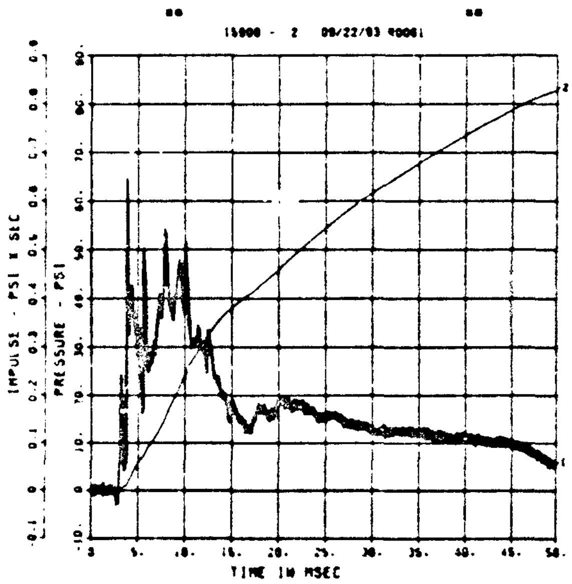

FEMA ELEM TEST D-1
IF-15
200000. HZ CAL= 99.40

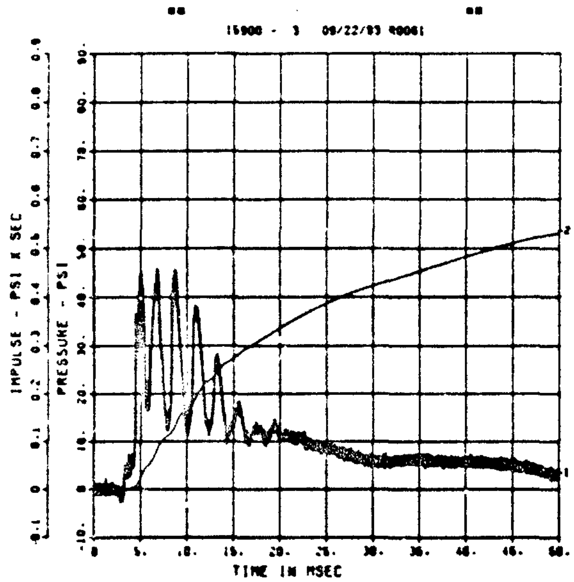

FEMA ELEM TEST D-1
IF-16
200000. HZ CAL= 87.60

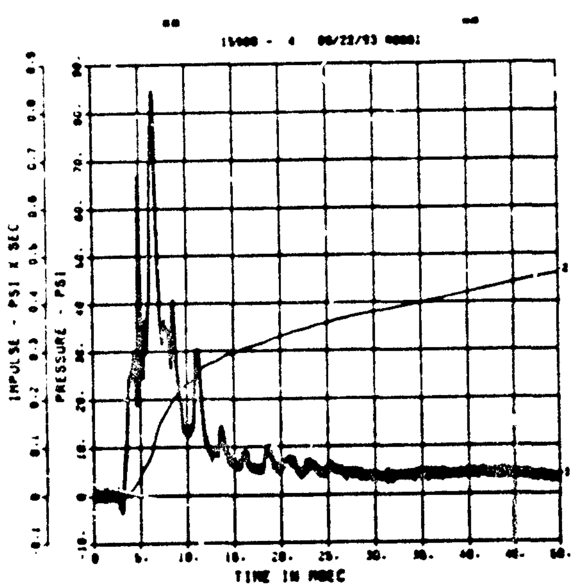

FEMA ELEM TEST D-1
IF-17
200000. HZ CAL= 255.3

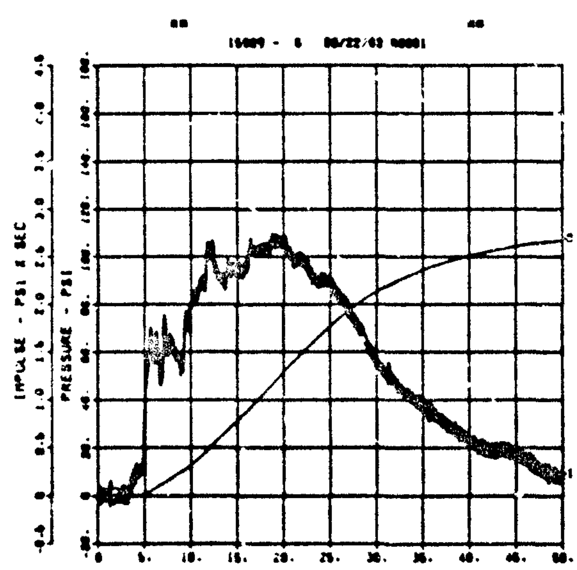

FEMA ELEM TEST D-1
IF-18
200000. HZ CAL= 166.8
LP4/0 70% CUTOFF= 3000. HZ

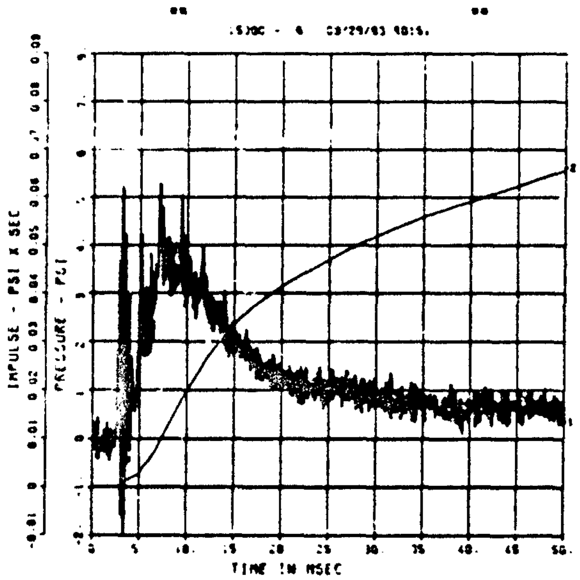

FEMA ELEM TEST D-1
IF-19
200000. HZ CAL= 51.70
LP4/0 70% CUTOFF= 3000. HZ

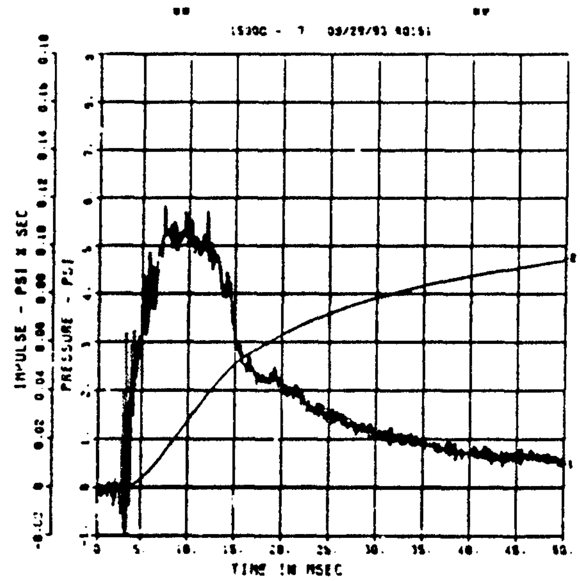

FEMA ELEM TEST D-1
IF-20
200000. HZ CAL= 26.76
LP2/0 70% CUTOFF= 15000. HZ

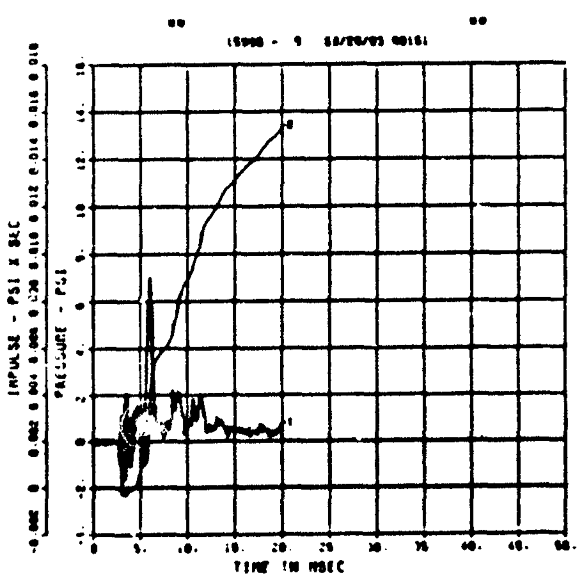

FEMA ELEM TEST D-1
IF-21
200000. HZ CAL= 51.10

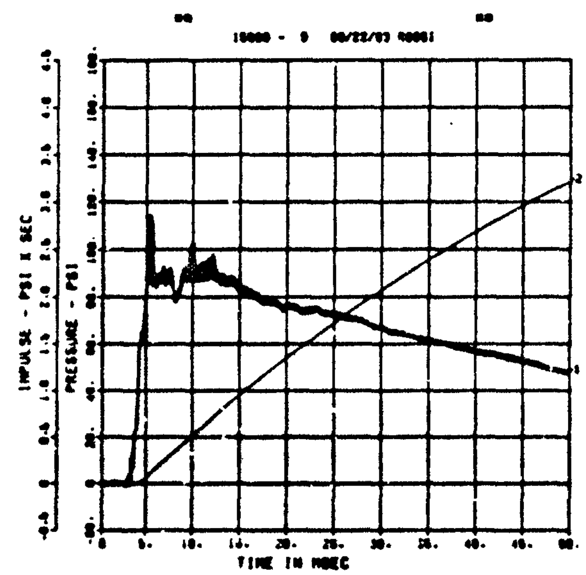

FEMA ELEM TEST D-1
IF-22
200000. HZ CAL= 247.0

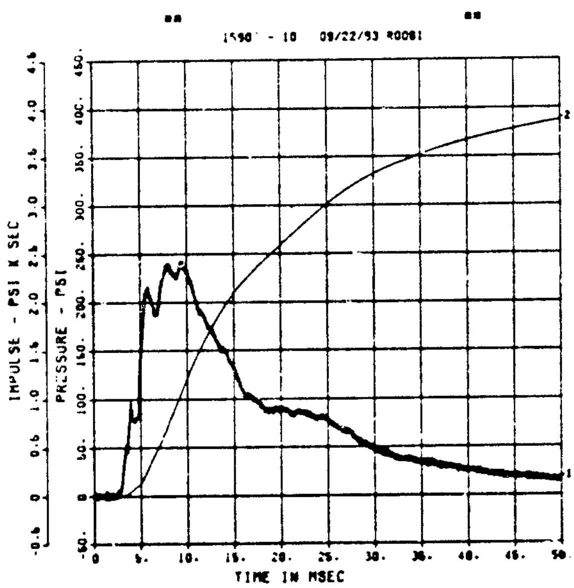

FEMA ELEM TEST D-1
EO-1
200000. HZ CAL= 20205.
LP2/0 70% CUTOFF= 18000. HZ

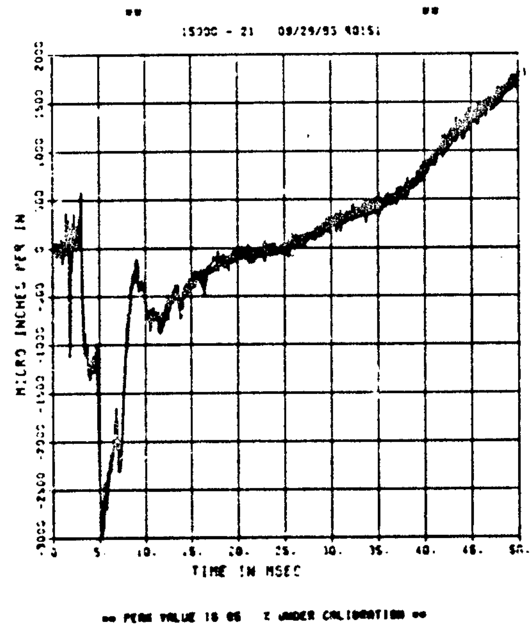

FEMA ELEM TEST D-1
EO-3
200000. HZ CAL= 10276.
LP4/0 70% CUTOFF= 8000. HZ

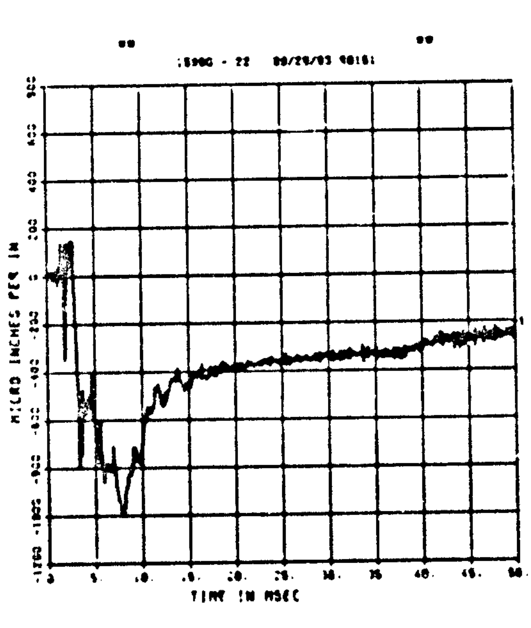

FEMA ELEM TEST D-1
EO-4
200000. HZ CAL= 20205.

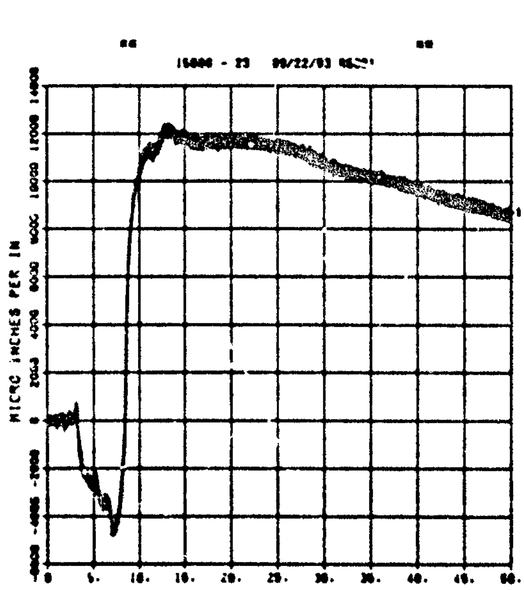

FEMA ELEM TEST D-1
EI-4
200000. HZ CAL= 10276.
LP2/0 70% CUTOFF= 15000. HZ

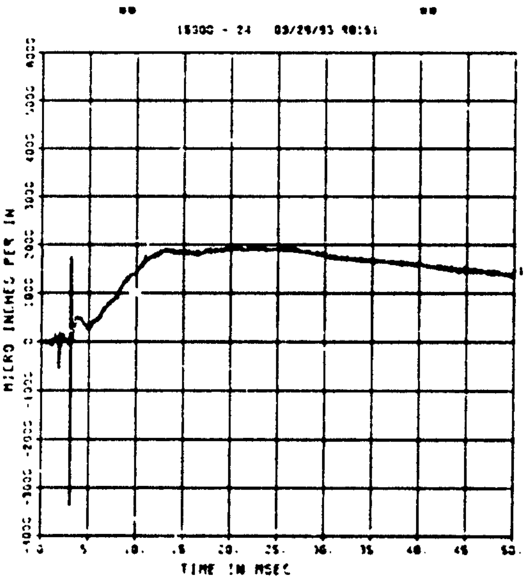

FEMA ELEM TEST D-1
EO-5
200000. HZ CAL= 6692.
LP4/0 70% CUTOFF= 9000. HZ

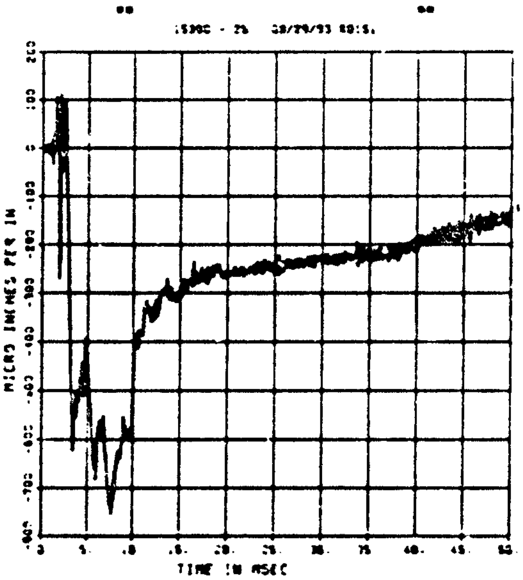

** PEAK VALUE IS 00 % UNDER CALIBRATION **

FEMA ELEM TEST D-1
EO-7
200000. HZ CAL= 6692.
LP4/0 70% CUTOFF= 9000. HZ

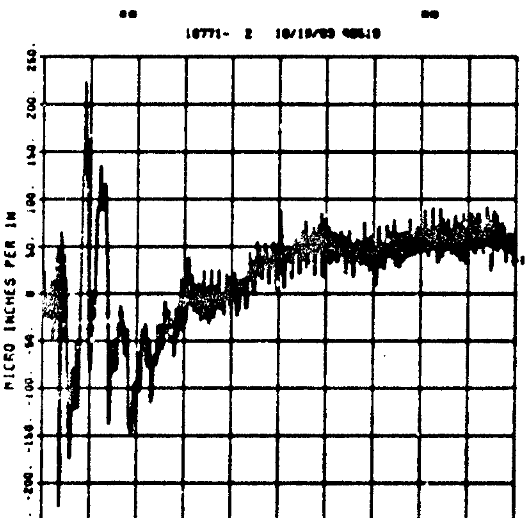

** PEAK VALUE IS 87. % UNDER CALIBRATION **

FEMA ELEM TEST D-1
EI-7
200000. HZ CAL= 6692.
LP4/0 70% CUTOFF= 9000. HZ

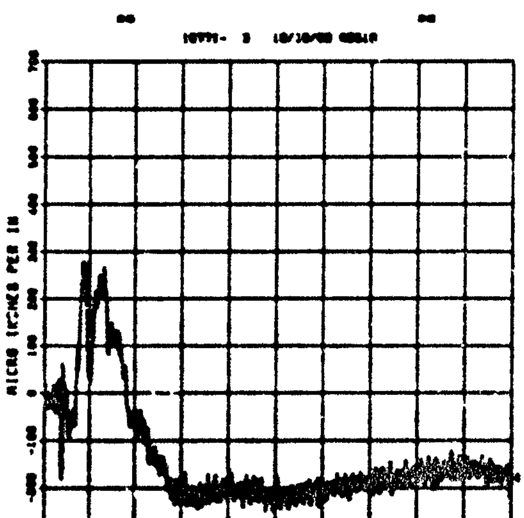

** PEAK VALUE IS 00 % UNDER CALIBRATION **

FEMA ELEM TEST D-1
EO-8
200000. HZ CAL= 6692.

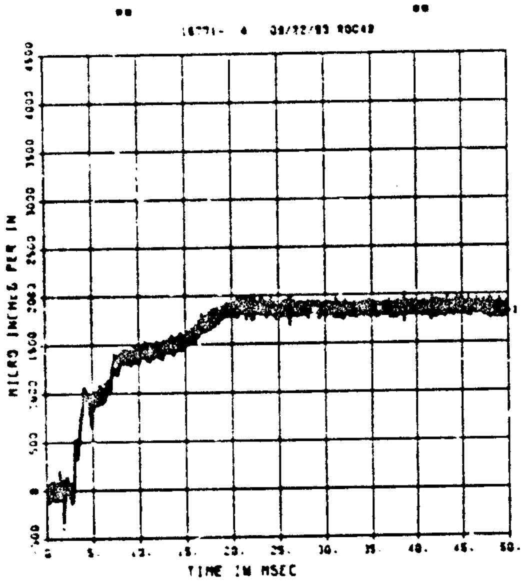

FEMA ELEM TEST D-1
EI-8
200000. HZ CAL= 6692.
LP4/0 70% CUTOFF= 9000. HZ

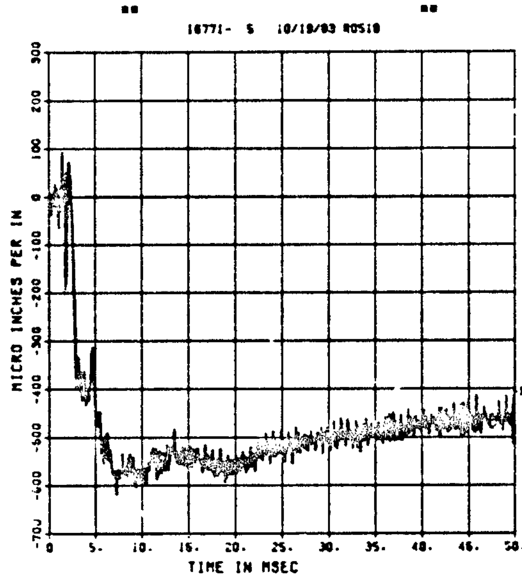

** PEAK VALUE IS 91 % UNDER CALIBRATION **

FEMA ELEM TEST D-1
EI-9
200000. HZ CAL= 20205.
LP4/0 70% CUTOFF= 9000. HZ

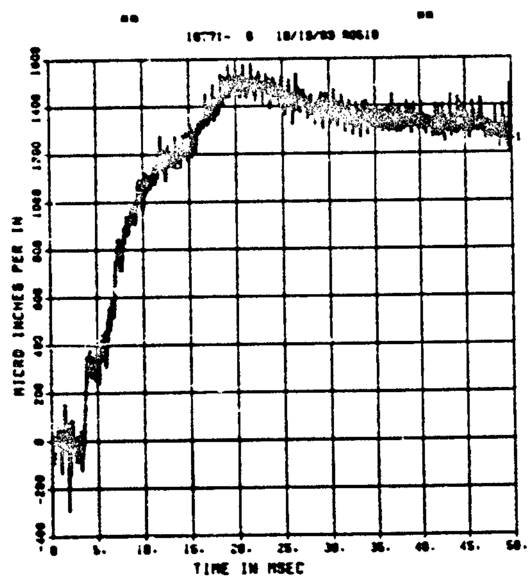

** PEAK VALUE IS 8 % UNDER CALIBRATION **

FEMA ELEM TEST D-1
EO-11
200000. HZ CAL= 10276.
LP4/0 70% CUTOFF= 9000. HZ

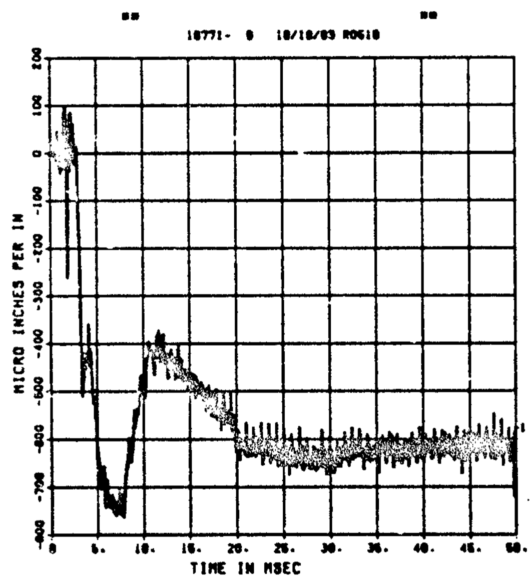

** PEAK VALUE IS 93 % UNDER CALIBRATION **

FEMA ELEM TEST D-1
EI-11
200000. HZ CAL= 28530.
LP4/0 70% CUTOFF= 9000. HZ

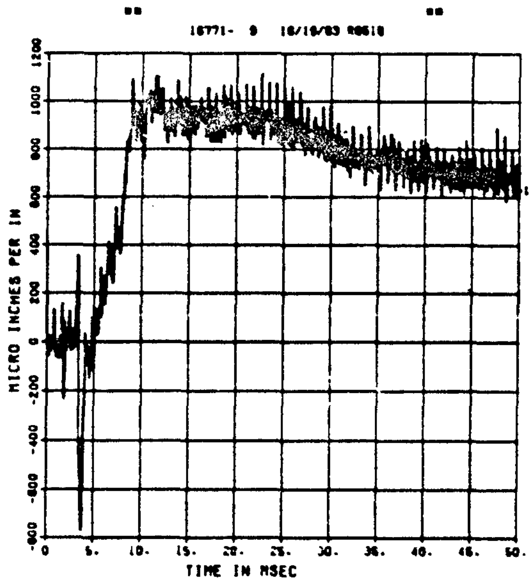

** PEAK VALUE IS 94 % UNDER CALIBRATION **

FEMA ELEM TEST D-1
EO-12
200000. HZ CAL= 20205.
LP4/0 70% CUTOFF= 9000. HZ

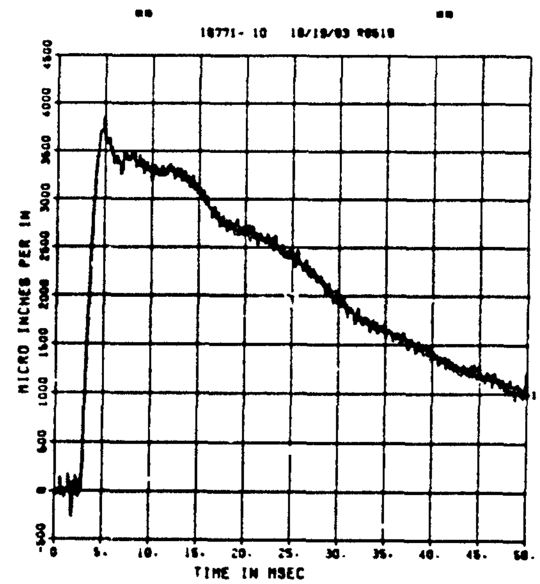

** PEAK VALUE IS 91 % UNDER CALIBRATION **

FEMA ELEM TEST D-1
EI-12
200000. HZ CAL= 10276.

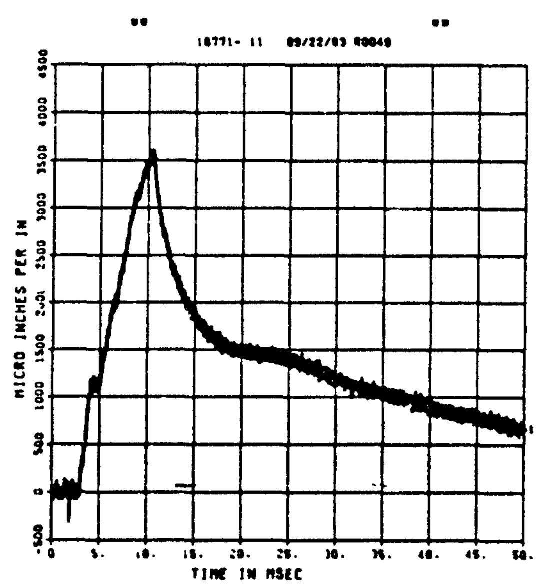

FEMA ELEM TEST D-1
GT-1
200000. HZ CAL= 2084.
LP4/0 70% CUTOFF= 9000. HZ

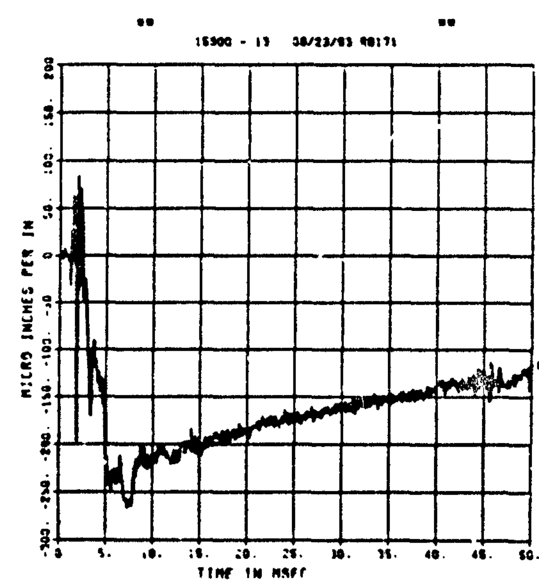

** PEAK VALUE IS 87 % UNDER CALIBRATION **

FEMA ELEM TEST D-1
GB-1
200000. HZ CAL= 2084.

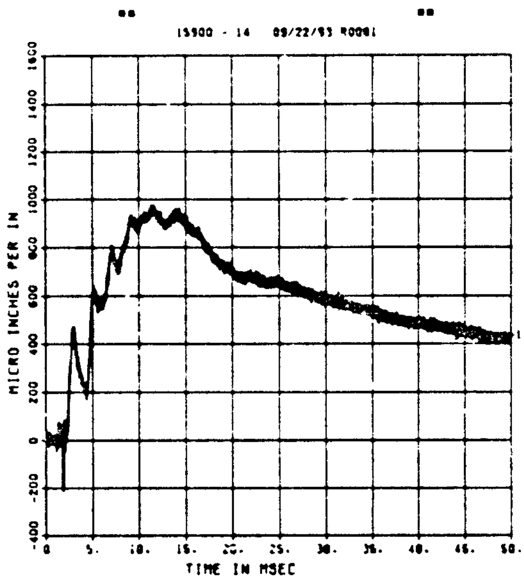

FEMA ELEM TEST D-1
GB-2
200000. HZ CAL= 2084.

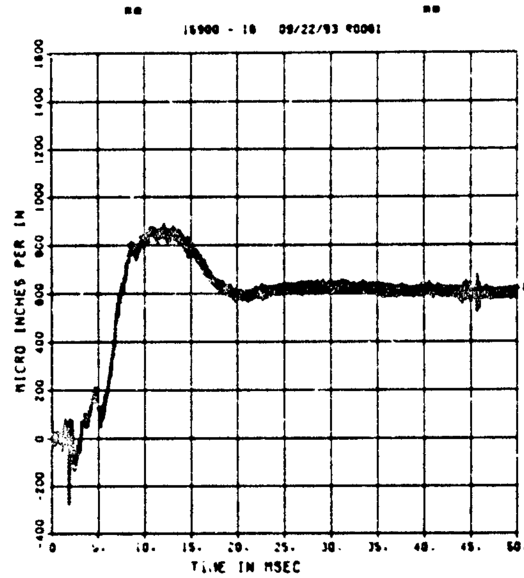

FEMA ELEM TEST D-1
GT-2
200000. HZ CAL= 2084.
LP4/0 70% CUTOFF= 9000. HZ

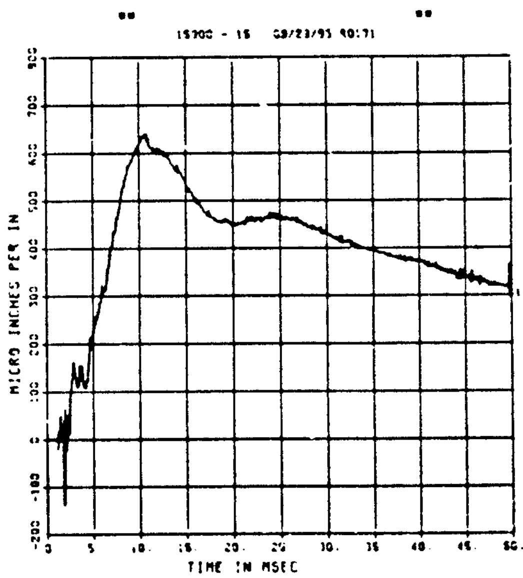

FEMA ELEM TEST D-1
GT-3
200000. HZ CAL= 4162.
LP4/0 70% CUTOFF= 9000. HZ

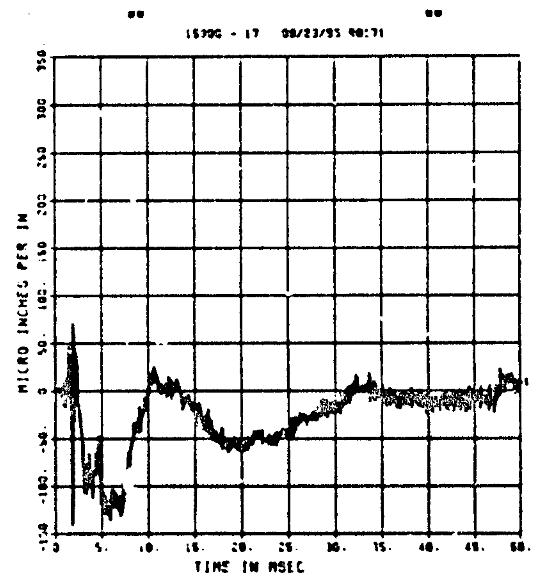

** PEAK VALUE IS 97 % UNDER CALIBRATION **

FEMA ELEM TEST D-1
GB-3
200000. HZ CAL= 4162.
LP2/0 70% CUTOFF= 10000. HZ

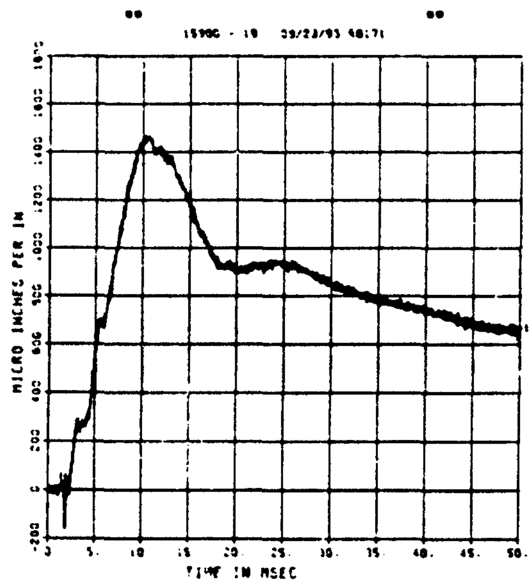

FEMA ELEM TEST D-1
GT-4
200000. HZ CAL= 4162.
LP2/0 70% CUTOFF= 10000. HZ

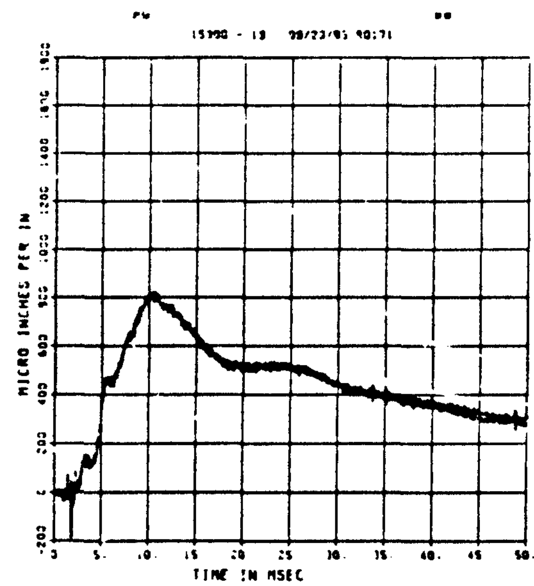

FEMA ELEM TEST D-1
GB-4
200000. HZ CAL= 4162.
LP2/0 70% CUTOFF= 10000. HZ

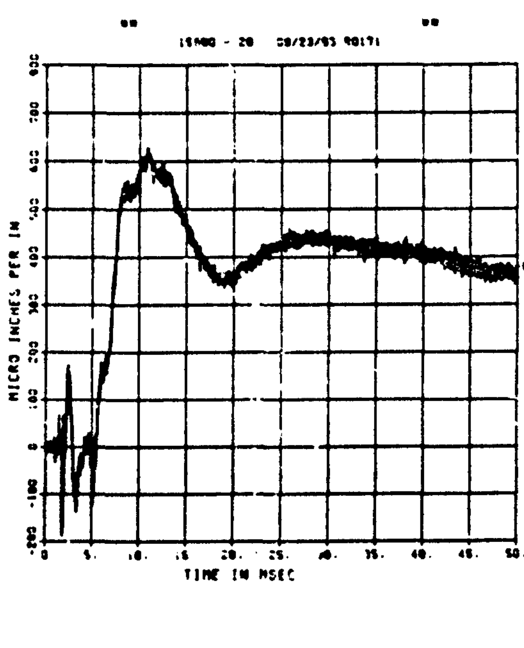

FEMA ELEM TEST D-1
LC-1
200000. HZ CAL= 119829.

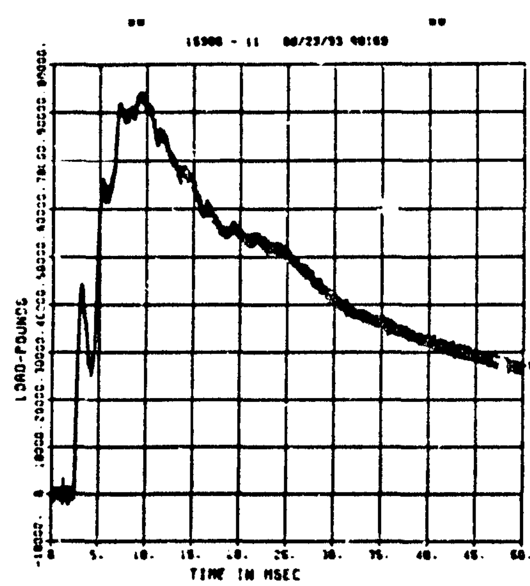

FEMA ELEM TEST D-1
LC-2
200000. HZ CAL= 135527.

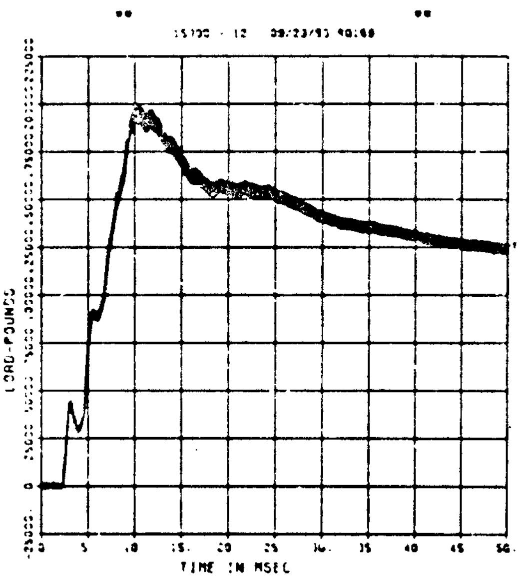

** PEAK VALUE IS 47 % OVER CALIBRATION **

FEMA ELEM TEST D-2
BP-1
50000. HZ CAL= 992.0
LP4/4 70% CUTOFF= 2250. HZ

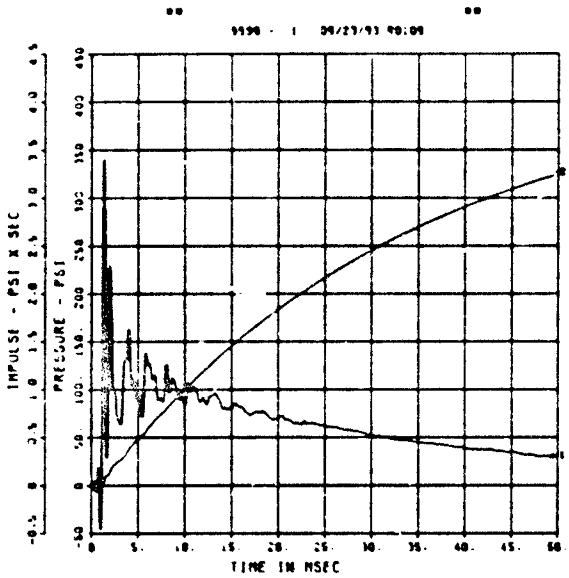

FEMA ELEM TEST D-2
BP-4
50000. HZ CAL= 1048.
LP4/4 70% CUTOFF= 2250. HZ

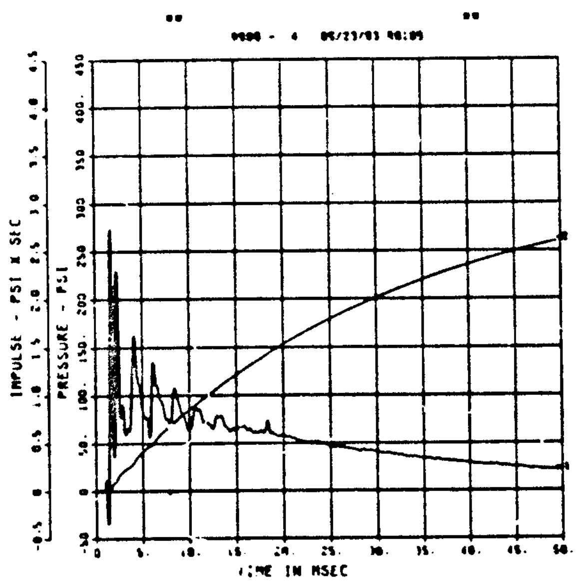

FEMA ELEM TEST D-2
SE-1
200000. HZ CAL= 339.2

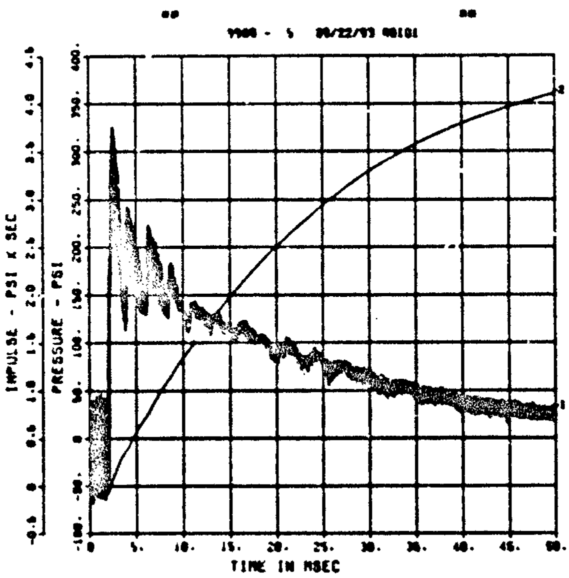

FEMA ELEM TEST D-2
SE-2
50000. HZ CAL= 130.9
LP4/4 70% CUTOFF= 2250. HZ

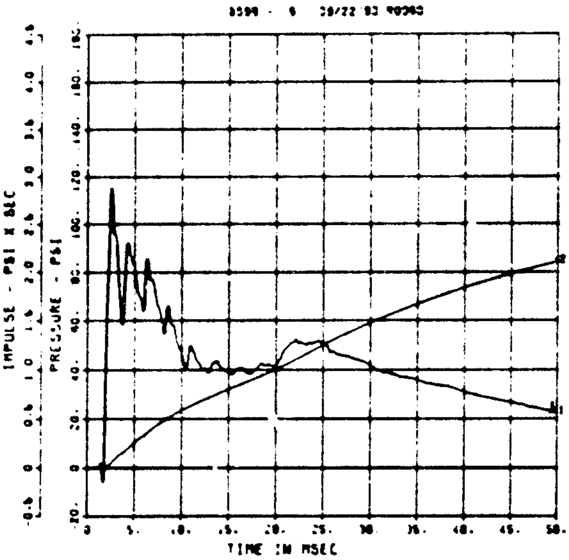

FEMA ELEM TEST D-2
SE-3
50000. HZ CAL= 257.8
LP4/4 70% CUTOFF= 2250. HZ

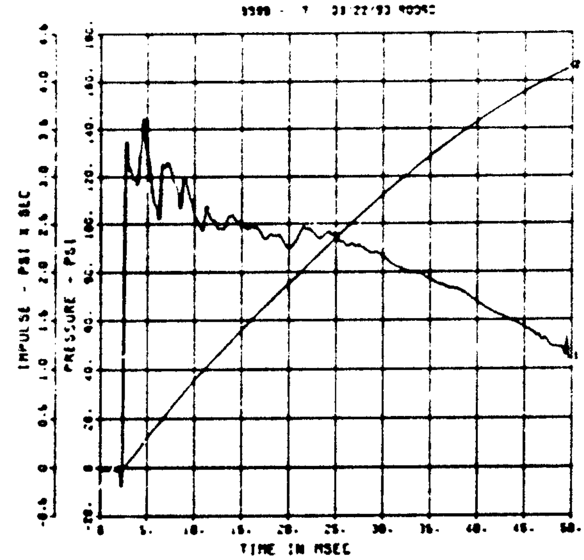

FEMA ELEM TEST D-2
SE-4
50000. HZ CAL= 252.7
LP4/4 70% CUTOFF= 2250. HZ

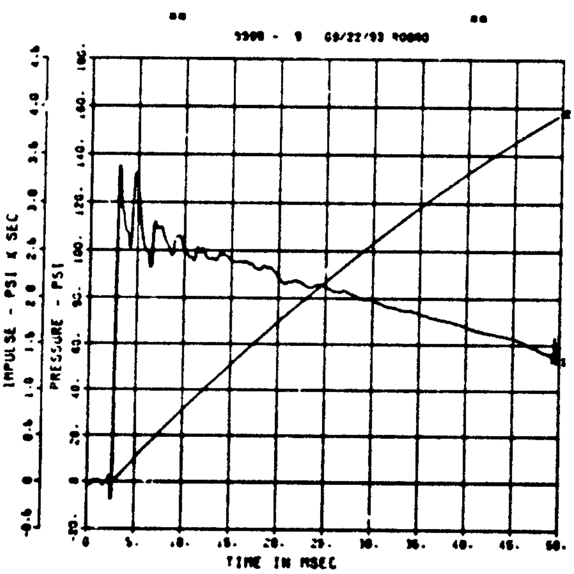

FEMA ELEM TEST D-2
SE-5
50000. HZ CAL= 194.9
LP4/4 70% CUTOFF= 2250. HZ

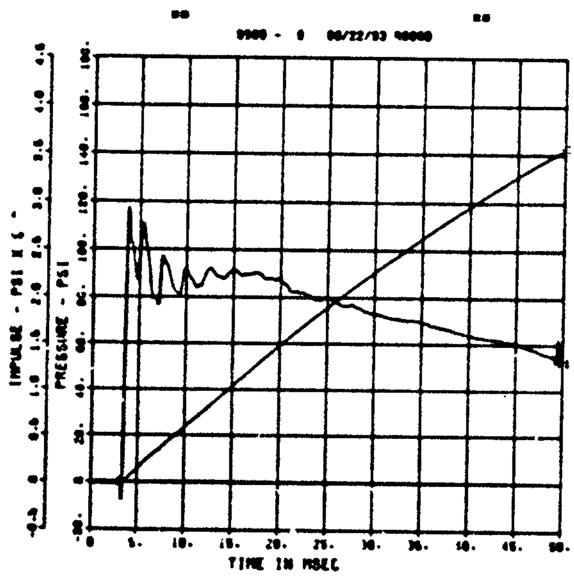

FEMA ELEM TEST D-2
SE-6
50000. HZ CAL= 249.0
LP4/4 70% CUTOFF= 2250. HZ

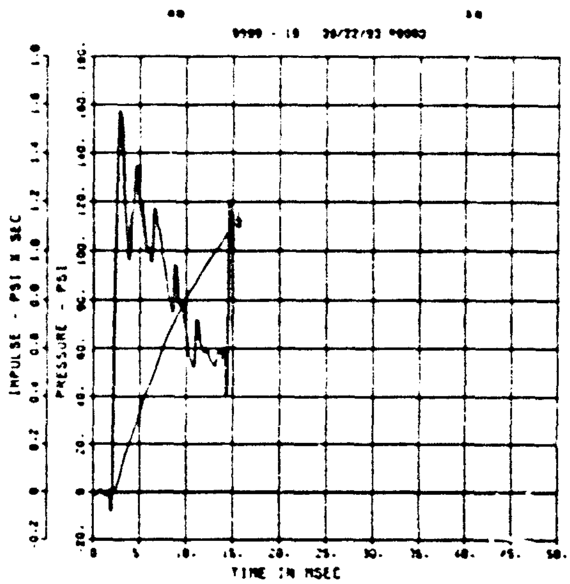

FEMA ELEM TEST D-2
SE-7
50000. HZ CAL= 122.6
LP4/4 70% CUTOFF= 2250. HZ

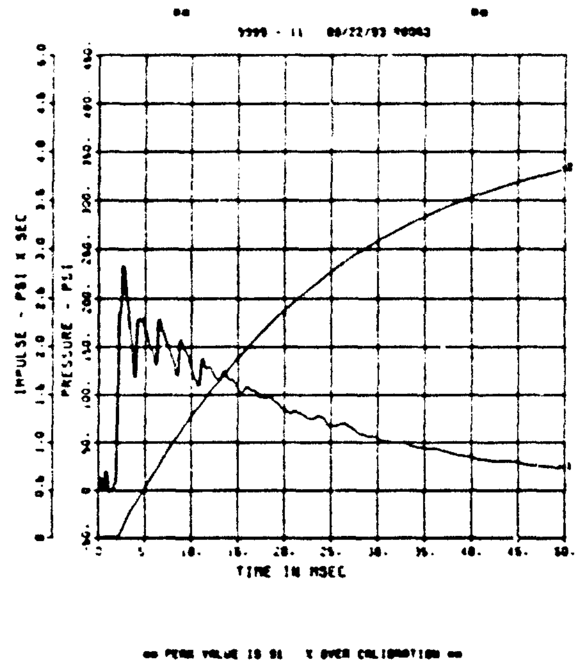

FEMA ELEM TEST D-2
AFF-1
200000. HZ CAL= 1137.

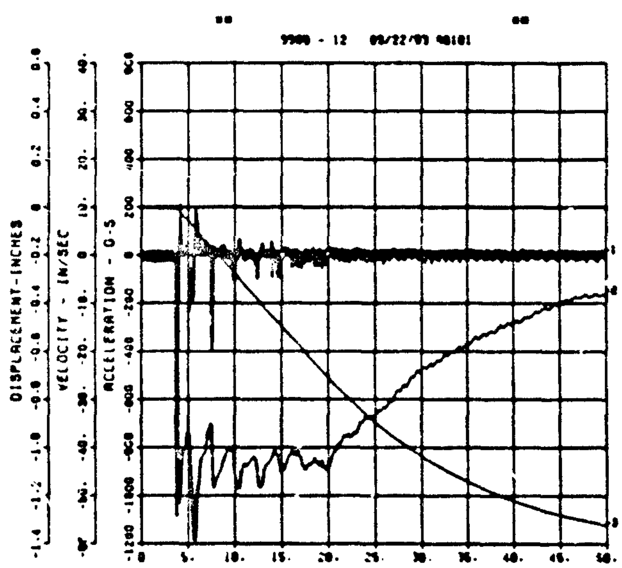

FEMA ELEM TEST D-2
A-2
200000. HZ CAL= 1230.

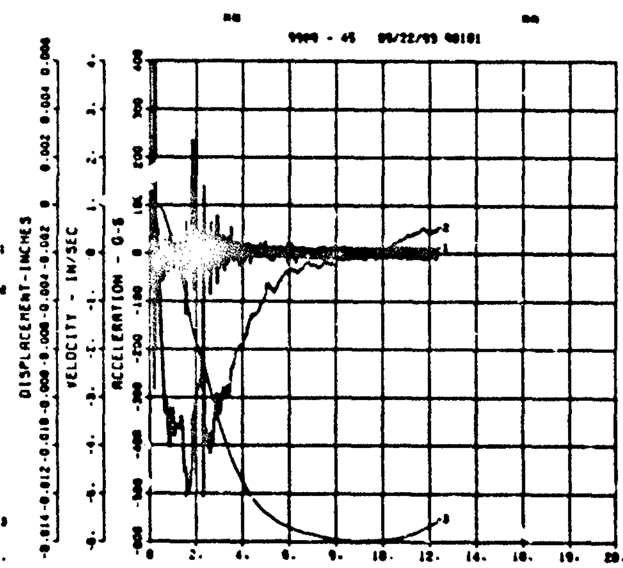

FEMA ELEM TEST D-2
IF-6
50000. HZ CAL= 215.3
LP4/4 70% CUTOFF= 2250. HZ

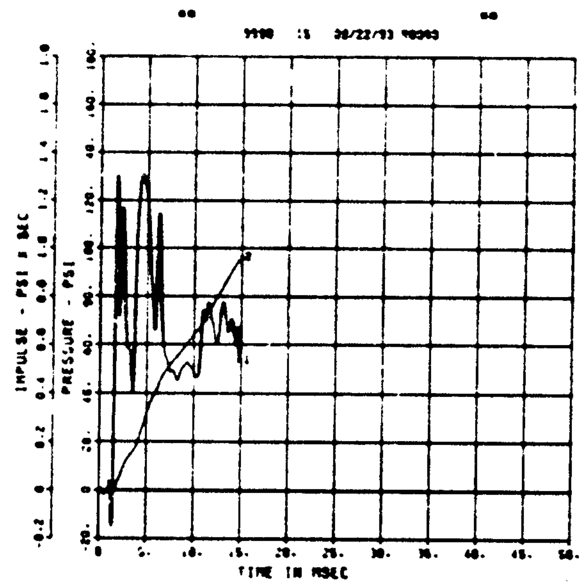

FEMA ELEM TEST D-2
IF-9
200000. HZ CAL= 129.1
LP4/3 70% CUTOFF= 9000. HZ

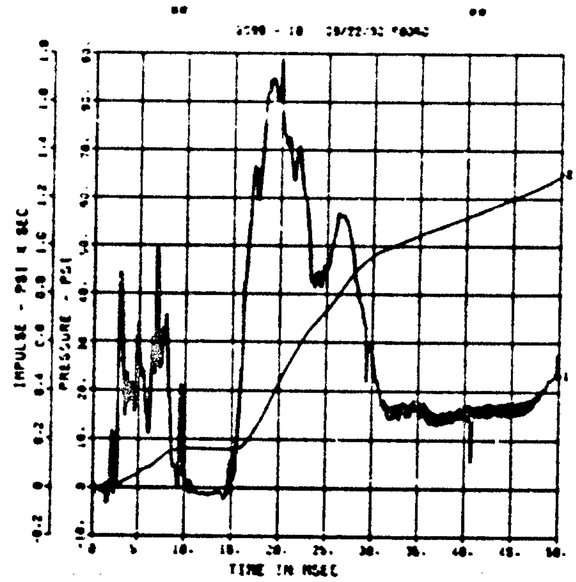

FEMA ELEM TEST D-2
IF-11
50000. HZ CAL= 165.8
LP4/4 70% CUTOFF= 2250. HZ

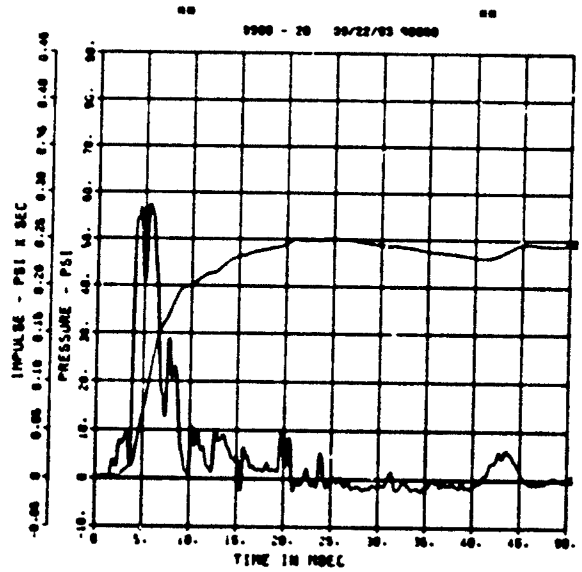

FEMA ELEM TEST D-2
IF-12
50000. HZ CAL= 166.7
LP4/4 70% CUTOFF= 2250. HZ

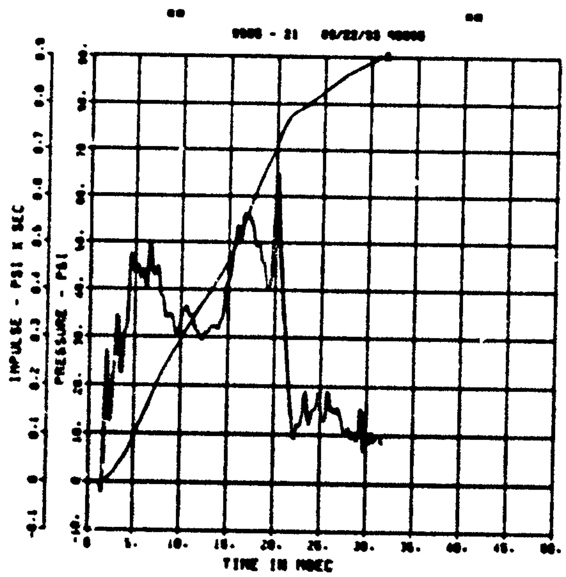

FEMA ELEM TEST D-2
IF-16
50000. HZ CAL= 345.3
LP4/4 70% CUTOFF= 2250. HZ

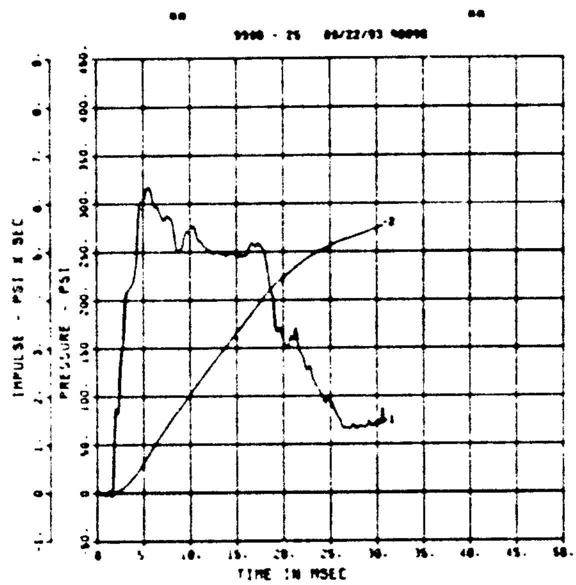

FEMA ELEM TEST D-2
EO-1
200000. HZ CAL= 39162.

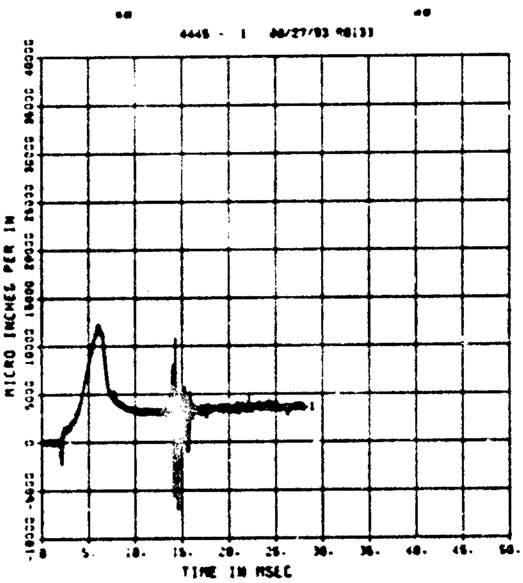

FEMA ELEM TEST D-2
EI-1
200000. HZ CAL= 39162.

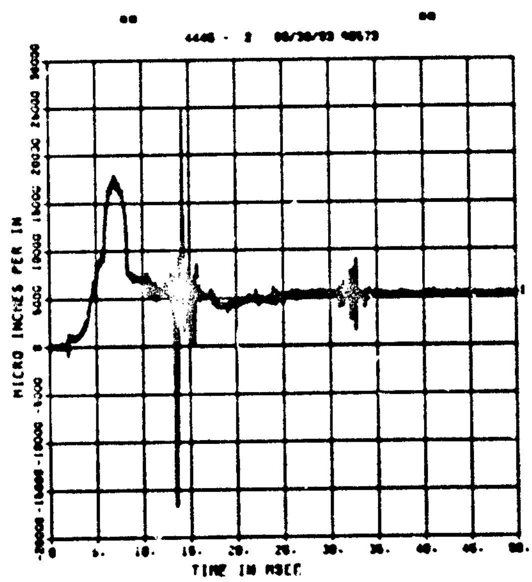

FEMA ELEM TEST D-2
EO-2
200000. HZ CAL= 39162.
LP4/0 70% CUTOFF= 9000. HZ

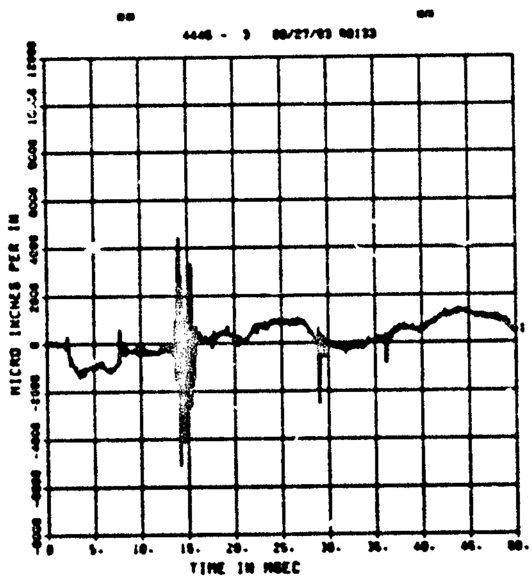

** PEAK VALUE IS 87 % UNDER CALIBRATION **

FEMA ELEM TEST D-2
EI-2
200000. HZ CAL= 39162.
LP4/0 70% CUTOFF= 9000. HZ

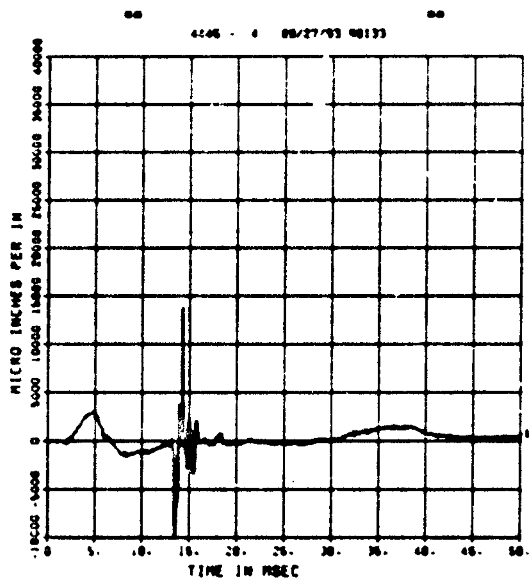

FEMA ELEM TEST D-2
EO-3
200000. HZ CAL= 39162.
LP4/0 70% CUTOFF= 9000. HZ

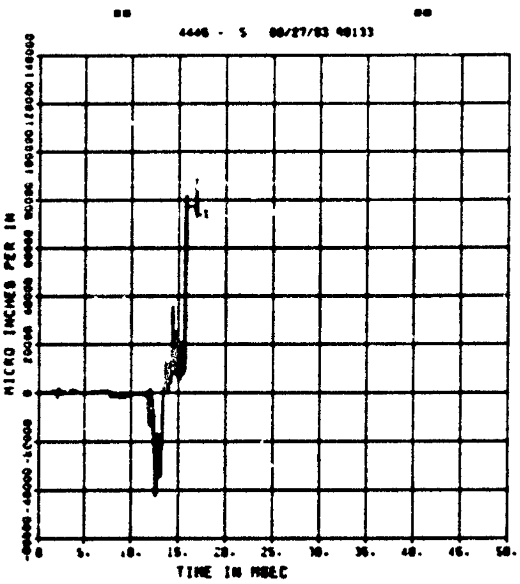

** PEAK VALUE IS 127 % OVER CALIBRATION **

FEMA ELEM TEST D-2
EO-4
200000. HZ CAL= 39162.

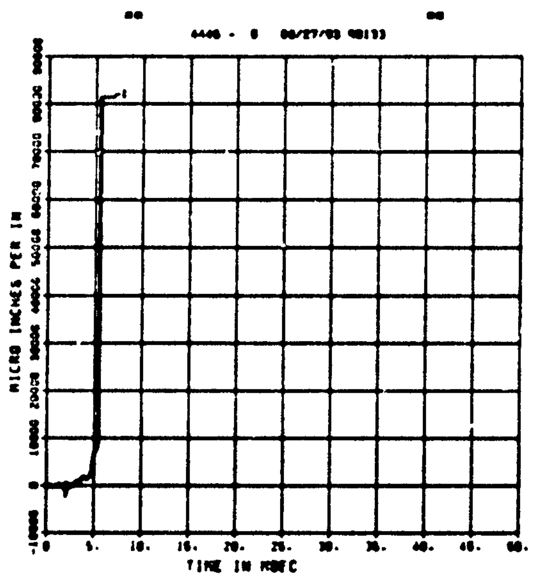

** PEAK VALUE IS 100 % OVER CALIBRATION **

FEMA ELEM TEST D-2
EO-5
200000. HZ CAL= 20205.
LP4/0 70% CUTOFF= 9000. HZ

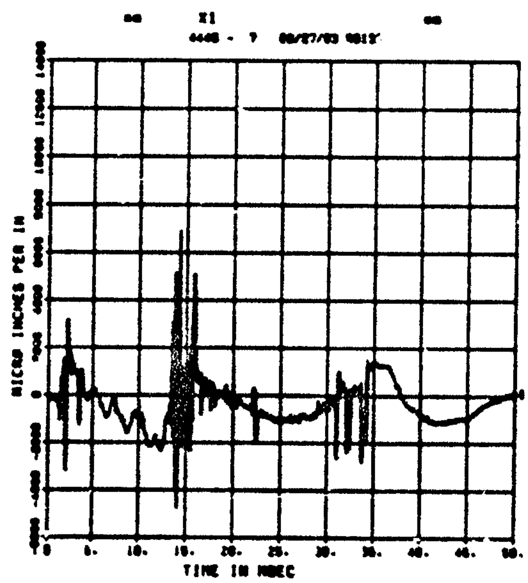

FEMA ELEM TEST D-2
EI-5
200000. HZ CAL= 20205.

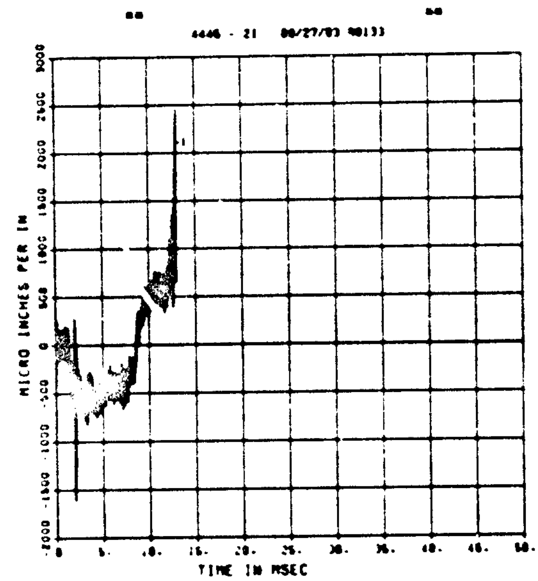

** PEAK VALUE IS 08 % UNDER CALIBRATION **

FEMA ELEM TEST D-2
EO-6
200000. HZ CAL= 10276.

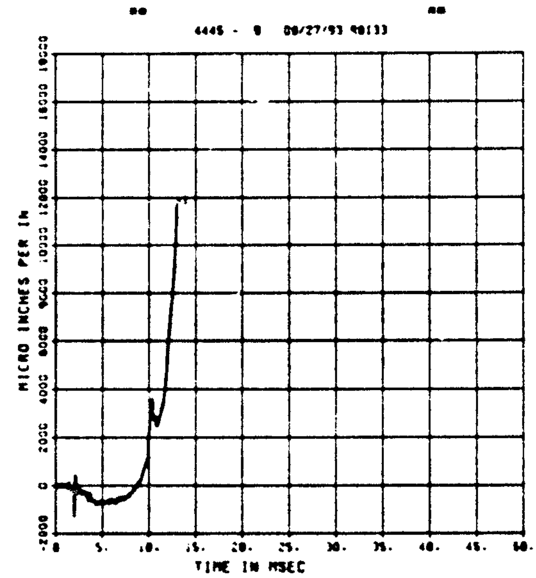

** PEAK VALUE IS 14 % OVER CALIBRATION **

FEMA ELEM TEST D-2
EI-6
200000. HZ CAL= 10276.
LP4/0 70% CUTOFF= 9000. HZ

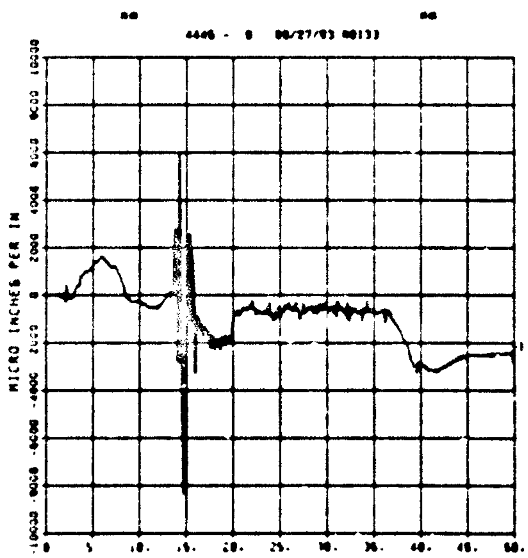

FEMA ELEM TEST D-2
EO-7
50000. HZ CAL= 10276.
LP4/4 70% CUTOFF= 2250. HZ

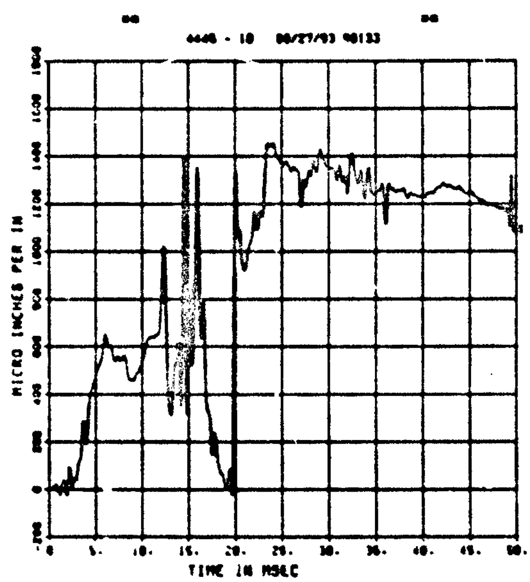

** PEAK VALUE IS 08 % UNDER CALIBRATION **

FEMA ELEM TEST D-2
EI-7
200000. HZ CAL= 10276.
LP4/0 70% CUTOFF= 9000. HZ

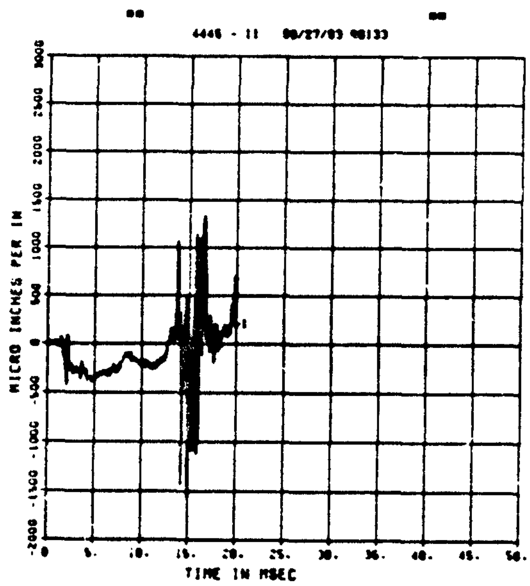

FEMA ELEM TEST D-2
EO-8
200000. HZ CAL= 39162.
LP4/0 70% CUTOFF= 9000. HZ

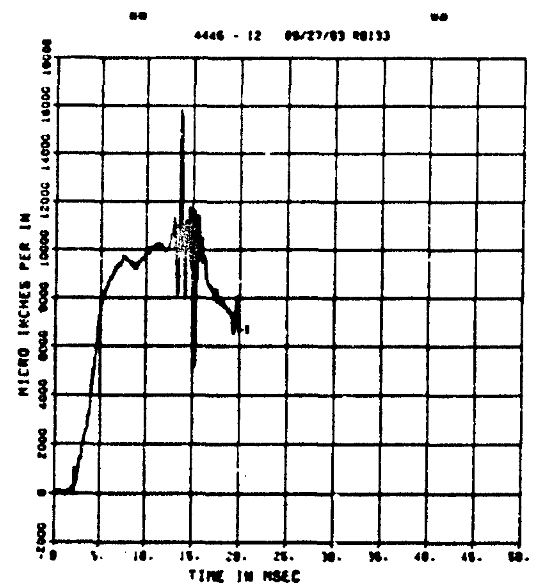

** PEAK VALUE IS 95 % UNDER CALIBRATION **

FEMA ELEM TEST D-2
EI-8
200000. HZ CAL= 39162.
LP4/0 70% CUTOFF= 9000. HZ

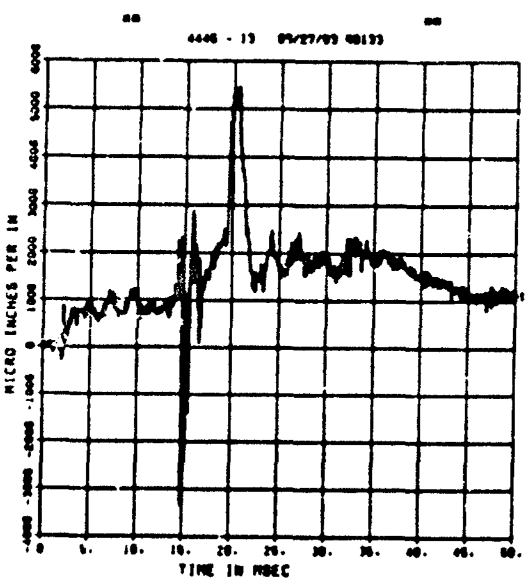

FEMA ELEM TEST D-2
EO-9
200000. HZ CAL= 20205.
LP4/0 70% CUTOFF= 9000. HZ

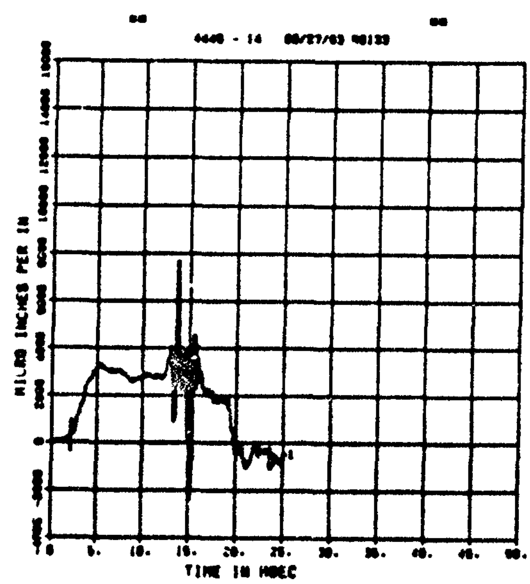

** PEAK VALUE IS 95 % UNDER CALIBRATION **

FEMA ELEM TEST D-2
EI-9
200000. HZ CAL= 20205.
LP4/0 70% CUTOFF= 9000. HZ

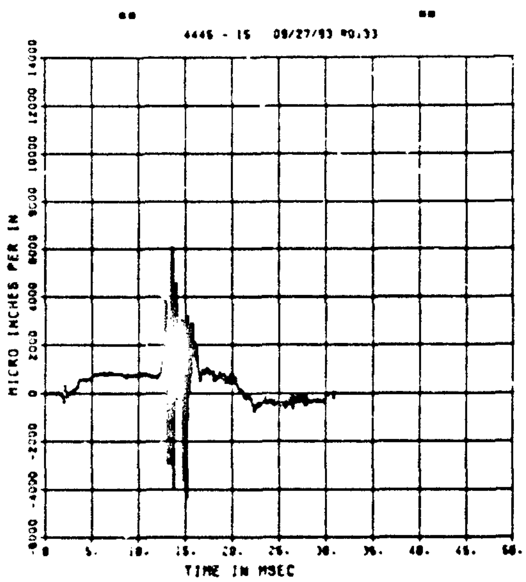

FEMA ELEM TEST D-2
EO-10
200000. HZ CAL= 20205.
LP4/0 70% CUTOFF= 9000. HZ

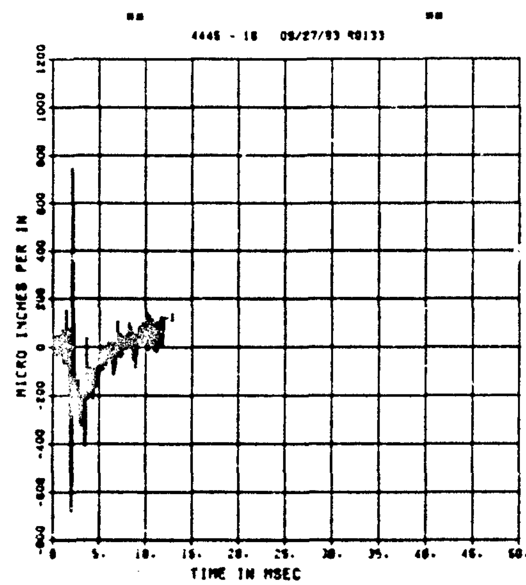

FEMA ELEM TEST D-2
EI-10
200000. HZ CAL= 20205.
LP4/0 70% CUTOFF= 9000. HZ

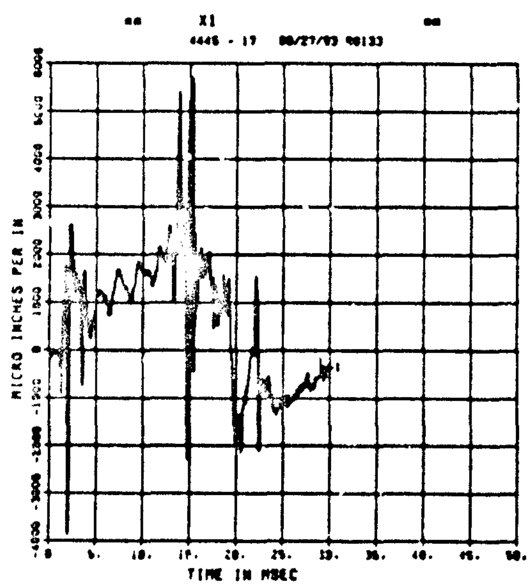

FEMA ELEM TEST D-2
EO-11
50000. HZ CAL= 39162.
LP4/4 70% CUTOFF= 2250. HZ

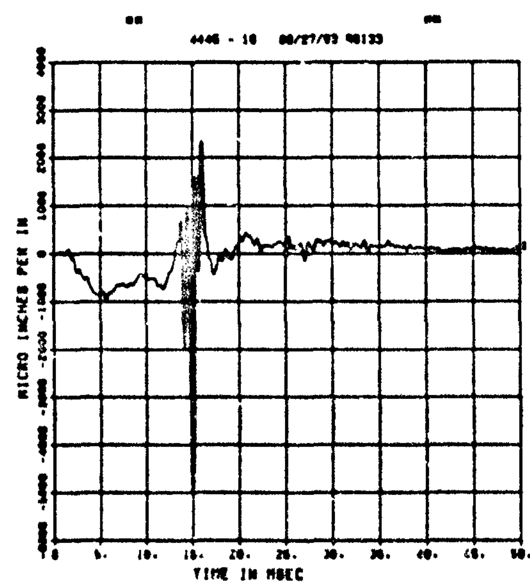

FEMA ELEM TEST D-2
EI-11
50000. HZ CAL= 39162.
LP4/4 70% CUTOFF= 2250. HZ

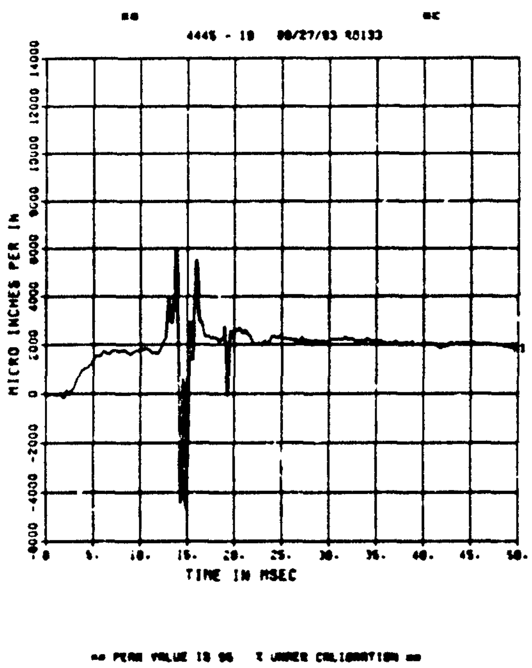

FEMA ELEM TEST D-3
BP-1
200000. HZ CAL= 291.3

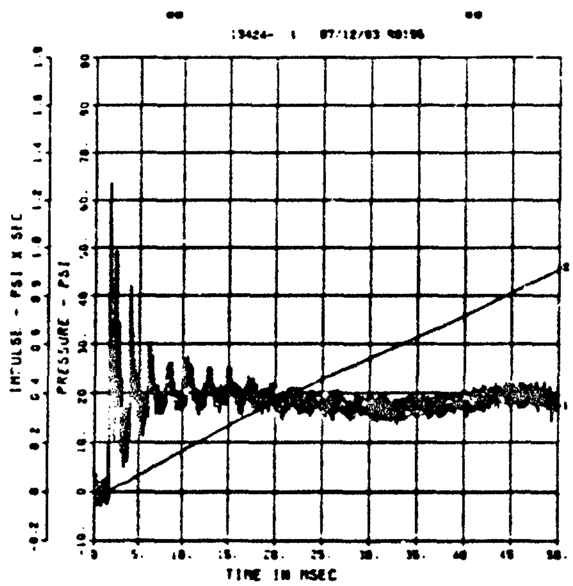

FEMA ELEM TEST D-3
BP-3
200000. HZ CAL= 224.9

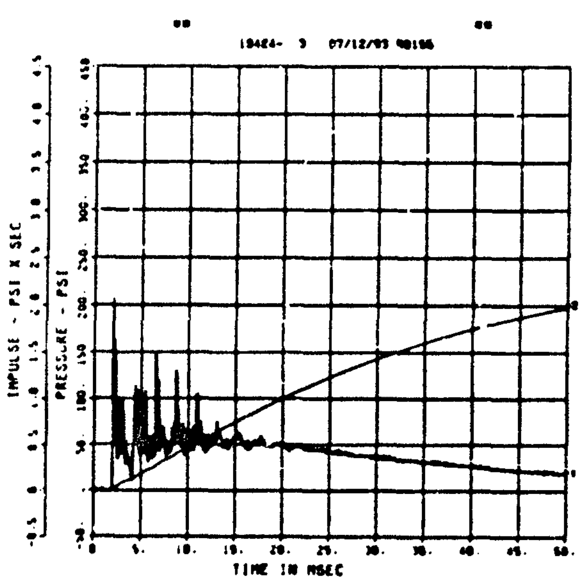

FEMA ELEM TEST D-3
BP-4
200000. HZ CAL= 284.1

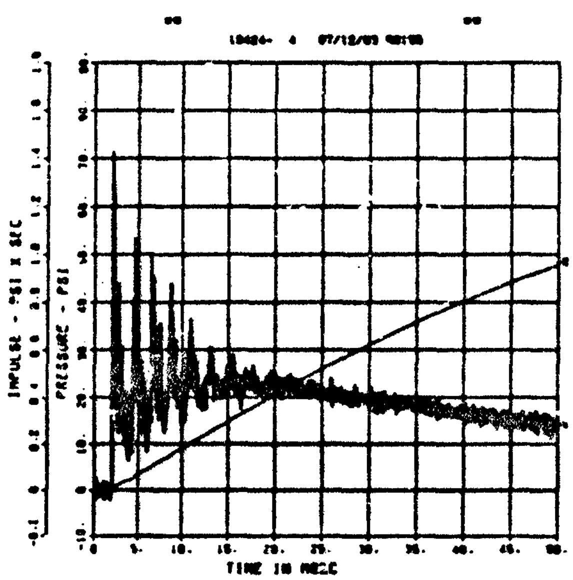

FEMA ELEM TEST D-3
SE-1
200000. HZ CAL= 191.5

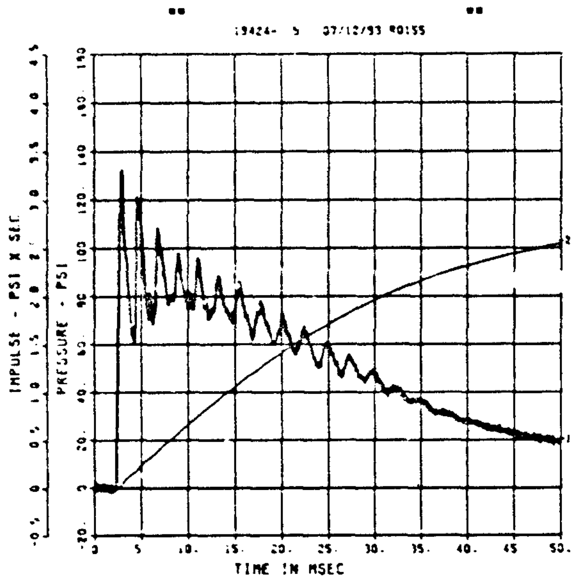

FEMA ELEM TEST D-3
SE-2
200000. HZ CAL= 130.9

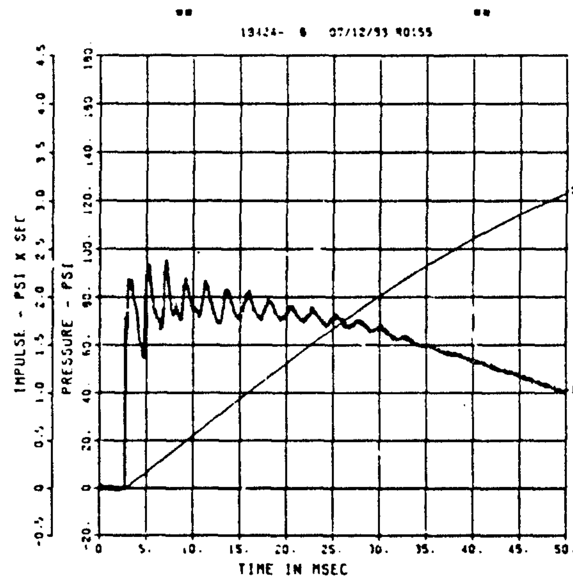

FEMA ELEM TEST D-3
SE-3
200000. HZ CAL= 198.2

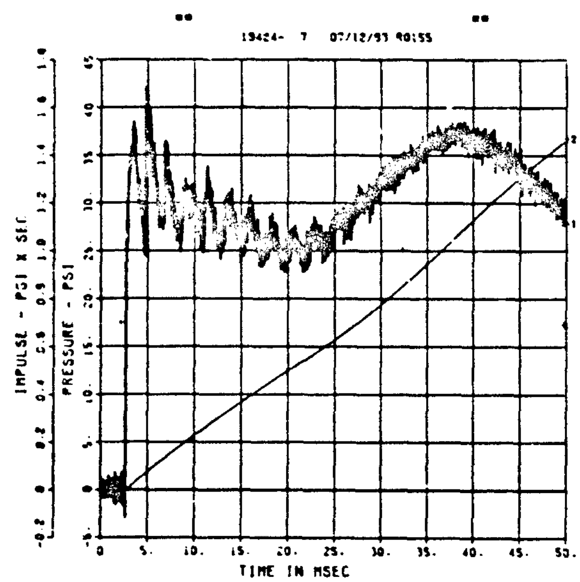

FEMA ELEM TEST D-3
SE-4
200000. HZ CAL= 81.60

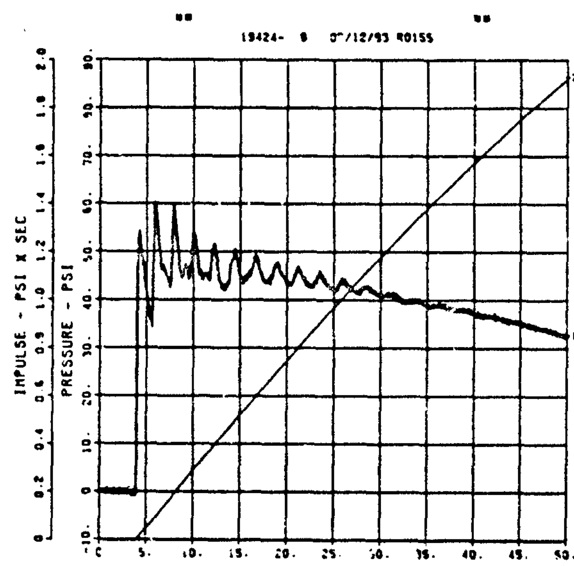

FEMA ELEM TEST D-3
SE-5
200000. HZ CAL= 81.80

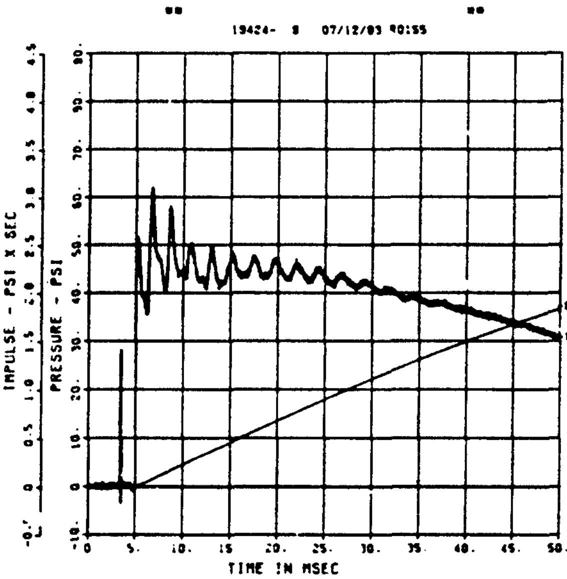

FEMA ELEM TEST D-3
SE-6
200000. HZ CAL= 196.2

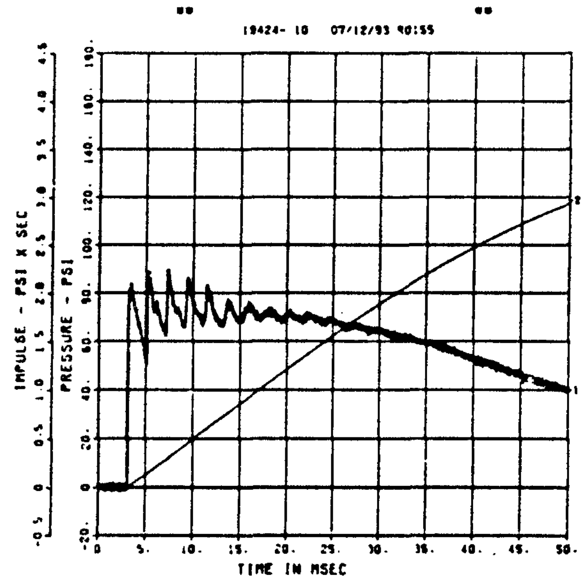

FEMA ELEM TEST D-3
SE-7
200000. HZ CAL= 75.50

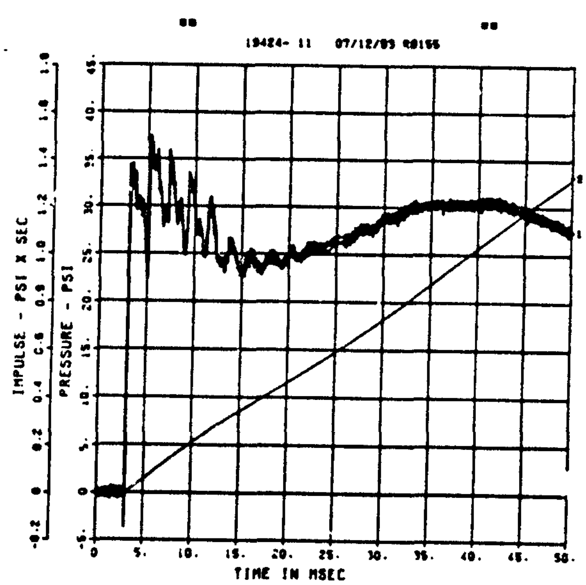

FEMA ELEM TEST D-3
AFF-1
200000. HZ CAL= 103.7

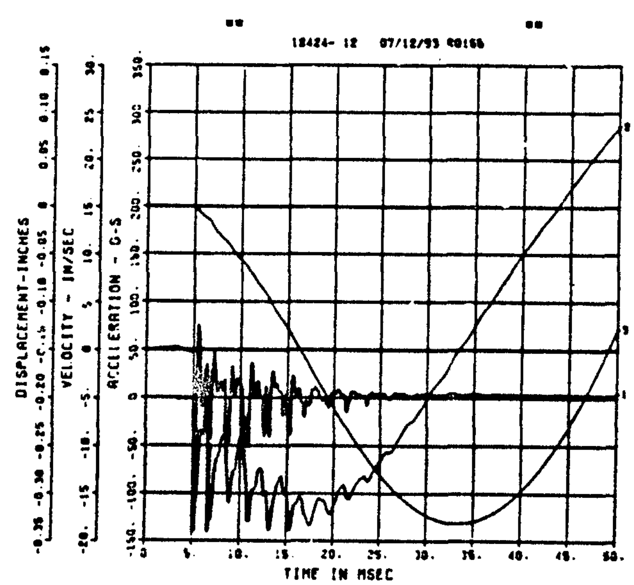

** PEAK VALUE IS 36 % OVER CALIBRATION **

FEMA ELEM TEST D-3
A-1
200000. HZ CAL= 186.7

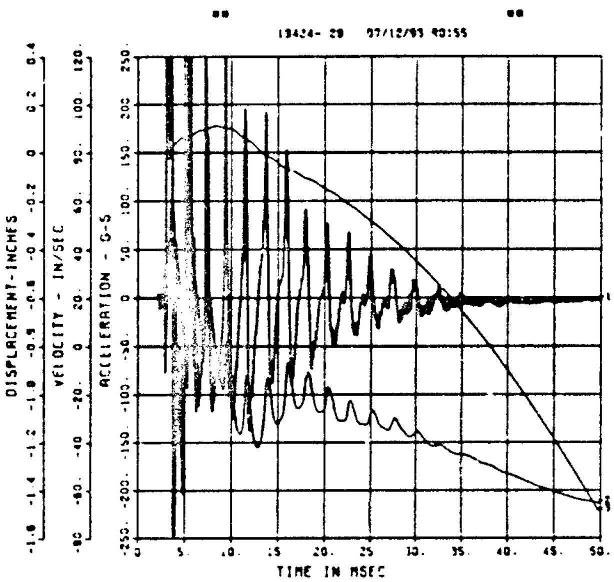

** PEAK VALUE IS 33 % OVER CALIBRATION **

FEMA ELEM TEST D-3
A-2
200000. HZ CAL= 104.6

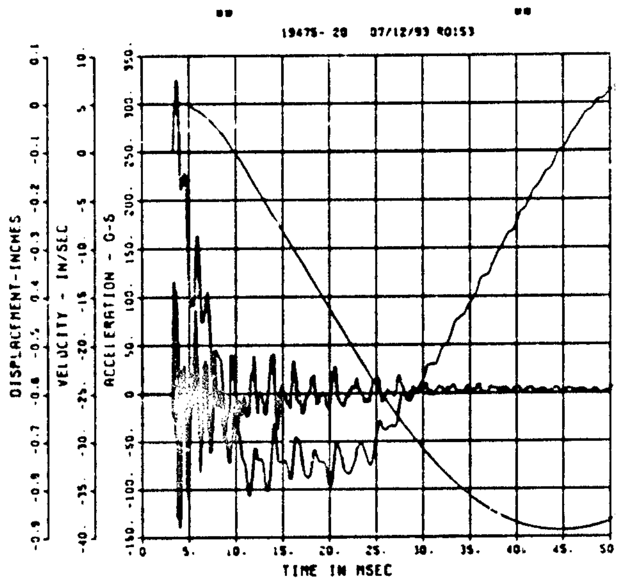

** PEAK VALUE IS 33 % OVER CALIBRATION **

FEMA ELEM TEST D-3
IF-1
200000. HZ CAL= 246.2

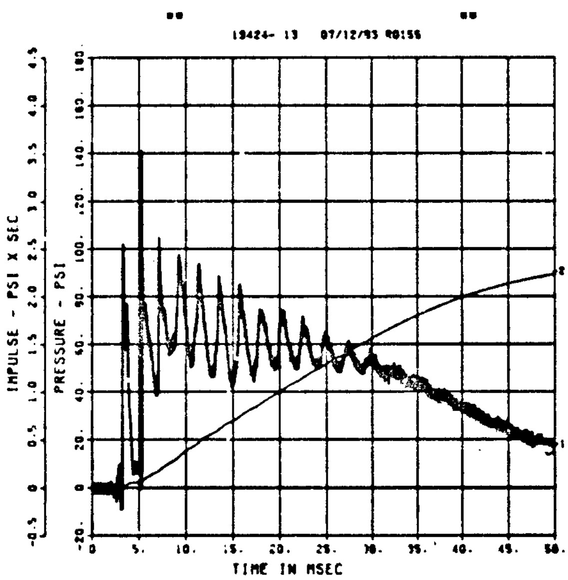

FEMA ELEM TEST D-3
IF-2
200000. HZ CAL= 246.7

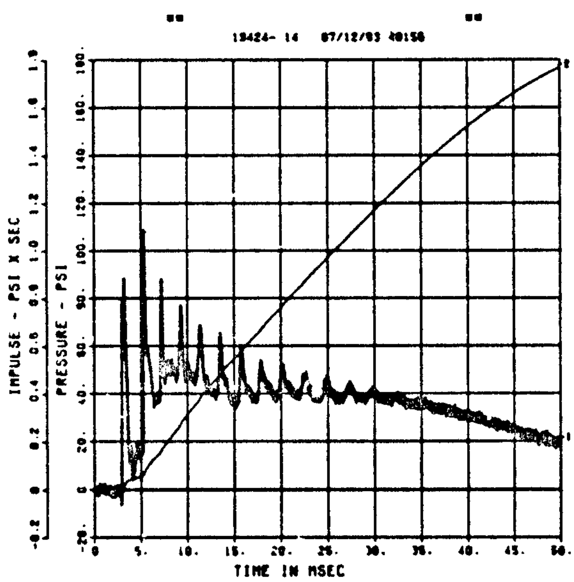

FEMA ELEM TEST D-3
IF-3
200000. HZ   CAL= 247.0

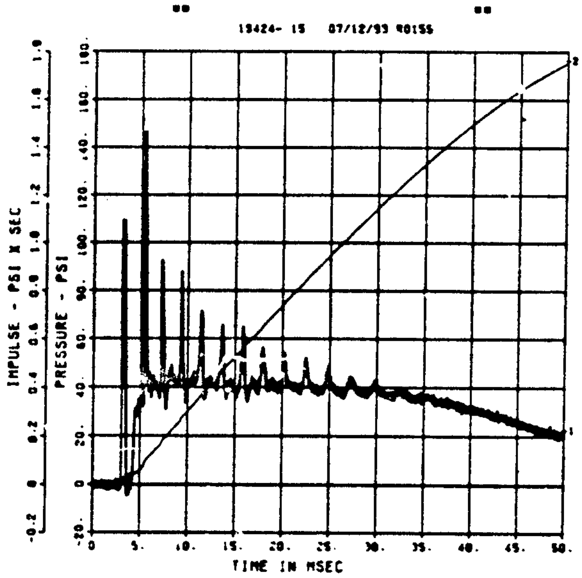

FEMA ELEM TEST D-3
IF-4
200000. HZ   CAL= 245.7

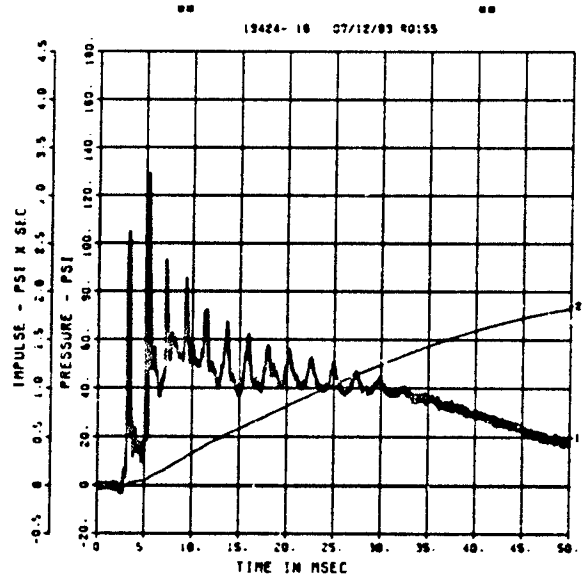

FEMA ELEM TEST D-3
IF-5
200000. HZ   CAL= 253.5

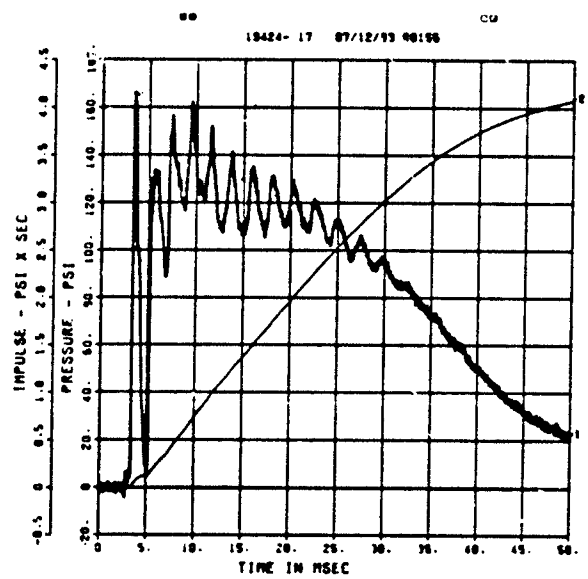

FEMA ELEM TEST D-3
IF-6
200000. HZ   CAL= 109.8

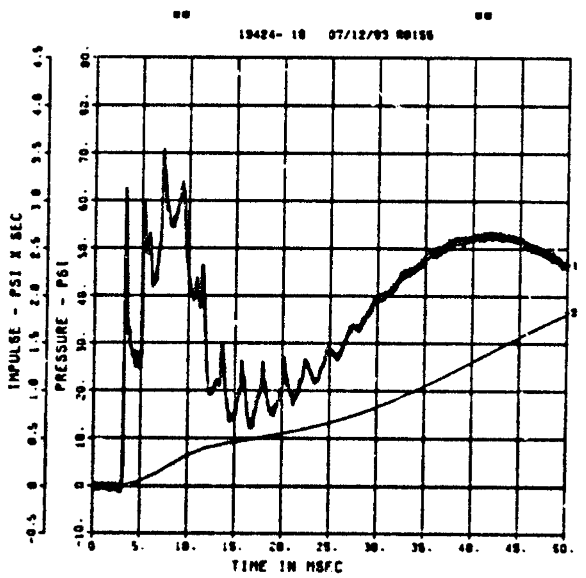

FEMA ELEM TEST D-3
IF-7
200000. HZ CAL= 128.5

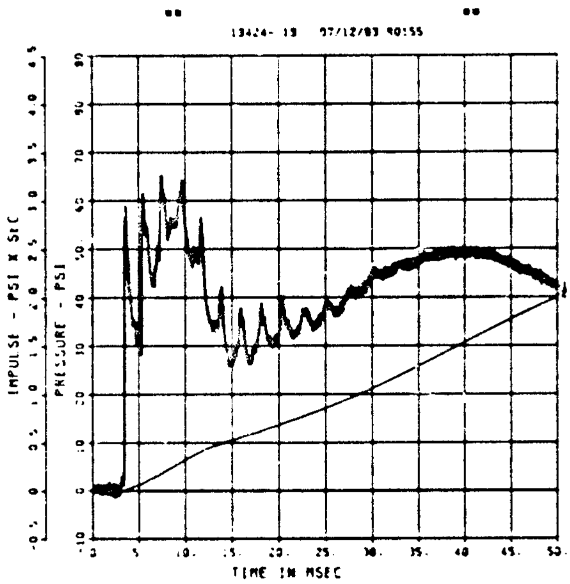

FEMA ELEM TEST D-3
IF-8
200000. HZ CAL= 85.40

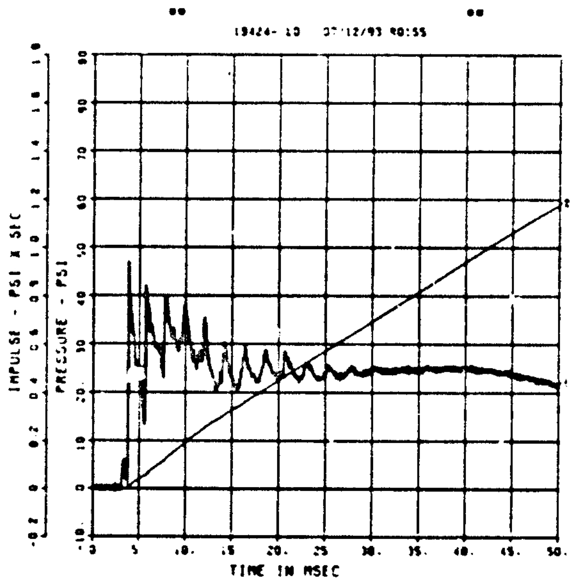

FEMA ELEM TEST D-3
IF-9
200000. HZ CAL= 84.10

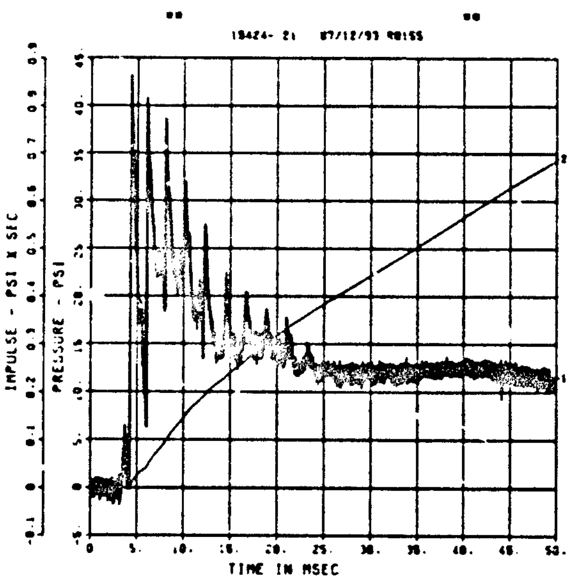

FEMA ELEM TEST D-3
IF-10
200000. HZ CAL= 51.70

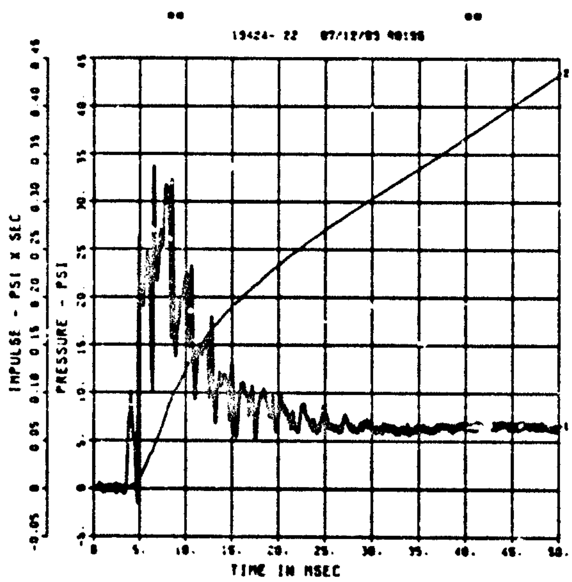

FEMA ELEM TEST D-3
IF-11
200000. HZ CAL= 52.80

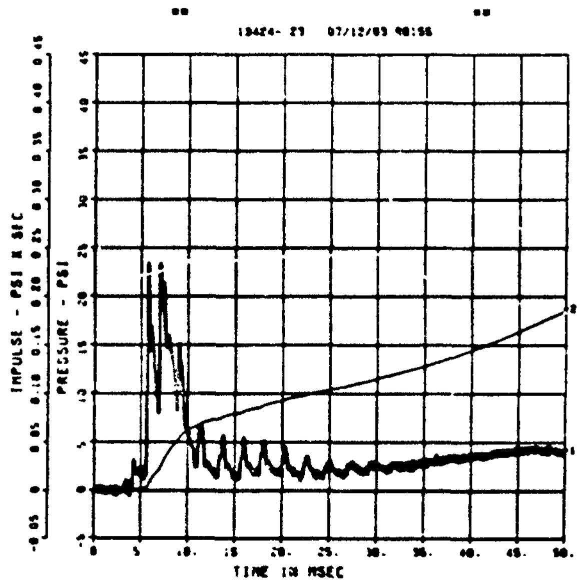

FEMA ELEM TEST D-3
IF-12
200000. HZ CAL= 124.4

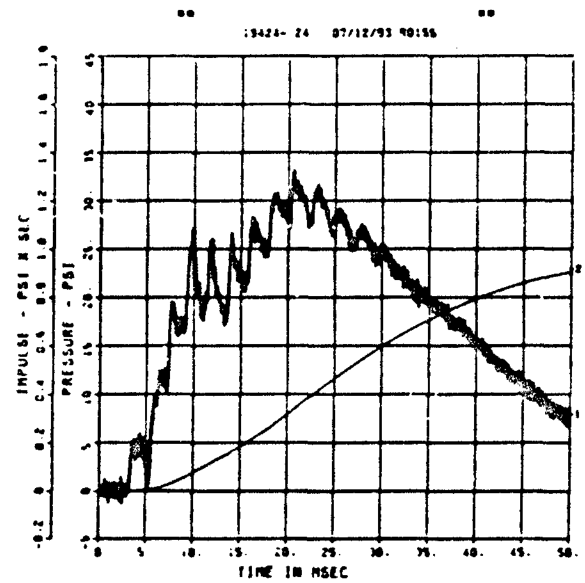

FEMA ELEM TEST D-3
IF-13
200000. HZ CAL= 125.9
LP4/0 70% CUTOFF= 9000. HZ

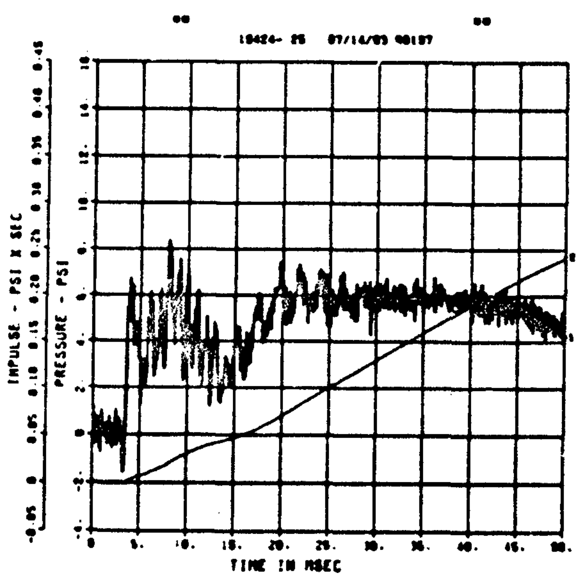

FEMA ELEM TEST D-3
IF-15
200000. HZ CAL= 124.8

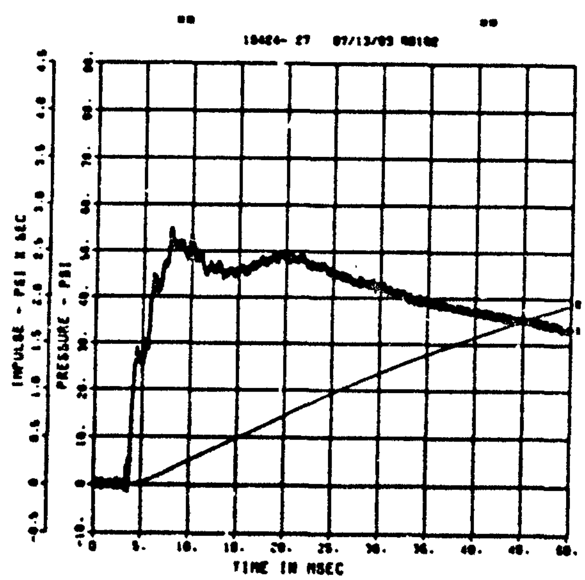

FEMA ELEM TEST D-3
IF-16
200000. HZ CAL= 126.1

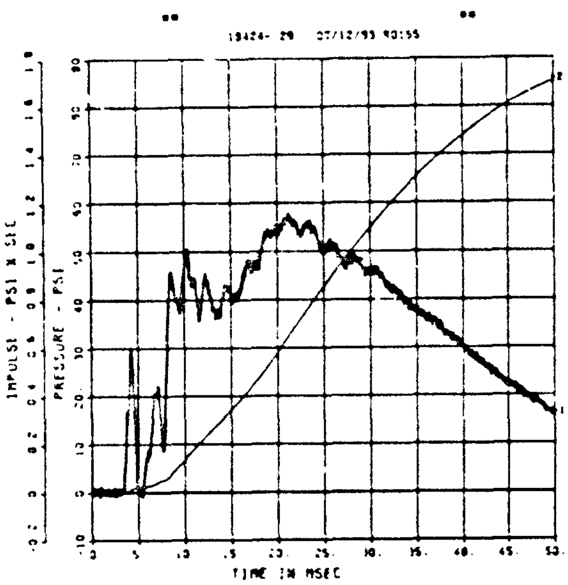

FEMA ELEM TEST D-3
EO-1
200000. HZ CAL= 20205.
LP4/0 70% CUTOFF= 9000. HZ

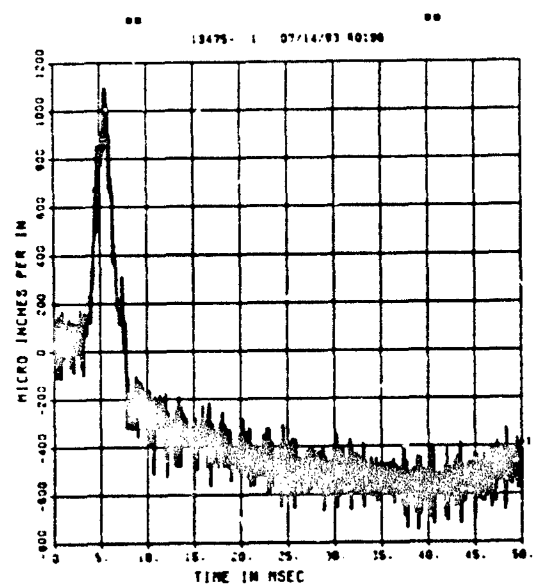

FEMA ELEM TEST D-3
EI-1
200000. HZ CAL= 20205.
LP4/0 70% CUTOFF= 9000. HZ

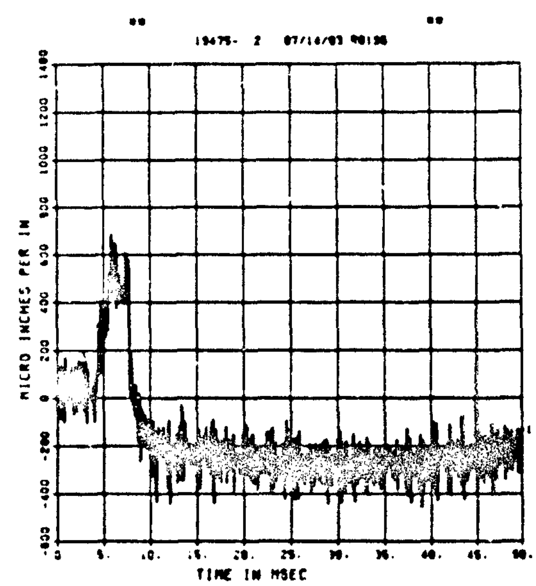

FEMA ELEM TEST D-3
EO-2
200000. HZ CAL= 20205.

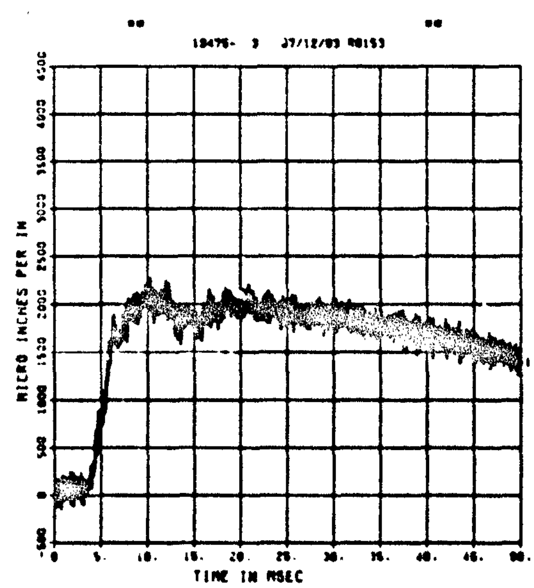

FEMA ELEM TEST D-3
EI-2
200000. HZ CAL= 20205.
LP4/0 70% CUTOFF= 9000. HZ

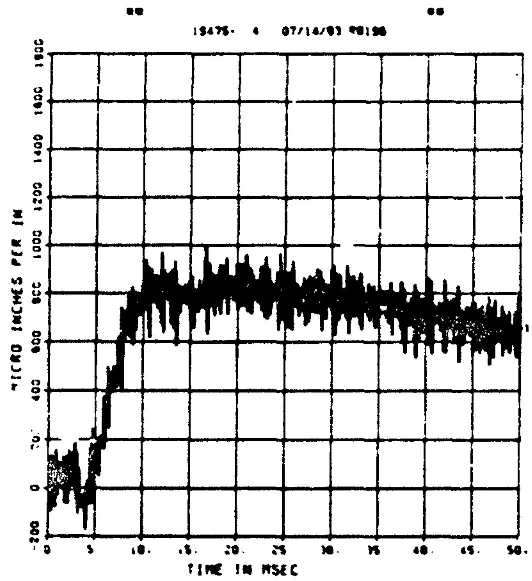

** PEAK VALUE IS 95 % UNDER CALIBRATION **

FEMA ELEM TEST D-3
EO-3
200000. HZ CAL= 10276.
LP4/0 70% CUTOFF= 9000. HZ

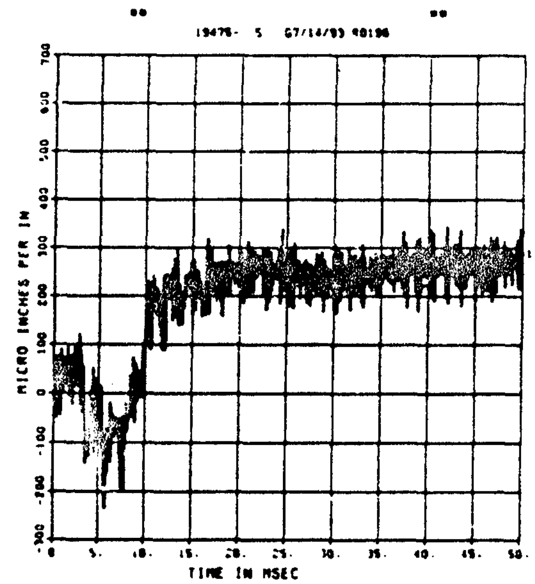

** PEAK VALUE IS 97 % UNDER CALIBRATION **

FEMA ELEM TEST D-3
EI-3
200000. HZ CAL= 10276.

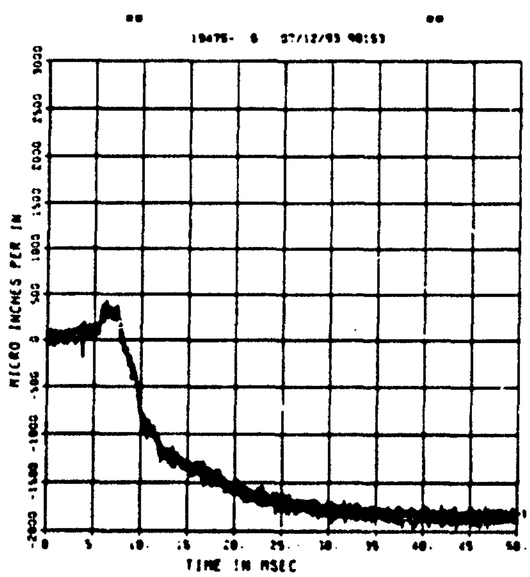

** PEAK VALUE IS 61 % UNDER CALIBRATION **

FEMA ELEM TEST D-3
EO-4
50000. HZ CAL= 20205.
LP4/4 70% CUTOFF= 2250. HZ

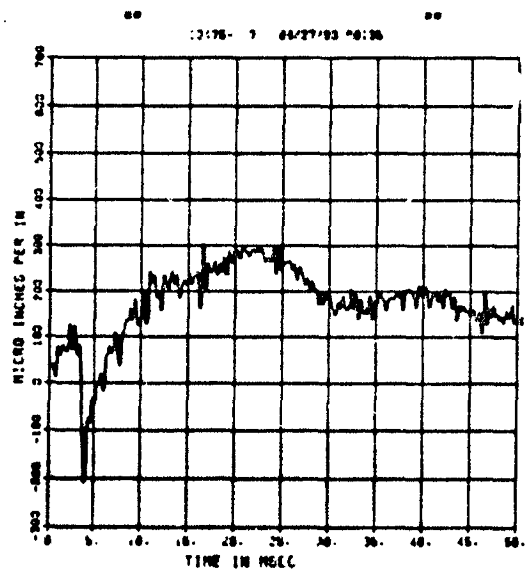

** PEAK VALUE IS 90 % UNDER CALIBRATION **

FEMA ELEM TEST D-3
E0-5
200000. HZ CAL= 20205.

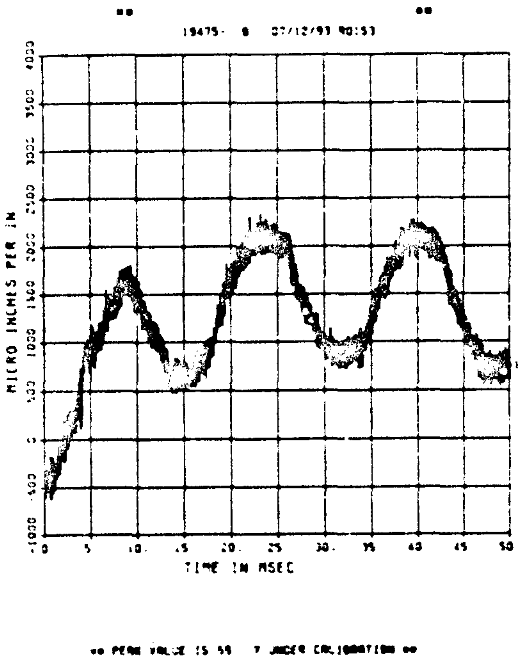

FEMA ELEM TEST D-3
EI-5
50000. HZ CAL= 20205.
LP4/4 70% CUTOFF= 2250 HZ

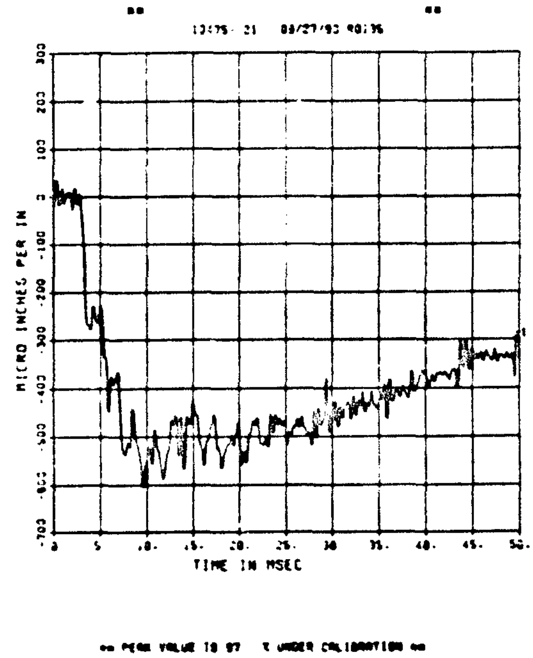

FEMA ELEM TEST D-3
E0-6
50000. HZ CAL= 20205.
LP4/4 70% CUTOFF= 2250. HZ

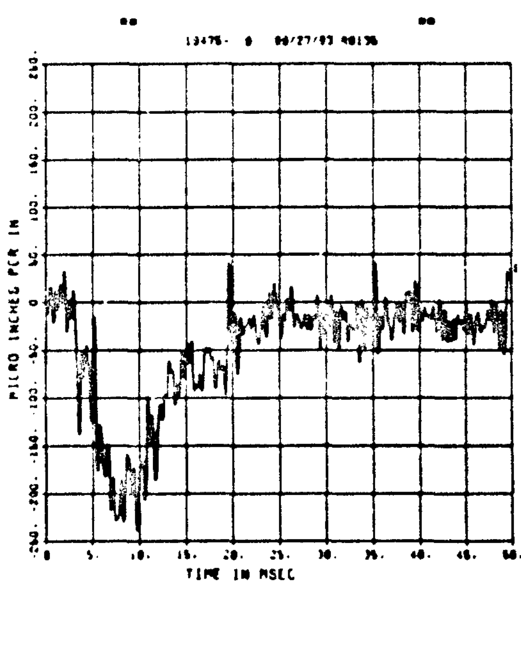

FEMA ELEM TEST D-3
EI-6
50000. HZ CAL= 20205.
LP4/4 70% CUTOFF= 2250. HZ

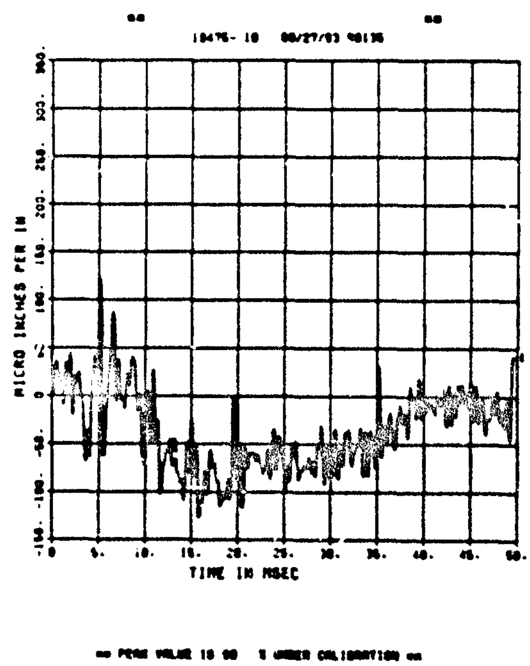

FEMA ELEM TEST D-3
EO-7
200000. HZ CAL= 10276.
LP4/0 70% CUTOFF= 9000. HZ

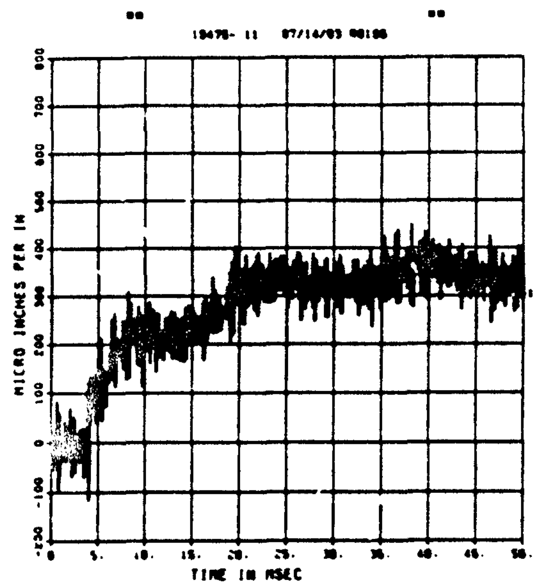

** PEAK VALUE IS 96 % UNDER CALIBRATION **

FEMA ELEM TEST D-3
EI-7
200000. HZ CAL= 10276.
LP4/0 70% CUTOFF= 9000. HZ

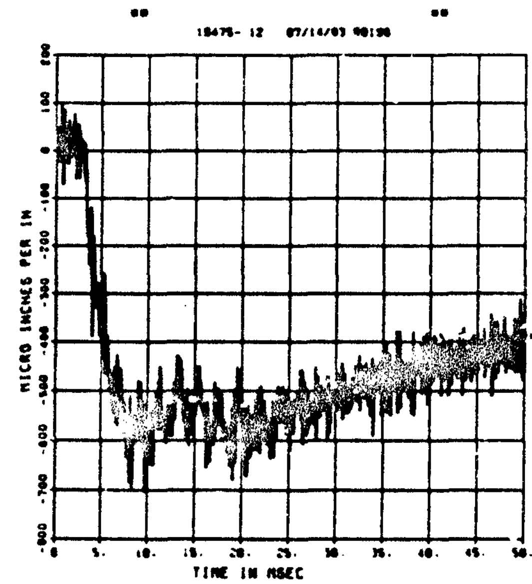

** PEAK VALUE IS 93 % UNDER CALIBRATION **

FEMA ELEM TEST D-3
EO-8
200000. HZ CAL= 10276.

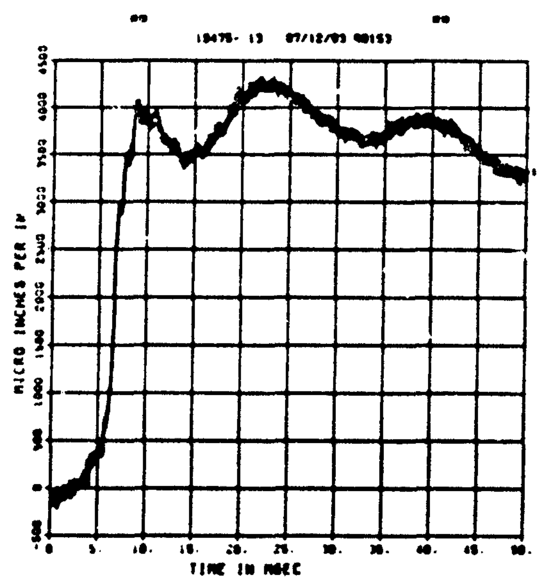

FEMA ELEM TEST D-3
EI-8
200000. HZ CAL= 10276.
LP4/0 70% CUTOFF= 9000. HZ

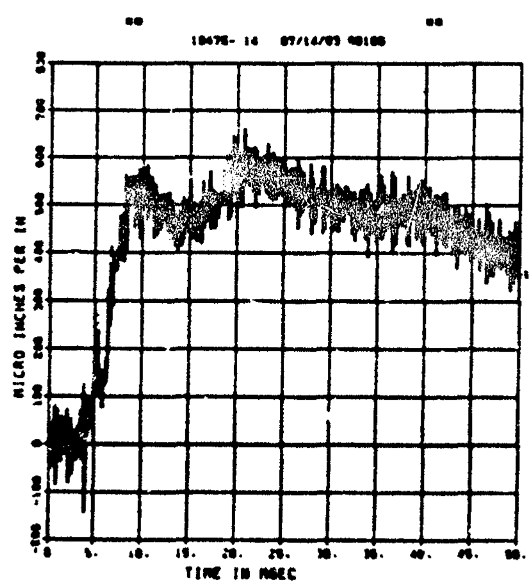

** PEAK VALUE IS 84 % UNDER CALIBRATION **

FEMA ELEM TEST D-3
EO-9
200000. HZ CAL= 10276.
LP4/0 70% CUTOFF= 9000. HZ

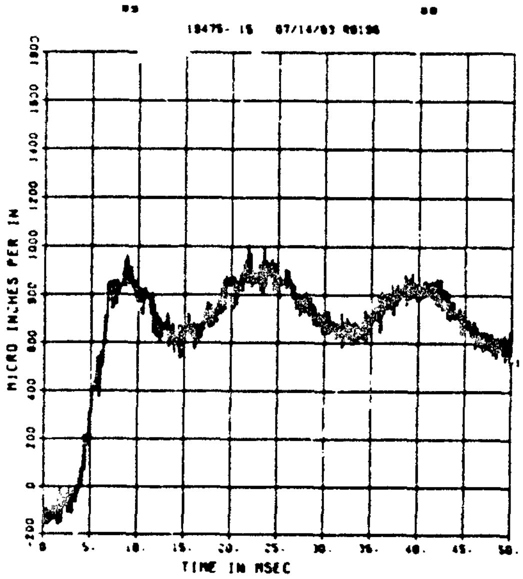

FEMA ELEM TEST D-3
EI-9
50000. HZ CAL= 10276.
LP4/4 70% CUTOFF= 2250. HZ

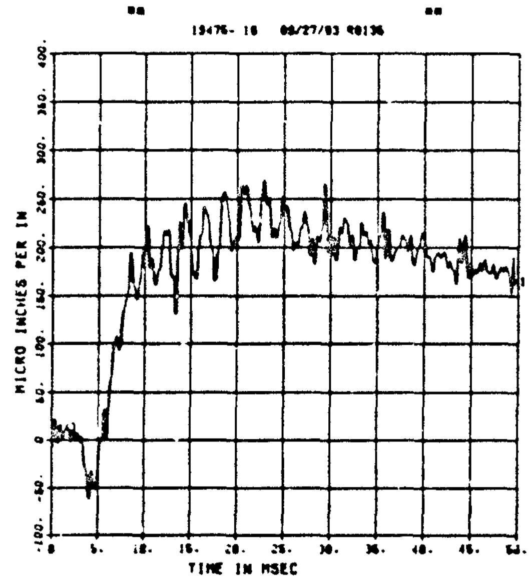

FEMA ELEM TEST D-3
EO-10
50000. HZ CAL= 10276.
LP4/4 70% CUTOFF= 2250. HZ

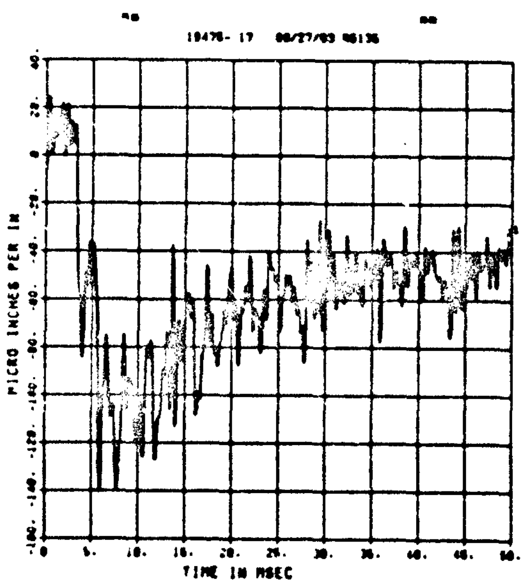

FEMA ELEM TEST D-3
EO-11
50000. HZ CAL= 10276.
LP4/4 70% CUTOFF= 2250. HZ

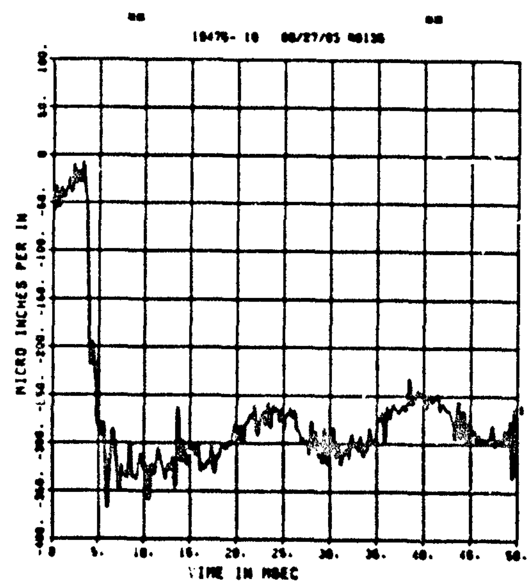

FEMA ELEM TEST D-3
EI-11
200000. HZ CAL= 10276.

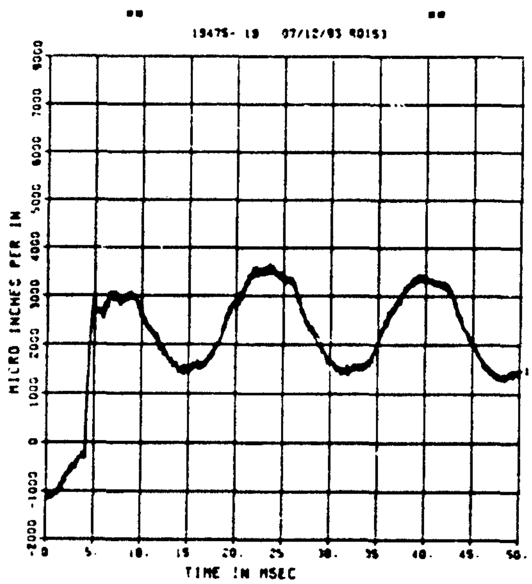

FEMA ELEM TEST D-3A
BP-1
200000. HZ CAL= 291.3

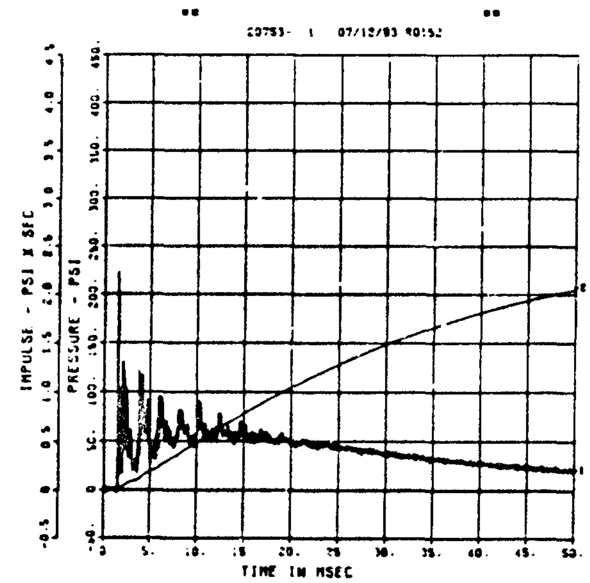

FEMA ELEM TEST D-3A
BP-3
200000. HZ CAL= 383.9

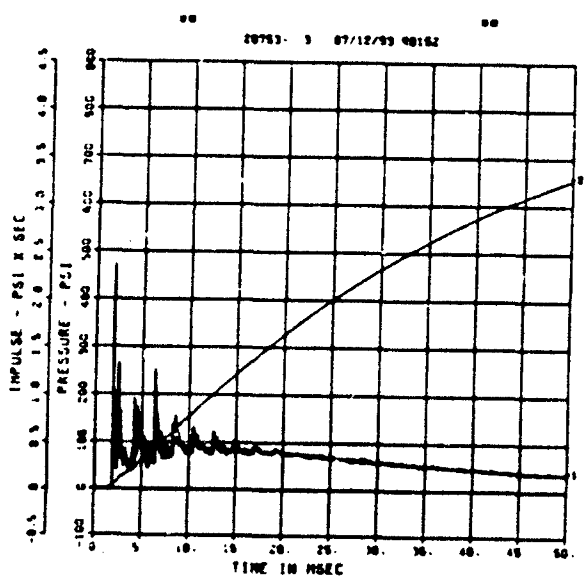

FEMA ELEM TEST D-3A
BP-4
200000. HZ CAL= 284.1

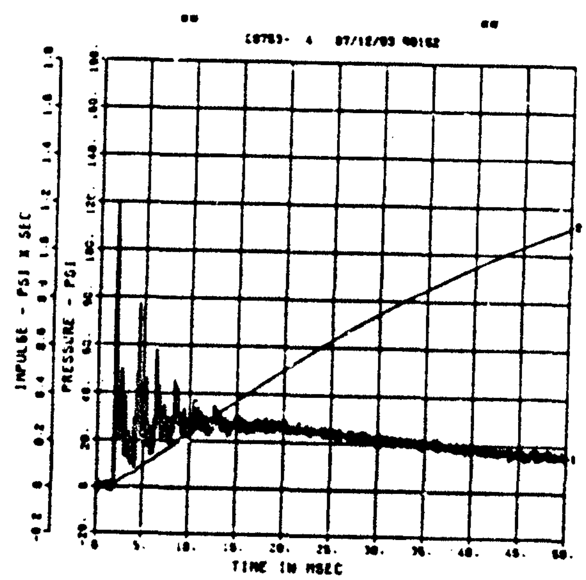

FEMA ELEM TEST D-3A
SE-1
200000. HZ CAL= 191.5

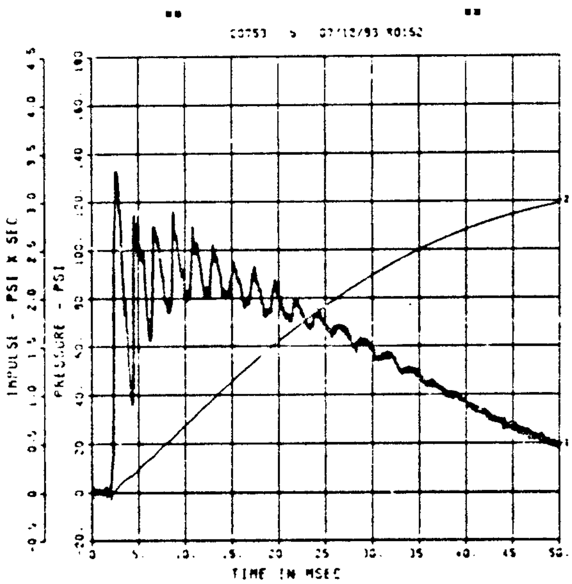

FEMA ELEM TEST D-3A
SE-2
200000. HZ CAL= 130.9

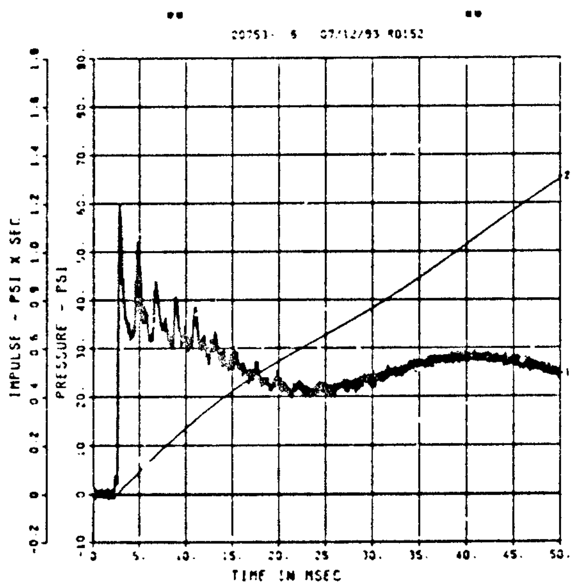

FEMA ELEM TEST D-3A
SE-3
200000. HZ CAL= 198.2

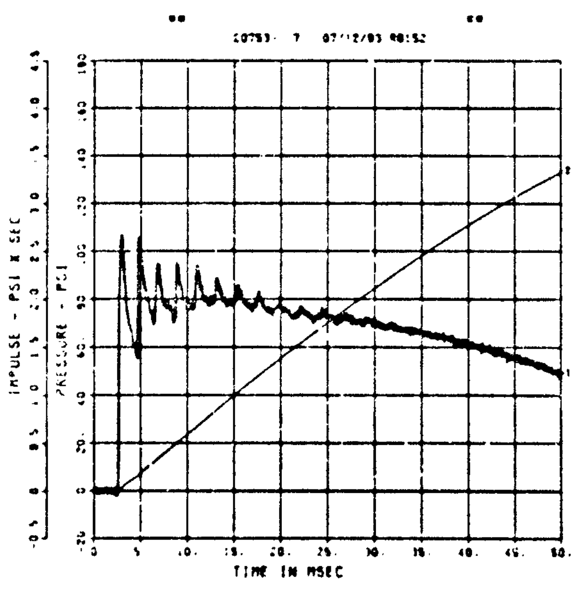

FEMA ELEM TEST D-3A
SE-4
200000. HZ CAL= 81.60

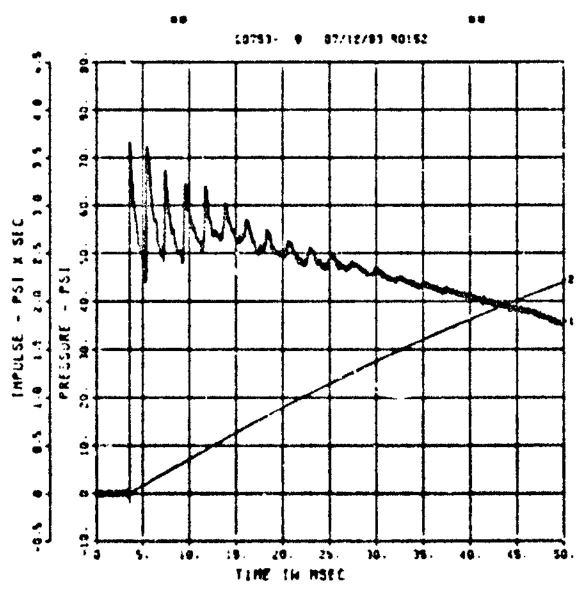

FEMA ELEM TEST D-3A
SE-5
200000. HZ CAL= 81.80

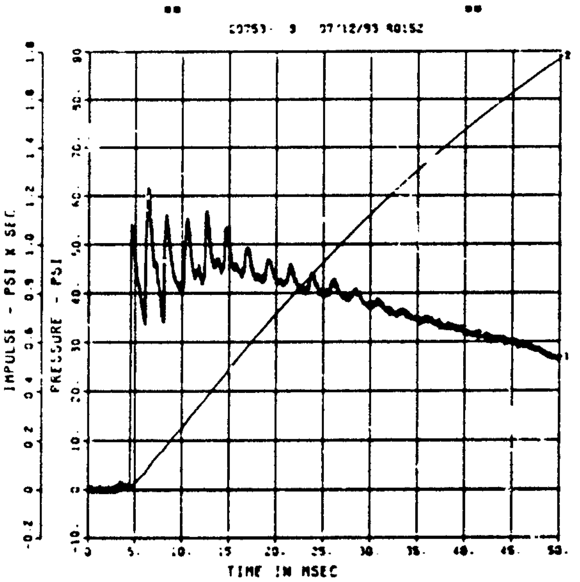

FEMA ELEM TEST D-3A
SE-6
200000. HZ CAL= 196.2

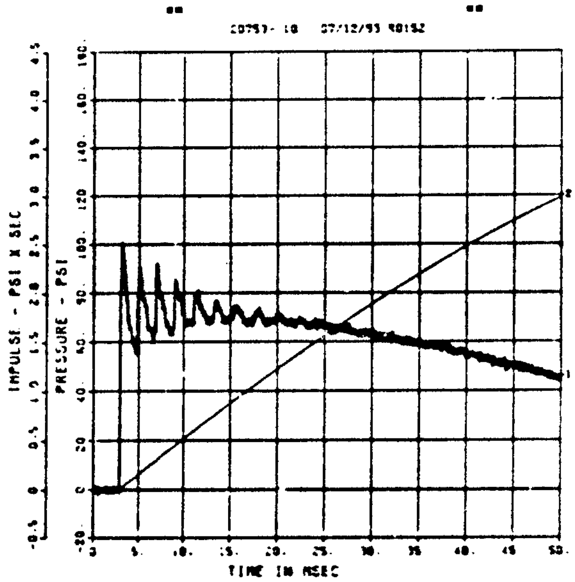

FEMA ELEM TEST D-3A
SE-7
200000. HZ CAL= 122.6

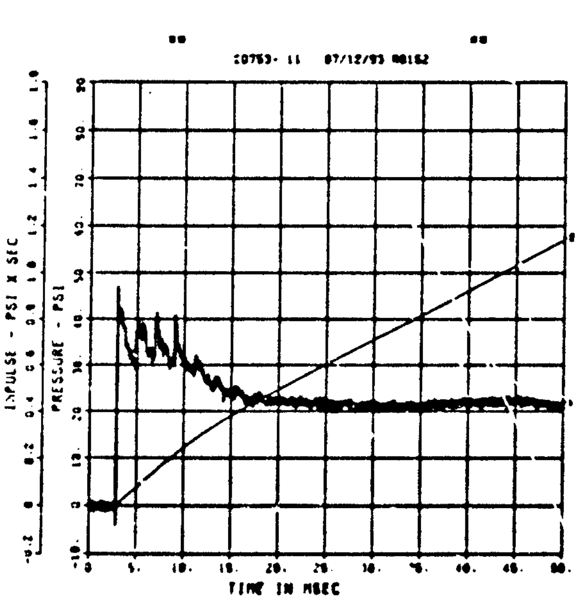

FEMA ELEM TEST D-3A
AFF-1
200000. HZ CAL= 221.8

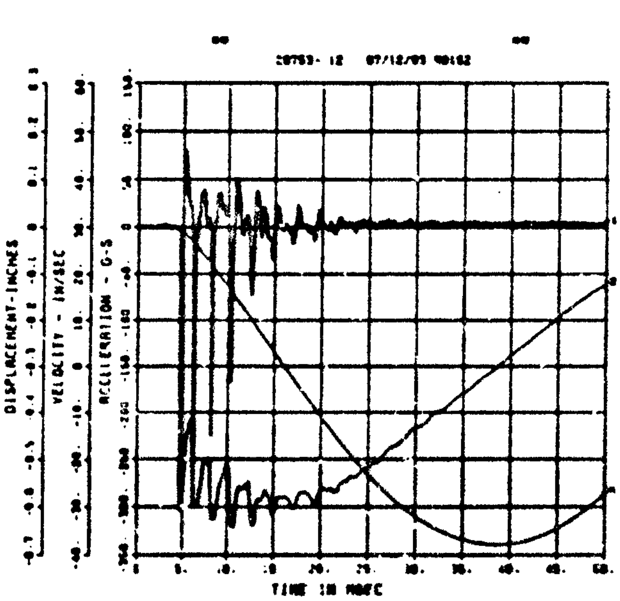

FEMA ELEM TEST D-3A
A-1
200000. HZ CAL= 2504.

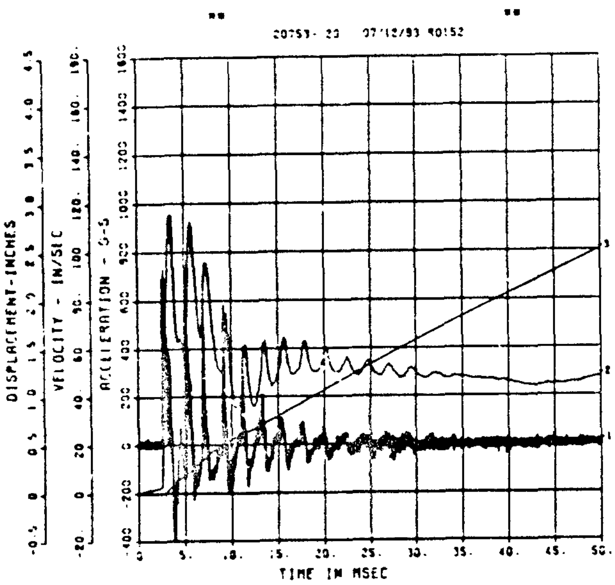

FEMA ELEM TEST D-3A
A-2
200000. HZ CAL= 221.4

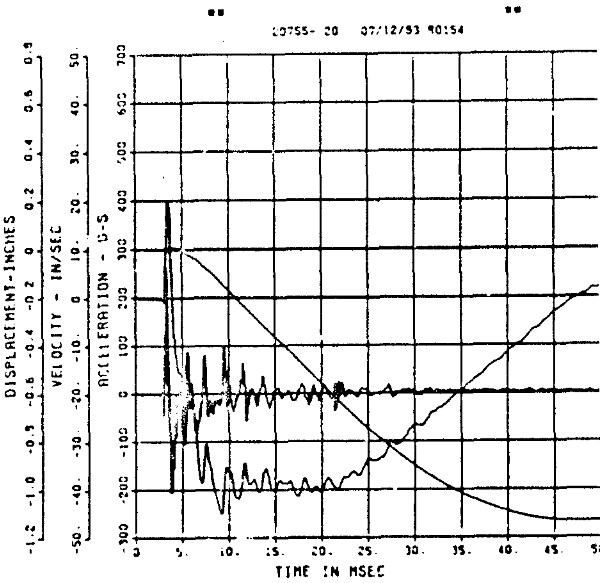

FEMA ELEM TEST D-3A
IF-1
200000. HZ CAL= 245.2

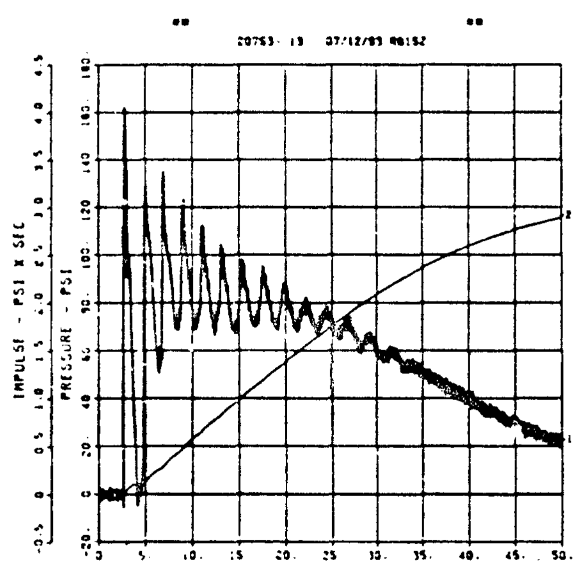

FEMA ELEM TEST D-3A
IF-2
200000. HZ CAL= 246.7

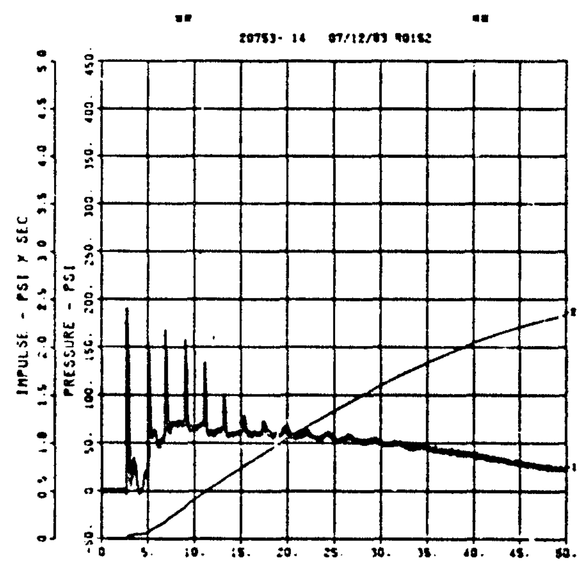

FEMA ELEM TEST D-3A
IF-3
200000. HZ CAL= 247.0

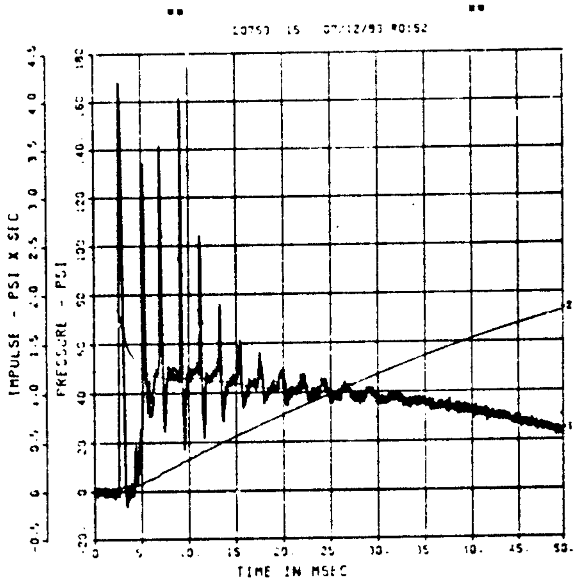

FEMA ELEM TEST D-3A
IF-4
200000. HZ CAL= 245.7

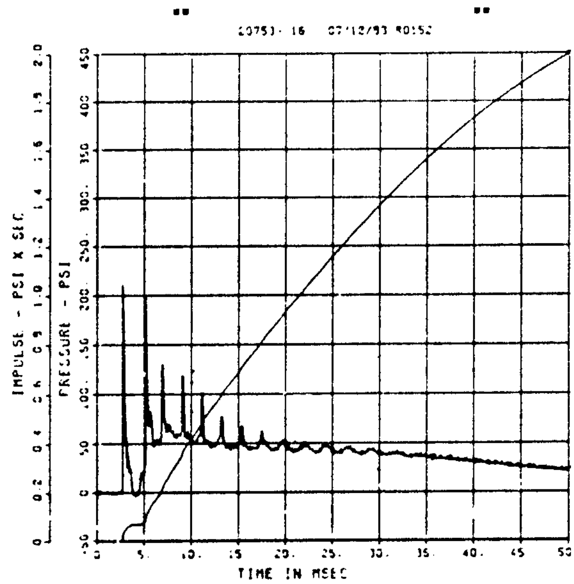

FEMA ELEM TEST D-3A
IF-5
200000. HZ CAL= 253.5

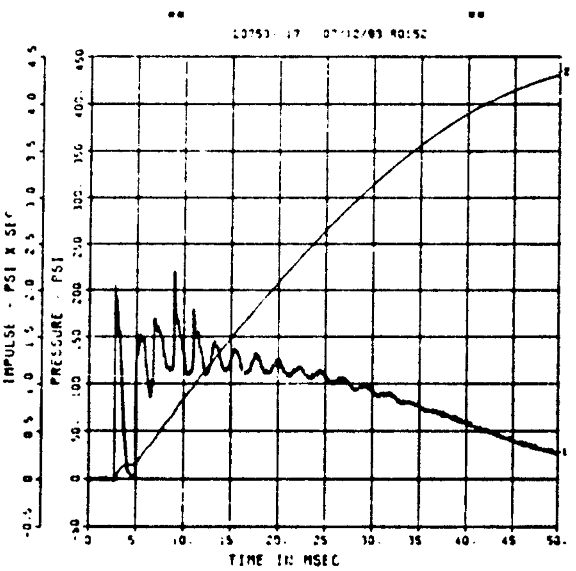

FEMA ELEM TEST D-3A
IF-6
200000. HZ CAL= 109.8

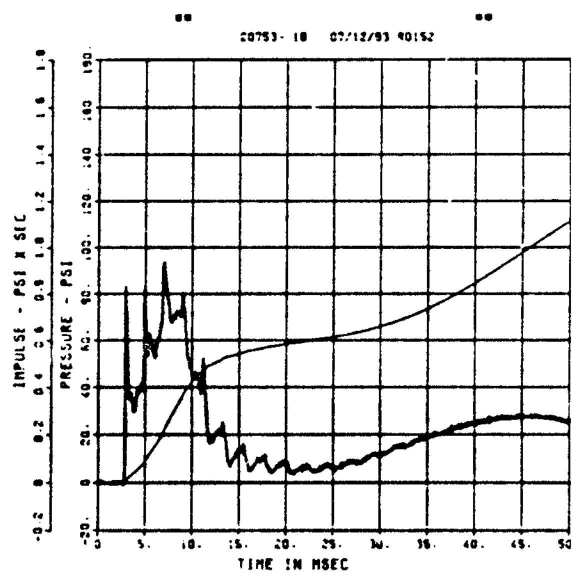

FEMA ELEM TEST D-3A
IF-7
200000. HZ CAL= 128.5

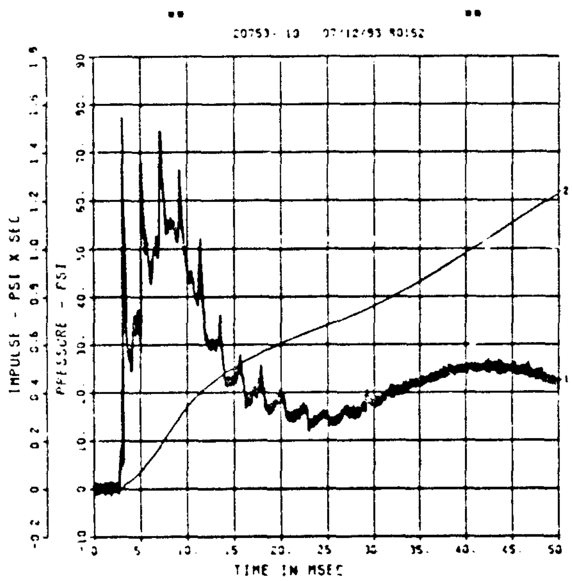

FEMA ELEM TEST D-3A
IF-8
200000. HZ CAL= 85.40

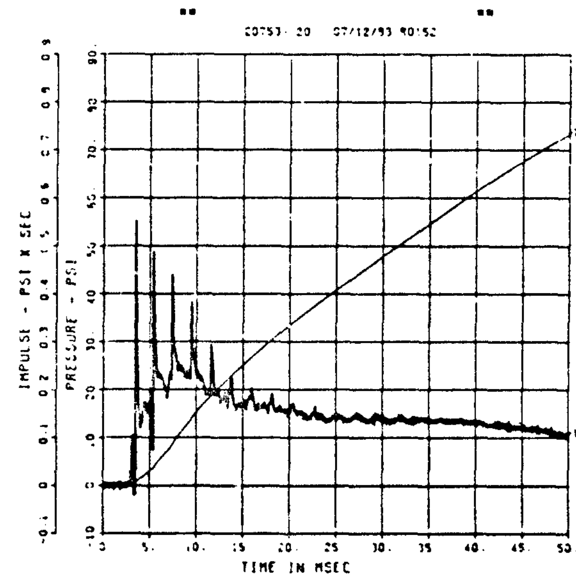

FEMA ELEM TEST D-3A
IF-9
200000. HZ CAL= 84.10

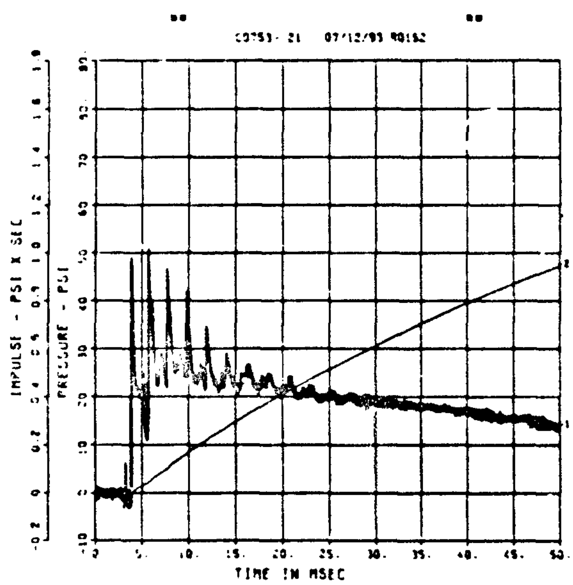

FEMA ELEM TEST D-3A
IF-10
200000. HZ CAL= 51.70

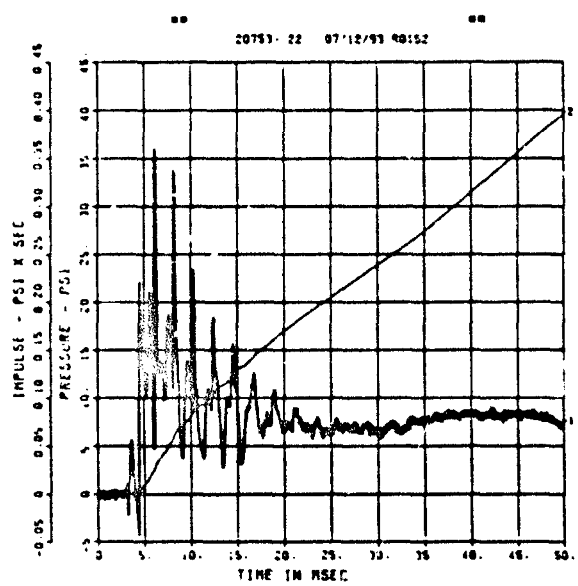

FEMA ELEM TEST D-3A
IF-11
200000. HZ CAL= 52.80

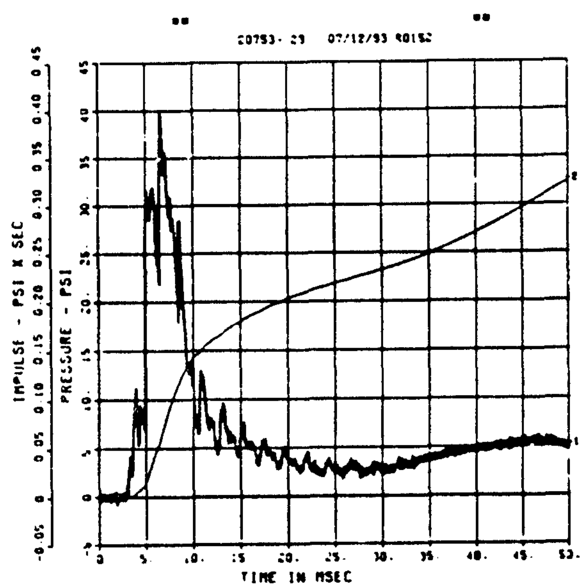

FEMA ELEM TEST D-3A
IF-12
200000. HZ CAL= 124.4

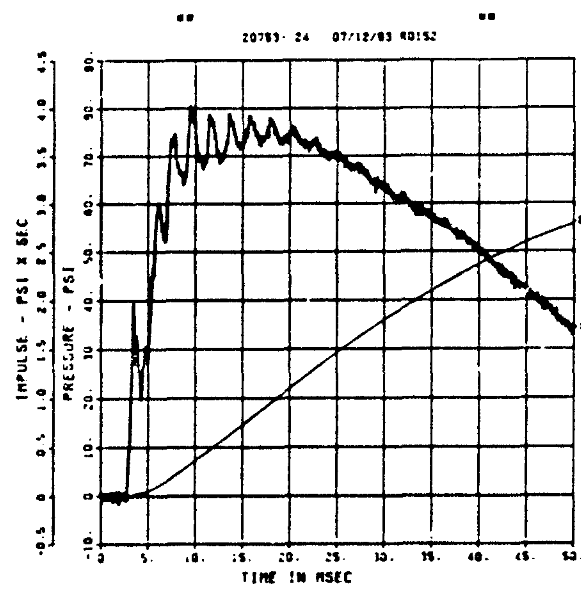

FEMA ELEM TEST D-3A
IF-13
200000. HZ CAL= 125.9
LP4/0 70% CUTOFF= 9000. HZ

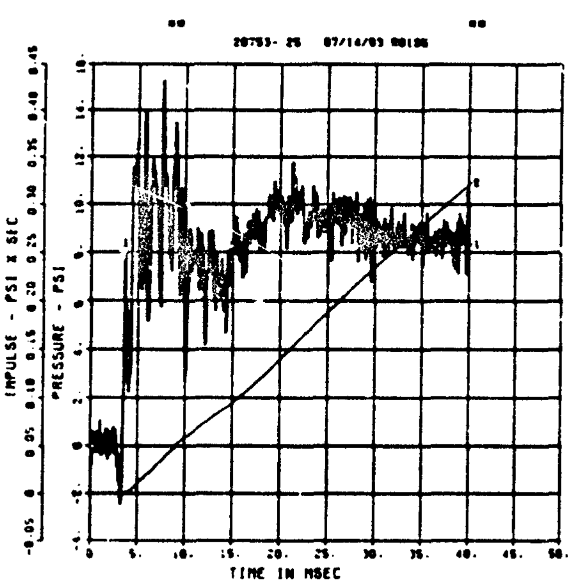

** PEAK VALUE IS 59 % UNDER CALIBRATION **

FEMA ELEM TEST D-3A
IF-14
200000. HZ CAL= 125.9
LP4/0 70% CUTOFF= 9000. HZ

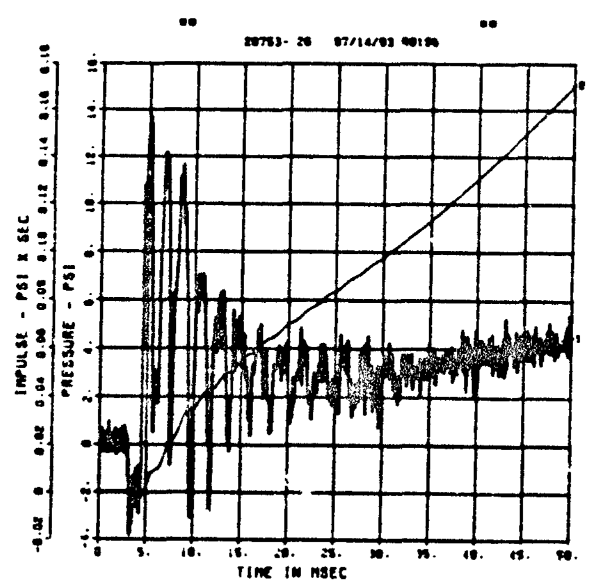

** PEAK VALUE IS 80 % UNDER CALIBRATION **

FEMA ELEM TEST D-3A
IF-15
200000. HZ CAL= 124.8

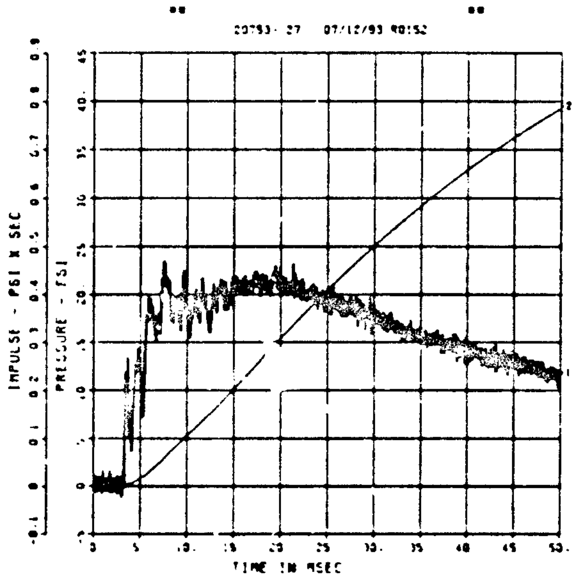

** PEAK VALUE IS 51 % UNDER CALIBRATION **

FEMA ELEM TEST D-3A
IF-16
200000. HZ CAL= 126.1

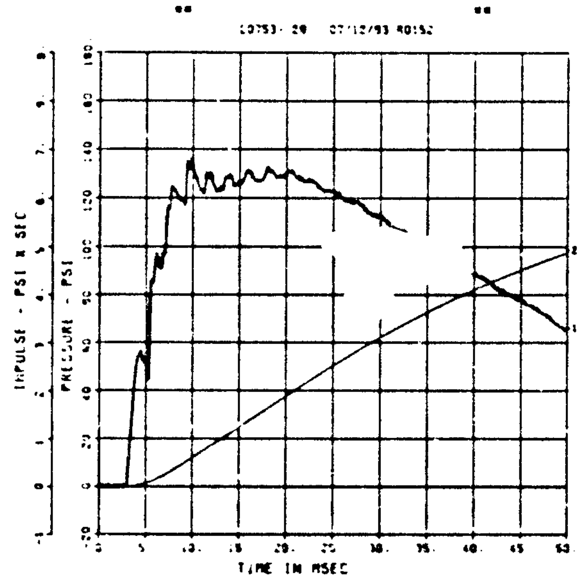

** PEAK VALUE IS 9 % OVER CALIBRATION **

FEMA ELEM TEST D-3A
EO-1
50000. HZ CAL= 20205.
LP4/4 70% CUTOFF= 2250. HZ

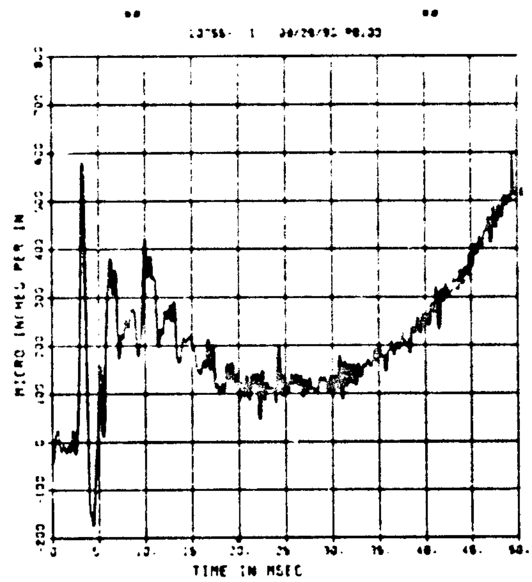

** PEAK VALUE IS 97 % UNDER CALIBRATION **

FEMA ELEM TEST D-3A
EI-1
200000. HZ CAL= 20205.
LP4/3 70% CUTOFF= 8000. HZ

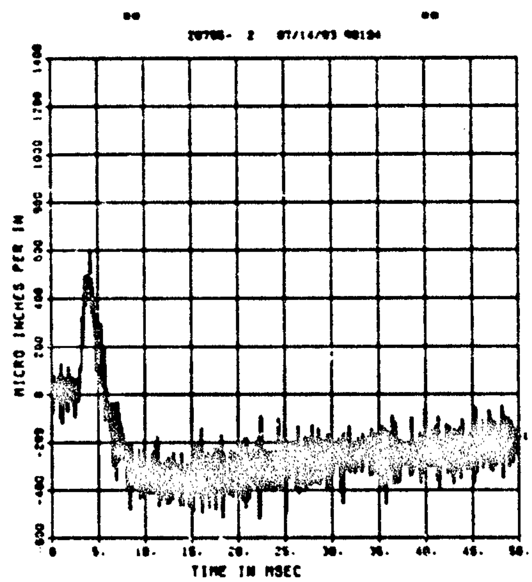

** PEAK VALUE IS 97 % UNDER CALIBRATION **

FEMA ELEM TEST D-3A
E0-2
200000. HZ CAL= 20205.

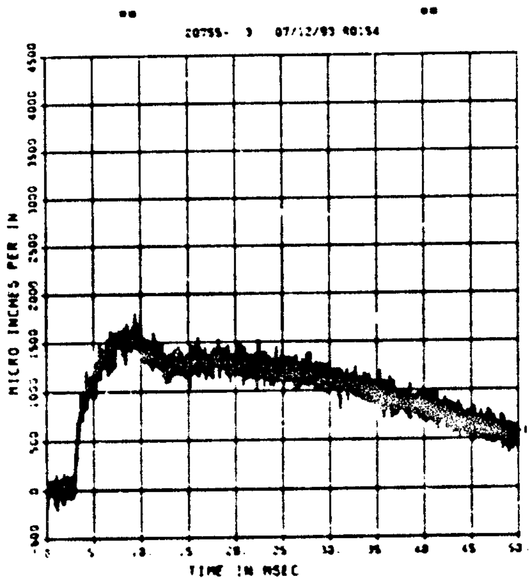

** PEAK VALUE IS 91 % UNDER CALIBRATION **

FEMA ELEM TEST D-3A
EI-2
200000. HZ CAL= 20205.

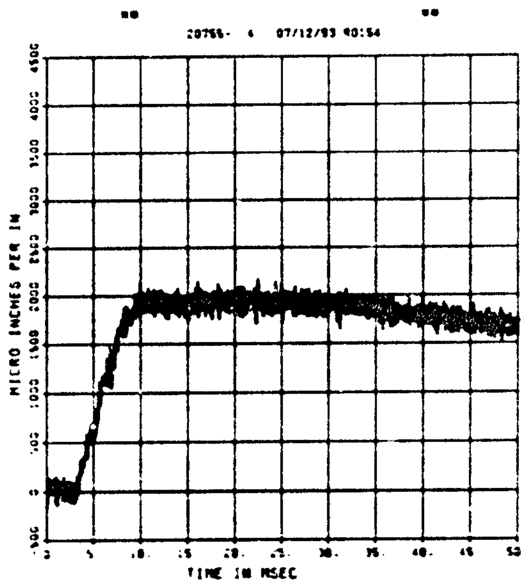

** PEAK VALUE IS 98 % UNDER CALIBRATION **

FEMA ELEM TEST D-3A
E0-3
200000. HZ CAL= 10276.
LP4/8 70% CUTOFF= 9000. HZ

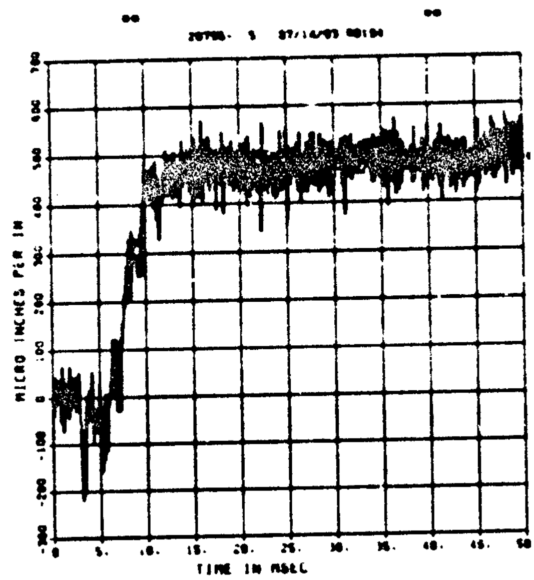

** PEAK VALUE IS 84 % UNDER CALIBRATION **

FEMA ELEM TEST D-3A
EI-3
200000. HZ CAL= 10276.

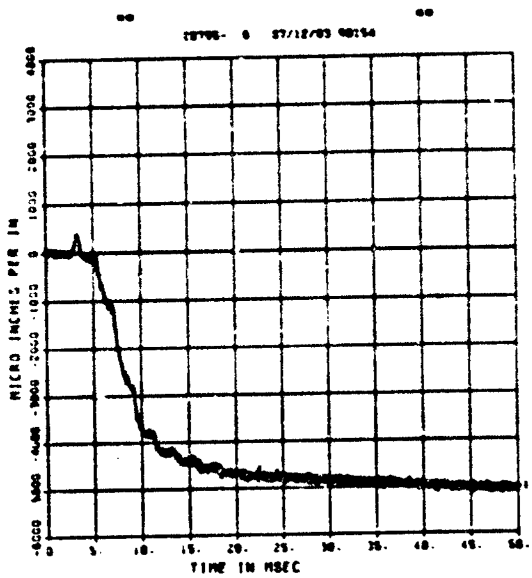

FEMA ELEM TEST D-3A
EO-4
50000. HZ CAL= 20205.
LP4/4 70% CUTOFF= 2250. HZ

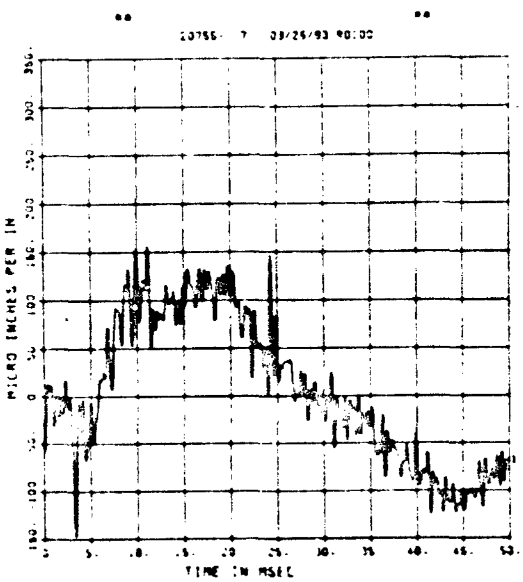

FEMA ELEM TEST D-3A
EO-5
200000. HZ CAL= 20205.

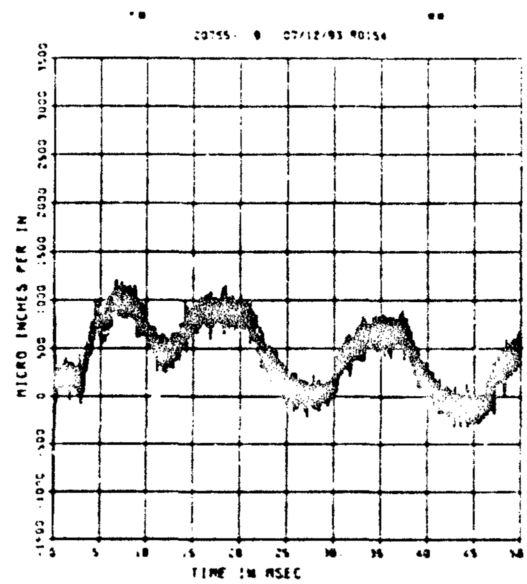

FEMA ELEM TEST D-3A
EI-5
200000. HZ CAL= 20205.

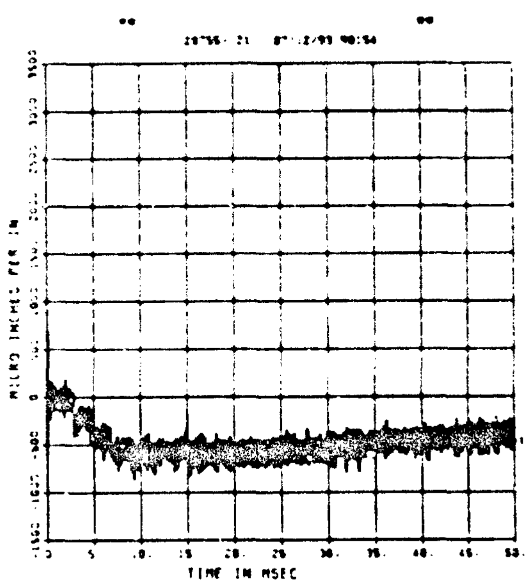

FEMA ELEM TEST D-3A
EO-6
50000. HZ CAL= 20205.
LP4/4 70% CUTOFF= 2250. HZ

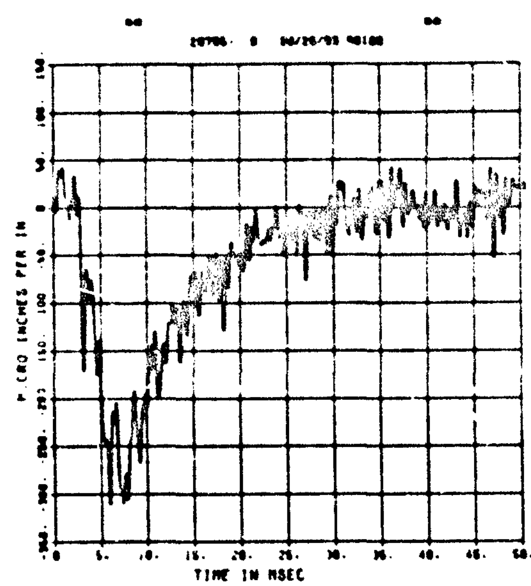

FEMA ELEM TEST D-3A
EI-6
50000. HZ CAL= 20205.
LP4/4 70% CUTOFF= 2250. HZ

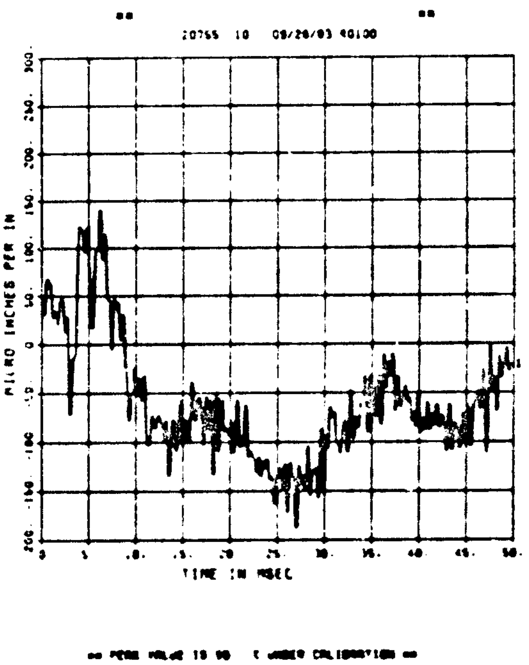

FEMA ELEM TEST D-3A
EO-7
50000. HZ CAL= 10276.
LP4/4 70% CUTOFF= 2250. HZ

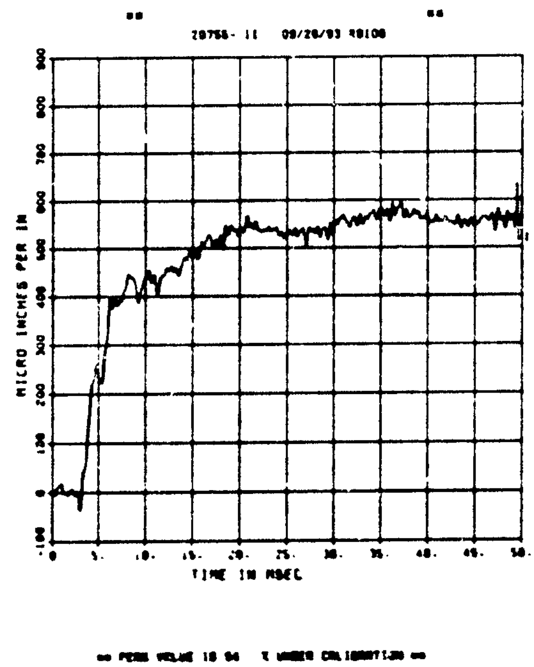

FEMA ELEM TEST D-3A
EI-7
50000. HZ CAL= 10276.
LP4/4 70% CUTOFF= 2250. HZ

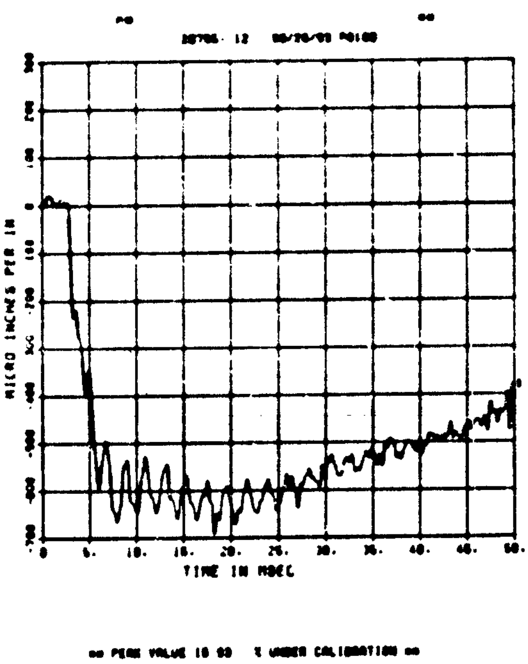

FEMA ELEM TEST D-3A
EO-8
200000. HZ CAL= 20205.

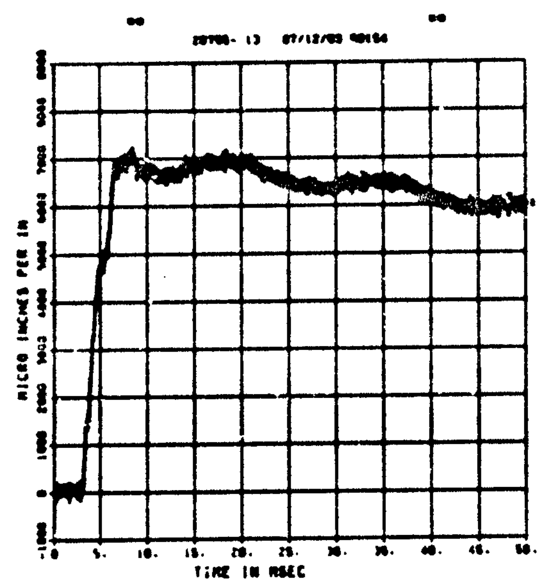

FEMA ELEM TEST D-3A
EI-8
200000. HZ CAL= 10276.
LP4/0 70% CUTOFF= 9000. HZ

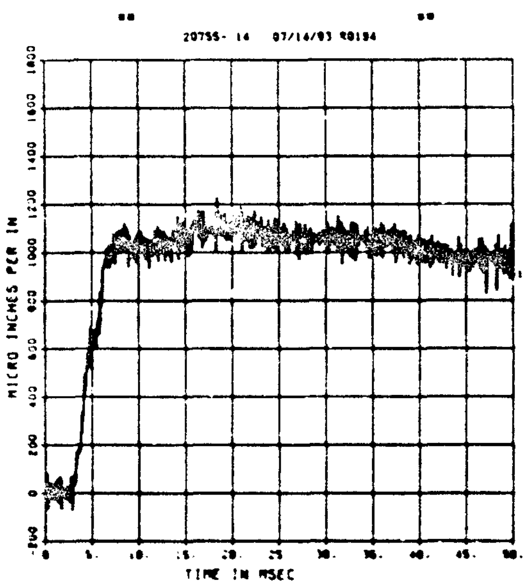

FEMA ELEM TEST D-3A
EO-9
200000. HZ CAL= 10276.

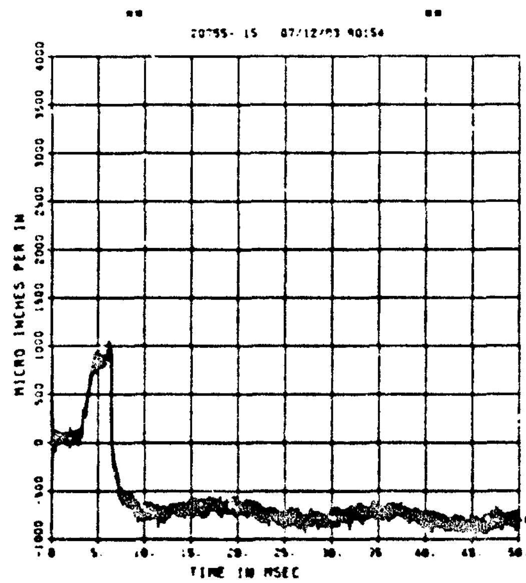

FEMA ELEM TEST D-3A
EI-9
200000. HZ CAL= 10276.

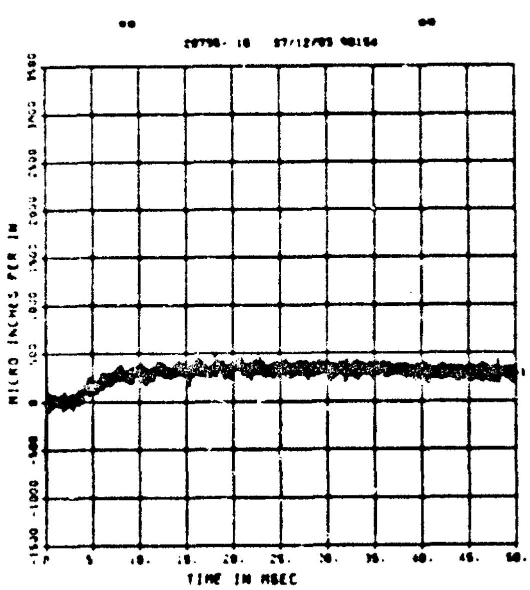

FEMA ELEM TEST D-3A
EO-10
50000. HZ CAL= 10276.
LP4/4 70% CUTOFF= 2250. HZ

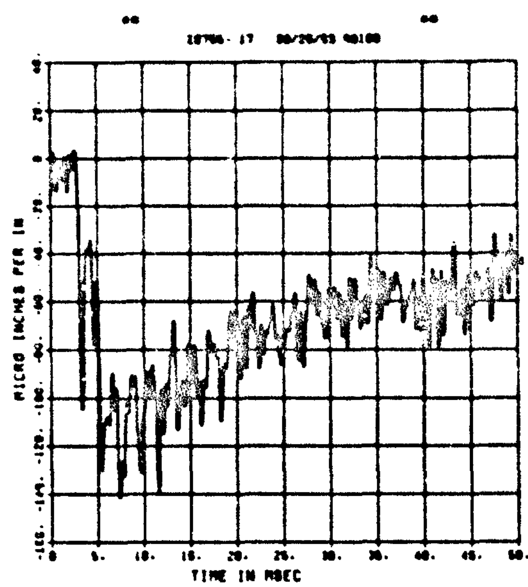

FEMA ELEM TEST D-3A
EO-11
50000. HZ CAL= 10276.
LP4/4 70% CUTOFF= 2250. HZ

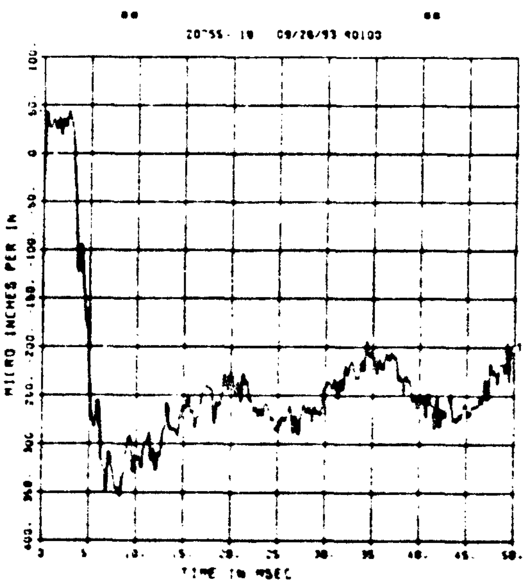

FEMA ELEM TEST D-3A
EI-11
200000. HZ CAL= 20205.

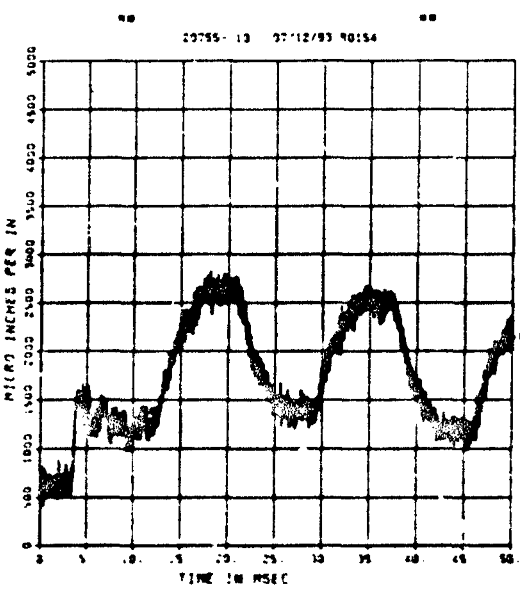

FEMA ELEM TEST D-3B
BP-1
200000. HZ CAL= 564.6

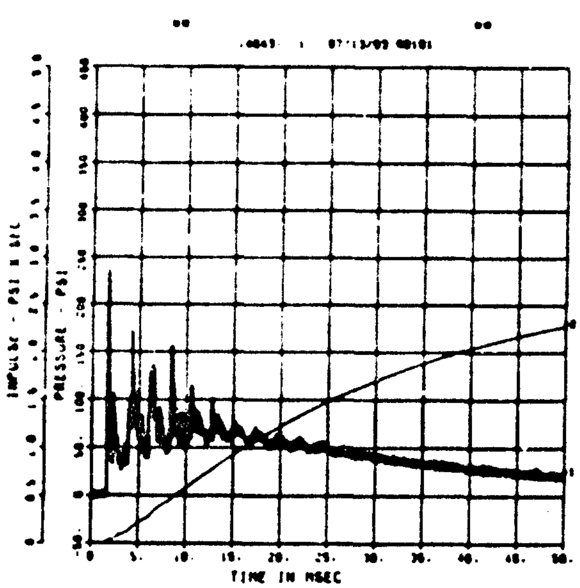

FEMA ELEM TEST D-3B
BP-2
200000. HZ CAL= 622.5

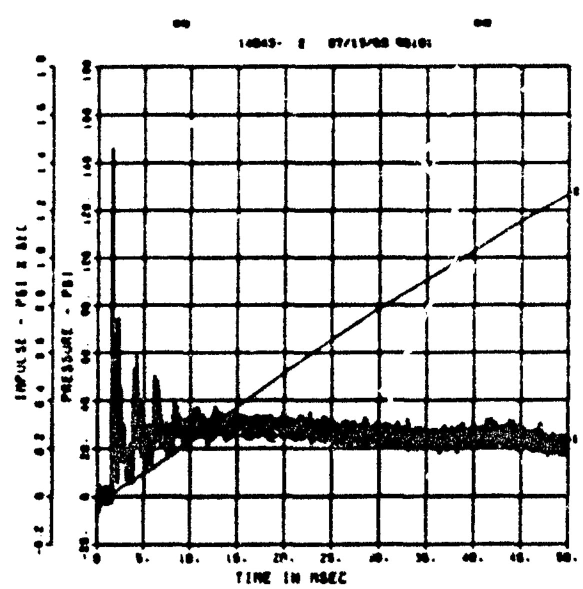

FEMA ELEM TEST D-3B
BP-3
200000. HZ CAL= 744.2

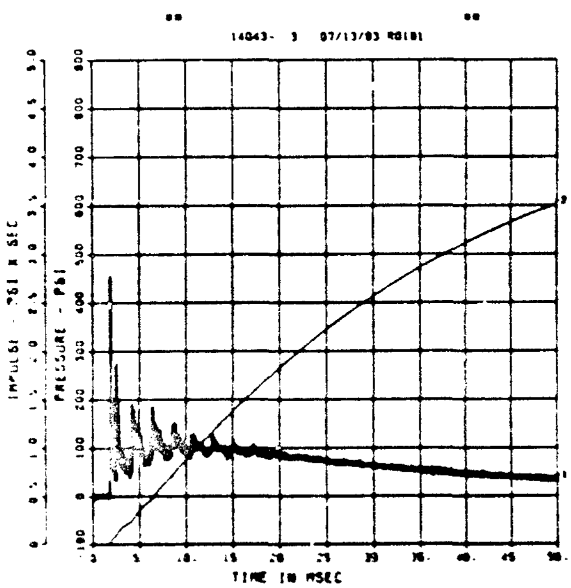

FEMA ELEM TEST D-3B
BP-4
50000. HZ CAL= 550.6
LP4/4 70% CUTOFF= 2250. HZ

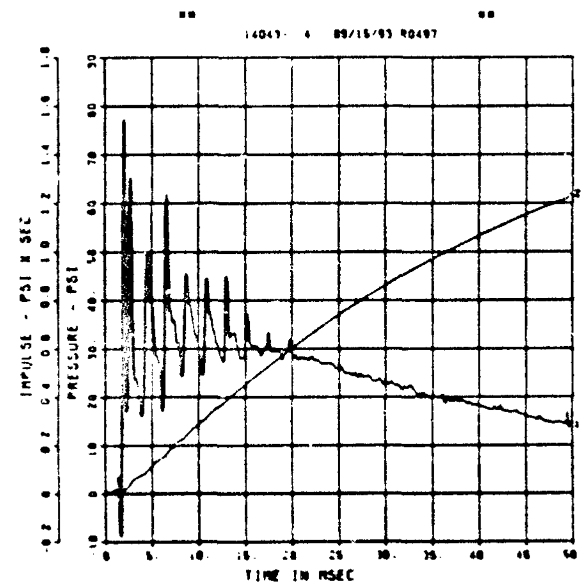

FEMA ELEM TEST D-3B
SE-1
200000. HZ CAL= 249.0

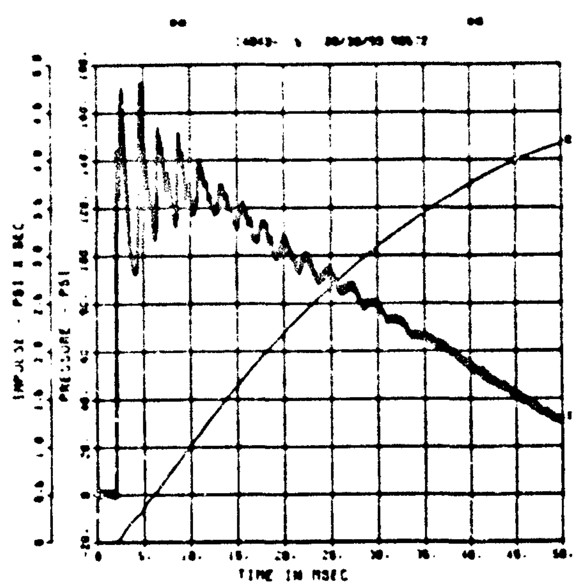

FEMA ELEM TEST D-3B
SE-2
200000. HZ CAL= 192.0

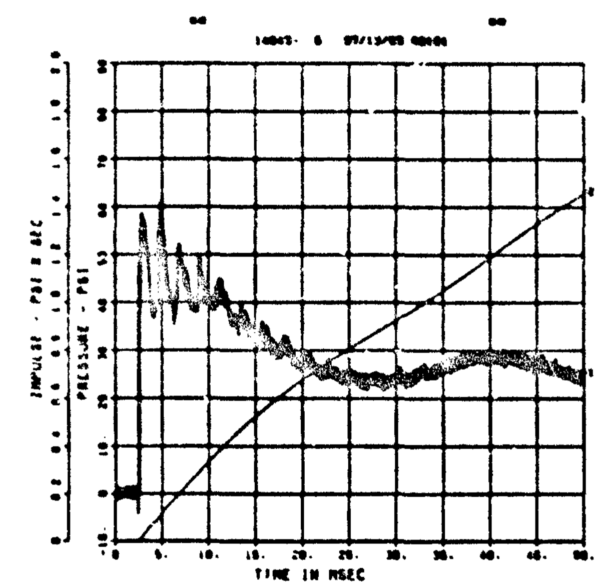

FEMA ELEM TEST D-3B
SE-3
200000. HZ CAL= 257.8

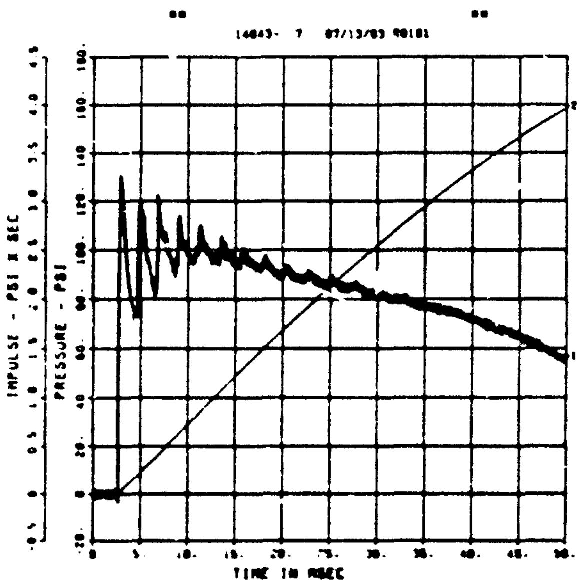

FEMA ELEM TEST D-3B
SE-4
200000. HZ CAL= 132.4

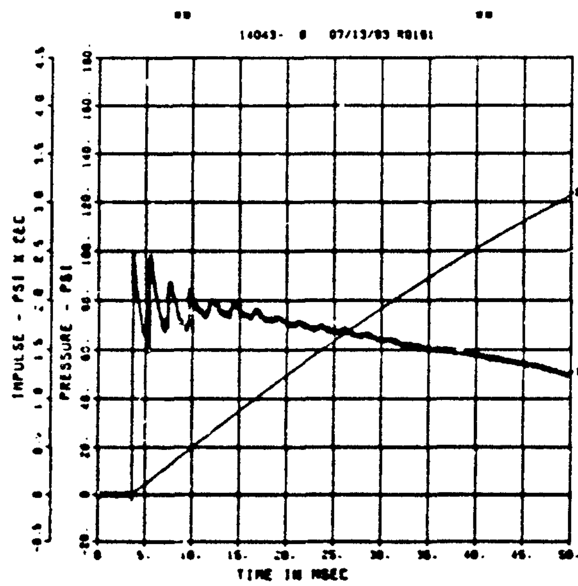

FEMA ELEM TEST D-3B
SE-5
200000. HZ CAL= 132.8

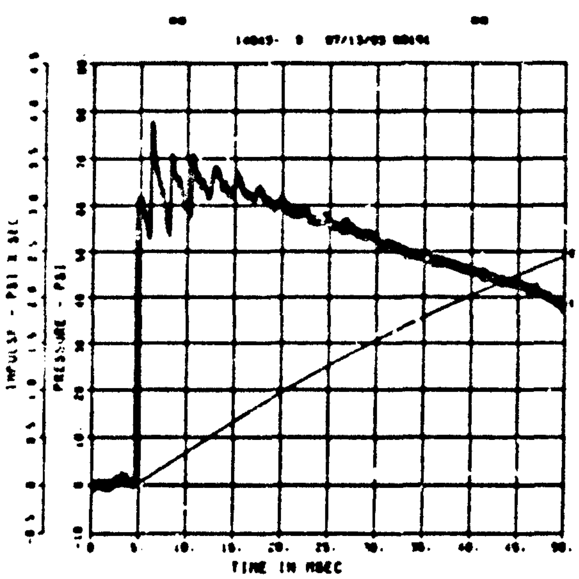

FEMA ELEM TEST D-3B
SE-6
200000. HZ CAL= 255.2

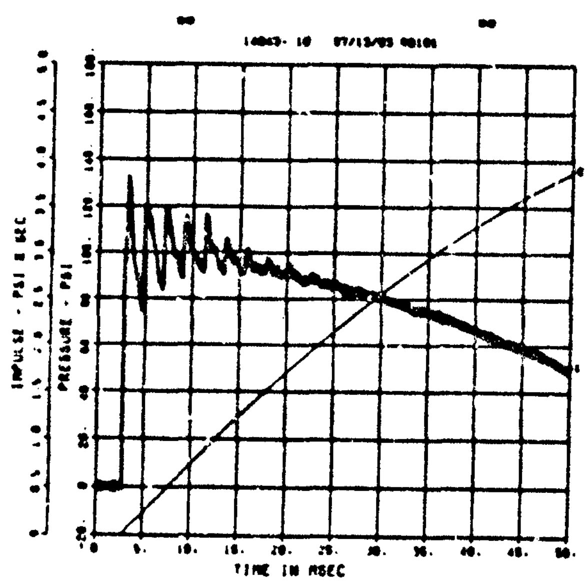

FEMA ELEM TEST D-3B
SE-7
200000. HZ CAL= 179.8

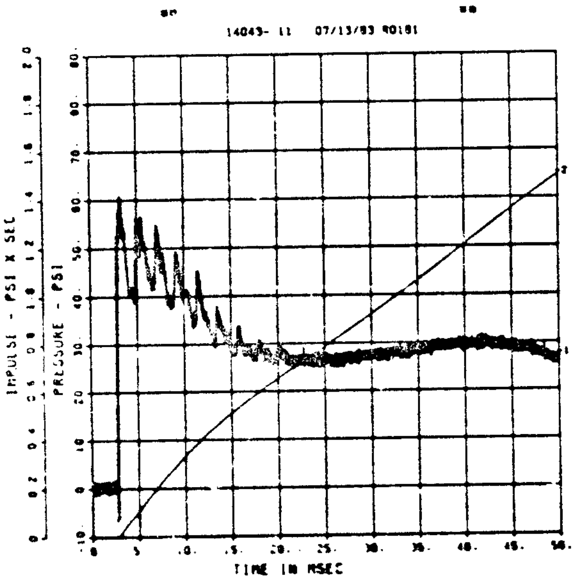

FEMA ELEM TEST D-3B
AFF-1
200000. HZ CAL= 1153.

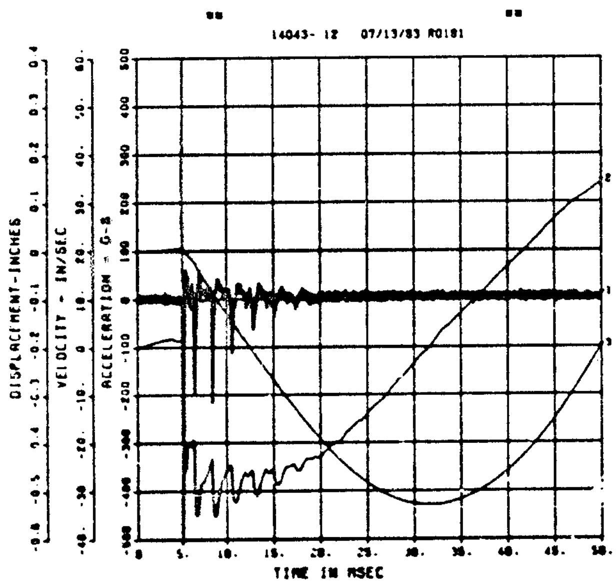

FEMA ELEM TEST D-3B
A-1
200000. HZ CAL= 1692.

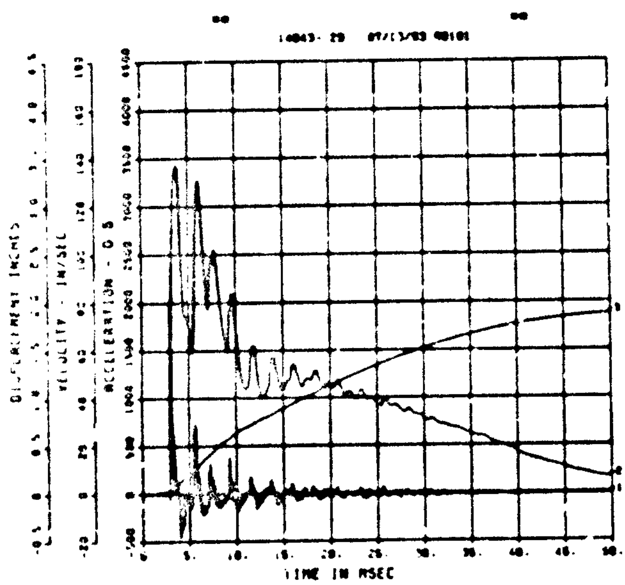

FEMA ELEM TEST D-3B
A-2
200000. HZ CAL= 1144.

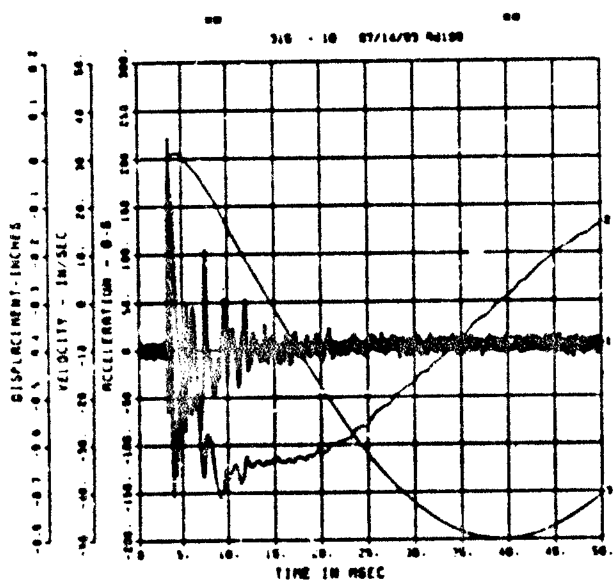

** PEAK VALUE IS 19 % OVER CALIBRATION **

** PEAK VALUE IS 91 % UNDER CALIBRATION **

FEMA ELEM TEST D-3B
IF-1
200000. HZ CAL= 246.2

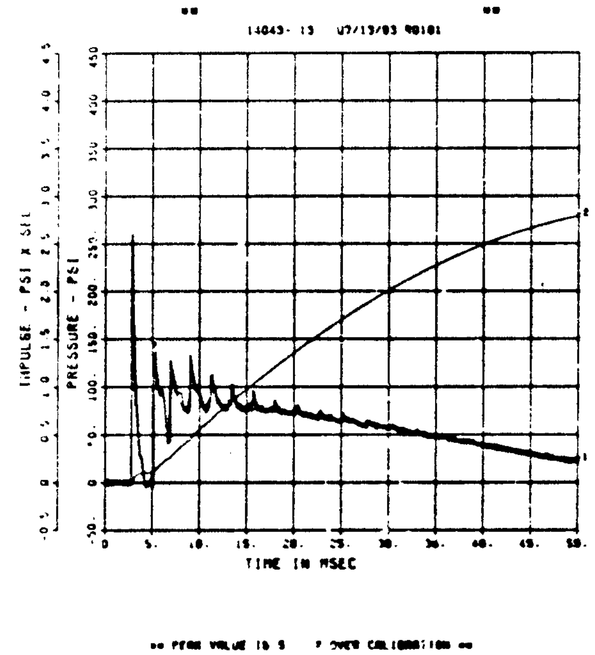

FEMA ELEM TEST D-3B
IF-2
200000. HZ CAL= 246.7

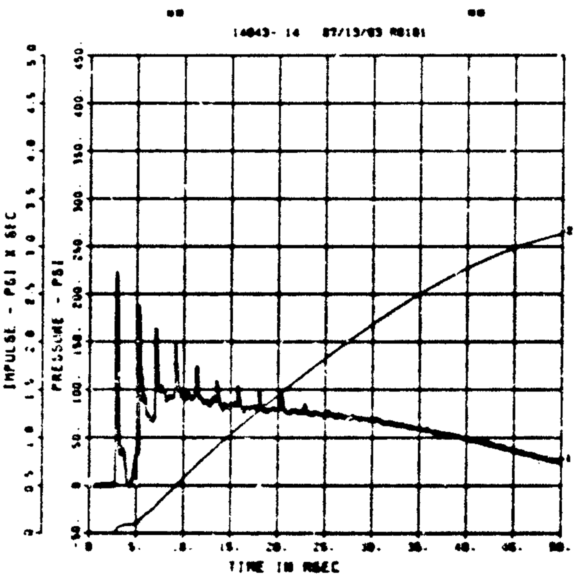

FEMA ELEM TEST D-3B
IF-3
200000. HZ CAL= 247.0

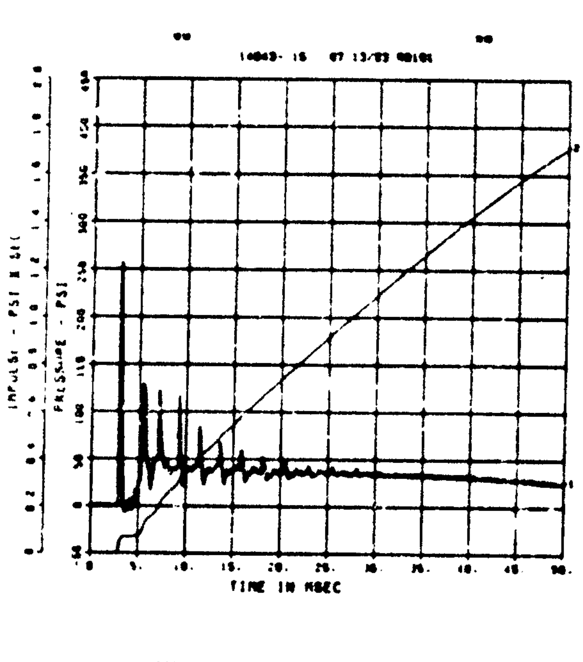

FEMA ELEM TEST D-3B
IF-4
200000. HZ CAL= 245.7

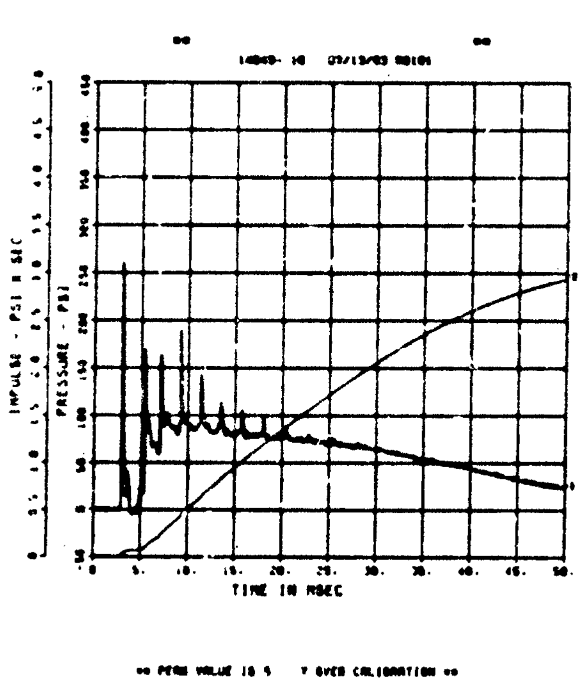

FEMA ELEM TEST D-3B
IF-5
200000. HZ CAL= 253.5

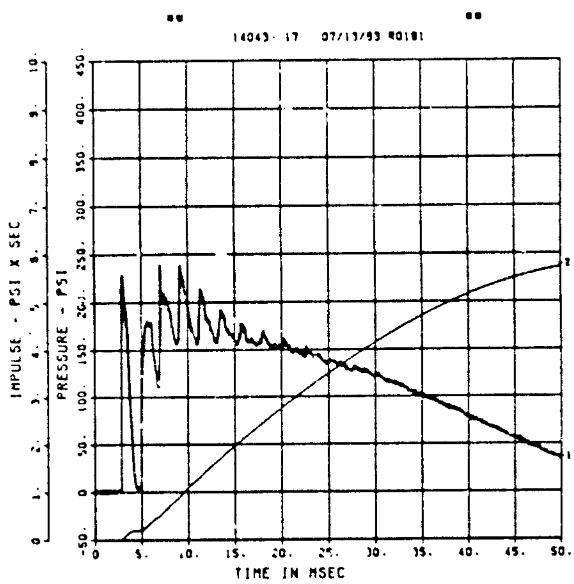

FEMA ELEM TEST D-3B
IF-6
200000. HZ CAL= 109.8

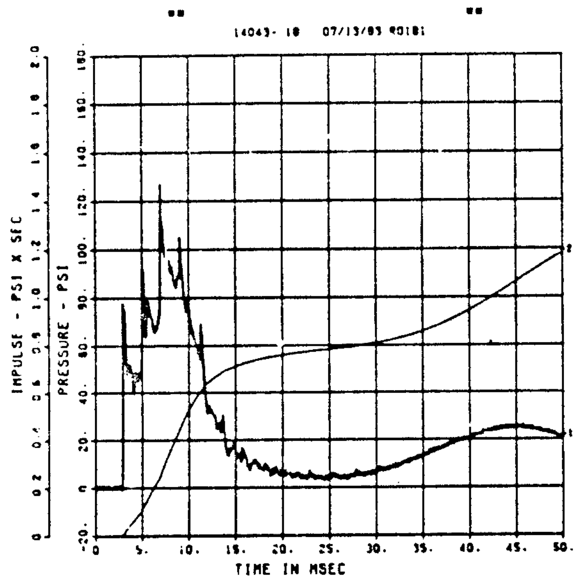

** PEAK VALUE IS 16 % OVER CALIBRATION **

FEMA ELEM TEST D-3B
IF-7
200000. HZ CAL= 128.5

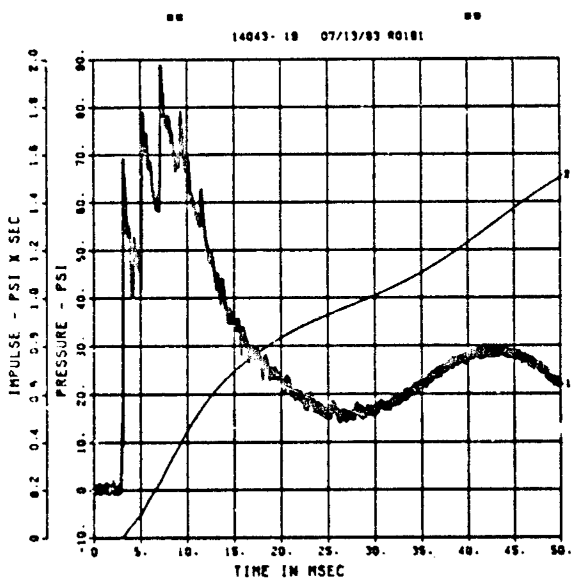

FEMA ELEM TEST D-3B
IF-8
200000. HZ CAL= 131.0

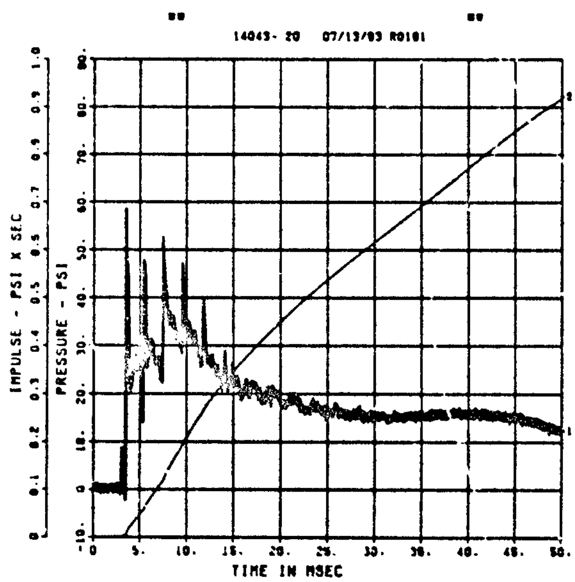

FEMA ELEM TEST D-3B
IF-9
200000. HZ CAL= 84.10

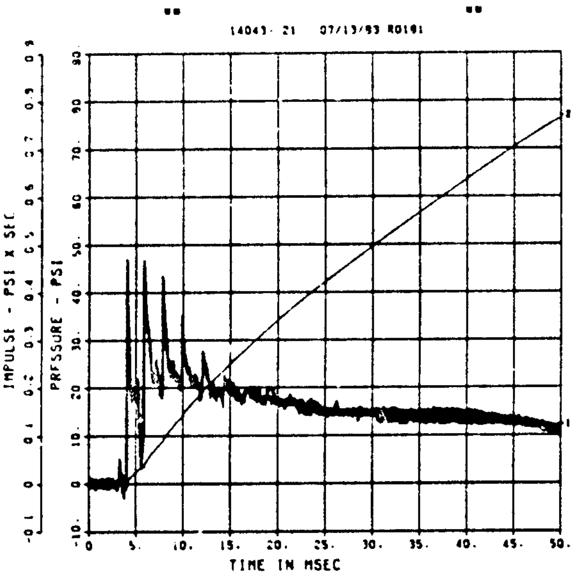

FEMA ELEM TEST D-3B
IF-10
200000. HZ CAL= 83.00

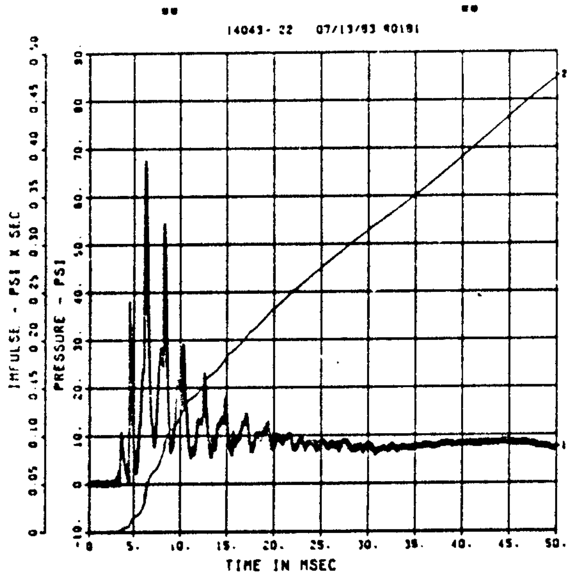

FEMA ELEM TEST D-3B
IF-11
200000. HZ CAL= 84.80

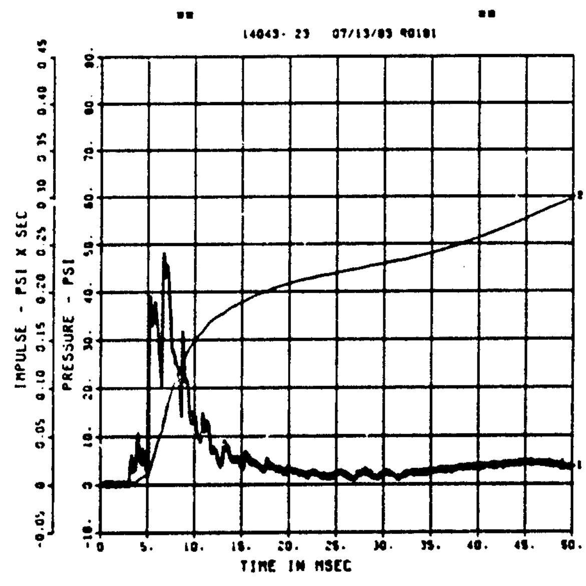

FEMA ELEM TEST D-3B
IF-12
200000. HZ CAL= 164.7

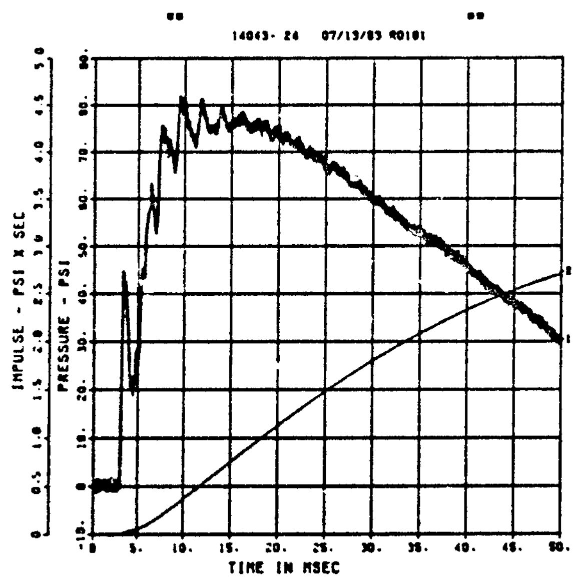

FEMA ELEM TEST D-3B
IF-13
50000. HZ CAL= 166.7
LP4/4 70% CUTOFF= 2250. HZ

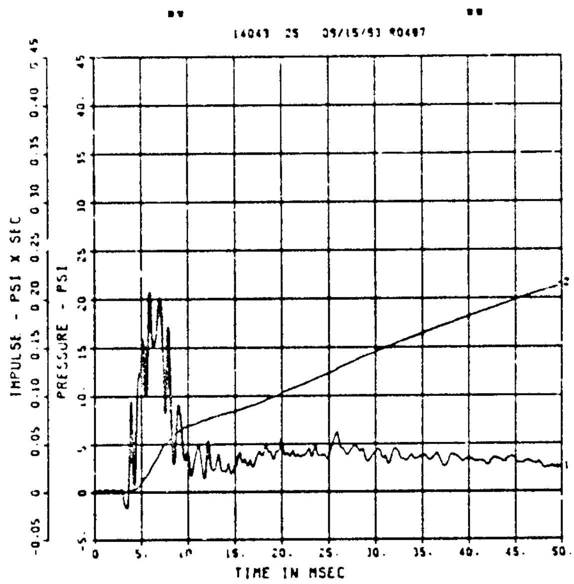

** PEAK VALUE IS 99 % UNDER CALIBRATION **

FEMA ELEM TEST D-3B
IF-14
50000. HZ CAL= 166.6
LP4/4 70% CUTOFF= 2250. HZ

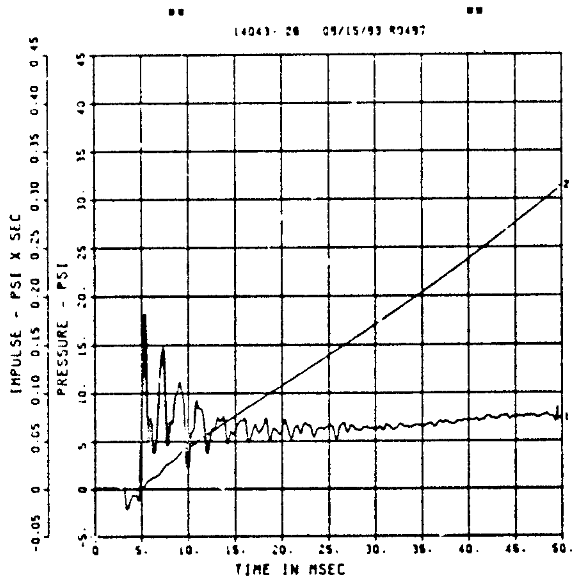

** PEAK VALUE IS 99 % UNDER CALIBRATION **

FEMA ELEM TEST D-3B
IF-15
50000. HZ CAL= 165.2
LP4/4 70% CUTOFF= 2250. HZ

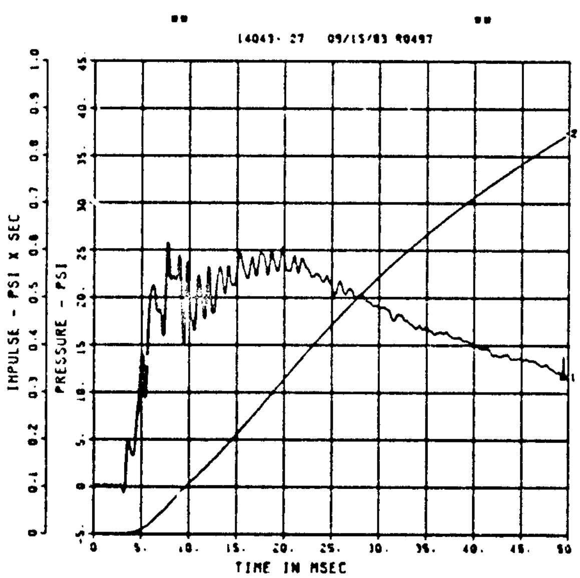

** PEAK VALUE IS 94 % UNDER CALIBRATION **

FEMA ELEM TEST D-3B
IF-16
200000. HZ CAL= 166.9

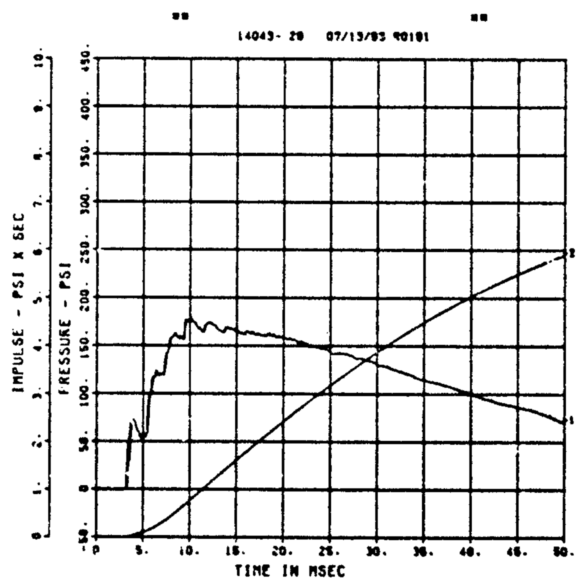

** PEAK VALUE IS [illegible] % OVER CALIBRATION **

FEMA ELEM TEST D-3B
EO-1
200000. HZ CAL= 20205.

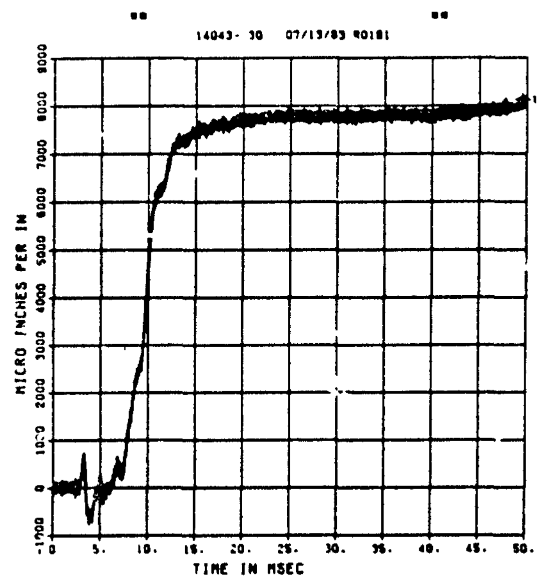

FEMA ELEM TEST D-3B
EI-1
50000. HZ CAL= 20205.
LP4/4 70% CUTOFF= 2250. HZ

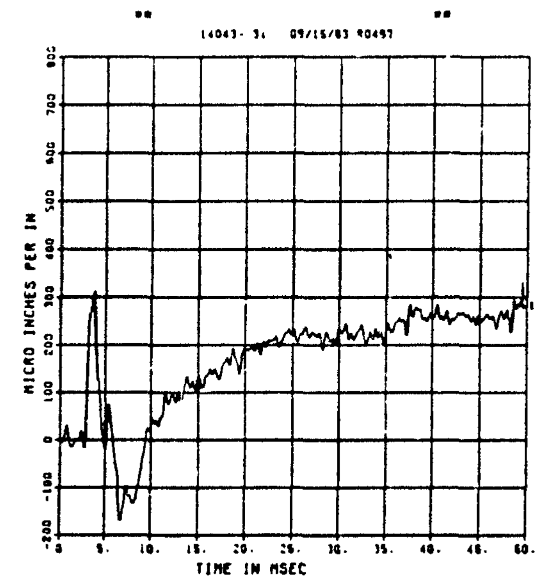

FEMA ELEM TEST D-3B
EO-2
200000. HZ CAL= 20205.

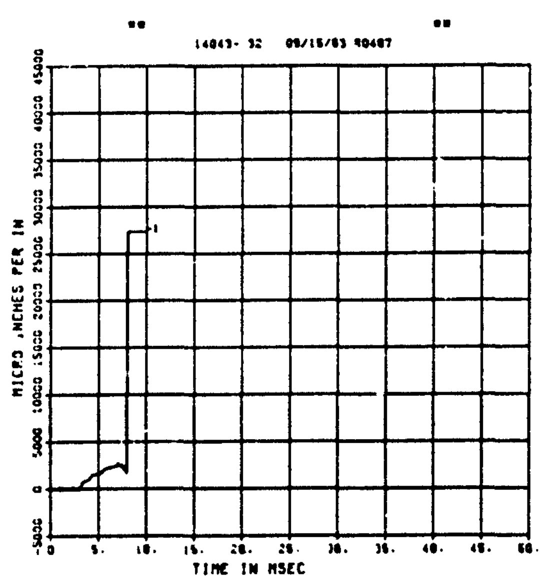

FEMA ELEM TEST D-3B
EI-2
50000. HZ CAL= 20205.
LP4/4 70% CUTOFF= 2250. HZ

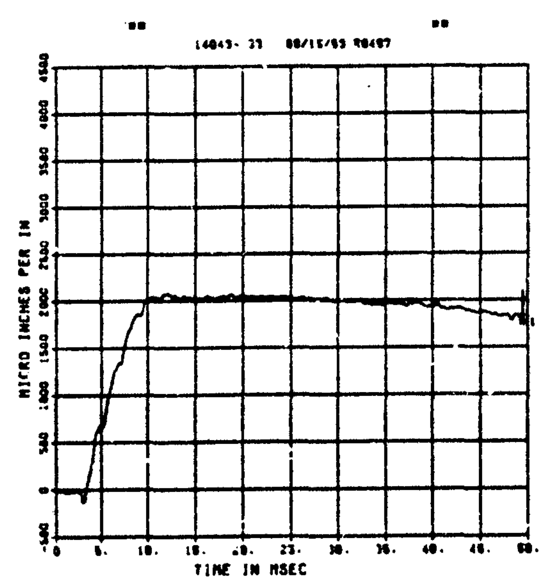

FEMA ELEM TEST D-3B
E0-3
50000. HZ CAL= 10276.
LP4/4 70% CUTOFF= 2250. HZ

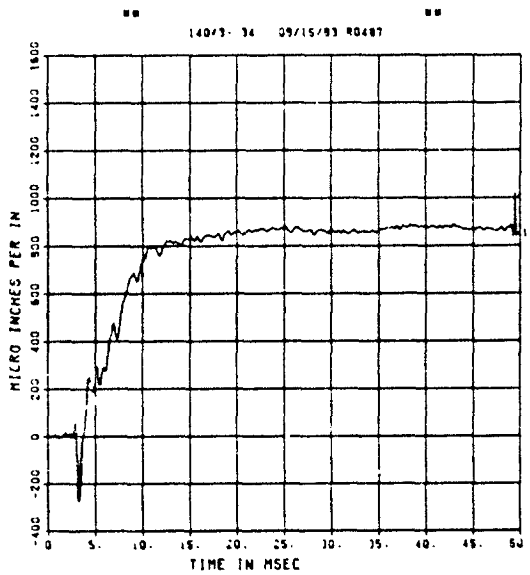

** PEAK VALUE IS 90 % UNDER CALIBRATION **

FEMA ELEM TEST D-3B
EI-3
200000. HZ CAL= 10276.

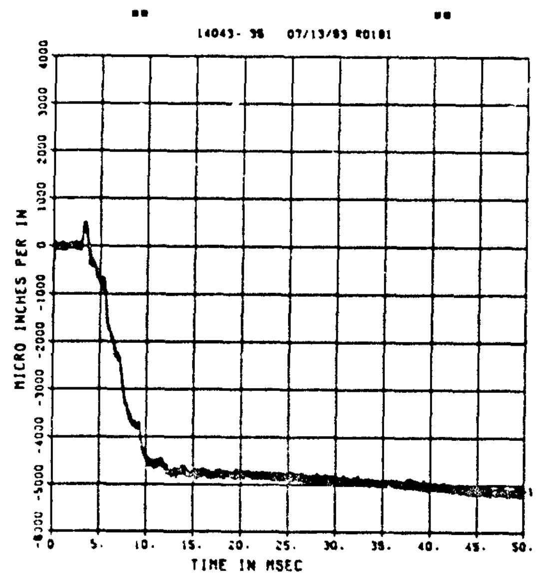

FEMA ELEM TEST D-3B
E0-4
50000. HZ CAL= 20205.
LP4/4 70% CUTOFF= 2250. HZ

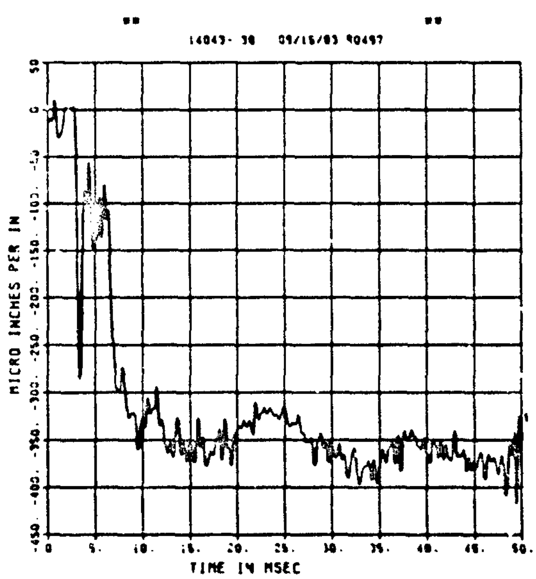

** PEAK VALUE IS 90 % UNDER CALIBRATION **

FEMA ELEM TEST D-3B
E0-5
50000. HZ CAL= 20205.
LP4/4 70% CUTOFF= 2250. HZ

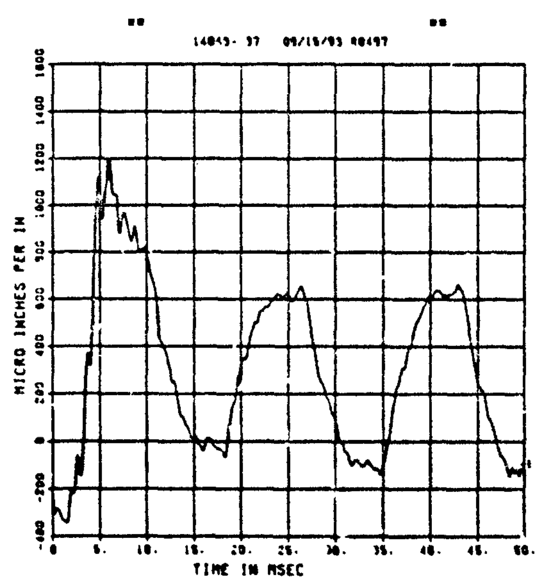

** PEAK VALUE IS 94 % UNDER CALIBRATION **

FEMA ELEM TEST D-3B
EI-5
50000. HZ CAL= 20205.
LP4/4 70% CUTOFF= 2250. HZ

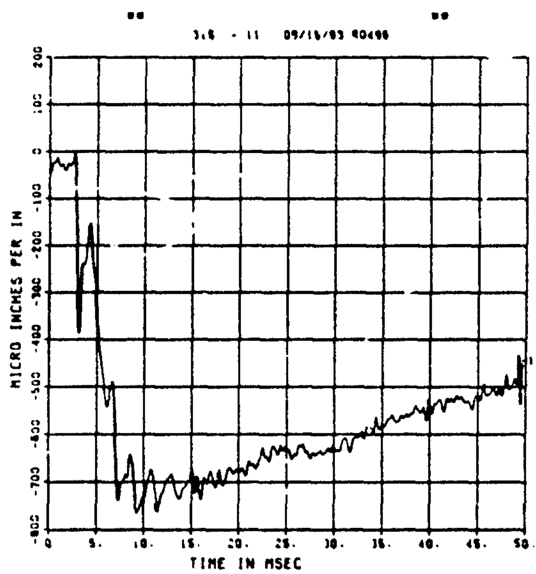

** PEAK VALUE IS 90 % UNDER CALIBRATION **

FEMA ELEM TEST D-3B
EO-6
50000. HZ CAL= 20205.
LP4/4 70% CUTOFF= 2250. HZ

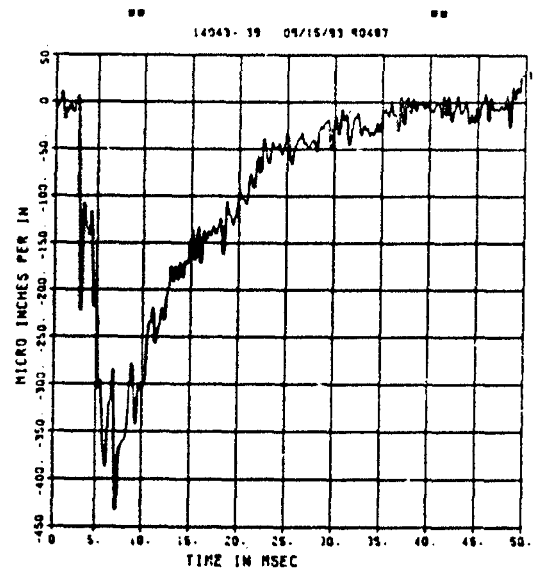

** PEAK VALUE IS 90 % UNDER CALIBRATION **

FEMA ELEM TEST D-3B
EI-6
50000. HZ CAL= 20205.
LP4/4 70% CUTOFF= 2250. HZ

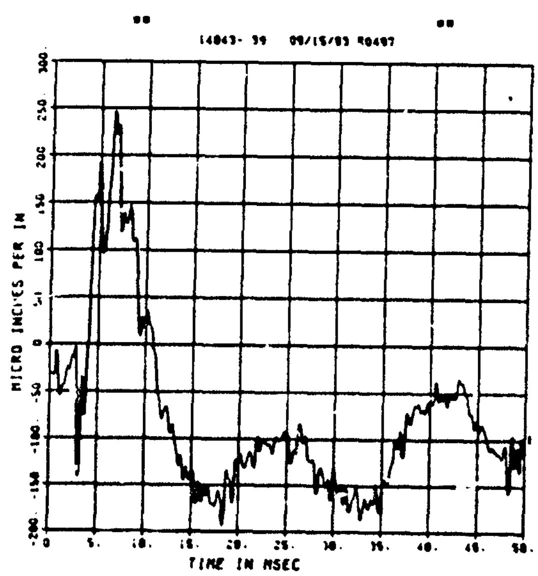

** PEAK VALUE IS 90 % UNDER CALIBRATION **

FEMA ELEM TEST D-3B
EO-7
50000. HZ CAL= 10276.
LP4/4 70% CUTOFF= 2250. HZ

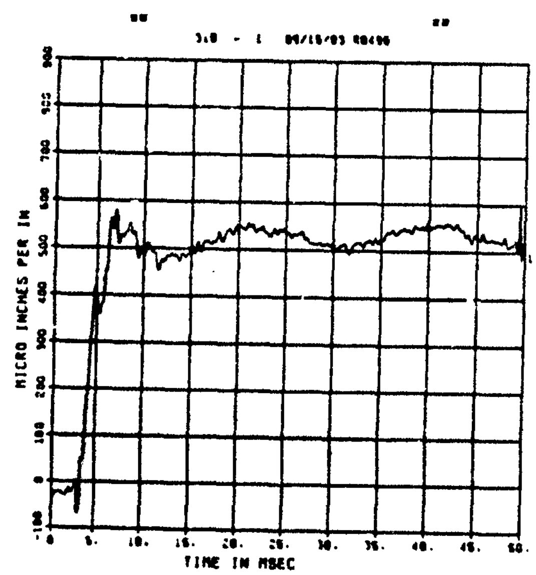

** PEAK VALUE IS 94 % UNDER CALIBRATION **

FEMA ELEM TEST D-3B
EI-7
50000. HZ CAL= 10276.
LP4/4 70% CUTOFF= 2250. HZ

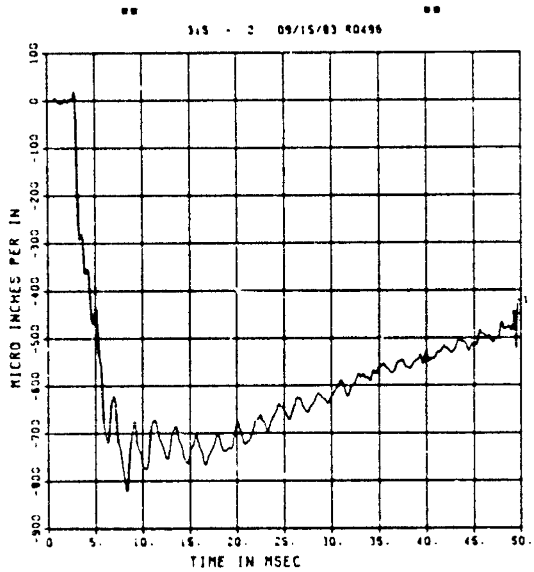

** PEAK VALUE IS 92 % UNDER CALIBRATION **

FEMA ELEM TEST D-3B
EO-8
200000. HZ CAL= 20205.

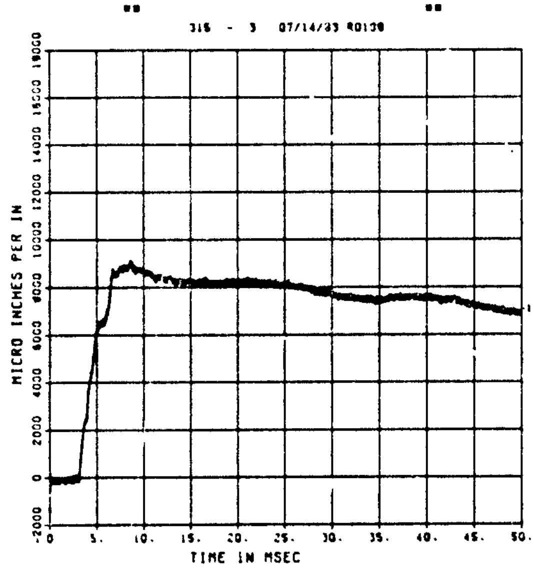

FEMA ELEM TEST D-3B
EI-8
50000. HZ CAL= 10276.
LP4/4 70% CUTOFF= 2250. HZ

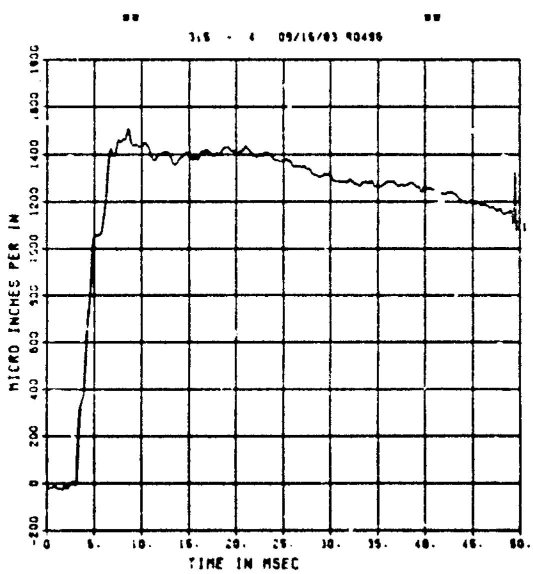

** PEAK VALUE IS 95 % UNDER CALIBRATION **

FEMA ELEM TEST D-3B
EO-9
200000. HZ CAL= 10276.

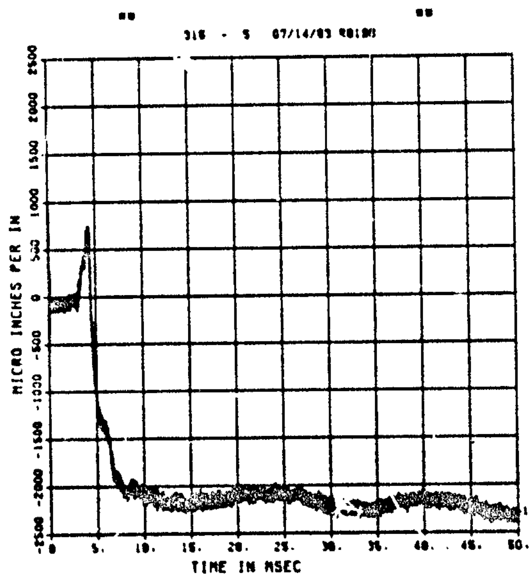

FEMA ELEM TEST D-3B
EI-9
200000. HZ CAL= 10276.

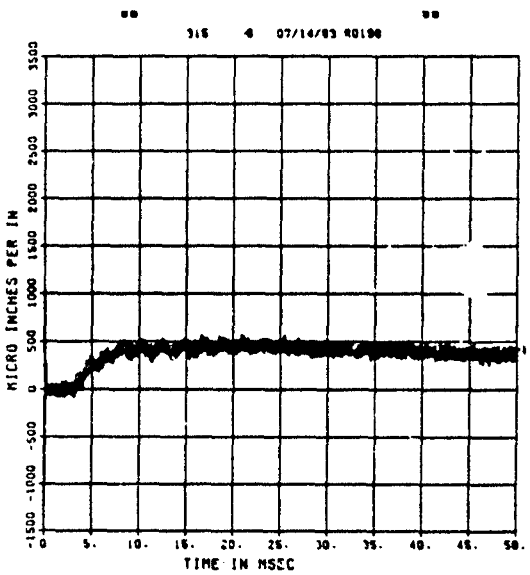

** PEAK VALUE IS 99 % UNDER CALIBRATION **

FEMA ELEM TEST D-3B
EO-10
200000. HZ CAL= 10276.

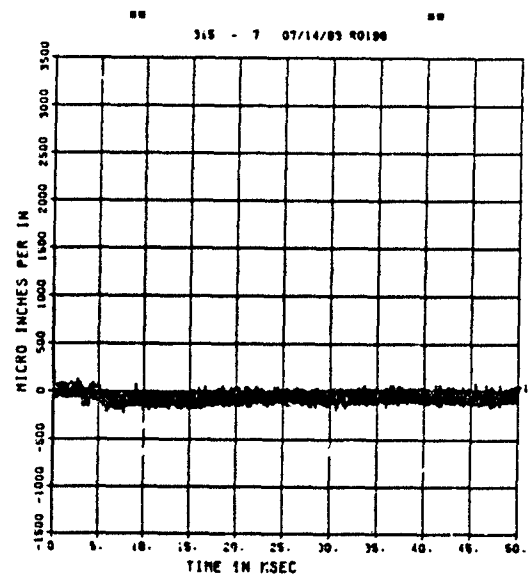

** PEAK VALUE IS 98 % UNDER CALIBRATION **

FEMA ELEM TEST D-3B
EO-11
200000. HZ CAL= 10276.

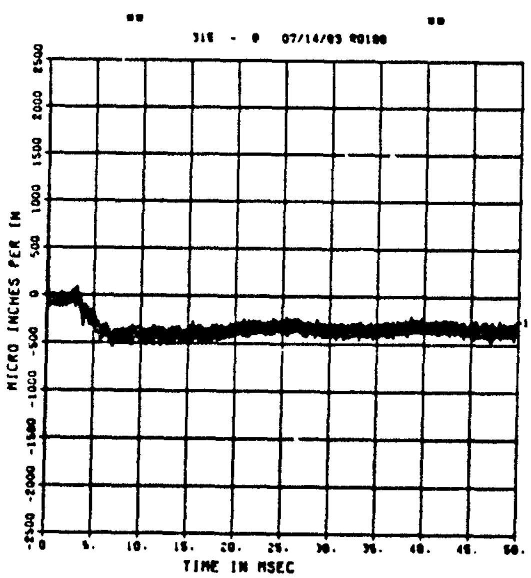

FEMA ELEM TEST D-3B
EI-11
50000. HZ CAL= 20205.
LP4/4 70% CUTOFF= 2250. HZ

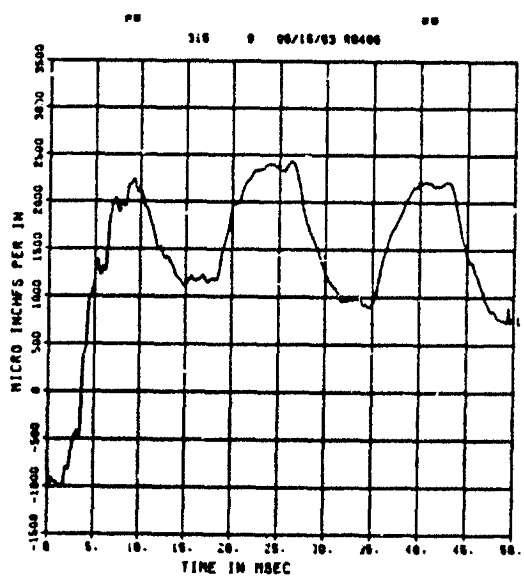

** PEAK VALUE IS 98 % UNDER CALIBRATION **

FEMA ELEM TEST D-3C
BP-1
200000. HZ CAL= 624.2

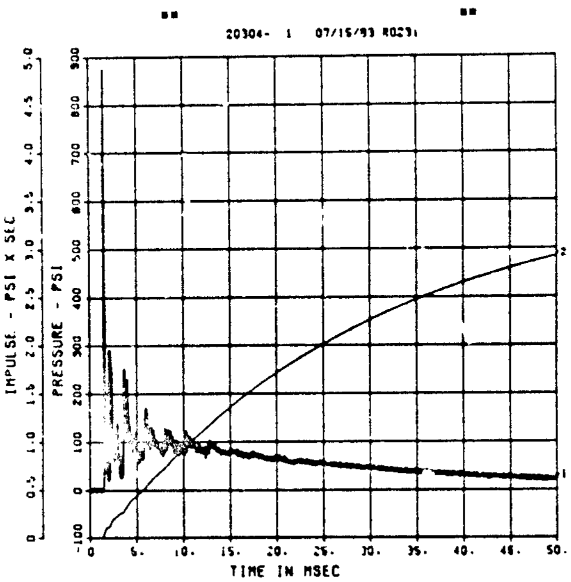

** PEAK VALUE IS 41 % OVER CALIBRATION **

FEMA ELEM TEST D-3C
BP-2
200000. HZ CAL= 575.9

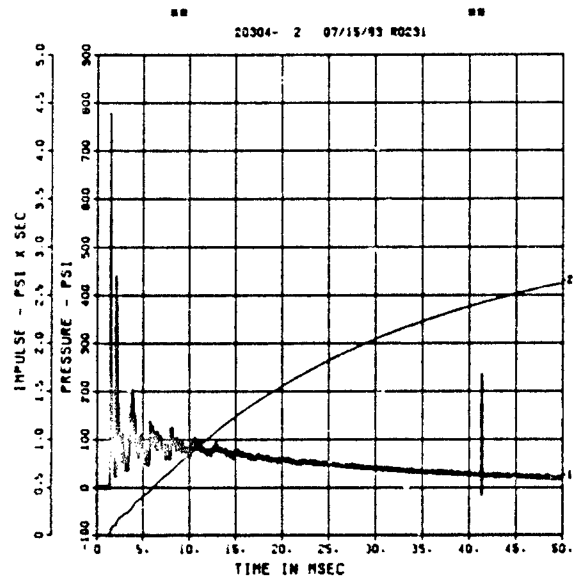

** PEAK VALUE IS 35 % OVER CALIBRATION **

FEMA ELEM TEST D-3C
BP-3
200000. HZ CAL= 744.2

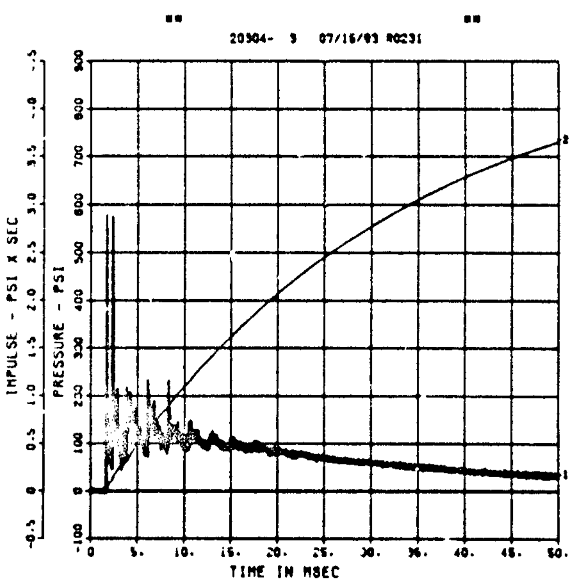

FEMA ELEM TEST D-3C
BP-4
200000. HZ CAL= 659.2 .

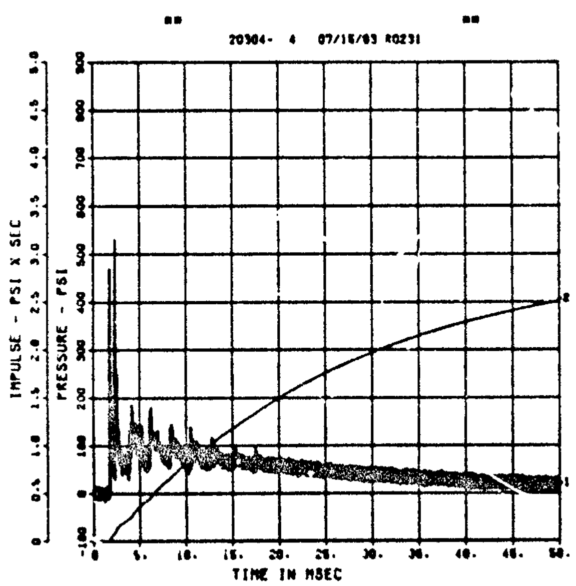

FEMA ELEM TEST D-3C
SE-1
200000. HZ CAL= 356.0

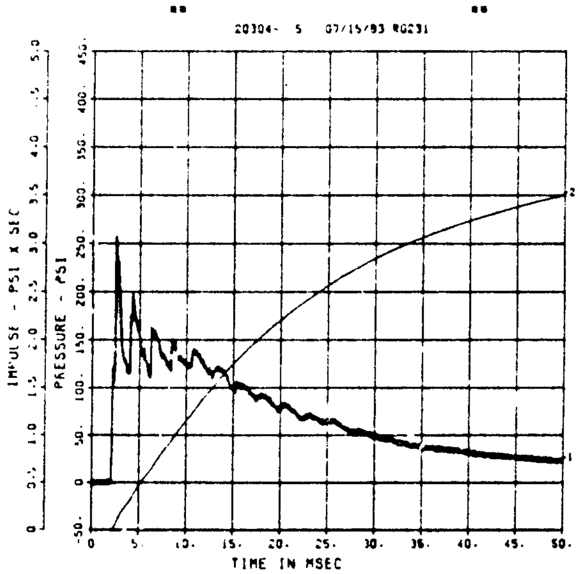

FEMA ELEM TEST D-3C
SE-2
200000. HZ CAL= 130.8

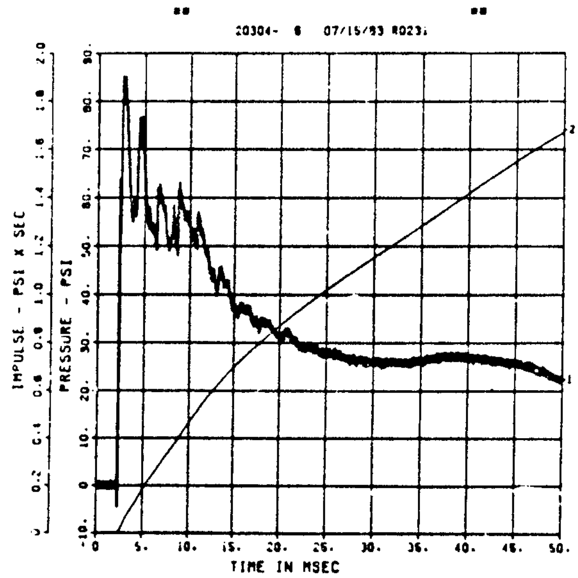

FEMA ELEM TEST D-3C
SE-3
200000. HZ CAL= 257.8

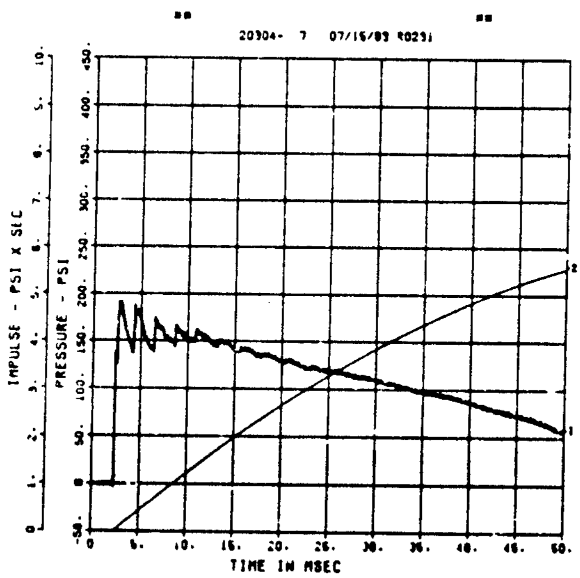

FEMA ELEM TEST D-3C
SE-4
200000. HZ CAL= 132.4

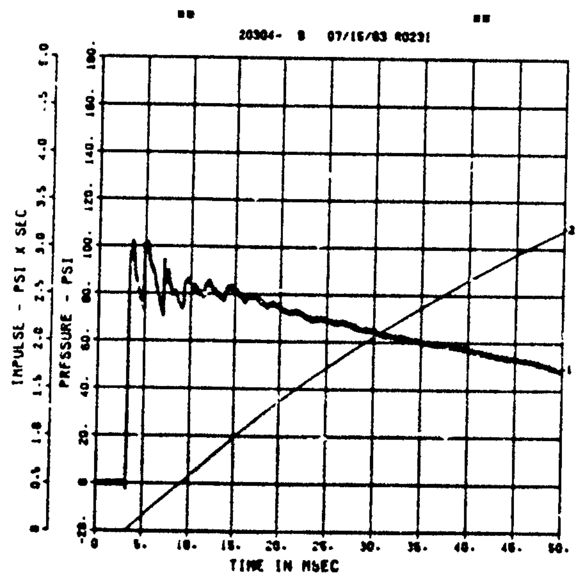

FEMA ELEM TEST D-3C
SE-5
200000. HZ CAL= 132.8

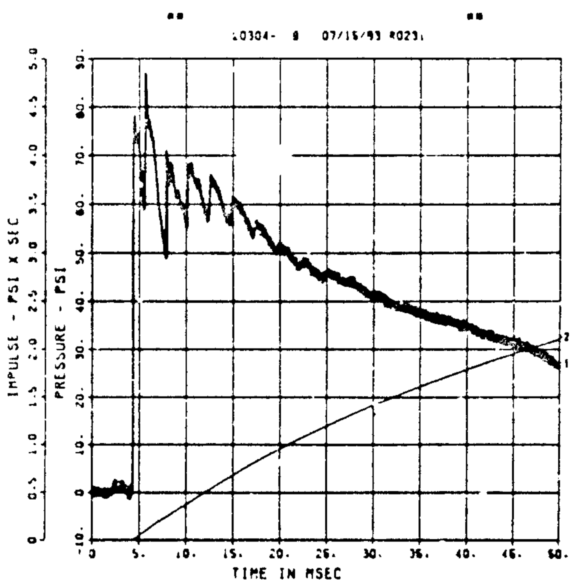

FEMA ELEM TEST D-3C
SE-6
200000. HZ CAL= 364.9

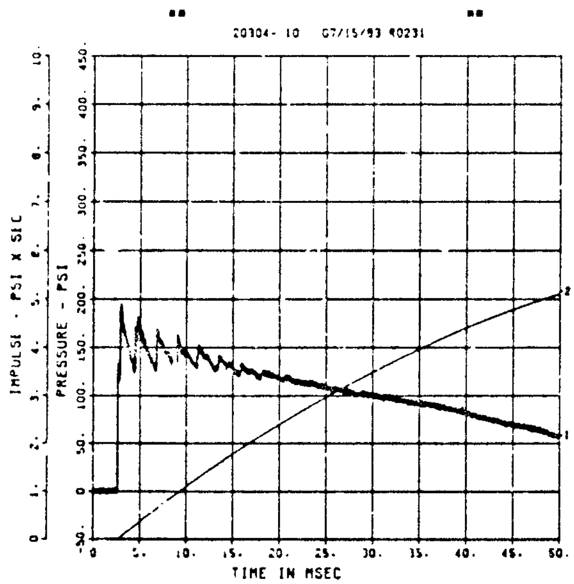

FEMA ELEM TEST D-3C
SE-7
200000. HZ CAL= 122.5

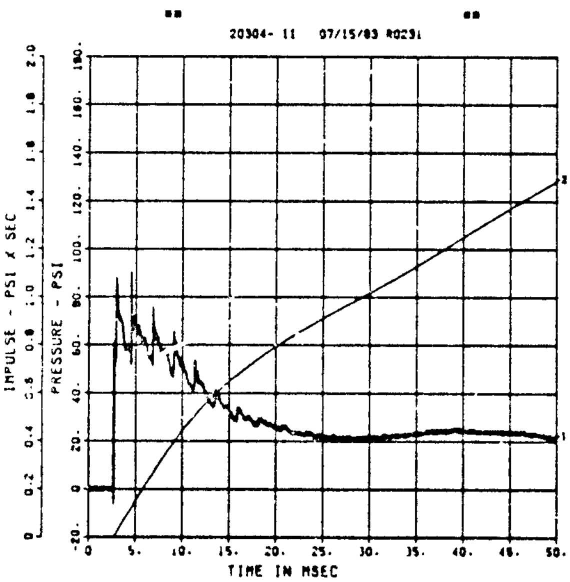

FEMA ELEM TEST D-3C
AFF-1
200000. HZ CAL= 553.1

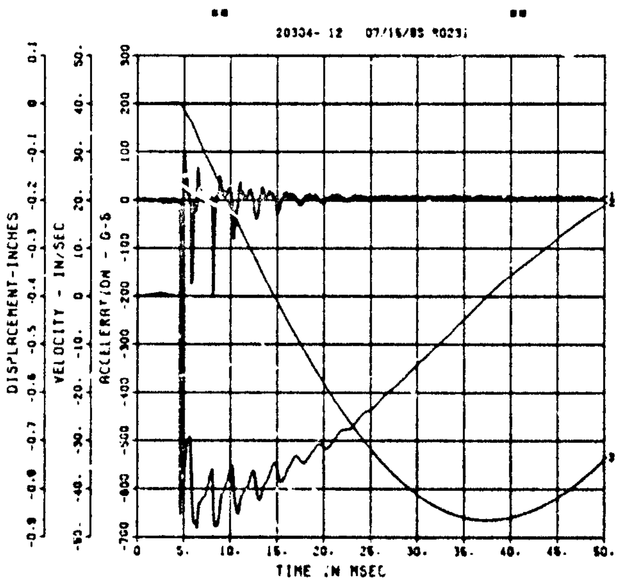

** PEAK VALUE IS 18 % OVER CALIBRATION **

FEMA ELEM TEST D-3C
A-1
200000. HZ CAL= 2504.

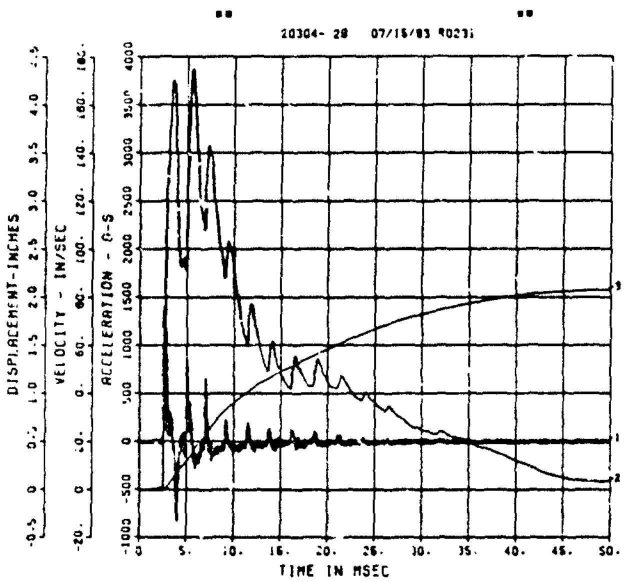

FEMA ELEM TEST D-3C
A-2
200000. HZ CAL= 812.4

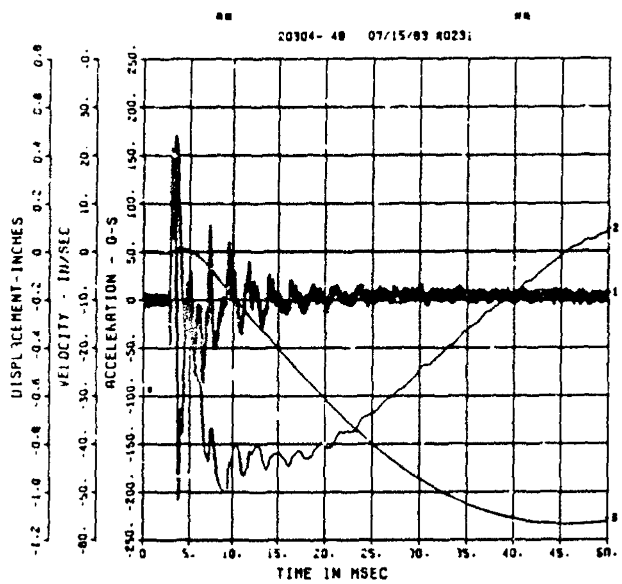

FEMA ELEM TEST D-3C
IF-1
200000. HZ CAL= 346.6

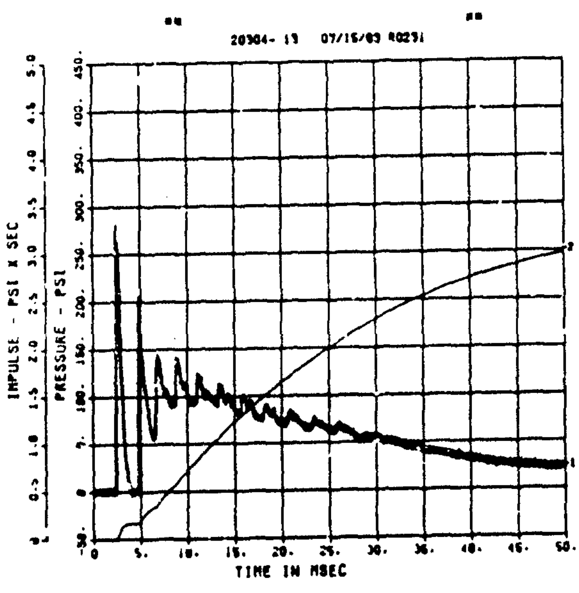

FEMA ELEM TEST D-3C
IF-2
200000. HZ CAL= 347.3

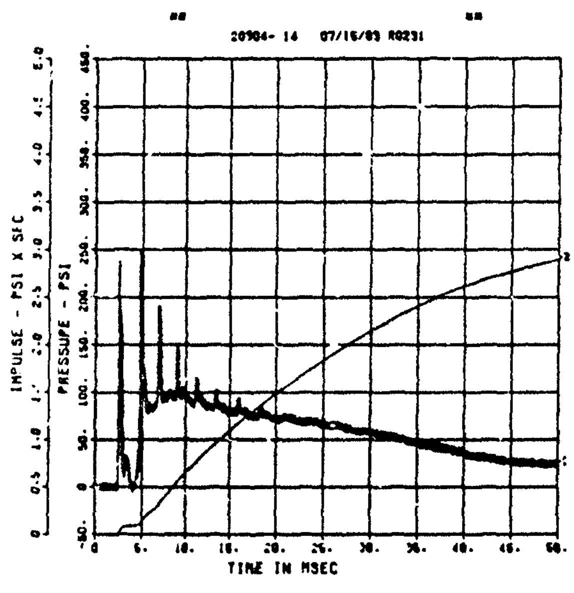

FEMA ELEM TEST D-3C
IF-3
200000. HZ CAL= 347.8

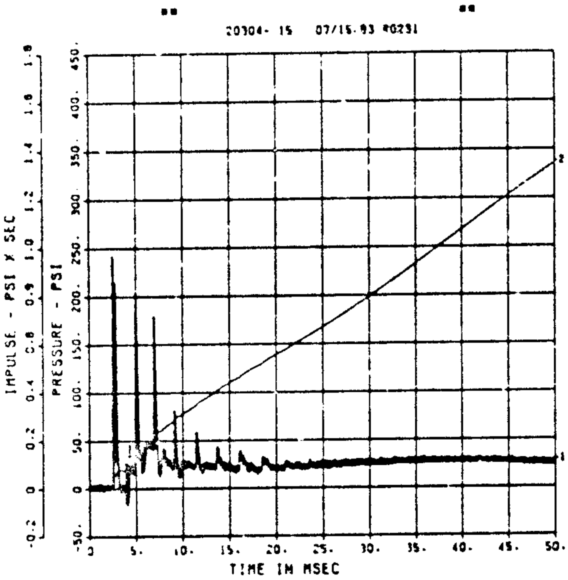

FEMA ELEM TEST D-3C
IF-4
200000. HZ CAL= 345.9

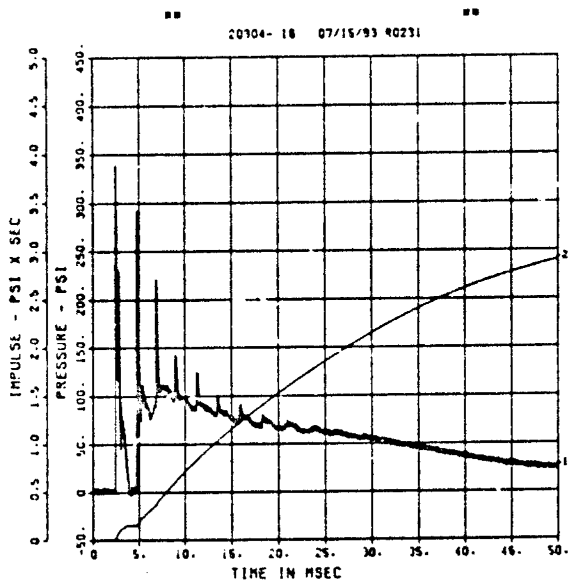

FEMA ELEM TEST D-3C
IF-5
200000. HZ CAL= 363.1

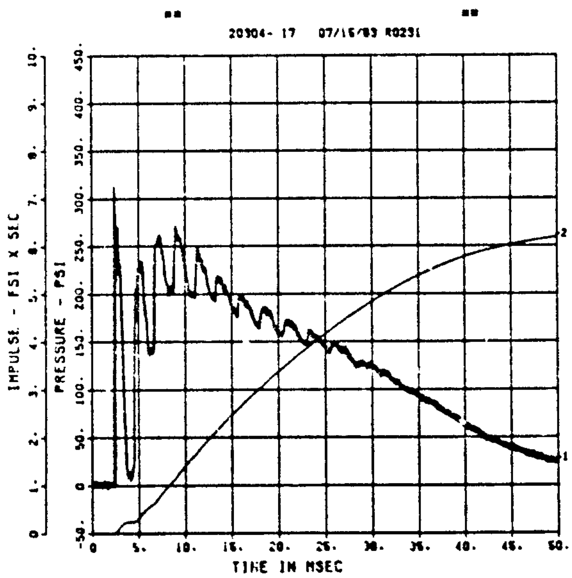

FEMA ELEM TEST D-3C
IF-6
200000. HZ CAL= 109.8

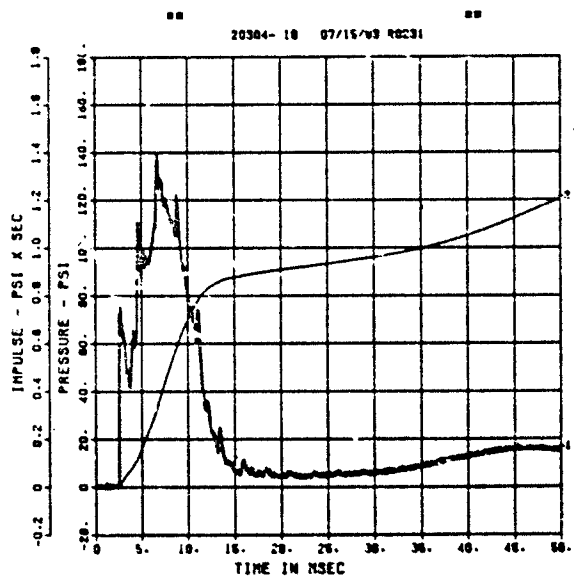

** PEAK VALUE IS 27 % OVER CALIBRATION **

FEMA ELEM TEST D-3C
IF-7
200000. HZ CAL= 128.5

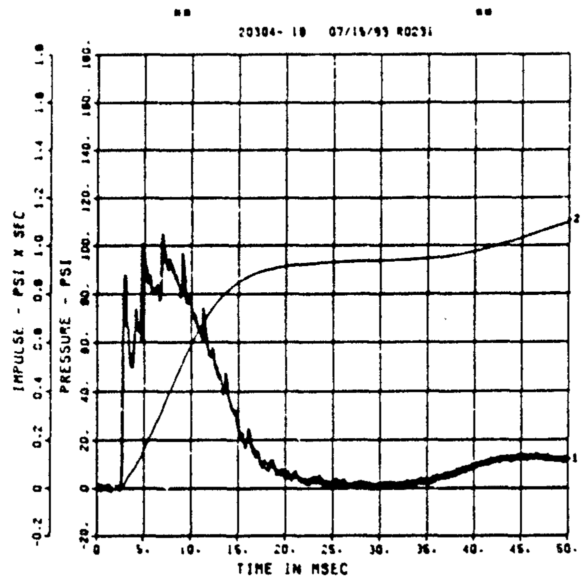

FEMA ELEM TEST D-3C
IF-8
200000. HZ CAL= 85.40

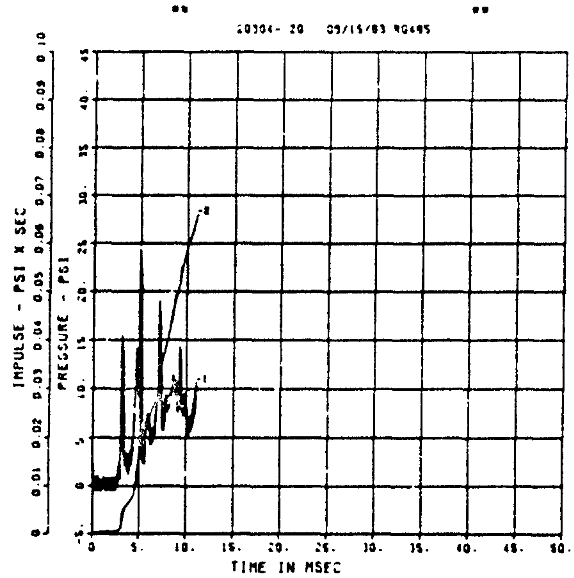

FEMA ELEM TEST D-3C
IF-9
200000. HZ CAL= 52.30

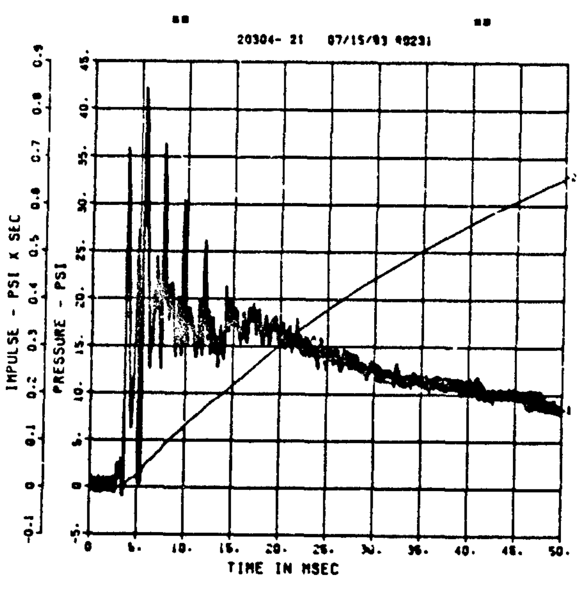

FEMA ELEM TEST D-3C
IF-10
200000. HZ CAL= 51.70

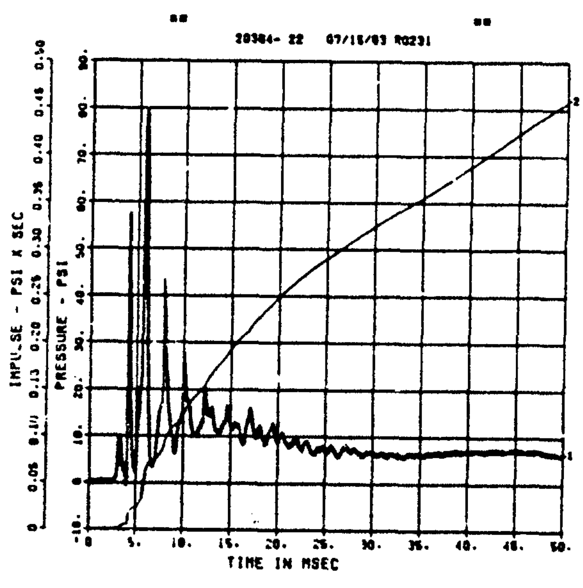

** PEAK VALUE IS 64 % OVER CALIBRATION **

FEMA ELEM TEST D-3C
IF-11
200000. HZ CAL= 52.80

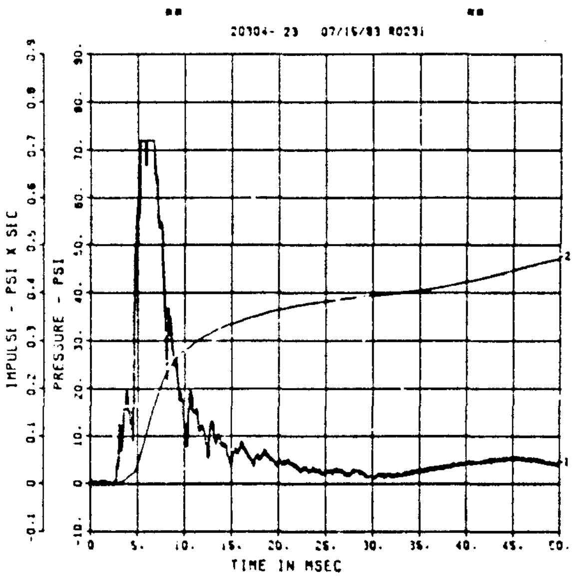

** PEAK VALUE IS 37 % OVER CALIBRATION **

FEMA ELEM TEST D-3C
IF-12
200000. HZ CAL= 243.7

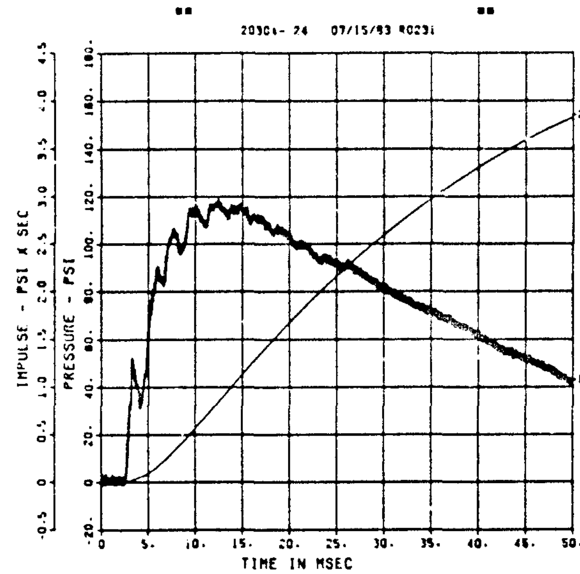

FEMA ELEM TEST D-3C
IF-13
200000. HZ CAL= 246.7

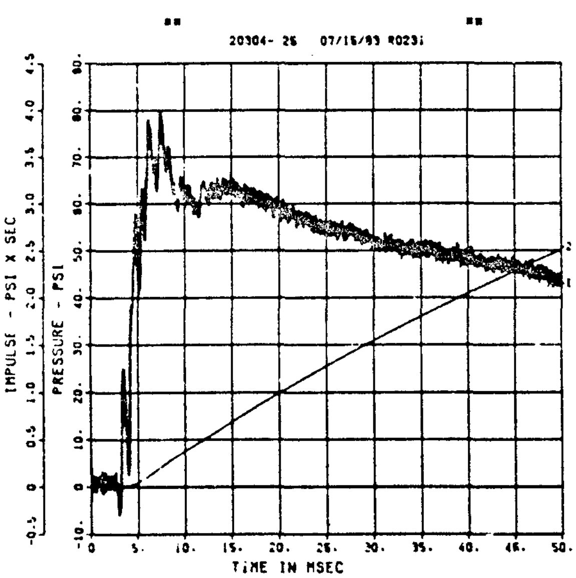

FEMA ELEM TEST D-3C
IF-14
50000. HZ CAL= 246.6
LP4/4 70% CUTOFF= 2250. HZ

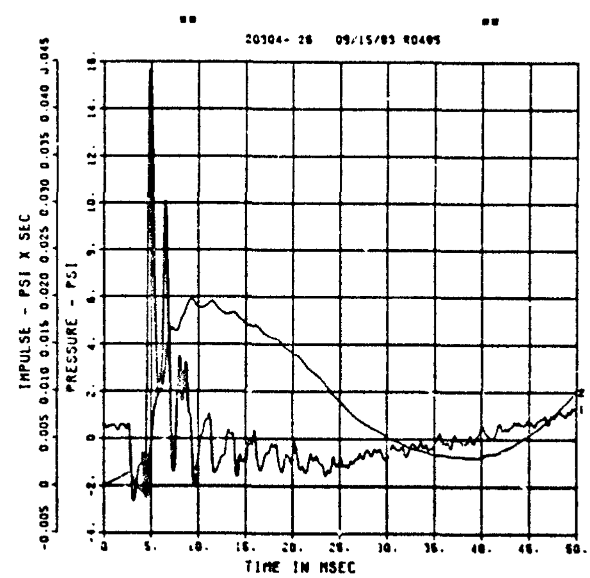

** PEAK VALUE IS 94 % UNDER CALIBRATION **

FEMA ELEM TEST D-3C
IF-15
50000. HZ CAL= 244.5
LP4/4 70% CUTOFF= 2250. HZ

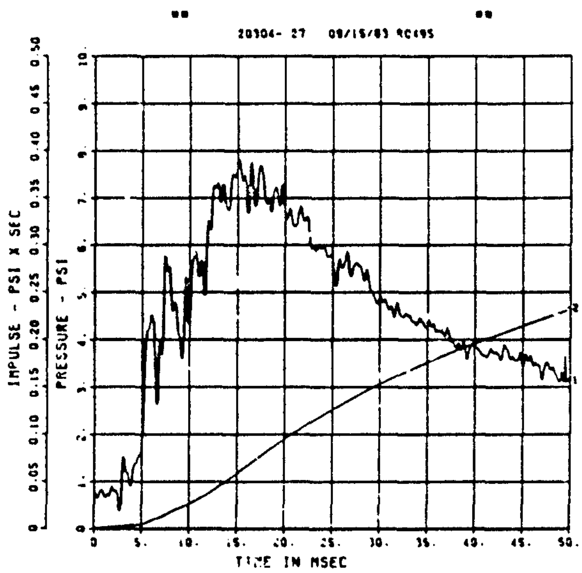

** PEAK VALUE IS 97 % UNDER CALIBRATION **

FEMA ELEM TEST D-3C
IF-16
200000. HZ CAL= 247.0

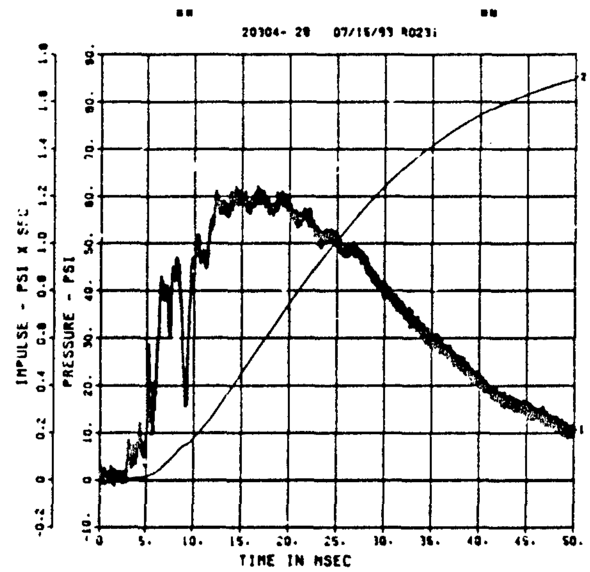

FEMA ELEM TEST D-3C
EO-1
50000. HZ CAL= 20205.
LP4/4 70% CUTOFF= 2250. HZ

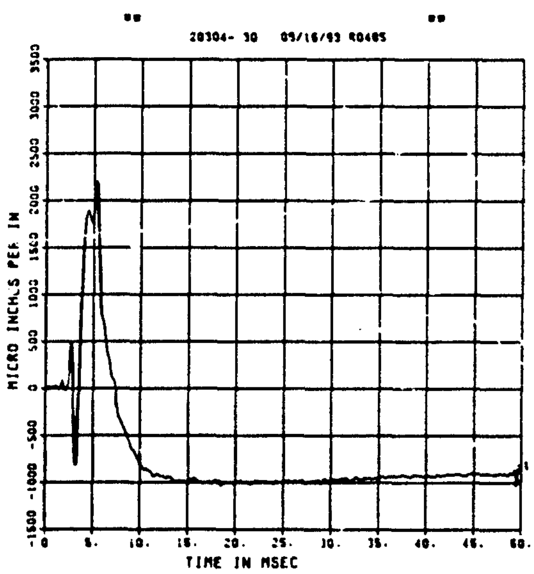

** PEAK VALUE IS 88 % UNDER CALIBRATION **

FEMA ELEM TEST D-3C
EI-1
50000. HZ CAL= 20205.
LP4/4 70% CUTOFF= 2250. HZ

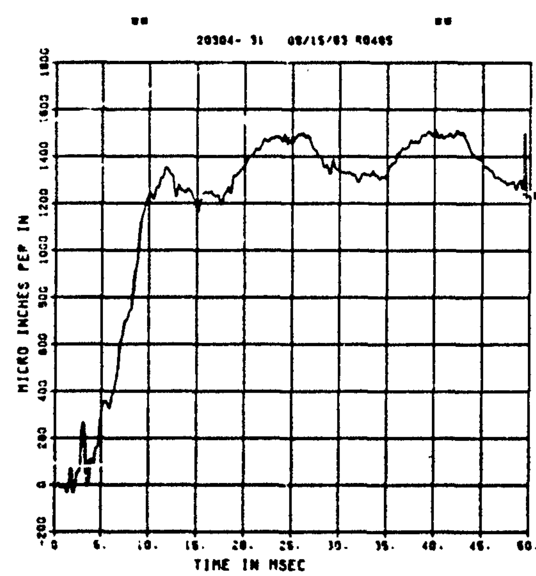

** PEAK VALUE IS 83 % UNDER CALIBRATION **

FEMA ELEM TEST D-3C
E0-2
200000. HZ CAL= 20205.

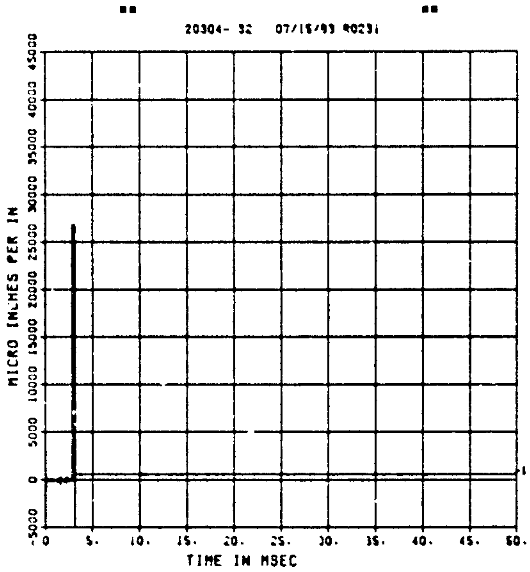

** PEAK VALUE IS 33 % OVER CALIBRATION **

FEMA ELEM TEST D-3C
EI-2
50000. HZ CAL= 20205.
LP4/4 70% CUTOFF= 2250. HZ

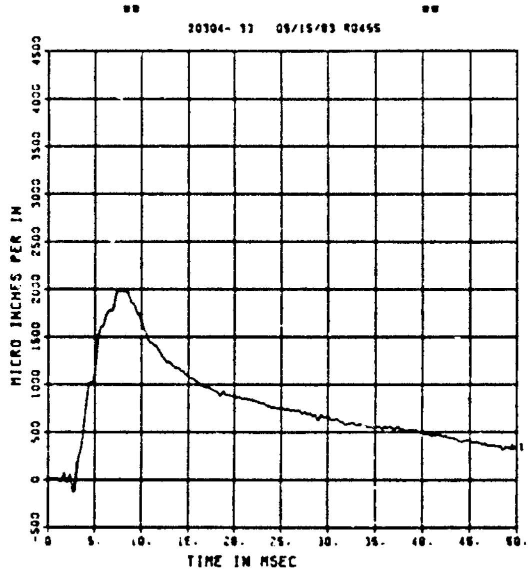

** PEAK VALUE IS 90 % UNDER CALIBRATION **

FEMA ELEM TEST D-3C
E0-3
50000. HZ CAL= 20205.
LP4/4 70% CUTOFF= 2250. HZ

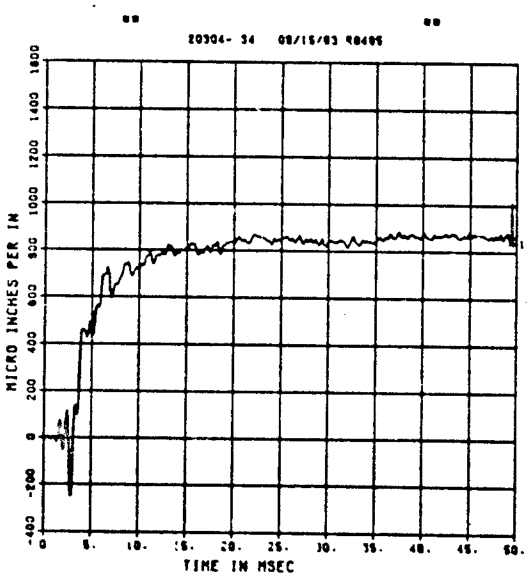

** PEAK VALUE IS 95 % UNDER CALIBRATION **

FEMA ELEM TEST D-3C
EI-3
200000. HZ CAL= 20205.

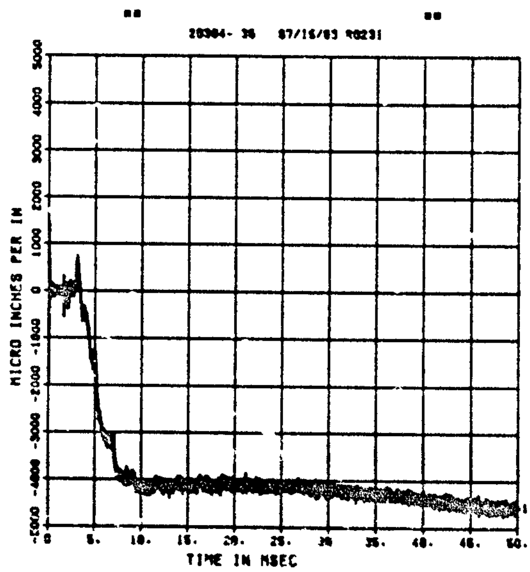

FEMA ELEM TEST D-3C
EO-4
50000. HZ CAL= 20205.
LP4/4 70% CUTOFF= 2250. HZ

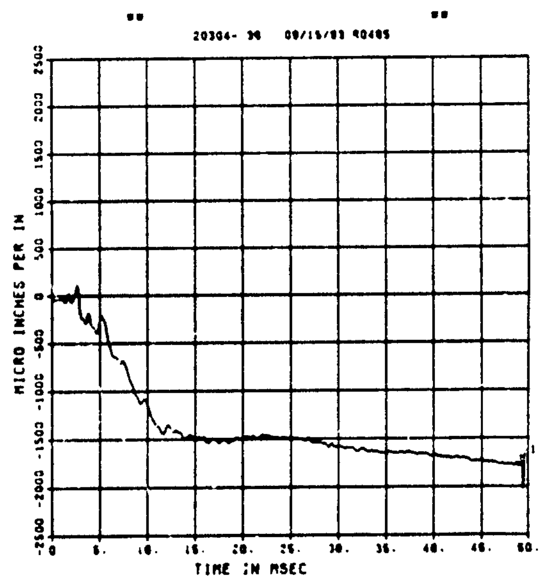

** PEAK VALUE IS 90 % UNDER CALIBRATION **

FEMA ELEM TEST D-3C
EO-5
50000. HZ CAL= 20205.
LP4/4 70% CUTOFF= 2250. HZ

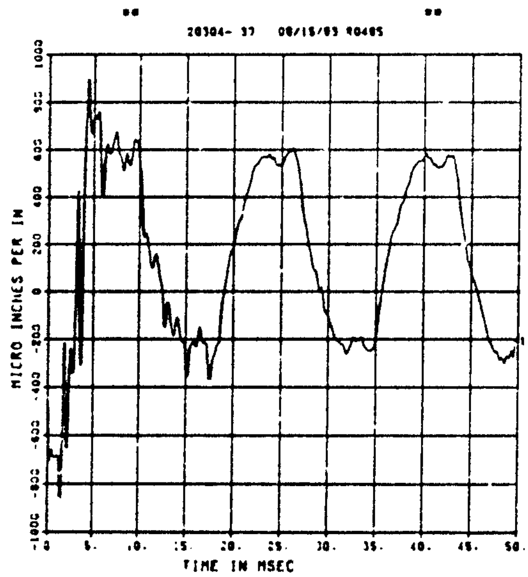

** PEAK VALUE IS 90 % UNDER CALIBRATION **

FEMA ELEM TEST D-3C
EI-5
50000. HZ CAL= 20205.
LP4/4 70% CUTOFF= 2250. HZ

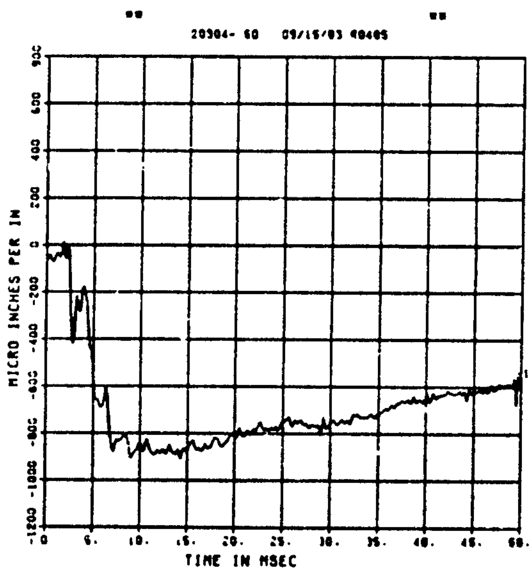

** PEAK VALUE IS 90 % UNDER CALIBRATION **

FEMA ELEM TEST D-3C
EO-6
50000. HZ CAL= 20205.
LP4/4 70% CUTOFF= 2250. HZ

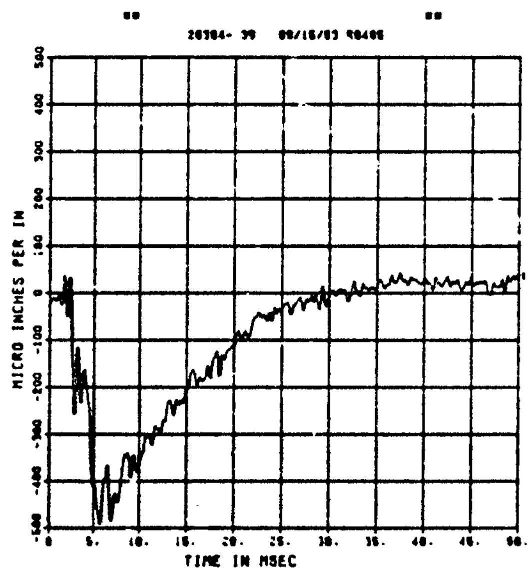

** PEAK VALUE IS 90 % UNDER CALIBRATION **

FEMA ELEM TEST D-3C
EI-6
50000. HZ CAL= 20205.
LP4/4 70% CUTOFF= 2250. HZ

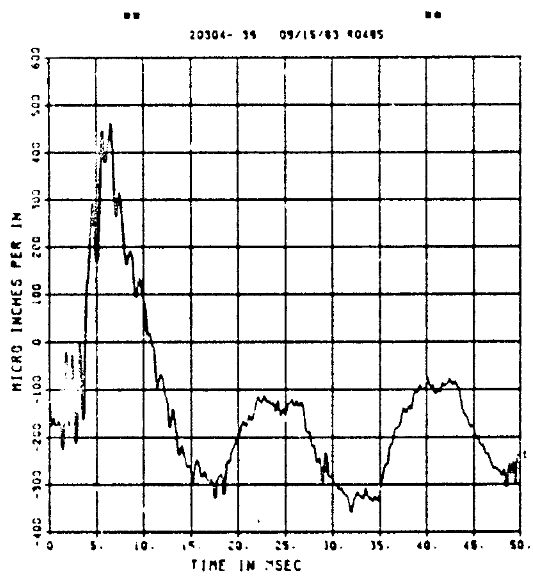

** PEAK VALUE IS 90 % UNDER CALIBRATION **

FEMA ELEM TEST D-3C
EO-7
50000. HZ CAL= 20205.
LP4/4 70% CUTOFF= 2250. HZ

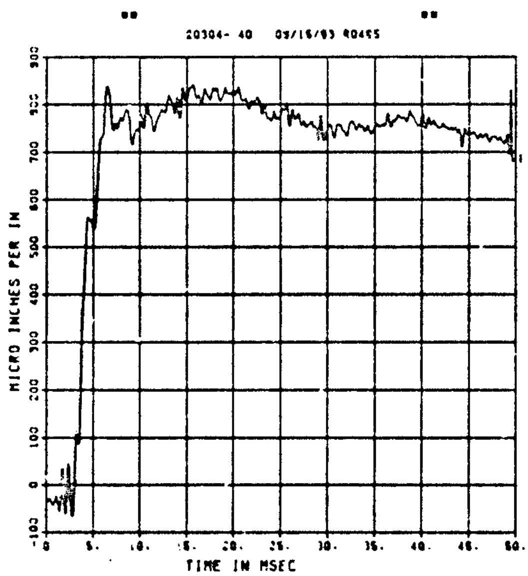

** PEAK VALUE IS 90 % UNDER CALIBRATION **

FEMA ELEM TEST D-3C
EI-7
50000. HZ CAL= 20205.
LP4/4 70% CUTOFF= 2250. HZ

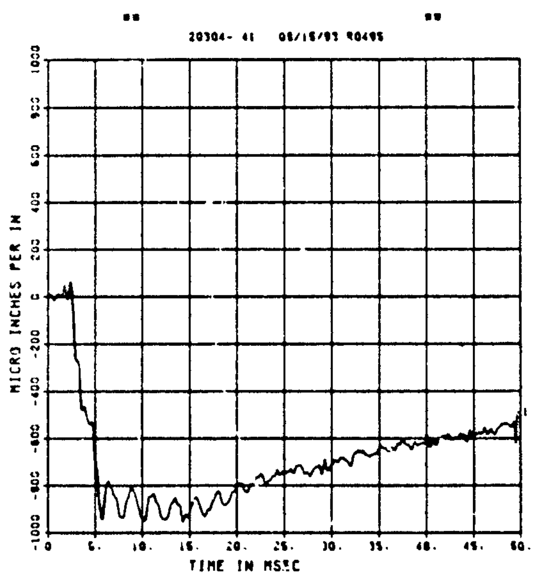

** PEAK VALUE IS 96 % UNDER CALIBRATION **

FEMA ELEM TEST D-3C
EO-8
200000. HZ CAL= 39162.

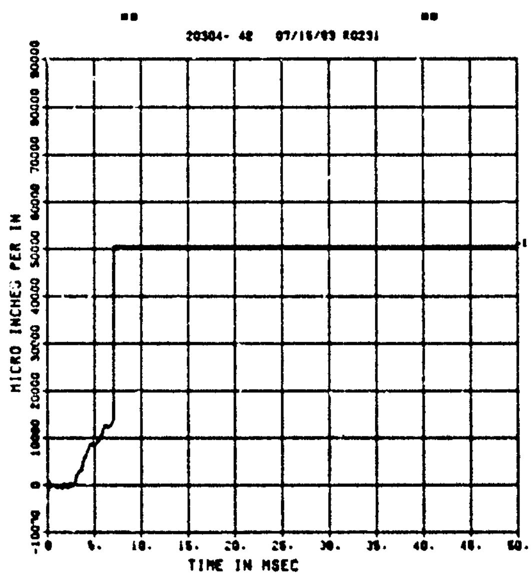

** PEAK VALUE IS 28 % OVER CALIBRATION **

FEMA ELEM TEST D-3C
EI-8
200000. HZ CAL= 10276.

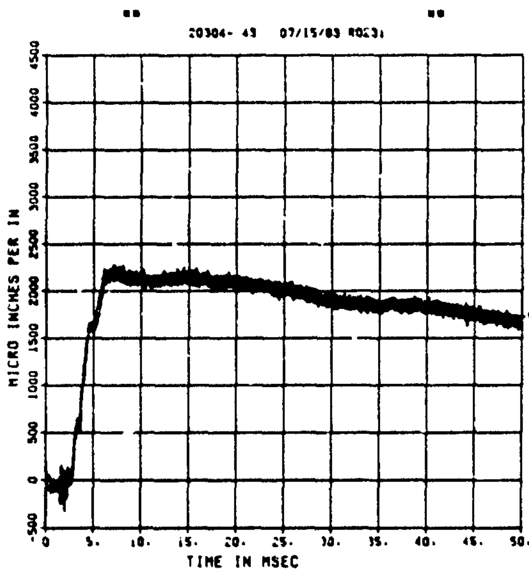

FEMA ELEM TEST D-3C
EO-9
200000. HZ CAL= 10276.

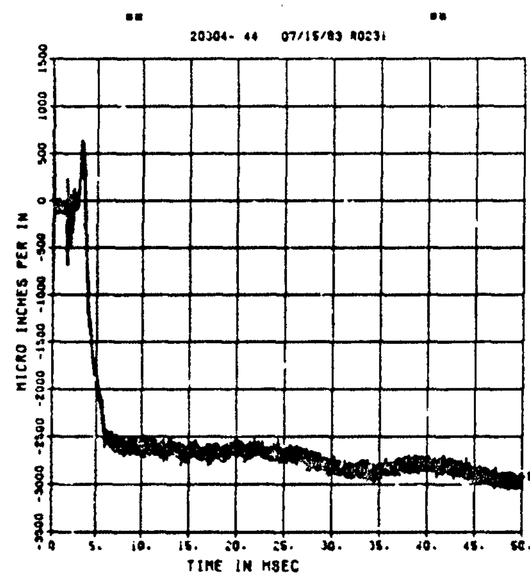

FEMA ELEM TEST D-3C
EI-9
50000. HZ CAL= 10276.
LP4/4 70% CUTOFF= 2250. HZ

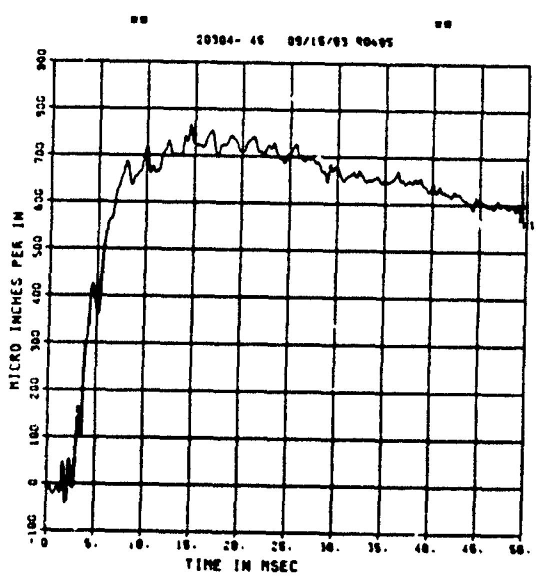

** PEAK VALUE IS 83 % UNDER CALIBRATION **

FEMA ELEM TEST D-3C
EO-10
50000. HZ CAL= 10276.
LP4/4 70% CUTOFF= 2250. HZ

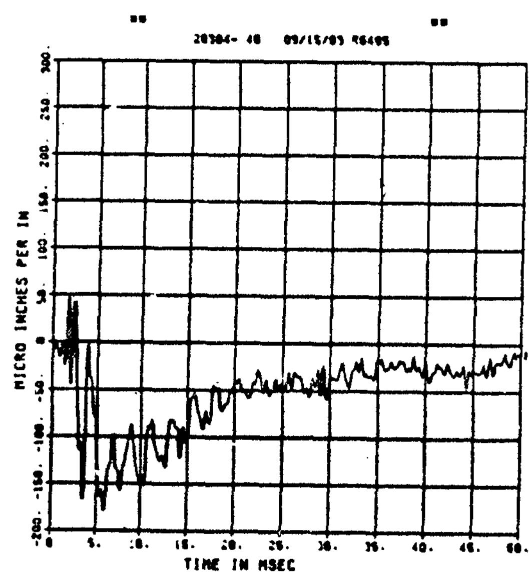

** PEAK VALUE IS 88 % UNDER CALIBRATION **

FEMA ELEM TEST D-3C
EO-11
50000. HZ CAL= 10276.
LP4/4 70% CUTOFF= 2250. HZ

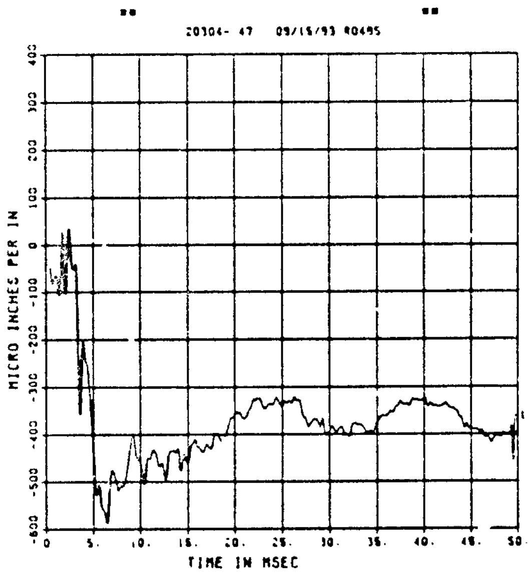

** PEAK VALUE IS 94 % UNDER CALIBRATION **

FEMA ELEM TEST D-3C
EI-11
50000. HZ CAL= 20205.
LP4/4 70% CUTOFF= 2250. HZ

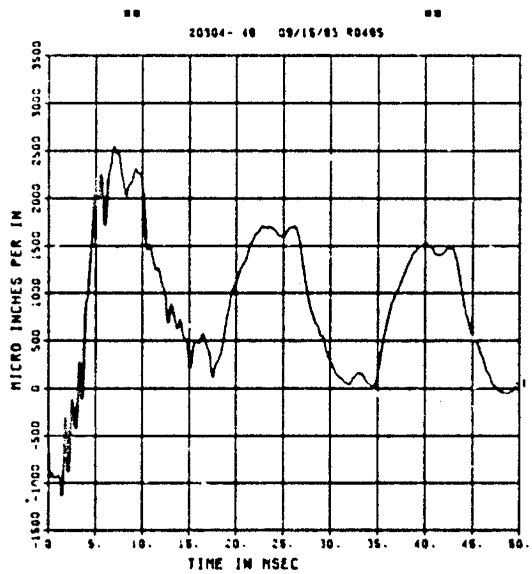

** PEAK VALUE IS 87 % UNDER CALIBRATION **

FEMA ELEM TEST D-4
BP-1
200000. HZ CAL= 989.0

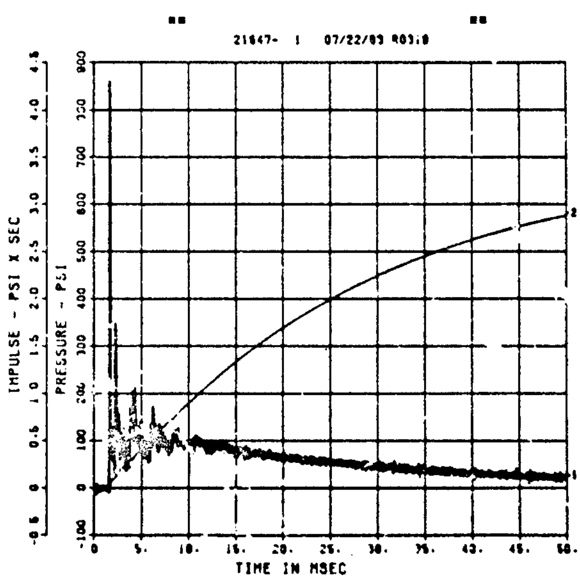

FEMA ELEM TEST D-4
BP-2
200000. HZ CAL= 912.5

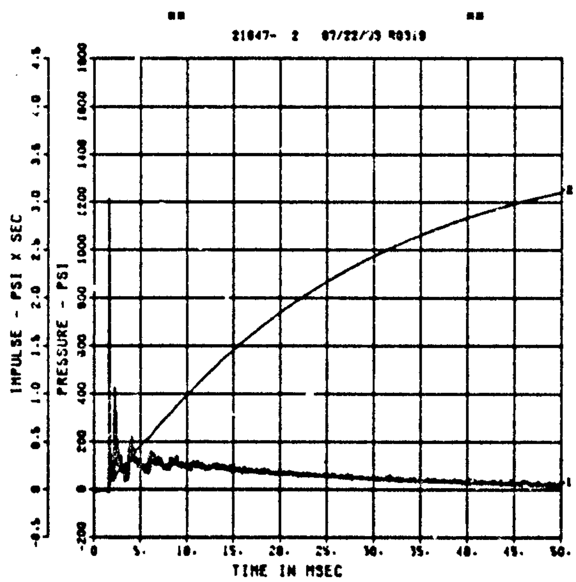

** PEAK VALUE 1.33 % OVER CALIBRATION **

FEMA ELEM TEST D-4
BP-3
200000. HZ CAL= 744.1

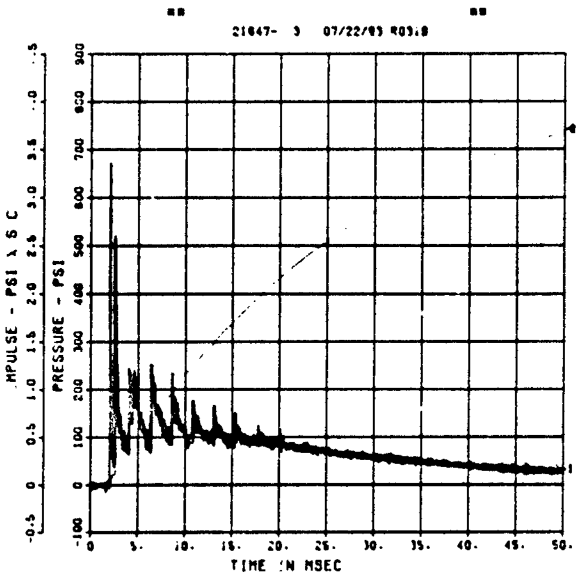

FEMA ELEM TEST D-4
BP-4
200000. HZ CAL= 1045.

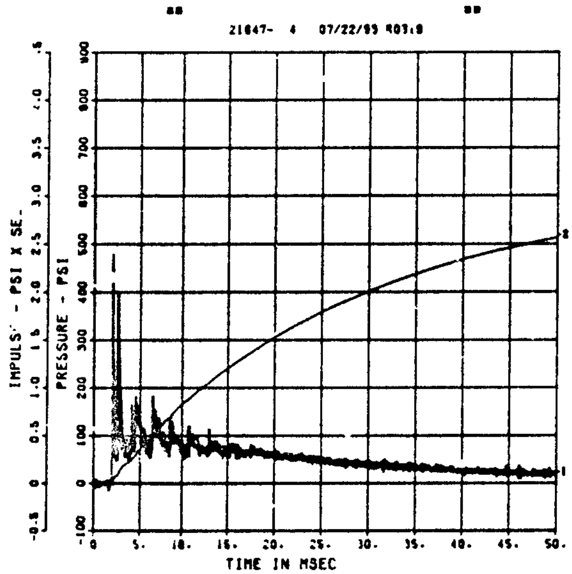

FEMA ELEM TEST D-4
SE-1
200000. HZ CAL= 356.1

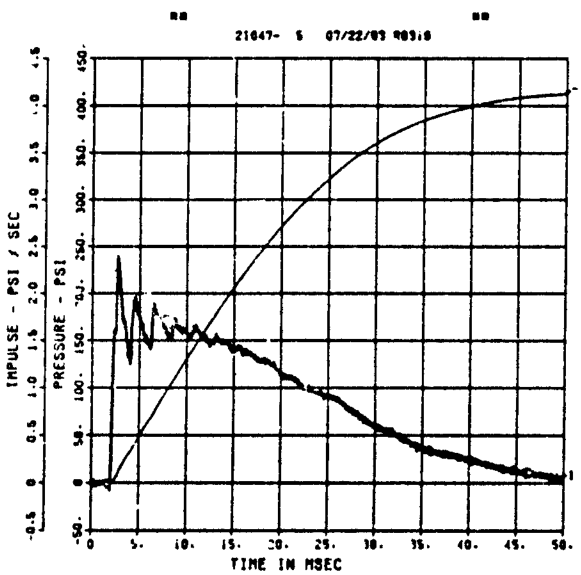

FEMA ELEM TEST D-4
SE-2
200000. HZ CAL= 130.8

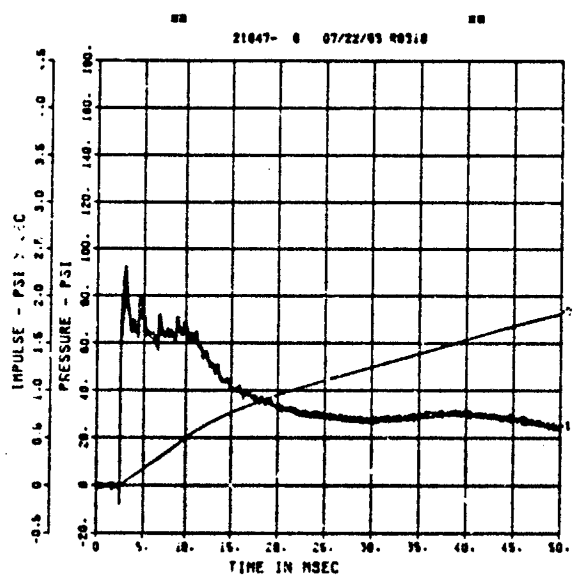

FEMA ELEM TEST D-4
SE-6
200000. HZ CAL= 364.9

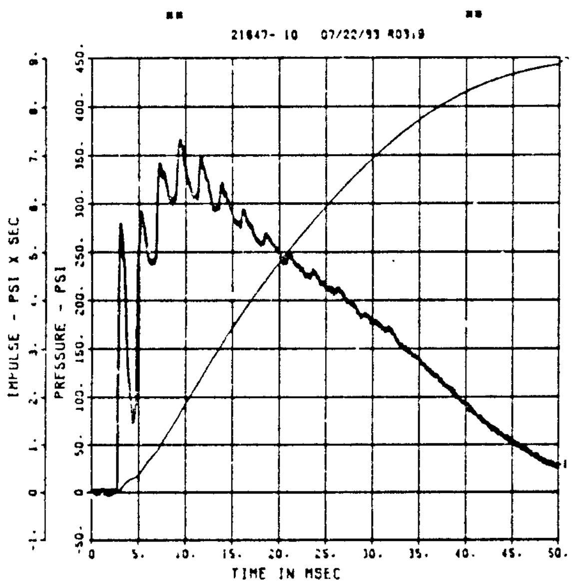

FEMA ELEM TEST D-4
SE-3
200000. HZ CAL= 257.8

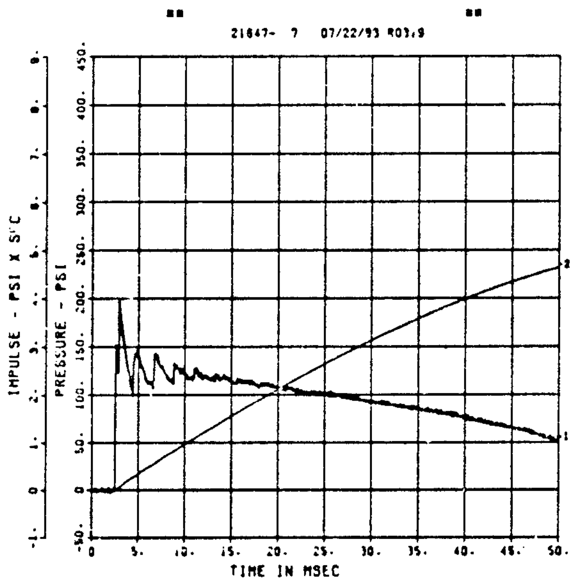

FEMA ELEM TEST D-4
SE-4
200000. HZ CAL= 132.5

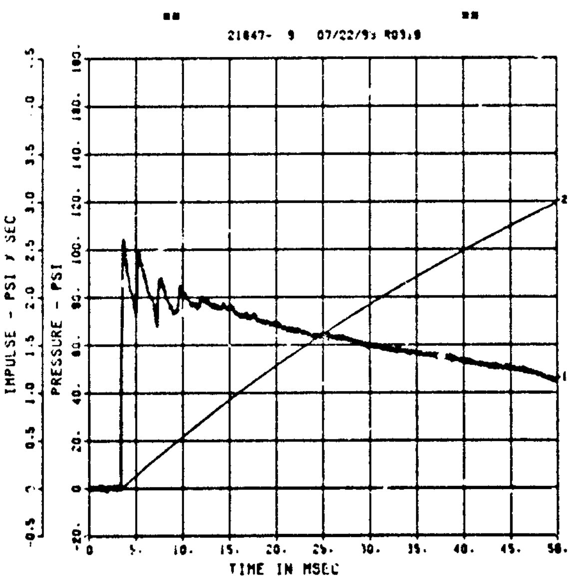

FEMA ELEM TEST D-4
SE-5
200000. HZ CAL= 132.9

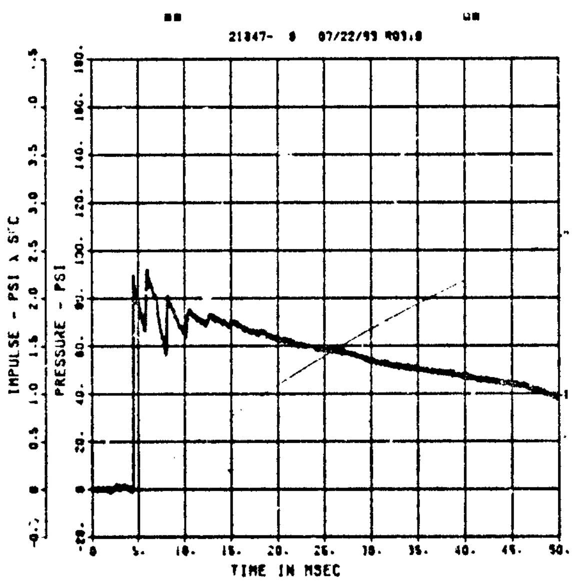

FEMA ELEM TEST D-4
SE-7
200000. HZ CAL= 122.6

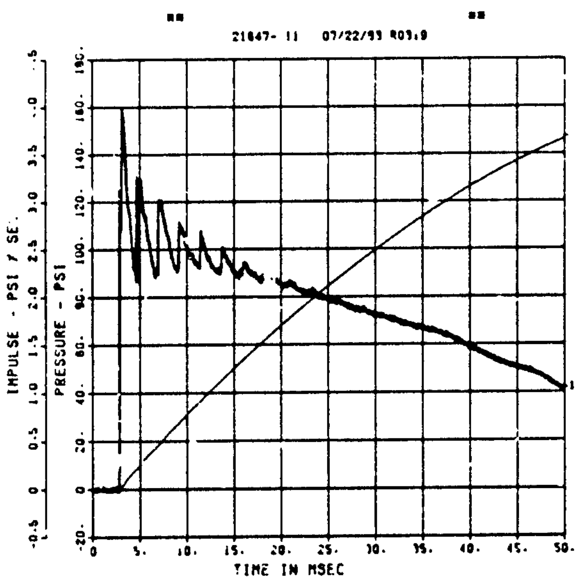

** PEAK VALUE IS 30 % OVER CALIBRATION **

FEMA ELEM TEST D-4
AFF-1
200000. HZ CAL= 810.6

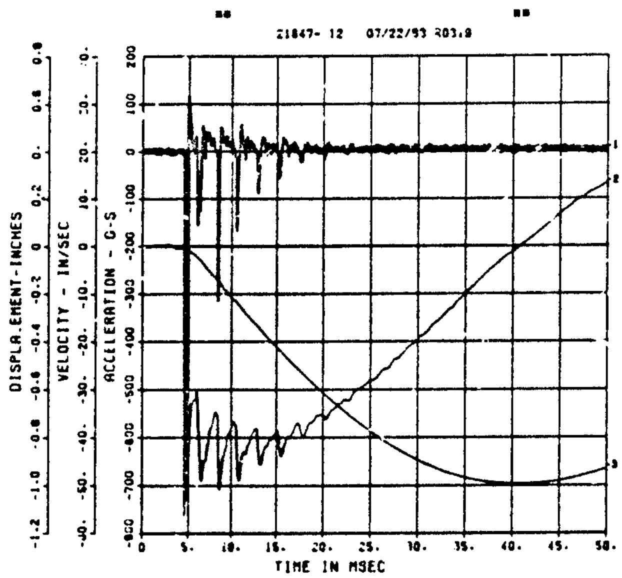

FEMA ELEM TEST D-4
A-1
200000. HZ CAL= 1692.

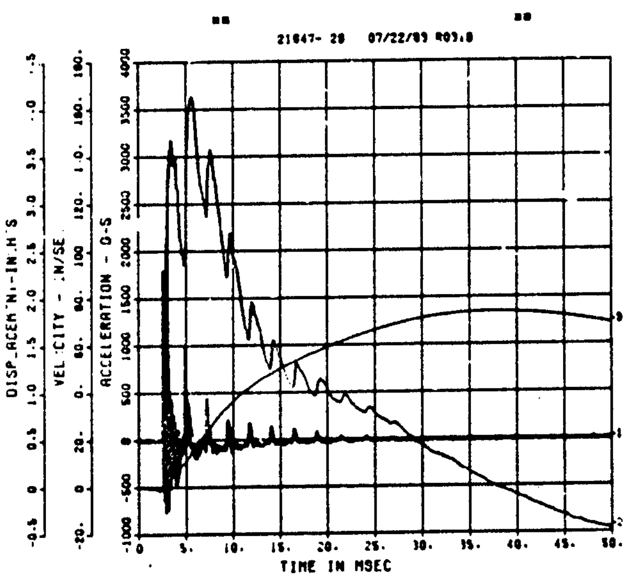

** PEAK VALUE IS 20 % OVER CALIBRATION **

FEMA ELEM TEST D-4
A-2
200000. HZ CAL= 414.6

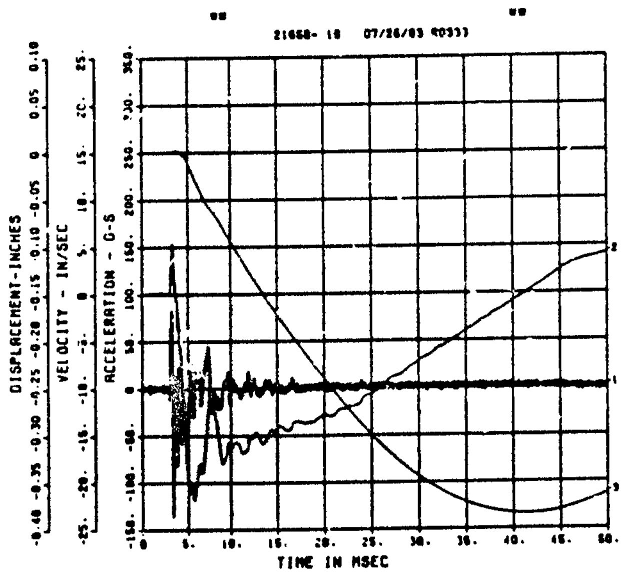

FEMA ELEM TEST D-4
IF-1
200000. HZ CAL= 349.5

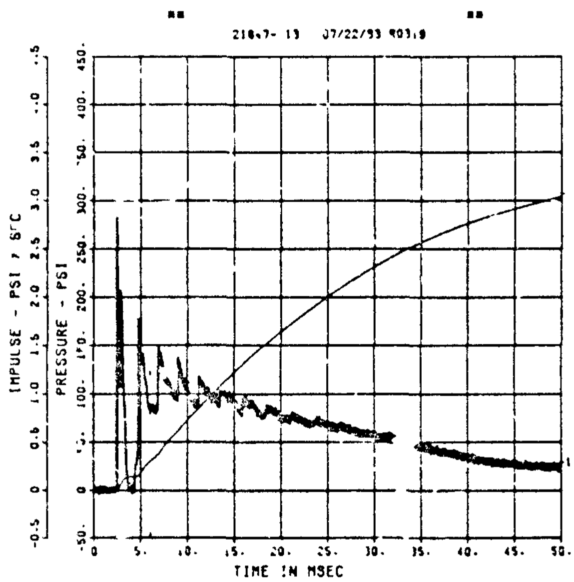

FEMA ELEM TEST D-4
IF-2
200000. HZ CAL= 347.3

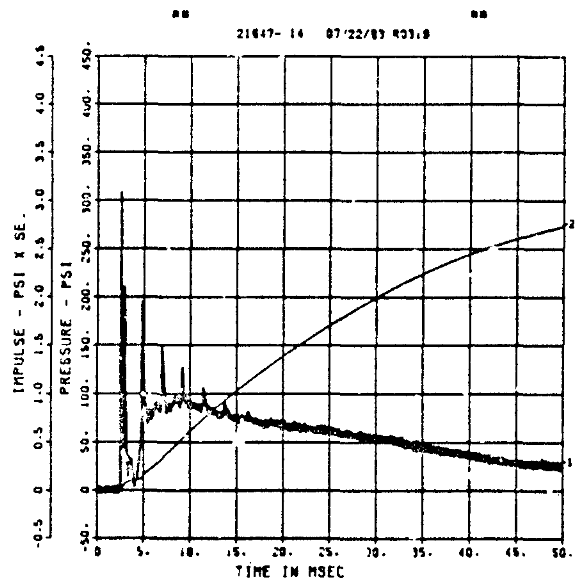

FEMA ELEM TEST D-4
IF-3
200000. HZ CAL= 347.9

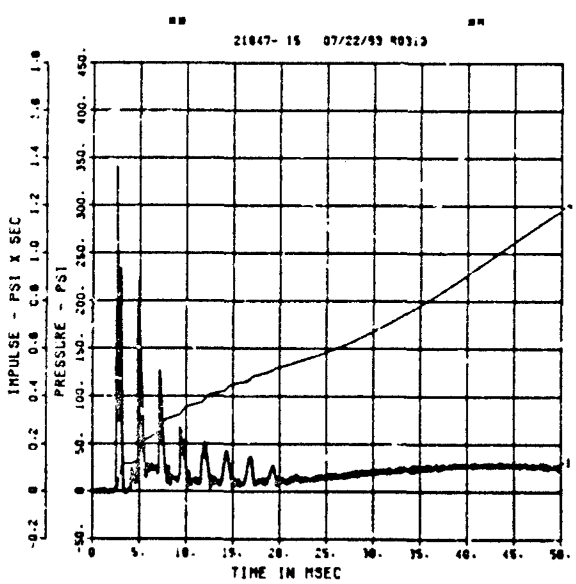

FEMA ELEM TEST D-4
IF-4
200000. HZ CAL= 345.9

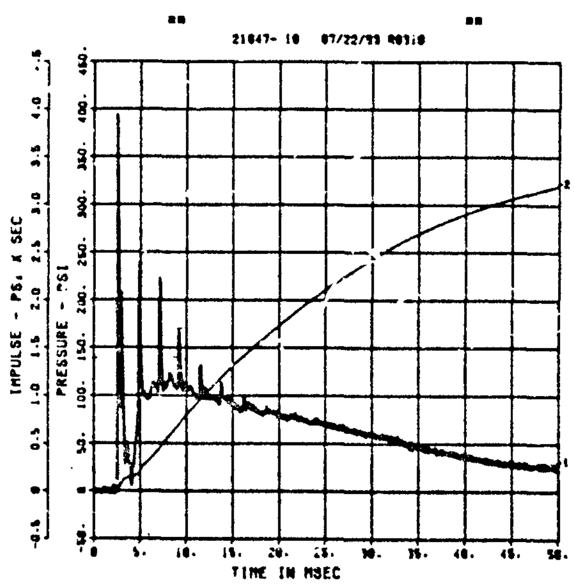

** PEAK VALUE IS 14 % OVER CALIBRATION **

FEMA ELEM TEST D-4
IF-6
200000. HZ CAL= 145.7

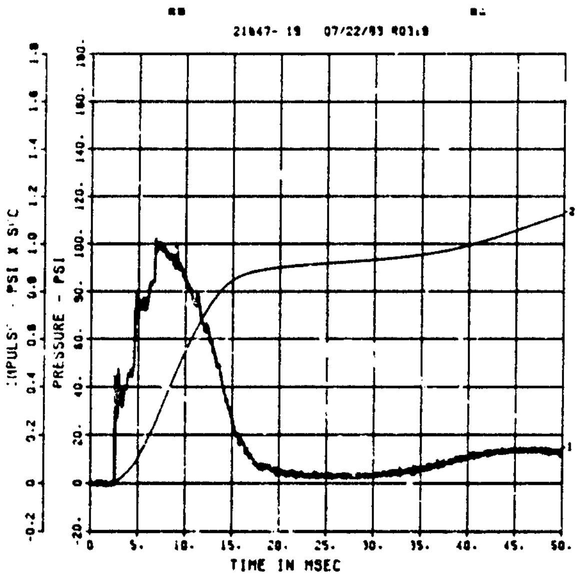

FEMA ELEM TEST D-4
IF-7
200000. HZ CAL= 128.6

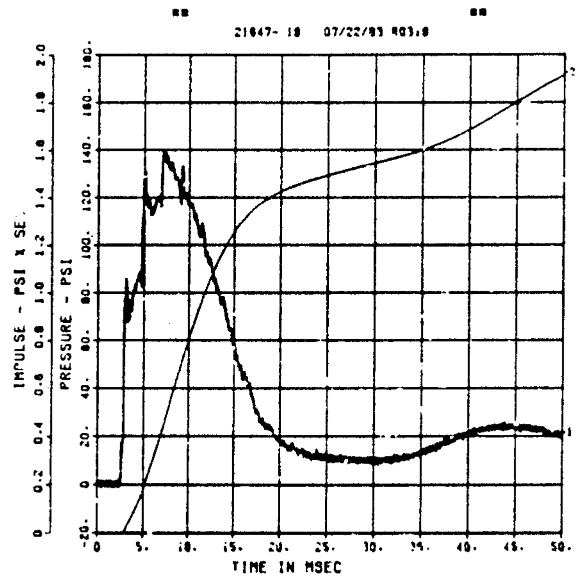

** PEAK VALUE ... X OVER CALIBRATION **

FEMA ELEM TEST D-4
IF-8
200000. HZ CAL= 127.9

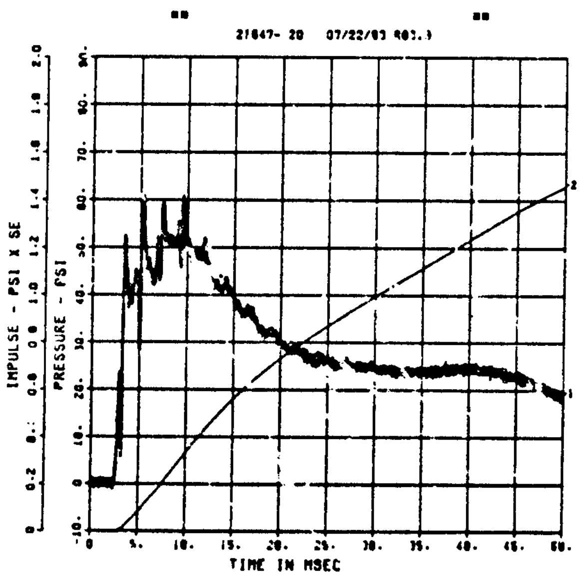

FEMA ELEM TEST D-4
IF-9
200000. HZ CAL= 84.10

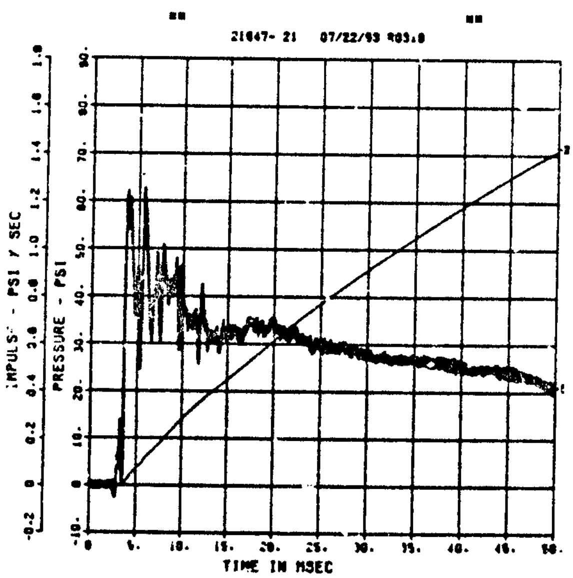

FEMA ELEM TEST D-4
IF-10
200000. HZ CAL= 83.10

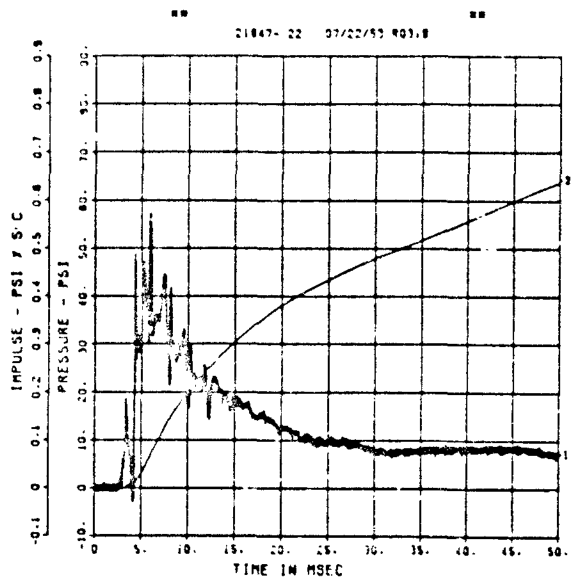

FEMA ELEM TEST D-4
IF-11
200000. HZ CAL= 84.80

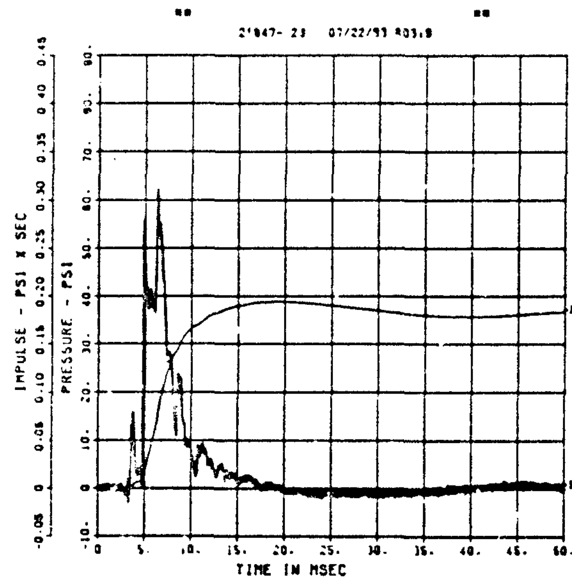

FEMA ELEM TEST D-4
IF-12
200000. HZ CAL= 243.7

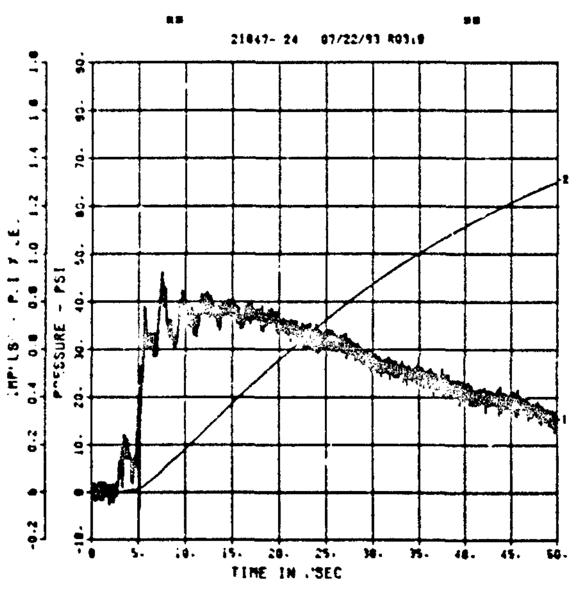

** PEAK VALUE IS 81 % UNDER CALIBRATION **

FEMA ELEM TEST D-4
IF-13
50000. HZ CAL= 166.8
LP4/4 70% CUTOFF= 2250. HZ

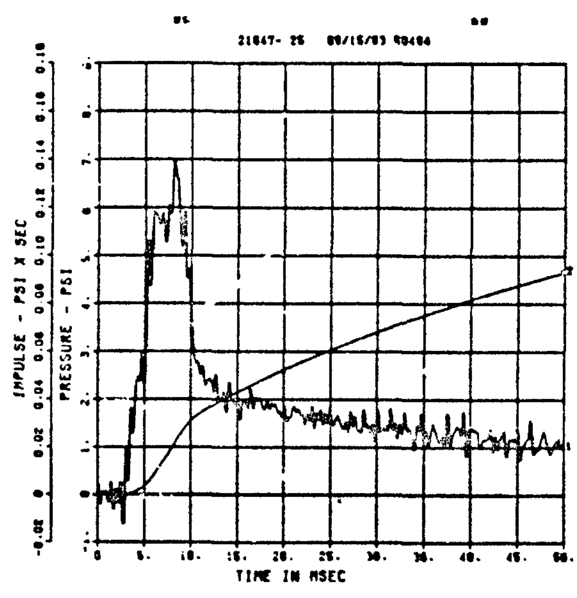

** PEAK VALUE IS 90 % UNDER CALIBRATION **

FEMA ELEM TEST D-4
IF-14
50000. HZ CAL= 125.8
LP4/4 70% CUTOFF= 2250. HZ

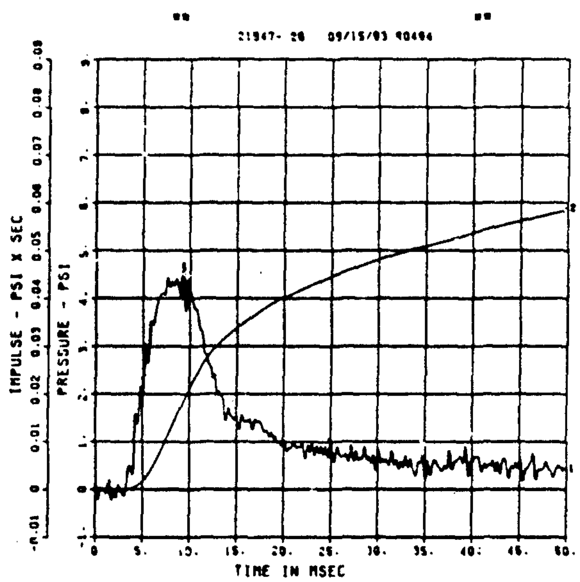

** PEAK VALUE IS 96 % UNDER CALIBRATION **

FEMA ELEM TEST D-4
IF-15
50000. HZ CAL= 165.3
LP4/4 70% CUTOFF= 2250. HZ

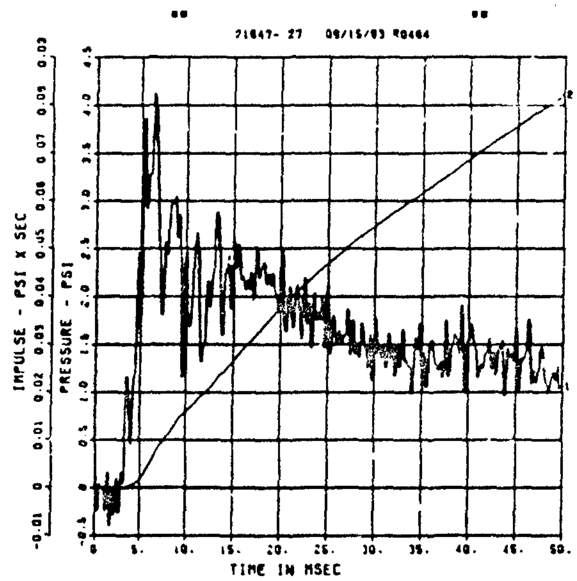

** PEAK VALUE IS 96 % UNDER CALIBRATION **

FEMA ELEM TEST D-4
IF-16
200000. HZ CAL= 247.0

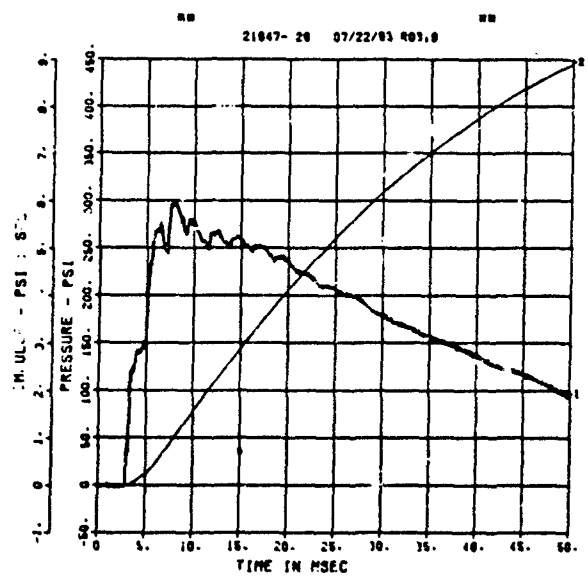

** PEAK VALUE IS 21 % OVER CALIBRATION **

FEMA ELEM TEST D-4
EO-1
200000. HZ CAL= 20205.

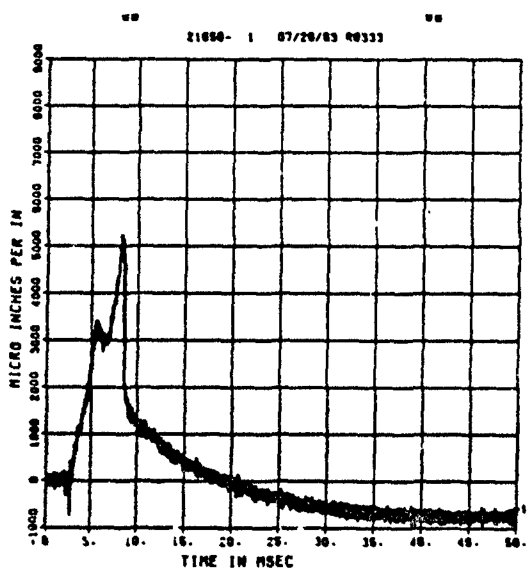

FEMA ELEM TEST D-4
EI-1
200000. HZ CAL= 10276.

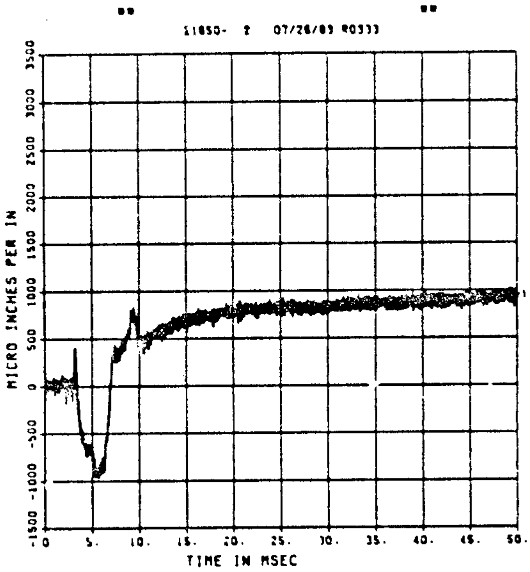

** PEAK VALUE IS 90 % UNDER CALIBRATION **

FEMA ELEM TEST D-4
EO-2
50000. HZ CAL= 39162.
LP4/4 70% CUTOFF= 2250. HZ

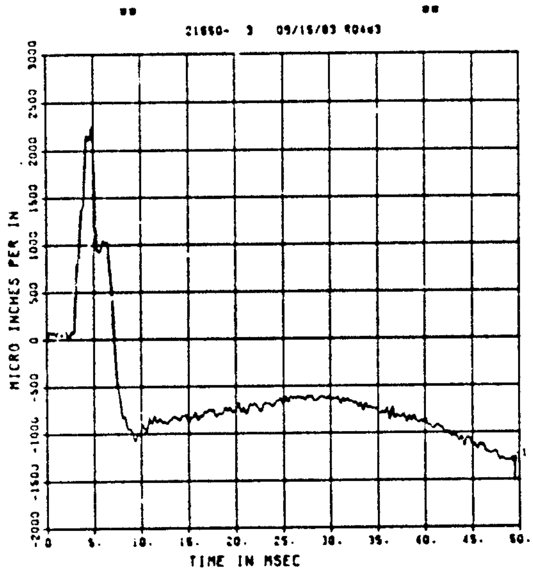

** PEAK VALUE IS 94 % UNDER CALIBRATION **

FEMA ELEM TEST D-4
EI-2
50000. HZ CAL= 10276.
LP4/4 70% CUTOFF= 2250. HZ

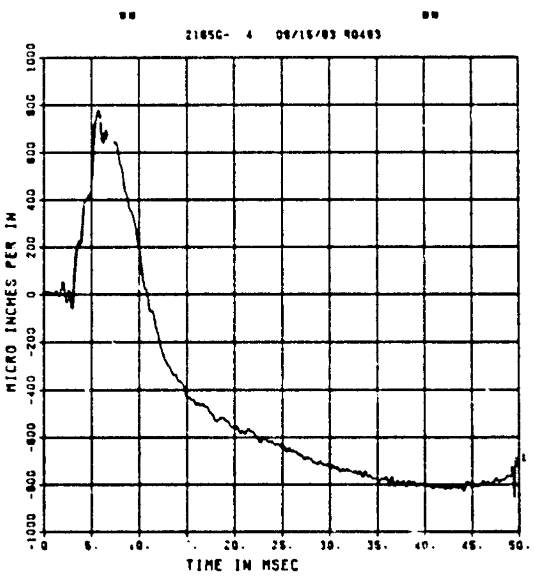

** PEAK VALUE IS 92 % UNDER CALIBRATION **

FEMA ELEM TEST D-4
EO-3
200000. HZ CAL= 10276.

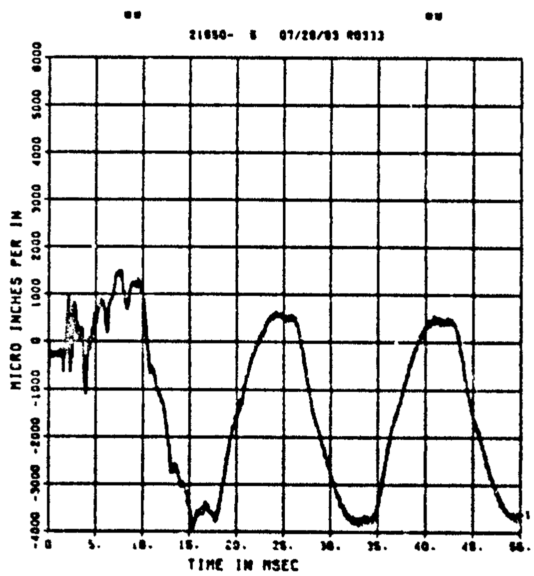

FEMA ELEM TEST D-4
EO-5
200000. HZ CAL= 10276.

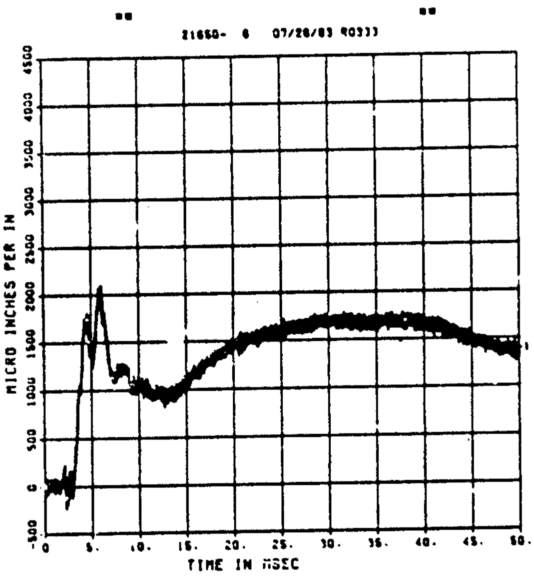

FEMA ELEM TEST D-4
EI-5
200000. HZ CAL= 10276.

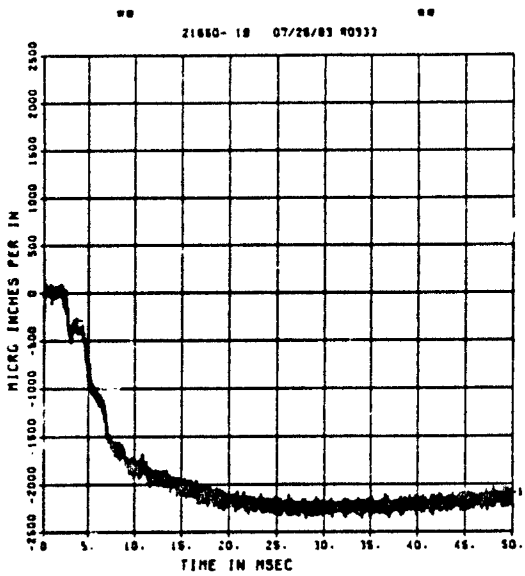

FEMA ELEM TEST D-4
EO-6
50000. HZ CAL= 6768.
LP4/4 70% CUTOFF= 2250. HZ

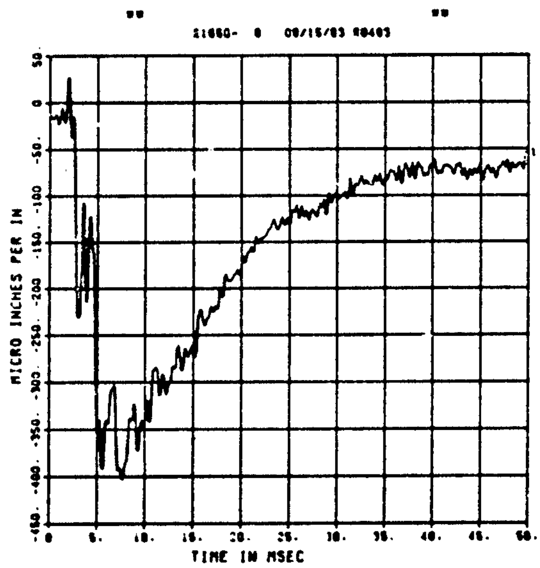

** PEAK VALUE IS 94 % UNDER CALIBRATION **

FEMA ELEM TEST D-4
EI-6
50000. HZ CAL= 6768.
LP4/4 70% CUTOFF= 2250. HZ

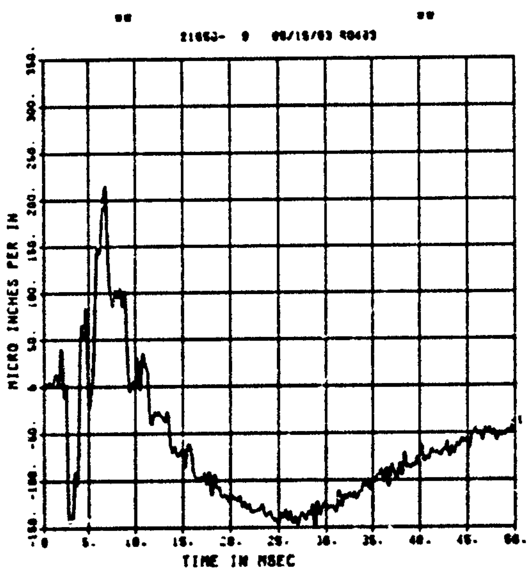

** PEAK VALUE IS 97 % UNDER CALIBRATION **

FEMA ELEM TEST D-4
EO-7
50000. HZ CAL= 6766.
LP4/4 70% CUTOFF= 2250. HZ

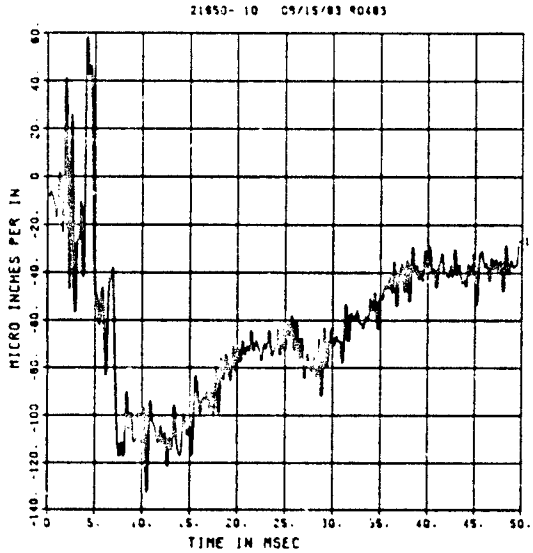

** PEAK VALUE IS 98 % UNDER CALIBRATION **

FEMA ELEM TEST D-4
EI-7
50000. HZ CAL= 6768.
LP4/4 70% CUTOFF= 2250. HZ

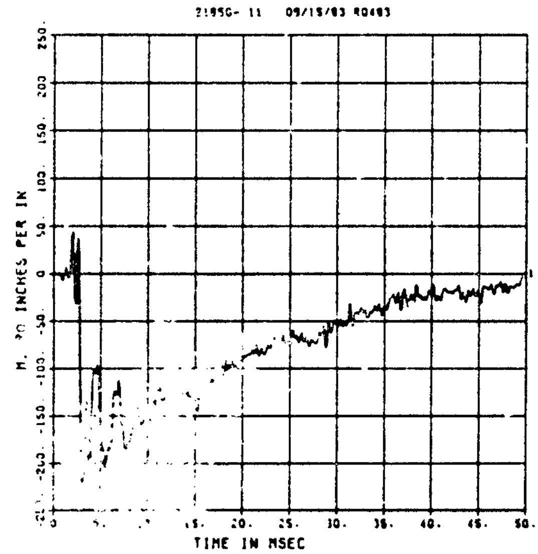

** PEAK VALUE IS 97 % UNDER CALIBRATION **

FEMA ELEM TEST D-4
EI-8
50000. HZ CAL= 10276.
LP4/4 70% CUTOFF= 2250. HZ

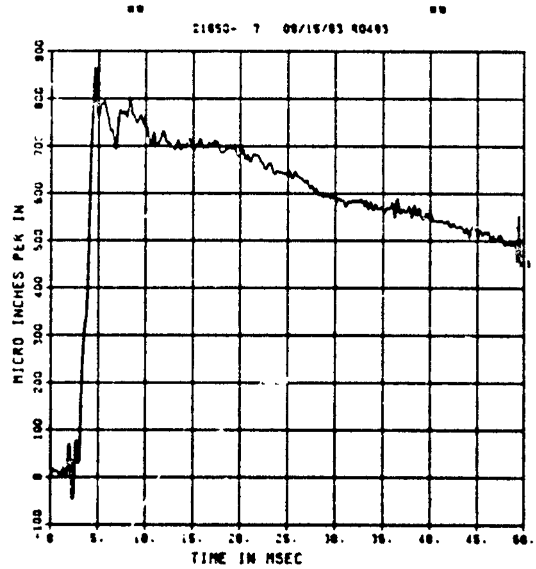

** PEAK VALUE IS 92 % UNDER CALIBRATION **

FEMA ELEM TEST D-4
EO-9
50000. HZ CAL= 10276.
LP4/4 70% CUTOFF= 2250. HZ

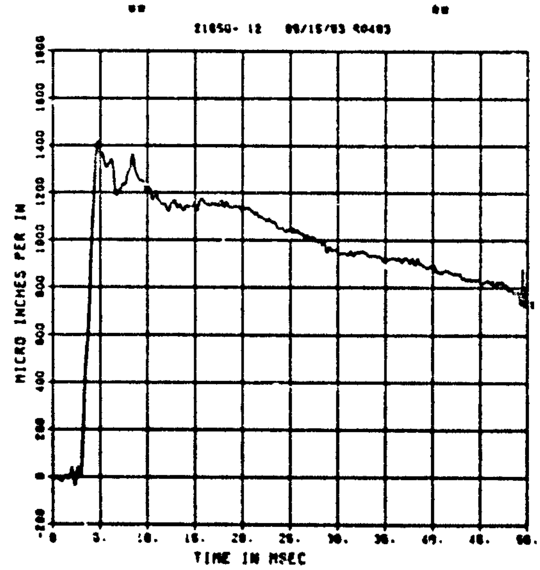

** PEAK VALUE IS 98 % UNDER CALIBRATION **

FEMA ELEM TEST D-4
EI-9
50000. HZ CAL= 10276.
LP4/4 70% CUTOFF= 2250. HZ

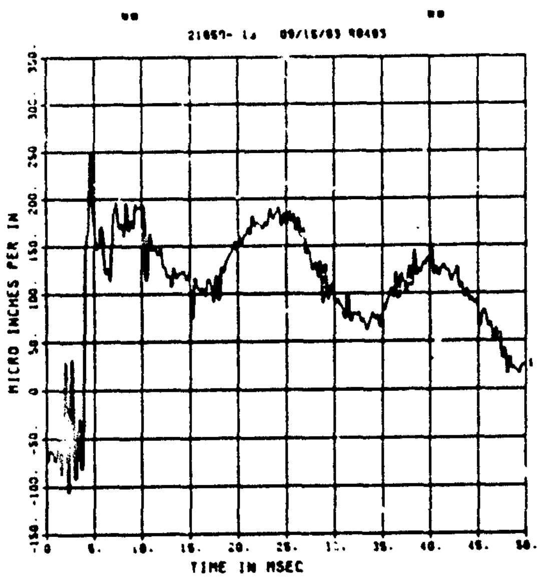

** PEAK VALUE IS 99 % UNDER CALIBRATION **

FEMA ELEM TEST D-4
EO-10
50000. HZ CAL= 6768.
LP4/4 70% CUTOFF= 2250. HZ

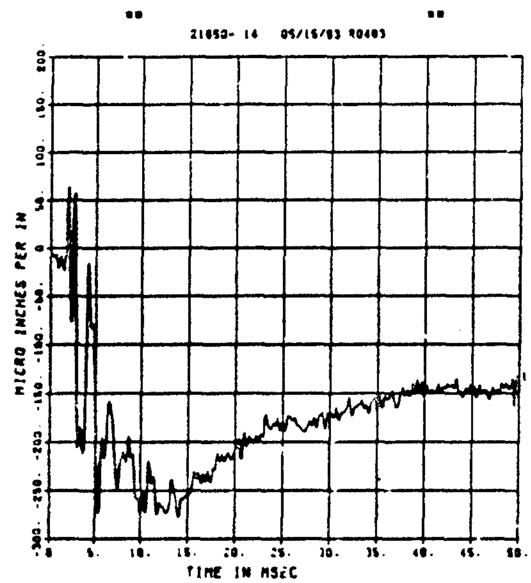

** PEAK VALUE IS 99 % UNDER CALIBRATION **

FEMA ELEM TEST D-4
EI-10
50000. HZ CAL= 6768.
LP4/4 70% CUTOFF= 2250. HZ

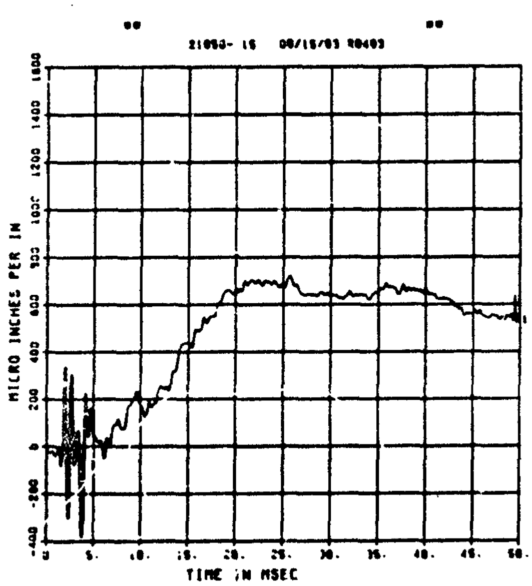

** PEAK VALUE IS 99 % UNDER CALIBRATION **

FEMA ELEM TEST D-4
EO-11
50000. HZ CAL= 10276.
LP4/4 70% CUTOFF= 2250. HZ

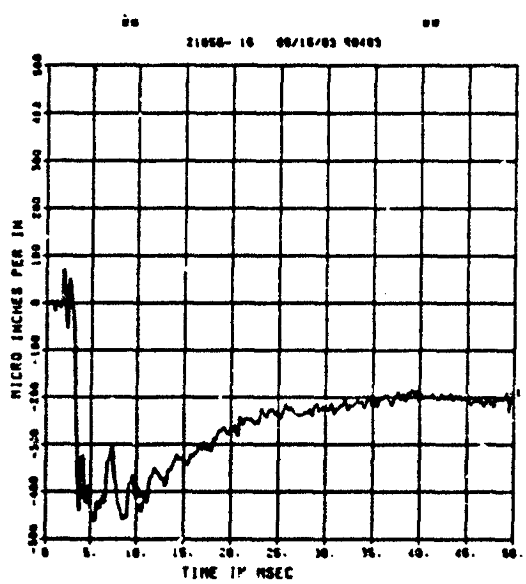

** PEAK VALUE IS 99 % UNDER CALIBRATION **

FEMA ELEM TEST D-4
EI-11
200000. HZ CAL= 10276.

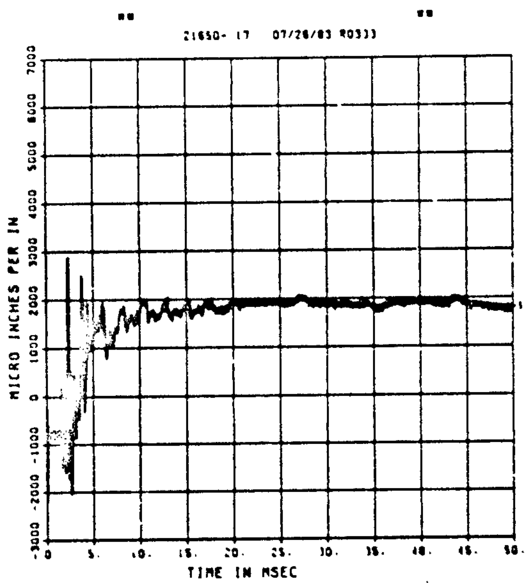

FEMA ELEM TEST D-5
BP-1
200000. HZ CAL= 624.1

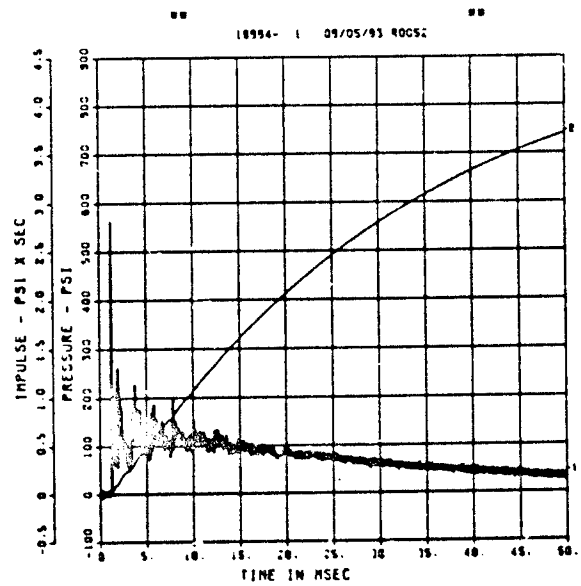

FEMA ELEM TEST D-5
BP-2
200000. HZ CAL= 575.9

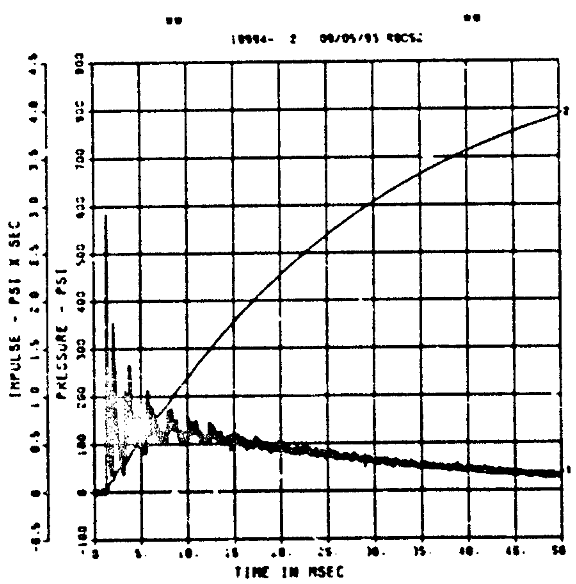

** PEAK VALUE IS 1 % OVER CALIBRATION **

FEMA ELEM TEST D-5
BP-3
200000. HZ CAL= 744.2

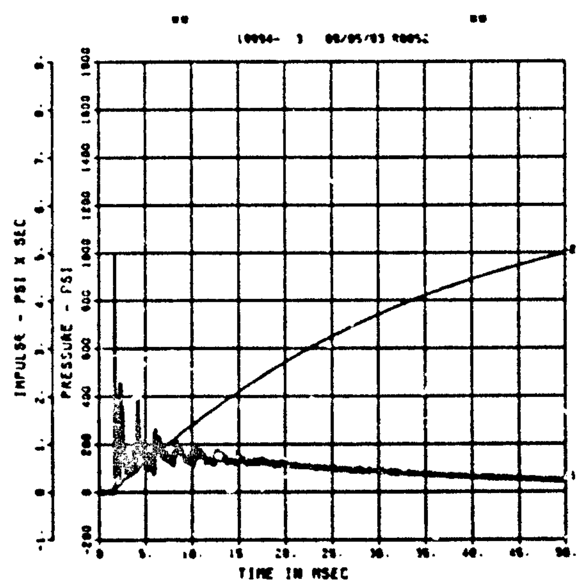

** PEAK VALUE IS 33 % OVER CALIBRATION **

FEMA ELEM TEST D-5
BP-4
200000. HZ CAL= 659.2

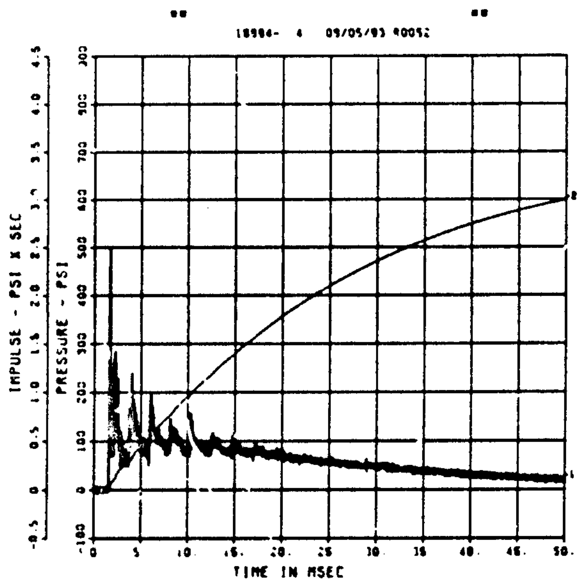

FEMA ELEM TEST D-5
BP-6
200000. HZ CAL= 1143.

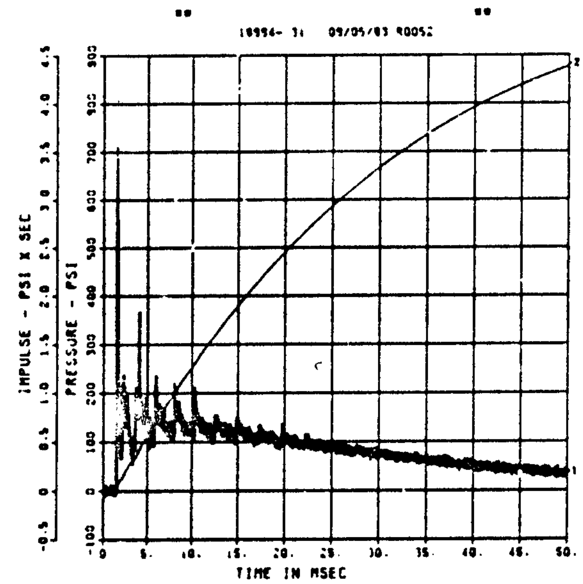

FEMA ELEM TEST D-5
SE-1
200000. HZ CAL= 356.1

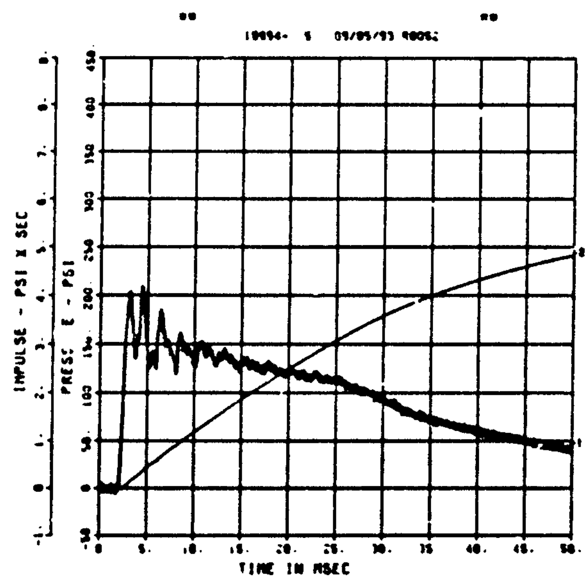

FEMA ELEM TEST D-5
SE-2
200000. HZ CAL= 138.8

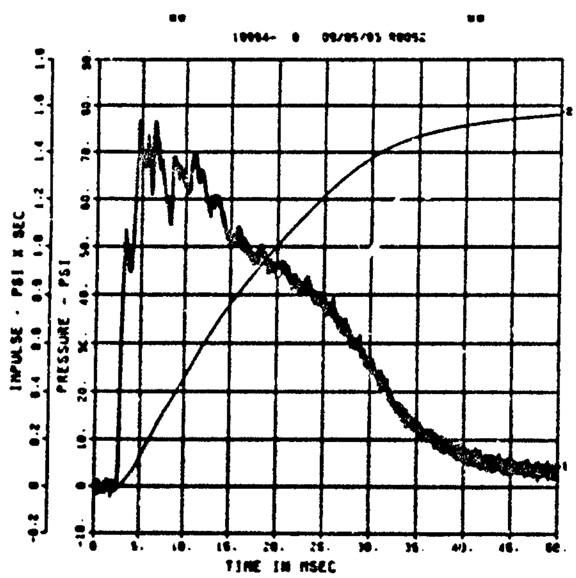

FEMA ELEM TEST D-5
SE-3
200000. HZ CAL= 198.2

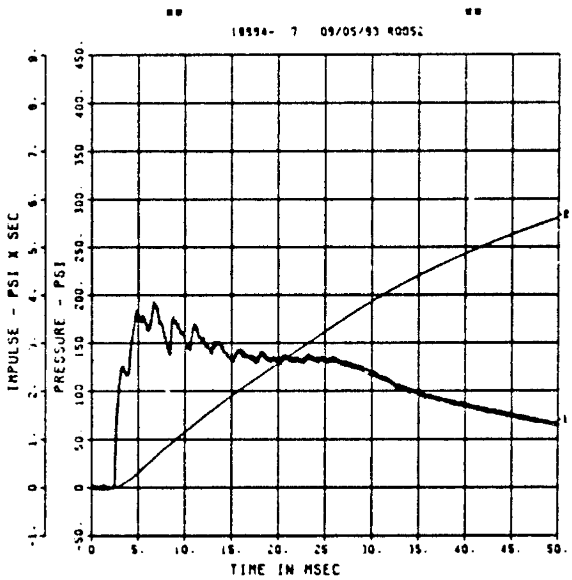

FEMA ELEM TEST D-5
SE-4
200000. HZ CAL= 132.5

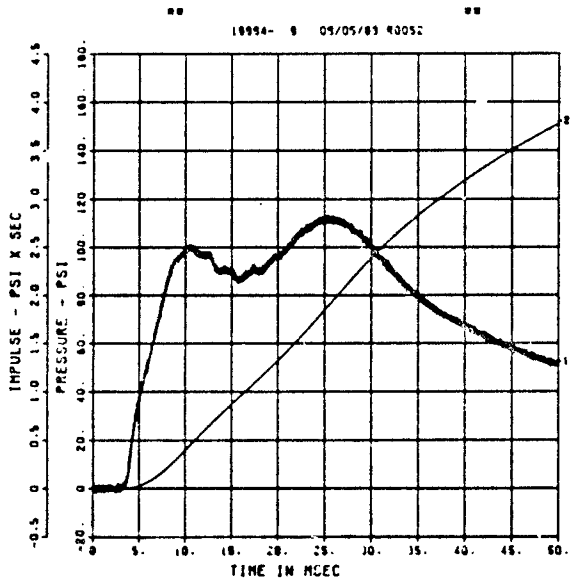

FEMA ELEM TEST D-5
SE-5
200000. HZ CAL= 132.8

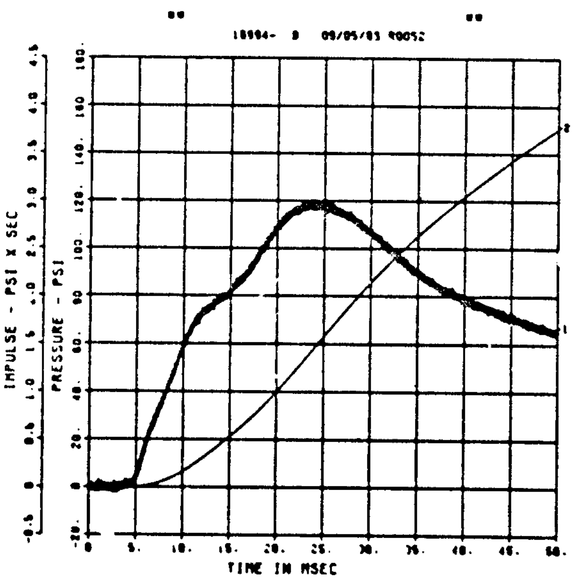

FEMA ELEM TEST D-5
SE-6
200000. HZ CAL= 364.9

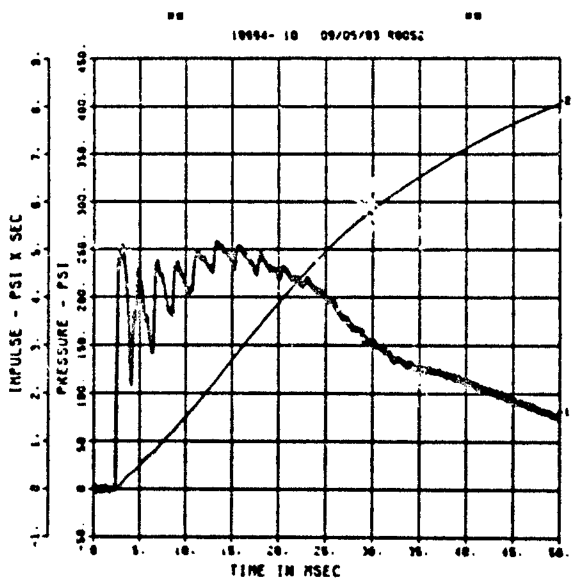

FEMA ELEM TEST D-5
SE-7
200000. HZ CAL= 233.9

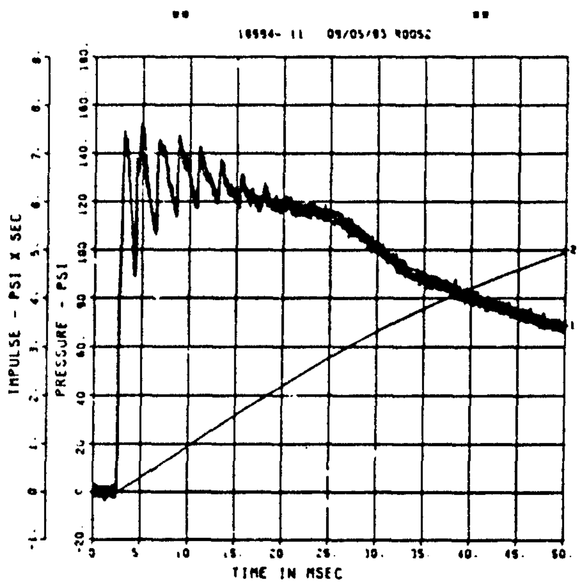

FEMA ELEM TEST D-5
AFF-1
50000. HZ CAL= 818.6
LP4/4 70% CUTOFF= 2250. HZ

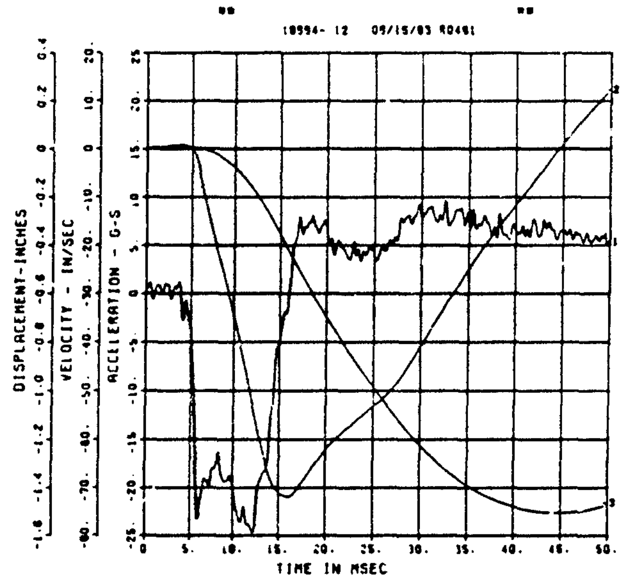

** PEAK VALUE IS 97 % UNDER CALIBRATION **

FEMA ELEM TEST D-5
A-1
200000. HZ CAL= 2504.

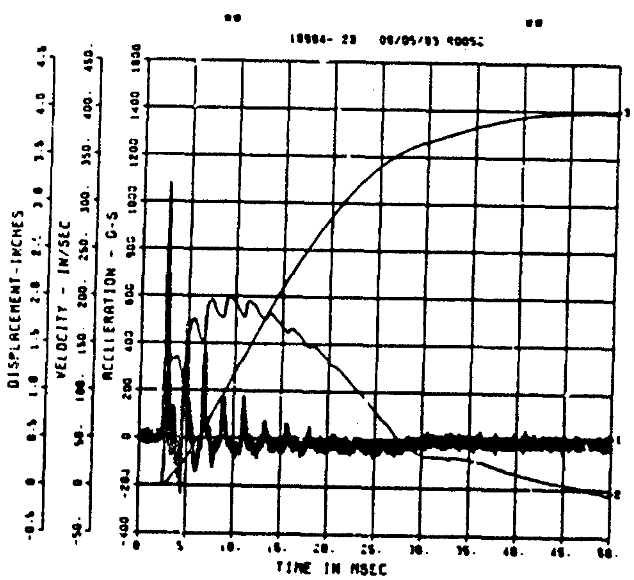

FEMA ELEM TEST D-5
A-2
200000. HZ CAL= 414.6

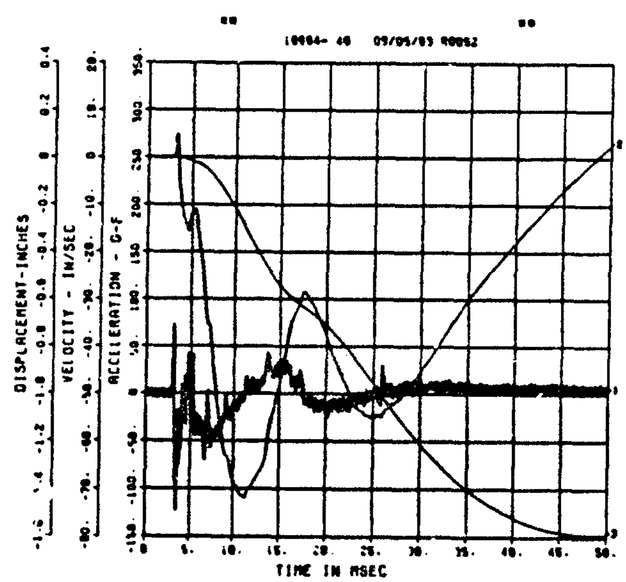

FEMA ELEM TEST D-5
IF-1
200000. HZ CAL= 344.8

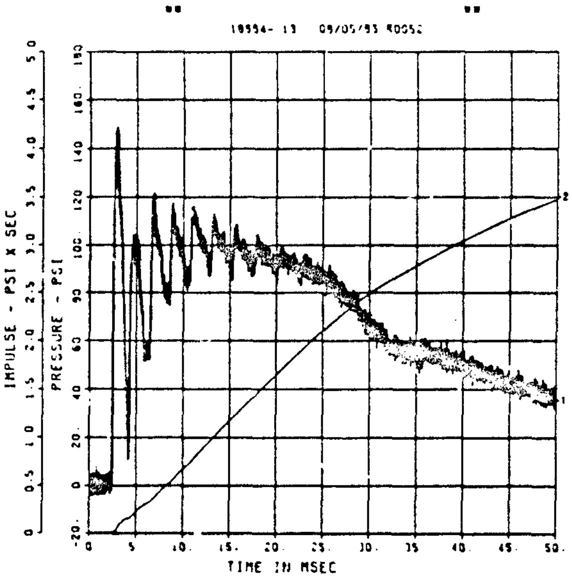

FEMA ELEM TEST D-5
IF-2
200000. HZ CAL= 335.9

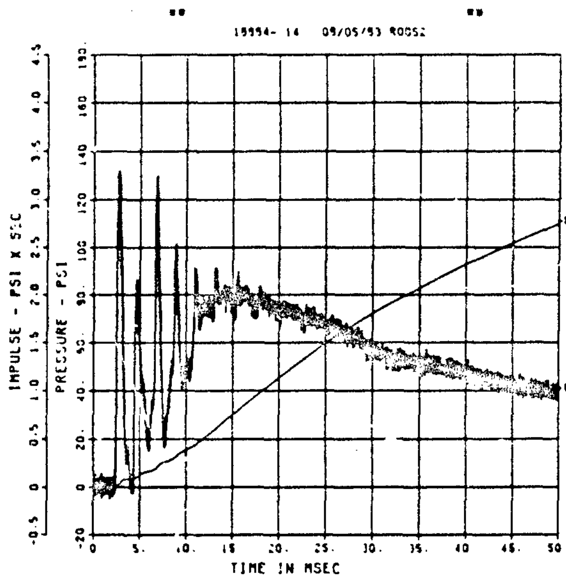

FEMA ELEM TEST D-5
IF-3
200000. HZ CAL= 343.2

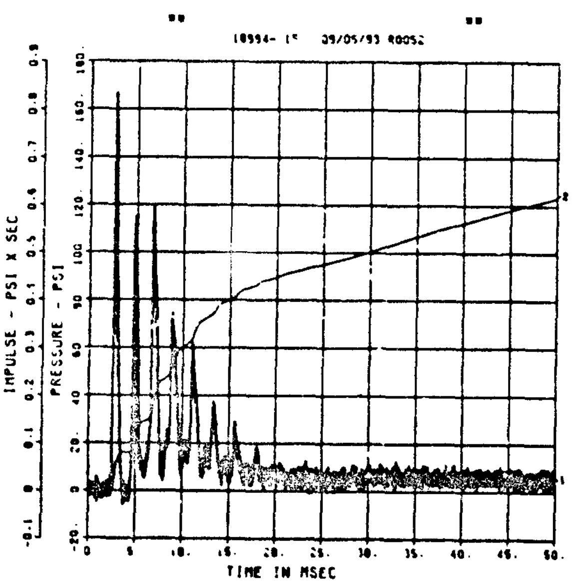

FEMA ELEM TEST D-5
IF-4
200000. HZ CAL= 341.1

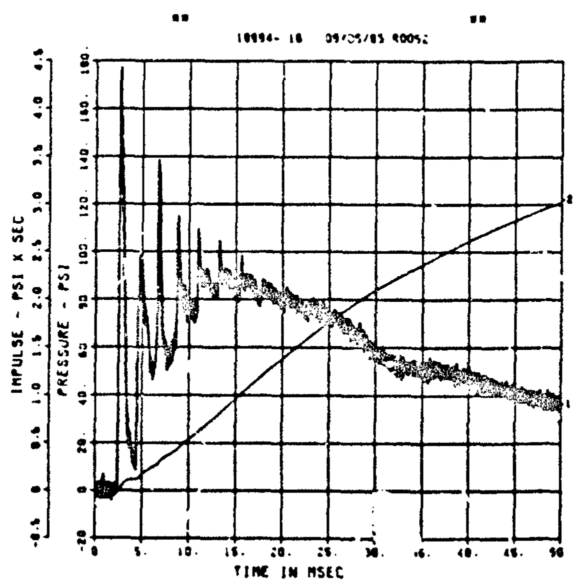

FEMA ELEM TEST D-5
IF-5
200000. HZ CAL= 358.3

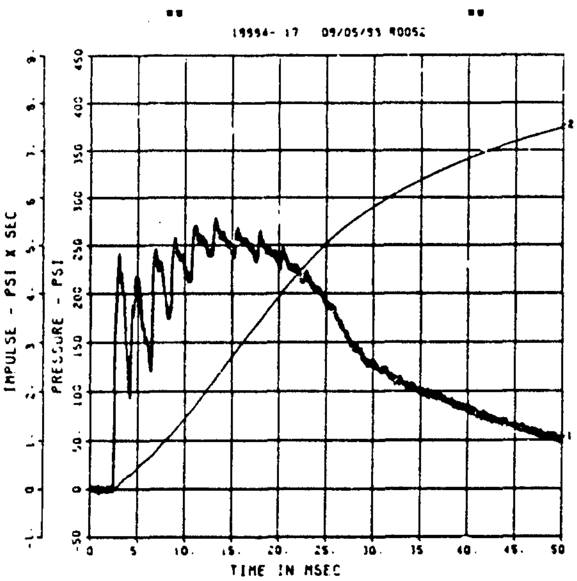

FEMA ELEM TEST D-5
IF-6
200000. HZ CAL= 145.5

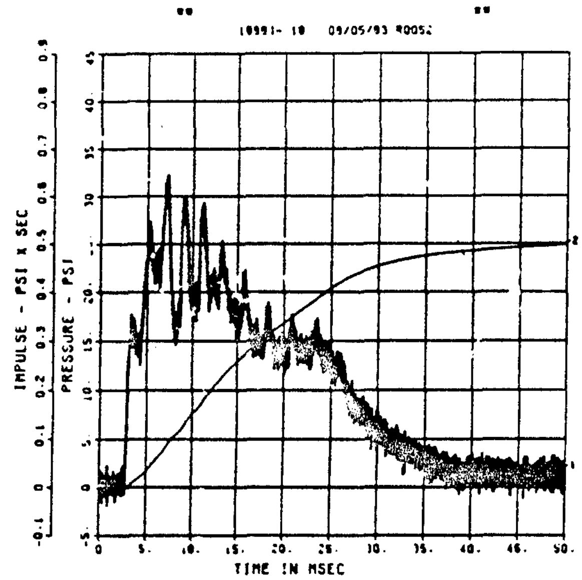

FEMA ELEM TEST D-5
IF-8
50000. HZ CAL= 83.40
LP4/4 70% CUTOFF= 2250. HZ

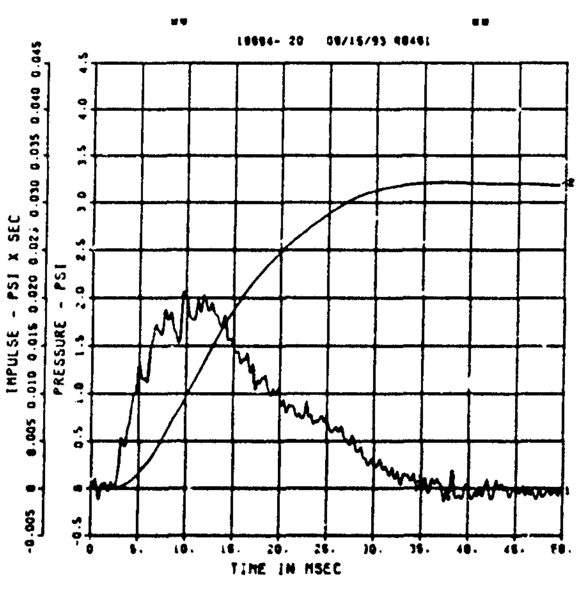

FEMA ELEM TEST D-5
IF-9
200000. HZ CAL= 84.10

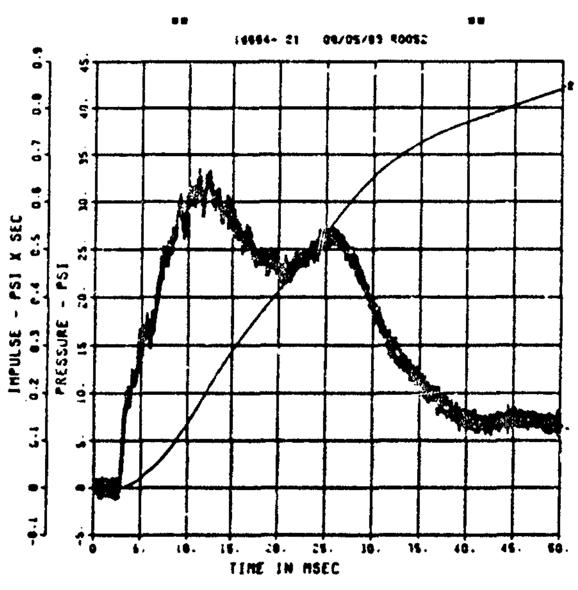

** PEAK VALUE IS 88 % UNDER CALIBRATION **

FEMA ELEM TEST D-5
IF-10
200000. HZ CAL= 83.00

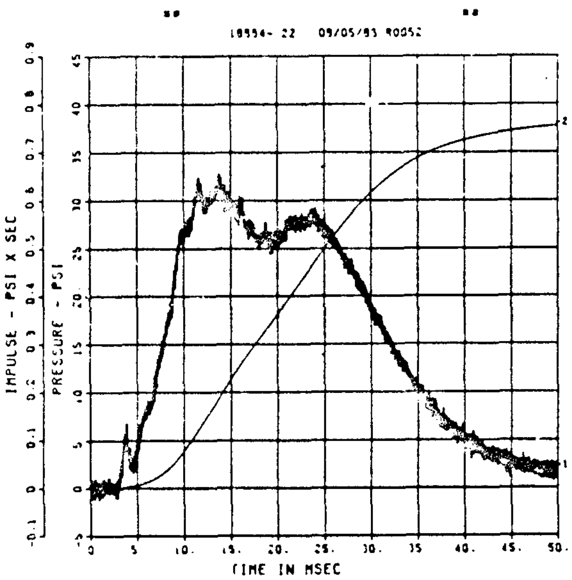

FEMA ELEM TEST D-5
IF-11
200000. HZ CAL= 81.60

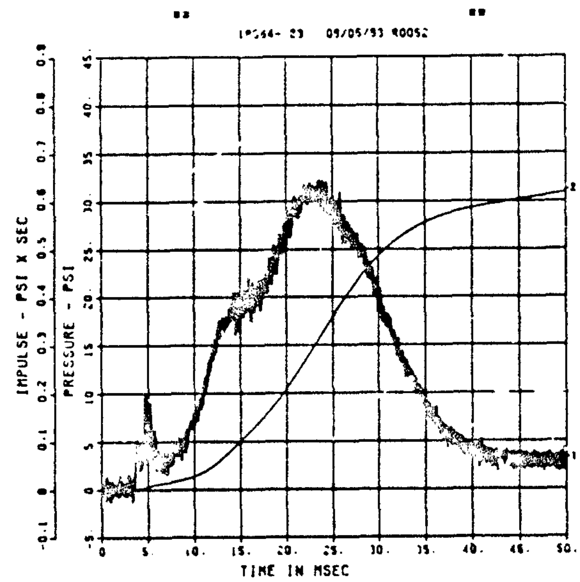

FEMA ELEM TEST D-5
IF-12
200000. HZ CAL= 124.4

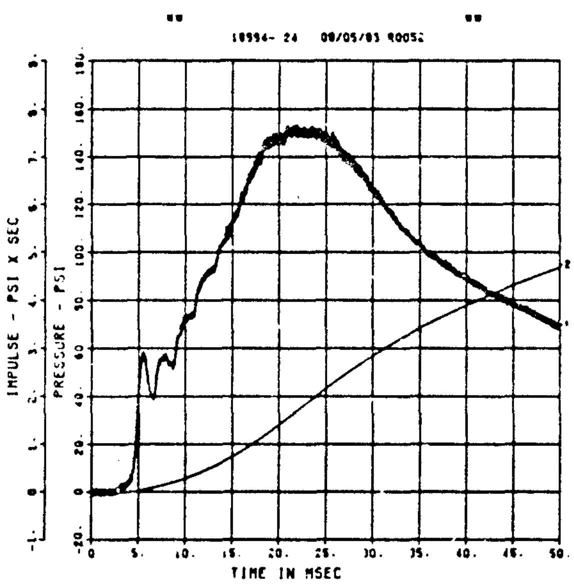

** PEAK VALUE IS 23 % OVER CALIBRATION **

FEMA ELEM TEST D-5
IF-13
200000. HZ CAL= 51.10

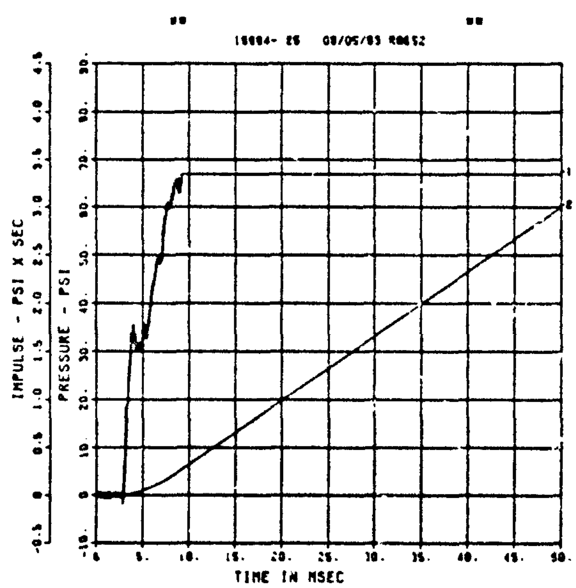

** PEAK VALUE IS 31 % OVER CALIBRATION **

FEMA ELEM TEST D-5
IF-14
50000. HZ CAL= 25.60
LP4/4 70% CUTOFF= 2250. HZ

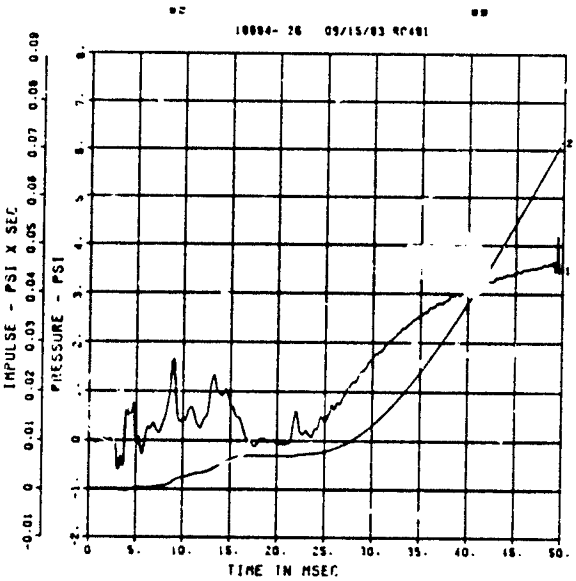

** PEAK VALUE IS 84 % UNDER CALIBRATION **

FEMA ELEM TEST D-5
IF-15
200000. HZ CAL= 25.40

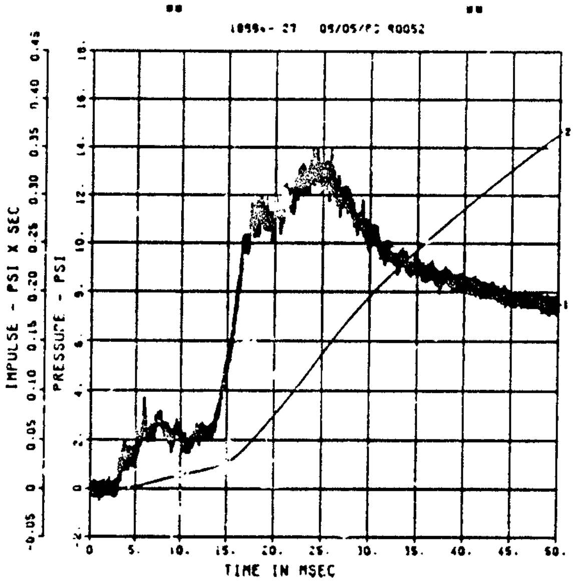

FEMA ELEM TEST D-5
IF-16
200000. HZ CAL= 247.0

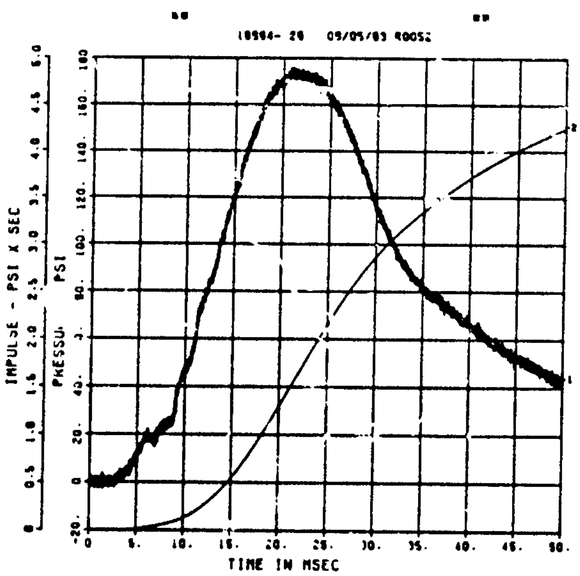

FEMA ELEM TEST D-5
EO-2
200000. HZ CAL= 20205.

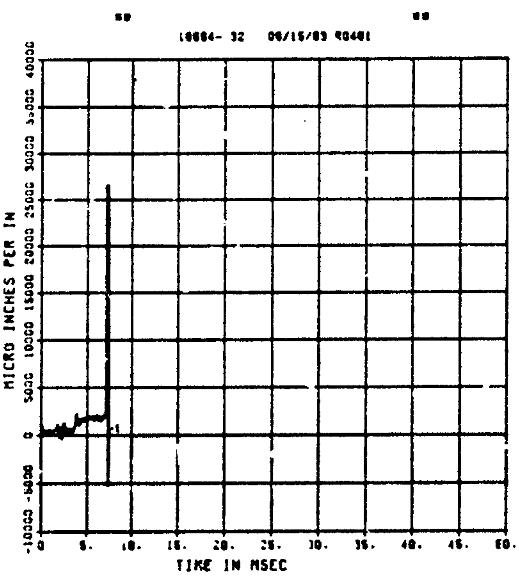

** PEAK VALUE IS 31 % OVER CALIBRATION **

FEMA ELEM TEST D-5
EO-3
50000. HZ CAL= 10276.
LP4/4 70% CUTOFF= 2250. HZ

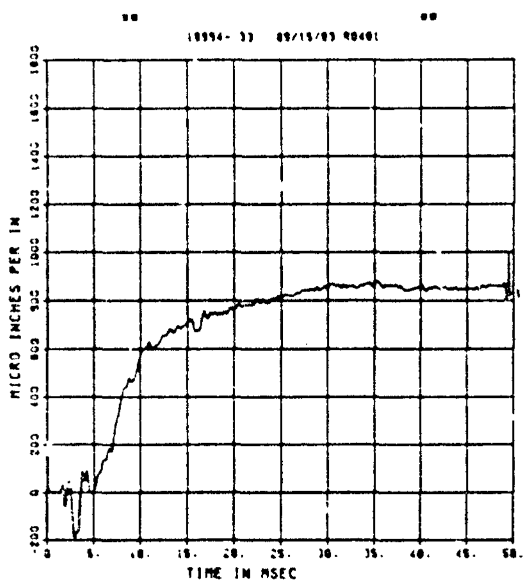

** PEAK VALUE IS 90 % UNDER CALIBRATION **

FEMA ELEM TEST D-5
EO-4
50000. HZ CAL= 10276.
LP4/4 70% CUTOFF= 2250. HZ

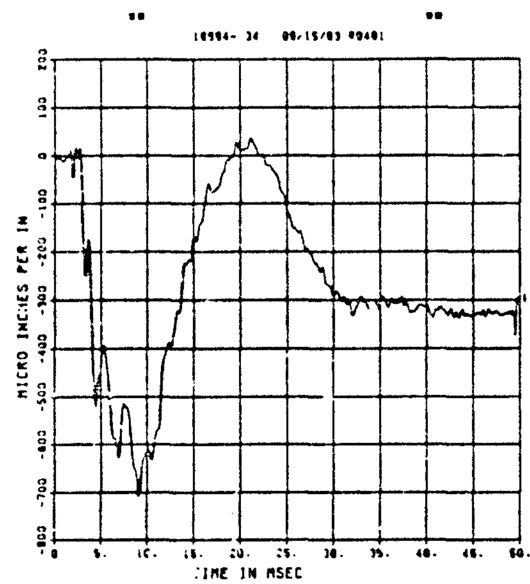

** PEAK VALUE IS 73 % UNDER CALIBRATION **

FEMA ELEM TEST D-5
EI-4
200000. HZ CAL= 39162.

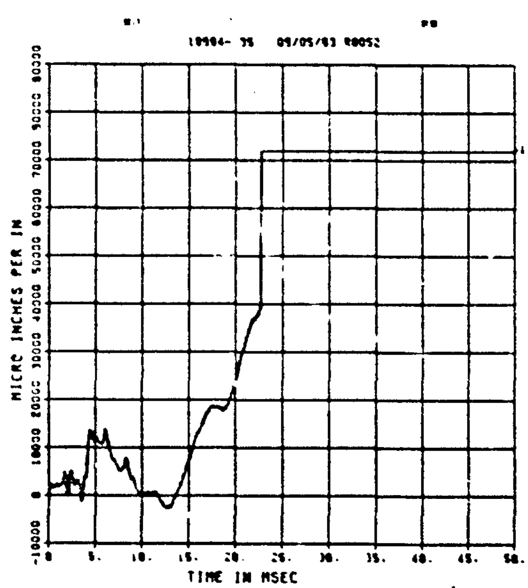

** PEAK VALUE IS 84 % OVER CALIBRATION **

FEMA ELEM TEST D-5
EO-5
50000. HZ CAL= 10276.
LP4/4 70% CUTOFF= 2250. HZ

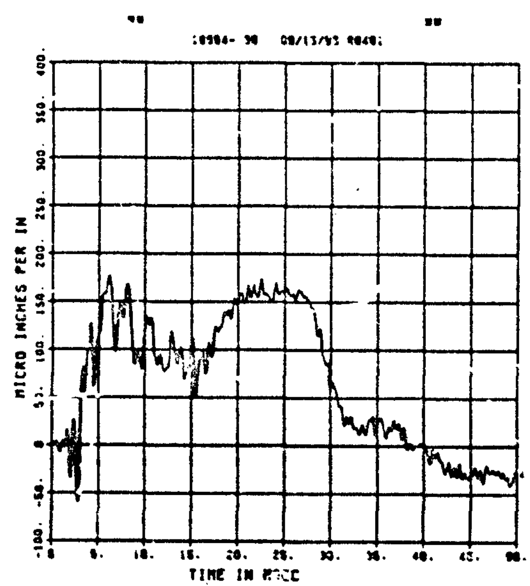

** PEAK VALUE IS 90 % UNDER CALIBRATION **

FEMA ELEM TEST D-5
EI-5
50000. HZ CAL= 6768.
LP4/4 70% CUTOFF= 2250. HZ

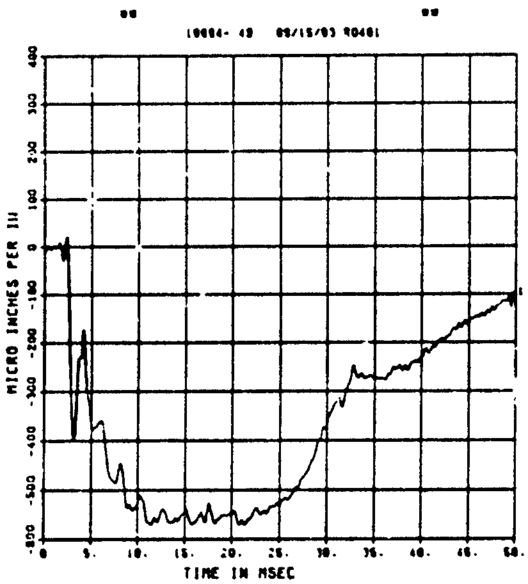

** PEAK VALUE IS 92 % UNDER CALIBRATION **

FEMA ELEM TEST D-5
EO-6
50000. HZ CAL= 6768.
LP4/4 70% CUTOFF= 2250. HZ

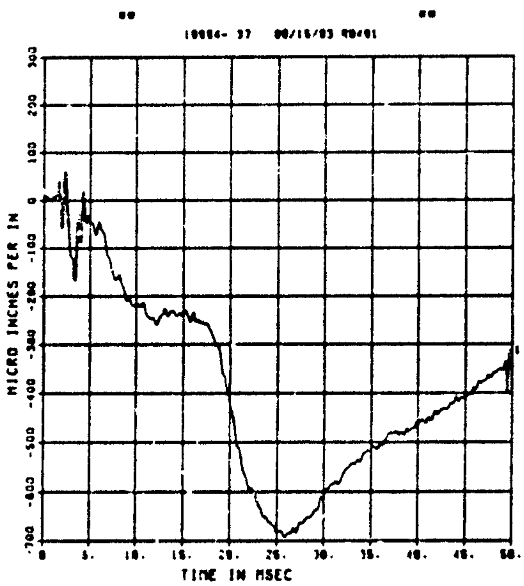

** PEAK VALUE IS 98 % UNDER CALIBRATION **

FEMA ELEM TEST D-5
EI-6
50000. HZ CAL= 6768.
LP4/4 70% CUTOFF= 2250. HZ

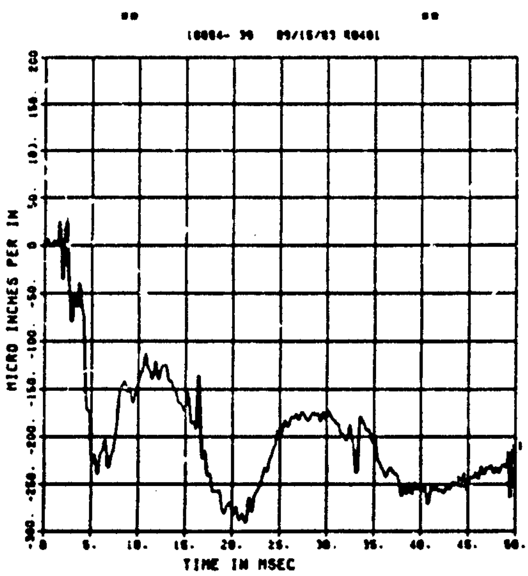

** PEAK VALUE IS 98 % UNDER CALIBRATION **

FEMA ELEM TEST D-5
EI-7
50000. HZ CAL= 6768.
LP4/4 70% CUTOFF= 2250. HZ

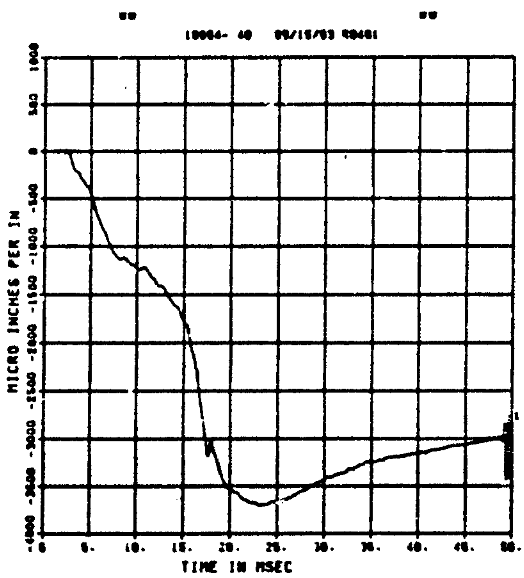

FEMA ELEM TEST D-5
EI-8
200000. HZ CAL= 10276.

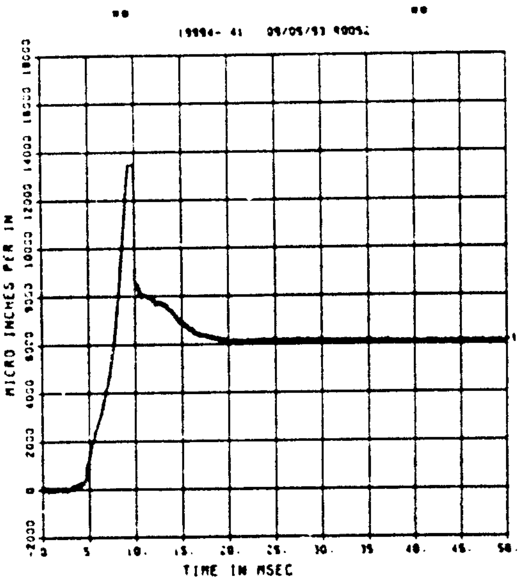

** PEAK VALUE IS 31 % OVER CALIBRATION **

FEMA ELEM TEST D-5
EO-9
200000. HZ CAL= 6768.

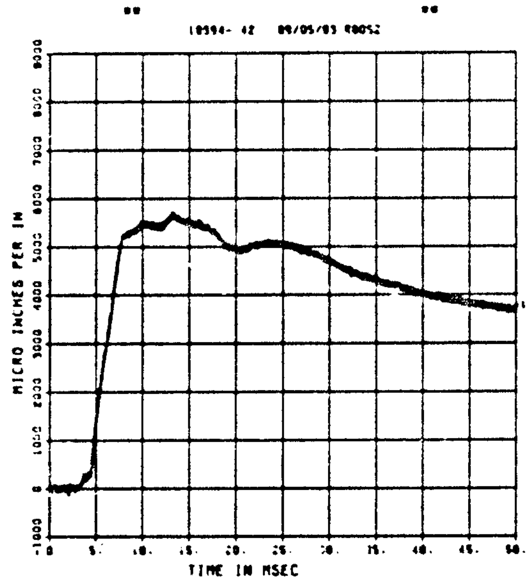

FEMA ELEM TEST D-5
EI-9
200000. HZ CAL= 6768.

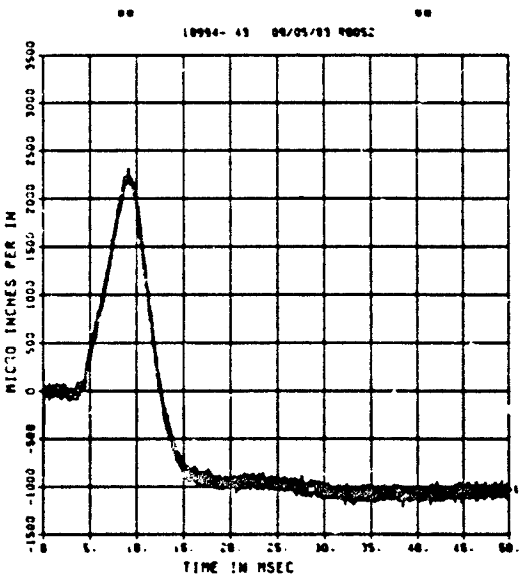

FEMA ELEM TEST D-5
EO-10
200000. HZ CAL= 6768.

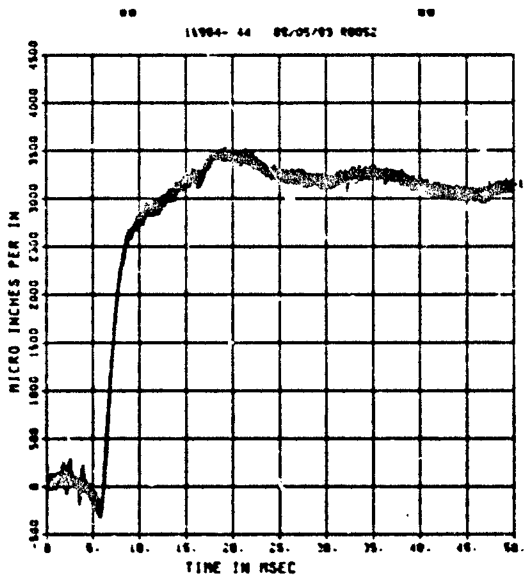

FEMA ELEM TEST D-5
EI-10
50000. HZ CAL= 6768.
LP4/4 70% CUTOFF= 2250. HZ

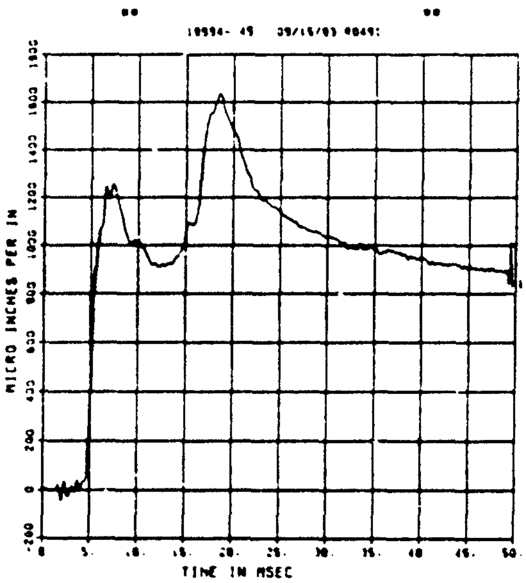

FEMA ELEM TEST D-5
EO-11
50000. HZ CAL= 10276.
LP4/4 70% CUTOFF= 2250. HZ

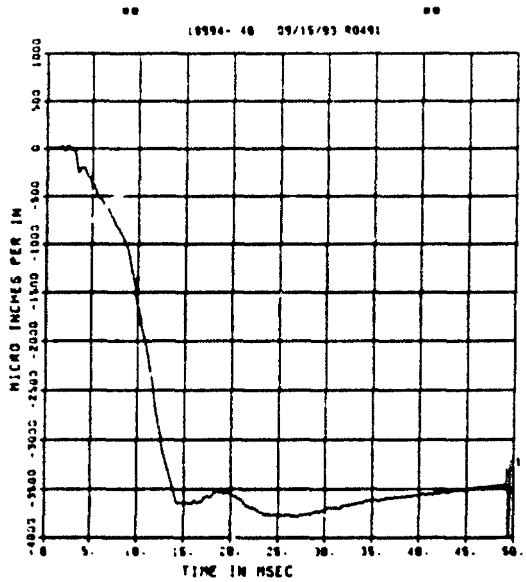

FEMA ELEM TEST D-5
EI-11
200000. HZ CAL= 10276.

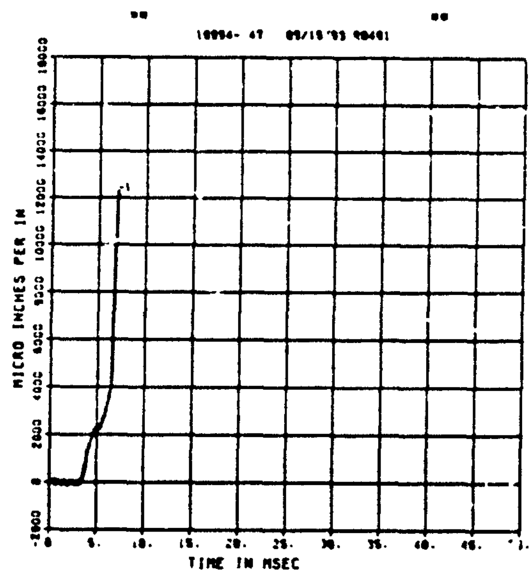

FEMA ELEM TEST D-6
BP-1
200000. HZ CAL= 969.0

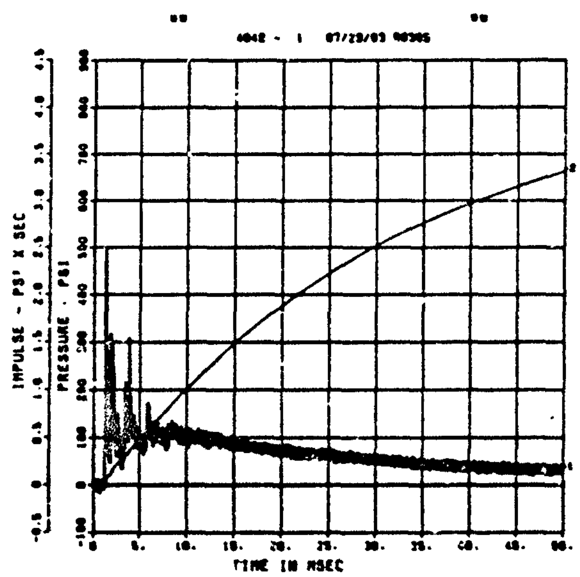

** PEAK VALUE IS 20 % OVER CALIBRATION **

FEMA ELEM TEST D-6
BP-2
200000. HZ CAL= 912.5

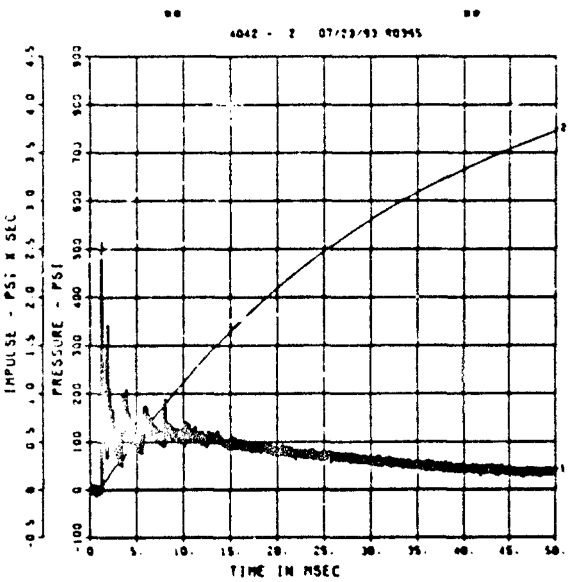

FEMA ELEM TEST D-6
BP-3
200000. HZ CAL= 744.1

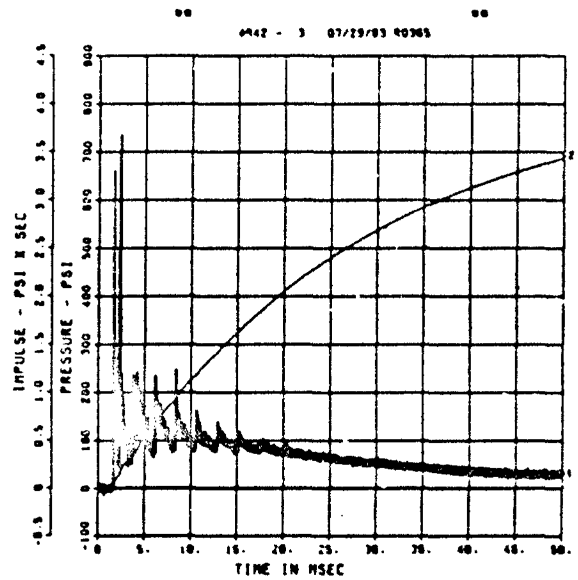

FEMA ELEM TEST D-6
BP-4
200000. HZ CAL= 659.2

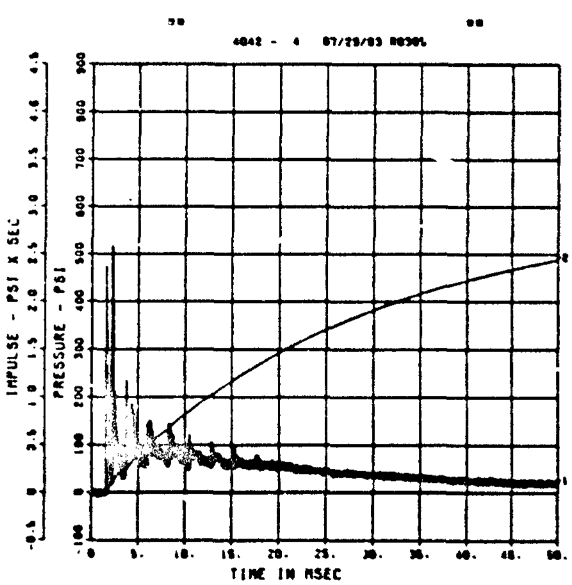

FEMA ELEM TEST D-6
SE-1
200000. HZ CAL= 249.0

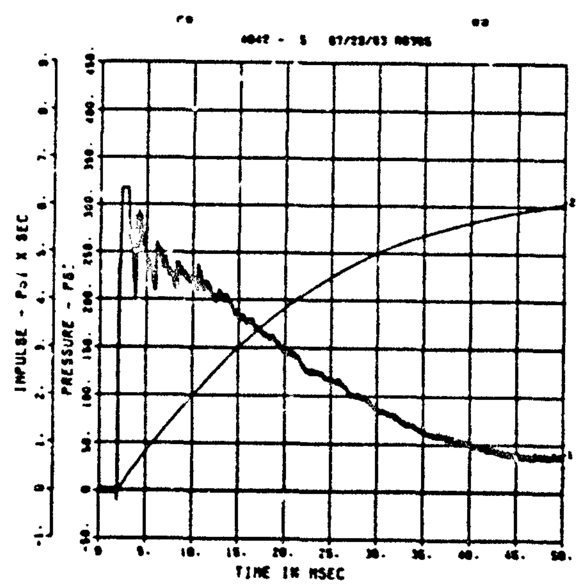

FEMA ELEM TEST D-6
SE-2
200000. HZ CAL= 130.8

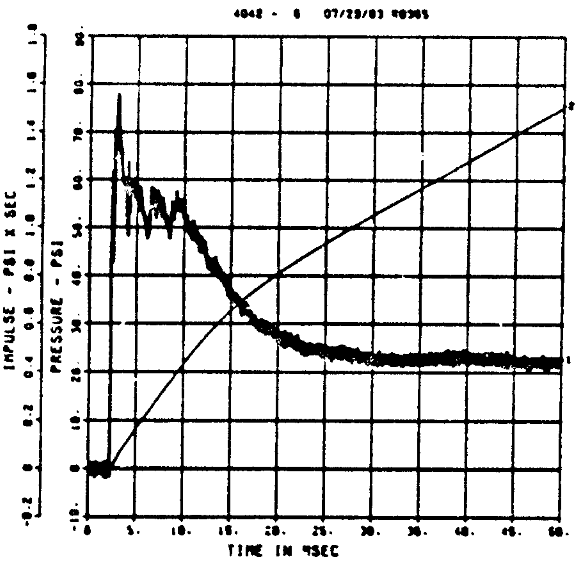

FEMA ELEM TEST D-6
SE-3
200000. HZ CAL= 198.2

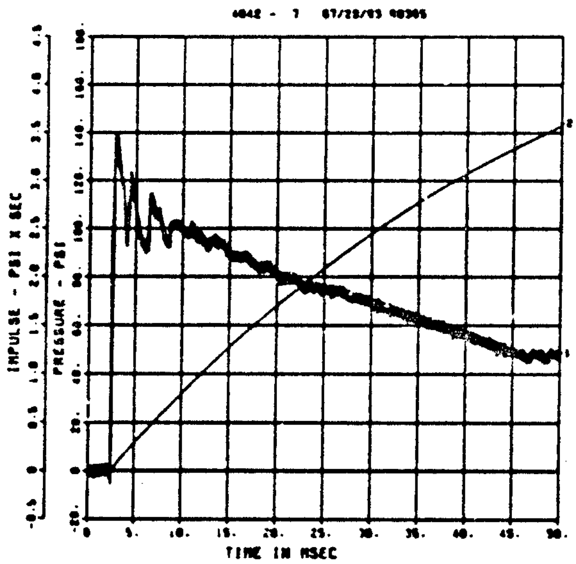

FEMA ELEM TEST D-6
SE-4
200000. HZ CAL= 132.6

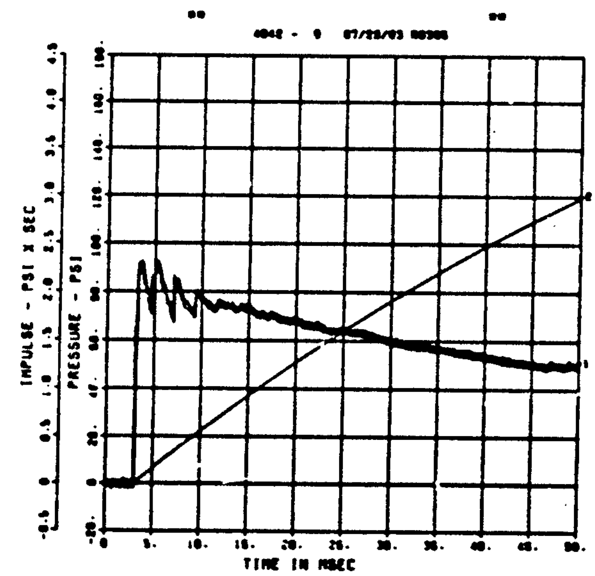

FEMA ELEM TEST D-6
SE-5
200000. HZ CAL= 132.1

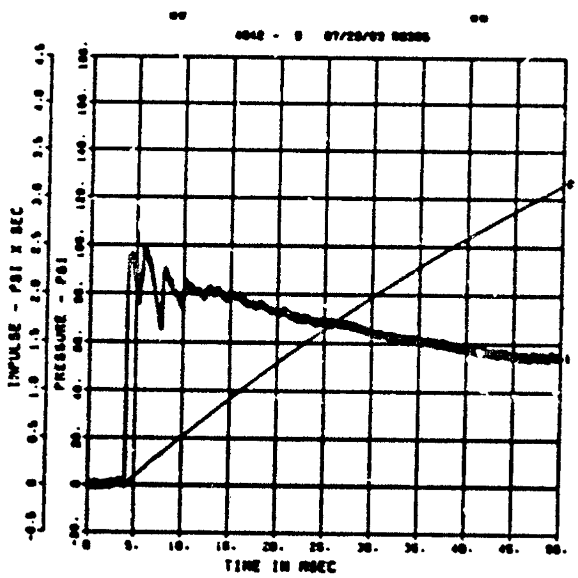

FEMA ELEM TEST D-6
SE-6
200000. HZ CAL= 364.9

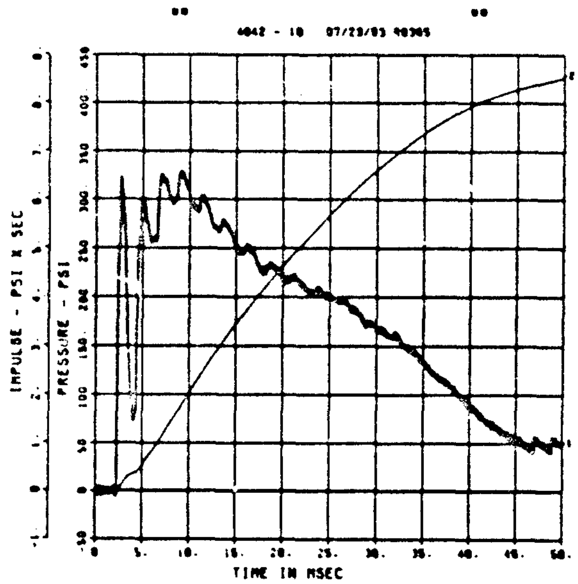

FEMA ELEM TEST D-6
SE-7
50000. HZ CAL= 233.9
LP4/4 70% CUTOFF= 2250. HZ

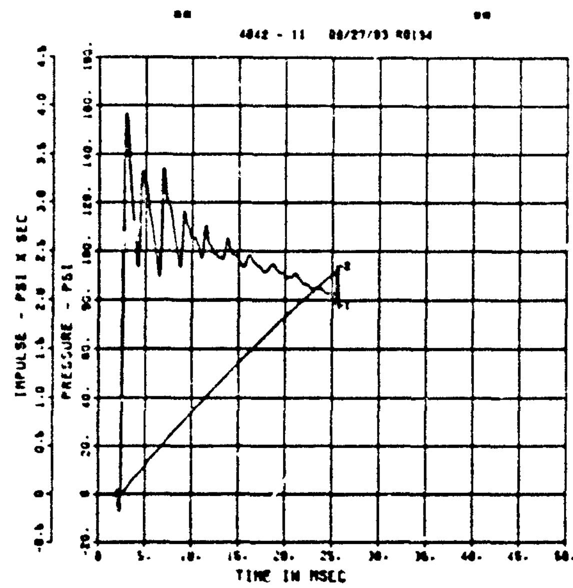

FEMA ELEM TEST D-6
AFF-1
200000. HZ CAL= 818.6

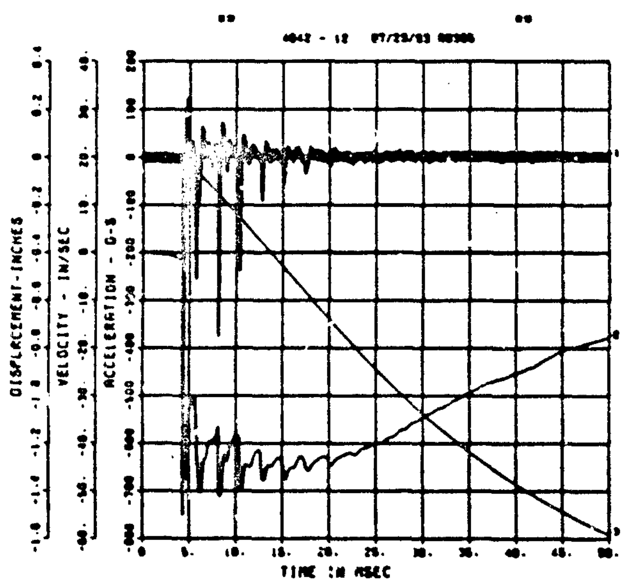

FEMA ELEM TEST D-6
A-1
200000. HZ CAL= 2504.

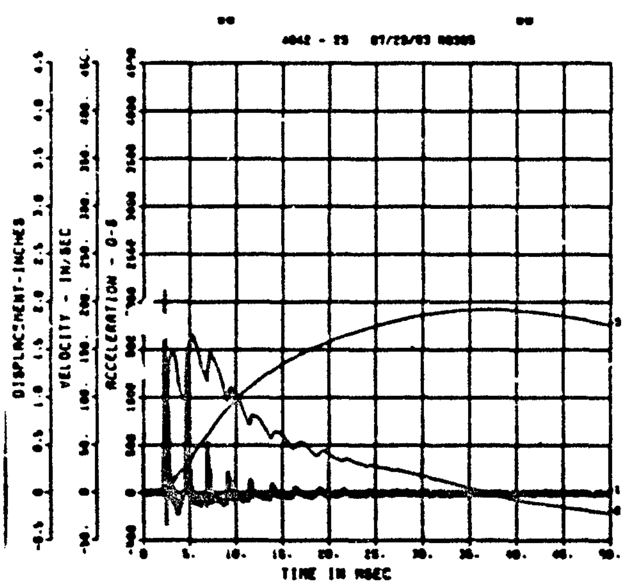

FEMA ELEM TEST D-6
A-2
200000. HZ CAL= 414.6

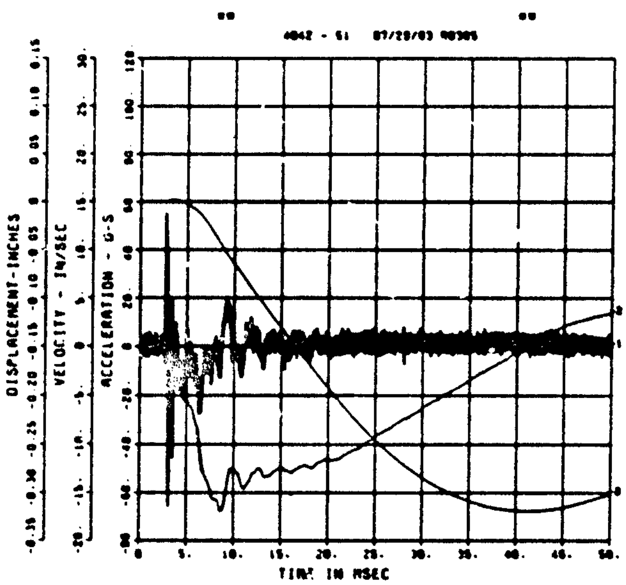

FEMA ELEM TEST D-6
IF-1
200000. HZ CAL= 344.8

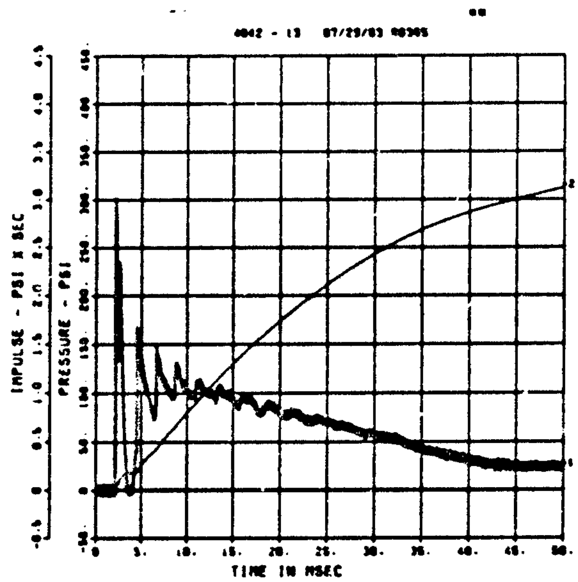

** PEAK VALUE IS 94 % UNDER CALIBRATION **

FEMA ELEM TEST D-6
IF-2
200000. HZ CAL= 342.7

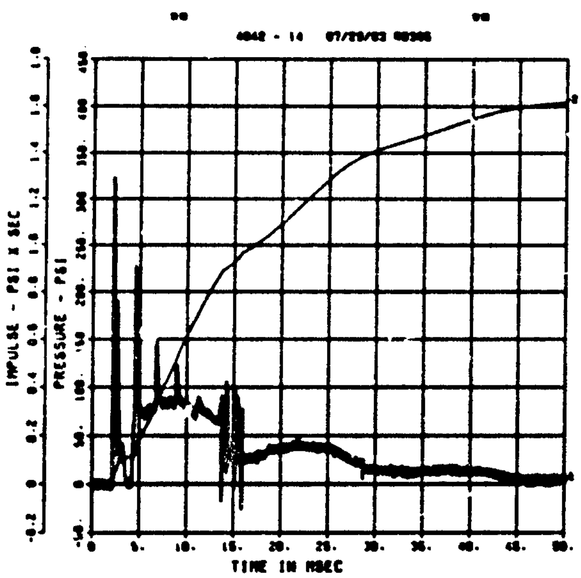

FEMA ELEM TEST D-6
IF-3
200000. HZ CAL= 343.2

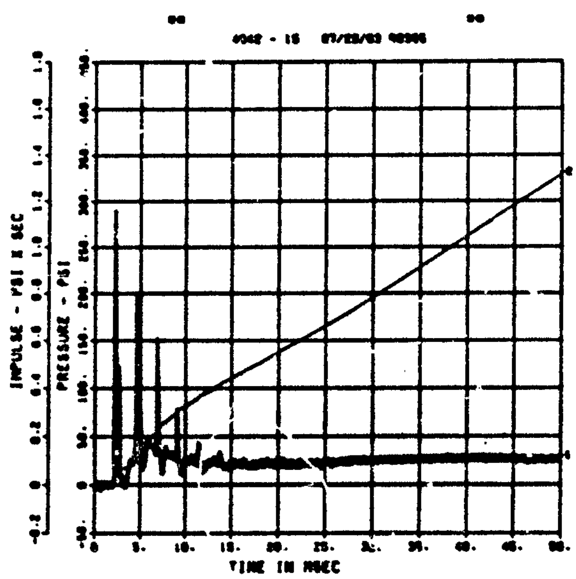

FEMA ELEM TEST D-6
IF-4
200000. HZ CAL= 341.2

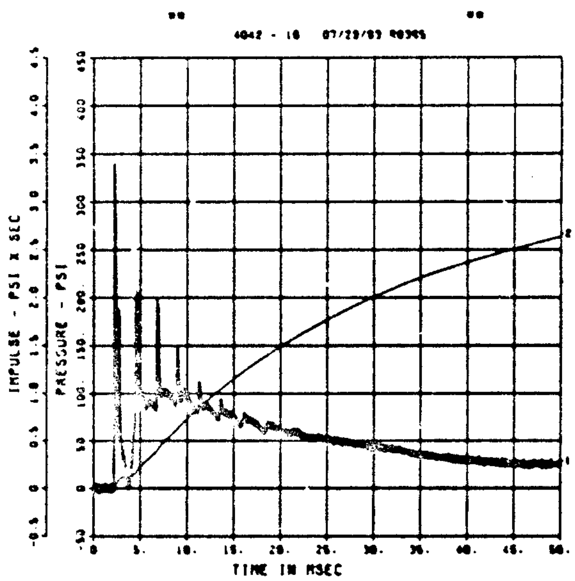

FEMA ELEM TEST D-6
IF-5
200000. HZ CAL= 358.4

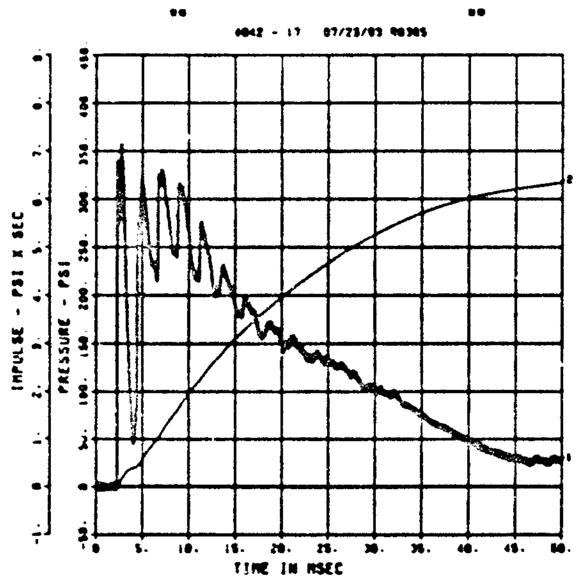

FEMA ELEM TEST D-6
IF-6
200000. HZ CAL= 145.5

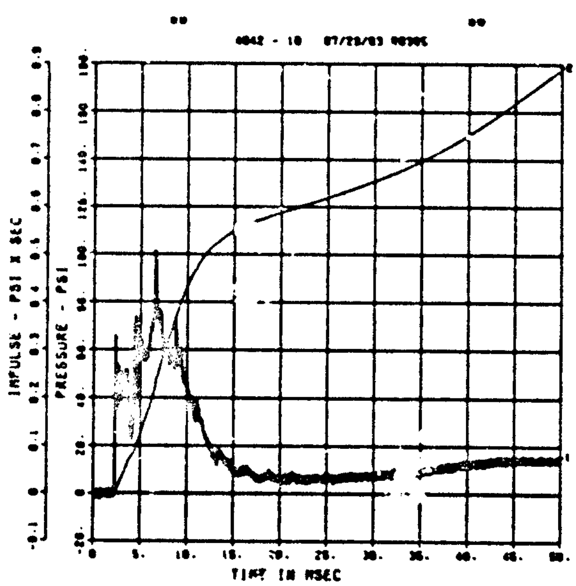

FEMA ELEM TEST D-6
IF-7
50000. HZ CAL= 128.4
LP4/4 70% CUTOFF= 2260. HZ

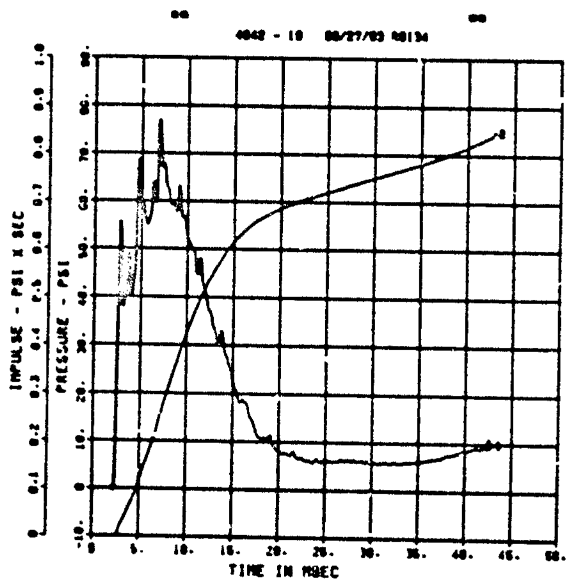

FEMA ELEM TEST D-6
IF-8
200000. HZ CAL= 83.40

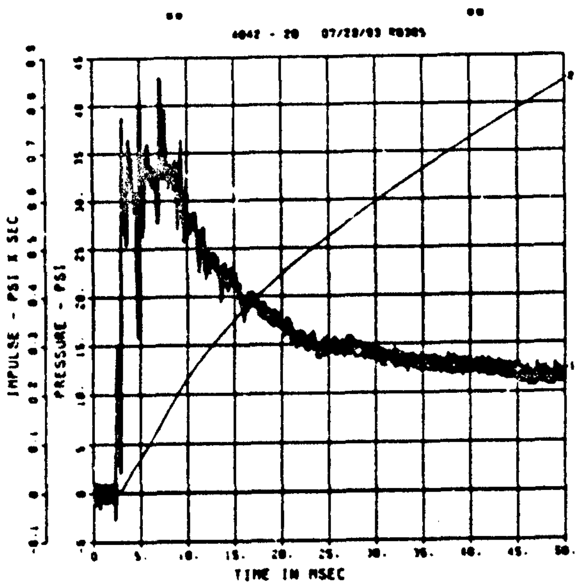

FEMA ELEM TEST D-6
IF-9
200000. HZ CAL= 84.10

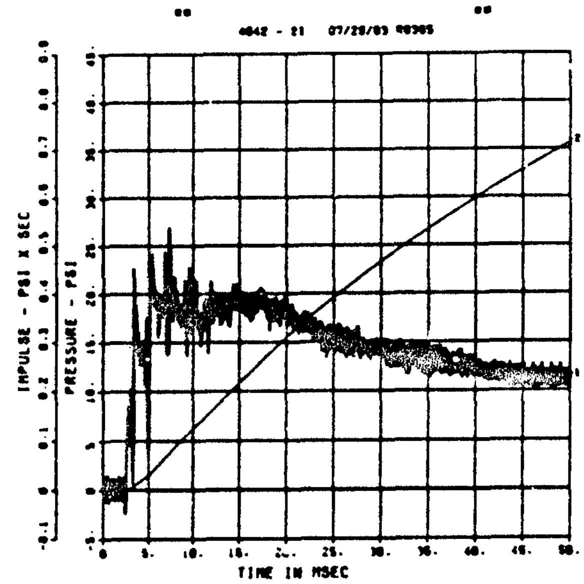

FEMA ELEM TEST D-6
IF-10
200000. HZ CAL= 83.10

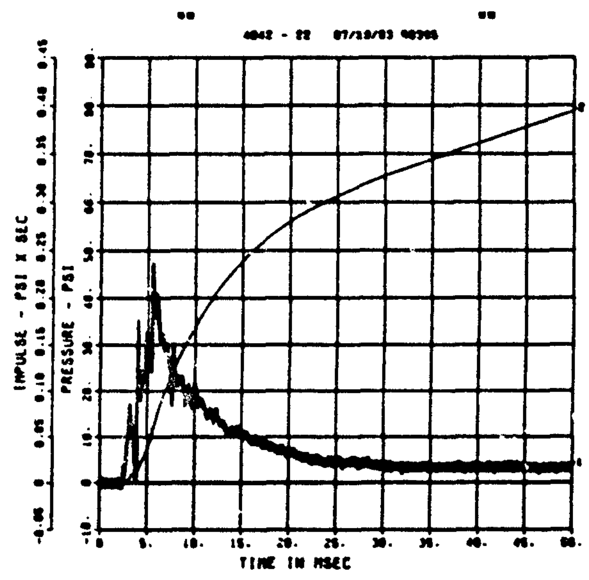

FEMA ELEM TEST D-6
IF-11
200000. HZ CAL= 61.60

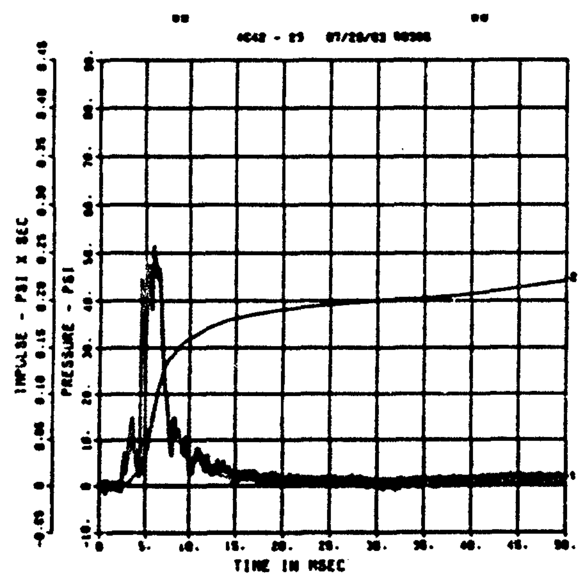

FEMA ELEM TEST D-6
IF-12
200000. HZ CAL= 81.10

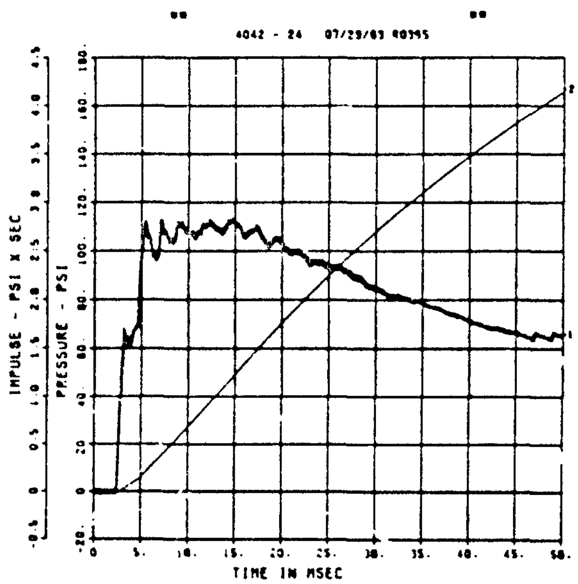

** PEAK VALUE IS 40 % OVER CALIBRATION **

FEMA ELEM TEST D-6
IF-13
50000. HZ CAL= 51.10
LP4/4 70% CUTOFF= 2250. HZ

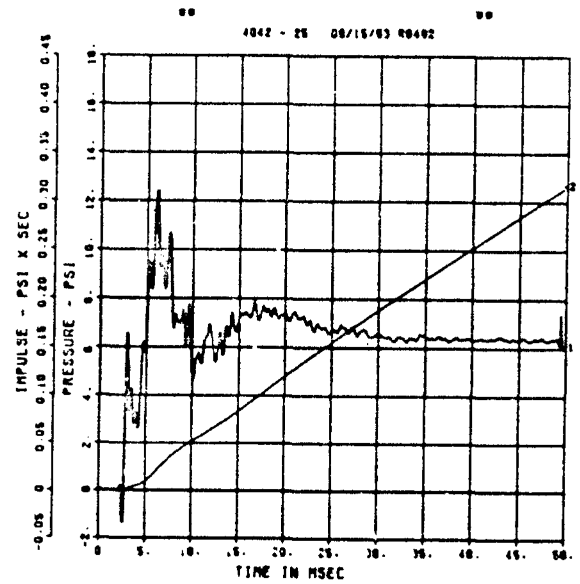

FEMA ELEM TEST D-6
IF-14
50000. HZ CAL= 51.10
LP4/4 70% CUTOFF= 2250. HZ

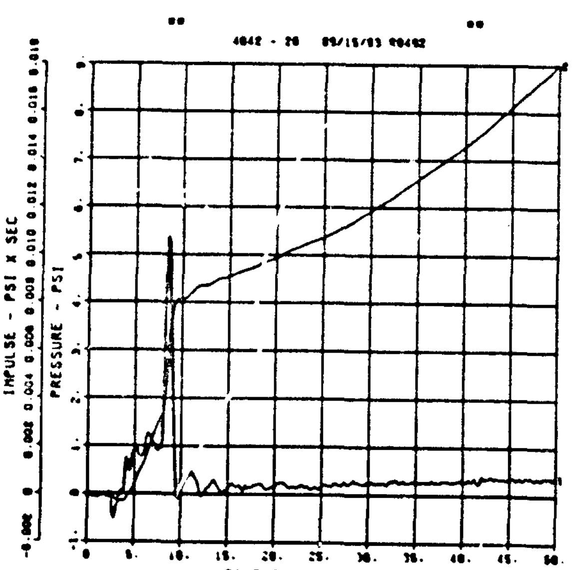

** PEAK VALUE IS 90 % UNDER CALIBRATION **

FEMA ELEM TEST D-6
IF-15
50000. HZ CAL= 50.60
LP4/4 70% CUTOFF= 2250. HZ

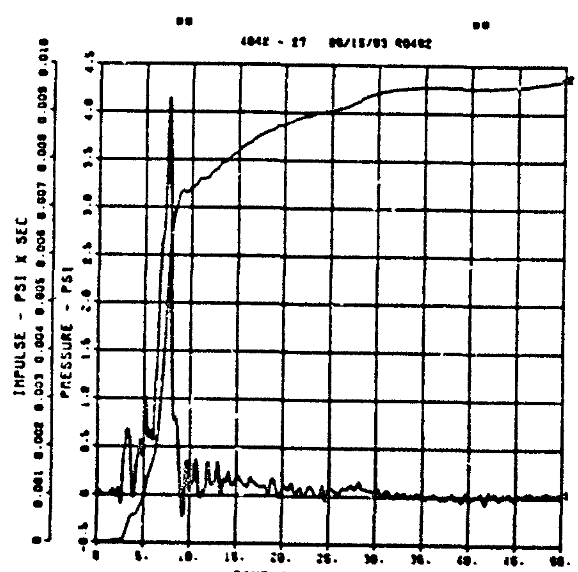

** PEAK VALUE IS 92 % UNDER CALIBRATION **

FEMA ELEM TEST D-6
IF-16
200000. HZ CAL= 343.2

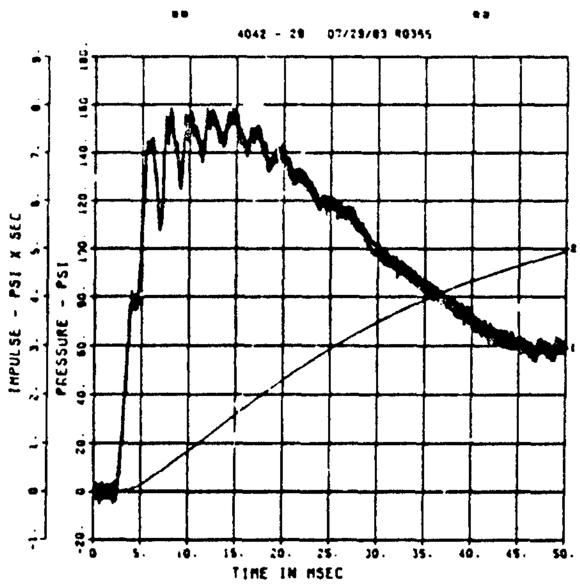

FEMA ELEM TEST D-6
EO-1
200000. HZ CAL= 20205.

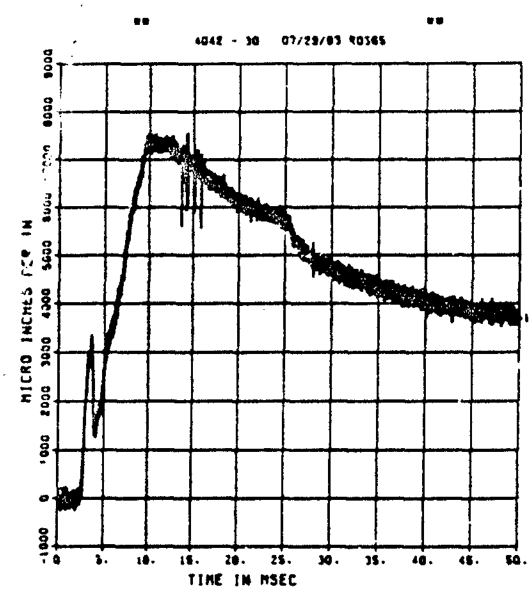

FEMA ELEM TEST D-6
EI-1
200000. HZ CAL= 10276.

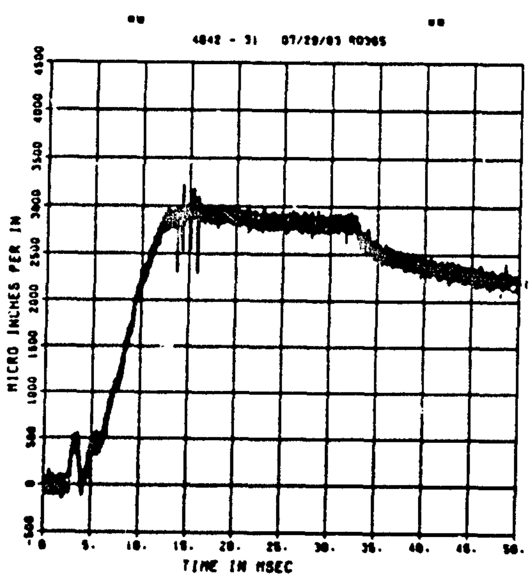

FEMA ELEM TEST D-6
EO-2
50000. HZ CAL= 39162.
LP4/4 70% CUTOFF= 2250. HZ

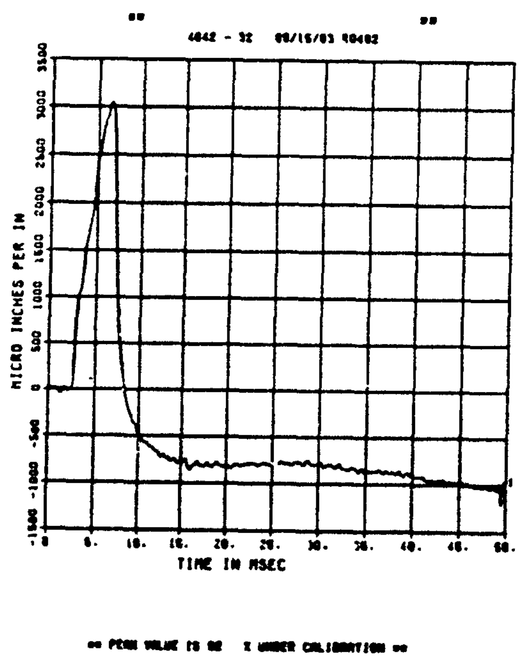

FEMA ELEM TEST D-6
EI-2
200000. HZ CAL= 10276.

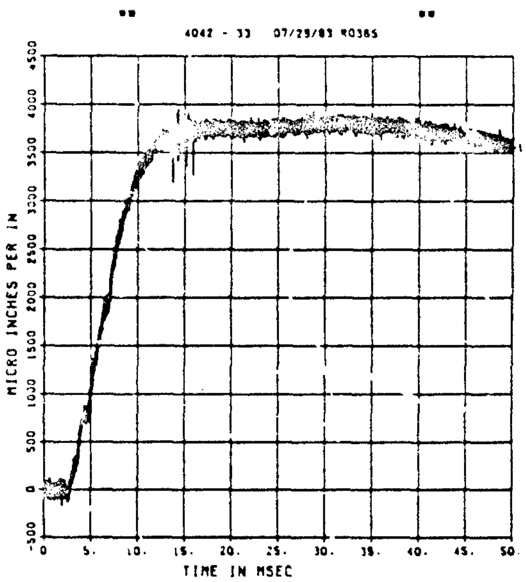

FEMA ELEM TEST D-6
EO-3
50000. HZ CAL= 10276.
LP4/4 70% CUTOFF= 2250. HZ

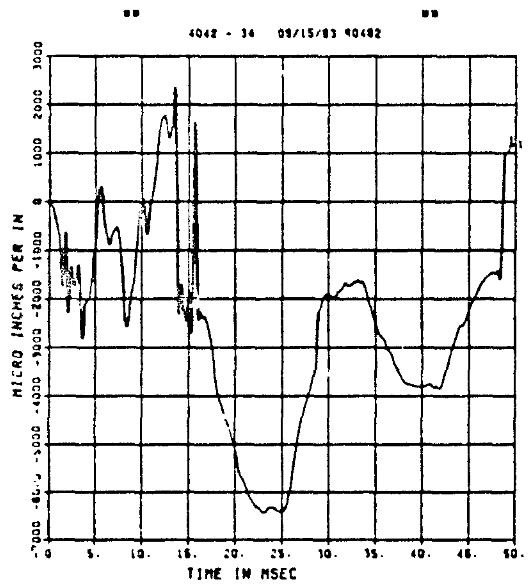

FEMA ELEM TEST D-6
EO-4
200000. HZ CAL= 10276.

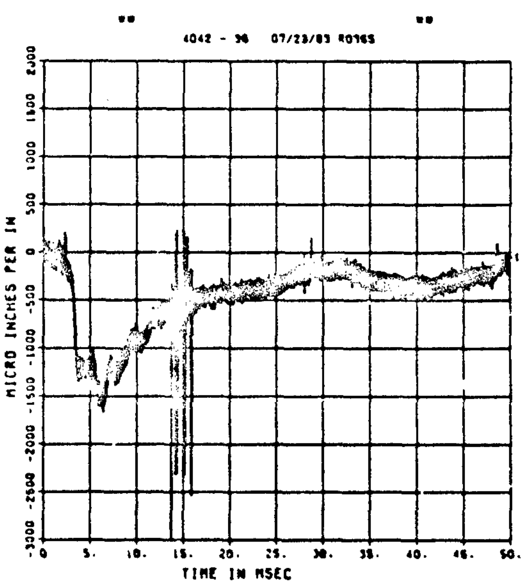

FEMA ELEM TEST D-6
EO-5
200000. HZ CAL= 10276.

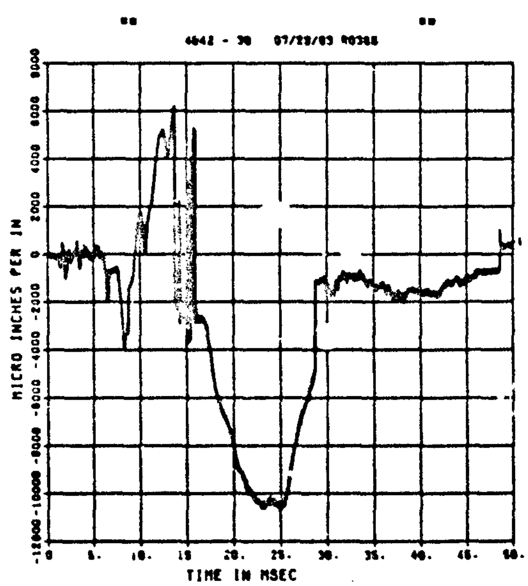

** PEAK VALUE IS 4 % OVER CALIBRATION **

FEMA ELEM TEST D-6
EI-5
50000. HZ CAL= 10276.
LP4/4 70% CUTOFF= 2250. HZ

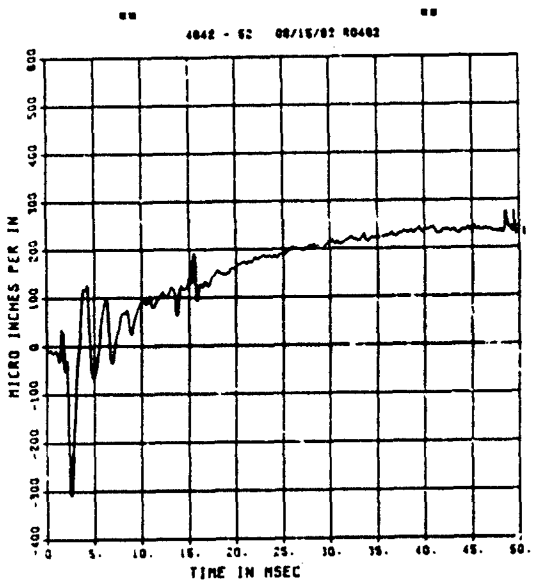

** PEAK VALUE IS 97 % UNDER CALIBRATION **

FEMA ELEM TEST D-6
EI-7
50000. HZ CAL= 6768.
LP4/4 70% CUTOFF= 2250. HZ

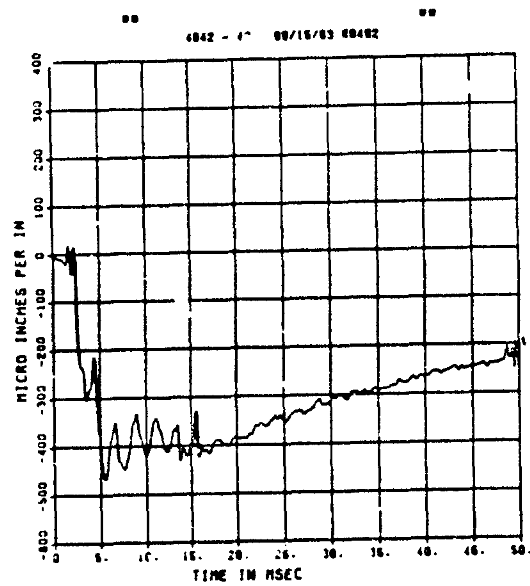

** PEAK VALUE IS 93 % UNDER CALIBRATION **

FEMA ELEM TEST D-6
EO-8
50000. HZ CAL= 20205.
LP4/4 70% CUTOFF= 2250. HZ

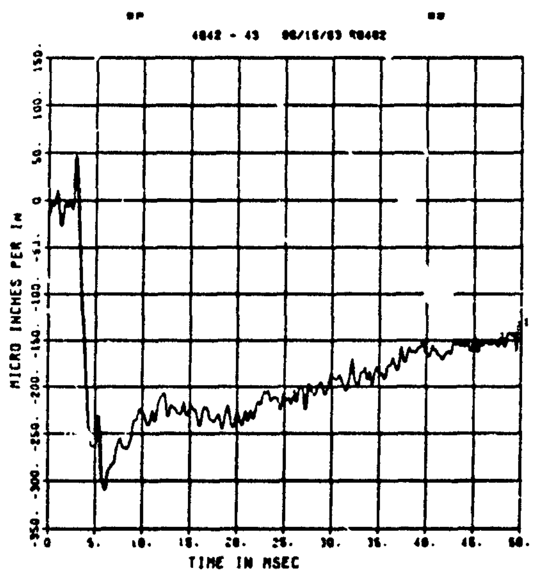

** PEAK VALUE IS 90 % UNDER CALIBRATION **

FEMA ELEM TEST D-6
EI-8
50000. HZ CAL= 10276.
LP4/4 70% CUTOFF= 2250. HZ

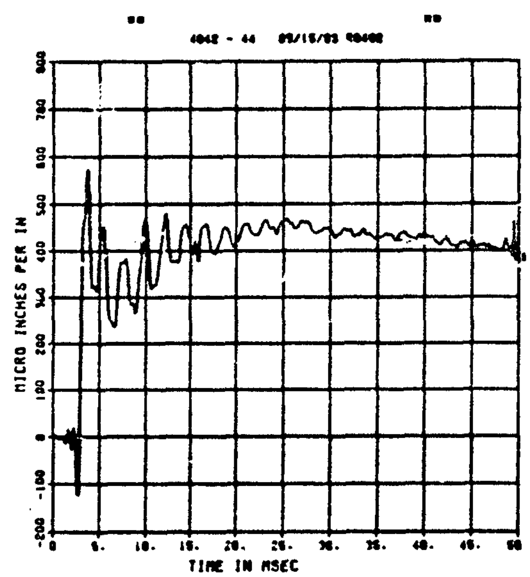

** PEAK VALUE IS 94 % UNDER CALIBRATION **

FEMA ELEM TEST D-6
E0-9
50000. HZ CAL= 10276.
LP4/4 70% CUTOFF= 2250. HZ

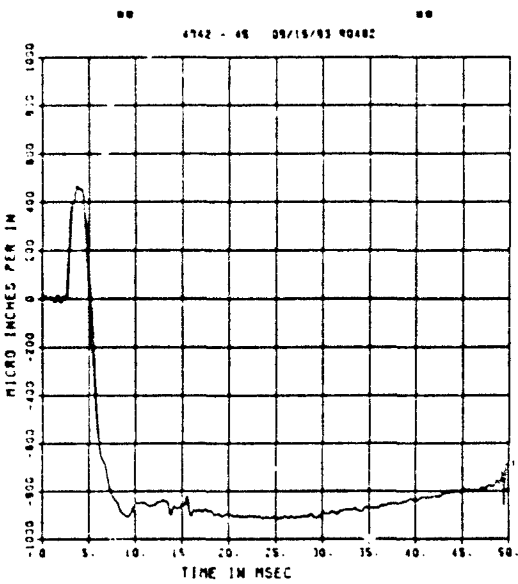

** PEAK VALUE IS 91 % UNDER CALIBRATION **

FEMA ELEM TEST D-6
EI-9
50000. HZ CAL= 10276.
LP4/4 70% CUTOFF= 2250. HZ

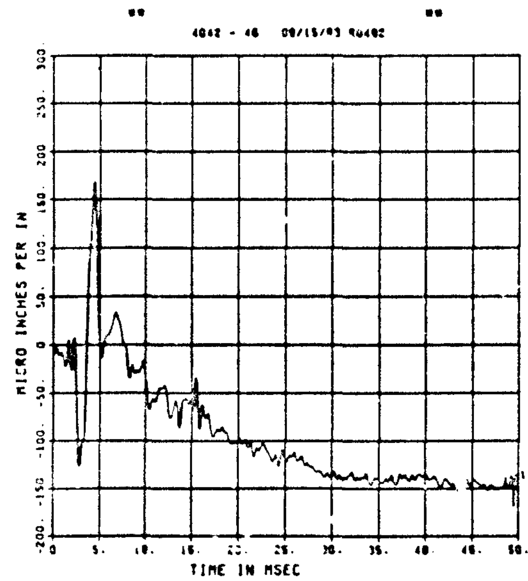

** PEAK VALUE IS 98 % UNDER CALIBRATION **

FEMA ELEM TEST D-6
E0-11
50000. HZ CAL= 10276.
LP4/4 70% CUTOFF= 2250. HZ

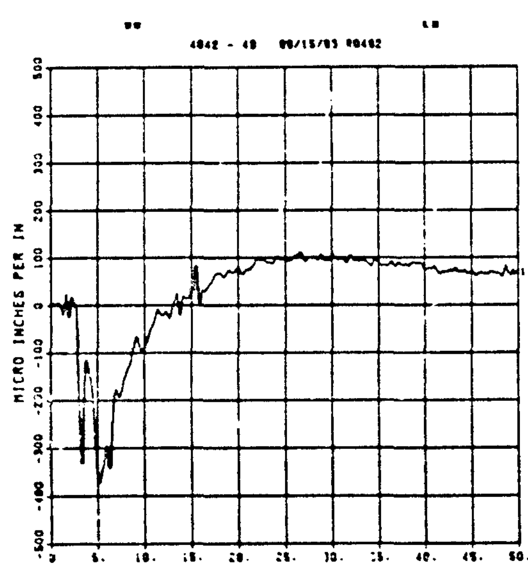

** PEAK VALUE IS 98 % UNDER CALIBRATION **

FEMA ELEM TEST D-6
EI-11
50000. HZ CAL= 10276.
LP4/4 70% CUTOFF= 2250. HZ

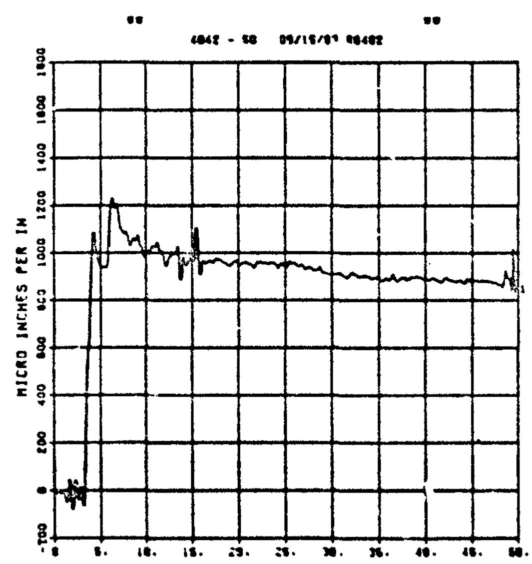

** PEAK VALUE IS 99 % UNDER CALIBRATION **

FEMA ELEM TEST D-7
BP-1
200000. HZ CAL= 992.0
LP2/0 70% CUTOFF= 18000. HZ

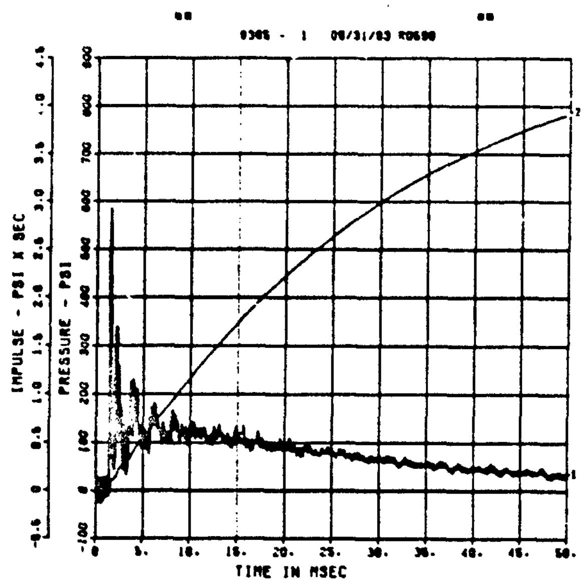

FEMA ELEM TEST D-7
BP-2
200000. HZ CAL= 915.2

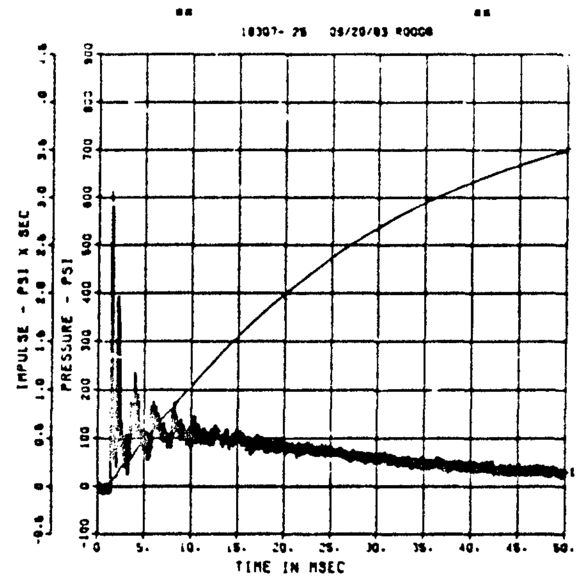

FEMA ELEM TEST D-7
BP-3
200000. HZ CAL= 744.1

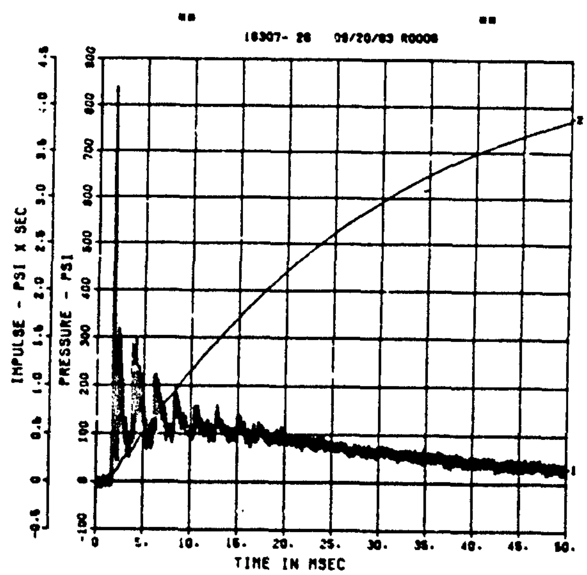

FEMA ELEM TEST D-7
BP-4
200000. HZ CAL= 1048.

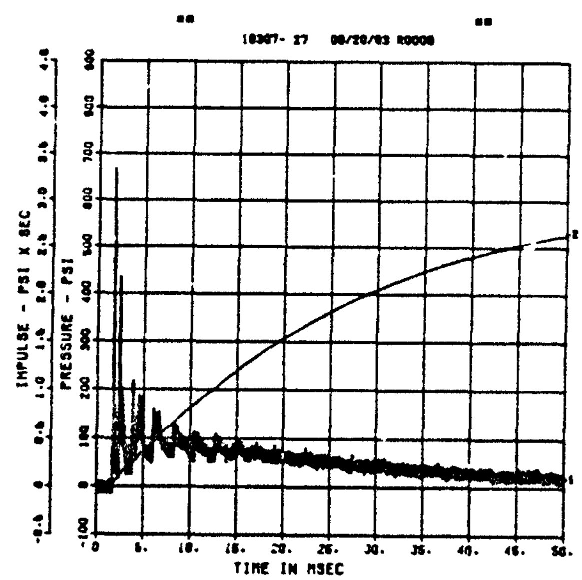

** PEAK VALUE IS 13 % OVER CALIBRATION **

FEMA ELEM TEST D-7
BP-6
200000. HZ CAL= 954.0
LP2/0 70% CUTOFF= 18000. HZ

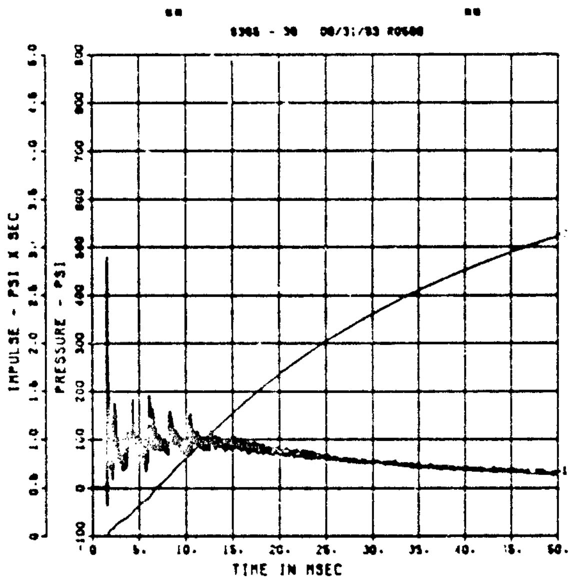

FEMA ELEM TEST D-7
SE-1
200000. HZ CAL= 339.2

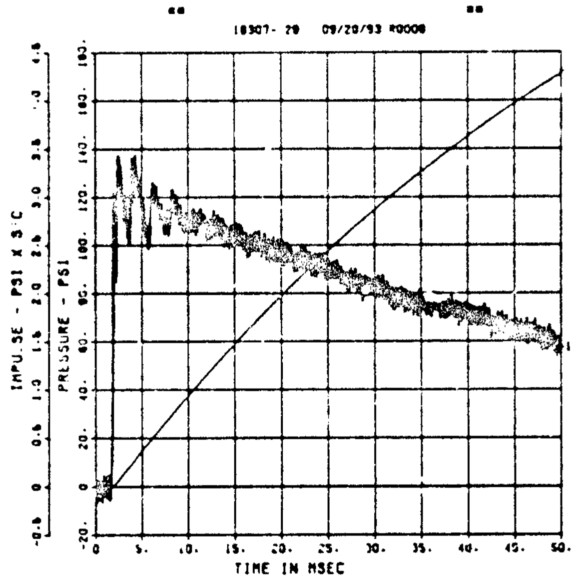

FEMA ELEM TEST D-7
SE-2
200000. HZ CAL= 192.0

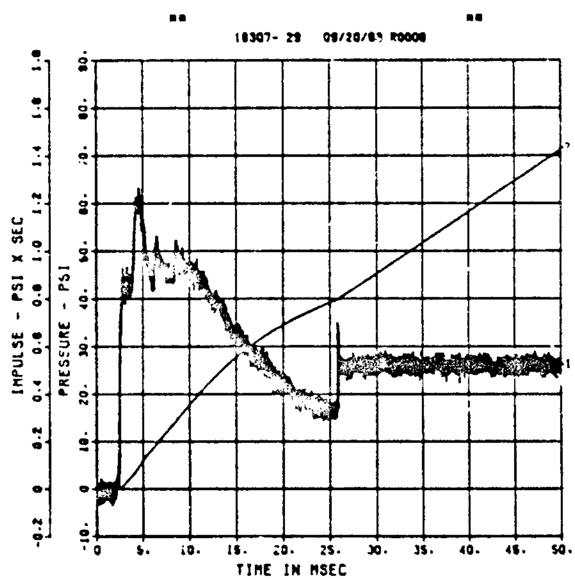

FEMA ELEM TEST D-7
SE-3
200000. HZ CAL= 198.2

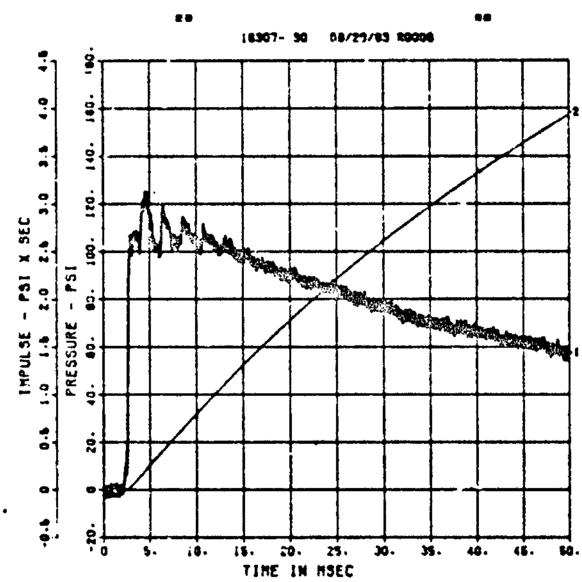

FEMA ELEM TEST D-7
SE-4
200000. HZ CAL= 132.5

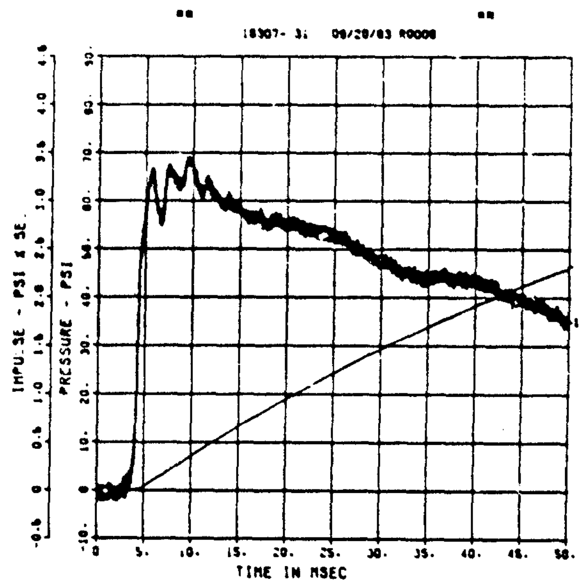

FEMA ELEM TEST D-7
SE-7 (REDO)
200000. HZ CAL= 324.5

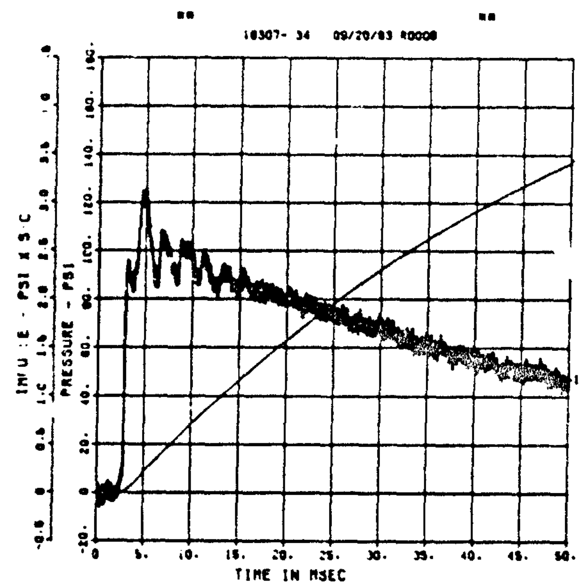

FEMA ELEM TEST D-7
AFF-1
200000. HZ CAL= 818.6

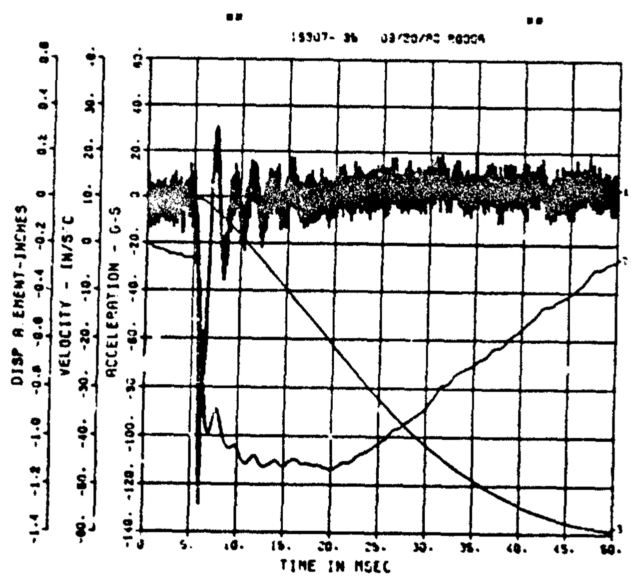

FEMA ELEM TEST D-7
A-1
200000. HZ CAL= 2504.

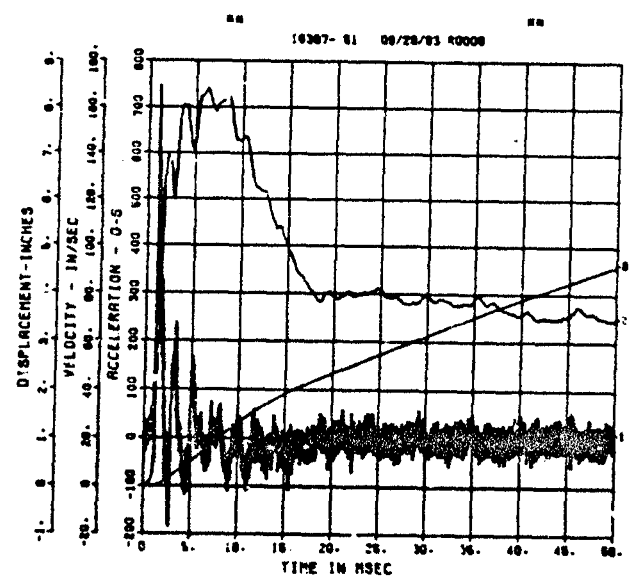

** PEAK VALUE IS 94 % UNDER CALIBRATION **

FEMA ELEM TEST D-7
A-2
200000. HZ CAL= 435.0
LP2/0 70% CUTOFF= 14000. HZ

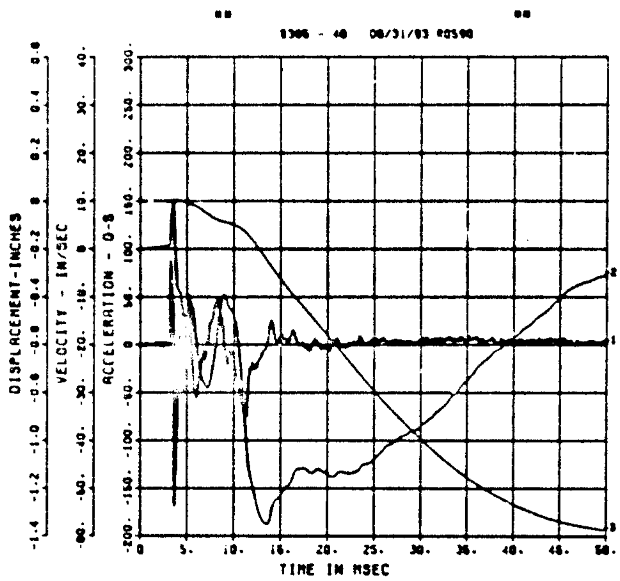

FEMA ELEM TEST D-7
IF-1
200000. HZ CAL= 248 2

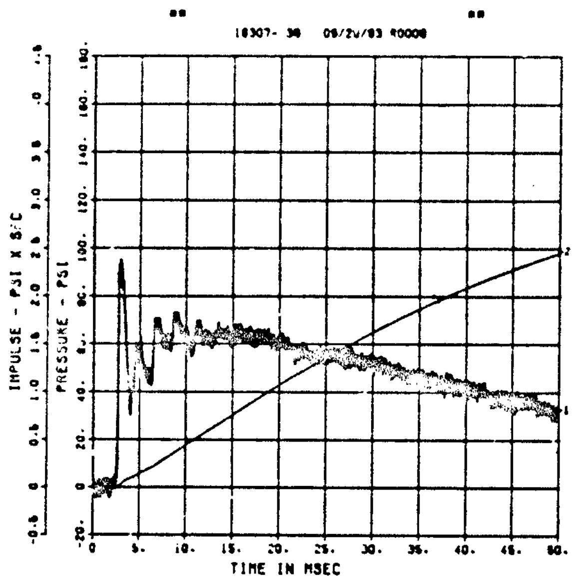

FEMA ELEM TEST D-7
IF-2
200000. HZ CAL= 241.7

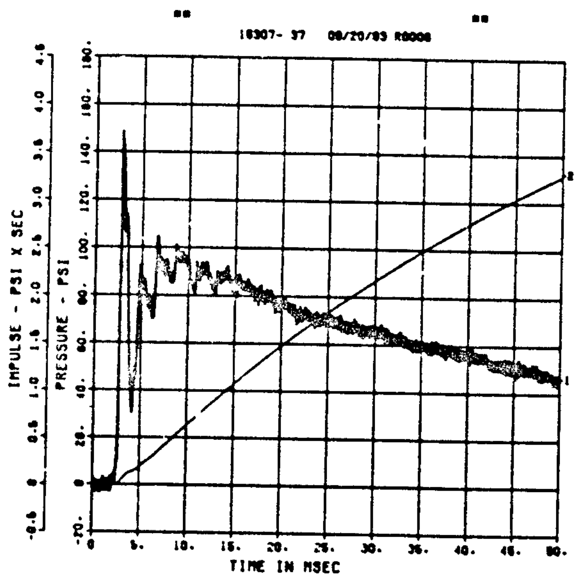

FEMA ELEM TEST D-7
IF-3
200000. HZ CAL= 247.0

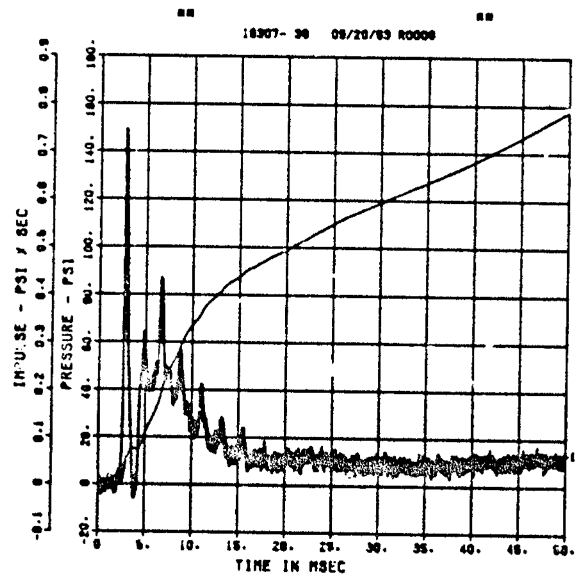

FEMA ELEM TEST D-7
IF-4
200000. HZ CAL= 245.6

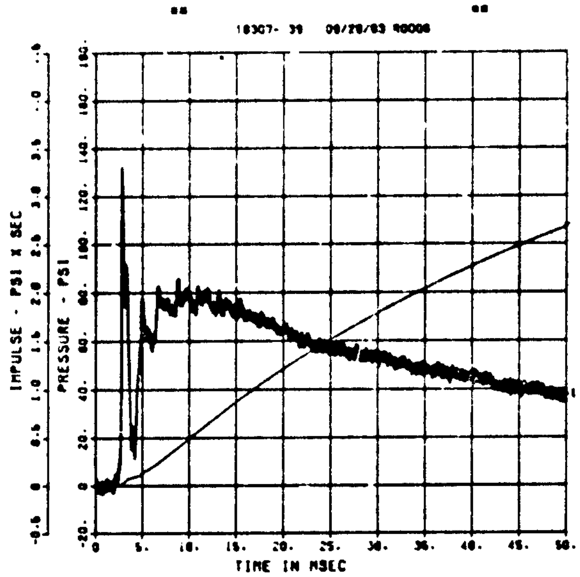

FEMA ELEM TEST D-7
IF-5
200000. HZ CAL= 357.9

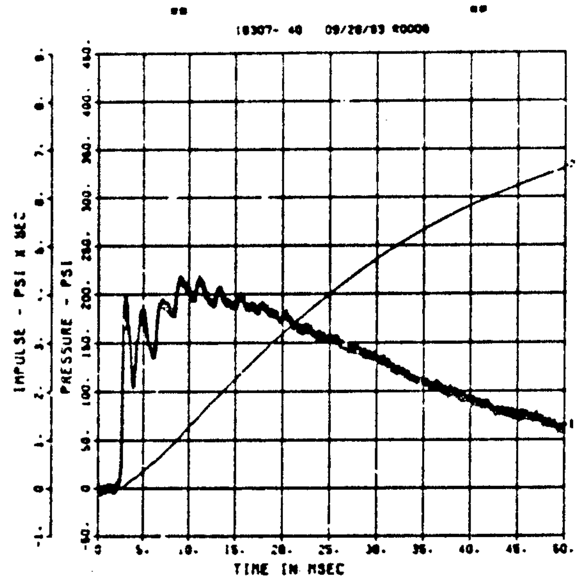

FEMA ELEM TEST D-7
IF-6
200000. HZ CAL= 128.1

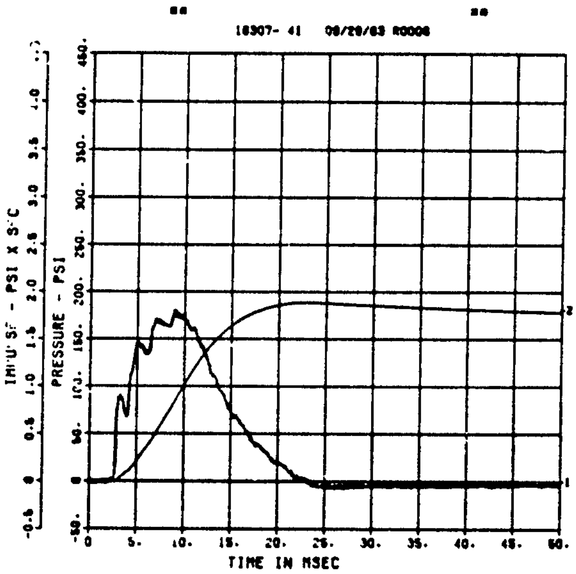

FEMA ELEM TEST D-7
IF-7
200000. HZ CAL= 126.8

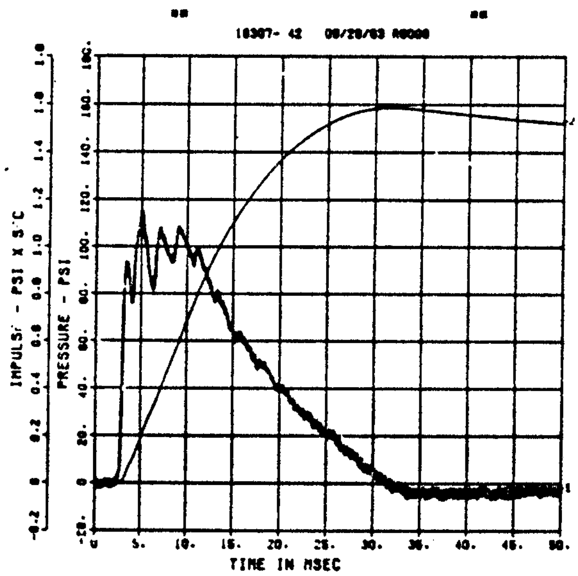

** PEAK VALUE IS 41 % OVER CALIBRATION **

FEMA ELEM TEST D-7
IF-8
200000. HZ CAL= 87.30

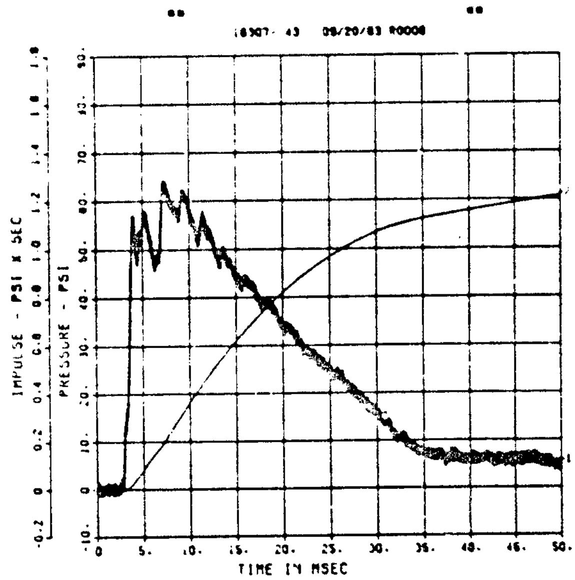

FEMA ELEM TEST D-7
IF-9
200000. HZ CAL= 86.40

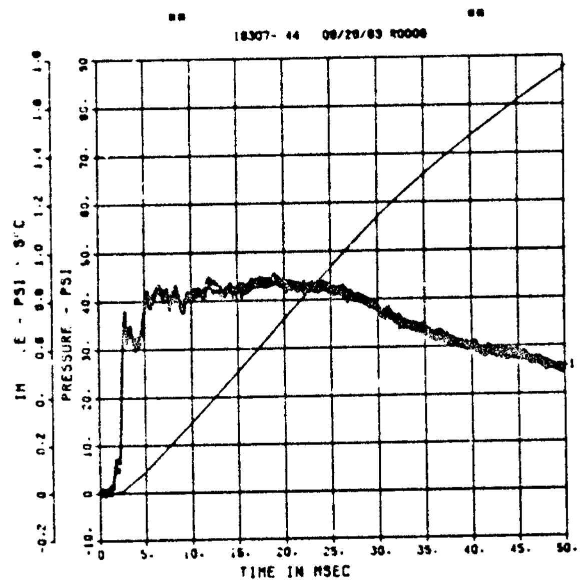

FEMA ELEM TEST D-7
IF-10
200000. HZ CAL= 85.20

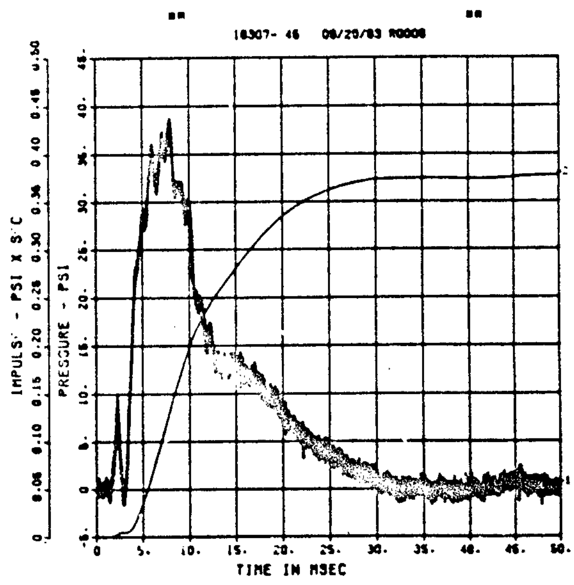

FEMA ELEM TEST D-7
IF-12
200000. HZ CAL= 166.7

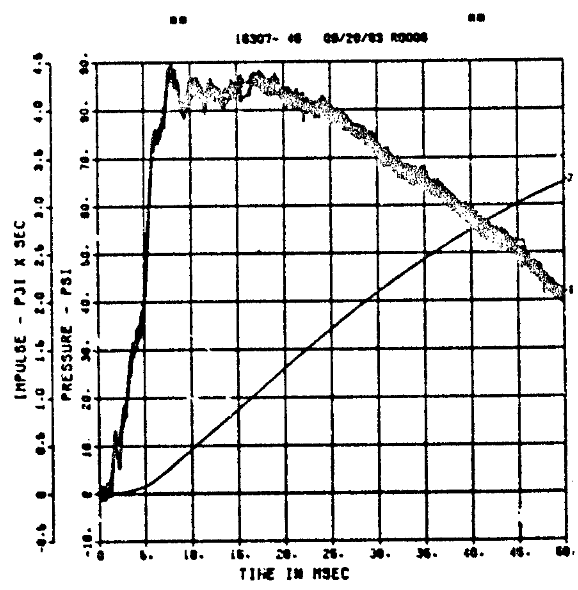

FEMA ELEM TEST D-7
IF-13
200000. HZ CAL= 125.9

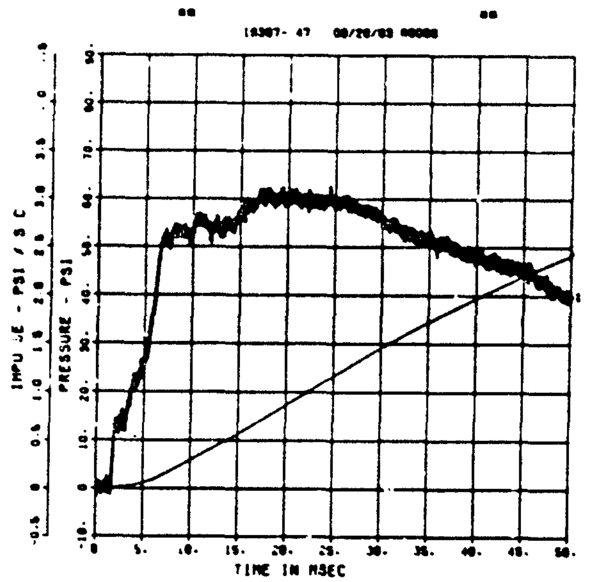

FEMA ELEM TEST D-7
IF-14
200000. HZ CAL= 25.50

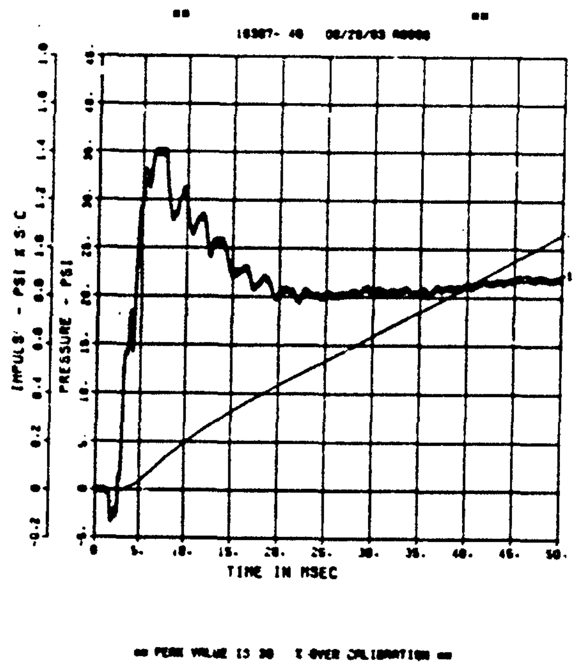

FEMA ELEM TEST D-7
IF-15
200000. HZ CAL= 31.00

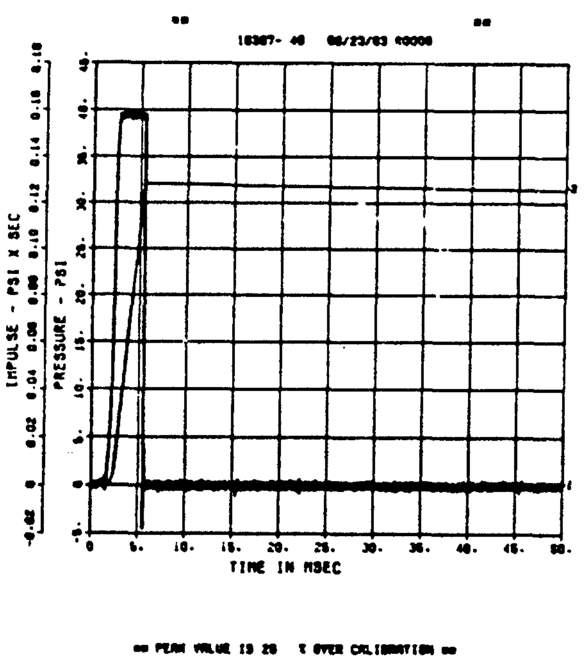

FEMA ELEM TEST D-7
IF-16
200000. HZ CAL= 240.5

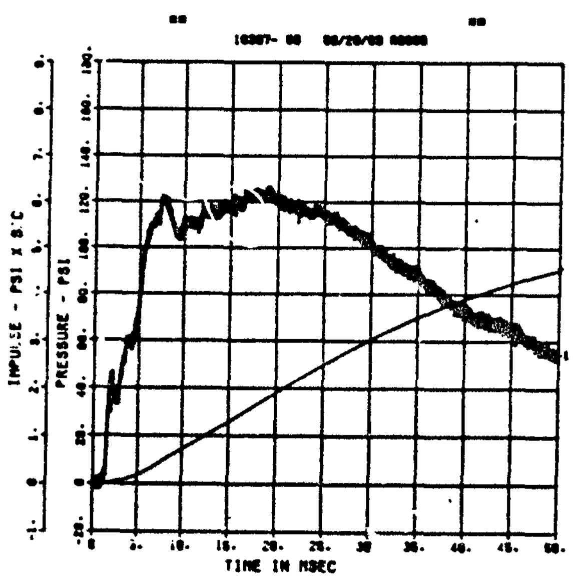

FEMA ELEM TEST D-7
EO-1
200000. HZ CAL= 39162.
LP2/0 70% CUTOFF= 18000. HZ

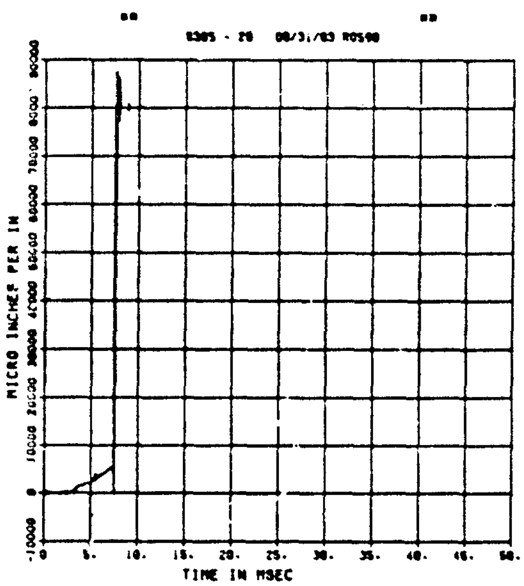

** PEAK VALUE IS 123 % OVER CALIBRATION **

FEMA ELEM TEST D-7
EI-1
200000. HZ CAL. 20205.
LP2/0 70% CUTOFF= 18000. HZ

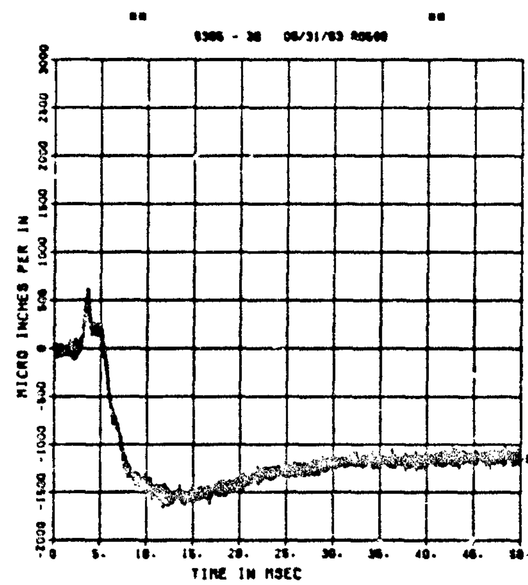

** PEAK VALUE IS 92 % UNDER CALIBRATION **

FEMA ELEM TEST D-7
EO-2
200000. HZ CAL= 39162.
LP2/0 70% CUTOFF= 18000. HZ

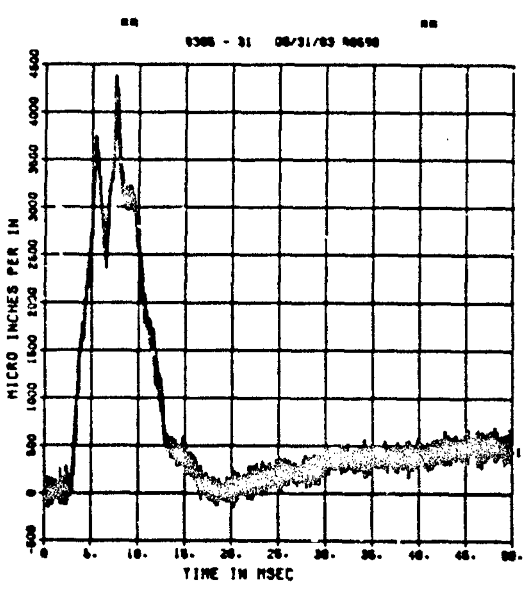

** PEAK VALUE IS 83 % UNDER CALIBRATION **

FEMA ELEM TEST D-7
EI-2
200000. HZ CAL= 20205.
LP2/0 70% CUTOFF= 18000. HZ

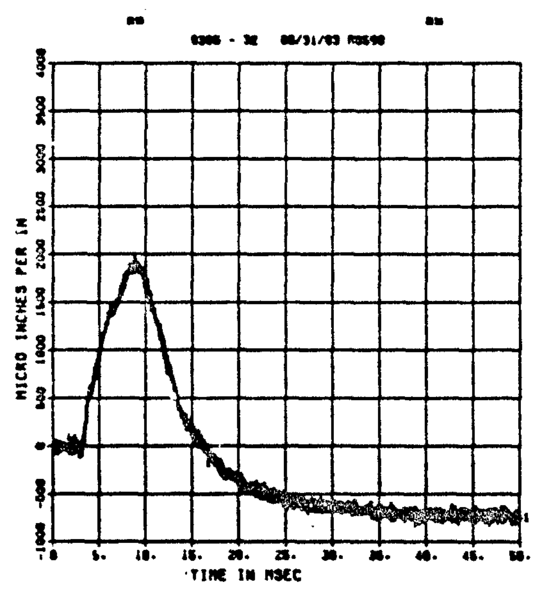

** PEAK VALUE IS 98 % UNDER CALIBRATION **

FEMA ELEM TEST D-7
EO-3
200000. HZ CAL= 10276.
LP2/0 70% CUTOFF= 18000. HZ

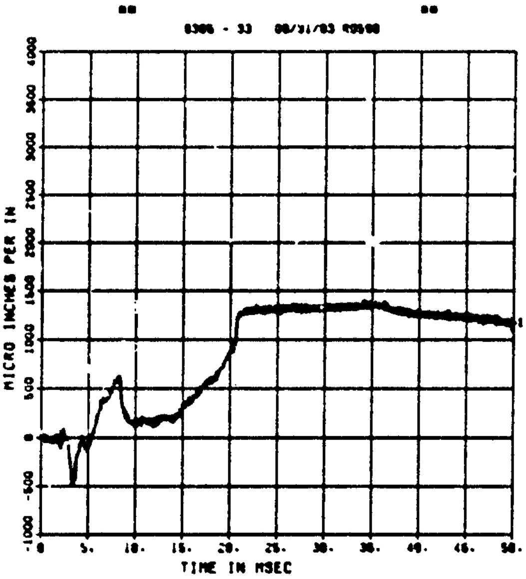

FEMA ELEM TEST D-7
EI-3
200000. HZ CAL= 10276.
LP2/0 70% CUTOFF= 18000. HZ

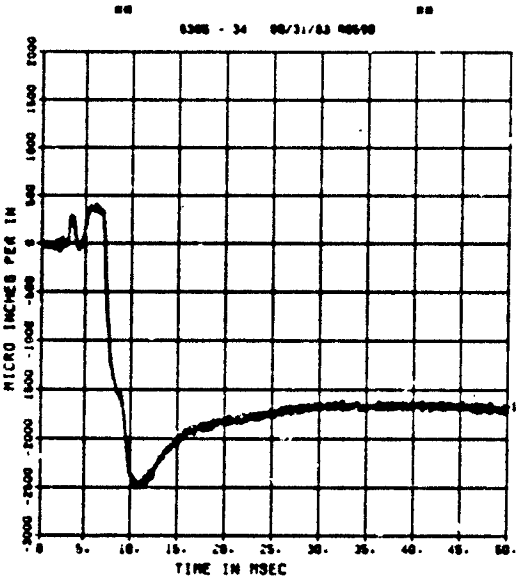

FEMA ELEM TEST D-7
EO-4
200000. HZ CAL= 10276.
LP2/0 70% CUTOFF= 18000. HZ

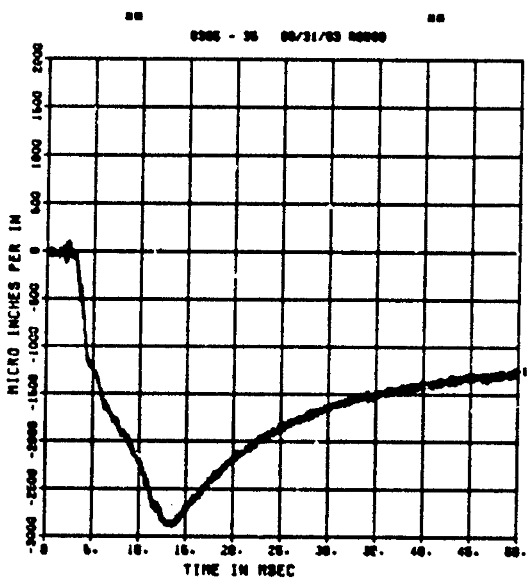

FEMA ELEM TEST D-7
EO-5
200000. HZ CAL= 10276.
LP2/0 70% CUTOFF= 18000. HZ

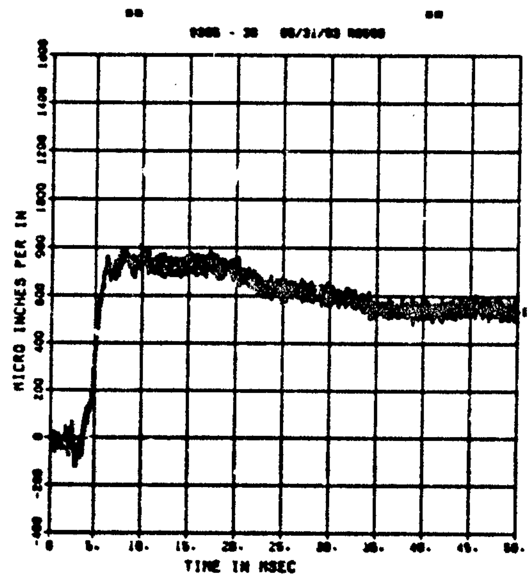

FEMA ELEM TEST D-7
EI-5
200000. HZ CAL= 10276.
LP4/0 70% CUTOFF= 9000. HZ

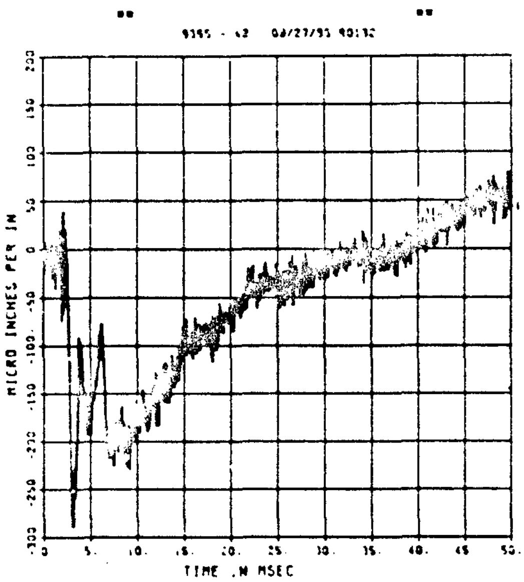

** PEAK VALUE IS 97 % UNDER CALIBRATION **

FEMA ELEM TEST D-7
EO-6
200000. HZ CAL= 6875.
LP2/0 70% CUTOFF= 18000. HZ

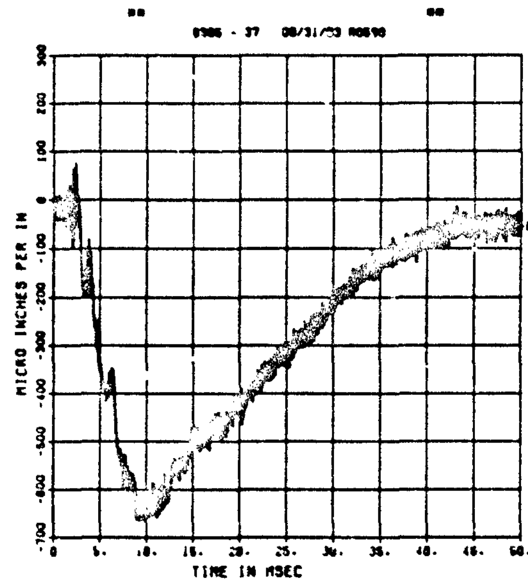

** PEAK VALUE IS 98 % UNDER CALIBRATION **

FEMA ELEM TEST D-7
EO-7
200000. HZ CAL= 6875.
LP2/0 70% CUTOFF= 18000. HZ

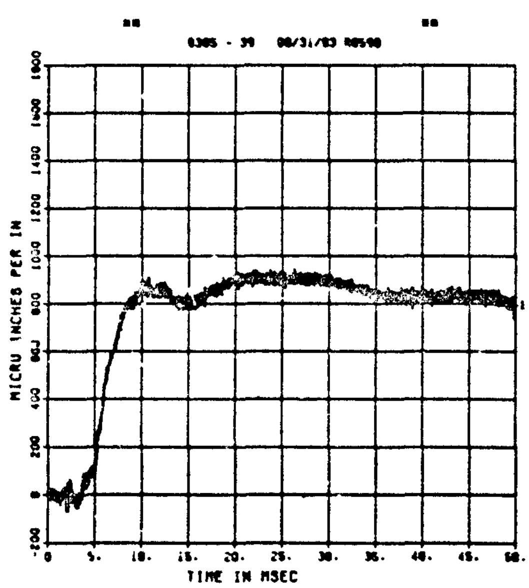

** PEAK VALUE IS 88 % UNDER CALIBRATION **

FEMA ELEM TEST D-7
EI-7
200000. HZ CAL= 6875.
LP4/0 70% CUTOFF= 9000. HZ

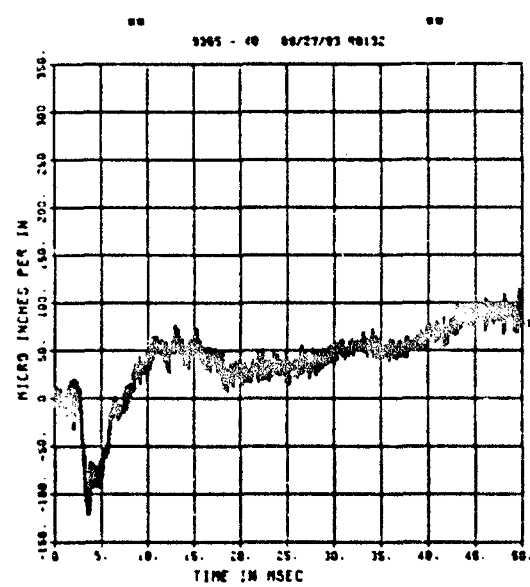

** PEAK VALUE IS 98 % UNDER CALIBRATION **

FEMA ELEM TEST D-7
E0-8
200000. HZ CAL= 20205.
LP2/0 70% CUTOFF= 18000. HZ

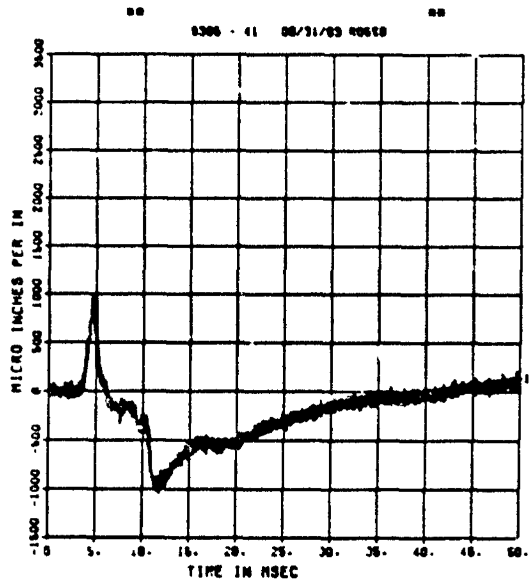

** PEAK VALUE IS 95 % UNDER CALIBRATION **

FEMA ELEM TEST D-7
E0-9
200000. HZ CAL= 6875.

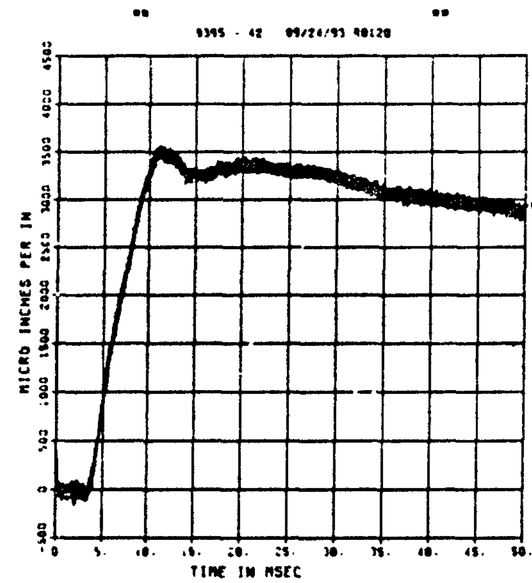

FEMA ELEM TEST D-7
EI-9
200000. HZ CAL= 6875.

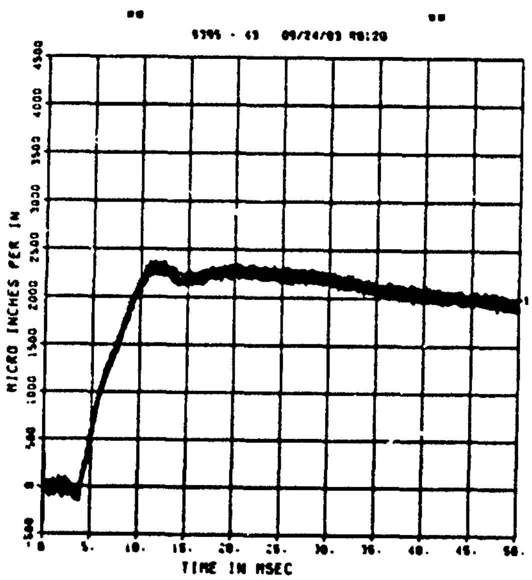

FEMA ELEM TEST D-7
E0-10
200000. HZ CAL= 6875.
LP2/0 70% CUTOFF= 18000. HZ

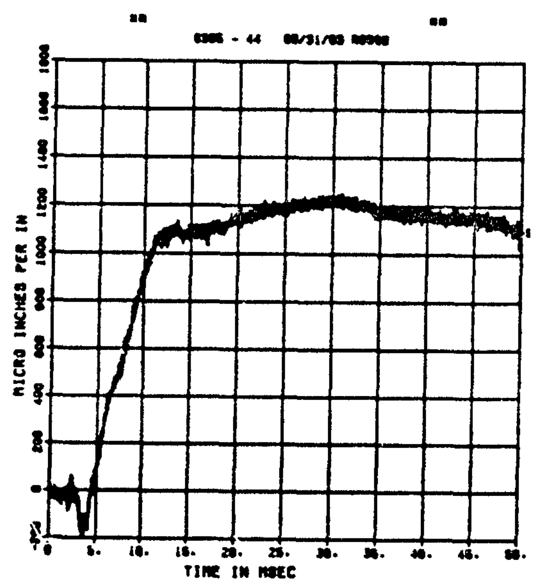

** PEAK VALUE IS 92 % UNDER CALIBRATION **

FEMA ELEM TEST D-7
EI-10
200000. HZ CAL= 6875.
LP2/0 70% CUTOFF= 18000. HZ

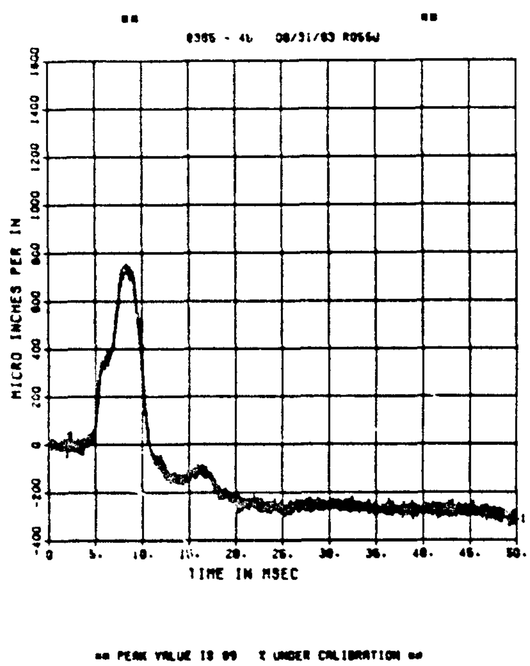

FEMA ELEM TEST D-7
EO-11
200000. HZ CAL= 10276.
LP4/0 70% CUTOFF= 5000. HZ

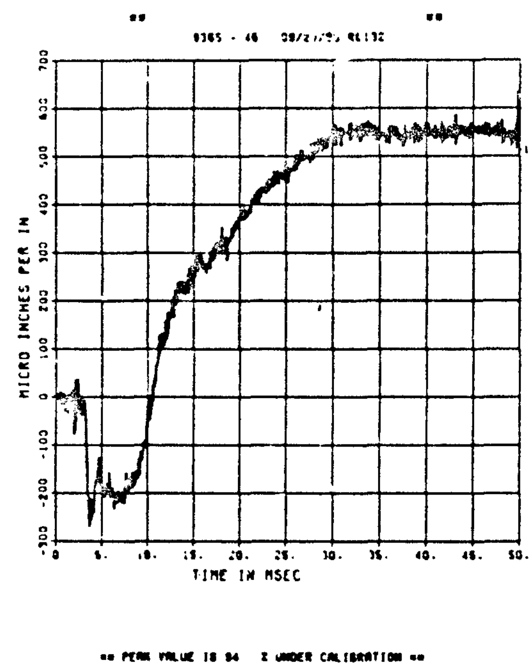

FEMA ELEM TEST D-7
EI-11
200000. HZ CAL= 39162.
LP2/0 70% CUTOFF= 18000. HZ

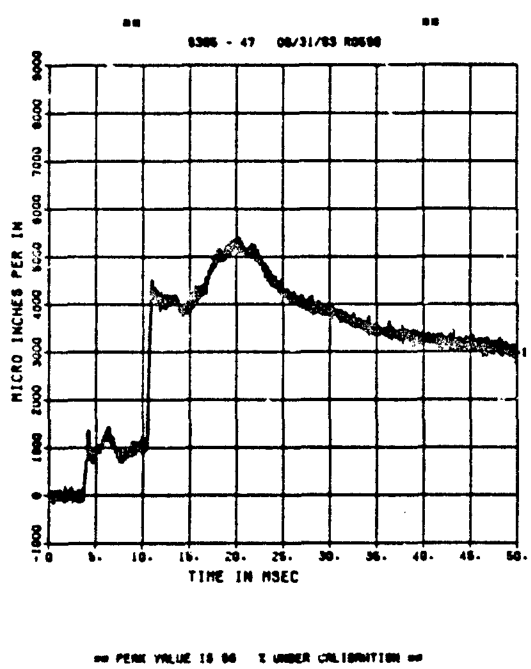

FEMA MULTI-HIT
BP-2
200000. HZ CAL= 915.2

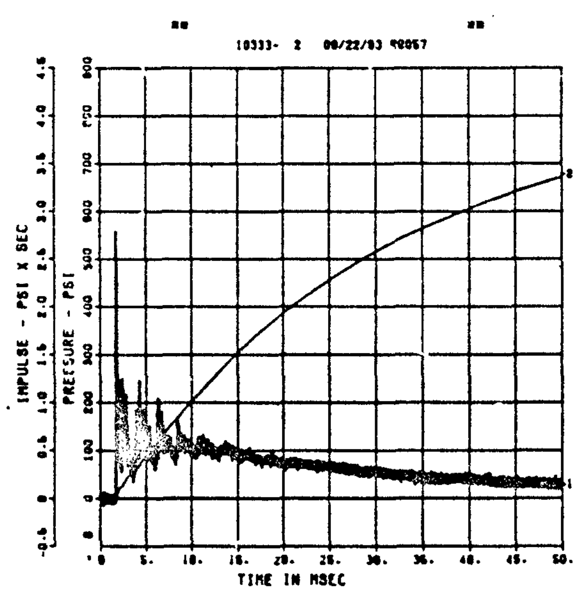

FEMA MULTI-HIT
BP-3
200000. HZ CAL= 744.2

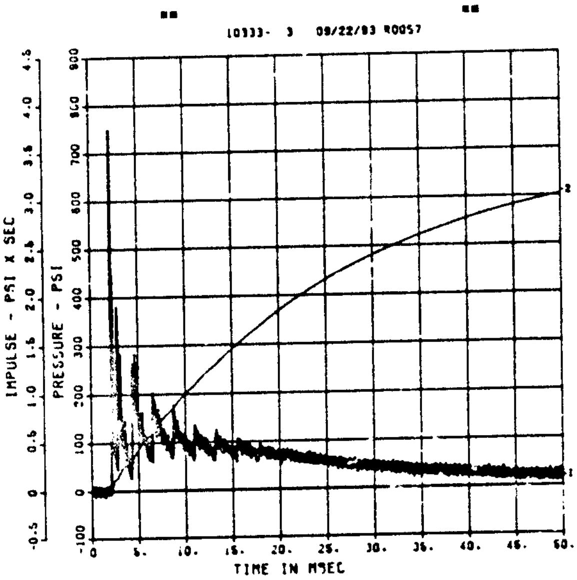

FEMA MULTI-HIT
BP-4
200000. HZ CAL= 659.2

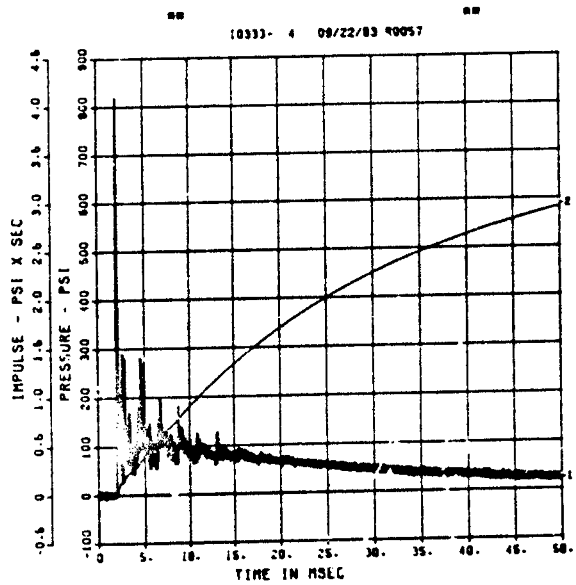

** PEAK VALUE IS 24 % OVER CALIBRATION **

FEMA MULTI-HIT
BP-6
200000. HZ CAL= 897.4

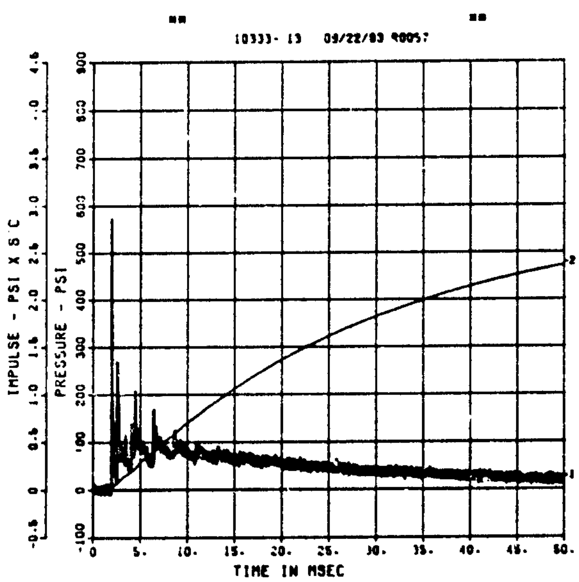

FEMA MULTI-HIT
SE-2
200000. HZ CAL= 357.0
LP3/0 70% CUTOFF= 11000. HZ

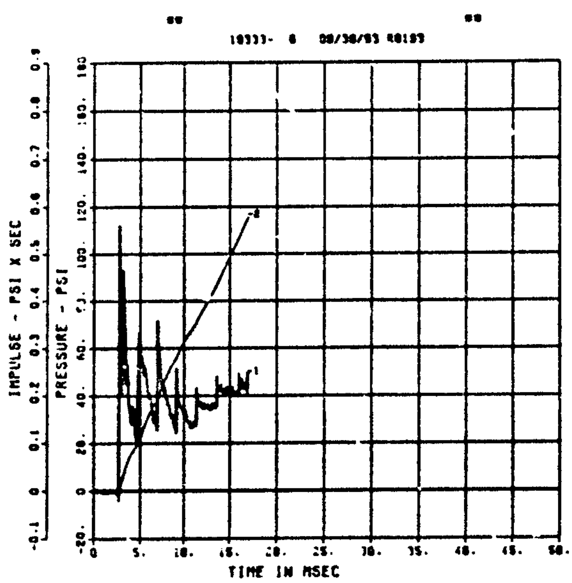

FEMA MULTI-HIT
SE-3
200000. HZ CAL= 257.8

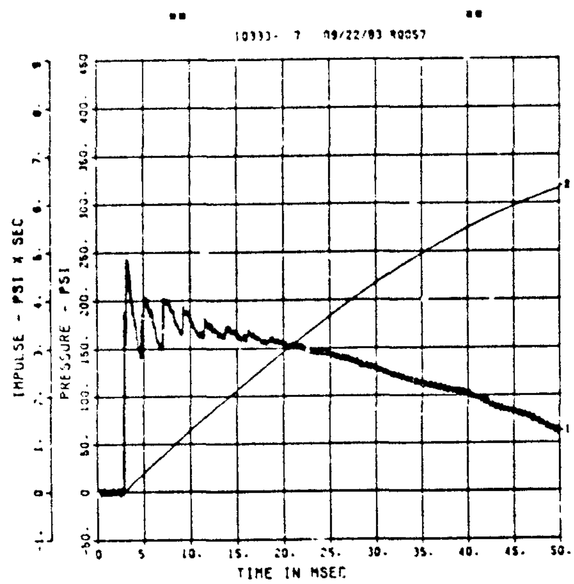

FEMA MULTI-HIT
SE-4
200000. HZ CAL= 361.4
LP3/0 70% CUTOFF= 11000. HZ

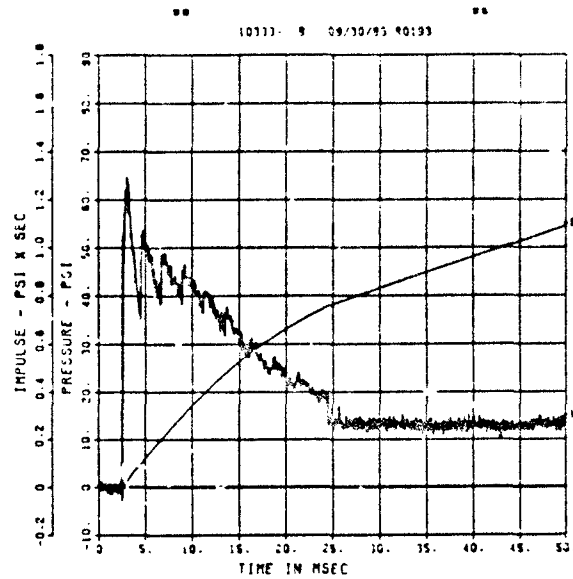

** PEAK VALUE IS 92 % UNDER CALIBRATION **

FEMA MULTI-HIT
SE-5
200000. HZ CAL= 253.5
LP3/0 70% CUTOFF= 11000. HZ

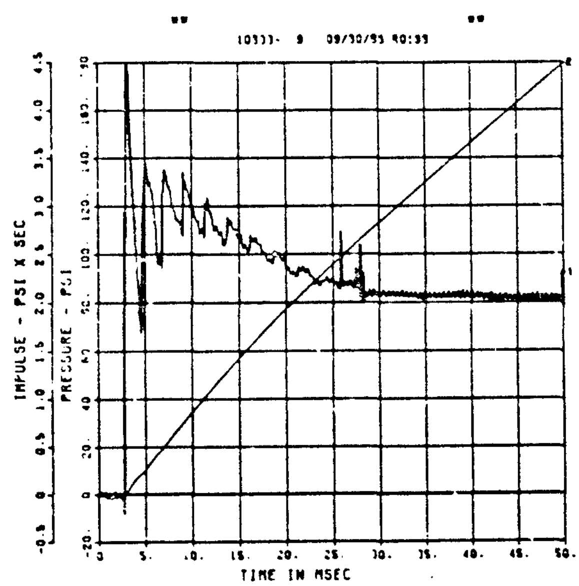

FEMA MULTI-HIT
SE-6
200000. HZ CAL= 364.9
LP3/0 70% CUTOFF= 11000. HZ

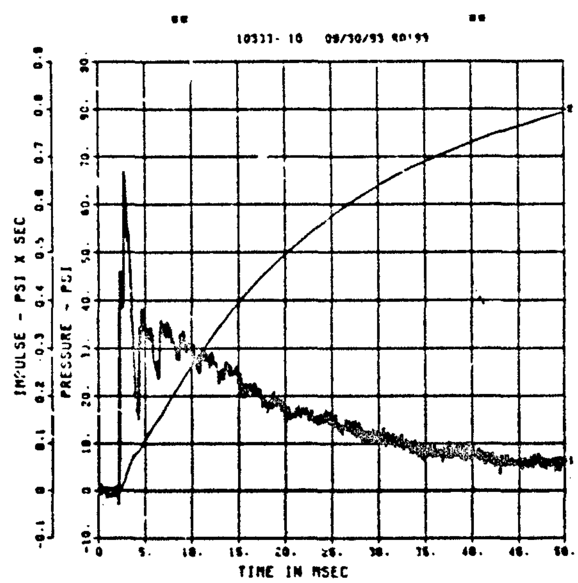

** PEAK VALUE IS 92 % UNDER CALIBRATION **

FEMA MULTI-HIT
SE-7
200000. HZ CAL= 334.4

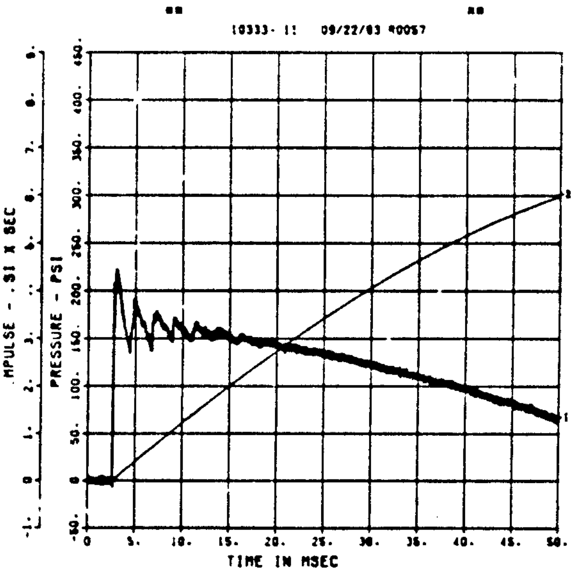

FEMA MULTI-HIT
IF-1
200000. HZ CAL= 355.1

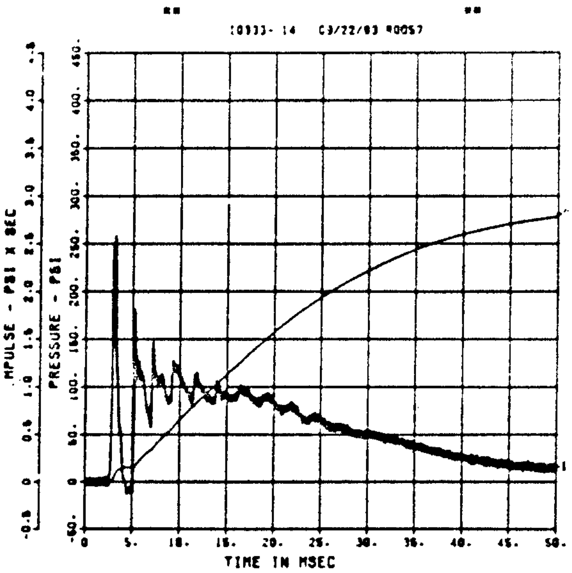

FEMA MULTI-HIT
IF-2
200000. HZ CAL= 335.9

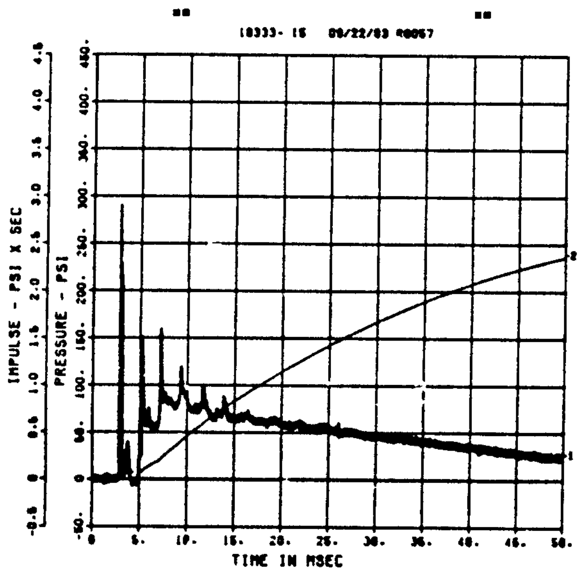

FEMA MULTI-HIT
IF-3
200000. HZ CAL= 348.9

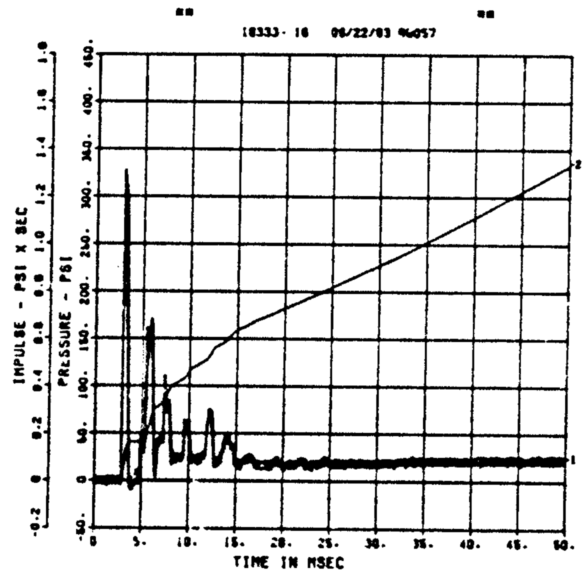

FEMA MULTI-HIT
IF-4
200000. HZ CAL= 342.1

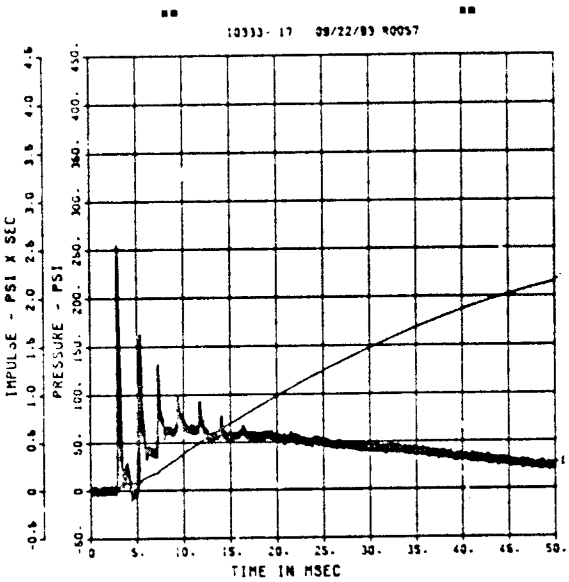

FEMA MULTI-HIT
IF-5
200000. HZ CAL= 345.2

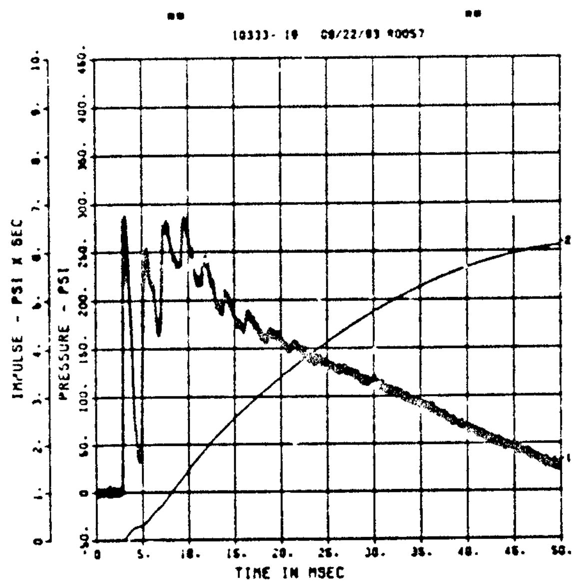

FEMA MULTI-HIT
IF-7
200000. HZ CAL= 523.8

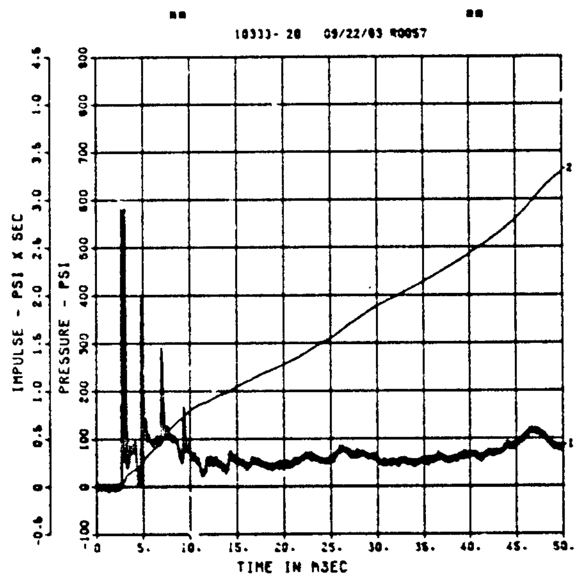

FEMA MULTI-HIT
IF-9
200000. HZ CAL= 465.2

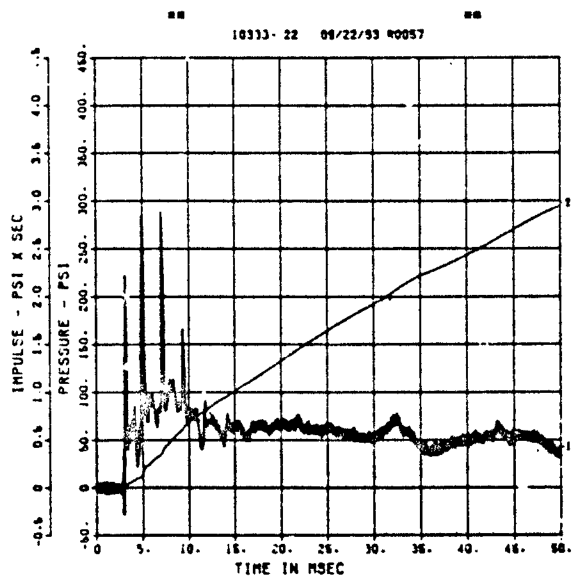

** PEAK VALUE IS 11 % OVER CALIBRATION **

FEMA MULTI-HIT
IF-10
200000. HZ CAL= 475.4

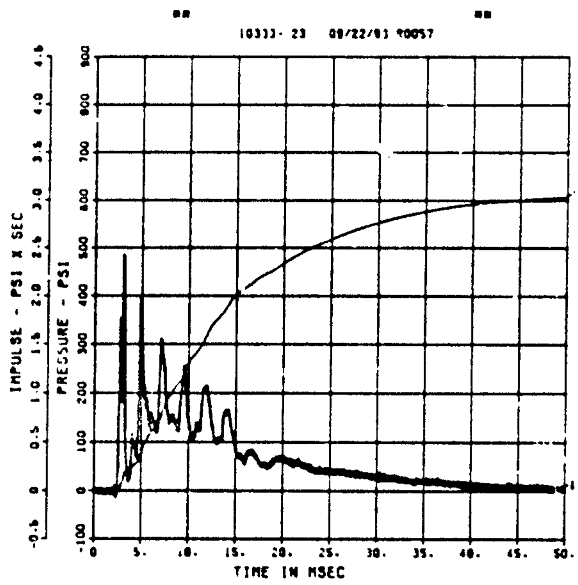

FEMA ELEM TEST D-8
BP-2
200000. HZ CAL= 1011.

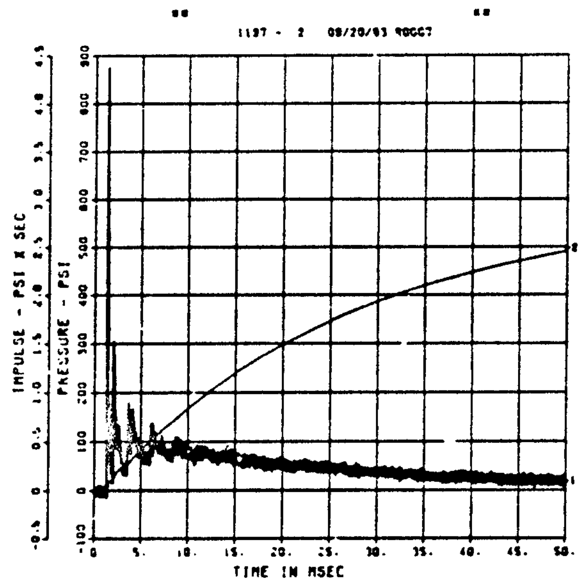

FEMA ELEM TEST D-8
BP-3
200000. HZ CAL= 1395.

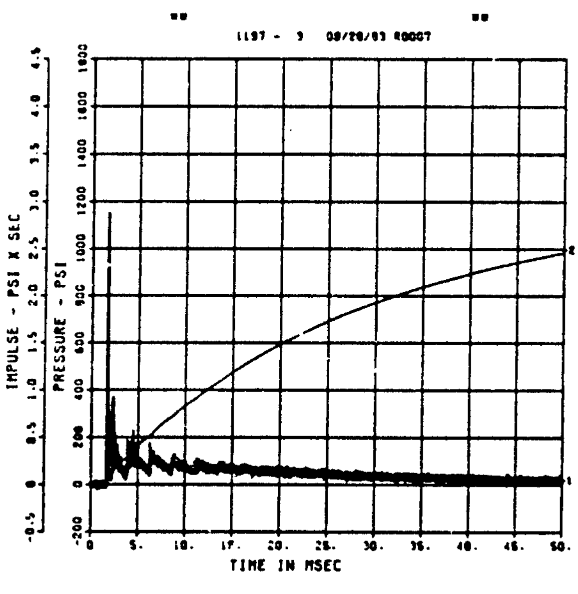

FEMA ELEM TEST D-8
BP-4
200000. HZ CAL= 1450.

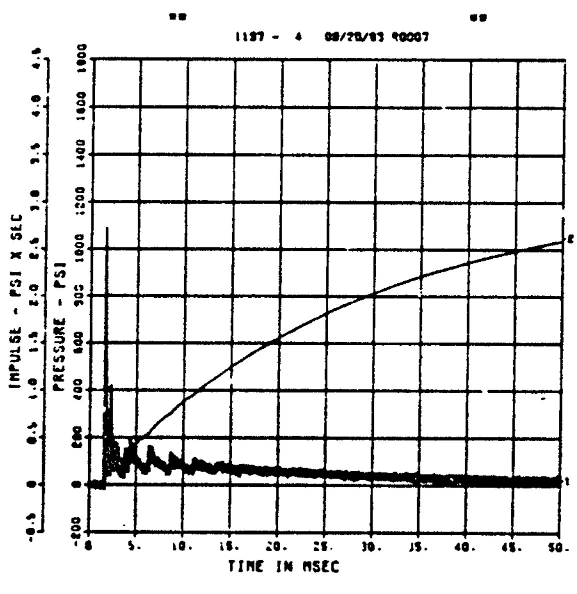

FEMA ELEM TEST D-8
BP-6
200000. HZ CAL= 1079.

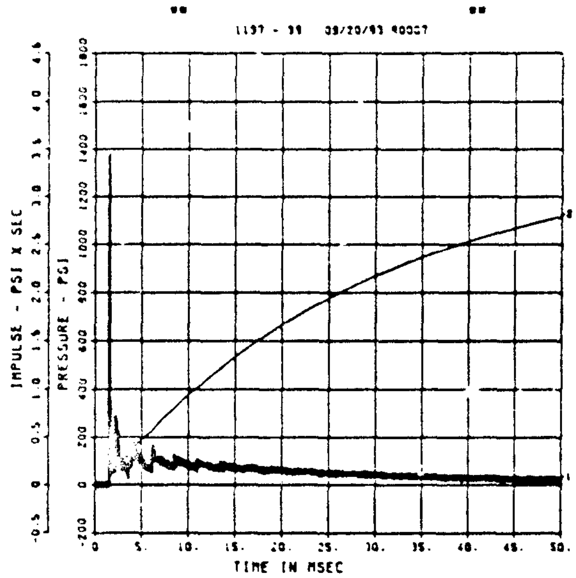

** PEAK VALUE IS 28 % OVER CALIBRATION **

FEMA ELEM TEST D-8
SE-1
200000. HZ CAL= 356.0

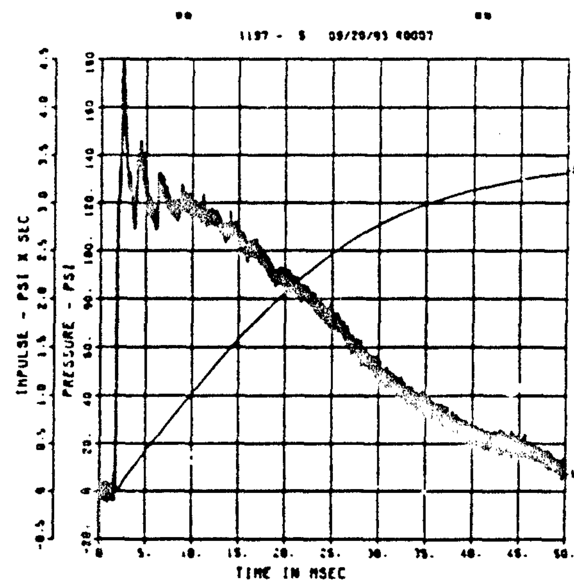

FEMA ELEM TEST D-8
SE-2
200000. HZ CAL= 204.7

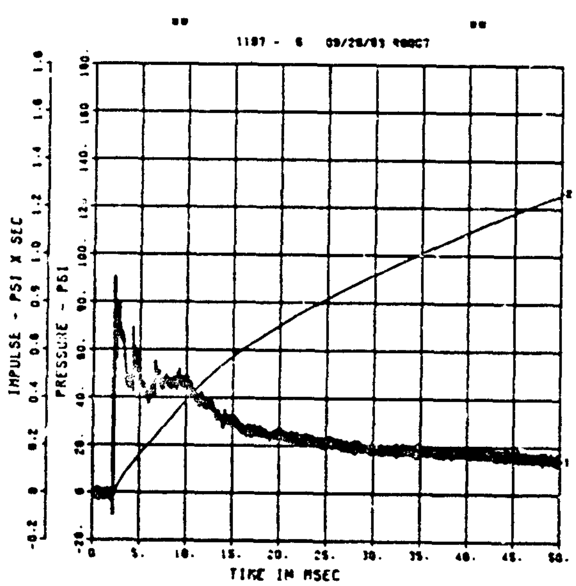

FEMA ELEM TEST D-8
SE-3
200000. HZ CAL= 368.7

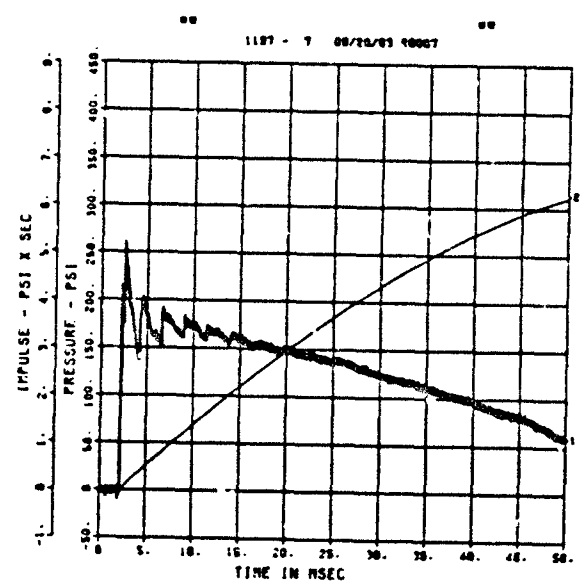

FEMA ELEM TEST D-8
SE-5
200000. HZ CAL= 132.8

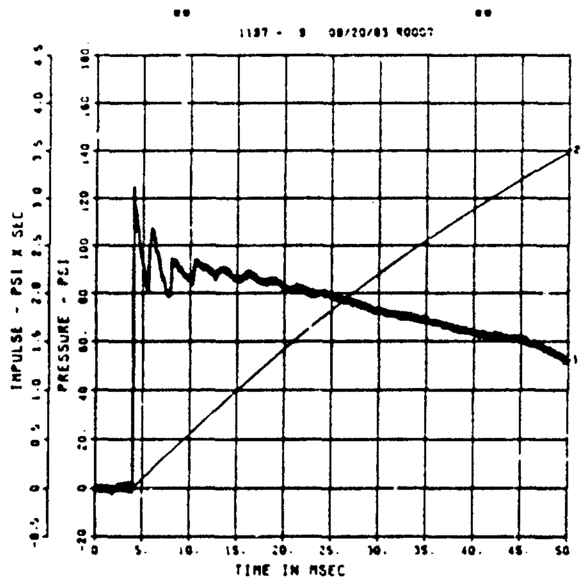

FEMA ELEM TEST D-8
SE-7
200000. HZ CAL= 179.8

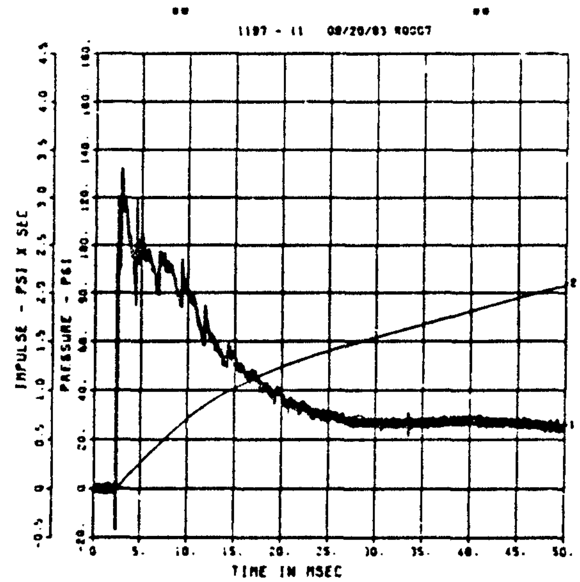

FEMA ELEM TEST D-8
AFF-1
200000. HZ CAL= 813.5

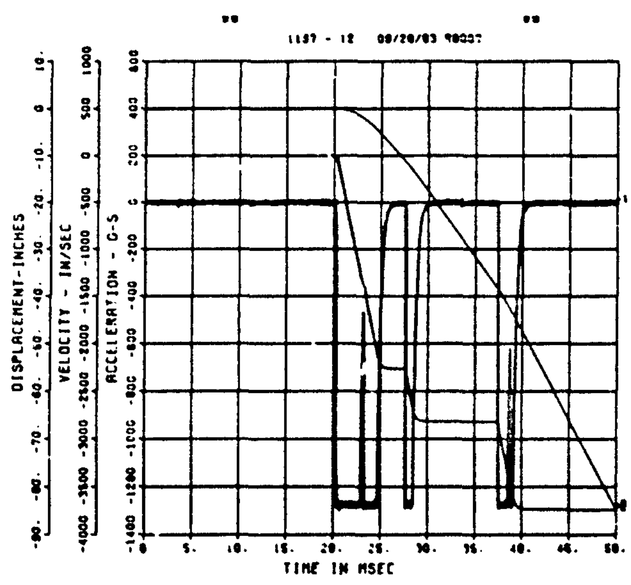

** PEAK VALUE IS 59 % OVER CALIBRATION **

FEMA ELEM TEST D-8
A-1
200000. HZ CAL= 2504.

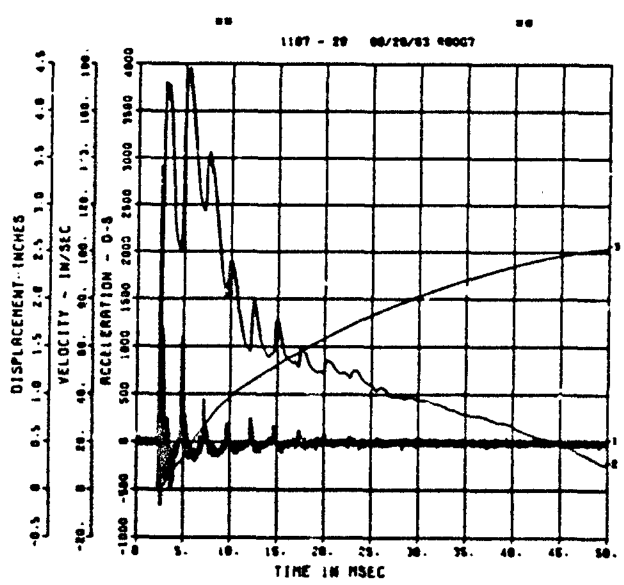

** PEAK VALUE IS 17 % OVER CALIBRATION **

FEMA ELEM TEST D-8
A-2
200000. HZ CAL= 549.0

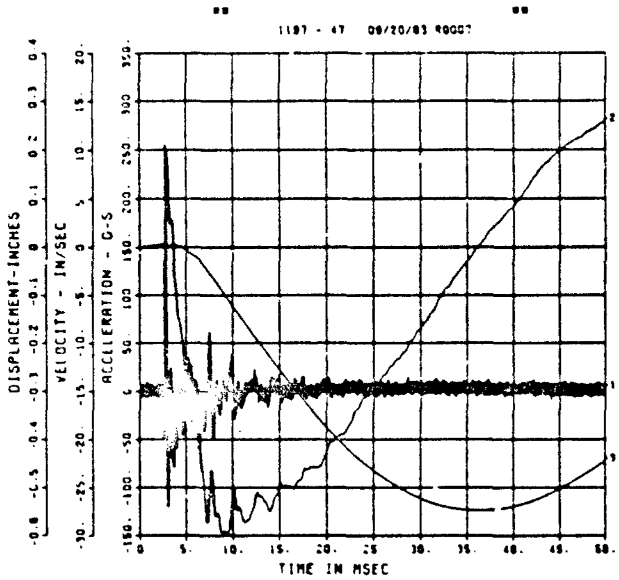

FEMA ELEM TEST D-8
IF-1
200000. HZ CAL= 461.8

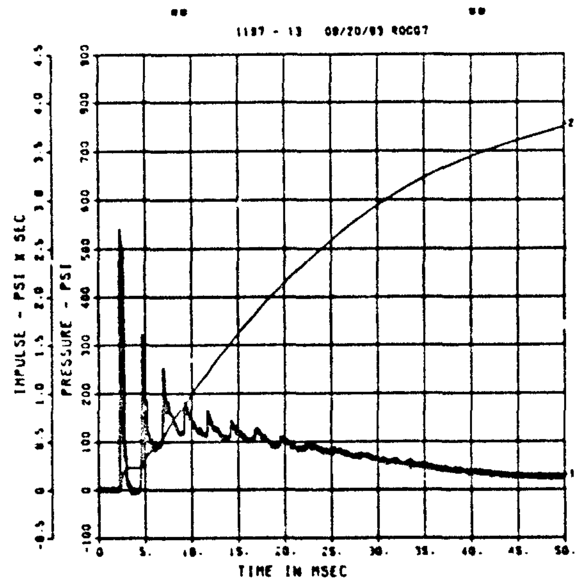

** PEAK VALUE IS 17 % OVER CALIBRATION **

FEMA ELEM TEST D-8
IF-2
200000. HZ CAL= 465.2

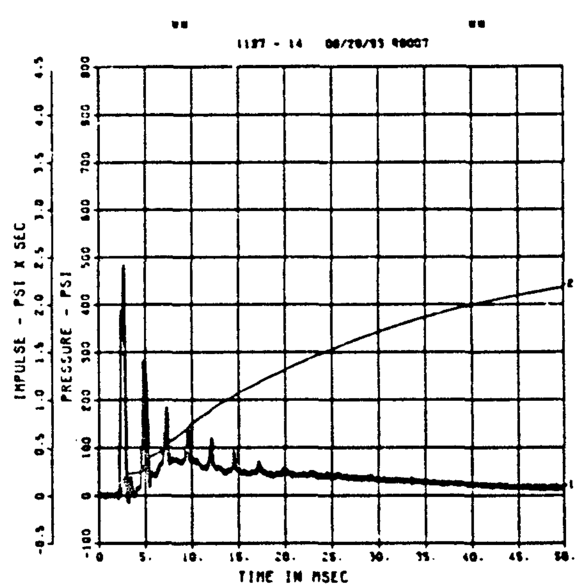

** PEAK VALUE IS 4 % OVER CALIBRATION **

FEMA ELEM TEST D-8
IF-5
200000. HZ CAL= 444.6

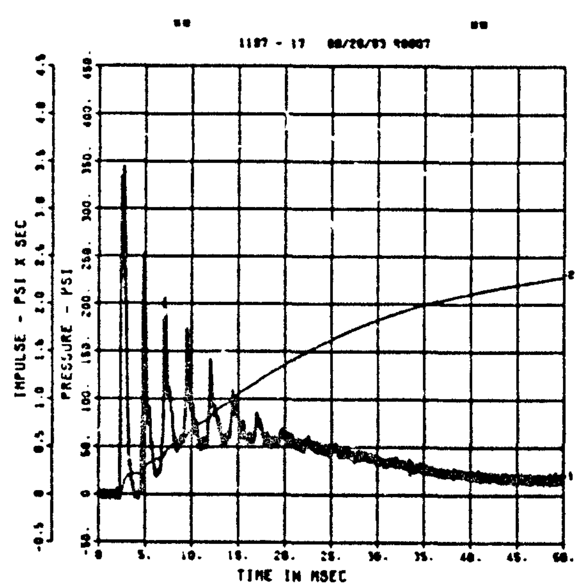

FEMA ELEM TEST D-8
IF-6
200000. HZ CAL= 254.9

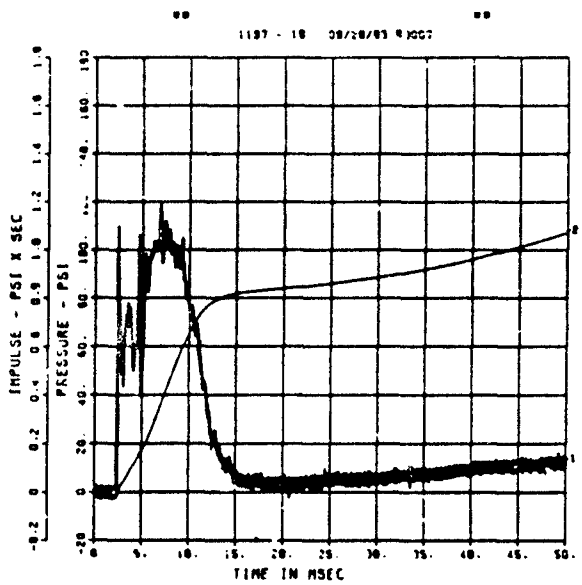

FEMA ELEM TEST D-8
IF-7
200000. HZ CAL= 246.7

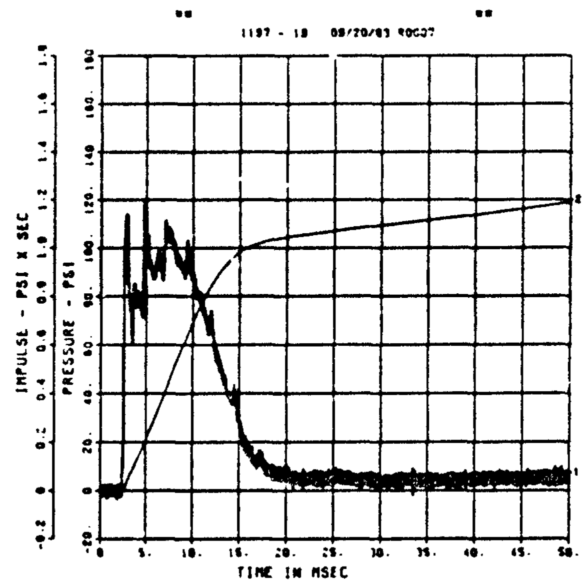

FEMA ELEM TEST D-8
IF-8
200000. HZ CAL= 166.8
LP4/0 70% CUTOFF= 9000. HZ

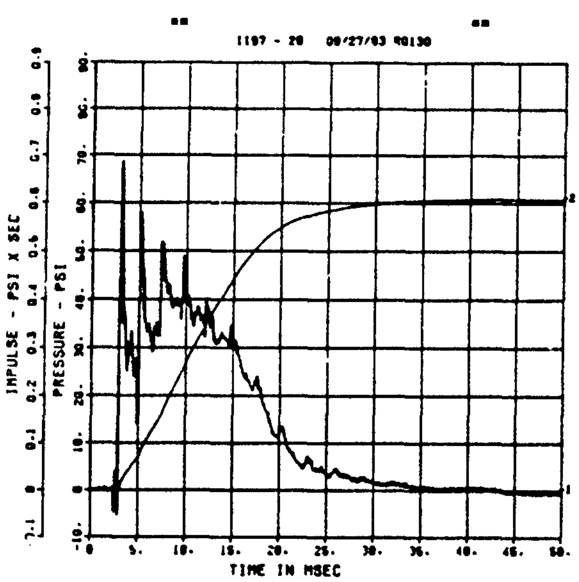

FEMA ELEM TEST D-8
IF-9
200000. HZ CAL= 174.3
LP4/0 70% CUTOFF= 9000. HZ

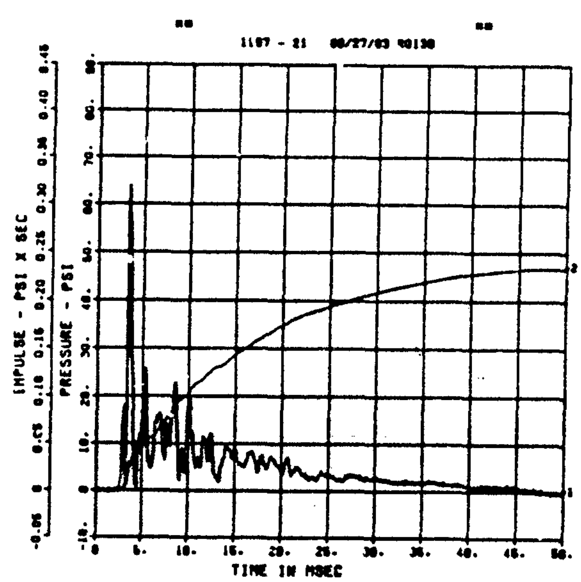

FEMA ELEM TEST D-8
IF-10
200000. HZ CAL= 125.3

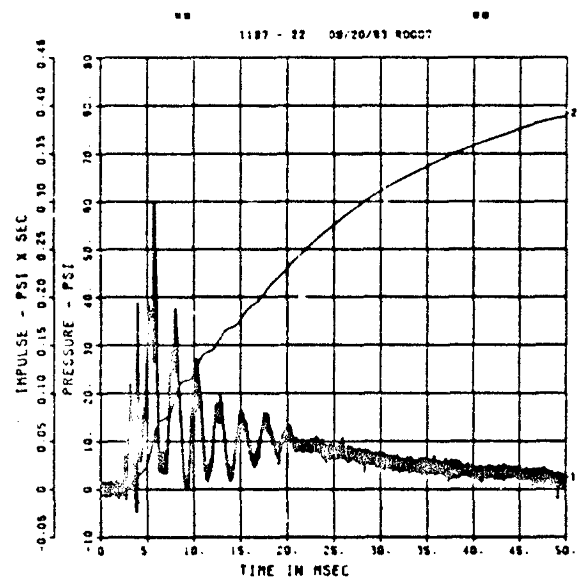

FEMA ELEM TEST D-8
IF-11
200000. HZ CAL= 125.6

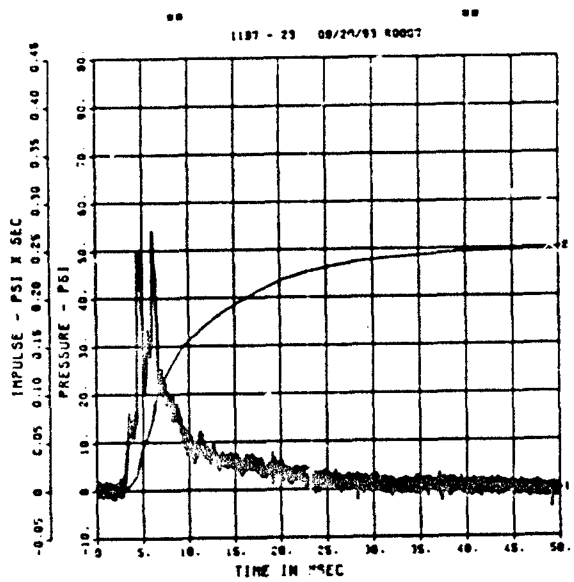

FEMA ELEM TEST D-8
IF-12
50000. HZ CAL= 166.9
LP4/4 70% CUTOFF= 2250. HZ

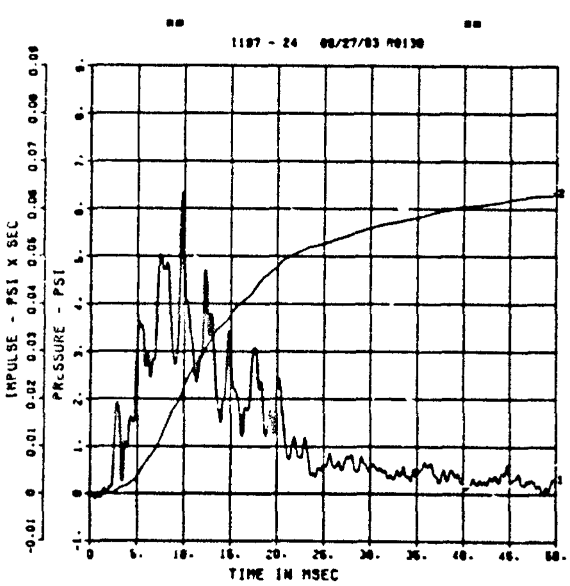

** PEAK VALUE IS 88 % UNDER CALIBRATION **

FEMA ELEM TEST D-8
IF-13
50000. HZ CAL= 126.8
LP4/4 70% CUTOFF= 2250. HZ

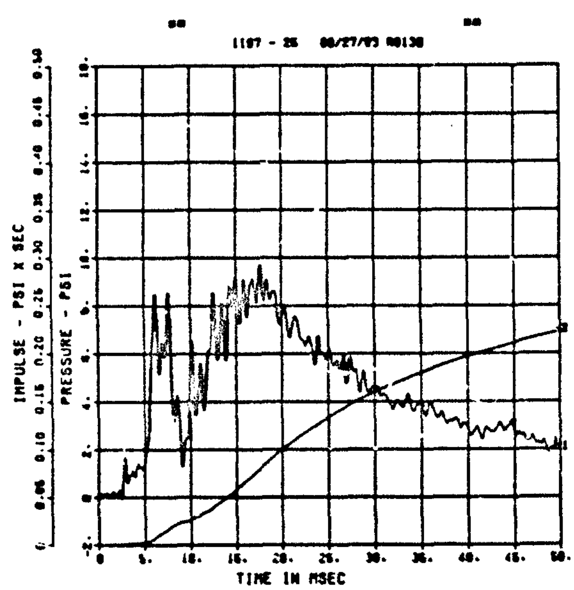

** PEAK VALUE IS 82 % UNDER CALIBRATION **

FEMA ELEM TEST D-8
IF-14
50000. HZ CAL= 85.20
LP4/4 70% CUTOFF= 2250. HZ

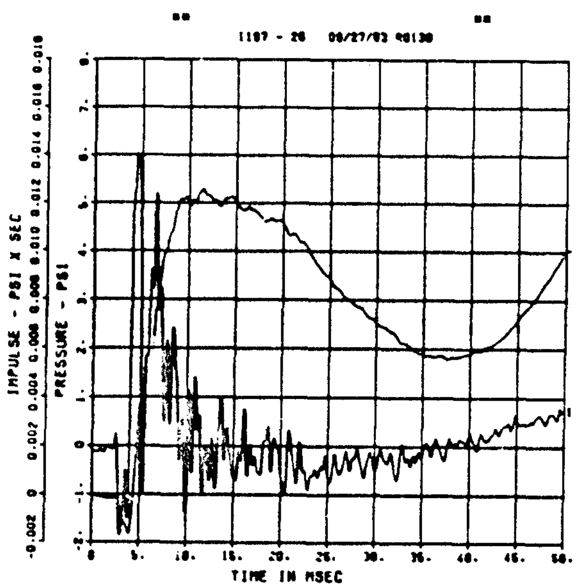

** PEAK VALUE IS 93 % UNDER CALIBRATION **

FEMA ELEM TEST D-8
IF-15
50000. HZ CAL= 83.70
LP4/4 70% CUTOFF= 2250. HZ

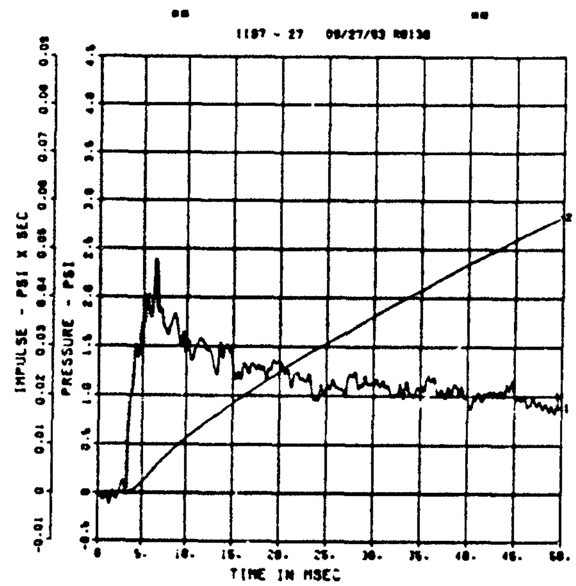

** PEAK VALUE IS 97 % UNDER CALIBRATION **

FEMA ELEM TEST D-8
IF-16
200000. HZ CAL= 355.0

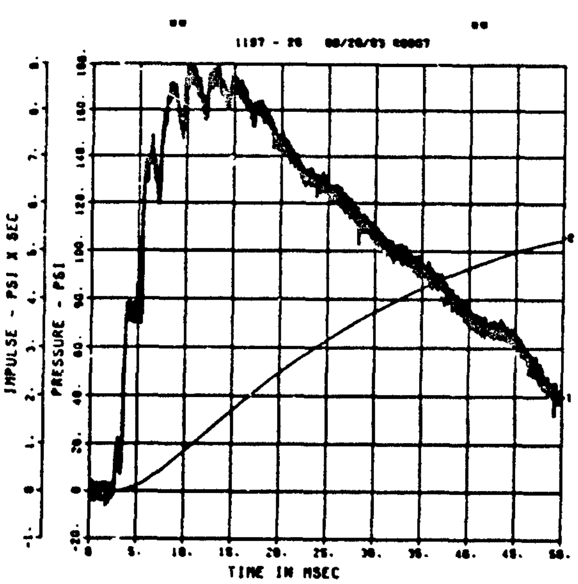

FEMA ELEM TEST D-8
EO-1
200000. HZ CAL= 39162.
LP4/0 70% CUTOFF= 9000. HZ

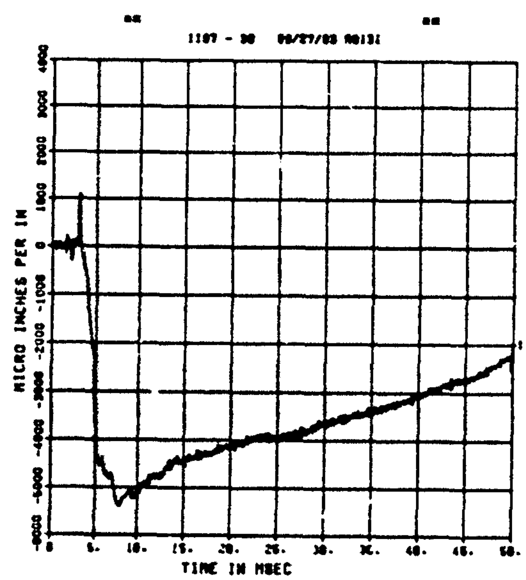

** PEAK VALUE IS 96 % UNDER CALIBRATION **

FEMA ELEM TEST D-8
EI-1
200000. HZ CAL= 20205.
LP4/0 70% CUTOFF= 9000. HZ

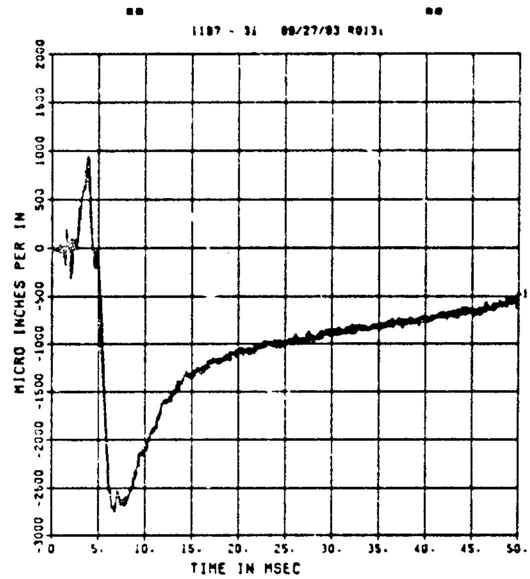

** PEAK VALUE IS 98 % UNDER CALIBRATION **

FEMA ELEM TEST D-8
EO-2
200000. HZ CAL= 39162.
LP3/0 70% CUTOFF= 11000. HZ

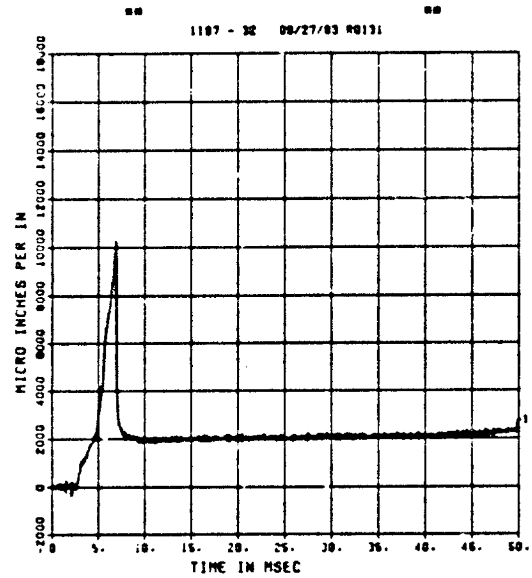

FEMA ELEM TEST D-8
EI-2
200000. HZ CAL= 20205.
LP4/0 70% CUTOFF= 9000. HZ

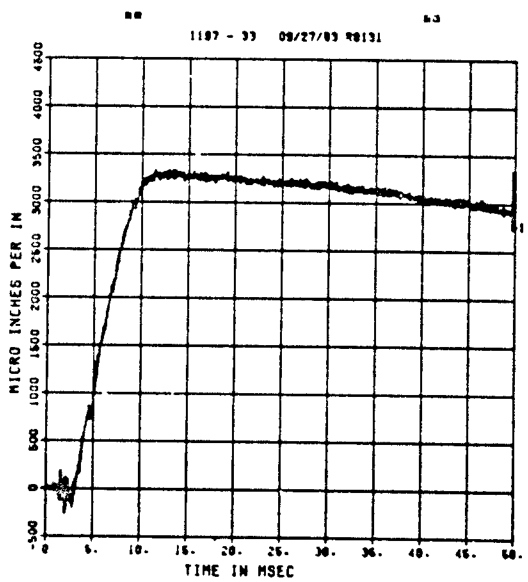

** PEAK VALUE IS 83 % UNDER CALIBRATION **

FEMA ELEM TEST D-8
EO-3
200000. HZ CAL= 1C?76.
LP3/0 70% CUTOFF= 11000. HZ

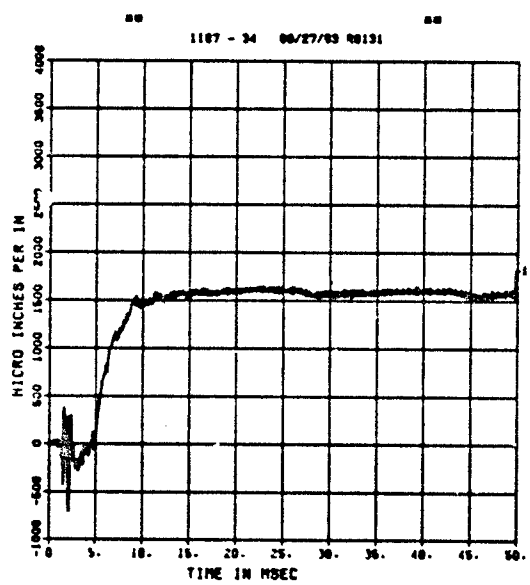

** PEAK VALUE IS 92 % UNDER CALIBRATION **

FEMA ELEM TEST D-8
EI-3
200000. HZ CAL= 10276.
LP3/0 70% CUTOFF= 11000. HZ

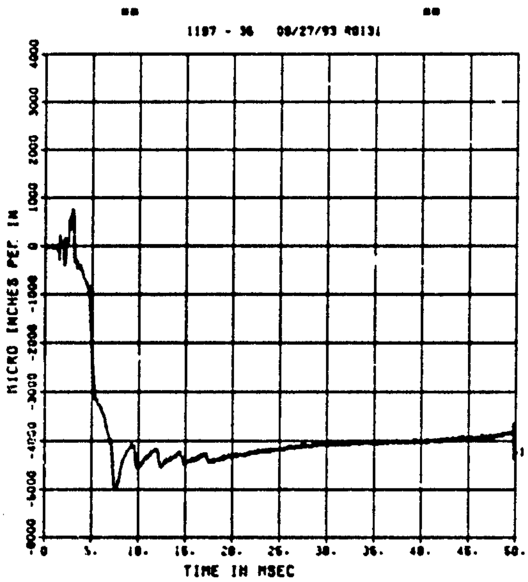

FEMA ELEM TEST D-8
EO-4
50000. HZ CAL= 20205.
LP4/4 70% CUTOFF= 2250. HZ

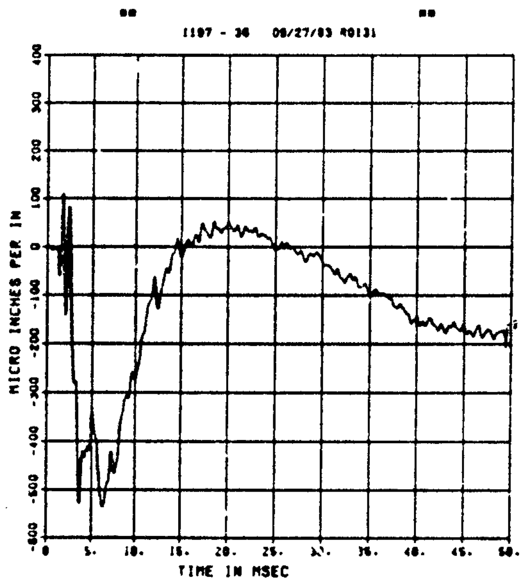

** PEAK VALUE IS 97 % UNDER CALIBRATION **

FEMA ELEM TEST D-8
EI-4
50000. HZ CAL= 39162.
LP4/4 70% CUTOFF= 2250. HZ

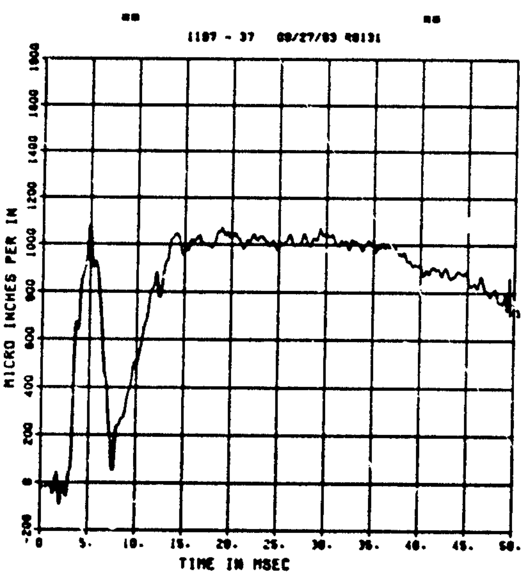

** PEAK VALUE IS 97 % UNDER CALIBRATION **

FEMA ELEM TEST D-8
EI-5
50000. HZ CAL= 10276.
LP4/4 70% CUTOFF= 2250. HZ

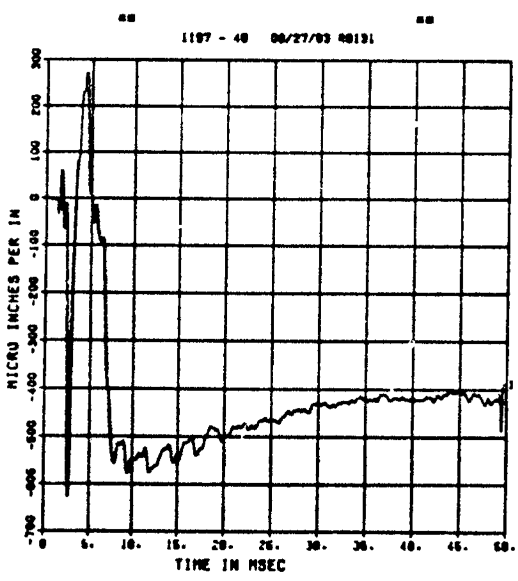

** PEAK VALUE IS 94 % UNDER CALIBRATION **

FEMA ELEM TEST D-8
EI-7
200000. HZ CAL= 6692.

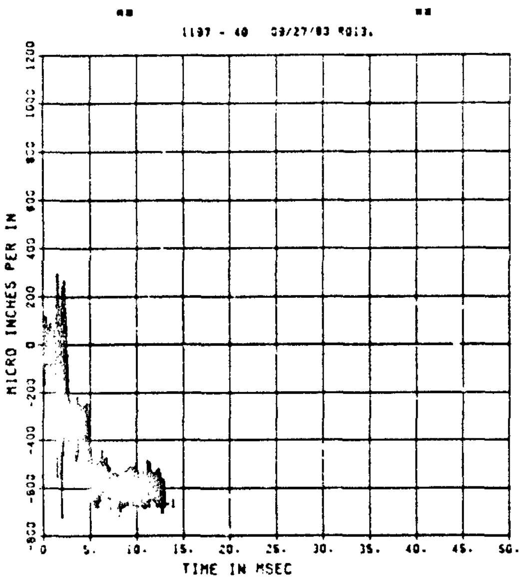

** PEAK VALUE IS 89 % UNDER CALIBRATION **

FEMA ELEM TEST D-8
EI-9
200000. HZ CAL= 10276.
LP4/0 70% CUTOFF= 9000. HZ

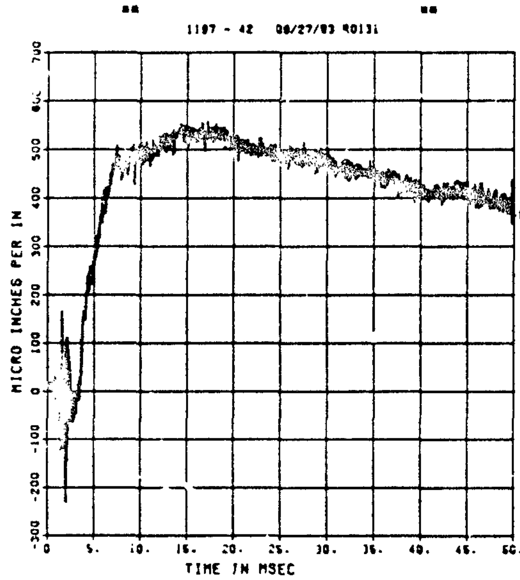

** PEAK VALUE IS 96 % UNDER CALIBRATION **

FEMA ELEM TEST D-8
EO-10
200000. HZ CAL= 6692.
LP4/0 70% CUTOFF= 9000. HZ

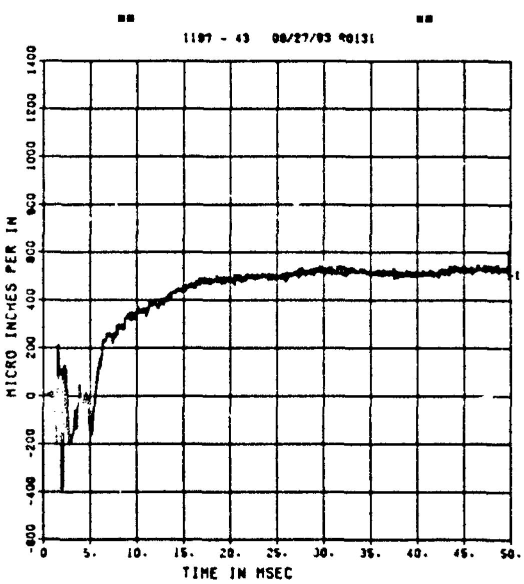

** PEAK VALUE IS 81 % UNDER CALIBRATION **

FEMA ELEM TEST D-8
EI-10
200000. HZ CAL= 6692.
LP4/0 70% CUTOFF= 9000. HZ

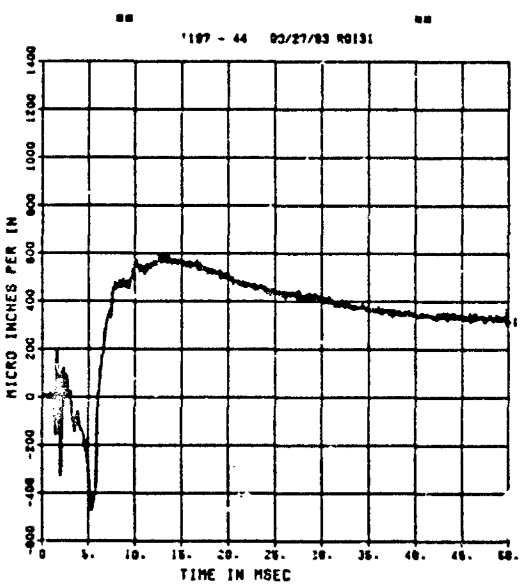

** PEAK VALUE IS 81 % UNDER CALIBRATION **

FEMA ELEM TEST D-8
EO-11
200000. HZ CAL= 10276.
LP4/0 70% CUTOFF= 9000. HZ

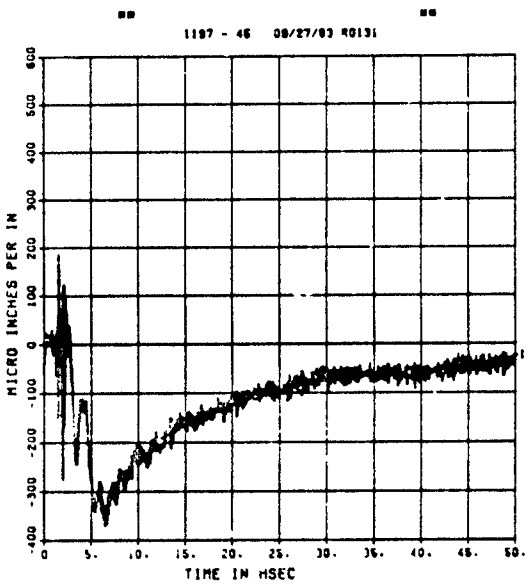

** PEAK VALUE IS 98 % UNDER CALIBRATION **

FEMA ELEM TEST D-8
EI-11
50000. HZ CAL= 39162.
LP4/4 70% CUTOFF= 2250. HZ

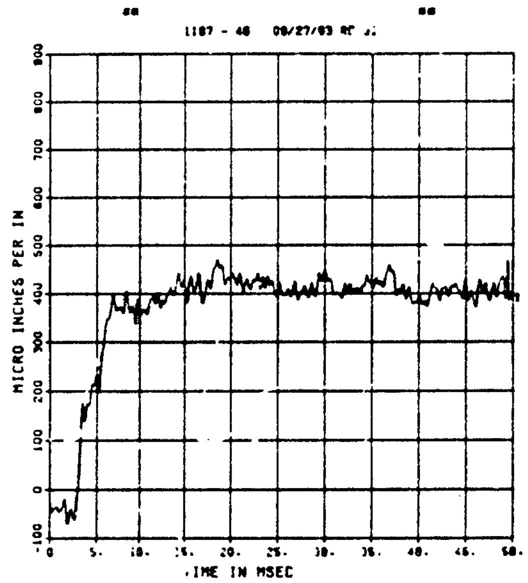

FEMA ELEM TEST S-1
SE-1

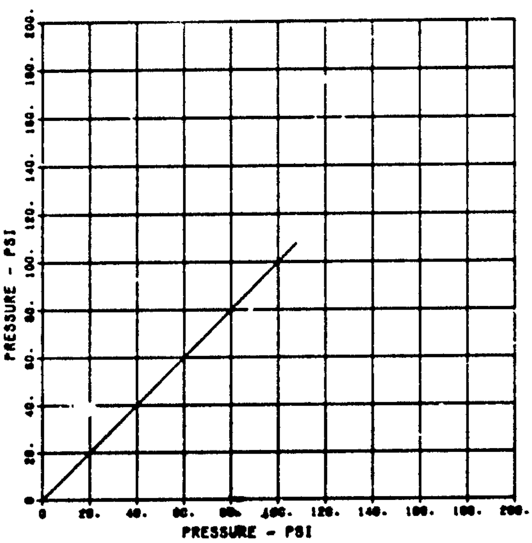

FEMA ELEM TEST S-1
SE-2

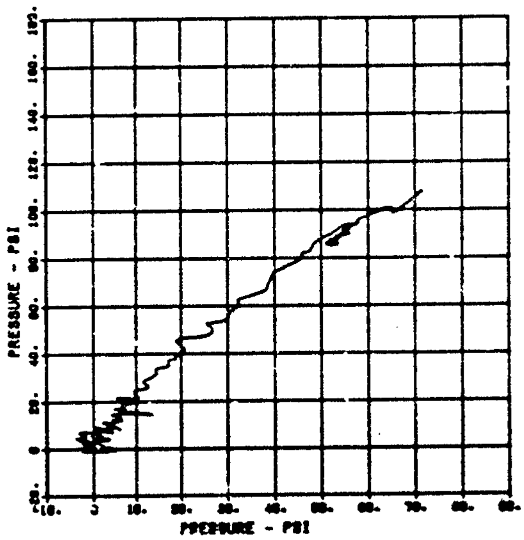

FEMA ELEM TEST S-1
SE-3

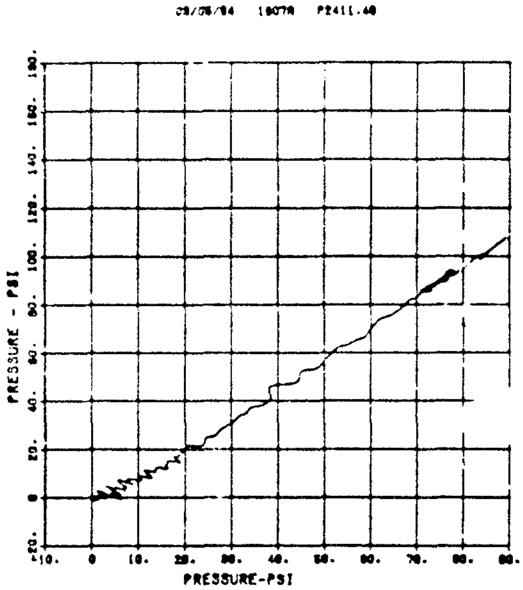

FEMA ELEM TEST S-1
SE-4

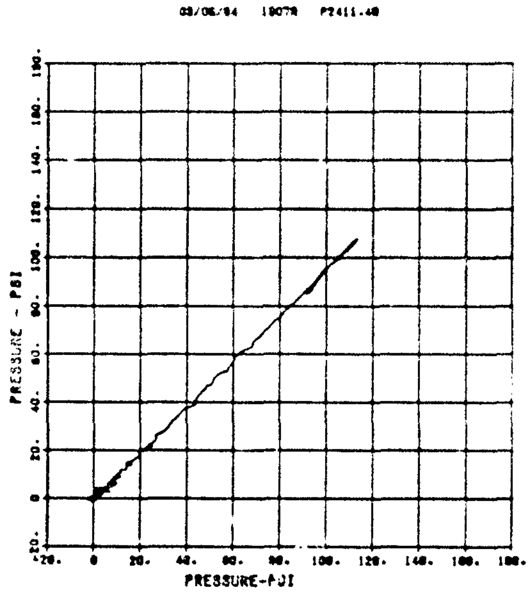

FEMA ELEM TEST S-1
SE-5

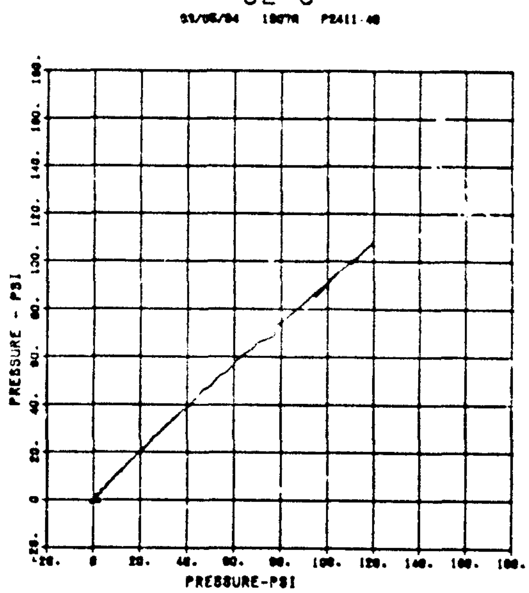

FEMA ELEM TEST S-1
SE-6

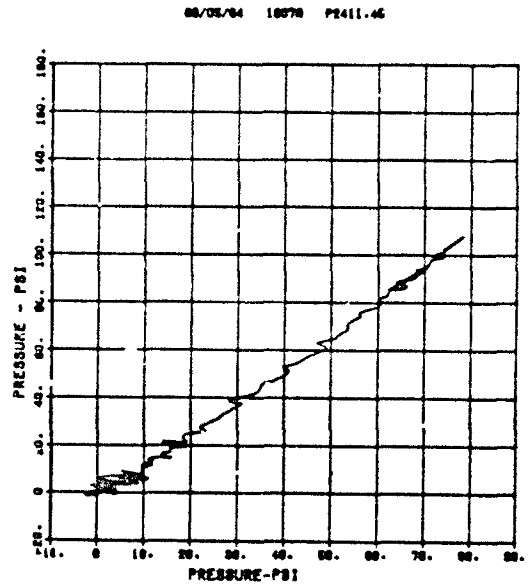

FEMA ELEM TEST S-1
SE-7
08/06/84 1007A P2411.40

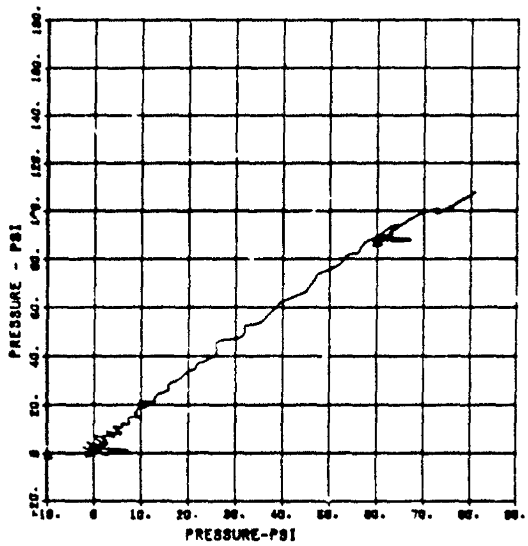

FEMA ELEM TEST S-1
D-1
04/04/84 1014C P2411.40

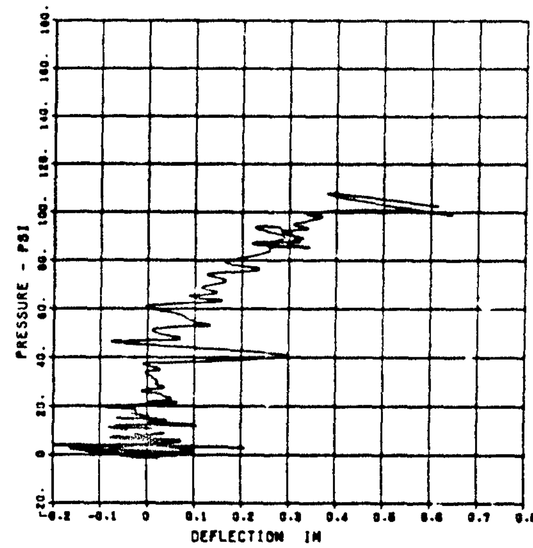

FEMA ELEM TEST S-1
D-2
04/04/84 1014C P2411.40

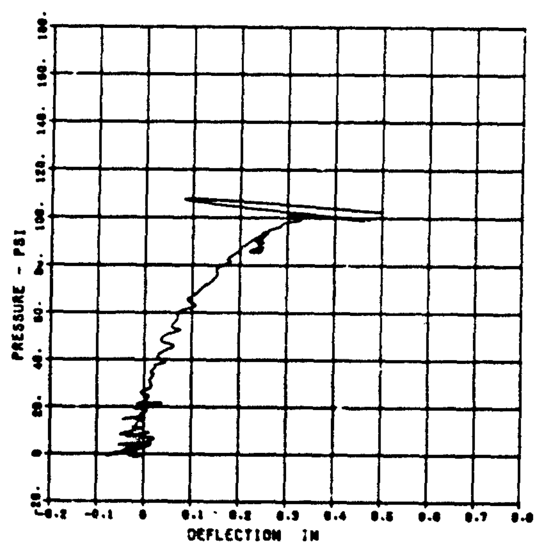

FEMA ELEM TEST S-1
IF-1

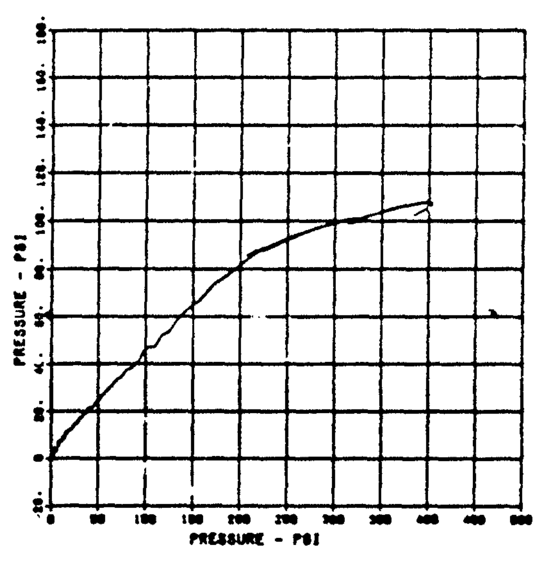

FEMA ELEM TEST S-1
IF-2

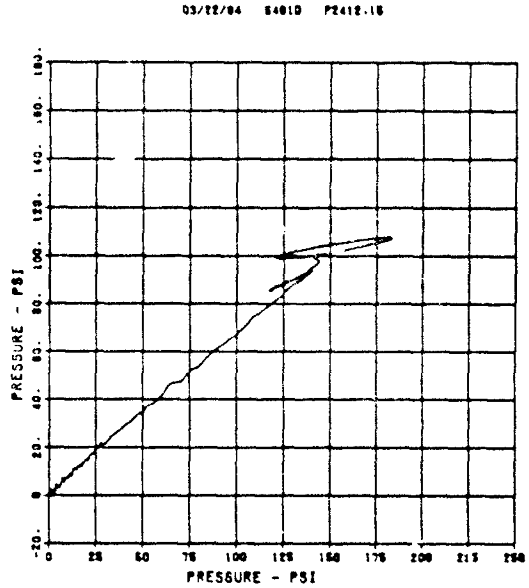

FEMA ELEM TEST S-1
IF-3

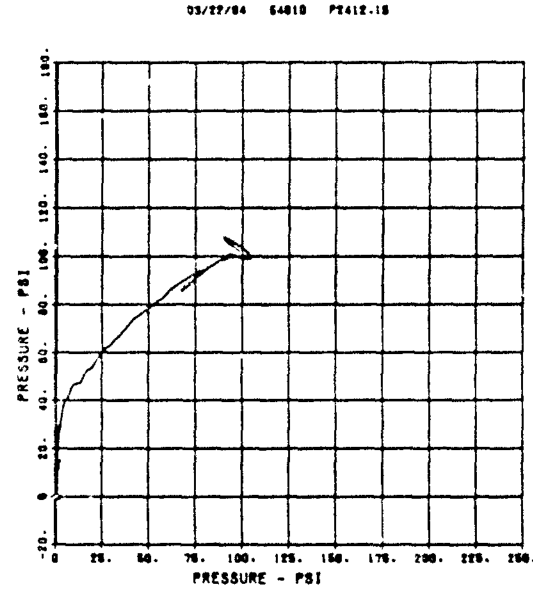

FEMA ELEM TEST S-1
IF-6

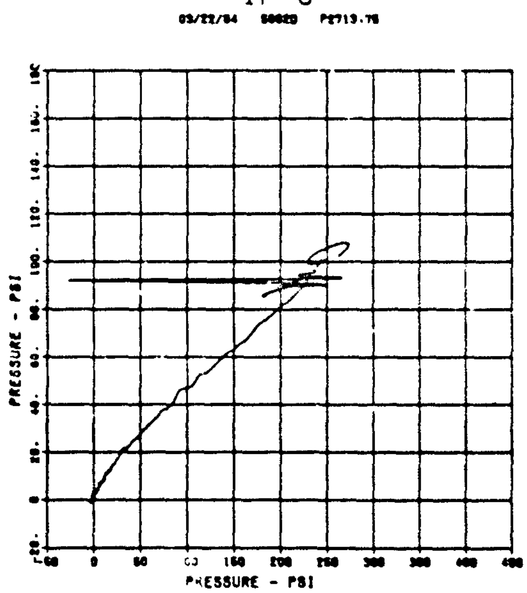

FEMA ELEM TEST S-1
IF-7

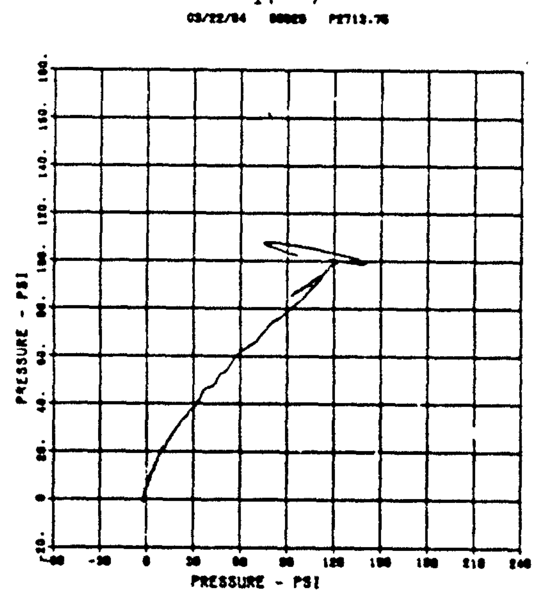

FEMA ELEM TEST S-1
IF-8

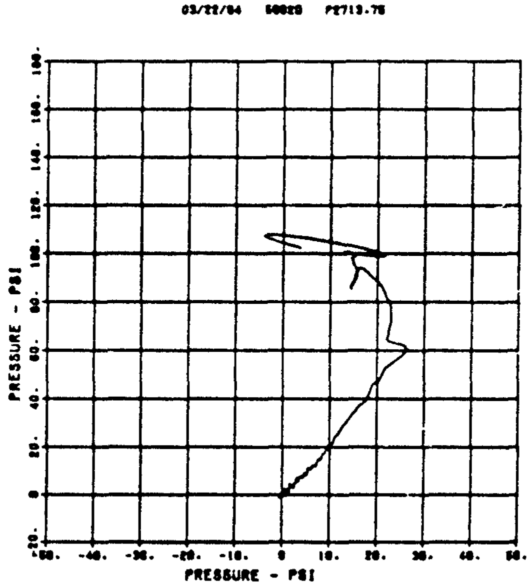

FEMA ELEM TEST S-1
IF-10

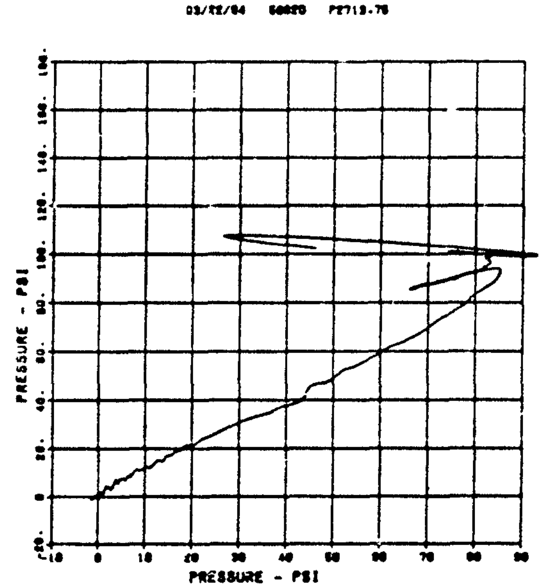

FEMA ELEM TEST S-1
IF-11

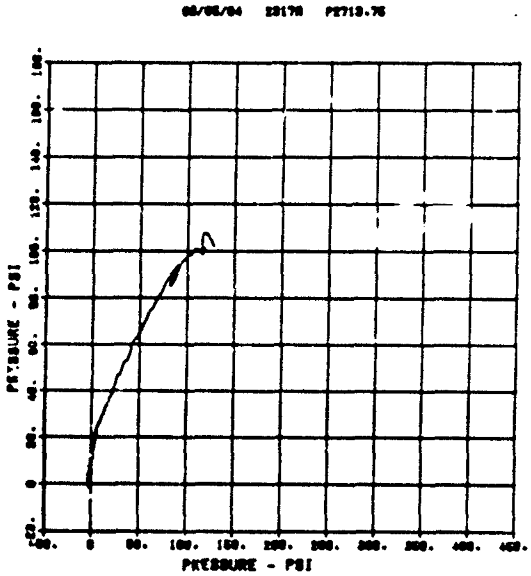

FEMA ELEM TEST S-1
IF-12

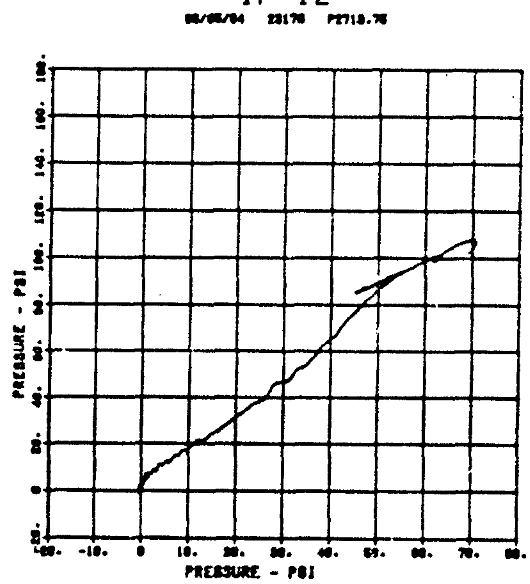

FEMA ELEM TEST S-1
IF - 13

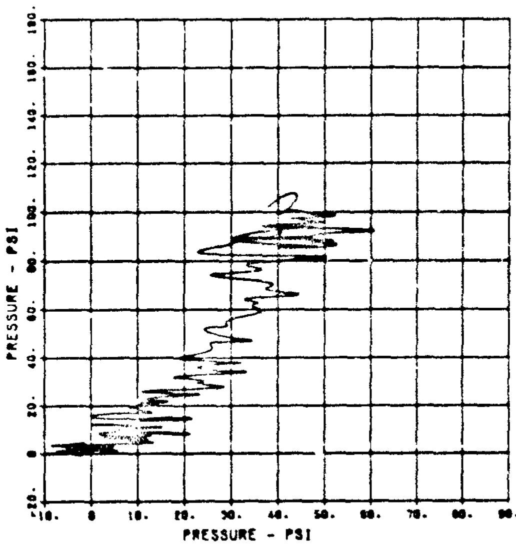

FEMA ELEM TEST S-1
IF-14

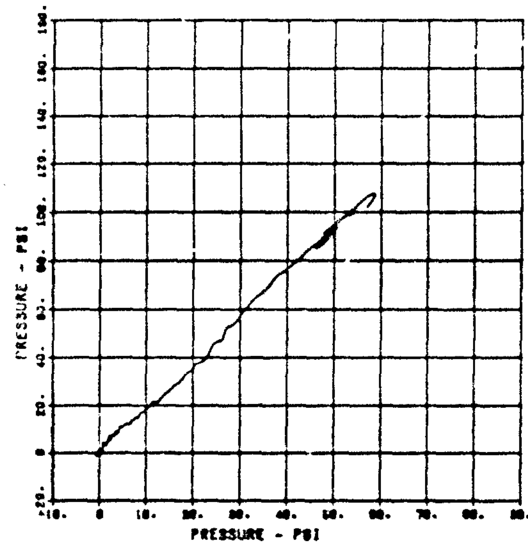

FEMA ELEM TEST S-1
IF-15

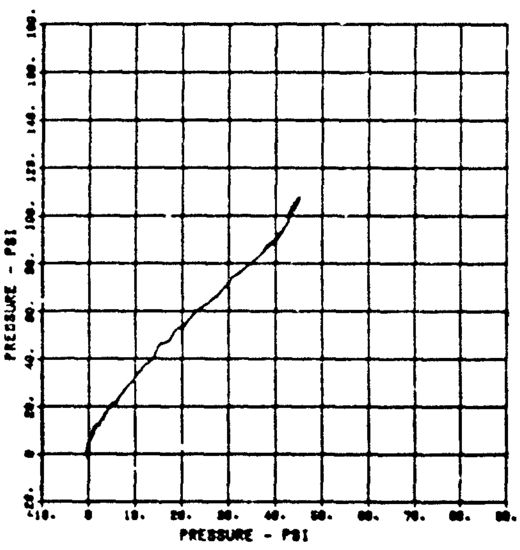

FEMA ELEM TEST S-1
IF-16

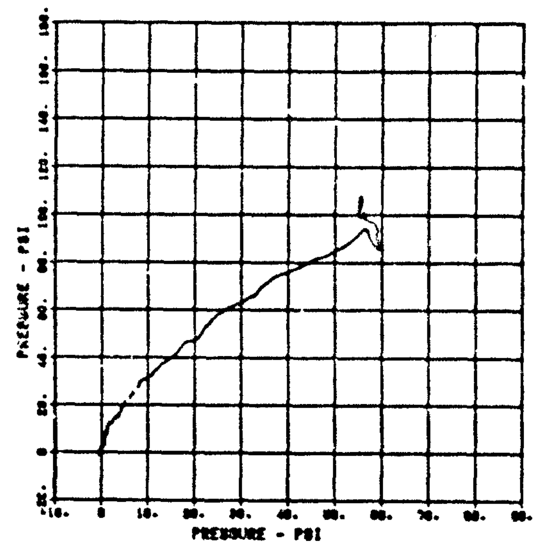

FEMA ELEm TEST S-1
IF-17

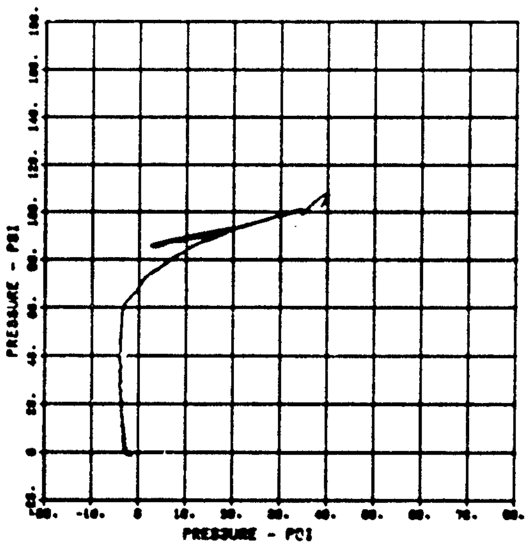

FEMA ELEM TEST S-1
IF-18

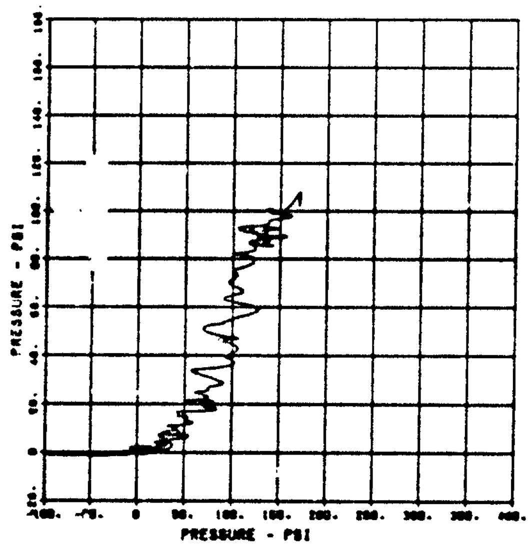

FEMA ELEM TEST S-1
IF-19

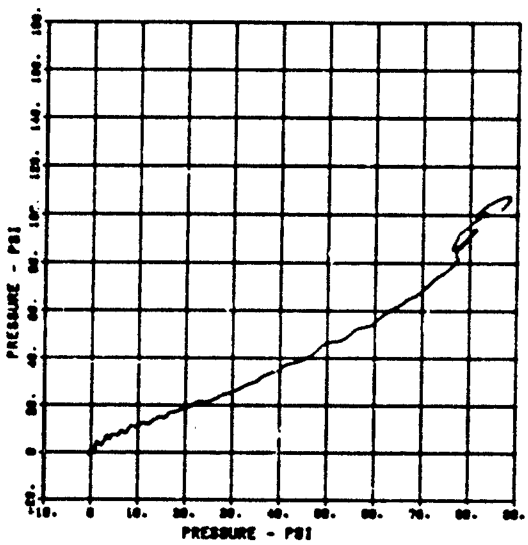

FEMA ELEM TEST S-1
IF-20

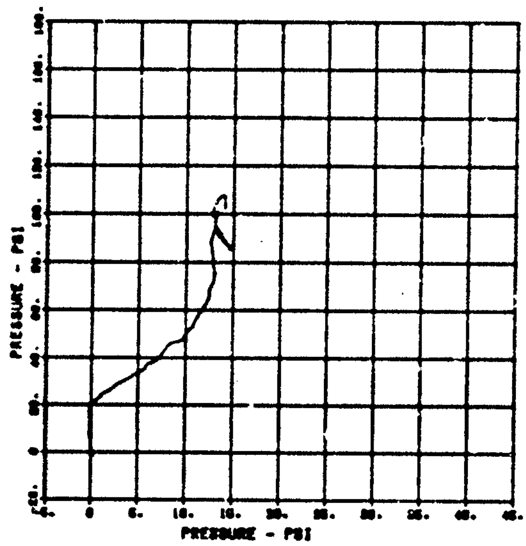

FEMA ELEM TEST S-1
IF-21

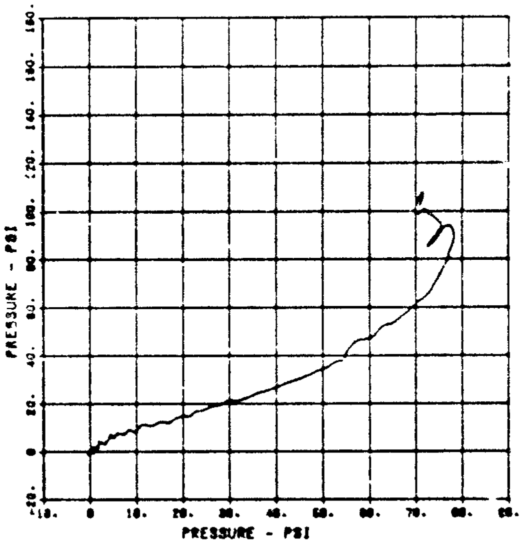

FEMA ELEM TEST S-1
IF-22

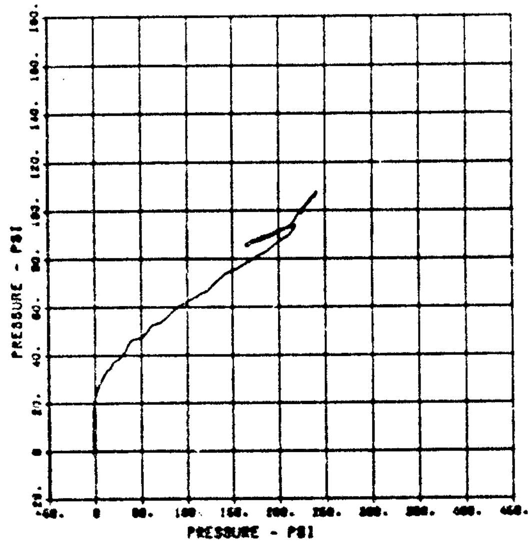

FEMA ELEM TEST S-1
LC-1

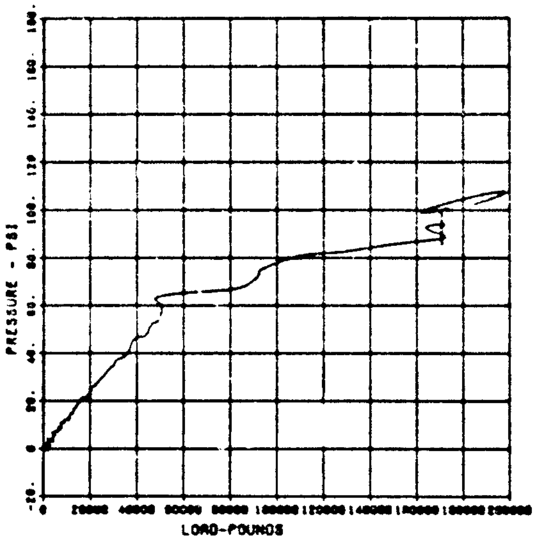

FEMA ELEM TEST S-1
LC-2

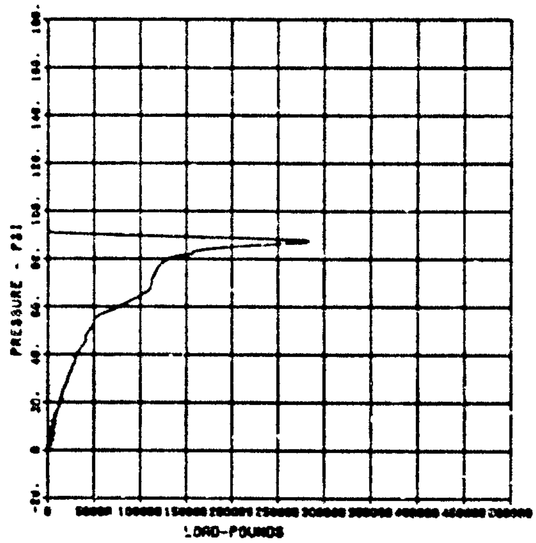

FEMA ELEM TEST S-1
EO-1

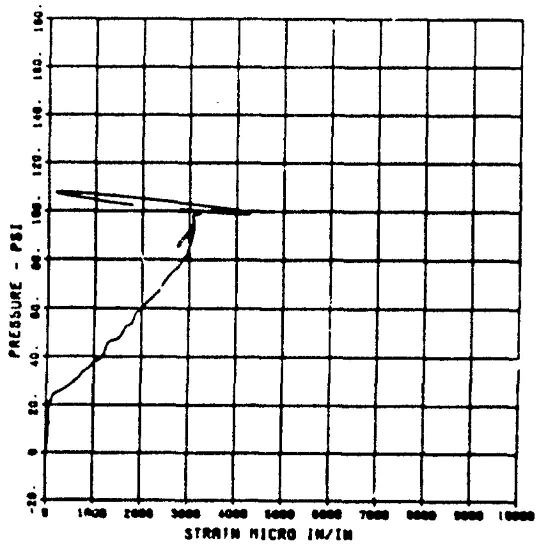

FEMA ELEM TEST S-1
EI-1

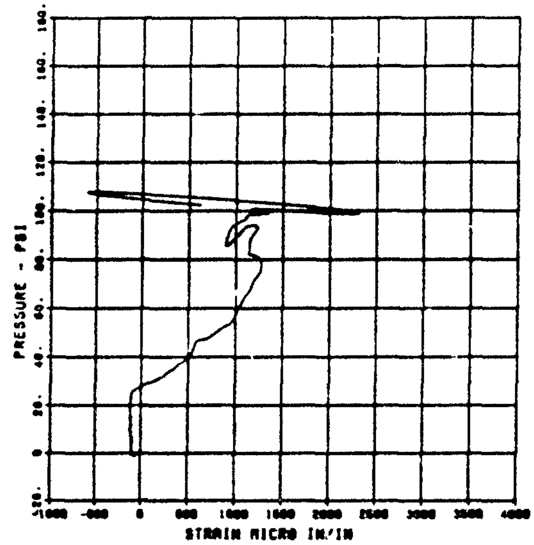

FEMA ELEM TEST S-1
EI-2

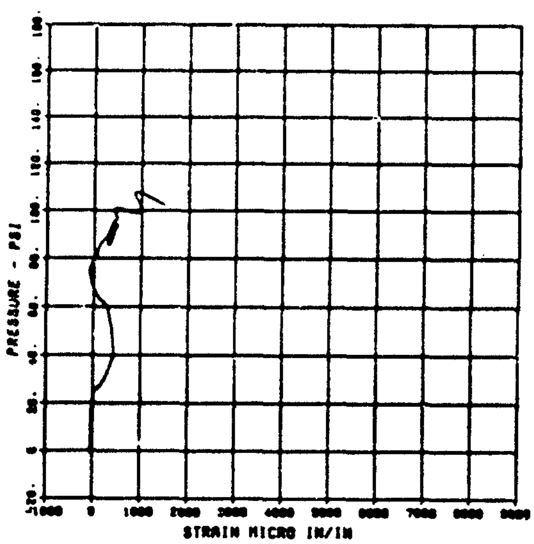

FEMA ELEM TEST S-1
EO-3

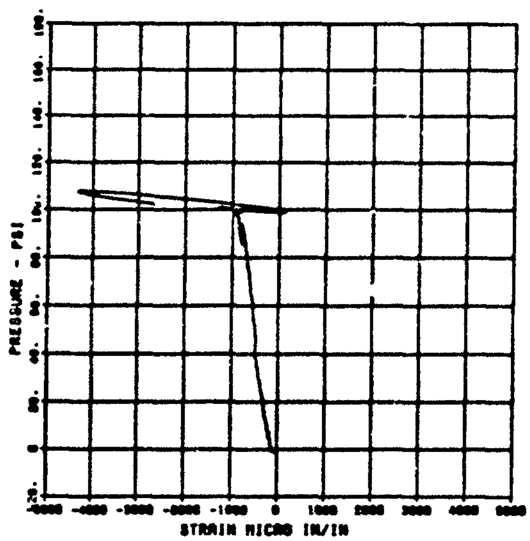

FEMA ELEM TEST S-1
EI-3
03/22/84 56770 P2412.00

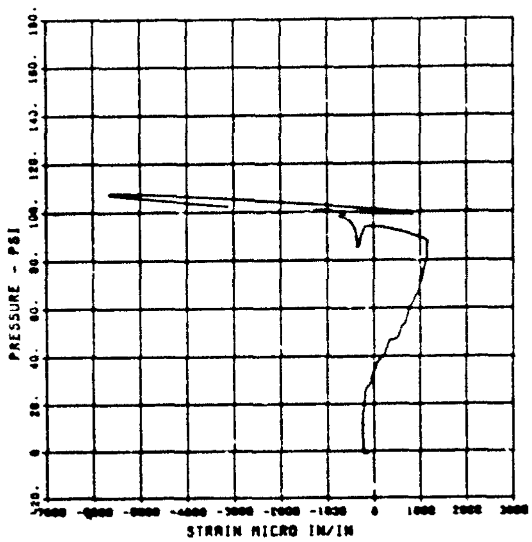

FEMA ELEM TEST S-1
EO-4
03/22/84 56770 P2412.00

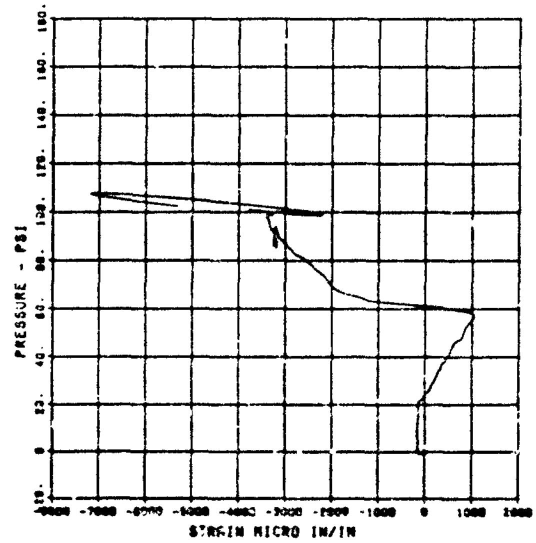

FEMA ELEM TEST S-1
EO-5
03/22/84 53000 P2411.40

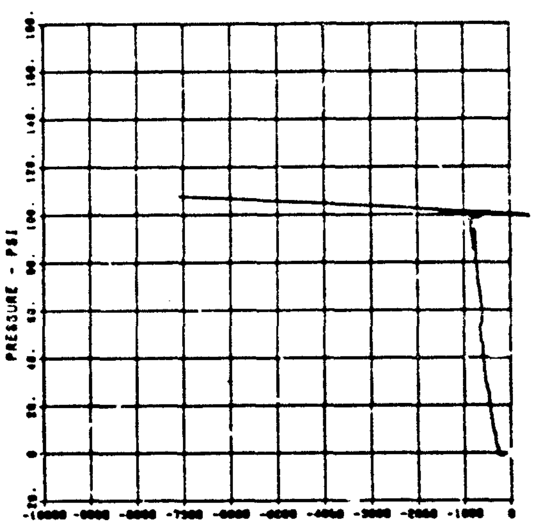

FEMA ELEM TEST S-1
EI-5

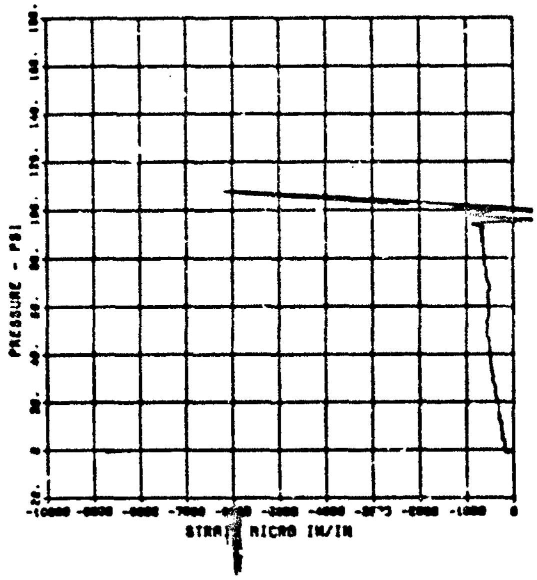

FEMA ELEM TEST S-1

EO-6

03/22/84 6422C P2713.41

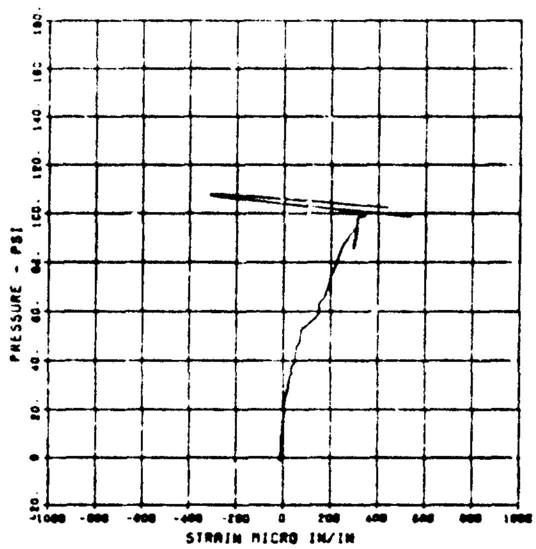

FEMA ELEM TEST S-1

EI-6

03/22/84 6422B P2713.41

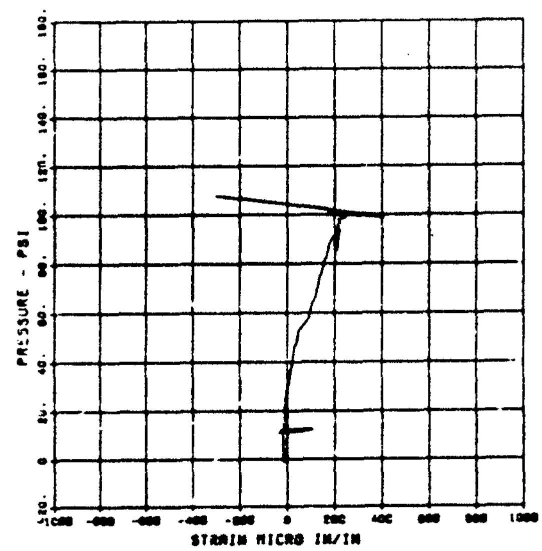

FEMA ELEM TEST S-1

EI - 7

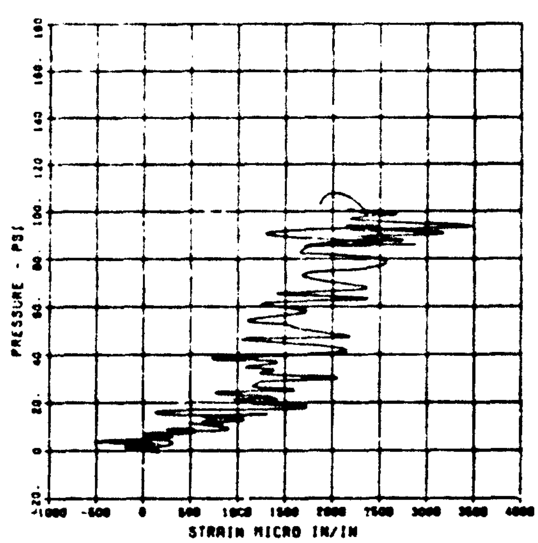

FEMA ELEM TEST S-1

EI-9

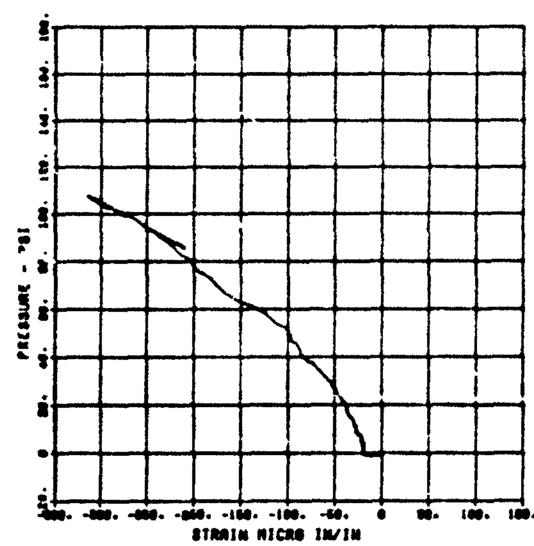

FEMA ELEM TEST S-1
EO-10

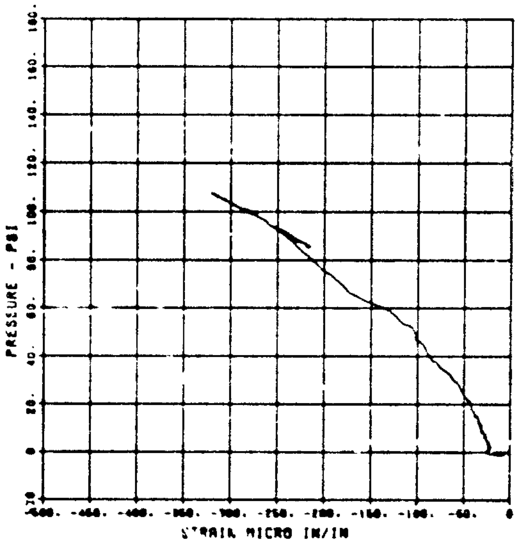

FEMA ELEM TEST S-1
EI-10

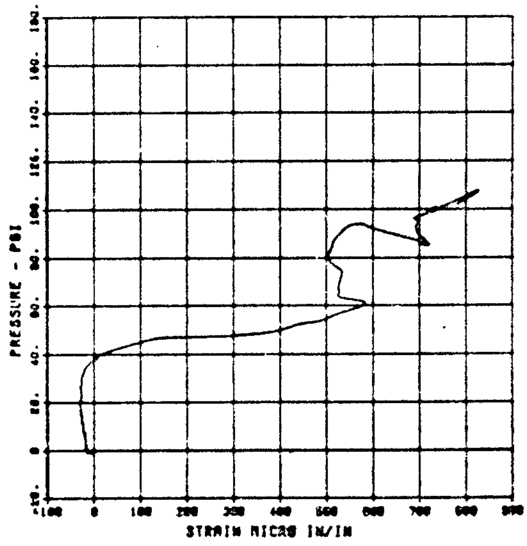

FEMA ELEM TEST S-1
EO-11

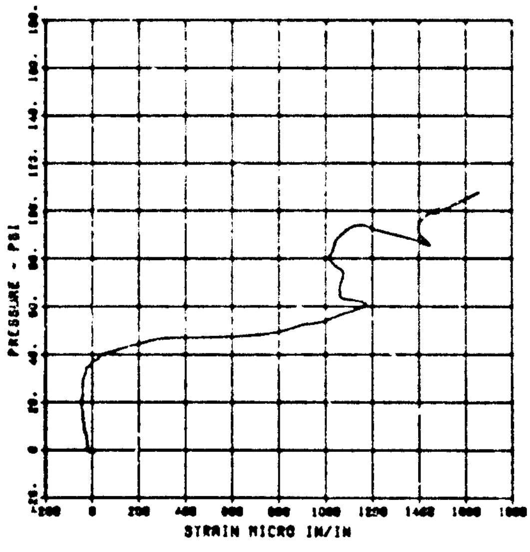

FEMA ELEM TEST S-1
EO-12

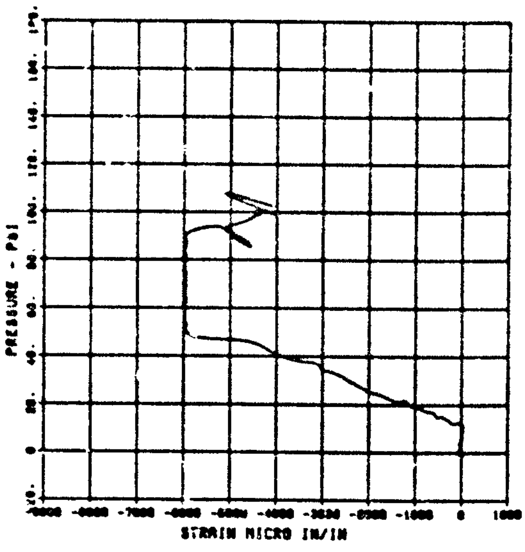

FEMA ELEM TEST S-1
EI-12

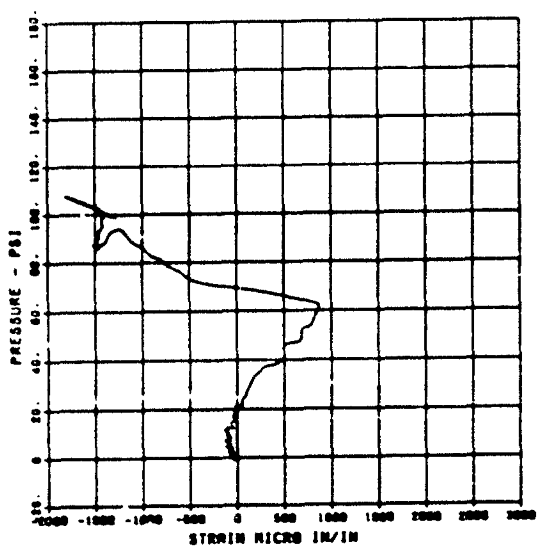

FEMA ELEM TEST S-1
EO-13

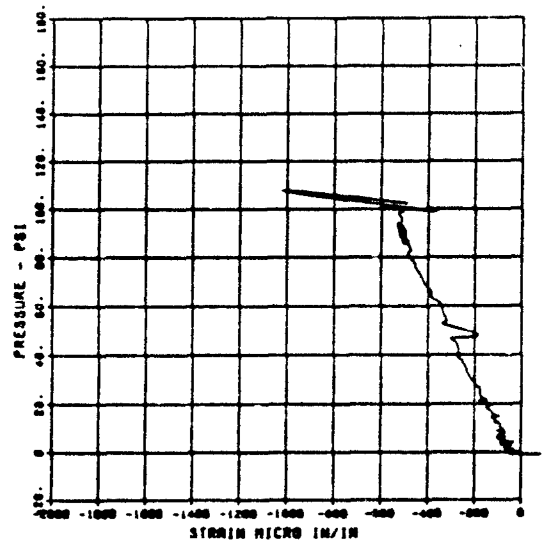

FEMA ELEM TEST S-1
EI-13

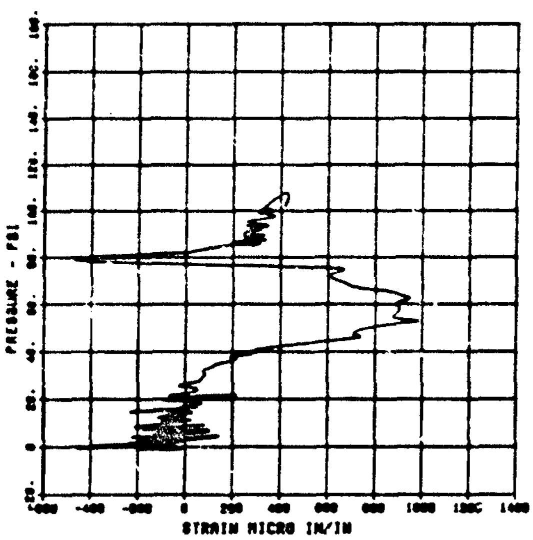

FEMA ELEM TEST S-1
GT-1

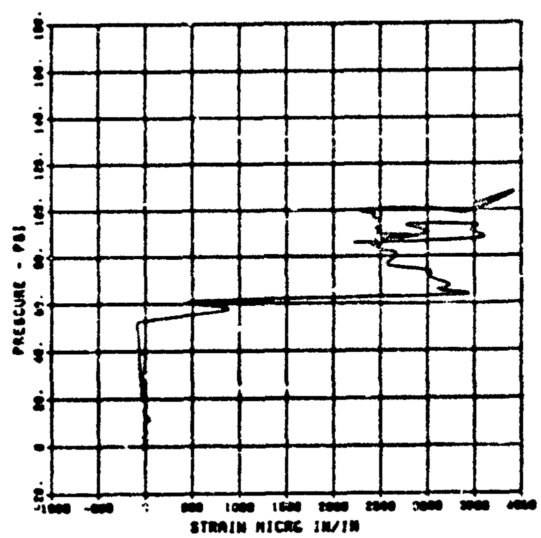

FEMA ELEM TEST S-1
GB-2

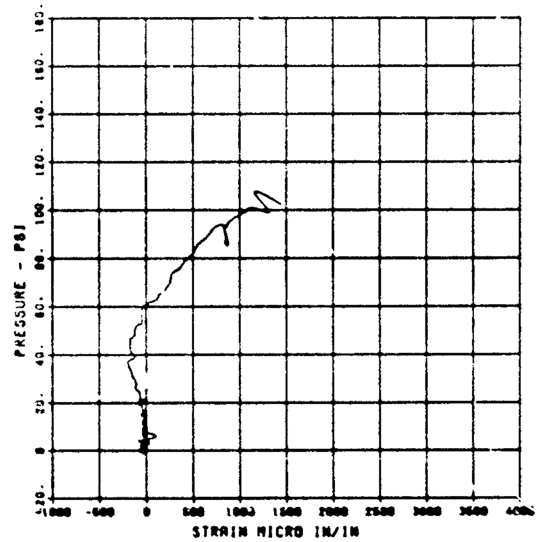

FEMA ELEM TEST S-1
GT-2

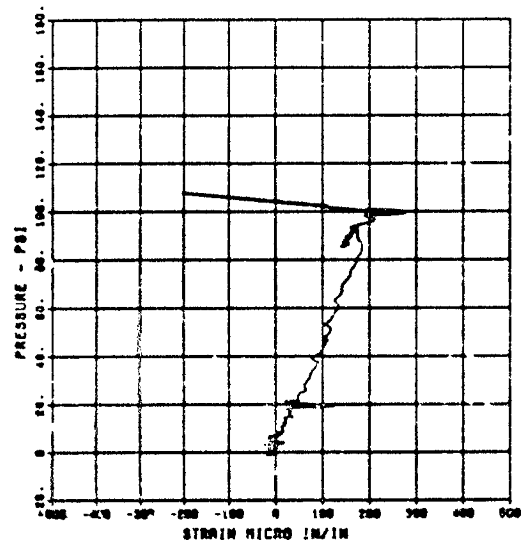

FEMA ELEM TEST
GT-

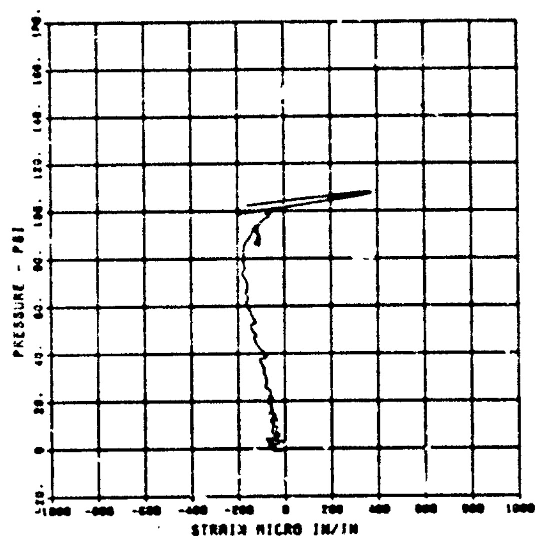

FEMA ELEM TEST S-1
GB-3

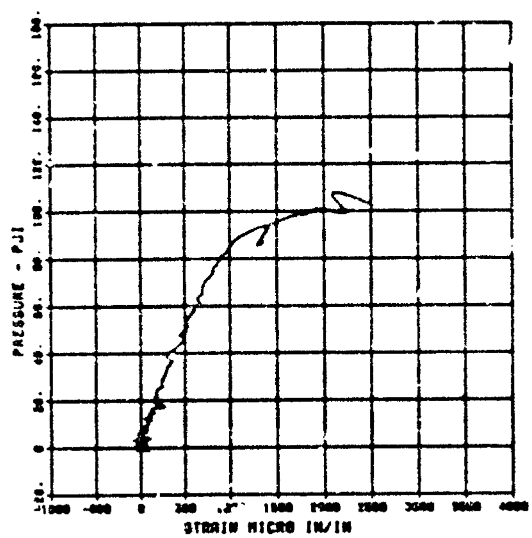

FEMA ELEM TEST S-1
GT-4

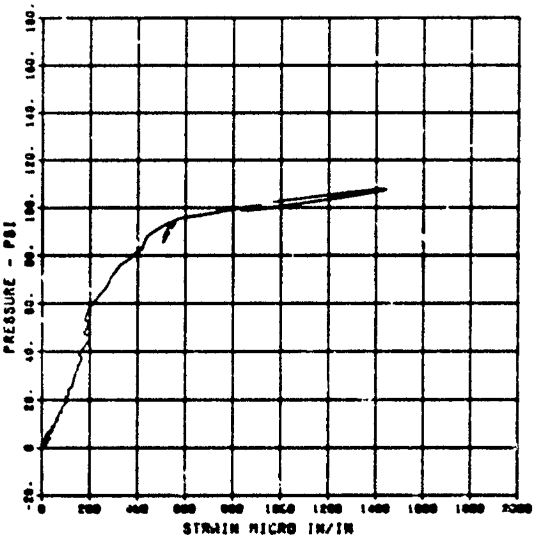

FEMA ELEM TEST S-1
GS-4

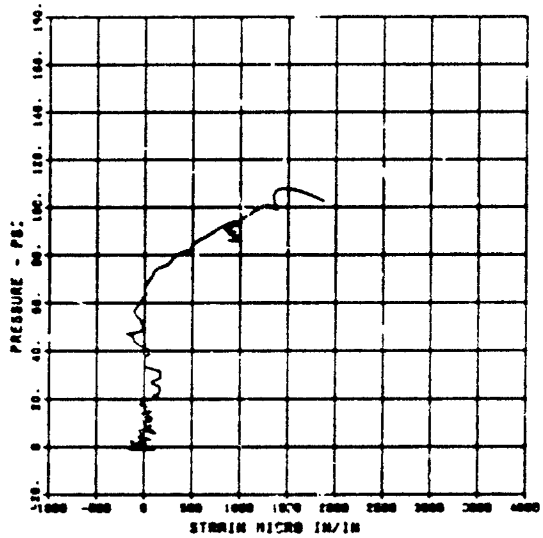

FEMA ELEM TEST S-3
SE-4
11/04/83

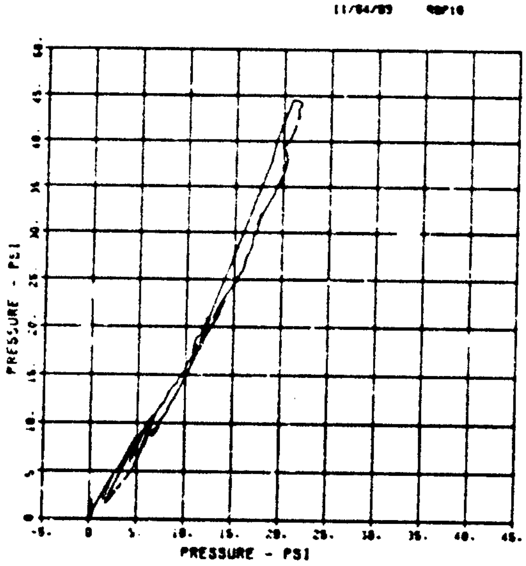

FEMA ELEM TEST S-3
SE-3
11/04/83

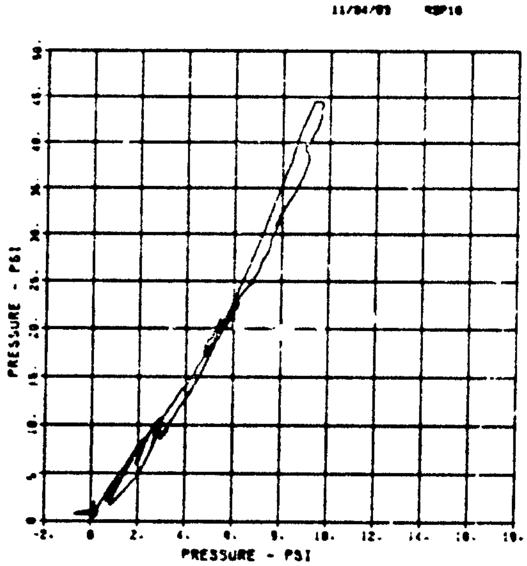

FEMA ELEM TEST S-3
D-1
MAXIMUM 5.2409 SIGMA CAL 1.5123 CAL VAL 5.9
F2
CHANNEL NO. 3 3938 3
11/05/93 ROP20

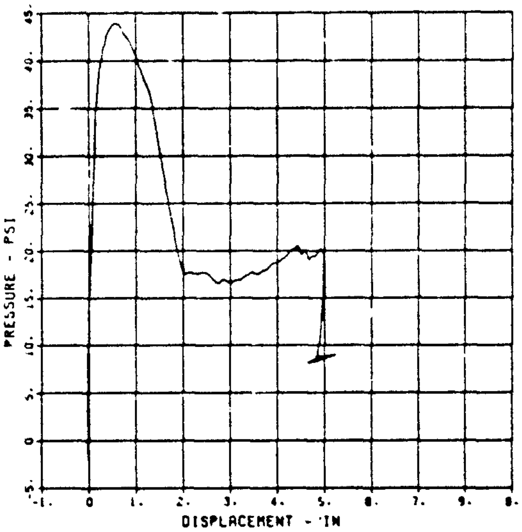

FEMA ELEM TEST S-3
IF-5
MAXIMUM [illegible] SIGMA CAL [illegible] CAL VAL 43.[illegible]
F2
CHANNEL NO. [illegible] 3903 [illegible]
11/04/93 ROP19

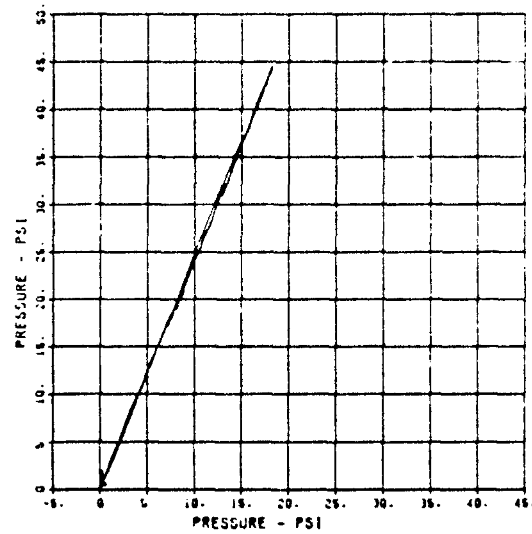

FEMA ELEM TEST S-3
IF-7
MAXIMUM 15.7524 SIGMA CAL 1.9430 CAL VAL 42.1
F2
CHANNEL NO 4 3903 1
11/04/93 ROP18

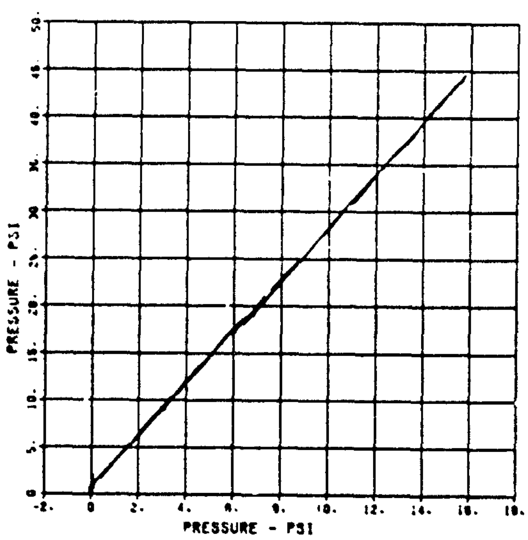

FEMA ELEM TEST S-3
IF-9
MAXIMUM 55.1774 SIGMA CAL 1.4320 CAL VAL 31.2
F2
CHANNEL NO. 5 3803 1
11/04/93 ROP18

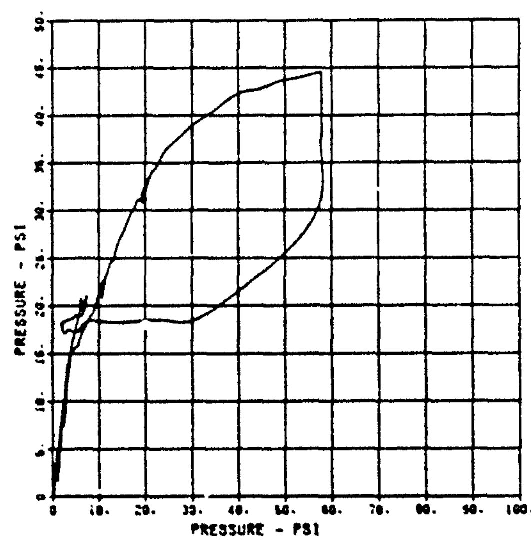

FEMA ELEM TEST S-3
IF-9
MAXIMUM 38.3230 SIGMA CAL 2.4549 CAL VAL 43.2
F2
CHANNEL NO. 6 9909 1
11/04/83 ROP18

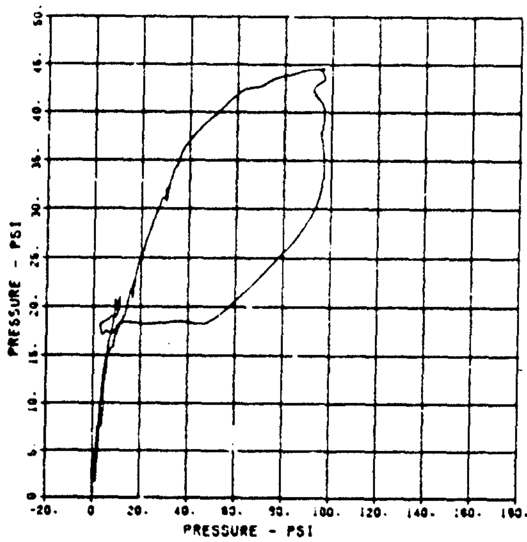

FEMA ELEM TEST S-3
IF-10
MAXIMUM 25.2578 SIGMA CAL 1.0279 CAL VAL 51.4
F2
CHANNEL NO. 5 9909 1
11/04/83 ROP18

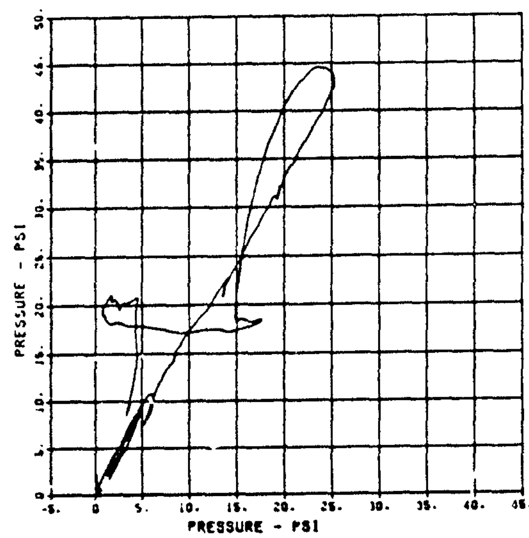

FEMA ELEM TEST S-3
EO-1
MAXIMUM 48694.8012 SIGMA CAL 1.8477 CAL VAL 22283.0
F2
CHANNEL NO. 4 99C8 1
11/05/83 ROP20

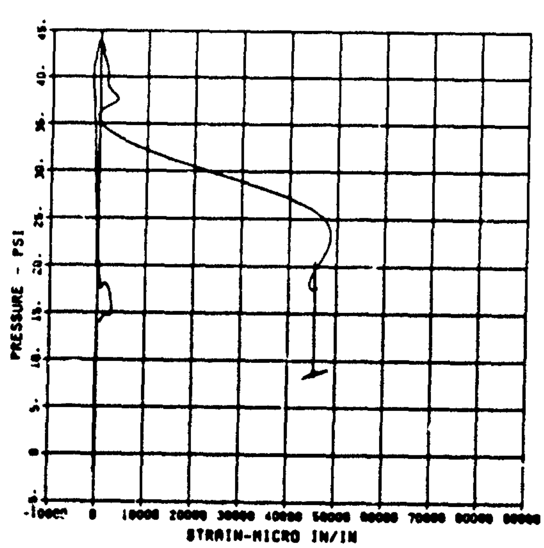

FEMA ELEM TEST S-3
EI-1
9808 3
03/28/84 R0071

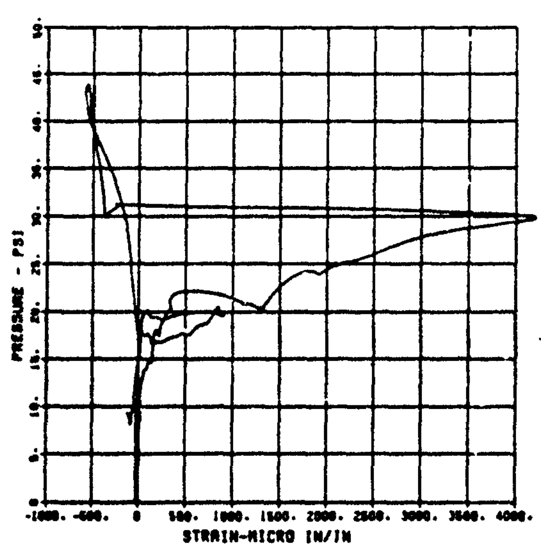

FEMA ELEM TEST S-3
EO-2
MAXIMUM 13508.9623 SIGMA CAL 2.6481 CAL VAL 32710.0
F2
CHANNEL NO. 8 9909 3
11/05/93 R0P20

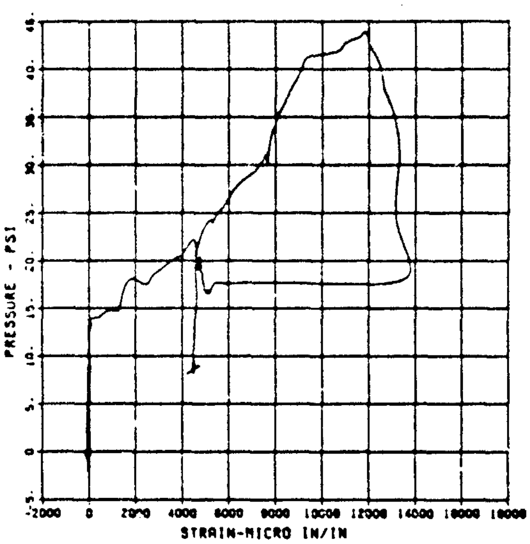

FEMA ELEM TEST S-3
EI-2
9909 3
01/28/94 R0071

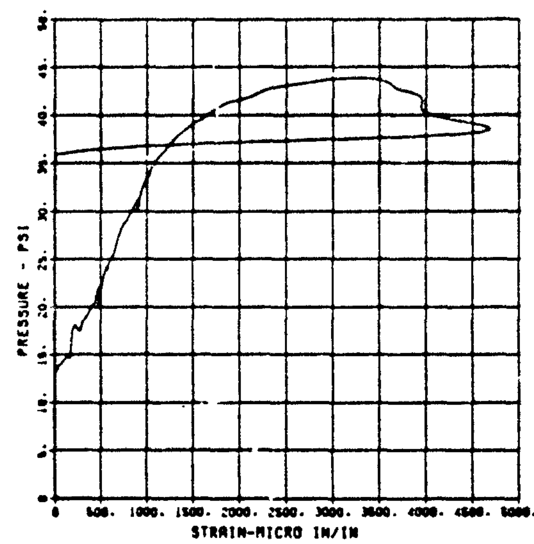

FEMA ELEM TEST S-3
EI-3
MAXIMUM -3811.7000 SIGMA CAL 1.0063 CAL VAL 4337.6
F2
CHANNEL NO. 5 9909 3
11/05/93 R0P20

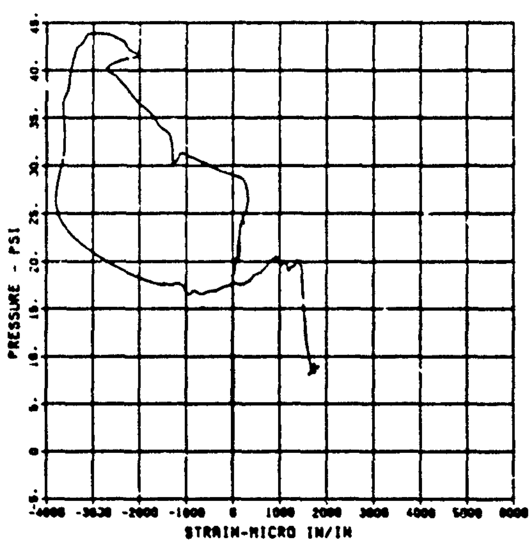

FEMA ELEM TEST S-3
EO-4
MAXIMUM -3817.0707 SIGMA CAL 1.2470 CAL VAL 22283.0
F2
CHANNEL NO. 6 9909 3
11/05/93 R0P20

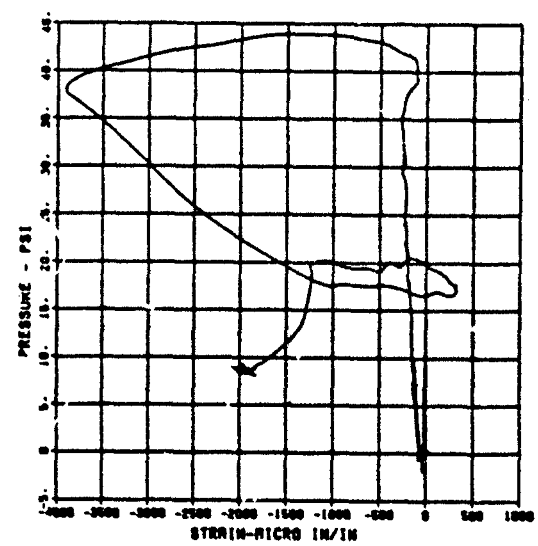

FEMA ELEM TEST S-3
E0-5
MAXIMUM 599.5032 SIGMA CAL 1.2252 CAL VAL 11401.0
F2
CHANNEL NO. 10 9909 3
11/05/93 R0P20

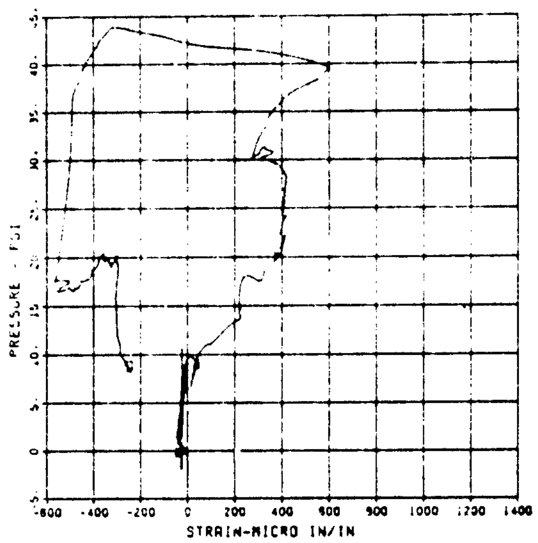

FEMA ELEM TEST S-3
EI-5
MAXIMUM 336.0957 SIGMA CAL 1.2501 CAL VAL 11401.0
F4
CHANNEL NO. 14 9909 3
04/08/94 R0180

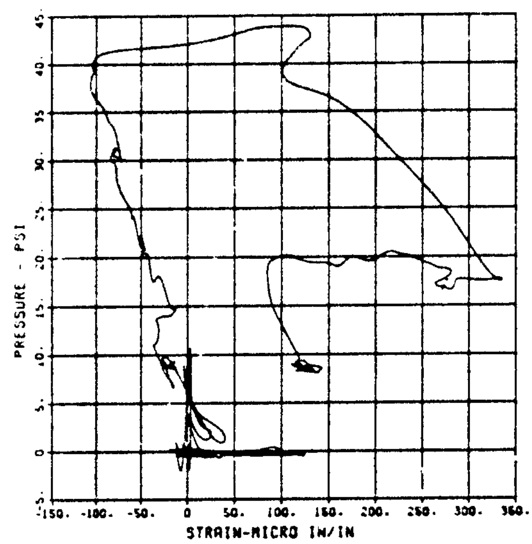

FEMA ELEM TEST S-3
E0 6
MAXIMUM 999.2192 SIGMA CAL 1.1752 CAL VAL 11401.0
F4
CHANNEL NO. 27 9909 4
04/08/94 R0195

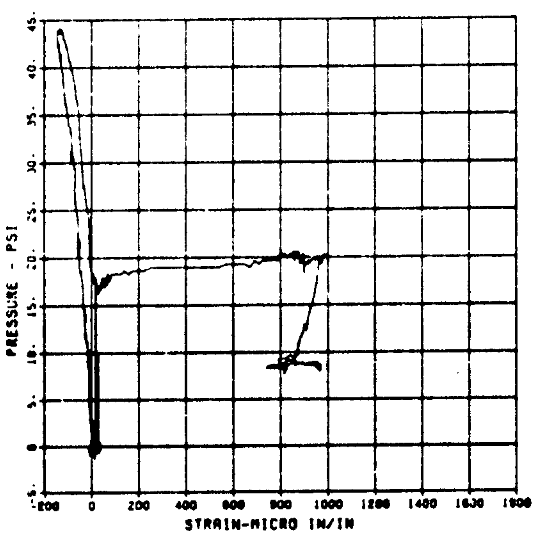

FEMA ELEM TEST S-3
EI-6

9909 4
03/26/94 R0071

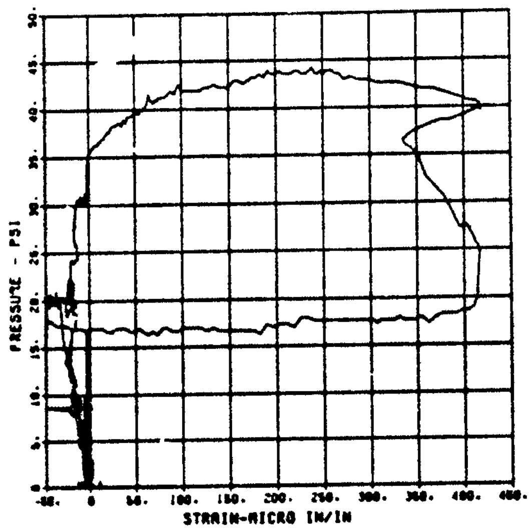

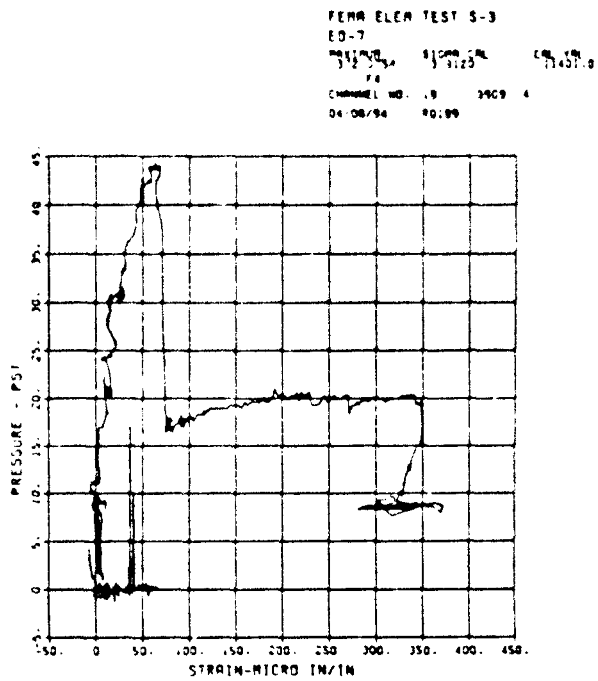
FEMA ELEM TEST S-3
EO-7
PRESSURE - PSI
STRAIN-MICRO IN/IN

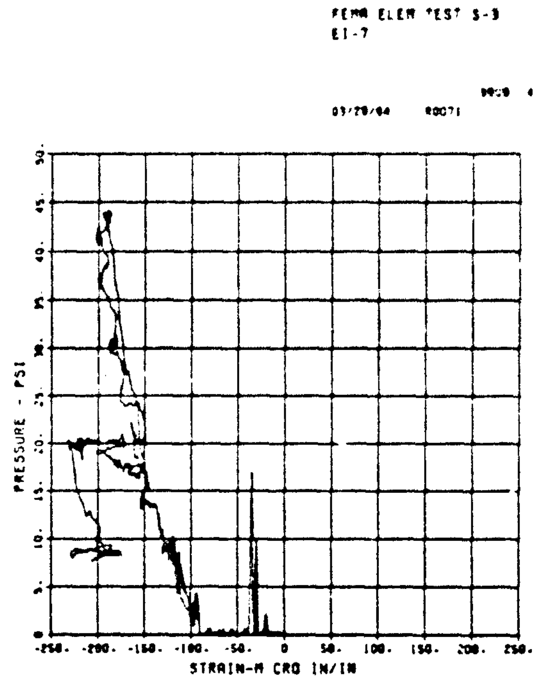
FEMA ELEM TEST S-3
EI-7
PRESSURE - PSI
STRAIN-MICRO IN/IN

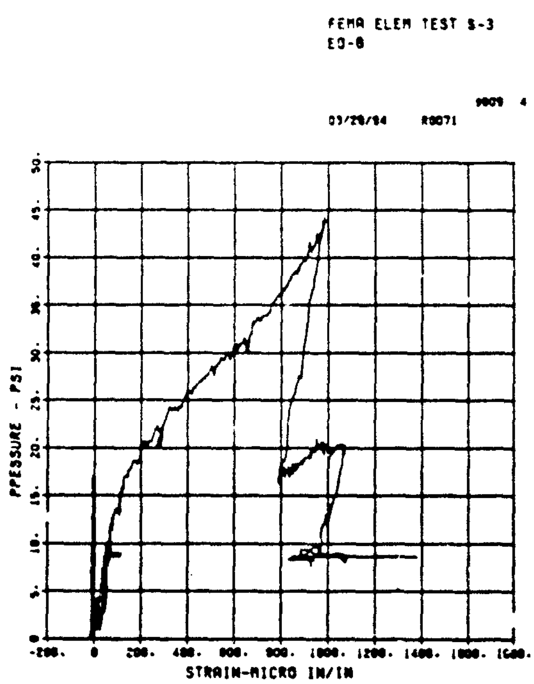
FEMA ELEM TEST S-3
EO-8
PRESSURE - PSI
STRAIN-MICRO IN/IN

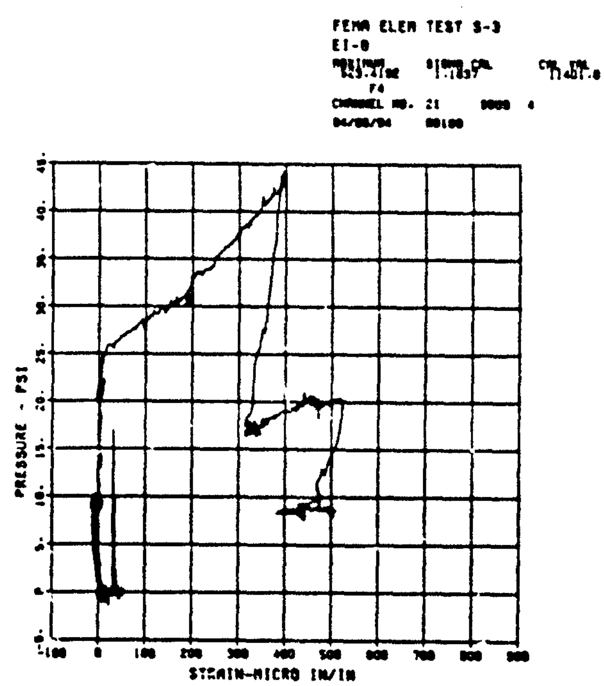
FEMA ELEM TEST S-3
EI-8
PRESSURE - PSI
STRAIN-MICRO IN/IN

FEMA ELEM TEST S-3
EO-9

9809 4
04/08/94 R0198

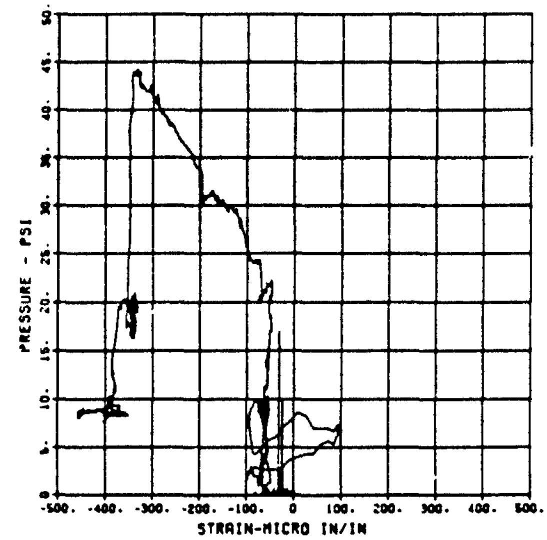

FEMA ELEM TEST S-3
EI-9

9809 4
04/08/94 R0189

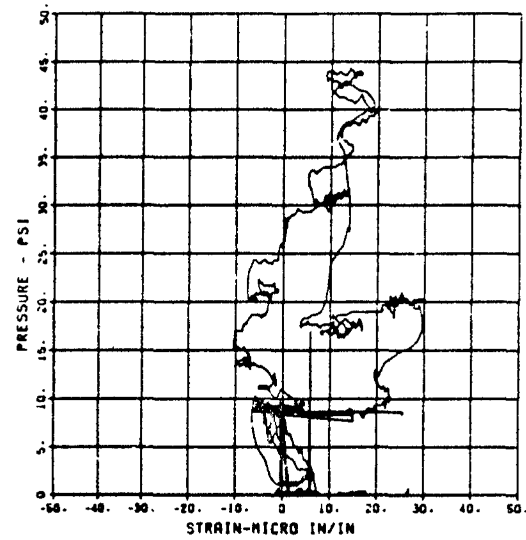

FEMA ELEM TEST S-3
EO-10
MAXIMUM -53.4423 SIGMA CAL 1.8797 CAL CAL 4337.0
F4
CHANNEL NO. 24 9809 4
04/08/94 R0198

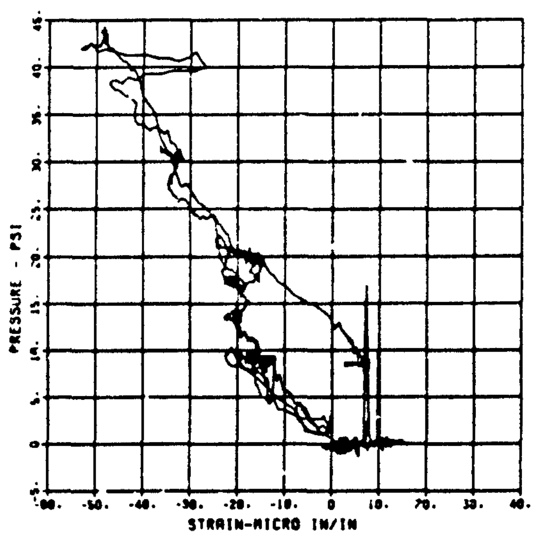

FEMA ELEM TEST S-3
EO-11

9809 4
04/08/94 R0198

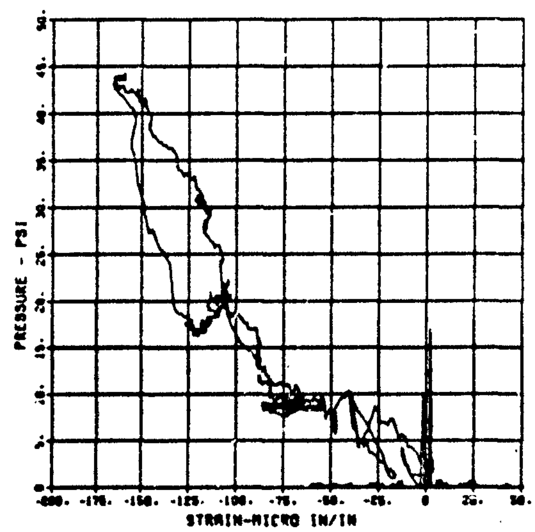

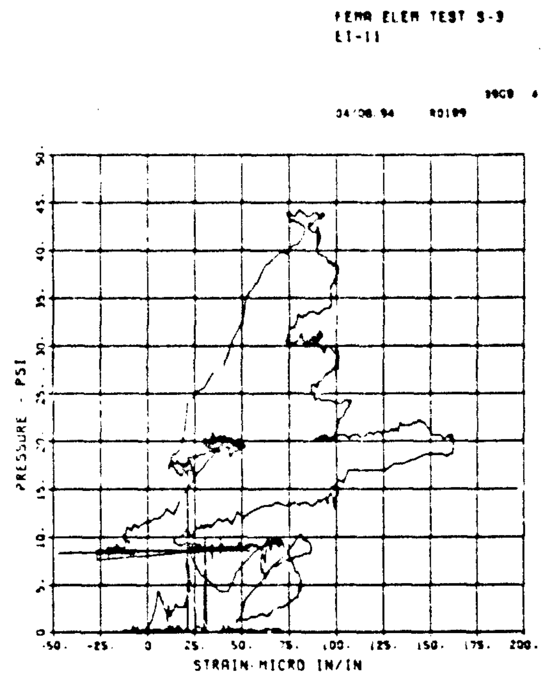
FEMA ELEM TEST S-3
EI-11
PRESSURE - PSI
STRAIN-MICRO IN/IN

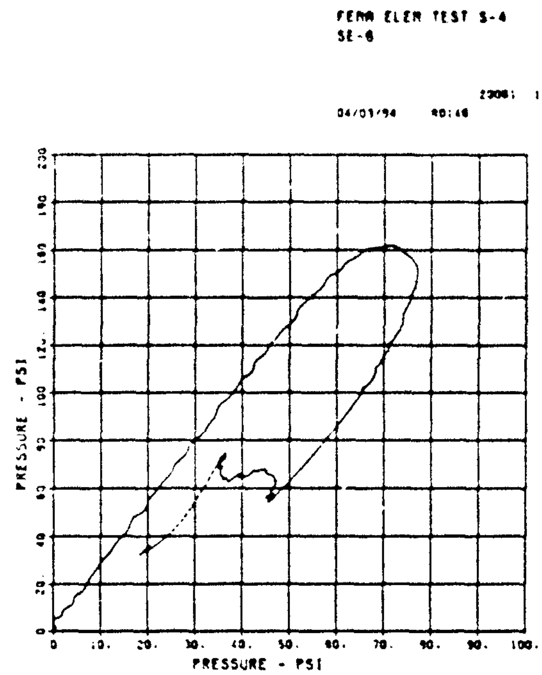
FEMA ELEM TEST S-4
SE-6
PRESSURE - PSI
PRESSURE - PSI

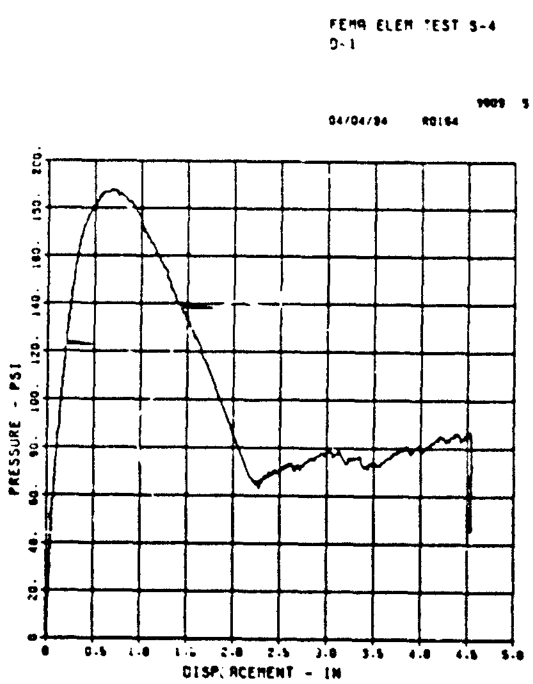
FEMA ELEM TEST S-4
D-1
PRESSURE - PSI
DISPLACEMENT - IN

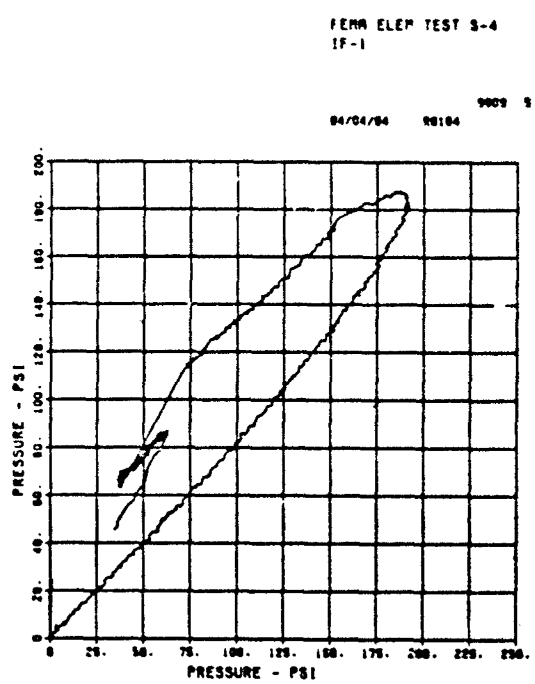
FEMA ELEM TEST S-4
IF-1
PRESSURE - PSI
PRESSURE - PSI

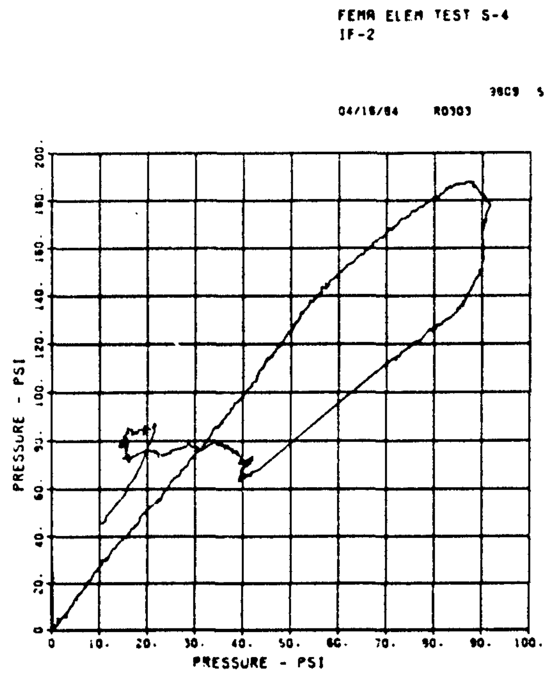
FEMA ELEM TEST S-4
IF-2
04/18/84
PRESSURE - PSI
PRESSURE - PSI

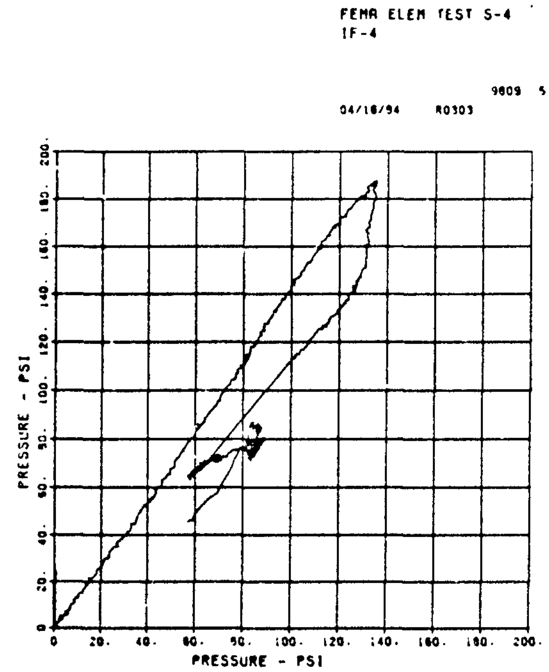
FEMA ELEM TEST S-4
IF-4
04/18/84
PRESSURE - PSI
PRESSURE - PSI

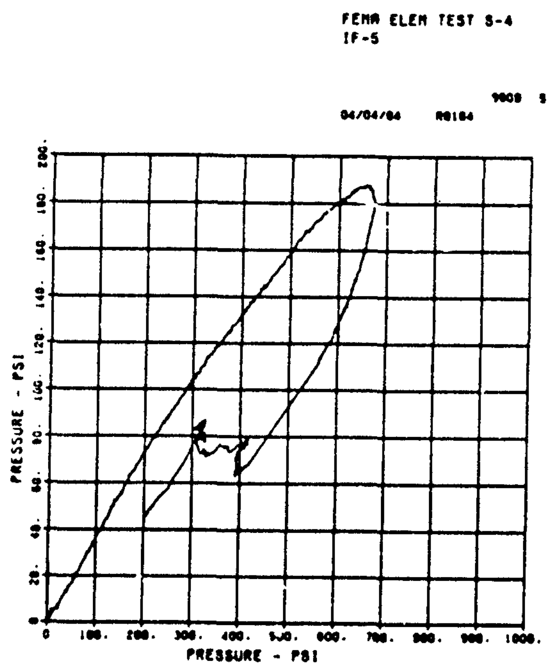
FEMA ELEM TEST S-4
IF-5
04/04/84
PRESSURE - PSI
PRESSURE - PSI

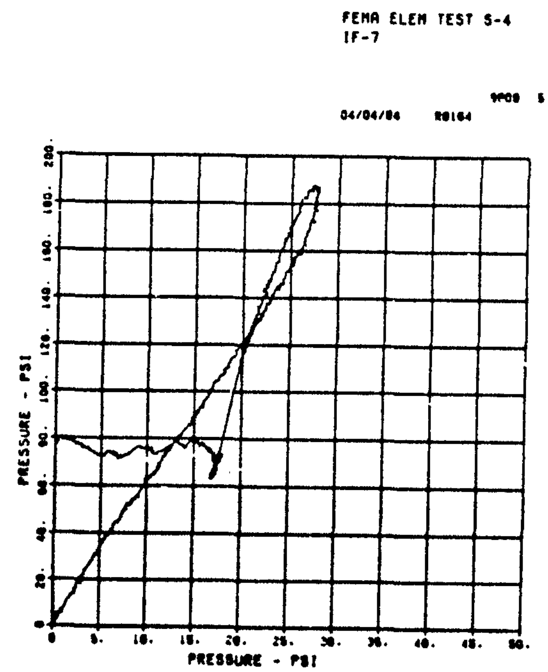
FEMA ELEM TEST S-4
IF-7
04/04/84
PRESSURE - PSI
PRESSURE - PSI

FEMA ELEM TEST S-4
TF-11

04/04/84

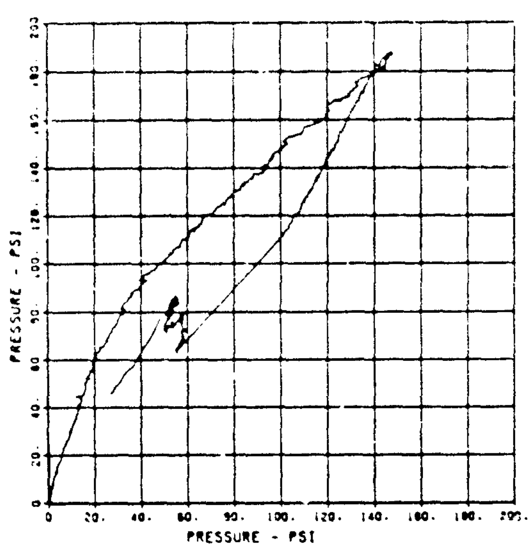

FEMA ELEM TEST S-4
EO-1

04/04/84

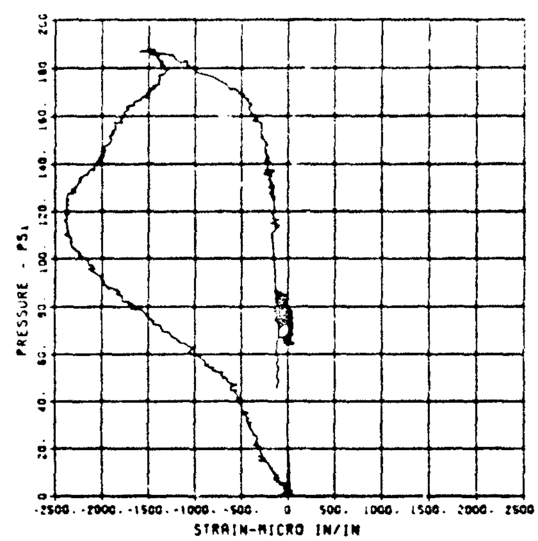

FEMA ELEM TEST S-4
EI-1

04/04/84

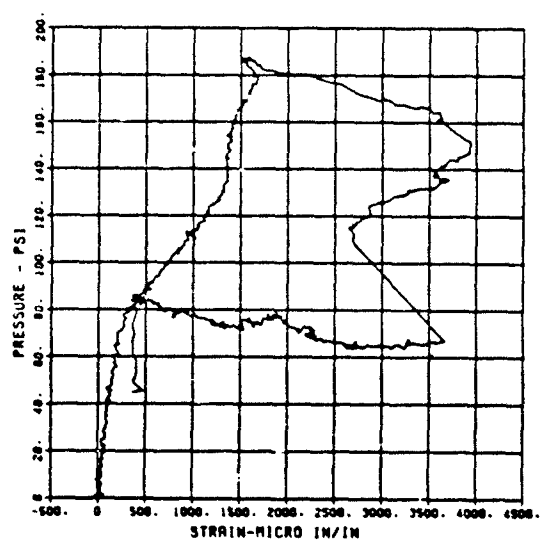

FEMA ELEM TEST S-4
EO-2

04/17/84

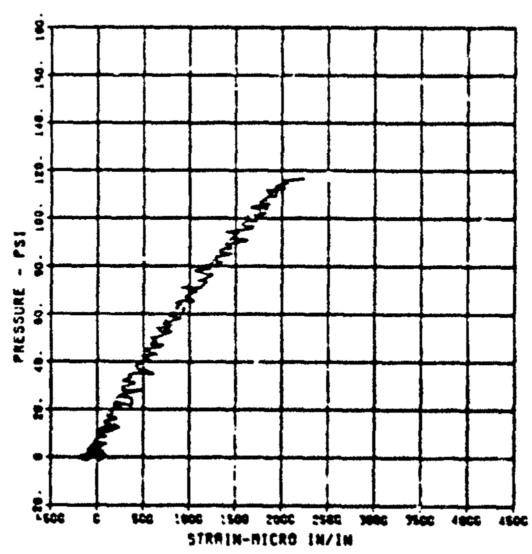

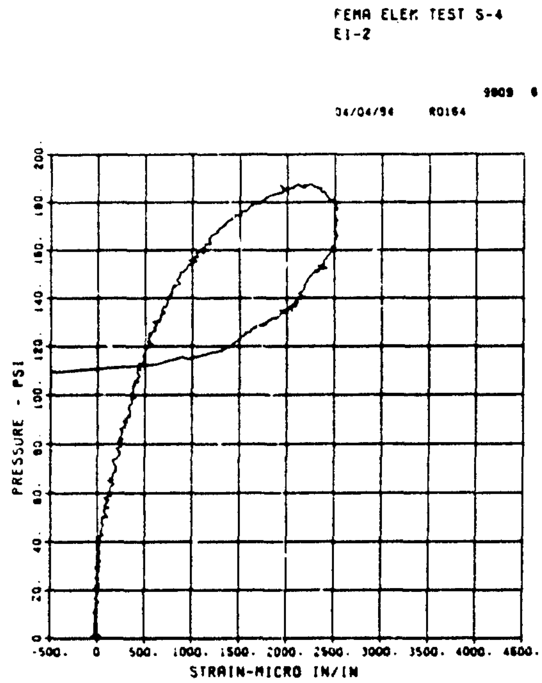
FEMA ELEM TEST S-4
EI-2
PRESSURE - PSI
STRAIN-MICRO IN/IN

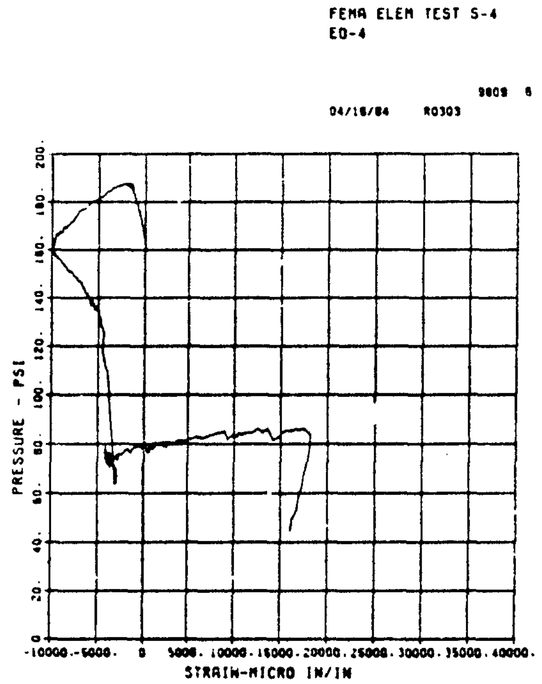
FEMA ELEM TEST S-4
EO-4
04/18/84 R0303
PRESSURE - PSI
STRAIN-MICRO IN/IN

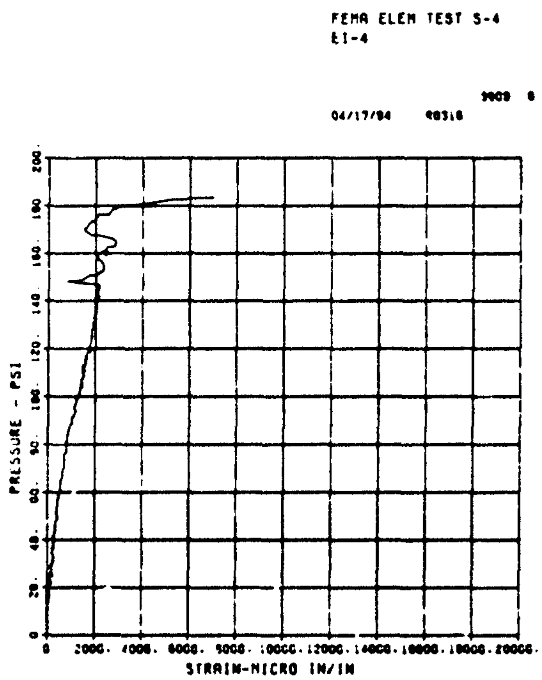
FEMA ELEM TEST S-4
EI-4
PRESSURE - PSI
STRAIN-MICRO IN/IN

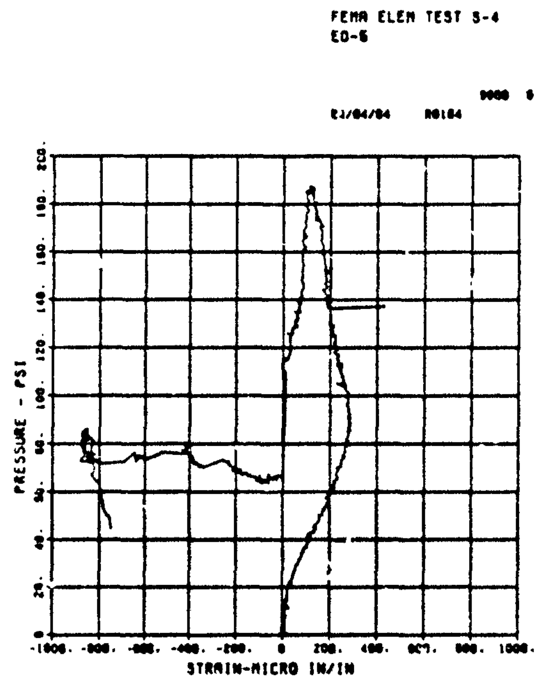
FEMA ELEM TEST S-4
EO-6
PRESSURE - PSI
STRAIN-MICRO IN/IN

FEMA ELEM TEST S-4
EI-5

3909 6
04/04/84 R0184

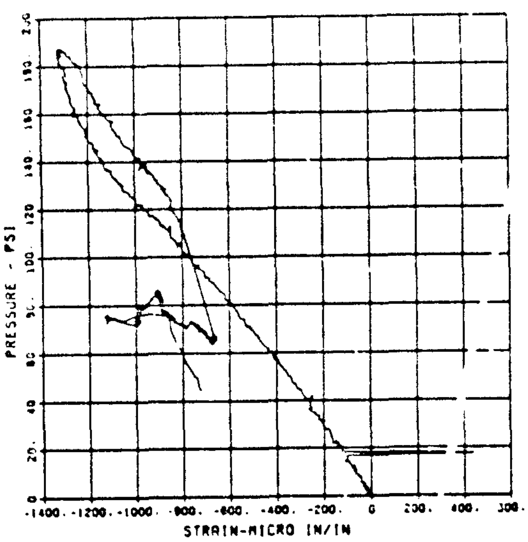

FEMA ELEM TEST S-4
EO-6

3909 6
04/04/84 R0184

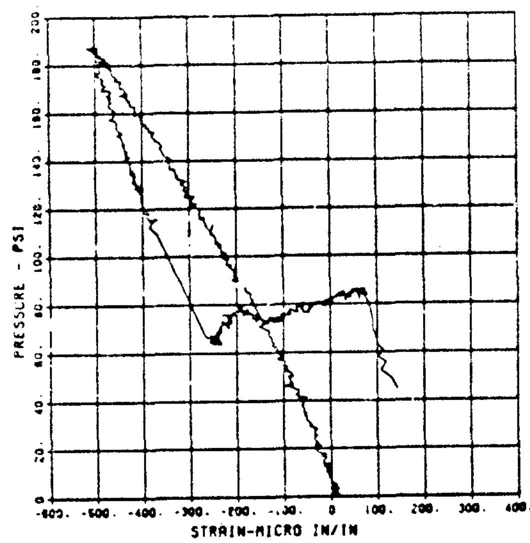

FEMA ELEM EST S-4
EI-6

3909 6
04/04/84 R0184

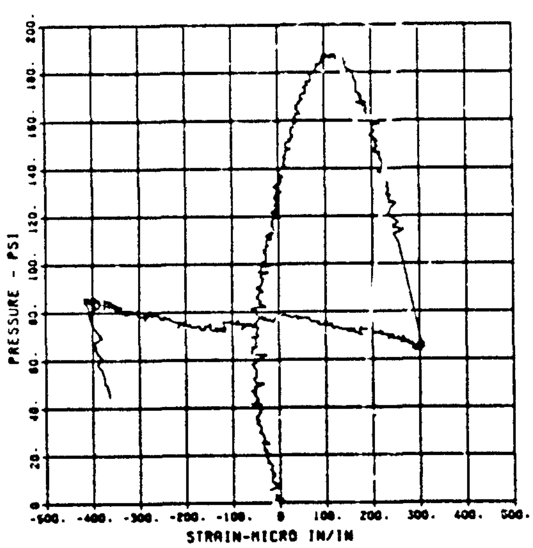

FEMA ELEM TEST S-4
EO-7

3909 6
04/04/84 R0184

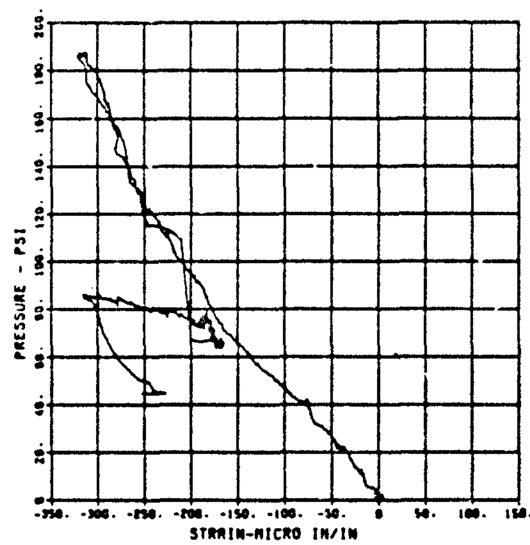

FEMA ELEM TEST S-4
E0-8

9909 5
04/18/84 R0303

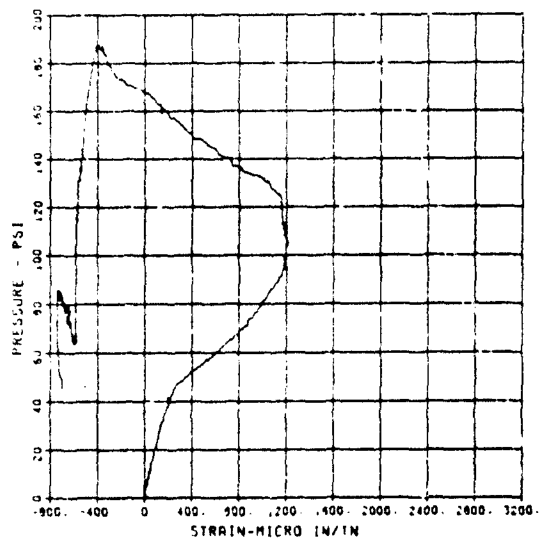

FEMA ELEM TEST S-4
E1-8

9309 6
04/04/84 R0164

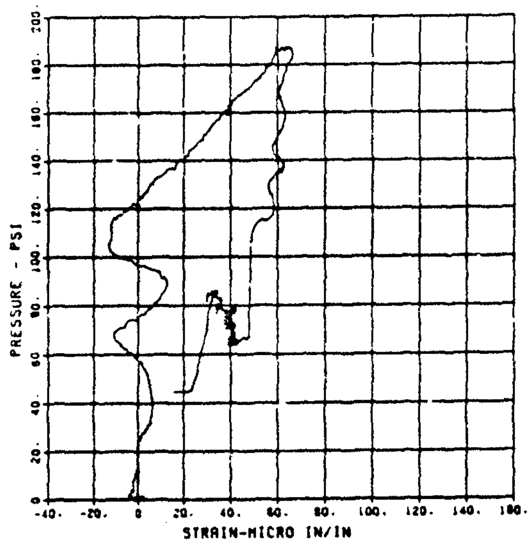

FEMA ELEM TEST S-4
E0-10
MAXIMUM SIGMA CAL CAL VAL
135.6195 3.5884 5760.0
F2
CHANNEL NO. 3 20061 1
04/18/84 R0305

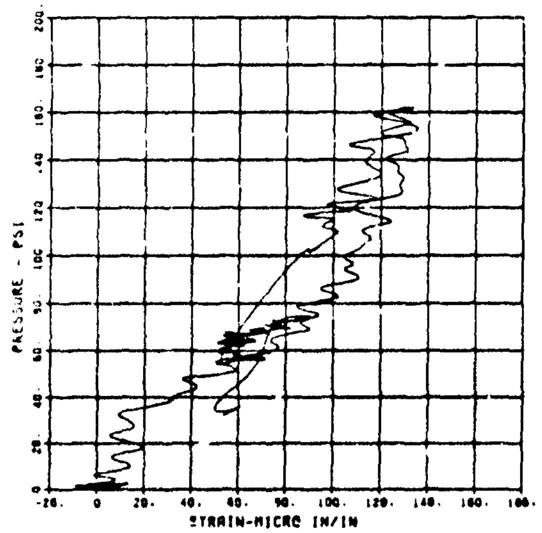

FEMA ELEM TEST S-4
E0-11
MAXIMUM SIGMA CAL CAL VAL
137.1492 3.2344 5760.0
F2
CHANNEL NO. 4 20061 1
04/03/84 R0148

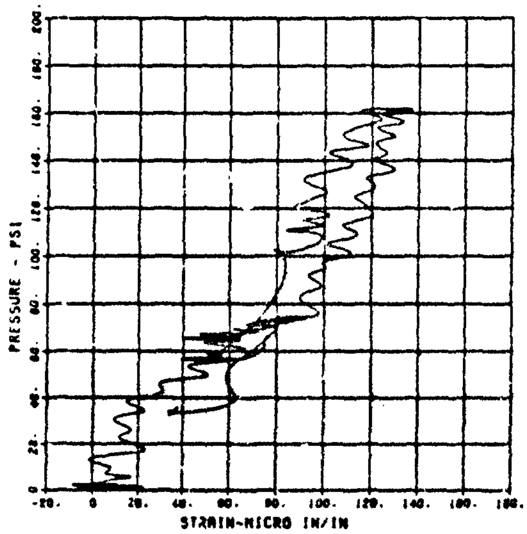

FEMA ELEM TEST S-5
SE-1

7214 1
03/30/84 R0097

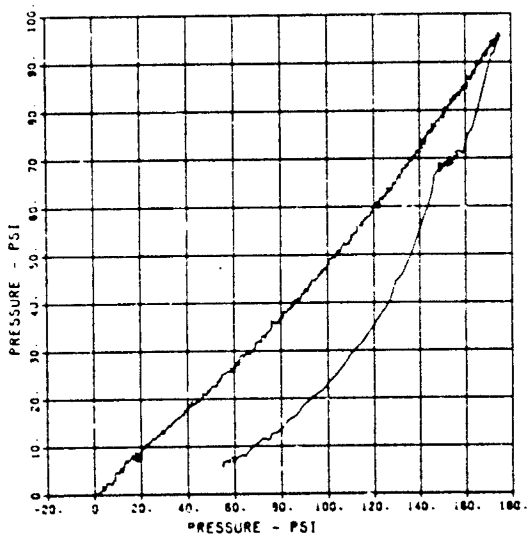

FEMA ELEM TEST S-5
SE-2

7214 1
03/30/84 R0097

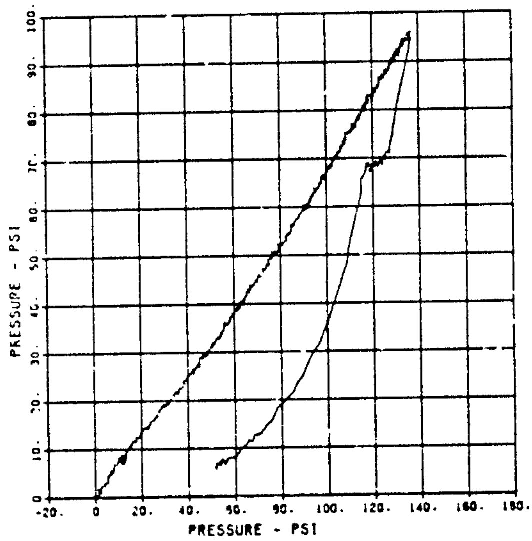

FEMA ELEM TEST S-5
SE-3

7214 1
03/30/84 R0097

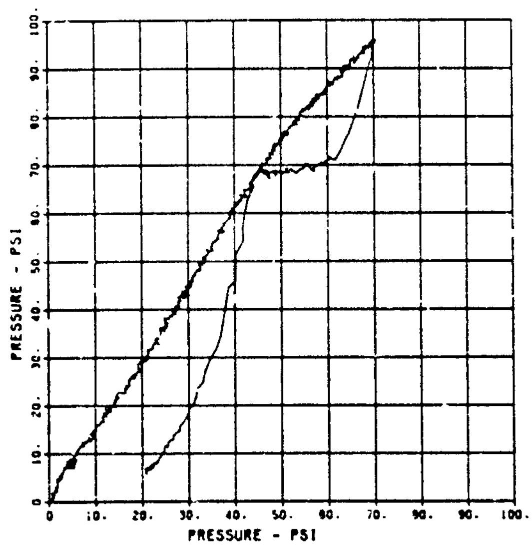

FEMA ELEM TEST S-5
SE-4

7214 1
03/30/84 R0097

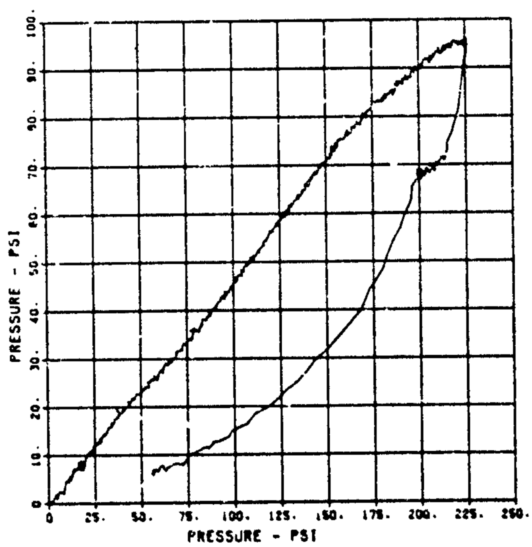

FEMA ELEM TEST S-5
SE-5

7214 1
03/30/84 R0097

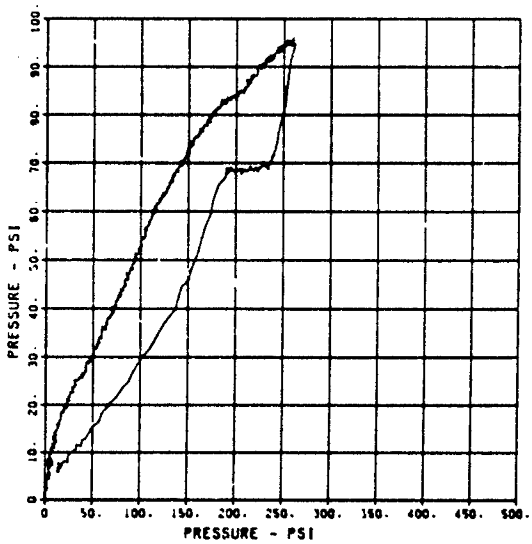

FEMA ELEM TEST S-5
SE-6

7214 1
03/30/84 R0097

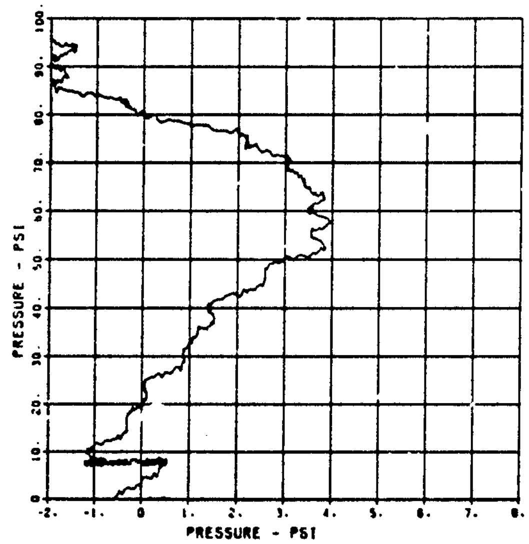

FEMA ELEM TEST S-5
D-1

7214 1
03/30/84 R0097

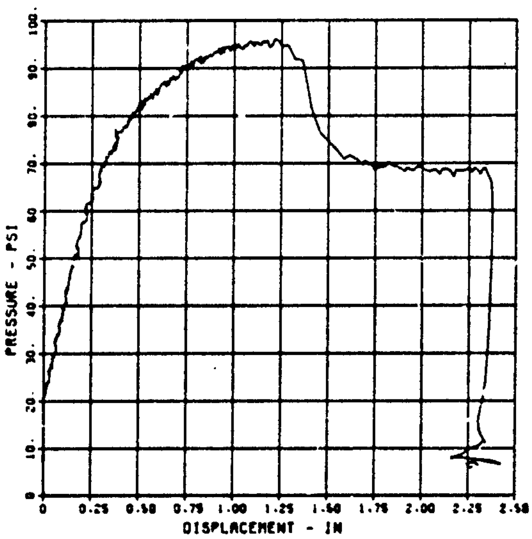

FEMA ELEM TEST S-5
IF-1

7214 1
03/30/84 R0097

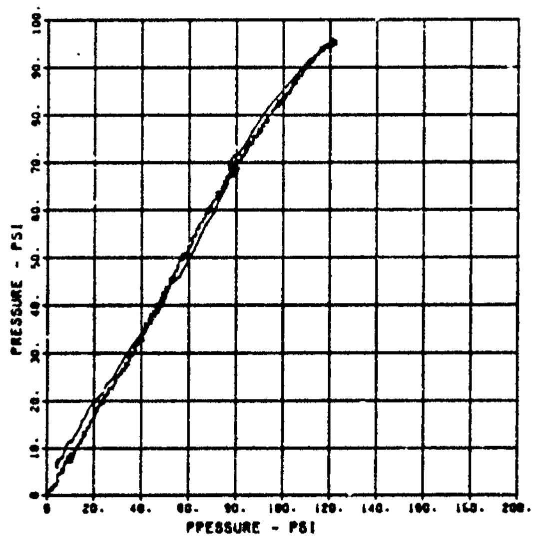

FEMA ELEM TEST S-5
IF-2

7214 1

03/30/94 R0097

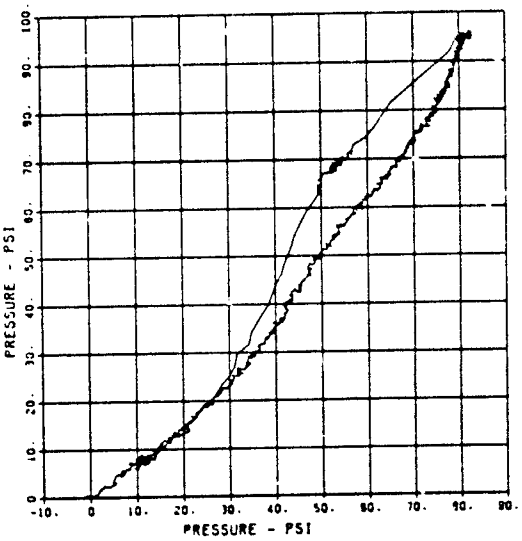

FEMA ELEM TEST S-5
IF-3

7214 1

03/30/94 R0097

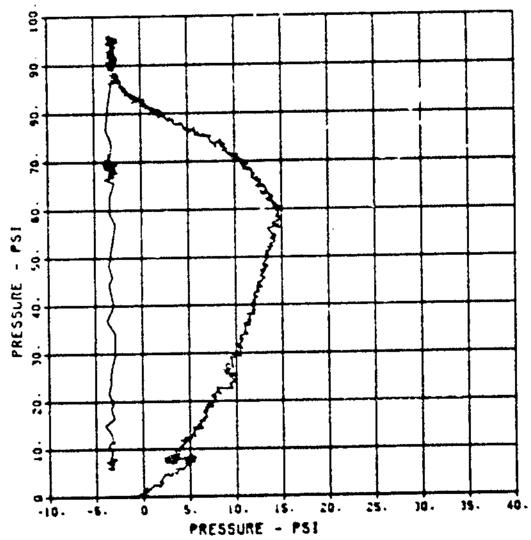

FEMA ELEM TEST S-5
IF-4

7214 1

03/30/94 R0097

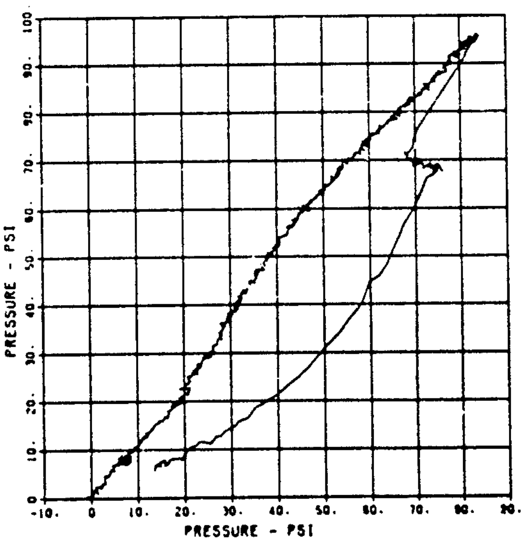

FEMA ELEM TEST S-5
IF-5

7214 1

03/30/94 R0097

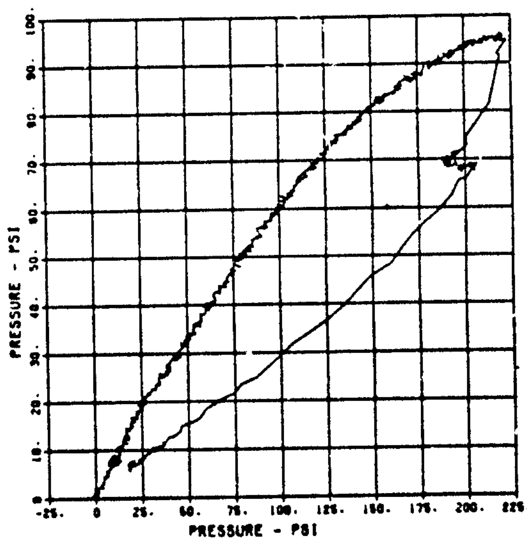

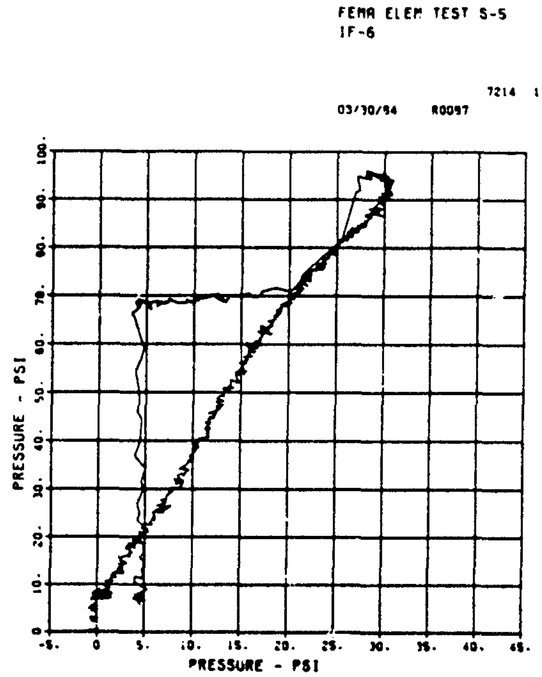
FEMA ELEM TEST S-5
IF-6
7214 1
03/30/84 R0097
PRESSURE - PSI
PRESSURE - PSI

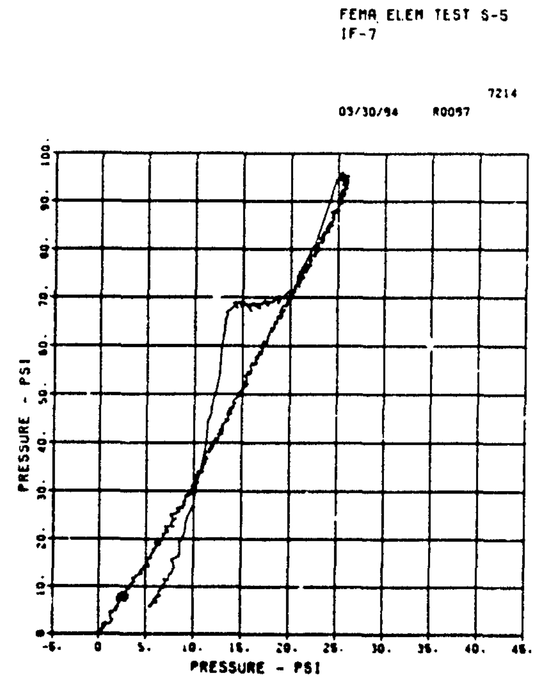
FEMA ELEM TEST S-5
IF-7
7214 1
03/30/84 R0097
PRESSURE - PSI
PRESSURE - PSI

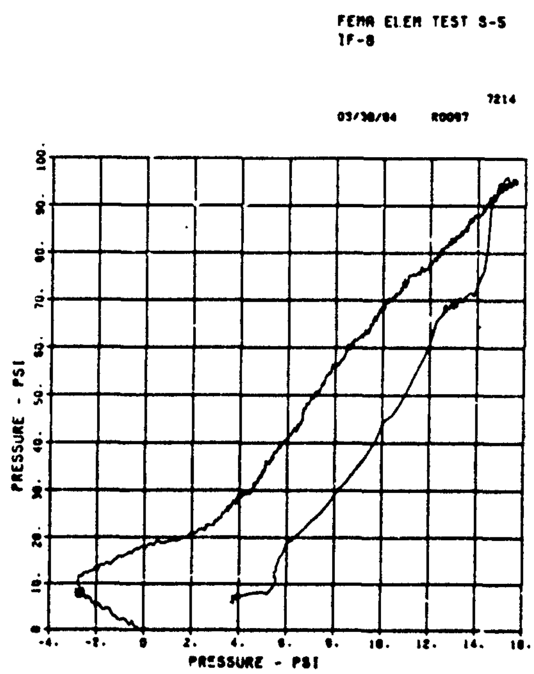
FEMA ELEM TEST S-5
IF-8
7214 1
03/30/84 R0097
PRESSURE - PSI
PRESSURE - PSI

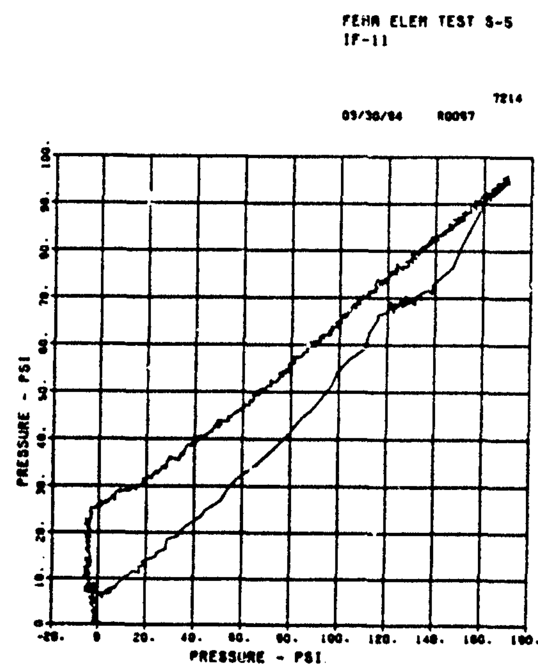
FEMA ELEM TEST S-5
IF-11
7214 1
03/30/84 R0097
PRESSURE - PSI
PRESSURE - PSI

FEMA ELEM TEST S-5
EO-1

7214 1
04/12/84 R0272

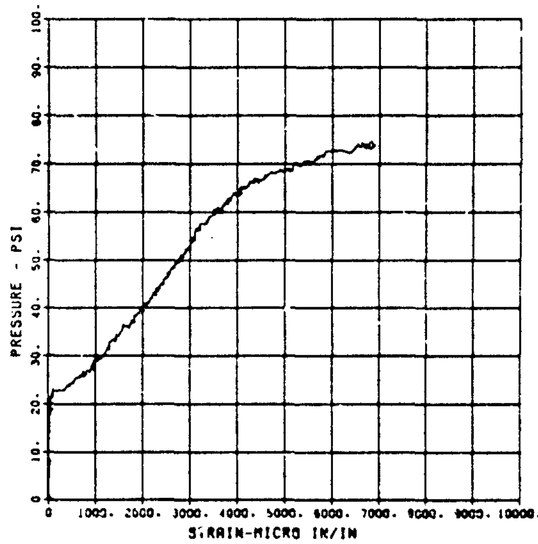

FEMA ELEM TEST S-5
EI-1

7214 1
04/12/84 R0272

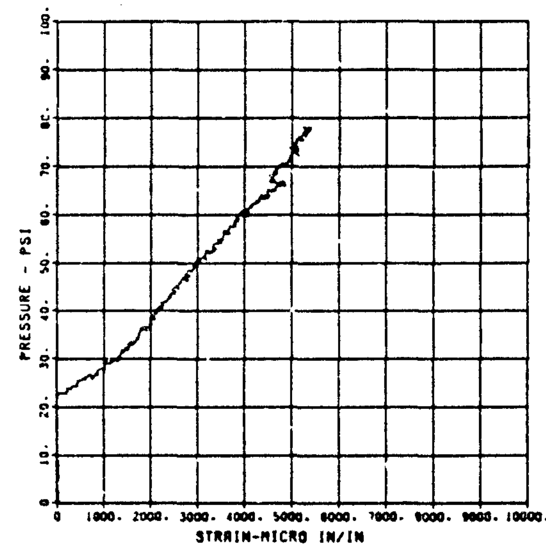

FEMA ELEM TEST S-5
EO-2

7214 1
03/30/84 R0007

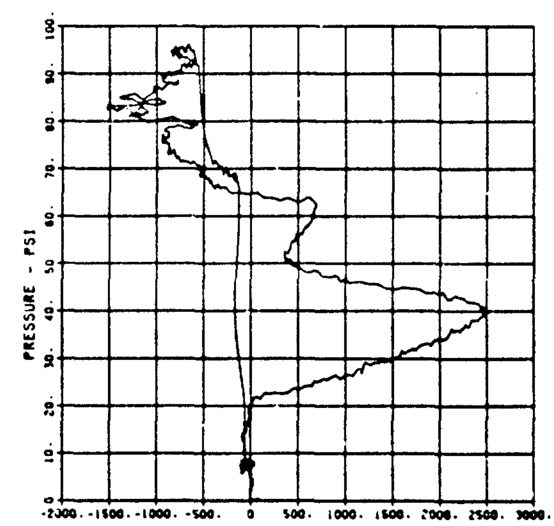

FEMA ELEM TEST S-5
EI-2

7214 1
03/30/84 R0007

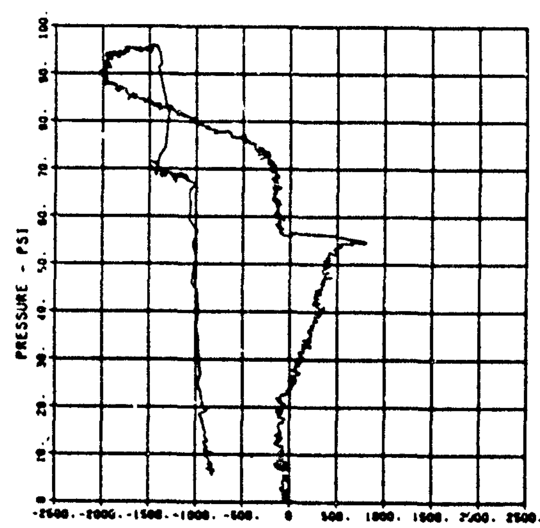

FEMA ELEM TEST S-5
EO-3

7214 1
03/30/84 R0097

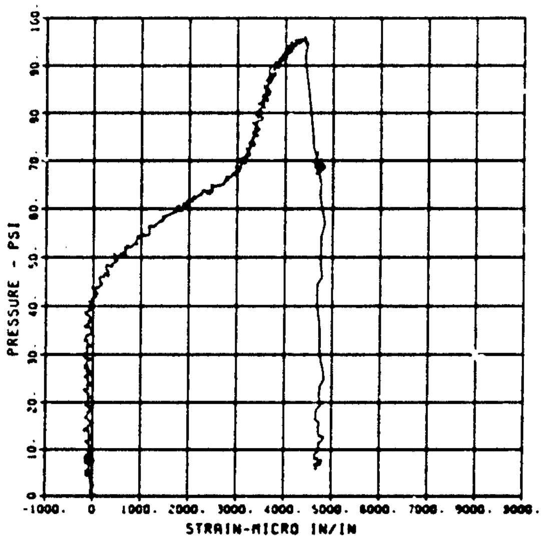

FEMA ELEM TEST S-5
EO-4

7214 1
03/30/84 R0097

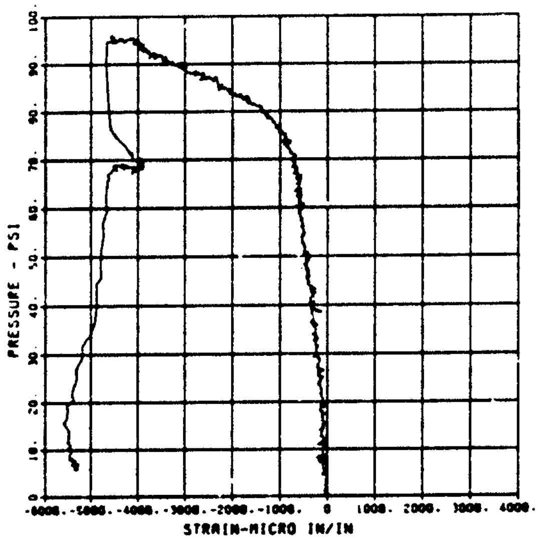

FEMA ELEM TEST S-6
EI-4
MAXIMUM 4447.8400 SIGMA CAL 3.3710 CAL VAL 32718.3

CHANNEL NO. 38 7214 1
04/12/84 R0E72

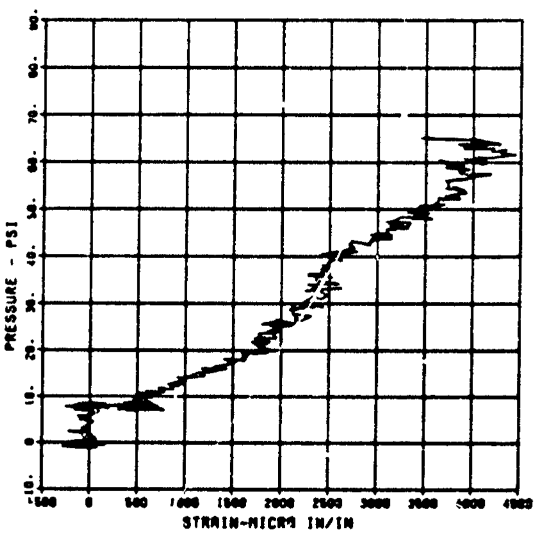

FEMA ELEM TEST S-5
EO-5

7214 1
03/30/84 R0097

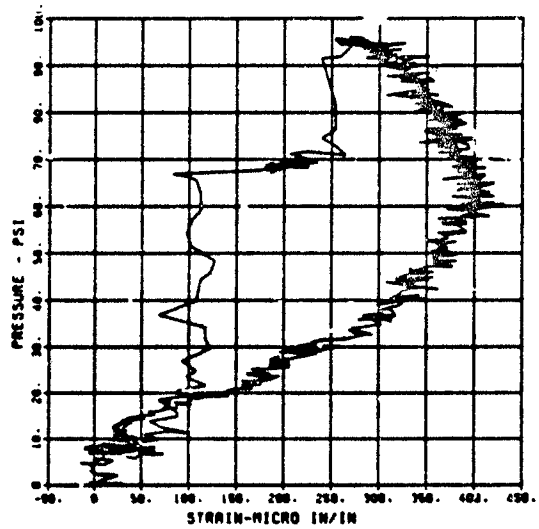

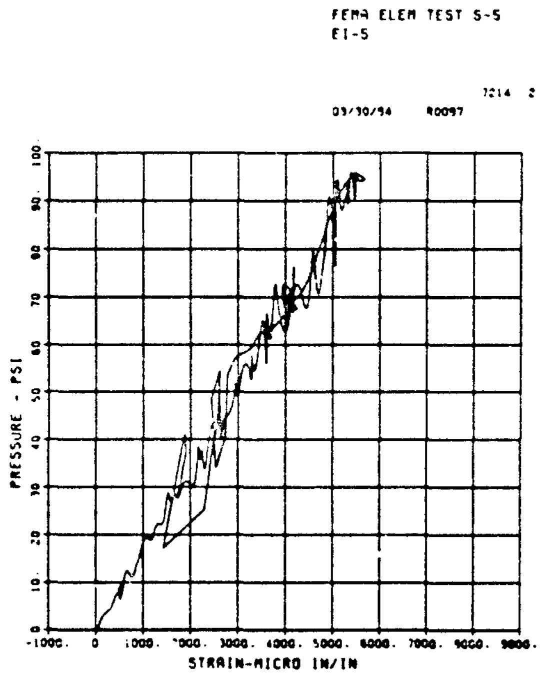
FEMA ELEM TEST S-5
EI-5
7214 2
03/30/94 R0097
PRESSURE - PSI
STRAIN-MICRO IN/IN

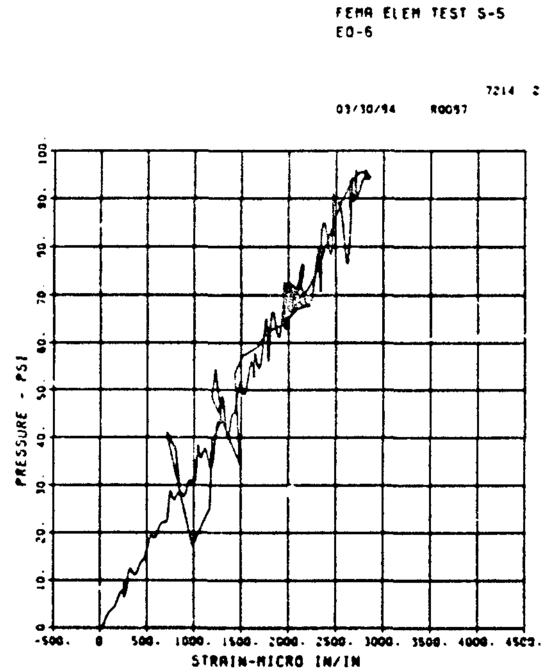
FEMA ELEM TEST S-5
EO-6
7214 2
03/30/94 R0097
PRESSURE - PSI
STRAIN-MICRO IN/IN

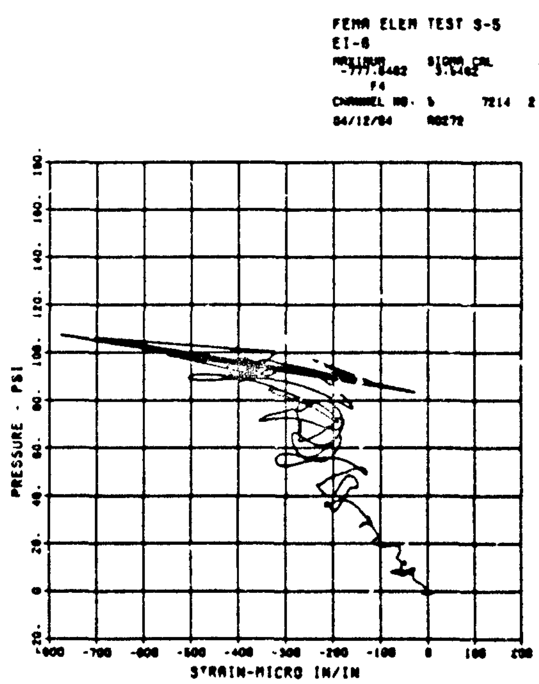
FEMA ELEM TEST S-5
EI-6
F4
7214 2
PRESSURE - PSI
STRAIN-MICRO IN/IN

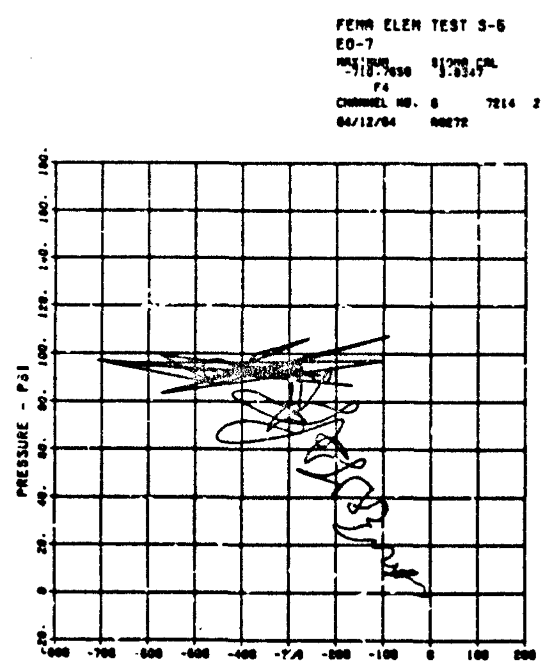
FEMA ELEM TEST S-6
EO-7
F4
7214 2
PRESSURE - PSI
STRAIN-MICRO IN/IN

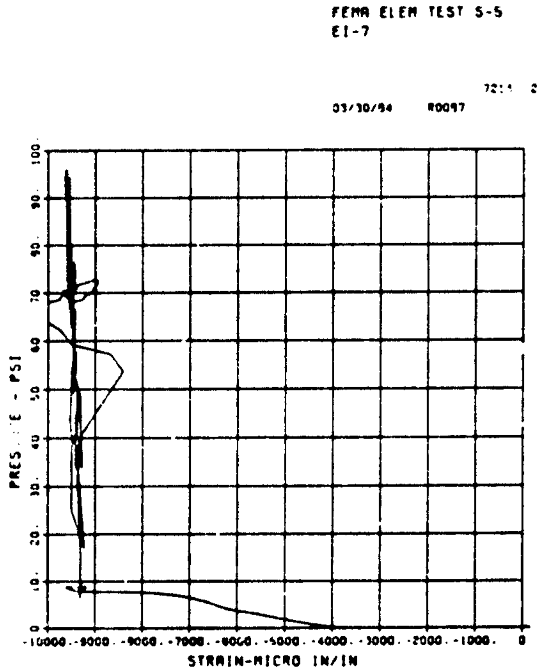
FEMA ELEM TEST S-5
EI-7
03/30/84
R0097
PRESSURE - PSI
STRAIN-MICRO IN/IN

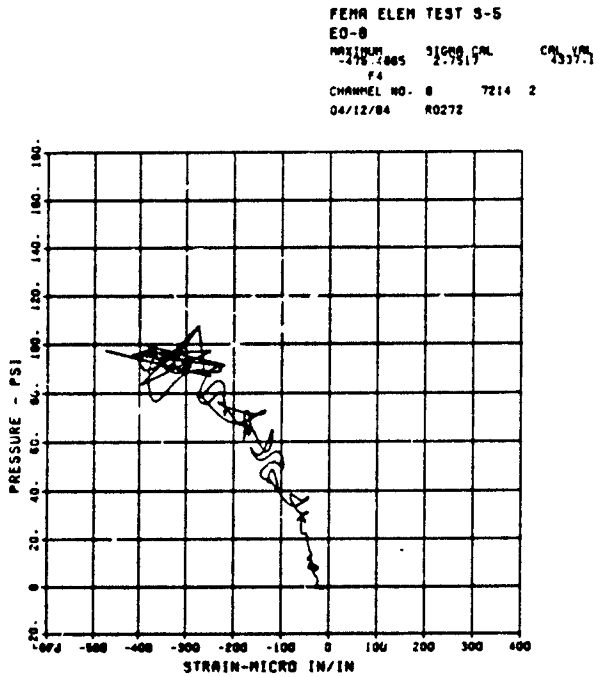
FEMA ELEM TEST S-5
EO-8
MAXIMUM
SIGMA CAL
CAL VAL
F4
CHANNEL NO. 8
7214 2
04/12/84
R0272
PRESSURE - PSI
STRAIN-MICRO IN/IN

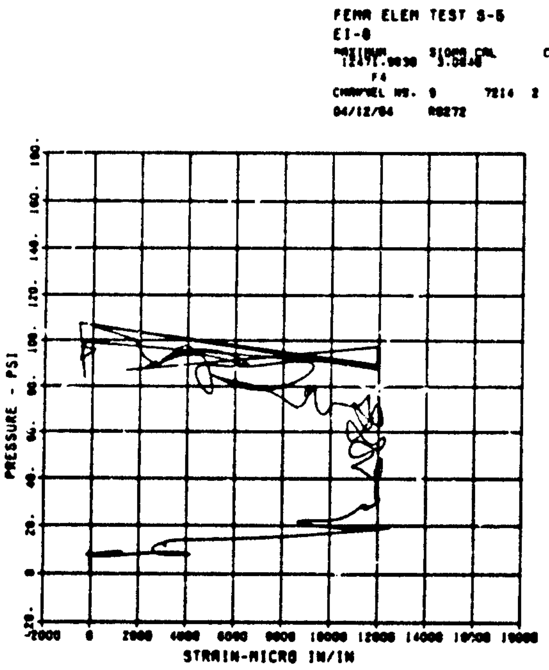
FEMA ELEM TEST S-5
EI-8
MAXIMUM
SIGMA CAL
CAL VAL
F4
7214 2
04/12/84
PRESSURE - PSI
STRAIN-MICRO IN/IN

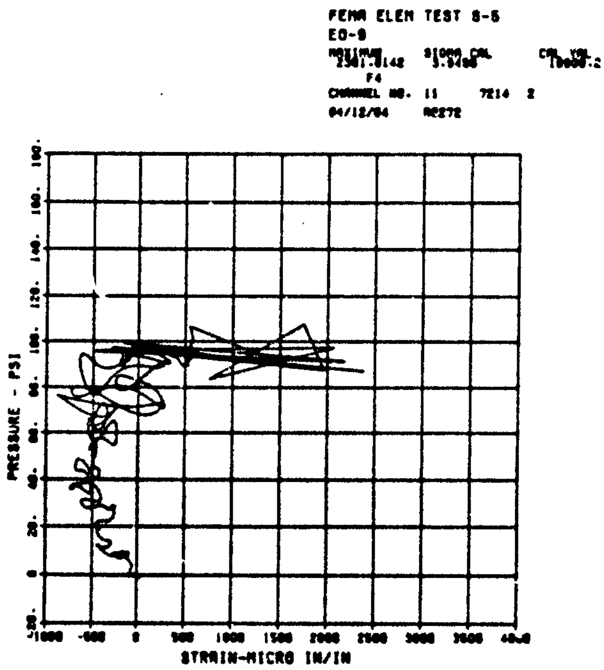
FEMA ELEM TEST S-5
EO-9
MAXIMUM
SIGMA CAL
CAL VAL
F4
7214 2
04/12/84
PRESSURE - PSI
STRAIN-MICRO IN/IN

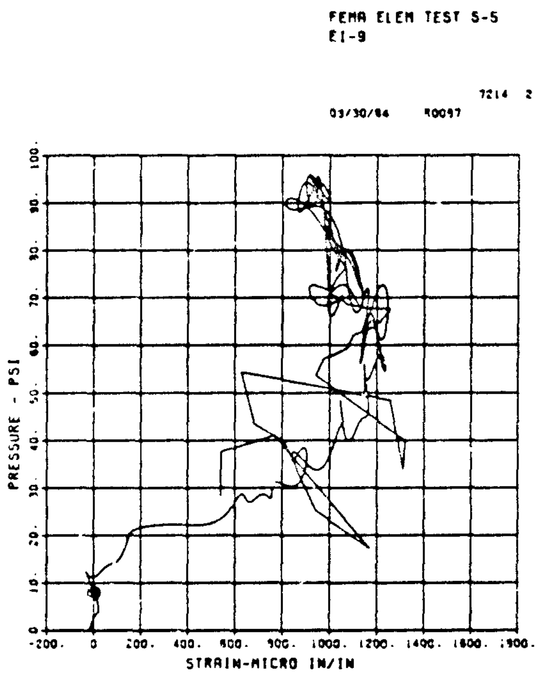
FEMA ELEM TEST S-5
EI-9
7214 2
03/30/84 R0097
PRESSURE - PSI
STRAIN-MICRO IN/IN

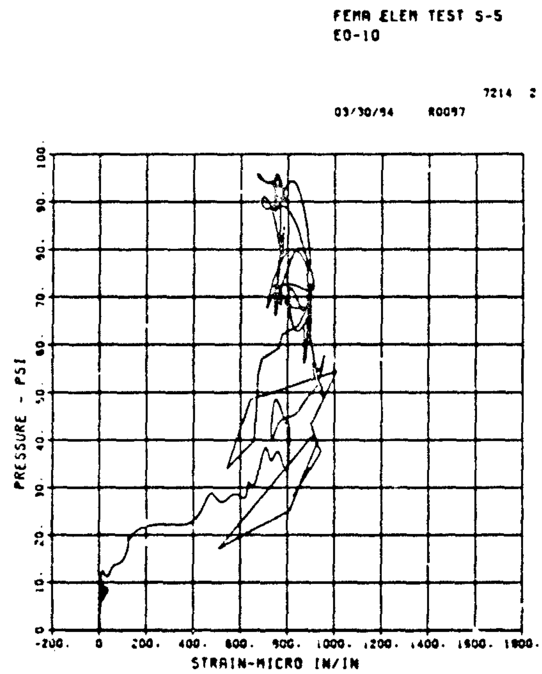
FEMA ELEM TEST S-5
EO-10
7214 2
03/30/84 R0097
PRESSURE - PSI
STRAIN-MICRO IN/IN

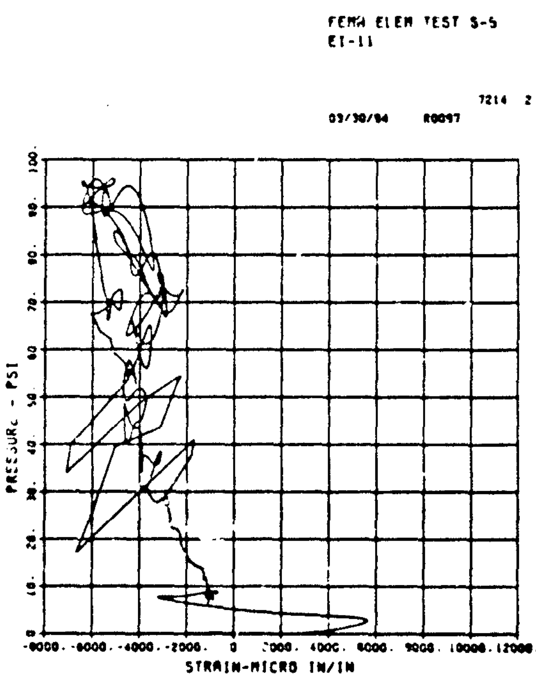
FEMA ELEM TEST S-5
EI-11
7214 2
03/30/84 R0097
PRESSURE - PSI
STRAIN-MICRO IN/IN

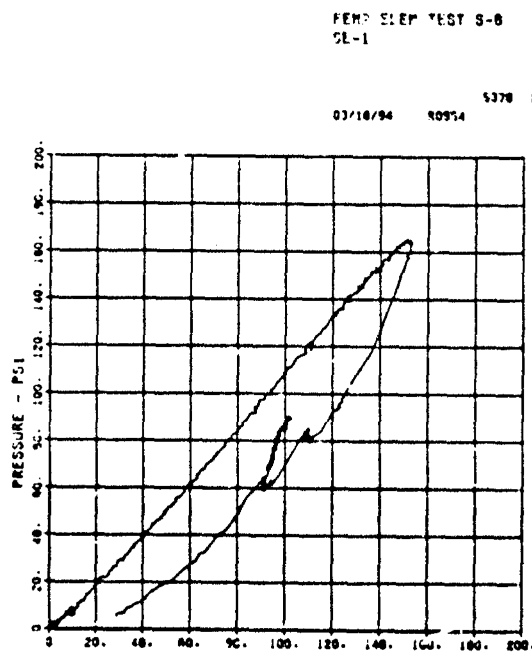
PRESSURE - PSI
PRESSURE - PSI

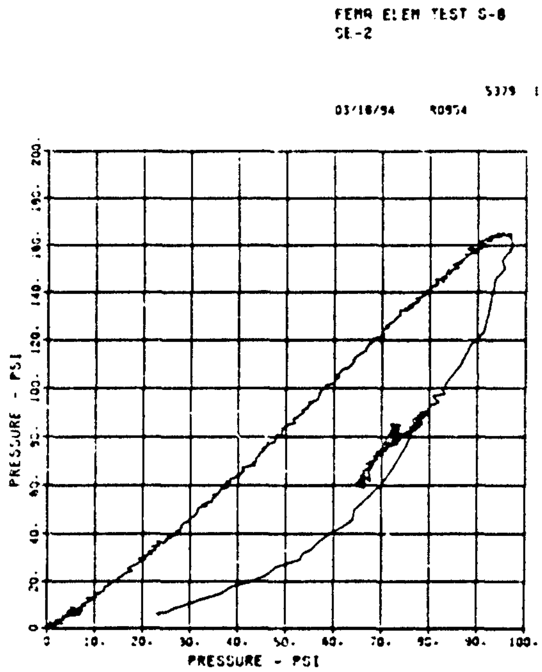
FEMA ELEM TEST S-8
SE-2
03/18/94
PRESSURE - PSI
PRESSURE - PSI

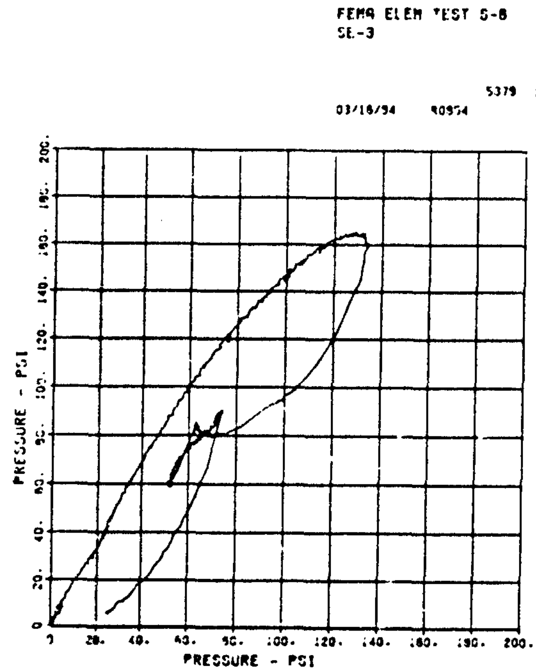
FEMA ELEM TEST S-8
SE-3
03/18/94
PRESSURE - PSI
PRESSURE - PSI

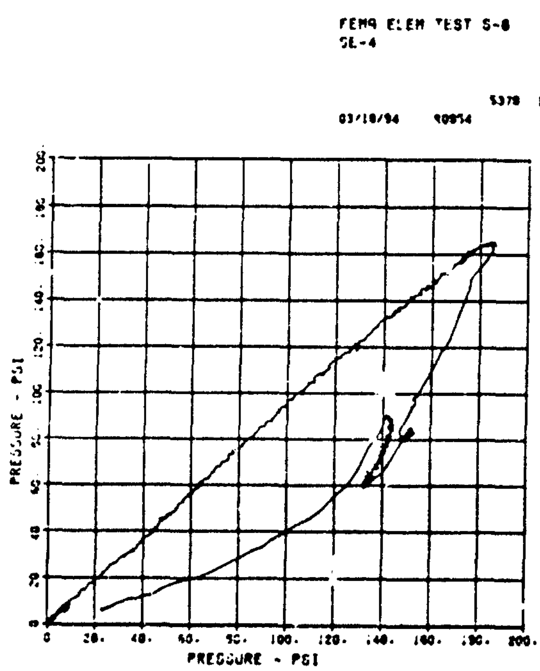
FEMA ELEM TEST S-8
SE-4
03/18/94
PRESSURE - PSI
PRESSURE - PSI

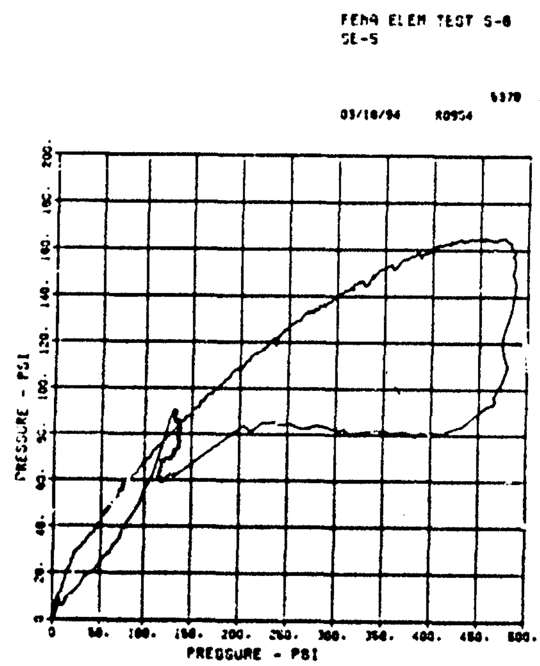
FEMA ELEM TEST S-8
SE-5
03/18/94
PRESSURE - PSI
PRESSURE - PSI

FEMA ELEM TEST S-6
D-1

5378 1
03/18/94 90954

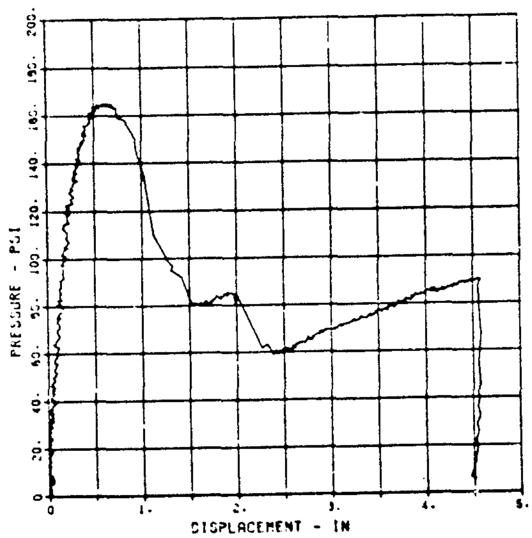

FEMA ELEM TEST S-6
IF-1

5378 1
03/18/94 90954

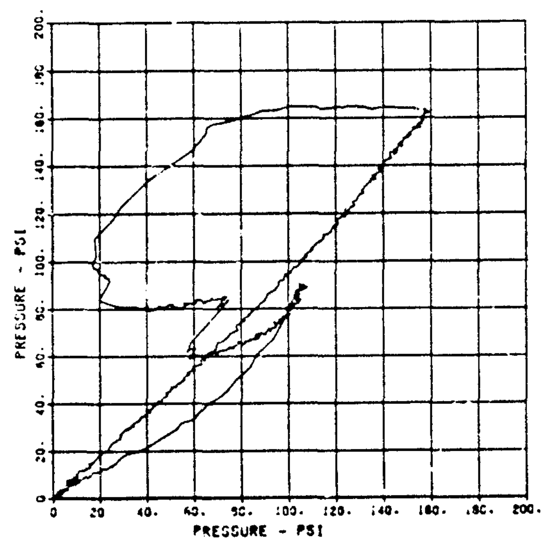

FEMA ELEM TEST S-6
IF-2

5378 1
03/18/94 90954

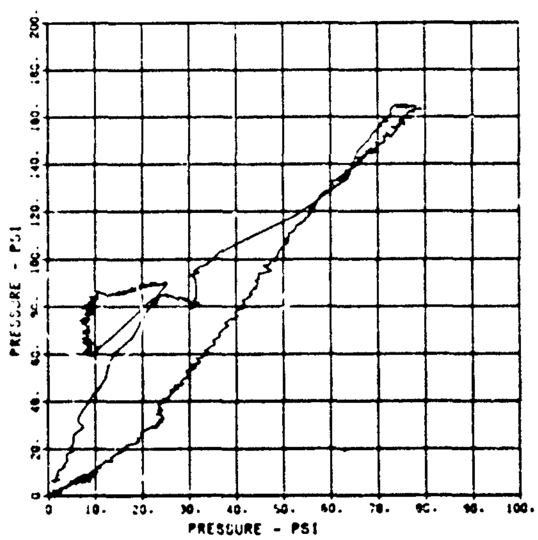

FEMA ELEM TEST S-6
IF-3

5378 1
03/18/94 90954

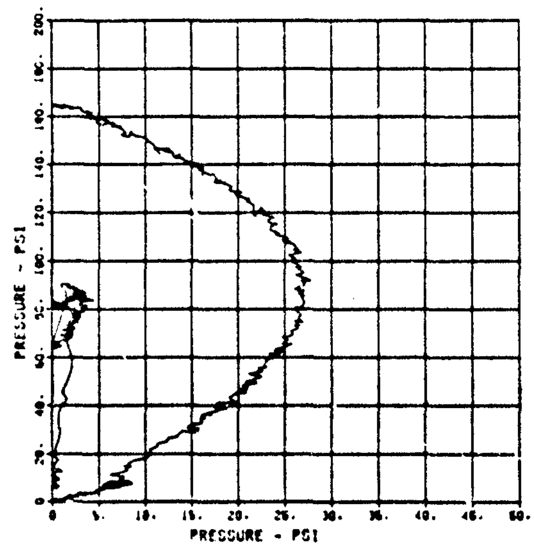

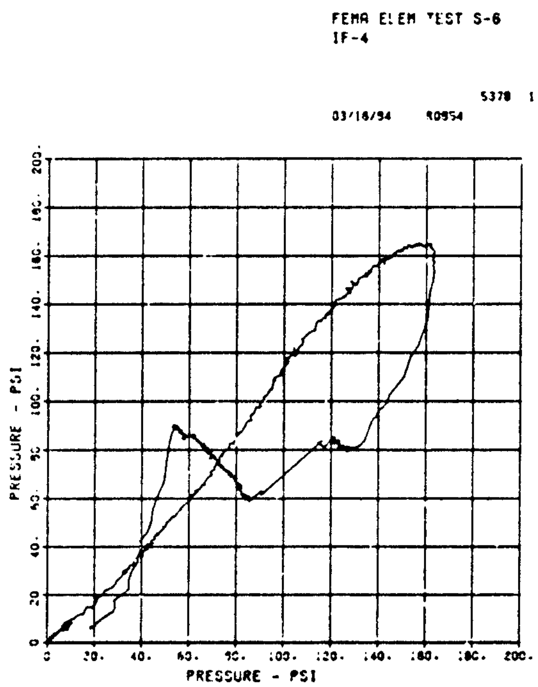
FEMA ELEM TEST S-6
IF-4
5378 1
03/18/94 R0954
PRESSURE - PSI
PRESSURE - PSI

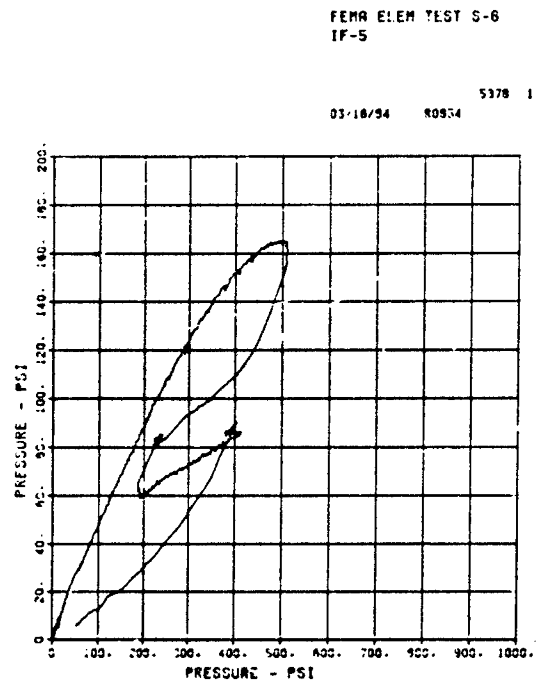
FEMA ELEM TEST S-6
IF-5
5378 1
03/18/94 R0954
PRESSURE - PSI
PRESSURE - PSI

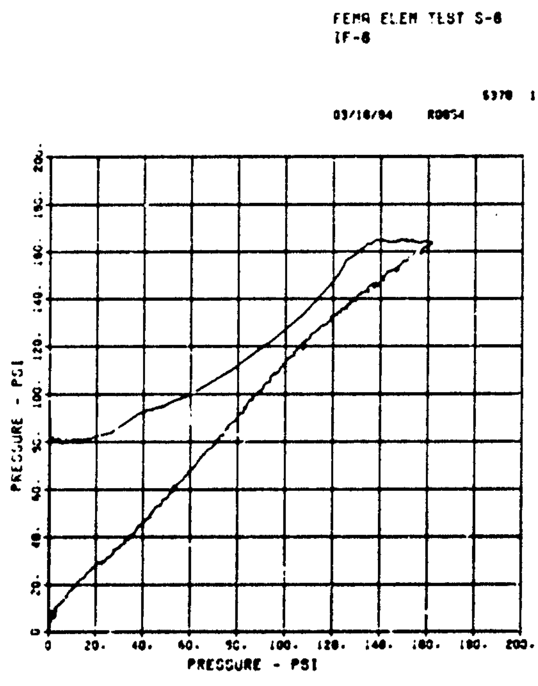
FEMA ELEM TEST S-6
IF-6
5378 1
03/18/94 R0954
PRESSURE - PSI
PRESSURE - PSI

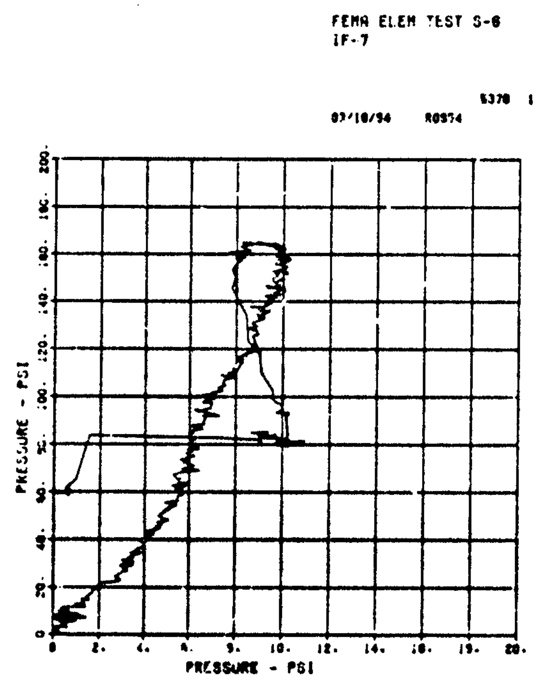
FEMA ELEM TEST S-6
IF-7
5378 1
03/18/94 R0954
PRESSURE - PSI
PRESSURE - PSI

FEMA ELEM TEST S-6
IF-9

5379 1
03/16/94 50954

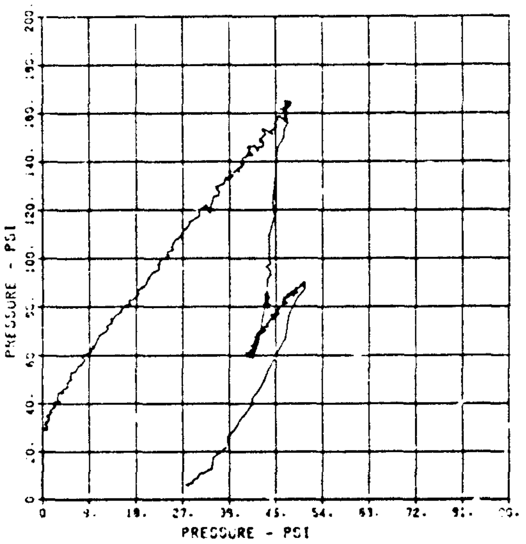

FEMA ELEM TEST S-6
IF-3

5379 1
03/16/94 50954

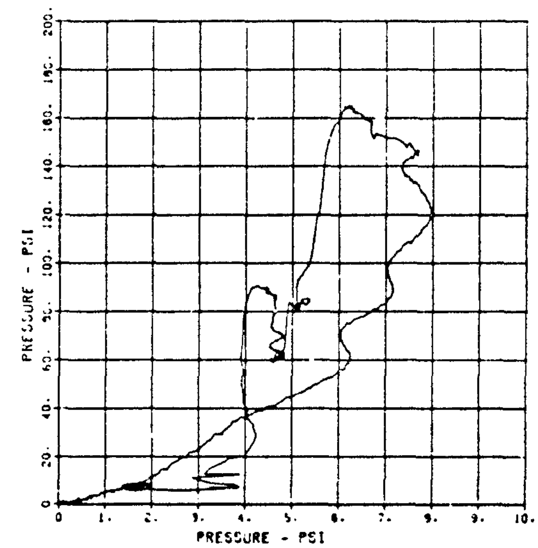

FEMA ELEM TEST S-6
IF-11

5378 1
03/16/94 50954

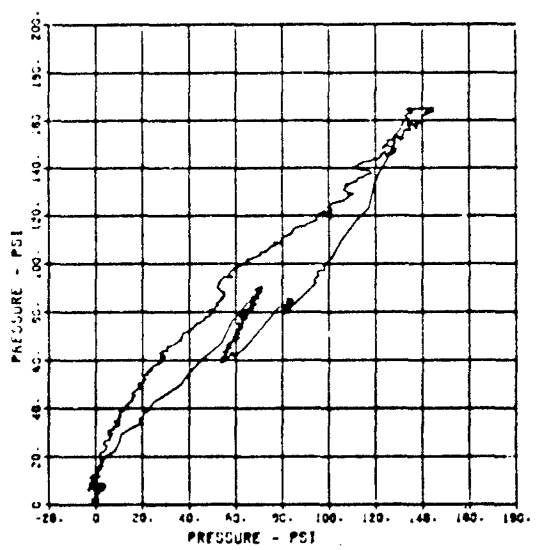

FEMA ELEM TEST S-6
EO-1

5378 1
04/13/84 80279

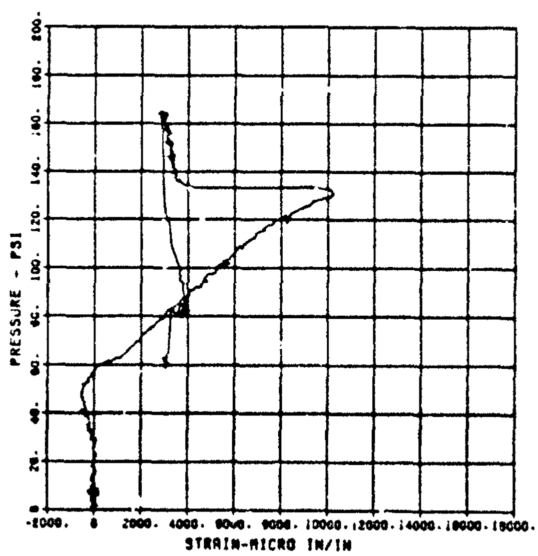

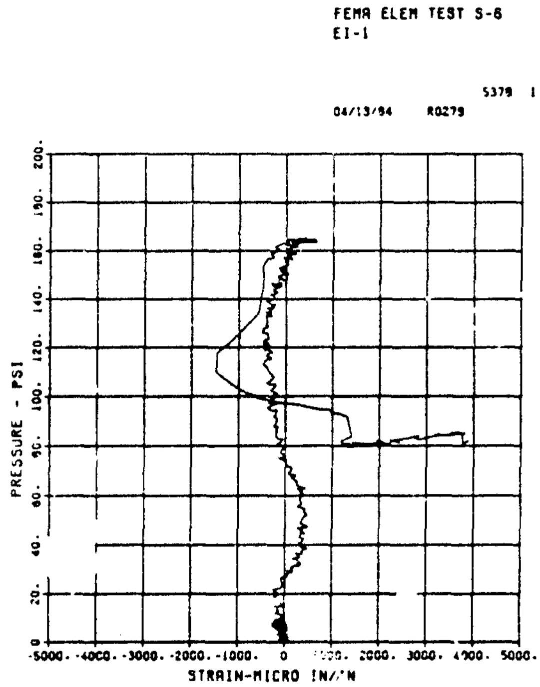
FEMA ELEM TEST S-6
EI-1
5379 1
04/13/94 R0279
PRESSURE - PSI
STRAIN-MICRO IN/IN

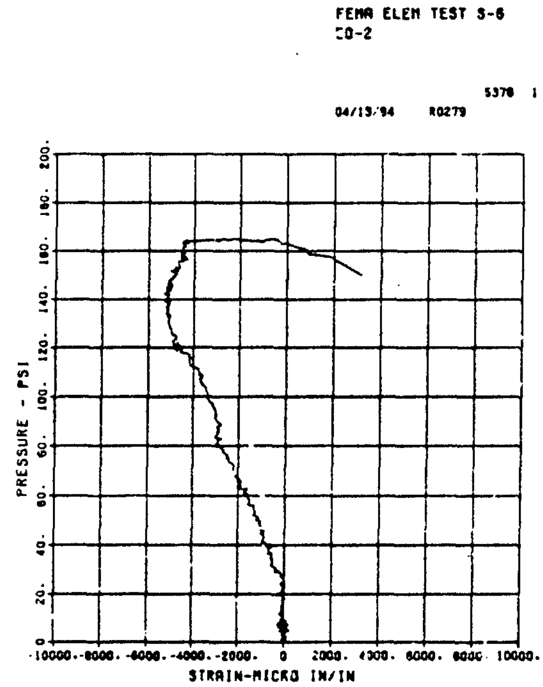
FEMA ELEM TEST S-6
EO-2
5378 1
04/13/94 R0279
PRESSURE - PSI
STRAIN-MICRO IN/IN

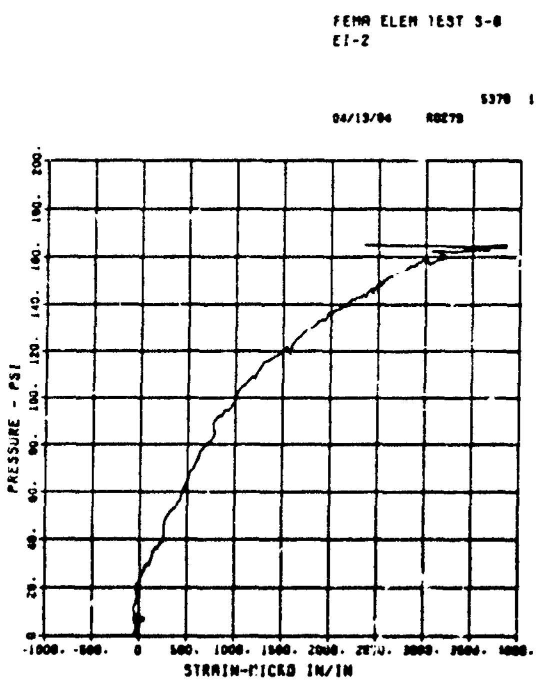
FEMA ELEM TEST S-6
EI-2
5379 1
04/13/94 R0279
PRESSURE - PSI
STRAIN-MICRO IN/IN

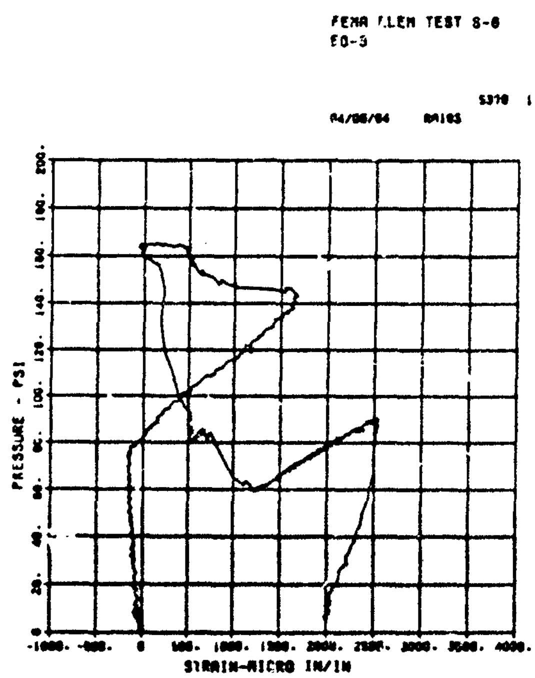
FEMA ELEM TEST S-6
EO-3
PRESSURE - PSI
STRAIN-MICRO IN/IN

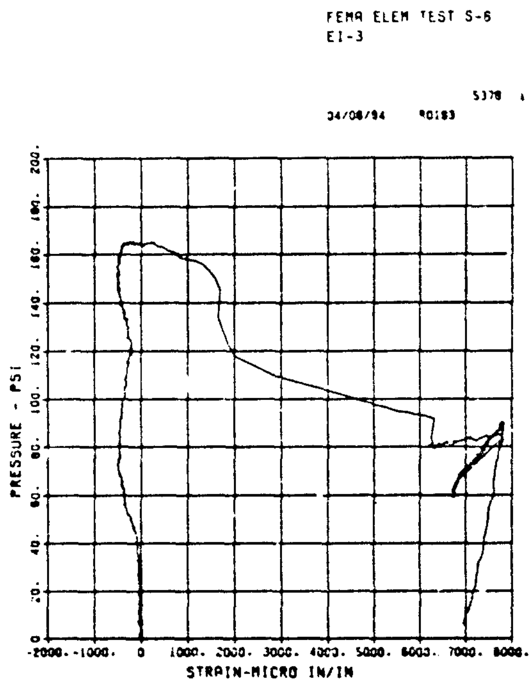
FEMA ELEM TEST S-6
EI-3
PRESSURE - PSI
STRAIN-MICRO IN/IN

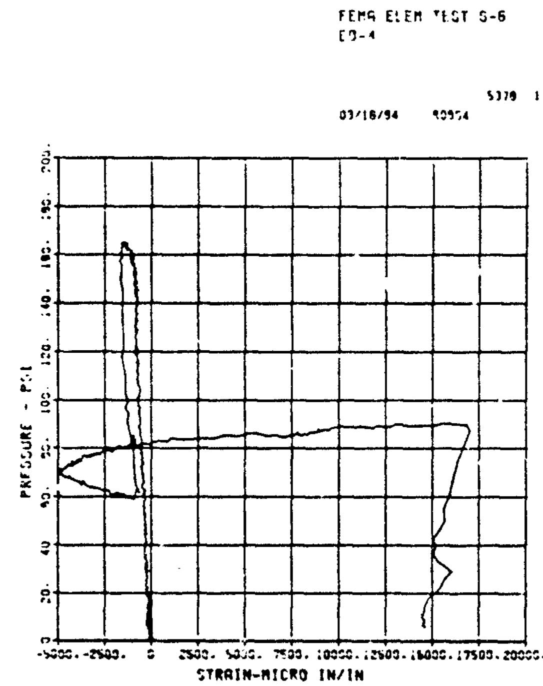
FEMA ELEM TEST S-6
PRESSURE - PSI
STRAIN-MICRO IN/IN

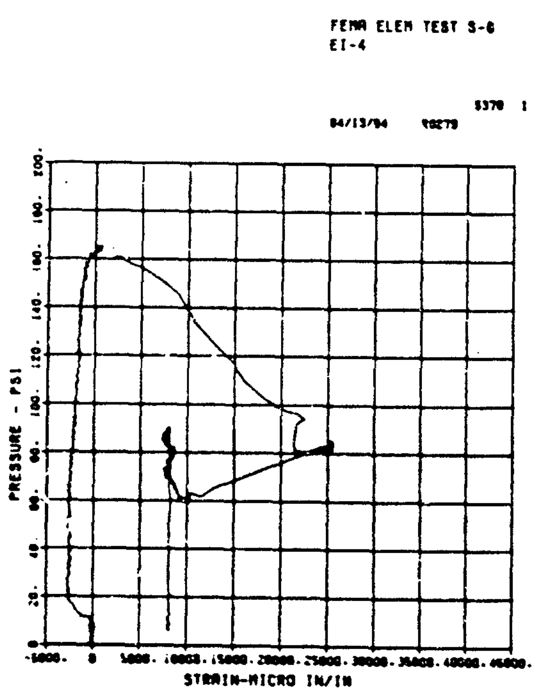
FEMA ELEM TEST S-6
EI-4
PRESSURE - PSI
STRAIN-MICRO IN/IN

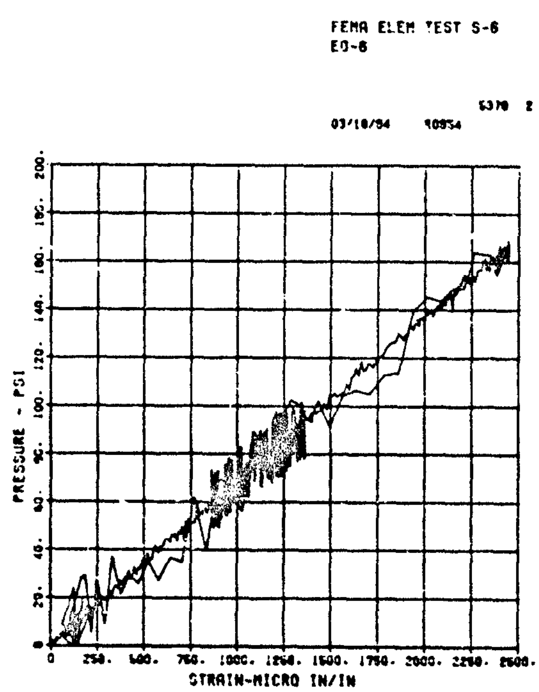
FEMA ELEM TEST S-6
EO-6
PRESSURE - PSI
STRAIN-MICRO IN/IN

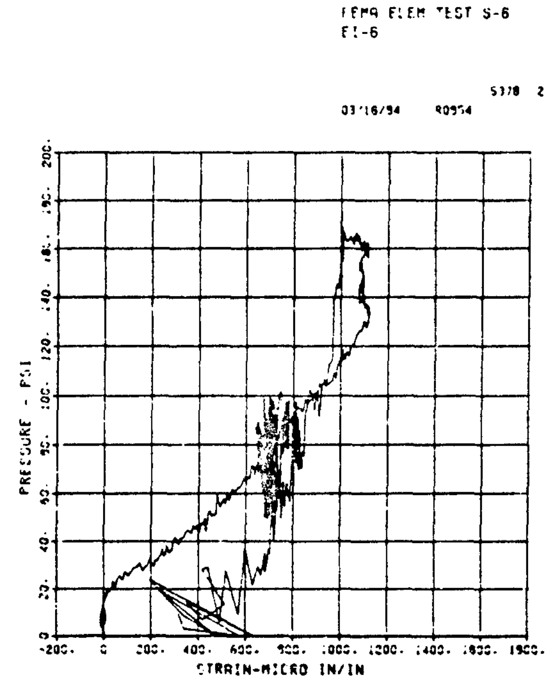
FEMA ELEM TEST S-6
EI-6
5378 2
03/16/84 R0954
PRESSURE - PSI
STRAIN-MICRO IN/IN

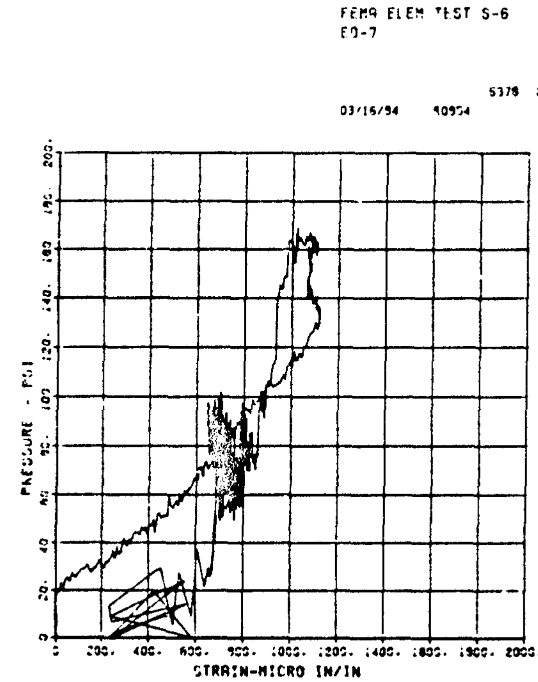
FEMA ELEM TEST S-6
EO-7
5378 2
03/16/84 R0954
PRESSURE - PSI
STRAIN-MICRO IN/IN

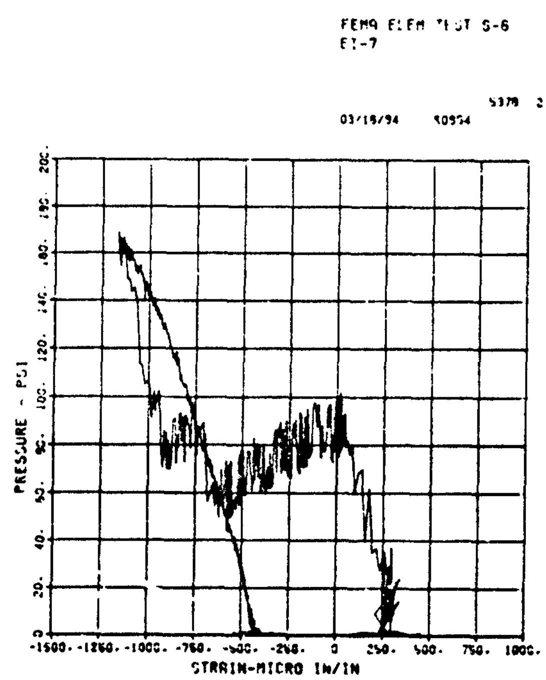
FEMA ELEM TEST S-6
EI-7
5378 2
03/16/84 R0954
PRESSURE - PSI
STRAIN-MICRO IN/IN

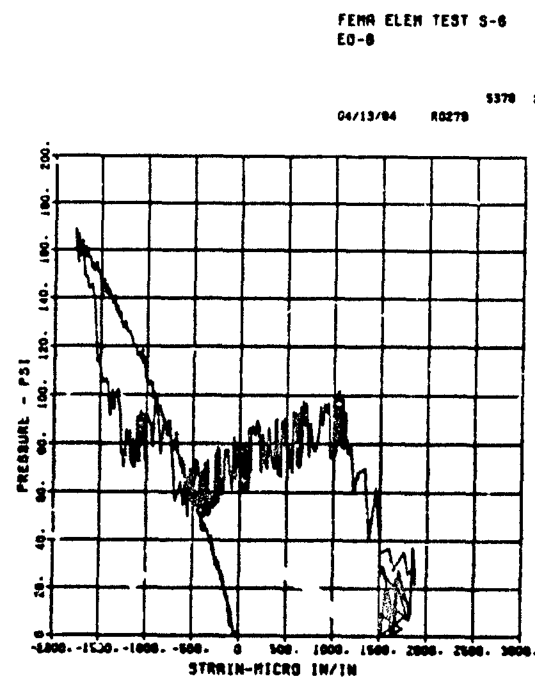
FEMA ELEM TEST S-6
EO-8
5378 2
04/13/84 R0278
PRESSURE - PSI
STRAIN-MICRO IN/IN

FEMA ELEM TEST S-6
EO-9

5378 2
04/06/84 R0183

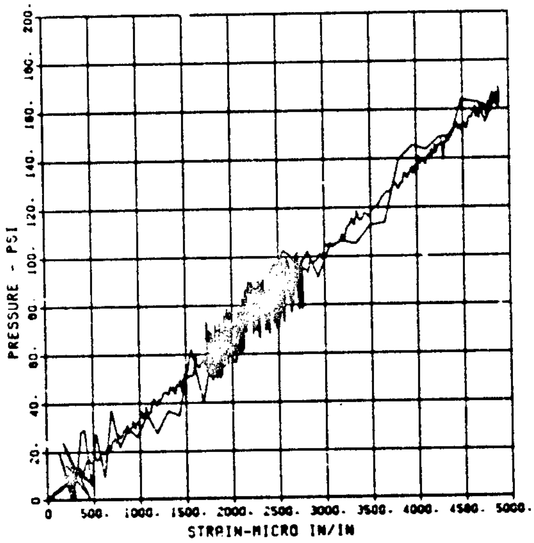

FEMA ELEM TEST S-6
EI-9

5379 2
04/13/84 R0279

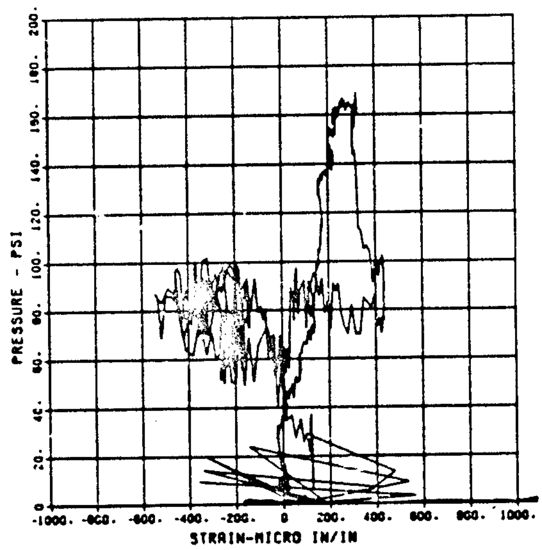

FEMA ELEM TEST S-6
EO-10

5378 2
03/16/84 R0954

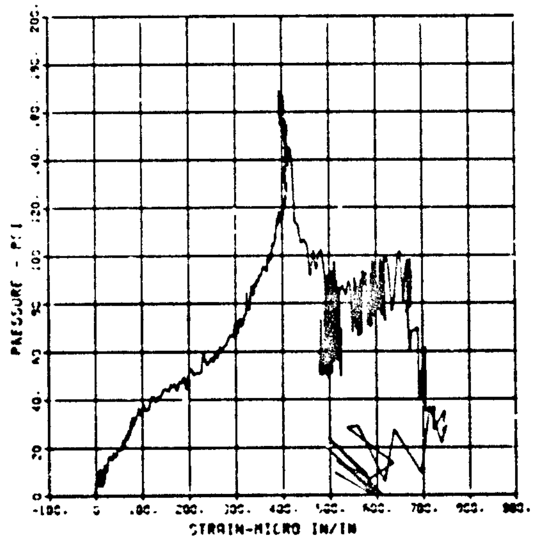

FEMA ELEM TEST S-6
EI-10

5378 2
04/13/84 R0279

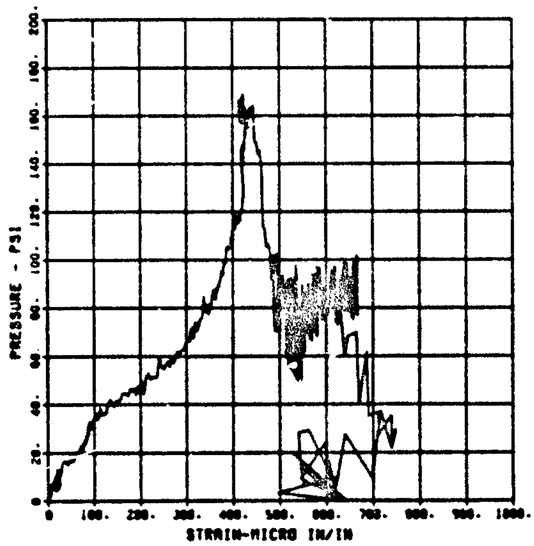

FEMA ELEM TEST S-7
SE-1

17779 2
04/02/84 R0106

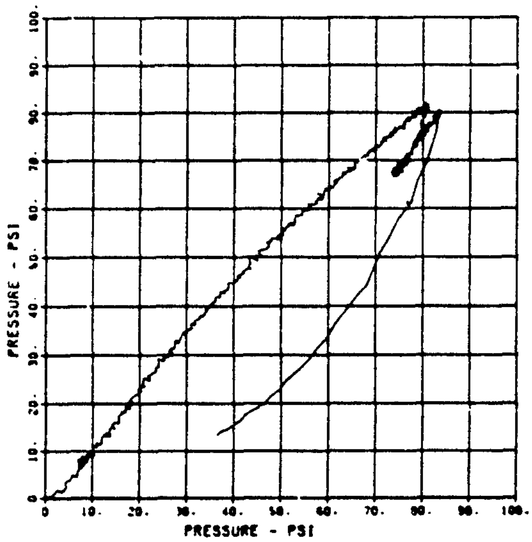

FEMA ELEM TEST S-7
SE-2

17779 2
04/02/84 R0106

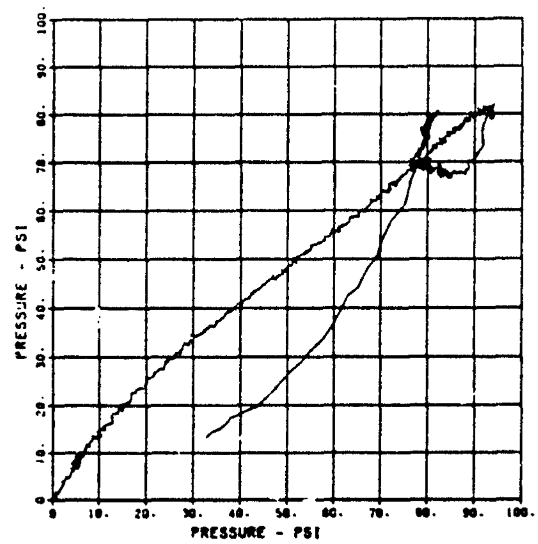

FEMA ELEM TEST S-7
SE-3

17779 2
04/02/84 R0106

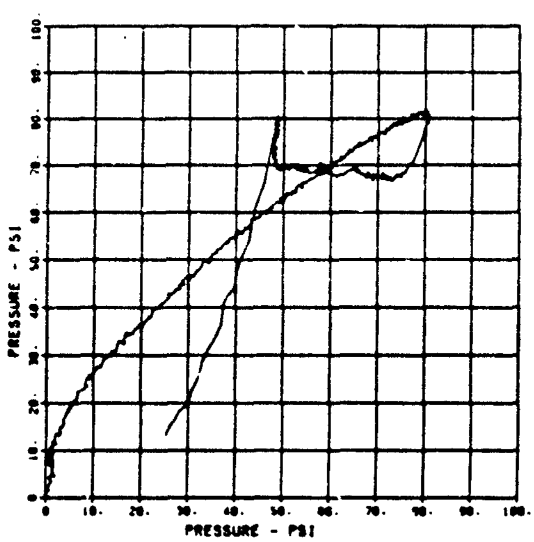

FEMA ELEM TEST S-7
SE-4

17779 2
04/02/84 R0106

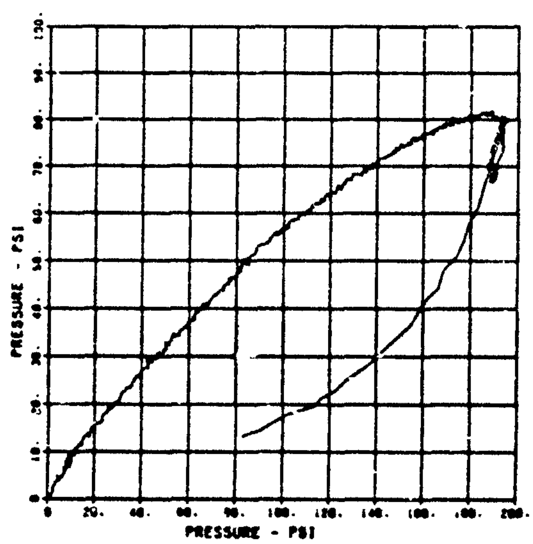

FEMA ELEM TEST S-7
SE-6

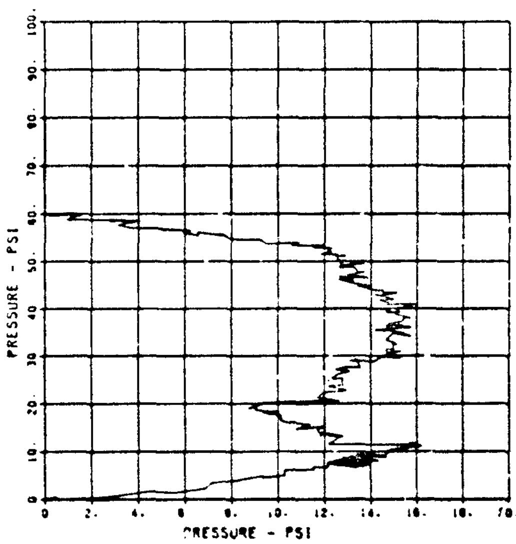

FEMA ELEM TEST S-7
D-1

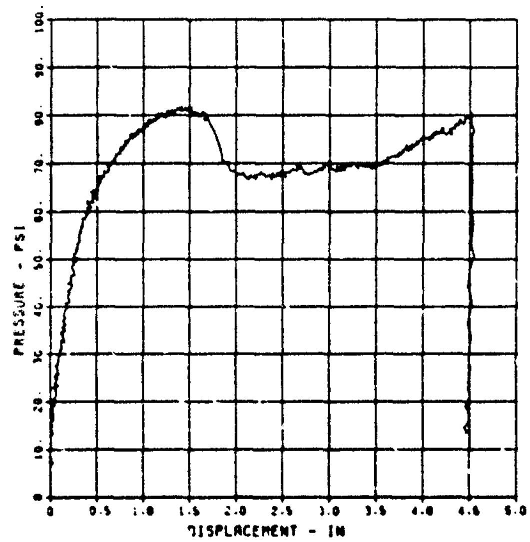

FEMA ELEM TEST S-7
IF-1

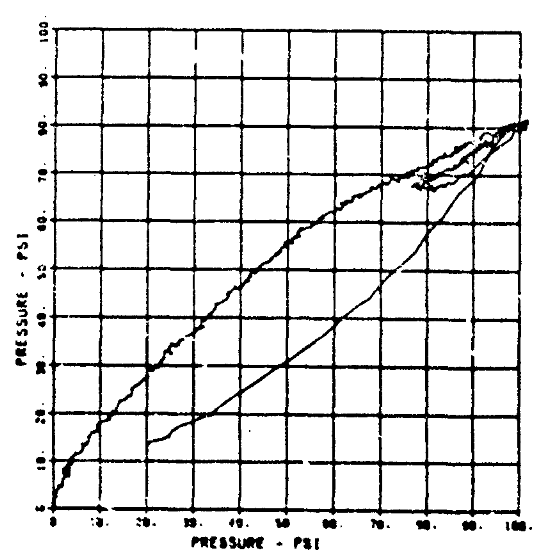

FEMA ELEM TEST S-7
IF-2

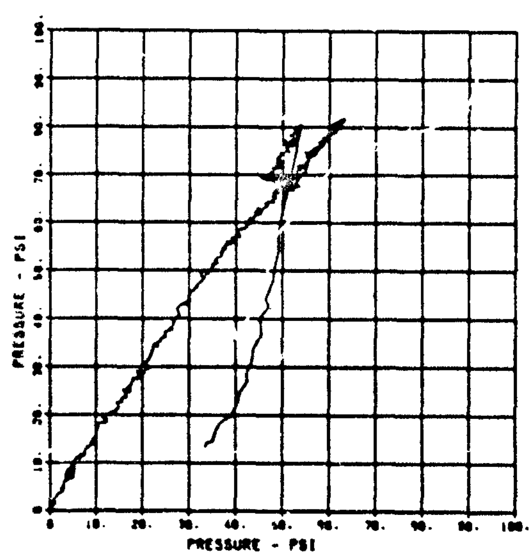

FEMA ELEM TEST S-7
IF-4

17779 2
04/02/84 R0106

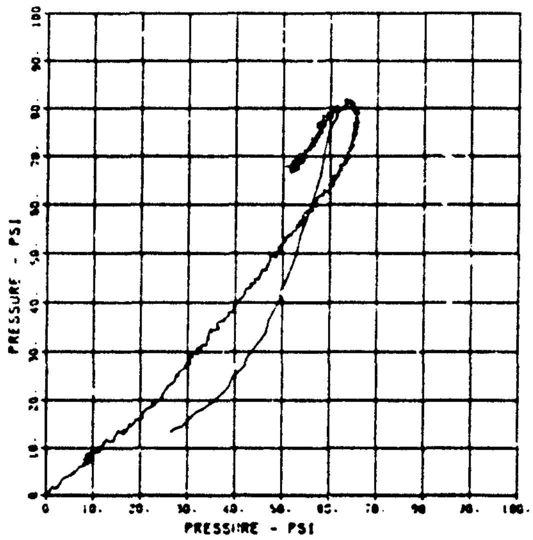

FEMA ELEM TEST S-7
IF-6

17779 2
04/02/84 R0106

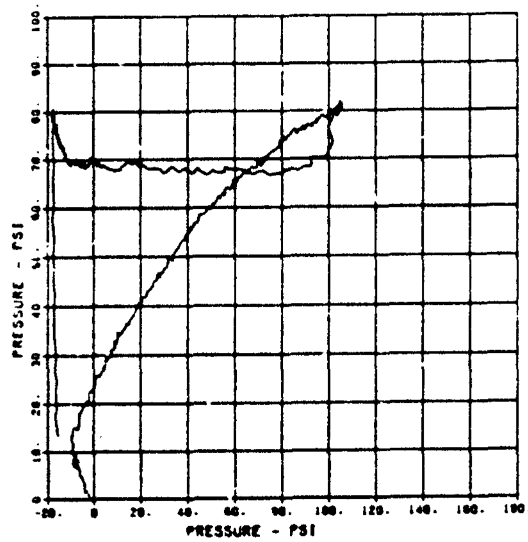

FEMA ELEM TEST S-7
IF-7

17779 2
04/02/84 R0106

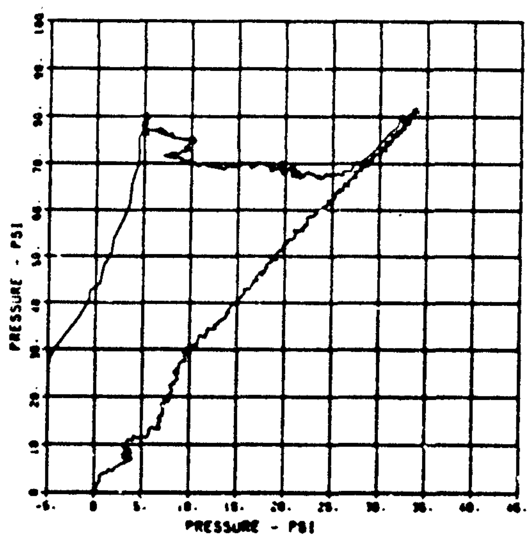

FEMA ELEM TEST S-7
IF-8

17779 2
04/02/84 R0106

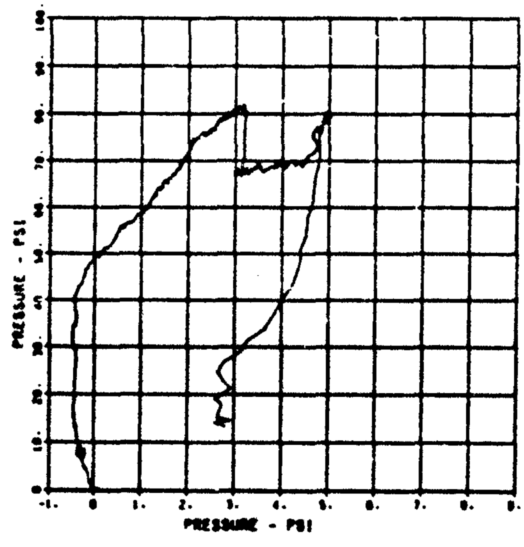

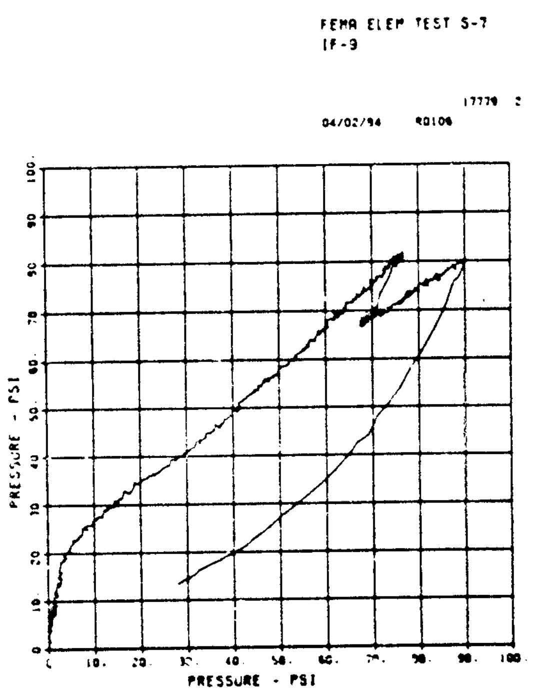

FEMA ELEM TEST S-7
IF-9
17779 2
04/02/94 R0106
PRESSURE - PSI
PRESSURE - PSI

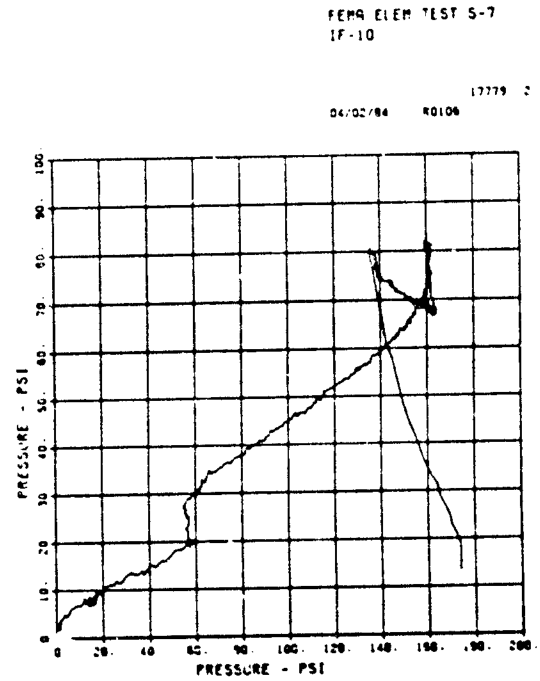

FEMA ELEM TEST S-7
IF-10
17779 2
04/02/84 R0106
PRESSURE - PSI
PRESSURE - PSI

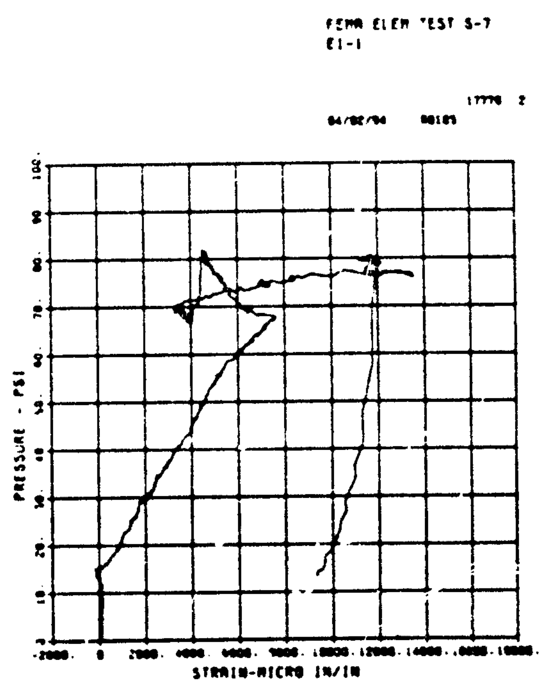

FEMA ELEM TEST S-7
EI-1
17779 2
PRESSURE - PSI
STRAIN-MICRO IN/IN

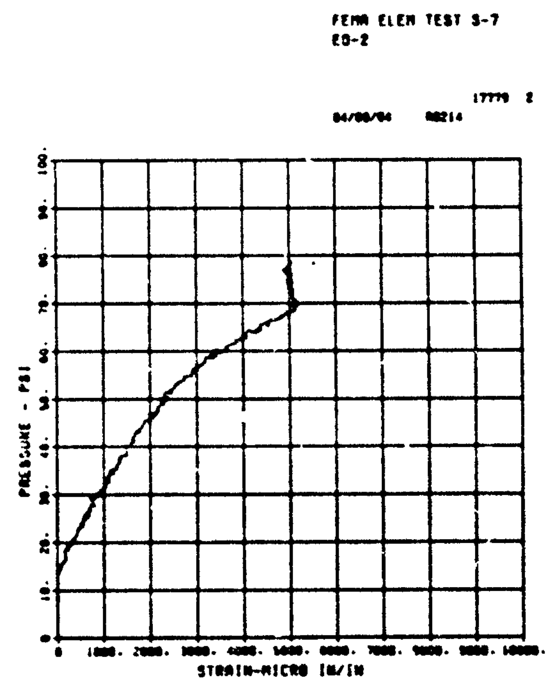

FEMA ELEM TEST S-7
EO-2
17779 2
PRESSURE - PSI
STRAIN-MICRO IN/IN

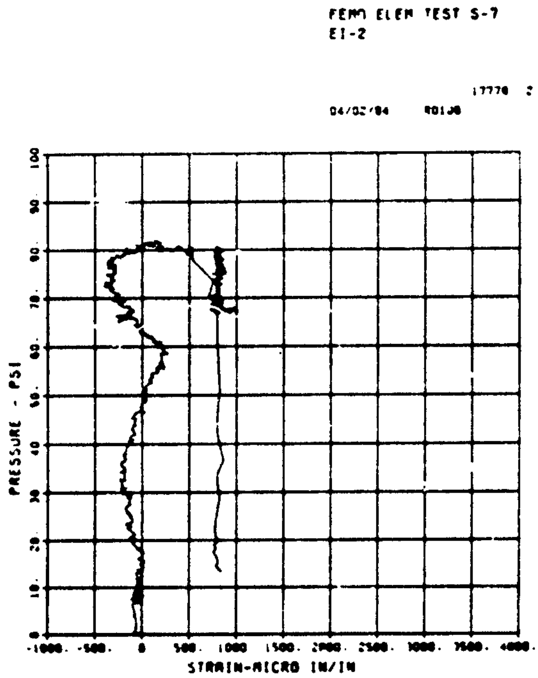
FEMA ELEM TEST S-7
EI-2
PRESSURE - PSI
STRAIN-MICRO IN/IN

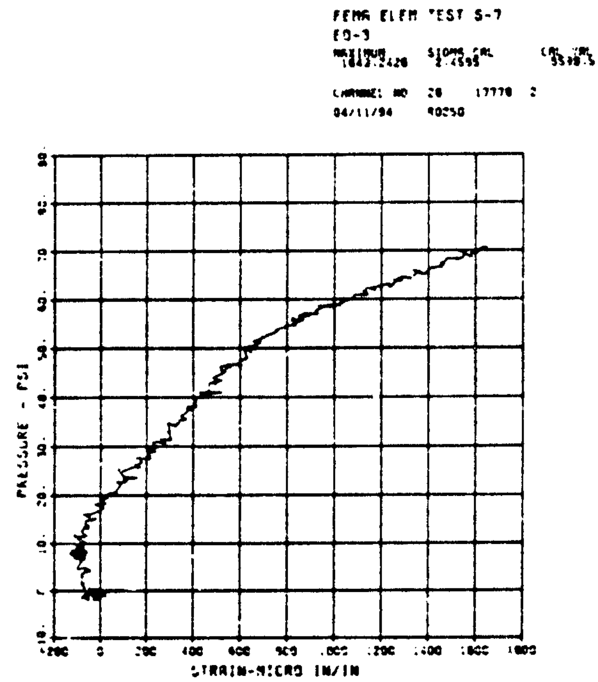
FEMA ELEM TEST S-7
EO-3
PRESSURE - PSI
STRAIN-MICRO IN/IN

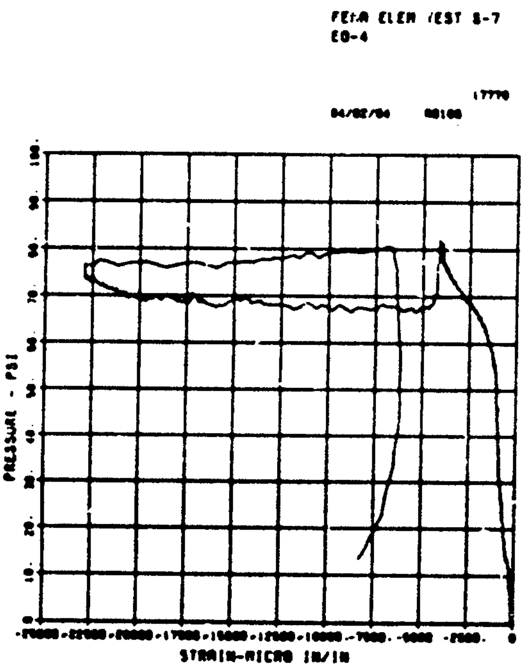
FEMA ELEM TEST S-7
EO-4
PRESSURE - PSI
STRAIN-MICRO IN/IN

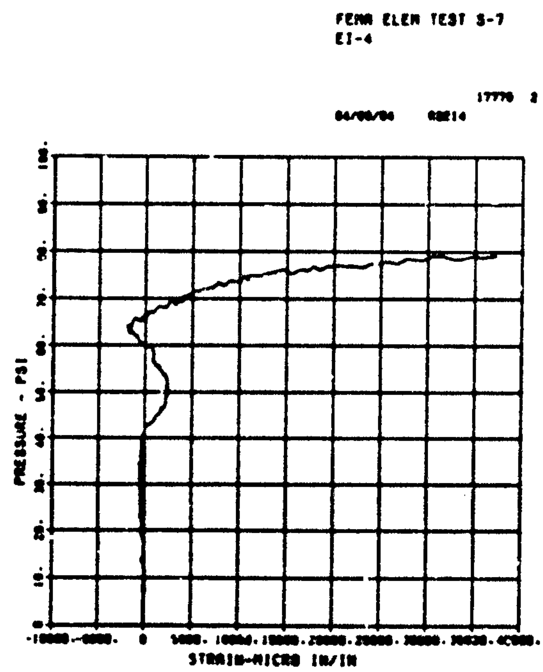
FEMA ELEM TEST S-7
EI-4
PRESSURE - PSI
STRAIN-MICRO IN/IN

FEMA ELEM TEST S-7
EO-5

17779 2
04/02/84 R0100

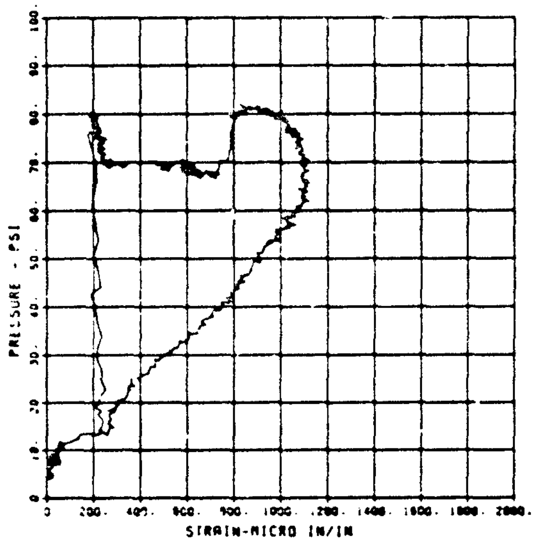

FEMA ELEM TEST S-7
EI-5

17779 1
04/02/84 R0100

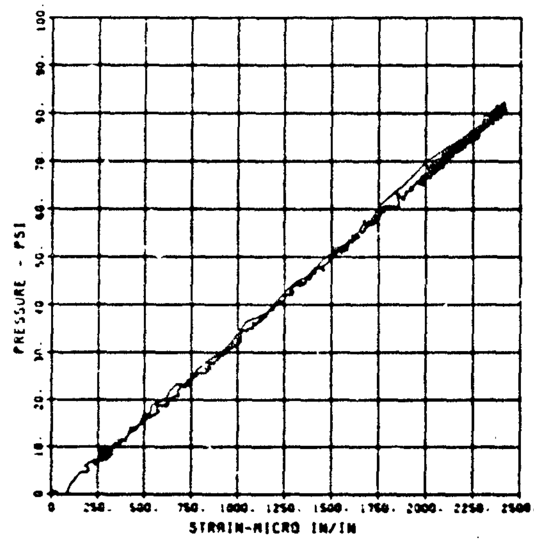

FEMA ELEM TEST S-7
EO-6

17779 1
04/02/84 R0100

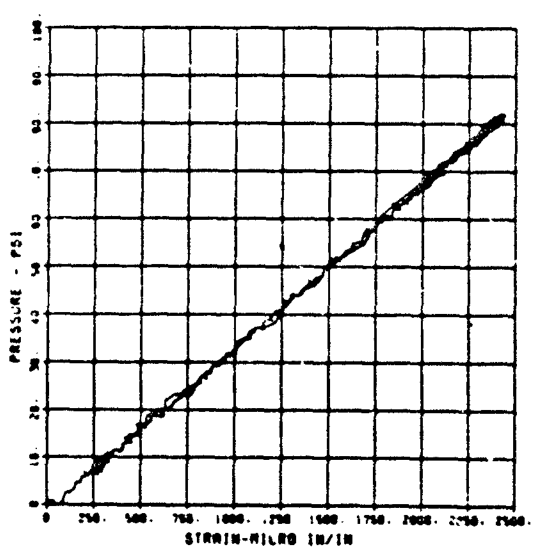

FEMA ELEM TEST S-7
EI-6

17779 1
04/02/84 R0100

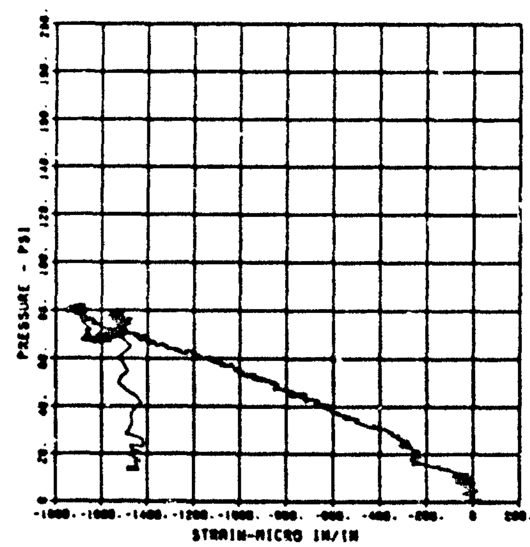

FEMA ELEM TEST S-7
E0-7

17778 1
04/02/84 R0106

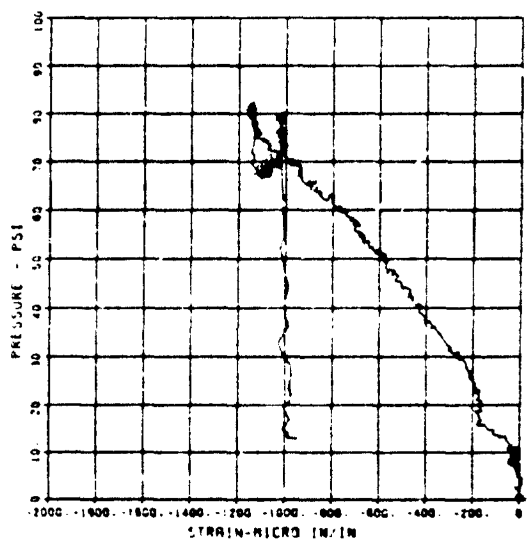

FEMA ELEM TEST S-7
EI-7

17778 1
04/02/84 R0106

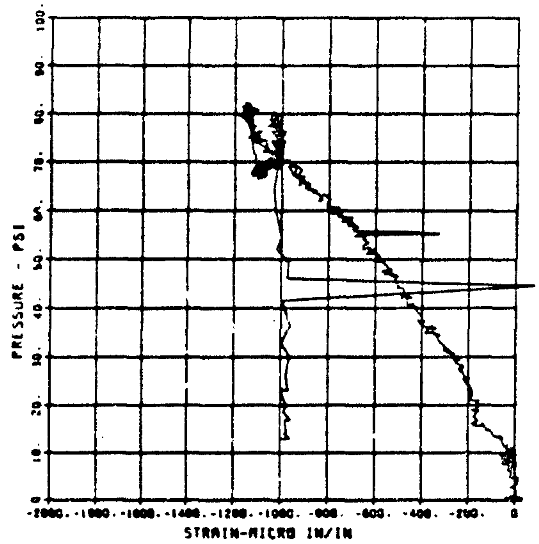

FEMA ELEM TEST S-7
E0-8

17778 1
04/02/84 R0106

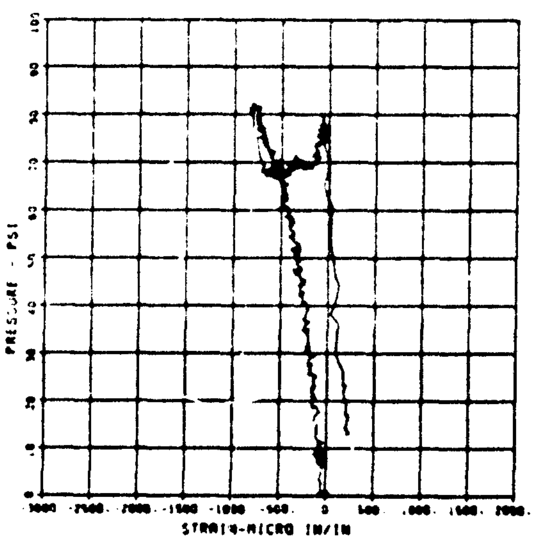

FEMA ELEM TEST S-7
EI-8

17778 1
04/02/84 R0106

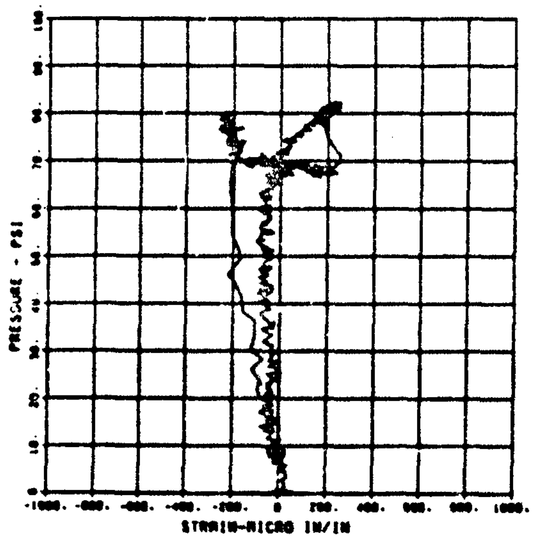

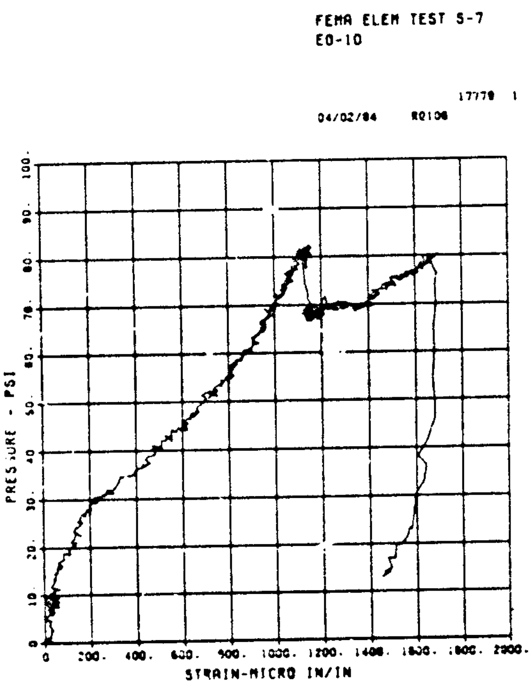
FEMA ELEM TEST S-7
EO-10
17778 1
04/02/84 R0106
PRESSURE - PSI
STRAIN-MICRO IN/IN

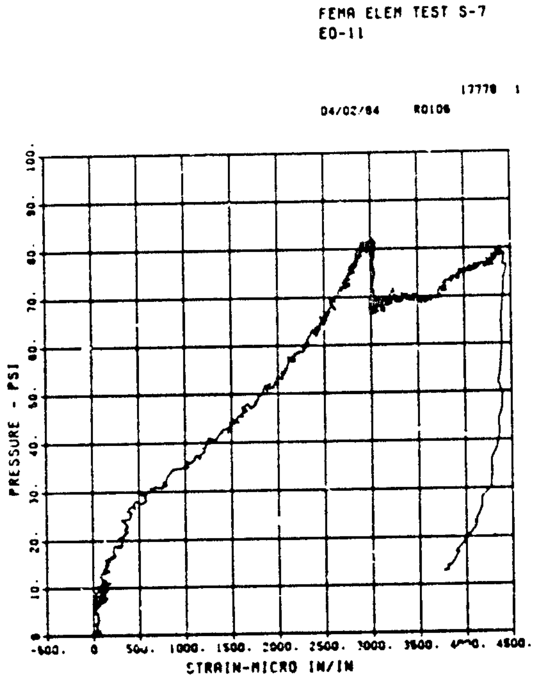
FEMA ELEM TEST S-7
EO-11
17778 1
04/02/84 R0106
PRESSURE - PSI
STRAIN-MICRO IN/IN

DISTRIBUTION LIST

Director, Federal Emergency Management Agency
ATTN: Mr. Tom Provenzano (25 Cys)
500 C St. SW
Washington, DC 20472

Commander, US Army Engineer District, Wilmington
ATTN: Pat Burns/Library
PO Box 1890
Wilmington, N. C. 28402

Headquarters, Department of Energy
ATTN: Library/G-049 MA-232.2/GTN
Washington, DC 20545

National Bureau of Standards
ATTN: Mr. Samuel Kramer
Dr. Lewis V. Spencer
Washington, DC 20234

Associate Director, Natural Resources and Commercial Services
Office of Science & Technology
ATTN: Mr. Phillip M. Smith
Executive Office Building
Washington, DC 20500

Director, Office of Administration
Program Planning and Control
Department of Housing and Urban Development
ATTN: Mr. Bert Greenglass
Washington, DC 20410

Director, Defense Nuclear Agency
ATTN: SPTD/Mr. Tom Kennedy
STTL/Technical Library
Washington, DC 20305

Director, Defense Intelligence Agency
ATTN: Mr. Carl Wiehle (DB-4C2)
Washington, DC 20301

Assistant Secretary of the Army (R&D)
ATTN: Assistant for Research
Washington, DC 20301

Office, Chief of Engineers,
Department of the Army
ATTN: DAEN-RDZ-A
DAEN-ECE-D
Washington, DC 20314

Sandia Corporation
ATTN: Dr. Clarence R. Mehl
Dept. 5230
Box 5800, Sandia Base
Albuquerque, N. Mex. 87115

Director, US Army Engineer Waterways Experiment Station
ATTN: Dr. S. A. Kiger
Mr. Bill Huff
Mr. Stan Woodson
3 cys Library
P. O. Box 631
Vicksburg, Miss. 39180

Defense Technical Information Center
12 cy ATTN: (DTIC-DDAB/Mr. Myer B. Kahn)
Cameron Station
Alexandria, Va. 22314

Commander, US Army Materials and Mechanics Research Center
ATTN: Technical Library
Watertown, Mass. 02172

Command and Control Technical Center
Department of Defense
Room 2E312 Pentagon
Washington, DC 20301

Los Alamos Scientific Laboratory
ATTN: Report Library MS-364
PO Box 1663
Los Alamos, N. Mex. 87544

Director, Ballistic Research Laboratory
ATTN: (DRXBR-TBD/Mr. George Coulter)
Aberdeen Proving Ground, Md. 21005

Commanding Officer, Office of Naval Research
Department of the Navy
Washington, DC 20390

Commanding Officer
US Naval Civil Engineering Laboratory
Naval Construction Battalion Center
ATTN: Library (Code L08A)
Port Hueneme, Calif. 93043

Commander, Air Force Weapons Laboratory/SUL
ATTN: Technical Library
Kirtland Air Force Base, N. Mex. 87117

Civil Engineering Center
AF/PRECET
Tyndall AFB, Fla. 32403

University of Florida
Civil Defense Technical Services
College of Engineering
Department of Engineering
Gainesville, Fla. 32601

Technical Reports Library
Kurt F. Wendt Library
College of Engineering
University of Wisconsin
Madison, Wisc. 53706

Agbabian Associates
250 N. Nash Street
El Segundo, Calif. 90245

AT&T Bell Laboratories
ATTN: Mr. E. Witt
Whippany, N. J. 07981

James E. Beck & Associates
4216 Los Palos Avenue
Palo Alto, Calif. 94306

Chamberlain Manufacturing Corp.
GARD, Inc.
7449 N. Natches Avenue
Niles, Ill. 60648

IIT Research Institute
ATTN: Mr. A. Longinow
10 West 35th Street
Chicago, Ill. 60616

H. L. Murphy Associates
Box 1727
San Mateo, Calif. 94401

RAND Corporation
ATTN: Document Library
1700 Main Street
Santa Monica, Calif. 90401

Research Triangle Institute
ATTN: Mr. Edward L. Hill
PO Box 12194
Research Triangle Park, N. C. 27709

Scientific Services, Inc.
517 East Bayshore Drive
Redwood City, Calif. 94060

US Army Engineer Division, Huntsville
ATTN: Mr. Paul Lahoud (10 cys)
PO Box 1600, West Station
Huntsville, AL 35807

STRUCTURAL ELEMENT TESTS IN SUPPORT OF THE KEYWORKER BLAST SHELTER PROGRAM.
Unclassified, US Army Engineer Waterways Experiment Station, October 1985, 321 pp.

At the initiation of this study, civil defense planning called for the evacuation of nonessential personnel to safe host areas during a time of crisis, and the construction of shelters to protect the keyworkers remaining behind. The Federal Emergency Management Agency tasked the US Army Engineer Division, Huntsville (HND), to design a 100-man keyworker shelter. The research documented in this report is in support of the HND design effort.

Six static tests and twelve dynamic tests were conducted on approximately 1/4-scale models of blast shelters. Specific objectives of these tests were to evaluate the preliminary structural design, to investigate structural response in various backfills, to investigate and recommend minimum concrete strength requirements, to evaluate structural response calculations, and to develop a data base on repeated hits so that structural response computational procedures can be developed to include the effects of repeated hits.

Test results indicate that the keyworker blast shelter design will resist a peak overpressure of 150 psi from a 1-MT nuclear weapon. Based on the results of this series of static and dynamic tests, it is recommended that: (1) minimum strength of concrete used in the keyworker blast shelter should be 3,000 psi; (2) backfill specifications can be reduced to include soils with a minimum angle of internal friction of 25° (30° for foundation materials); (3) a minimum depth of burial of 4 ft (30 percent of the unsupported roof span) should be used; (4) the interior structural steel frames should be replaced with precast or cast-in-place reinforced concrete walls.

STRUCTURAL ELEMENT TESTS IN SUPPORT OF THE KEYWORKER BLAST SHELTER PROGRAM.
Unclassified, US Army Engineer Waterways Experiment Station, October 1985, 321 pp.

At the initiation of this study, civil defense planning called for the evacuation of nonessential personnel to safe host areas during a time of crisis, and the construction of shelters to protect the keyworkers remaining behind. The Federal Emergency Management Agency tasked the US Army Engineer Division, Huntsville (HND), to design a 100-man keyworker shelter. The research documented in this report is in support of the HND design effort.

Six static tests and twelve dynamic tests were conducted on approximately 1/4-scale models of blast shelters. Specific objectives of these tests were to evaluate the preliminary structural design, to investigate structural response in various backfills, to investigate and recommend minimum concrete strength requirements, to evaluate structural response calculations, and to develop a data base on repeated hits so that structural response computational procedures can be developed to include the effects of repeated hits.

Test results indicate that the keyworker blast shelter design will resist a peak overpressure of 150 psi from a 1-MT nuclear weapon. Based on the results of this series of static and dynamic tests, it is recommended that: (1) minimum strength of concrete used in the keyworker blast shelter should be 3,000 psi; (2) backfill specifications can be reduced to include soils with a minimum angle of internal friction of 25° (30° for foundation materials); (3) a minimum depth of burial of 4 ft (30 percent of the unsupported roof span) should be used; (4) the interior structural steel frames should be replaced with precast or cast-in-place reinforced concrete walls.

STRUCTURAL ELEMENT TESTS IN SUPPORT OF THE KEYWORKER BLAST SHELTER PROGRAM.
Unclassified, US Army Engineer Waterways Experiment Station, October 1985, 321 pp.

At the initiation of this study, civil defense planning called for the evacuation of nonessential personnel to safe host areas during a time of crisis, and the construction of shelters to protect the keyworkers remaining behind. The Federal Emergency Management Agency tasked the US Army Engineer Division, Huntsville (HND), to design a 100-man keyworker shelter. The research documented in this report is in support of the HND design effort.

Six static tests and twelve dynamic tests were conducted on approximately 1/4-scale models of blast shelters. Specific objectives of these tests were to evaluate the preliminary structural design, to investigate structural response in various backfills, to investigate and recommend minimum concrete strength requirements, to evaluate structural response calculations, and to develop a data base on repeated hits so that structural response computational procedures can be developed to include the effects of repeated hits.

Test results indicate that the keyworker blast shelter design will resist a peak overpressure of 150 psi from a 1-MT nuclear weapon. Based on the results of this series of static and dynamic tests, it is recommended that: (1) minimum strength of concrete used in the keyworker blast shelter should be 3,000 psi; (2) backfill specifications can be reduced to include soils with a minimum angle of internal friction of 25° (30° for foundation materials); (3) a minimum depth of burial of 4 ft (30 percent of the unsupported roof span) should be used; (4) the interior structural steel frames should be replaced with precast or cast-in-place reinforced concrete walls.

STRUCTURAL ELEMENT TESTS IN SUPPORT OF THE KEYWORKER BLAST SHELTER PROGRAM.
Unclassified, US Army Engineer Waterways Experiment Station, October 1985, 321 pp.

At the initiation of this study, civil defense planning called for the evacuation of nonessential personnel to safe host areas during a time of crisis, and the construction of shelters to protect the keyworkers remaining behind. The Federal Emergency Management Agency tasked the US Army Engineer Division, Huntsville (HND), to design a 100-man keyworker shelter. The research documented in this report is in support of the HND design effort.

Six static tests and twelve dynamic tests were conducted on approximately 1/4-scale models of blast shelters. Specific objectives of these tests were to evaluate the preliminary structural design, to investigate structural response in various backfills, to investigate and recommend minimum concrete strength requirements, to evaluate structural response calculations, and to develop a data base on repeated hits so that structural response computational procedures can be developed to include the effects of repeated hits.

Test results indicate that the keyworker blast shelter design will resist a peak overpressure of 150 psi from a 1-MT nuclear weapon. Based on the results of this series of static and dynamic tests, it is recommended that: (1) minimum strength of concrete used in the keyworker blast shelter should be 3,000 psi; (2) backfill specifications can be reduced to include soils with a minimum angle of internal friction of 25° (30° for foundation materials); (3) a minimum depth of burial of 4 ft (30 percent of the unsupported roof span) should be used; (4) the interior structural steel frames should be replaced with precast or cast-in-place reinforced concrete walls.